Examination of Vascular Smooth Muscle Cell-specific NADPH Oxidase 5 in the Context of Age, Sex, and Angiotensin II-induced Hypertension: Implications for Cerebrovascular Disease

Zachariel Steven L Blaikie

BSc (Hons), MSc, GMBPsS

Thesis submitted in the fulfilment of the requirements of the degree of Doctor of Philosophy (PhD)

University of Glasgow

School of Cardiovascular and Metabolic Health

College of Medical, Veterinary, & Life Sciences

University of Glasgow

April 2025

COVID-19 Impact Statement

The COVID-19 pandemic significantly disrupted the progress of my MVLS DTP-funded PhD research. Central to my project was the use of 20- and 35-week-old vascular smooth muscle-specific Nox5 knock-in mice. The extended closure of research facilities from 23rd March 2020 to 15th August 2020 resulted in the cessation of mouse breeding programs vital for my research. Even after the reopening of facilities this was at a reduced capacity (30%) for ~12 months due to social distancing regulations and the production of experimental mice and associated experiments were severely hindered. Given that only 25% of offspring are expected to be the correct genotype, the prolonged disruption directly delayed experiments and caused the cancellation of some planned studies due to an insufficient number of suitable mice. Furthermore, training opportunities for learning new experimental techniques were also impacted due to social distancing regulations in the research laboratories, further stalling the planned methodological advancements within my project. Although archived material provided some avenues for analysis, the lack of new experimental material severely constrained progress.

Summary

NADPH oxidase 5 (NOX5) is a complex multi-domain reactive oxygen species (ROS) producing protein that is unique among NOX isoform family members due to Ca^{2+} binding being required for its enzymatic activation rather than regulatory proteins. Furthermore, whilst *NOX5* is expressed in human vascular smooth muscle cells (VSMCs), endothelial cells (ECs) and fibroblasts, the *NOX5* gene is absent in mice and rats resulting in limited understanding of the role of NOX5 in the vasculature. To assess potential vascular roles of NOX5, transgenic models expressing human *NOX5* have been generated. Whilst many studies have identified a deleterious role for NOX5 in peripheral vascular tissues, contributing to hypercontractility, hypertension and tissue damage, NOX5 remains poorly understood in the brain. Previous research demonstrated that endothelial-specific NOX5 expression in mice contributes to increased oxidative stress, blood-brain barrier (BBB) dysfunction in *post*-stroke surgical models, with further research identifying that ageing in the brains of endothelial-specific NOX5 mice contributes to a hypertensive phenotype and poorer cognitive and neurological outcomes. However, no research has examined the role of VSMC-specific NOX5 overexpression in the brains of mice. Given the central role for Ca^{2+} in cerebrovascular autoregulation and cerebral blood flow (CBF) dynamics, and mesenteric artery dysfunction and hypercontractility in mice expressing VSMC-specific NOX5, VSMC NOX5 could play a key role in contributing to pathophysiological processes that disrupt cerebrovascular function. Furthermore, to date, no studies have specifically assessed the role of cerebral VSMC-specific NOX5 overexpression in the context of sex differences and angiotensin II (Ang II) mediated hypertension despite compelling evidence from previous research that associates sex hormones and Ang II as critical regulators of NOX5 activity. As such, this thesis aimed to examine these critical gaps in the existing research literature.

The data presented in Chapter 3 of this thesis characterise the role of VSMC-specific NOX5 overexpression in the brains of male and female young (20-week-old) mice. This was achieved by utilising *ex vivo* molecular techniques to examine neurovascular function proteins, alternative NOX isoform protein and gene expression levels, markers of ROS bioavailability, oxidative stress and endoplasmic reticulum (ER) stress, and the NOTCH3 signalling axis in whole brain homogenates of these mice. Additionally, contraction and endothelial-independent vasorelaxation was assessed by wire

myography in the carotid arteries of these mice. It was hypothesised that VSMC-specific NOX5 would lead to increased ROS bioavailability, markers of oxidative and ER stress, dysregulated NOTCH3 signalling, and impaired vascular function. Furthermore, given the role of sex hormones in vascular disease, whereby oestrogen has been identified to act protectively, this study further hypothesised that these effects would be worsened in male VSMC-specific NOX5 mice. In male mice, VSMC-specific NOX5 was associated with increased ROS bioavailability, increased BIP protein levels, downregulated GFAP levels, and impaired endothelial-independent vasorelaxation in carotid arteries compared to WT mice. These data support the hypothesis that VSMC-specific NOX5 would increase ROS bioavailability and impair endothelial-independent vasorelaxation, indicating carotid artery vascular dysfunction. Conversely, in female VSMC-specific NOX5 mice there were reduced markers of oxidative stress and increased antioxidant gene expression, indications of non-canonical NOTCH3 signalling, with no observed changes to carotid artery vascular function compared to WT mice. These data indicate that sex hormones may play a key role in the regulation of NOX5 and NOX5 associated signalling cascades such as NOTCH3. However, the dynamics and exact mechanisms behind the influence of sex hormone regulation requires further study.

In Chapter 4 of this thesis, the aim was to examine the role of VSMC-specific NOX5 in the context of ageing. As ageing is associated with a decline in vascular health, it was hypothesised that the protective effects observed in chapter 3 in female VSMC-specific NOX5 mice would diminish as a consequence of age-related reductions in oestrogen bioavailability contributing to increased markers of ROS bioavailability, oxidative stress, dysregulated NOTCH3 signalling, and impaired vascular function. In male VSMC-specific NOX5 mice, it was hypothesised that ageing would contribute to further impairments of neurovascular proteins, increases in ROS bioavailability, enhanced ER stress and further impairments to vascular function, whilst also contributing to NOTCH3 dysregulation. The same analyses utilised in Chapter 3 were used to compare 35-week-old WT and VSMC-specific NOX5 mice with 20-week-old mice. In 35-week-old male mice, VSMC-specific NOX5 was associated with downregulation of NOX1 and upregulation of NOX2 protein levels. Whilst aged male WT mice exhibited decreases in irreversible protein tyrosine phosphatase oxidation and peroxiredoxin hyperoxidation, this effect was prevented in the brains of VSMC-specific NOX5 mice. Furthermore, male VSMC-specific NOX5 in the context of ageing contributed to altered cerebrovascular NOTCH3 signalling and the activation of downstream NOTCH3 transcription targets,

indicating that ageing in male VSMC-specific NOX5 mice contributes to canonical NOTCH3 signalling. These findings indicate a potential cerebral small vessel disease (CSVD) phenotype that was in agreement with impaired endothelial-independent vasorelaxation and hypercontractility observed in the carotid arteries of 35-week-old male VSMC-NOX5 mice. However, ageing did not affect the altered GFAP, BIP or ROS levels identified in young VSMC-NOX5 mice in chapter 3. In 35-week-old female mice, VSMC-specific NOX5 was associated with downregulated NOX1 and NOX4 levels, and an upregulation of *Nox2* mRNA expression. Furthermore, NOX2 levels were increased in female WT mice with age, but not in female VSMC-NOX5 mice. Aged female VSMC-specific NOX5 mice continued indicate a role for non-canonical NOTCH3 signalling. Additionally, VSMC-specific NOX5 in aged female mice promoted improved endothelial-independent vasorelaxation, with no changes in WT mice being identified, indicating a potentially vasoprotective role for NOX5 in female mice. These findings provide evidence that VSMC-specific NOX5 acts simultaneously vasoprotective and vasodeleterious with age with age in a sex-dependent manner.

In Chapter 5 of this thesis, the aim was to examine the role of VSMC-specific NOX5 in the context of Ang II-induced hypertension. As Ang II induces NOX activation and a hypertensive phenotype, it was hypothesised that in both male and female mice expressing VSMC-specific NOX5 it would contribute to impairment of the neurovascular unit, increase ROS bioavailability and additionally contribute to NOTCH3 dysregulation. WT and VSMC-specific NOX5 mice that had undergone a 4-week treatment with Ang II were compared to 'non-treated' (NT) normotensive counterparts. As in chapters 3 and 4, levels of neurovascular function proteins, other NOX isoform protein and gene expression levels, markers of ROS bioavailability, oxidative stress and ER stress, and the NOTCH3 signalling axis in whole brain homogenates from male and female 20-week-old Ang II treated and NT WT and VSMC-specific NOX5 mice were altered. Ang II treatment of WT males led to an increase in NOX4 protein levels that were not identified in Ang II-treated VSMC-specific NOX5 male mice. However, NOX1 protein expression was increased. Whilst markers of oxidative stress were identified, ROS and lipid peroxidation markers were downregulated in the brains of male Ang II treated VSMC-NOX5 mice whilst antioxidant response element mRNA expression was downregulated when compared to male NT VSMC-NOX5 mice. Additionally, markers of canonical NOTCH3 signalling were identified. Collectively, these results indicate a potential role for a VSMC-specific NOX5-mediated oxidative stress and CSVD phenotype that could contribute to severe

pathologies such as CADASIL. Conversely in female WT mice, Ang II upregulated cerebral NOX1 and downregulated NOX2 protein levels, effects that were absent in VSMC-specific NOX5 mice. Interestingly, no cerebral markers of oxidative stress were identified in Ang II-treated female VSMC-NOX5 mice, although BIP levels were increased which may indicate ER stress. Finally, assessment of NOTCH3 signalling identified no effect of VSMC-specific NOX5 overexpression in female mice other than downregulation of the mRNA expression of the downstream NOTCH3 target *Hey1*. These findings suggest sexual dimorphic effects of Ang II treatment in the brains of VSMC-specific NOX5 mice.

Taken collectively, the findings of this thesis present novel evidence that there is a sexual dimorphism in the response to VSMC-specific NOX5 overexpression in mice with respect to cerebrovascular function. In the brains and carotid arteries of males, VSMC-specific NOX5 was associated with progressive age-related cerebrovascular dysfunction linked with canonical NOTCH3 signalling. Conversely, in the brains of female mice, VSMC-specific NOX5 was associated with improved endothelial-independent vasorelaxation, whilst also contributing to non-canonical NOTCH3 signalling with age and may indicate that NOX5 in a VSMC-specific manner may contribute to vasoprotective effects, however the exact mechanisms are unclear warranting further study. Furthermore, in the context of Ang II-induced hypertension, a similar pattern of sex-specific differences in canonical and non-canonical NOTCH3 signalling was also observed. These findings highlight intriguing questions for future research examining VSMC-specific NOX5 in the brain. Firstly, do sex hormones modulate NOX5 activity and/or the NOX5-NOTCH3 signalling axis directly or through indirect signalling mechanisms? Secondly, do the effects identified in this thesis contribute to a CSVD phenotype, impaired CBF, and increased risk of cerebrovascular diseases such as CADASIL, stroke and vascular dementia? To fully elucidate the findings of this thesis, comprehensive *in vivo* models and *ex vivo* molecular characterisation is required to fully inform the signalling cascades influenced by VSMC-specific NOX5 and their effects in cerebrovascular dysfunction and may inform the development of targeted pharmacological therapeutic strategies to mitigate the risk of cerebrovascular disease.

Table of Contents

List of Tables

List of Figures

Acknowledgments

I would like to sincerely thank the University of Glasgow MVLS Doctoral Training Partnership for accepting me onto this programme and funding my research. When I got the call that I had been accepted, it was lifechanging for me. This opportunity allowed me to live my dream of becoming a scientist. I would also like to thank the school of cardiovascular and metabolic health janitorial and administrative staff. The work that you do behind the scenes to support and promote the amazing science produced in this institute, particularly during the COVID-19 pandemic, is fundamental and always appreciated.

A project as fascinating as NOX5 required excellent supervision, and I was fortunate to have been supervised and mentored by the very best. I would first like to thank my supervisor Professor Rhian Touyz. To have worked under you and to learn from your almost infinite wisdom, knowledge, and expertise has been an extraordinary privilege. You always did your best to take time out of your incredibly busy (and very important) work schedule to give exceptional guidance, insightful feedback, and personal support. I will always be able to say with pride that I worked under your supervision. A heartfelt thank you goes to Dr Augusto Montezano. From the beginning of my mini-project rotations in 2019 through the start of my PhD and now as I reach the end of my journey, you have been a constant source of guidance, leadership and support. We have been on an incredible journey, and I am deeply grateful for your guidance in my development both scientifically and personally. Your encouragement lifted me when I needed it the most and your honest feedback challenged me to be better. I am profoundly thankful for the opportunities you provided me and for having you not only as supervisor, but also as a mentor and a friend.

Whilst the Touyz lab is so vast that I cannot possibly mention all the incredible people I worked with, I would like to give a special mention to Dr Fransico Rios and Dr Livia Camargo. Put it simply, your knowledge and enthusiasm were inspiring, and you were always there to support me whenever I asked, which was priceless for me. Fran, your personal support in 2021 will never be forgotten. I would also like to express huge thanks to Mrs Wendy Beattie – I will never have the words to thank you for your help both academically and personally, and I am proud to be able to call you a colleague and a friend. I would also like to thank my amazing friend Dr Jithin Kuriakose. The first time we ever spoke was when you asked to join me and Wendy in an RNA extraction demonstration; little did I know that I had just met one of the closest friends I will ever

have. I have so many fond memories to reminisce over, from teaching each other experimental protocols, to offering one another our perspectives on research findings, it was a blessing to work together. A beautiful lab partnership that ended on the highest of highs, with a trip to the ISH conference in Japan. Although the PhD was a temporary phase in our life journey, our friendship will last forever.

I give thanks to Dr Alyson Miller for coming on board to the project when my supervisors left for Canada. The support, particularly in the first few months where you taught me wire myography, will always be appreciated.

To Dr Ian Salt, words cannot express my gratitude to you. You came onto the project at my most challenging point and your support was incredible. Discussing my project with you and getting your expert advice, as well as being able to do some experiments under your supervision, was a high point on which to end my PhD research. You were instrumental in getting this PhD over the line.

I would like to give special thanks to Dr Lorraine Work for your guidance and support throughout my PhD journey. We shared and faced many challenges throughout; from a pandemic to changes in supervisory set ups, there wasn't a single year of my PhD where something fundamental to the project hadn't changed and it is here, at the end of it all, that I realise just how much you did to support me. I deeply appreciate the time and effort you invested in me and my work, and how your insights and expertise has influenced my growth both as a researcher, and as a person.

I would also like thank my undergraduate supervisor Dr Jamal Mansour and my masters supervisor Dr Debbie Dewar for giving me the opportunities earlier in my academic career that opened the door to PhD.

A special mention has to also be made for Ms Denise Frame and Mrs Evelyn Craig. You were instrumental during my early life when not many gave me a chance to succeed, without your care, support and teachings, simply I wouldn't have got this far.

On a personal note, I would like to thank my mum and dad who supported me through so much, from school, to the military, and throughout my PhD. Your hard work and patience have allowed me to get to this point.

To my loving partner Dr Lauren Murray, it takes a remarkable woman to endure a second PhD, especially when the second PhD isn't her own. We have been through so much together, and your endless support, patience and encouragement has provided me with the motivation to succeed.

Finally, to my children Greyson and Theia, you both are the world to me. Whenever I had a difficult day of lab experiments, analysis, or writing, you were always in my thoughts and provided a welcome distraction. Everything I have accomplished here and everything I do going forward is for you, and my love for you both is what drives me on to succeed.

Author's Declaration

I declare that this thesis has been written entirely by myself, and all experimental data has been carried out by myself except where otherwise acknowledged, cited, or listed below:

- Breeding and genotyping of the mice used in this study was conducted by myself and Mrs Wendy Beattie
- Tail cuff plethysmography for BP measurement in mice was conducted by the Touyz Lab, notably Dr Augusto Montezano and Mrs Wendy Beattie.
- Surgical implantation of the mini-pump used for Angiotensin II experiments in this study was conducted by various members of the Touyz lab.

This thesis has not, in whole or part, been submitted for any other higher degree. The research was conducted at the School of Cardiovascular and Metabolic Health, University of Glasgow under the supervision of Dr Lorraine Work, Dr Augusto Montezano, Dr Ian Salt, Dr Alyson Miller, and Professor Rhian Touyz and was funded by the University of Glasgow Medical, Veterinary, and Life Sciences Doctoral Training Partnership.

Zachariel S L Blaikie
April 2025

Abbreviations

[Ca2+]i……Intracellular calcium ion concentration

•OH……hydroxyl radical

ACE……angiotensin converting enzyme

ADAM……A disintegrin and metalloproteinase

AGT……...angiotensinogen

AMPA……..α-amino-3-hydroxy-5-methyl-4-propionate acid

Amplex-Red……..……..10-acetyl-3,7-didroxyphenoxazine

Ang II……angiotensin II

ARE……antioxidant response element

AT_1R……angiotensin type 1 receptor

AT_2R……..angiotensin II type 2 receptor

ATP……...adenosine triphosphatase

BBB……blood brain barrier

BCA……bicinchoninic acid

BCAS……...bilateral carotid artery stenosis

BDNF……...brain derived neurotrophic factor

BIP……binding immunoglobulin protein

BP……..blood pressure

BSA……...bovine serum albumin

Ca^{2+}……calcium ion

CAA……cerebral amyloid angiopathy

CADASIL……
cerebral autosomal dominant arteriopathy with subcortical infarcts and leukoencephalopathy

CaM……calmodulin

cAMP……..cyclic adenosine 3',5'-monophosphate

CaV…….L-type voltage-gated Ca2+ channels

CBF……cerebral blood flow

CCRC…….cumulative concentration response curves

cGMP……...cyclic guanosine monophosphate

Cl^-……..chloride ion

CNS……..central nervous system

COX2……..cyclooxygenase

CPP……cerebral perfusion pressure

CSVD……..cerebral small vessel disease

DAPI……4′,6-diamidino-2-phenylindole

Delta……..delta-like protein ligands

DNA……..……deoxyribonucleic acid

E_1…….oestrone

E_2……..17β-oestradiol

E_3…….oestriol

EC…….endothelial cell

EF-hand…….Ca^{2+} binding helix-loop-helix structural domain

EGF…….epidermal growth factor-like

ELISA……enzyme linked-immunosorbent assay

eNOS……..……...endothelial nitric oxide synthase

ER…….endoplasmic reticulum

ERK……...extracellular signal-regulated kinases

ERα……...……oestrogen receptor-alpha

Erβ……...oestrogen receptor-beta

Fe^{2+}…….ferrous iron

Fe^{3+}……...ferric iron

GFAP……...glial fibrillary acidic protein

GOI……...gene of interest

GPCR……G-protein coupled receptor

GPER……..G-protein-coupled oestrogen receptors

GTP……..guanosine triphosphate

H_20_2.....hydrogen peroxide

Hes……...hairy/enhancer-of-split

Hey…….hairy/enhancer-of-split related YRPW motif protein

HKG…….housekeeeping gene

HO1…….. Haem oxygenase 1

HRP……..horseradish peroxidase

ICH……...…intercranial haemorrhage

IHC……..immunohistochemistry

IL…….....interleukin

iNOS…….inducible nitric oxide synthase

IP_3……inositol triphosphate

IP_3R……inositol triphosphate receptor

IRI……...ischaemic reperfusion injury

Jag…….……..jagged protein ligand

JAK/STAT……...janus kinase/signal transducers and activators of transcription

JAM……..junctional adhesion molecules

JNK…….c-jun N-terminal kinase

K^+……..potassium ion

KPSS…….high potassium physiological salt solution

LinA3…….….low-dose Ang II and NOS inhibition

L-NAME……..……L-N^G-Nitro arginine methyl ester

MAML……...mastermind-like protein

MAPK…….mitogen-activated protein kinases

MasR……mas receptor

MCA……..middle cerebral artery

MCAO……...middle cerebral artery occlusion

MDA…….malondialdehyde

MLC……myosin light chain

MLCK……..myosin light chain kinase

MOMP…….mitochondrial outer membrane permeabalisation

MRI…….magnetic resonance imaging

mRNA……...messenger ribonucleic acid

N3-ECD……..NOTCH3 extracellular domain

N3-ICD……NOTCH3 intracellular domain

Na^+…….sodium ion

NADPH……..nicotinamide dinucleotide phosphate

NEP……..neprilysin

NF-kB……...nuclear factor kappa light chain enhancer of activated B cells

NMDA……...N-methyl-D-aspartate

nNOS…….neuronal nitric oxide synthase

NO……..nitric oxide

NOTCH3……neurogenic locus notch homolog protein 3

NOX……...NADPH oxidase

NQO1……NADPH quinone oxidoreductase 1

NRF2……...nuclear factor erythroid 2-regulated factor 2

NVU……neurovascular unit

O_2……..oxygen

$O_2^{\bullet-}$……..superoxide

ONOO−……...peroxynitrite

PBS……..phosphate buffer solution

PGC-1α…….peroxisome proliferator-activated receptor gamma coactivator 1-alpha

PIP2……..phosphatidylinositol 4,5-bisphosphate

PKC……protein kinase C

PKG……protein kinase G

PLC……phospholipase C

PMA……...phorbol 12-myristate 13-acetate

PPIA……..peptidylprolyl isomerase A

PRDX…….peroxiredoxin

PRDX-SO_3……peroxiredoxin hyperoxidation

PSS……..……physiological salt solution

PTP…….protein tyrosine phosphatase

PTP-SO_3.....irreversible protein tyrosine phosphatase

PUFA…….polyunsaturated fatty acids

RAAS…….renin angiotensin aldosterone system

RBP-Jκ…….recombinant signal-binding protein for immunoglobulin kappa J region

RF-H_2O……...…….RNAse free water

RhoA……ras homolog family member A

RNA……ribonucleic acid

RNS……...reactive nitrogen species

ROCK……...rho kinase

ROS……reactive oxygen species

SAH……...subarachnoid haemorrhage

SDS-PAGE……...sodium dodecyl sulphate polyacrylamide gel electrophoresis

SERCA……sarco/endoplasmic reticulum Ca2+ ATPase

sGC……..soluble guanylate cyclase

SHR…….……....spontaneously hypertensive rat

SHRSP……....stroke prone spontaneously hypertensive rat

SNP…….sodium nitroprusside

SOD……superoxide dismutase

TACE……TNF-α-converting enzyme

TBARS…….thiobarbituric acid reactive substances

TBS…….tris-buffered saline

TBS-T……tris-buffered saline-tween 20

TCA……...trichloroacetic acid

TJ……tight junction

TNF-a……..tumour necrosis factor alpha

tMCAO……...transient middle cerebral artery occlusion

TXA_2R…….thromboxane A2 receptor

TXA_2S ……...thromboxane A_2 synthase

UPR…….unfolded protein response

VaD……..vascular dementia

VCI……...vascular cognitive impairment

VEGF…….vascular endothelial growth factor

VEGFR2……...…vascular endothelial growth factor receptor 2

VSMC……..……vascular smooth muscle cell

WMH…….white matter hyperintensities

WNT…….wingless-type MMTV integration site

WT……...….wild type

αSMA……..……...alpha smooth muscle actin

Publications, Presentations, and Awards

List of Publications:

- Touyz, RM, Camargo, LL, Rios, FJ, Alves-Lopes, R, Neves, KB, Eluwole, O, Maseko, MJ, Lucas-Herald, A, **Blaikie, Z**, Montezano, AC & Feldman, RD 2022, Arterial hypertension. T Kenakin (ed.), *Comprehensive Pharmacology*., 4.20, Amsterdam, pp. 469-487. doi: https://doi.org/10.1016/B978-0-12-820472-6.00192-4

List of Published Abstracts:

- **Blaikie, Z.,** Montezano, A., Miller, A., Touyz, R., and Work, L. (2023). PS-B01-12: Sexual dimorphism of cerebrovascular NOX5-NOTCH3 signalling in angiotensin II-induced hypertension. *Journal of Hypertension*. 41(1): e174. doi: http://dx.doi.org/10.1097/01.hjh.0000914428.69803.90

- Montezano, A., Rios, F., **Blaikie, Z.,** Saad, T., Camargo, L., Palacios-Ramirez, R., Tarjus, A., Sagan, A., Beattie, W., Guzik, T., Jaisser, F., Graham, D., and Touyz, R. (2022). PS-B01-7 Vascular smooth muscle cell NOX5 regulates fibroblast phenotypic switch and cardiovascular fibrosis. *Journal of Hypertension*. 41(1): e172. doi: http://dx.doi.org/10.1097/01.hjh.0000914408.16750.f6.

- Montezano, A., Rios, F., **Blaikie, Z.,** Saad, T., Camargo, L., Beattie, W., Jaisser, F., Guzik, T., Graham, D., and Touyz, R. (2023). Nox5 expression in a vascular smooth muscle cell-specific manner induces fibroblast to myofibroblast differentiation. *Hypertension*. 79 (1). doi: http://dx.doi.org/10.1161/hyp.79.suppl_1.127

- Montezano, A., Rios, F., **Blaikie, Z.,** Saad, T., Camargo, L., Beattie, W., Jaisser, F Guzik, T., Graham, D., Touyz, R. (2022). Nox5 expression in a vascular smooth muscle cell-specific manner induces phenotypic switch and pro-fibrotic effects. *Journal of Hypertension*. 40 (1):e37. doi: http://dx.doi.org/10.1097/01.hjh.0000835588.67477.1c

- **Blaikie, Z.,** Touyz, R., Montezano, A., and Work, L. (2022). Cerebrovascular profiling of vascular smooth muscle cell-specific NOX5 expression in mice. Journal of Cerebral Blood Flow & Metabolism. 42(15):254.

Oral and Poster Presentations:

- **Blaikie, Z. S.,** Touyz, RM., Montezano, AC., and Work, LM. Sex differences in cerebrovascular effects of smooth muscle cell-specific Nox5 mice. **[Poster presentation]** *Canadian Hypertension Congress,* Online 2022.

- **Blaikie, Z. S.,** Touyz, RM., Montezano, AC., and Work, LM. Cerebrovascular profiling of vascular smooth muscle cell-specific NOX5 expression in mice. **[Poster presentation]** *Brain and Brain PET,* Glasgow, U.K., 2022.

- **Blaikie, Z. S.,** Touyz, RM., Montezano, AC., and Work, LM. Cerebrovascular profiling of vascular smooth muscle cell-specific NOX5 expression in mice. **[Poster presentation]** *ARUK Annual Network Event,* St Andrews, U.K., 2022.

- **Blaikie, Z. S.,** Montezano, AC., Miller, AA., Touyz, RM., Work., LM. Sexual dimorphism of cerebrovascular NOX5-NOTCH3 signalling in angiotensin-II induced hypertension. **[Oral presentation]** *International Society of Hypertension New Investigators Network*, Kyoto, Japan, 2022.

- **Blaikie, Z. S.,** Montezano, AC., Miller, AA., Touyz, RM., Work., LM. Sexual dimorphism of cerebrovascular NOX5-NOTCH3 signalling in angiotensin-II induced hypertension. **[Poster presentation]** *International Society of Hypertension*, Kyoto, Japan, 2022.

Awards

- ***Outstanding Poster Presentation award:*** The 10th Canadian Hypertension Congress, 2022 [Online]

- ***Best Oral Presentation winner:*** The 29th Scientific Meeting of the International Society of Hypertension Conference 2022 [Kyoto, Japan], 600 USD prize.

- **New Investigator Spotlight for outstanding new researcher of the month:** International Society of Hypertension**:** https://ish-world.com/portfolio/january-2023-zach-blaikie-uk/.

- **University of Glasgow MVLS travel grant:** For attendance to the *BRAIN & BRAIN PET Conference*, 2022 [Glasgow, U.K], 400 GBP.

- **The 29th Meeting of the International Society of Hypertension Travel Grant**: For attendance to the *International Society of Hypertension Conference*, [Kyoto, Japan], 2022. 600 USD.

- **Guarantors of Brain Travel Grant**: For attendance to the *International Society of Hypertension Conference*, 2022 [Kyoto, Japan], 1000 GBP.

Chapter 1

Introduction

1.1 Introduction

Cerebrovascular diseases contribute significantly to neurological and cognitive decline and are some of the leading causes of morbidity and death worldwide (Verdelho *et al*., 2021, Hachinski *et al*., 2019). Cerebral small vessel disease (CSVD), stroke and vascular dementia (VaD) contribute significantly to this challenge and are characterised by progressive impairment of cerebral blood flow (CBF), cerebrovascular dysfunction, hypoperfusion, and brain tissue damage (Hachinski *et al*., 2019, Verdelho *et al*., 2021). Amongst the various contributing risk factors to these diseases, ageing and hypertension have both been identified as key mediators of cerebrovascular dysfunction and pathological risk (Hainsworth *et al*., 2024, Boehme *et al*., 2017). Moreover, increasing evidence has also identified that sex differences could play a key role in pathologies such as CSVD, stroke and VaD (Kremer *et al*., 2023). All of these risk factors share a common pathophysiological mechanism that plays a central and key role in cerebrovascular dysfunction – reactive oxygen species (ROS) mediated oxidative stress (Wu *et al*., 2020, Lloret *et al*., 2021). A critical source of ROS and oxidative stress in the vascular pathophysiology are nicotinamide adenine dinucleotide phosphate (NADPH) oxidases (NOX) which are expressed in different vascular cell types including vascular smooth muscle cells (VSMC). NOX5 has recently been identified as Ca^{2+}-mediated, superoxide producing, pro-contractile NOX and a driver of systemic diseases such as hypertension and atherosclerosis. In the brain, mice expressing NOX5 in an endothelial-specific manner, have been linked to worsened *post*-stroke outcomes (Montezano *et al*., 2018, Casas *et al*., 2019). However, the role of NOX5 has not been assessed in a VSMC-specific manner.

This thesis aims to investigate the role of VSMC-specific NOX5 and how it may contribute to molecular mechanisms that lead to vascular dysfunction and potential CSVD, stroke and VaD risk. By exploring the mechanism through which VSMC-specific NOX5-mediated oxidative stress influences cerebrovascular function, this research contributes to the understanding of how NOX5 may influence molecular mechanisms that drive cerebrovascular disease pathology, which is critical for developing more effective therapeutic interventions aimed at reducing the burden of cerebrovascular diseases and their associated neurological and cognitive sequelae. This thesis will discuss the physiological function of the cerebrovasculature, followed by in-depth assessment of cerebrovascular diseases CSVD, stroke and VaD, and their shared risk factors and pathological mechanisms, with focus on how NADPH oxidases contribute to oxidative

damage by looking at the current literature on NOX5, before disseminating the research examining the molecular and functional mechanisms of cerebral VSMC-specific NOX5. Through this research, this thesis will contribute to a growing body of research identifying how NOX5 plays a complex, yet key, role in driving vascular dysfunction, increasing the risk of diseases such as CSVD, stroke and VaD.

1.2 Cerebrovascular Circulation, Physiology and Anatomy

The central nervous system (CNS) is the most metabolically active organ in the body, that despite accounting for only 2% of total body mass, requires approximately 15-20% of the body's cardiac output. Moreover, brain tissue is limited in its capacity for anaerobic metabolism, consequently making the brain highly susceptible to hypoxic and ischaemic insults (Xing *et al*., 2017). As such, the brain requires a constant and intricately regulated supply of oxygen and glucose for sustained metabolic energy and cerebral function. This is achieved by a cerebrovascular network of large and small vessels which play distinct, yet complementary functions in maintaining adequate CBF and perfusion to neuronal and glial cells to maintain brain function (Claassen *et al*., 2021). Normal CBF in humans is approximately 50-60 mL/100 g/min and is delivered through a network of cerebrovascular vessels (Lee *et al*., 2005). The cerebrovascular network comprises of bilateral carotid and cerebral arteries that are essential for delivering blood from systemic circulation to the Circle of Willis, an anastomotic structure that connects to the basilar, internal carotid and posterior arteries via the anterior and posterior communicating arteries, providing collateral circulation in instances of reduced CBF (Ahn and Prince, 2013, Agarwal and Carare, 2021). Major branches of the internal carotid arteries include the anterior arteries and middle cerebral arteries (MCA) with MCA giving rise to lenticulostriate arteries that supply subcortical structures such as the caudate nucleus, thalamus, and the basal ganglia (Xu *et al*., 2021). Branches of the anterior, posterior arteries and MCA form networks within the pia-arachnoid membrane connecting to small penetrating arteries and capillary networks that penetrate grey matter tissue, transitioning into parenchymal arteries that distribute to the cerebral parenchyma for adequate cerebral perfusion. (Agarwal and Carare, 2021, Bergers and Song, 2005).

1.2.1 Cerebrovascular Vessel Structure

Cerebrovascular arteries consist of three distinct layers, each layer playing an interdependent role in contributing to vessel function and integrity. The innermost layer, known as the *tunica intima*, is a single layer of endothelial cells (EC). ECs ensheathe the internal elastic lamina, a layer of connective tissue that provides vascular elasticity in response blood pressure (BP) changes. The next layer of cerebrovascular arteries is known as the *tunica media*, consisting of VSMC, that are interspersed with collagen and elastin fibres. The outermost layer is known as the *tunica adventitia*/*tunica externa* predominantly comprising collagen fibres. As large arteries connect to capillaries, the vessel size decreases (**Figure 1-1**). Whilst larger arteries contain 20 layers of VSMC within the *tunica media*, smaller pial vessels typically only possess 2-3 VSMC layers and penetrating arteries possess only a single VSMC layer. In smaller arterioles and capillaries, VSMC are progressively replaced by pericytes (Agarwal and Carare, 2021). It was initially thought that pericytes played no role in changes in cerebral capillary vasomodulation as there was no detection of contractile proteins, and this was instead regulated by arteriolar VSMCs due to the inability to detect contractile proteins (Hill *et al*., 2015). However, pericytes were recently identified as expressing the contractile myofilaments alpha-smooth muscle actin (αSMA) and SM22 (Yao *et al*., 2014, Alarcon-Martinez *et al*., 2018), indicating that pericytes do contain contractile mechanisms. Seminal research assessing the role of capillary pericytes in the regulation of CBF identified glutamate-mediated pericyte relaxation by prostaglandin E_2, and nitric oxide (NO) suppression of the vasoconstrictive 20-hydorxyeicosatetraenoic acid synthesis, leading to capillary dilation (Hall *et al*., 2014). Further research identified a key role for pericyte calcium ion (Ca^{2+}) dynamics with L-type voltage-gated Ca^{2+} channels (CaVs) being a key regulator of intracellular Ca^{2+} ($[Ca^{2+}]i$) concentrations, ROS production, inflammation and impaired microvascular flow (Korte *et al*., 2024).

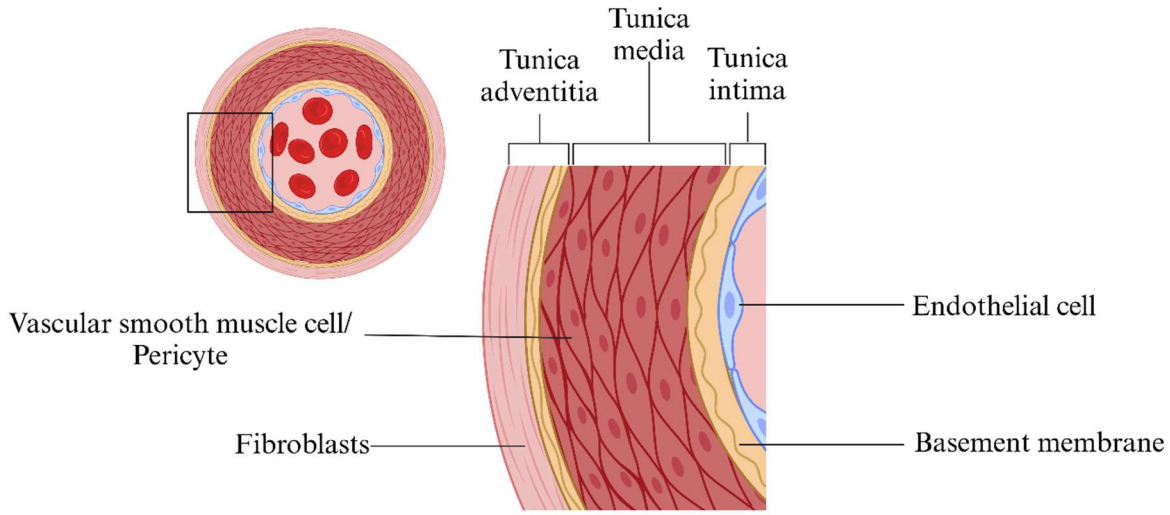

Figure 1-1. Anatomical structural of the vasculature wall. This figure illustrates the three primary layers of the vasculature wall: the tunica intima, tunica media and the tunica adventitia. First, the tunica intima consists of ECs and the basement membrane, which maintains blood flow homeostasis and regulates selective permeability of molecules. The tunica media is primarily composed of VSMCs, which are arranged in concentric layers within arteries and arterioles, controlling vascular contraction and relaxation in response to physiological stimuli. In contrast, pericytes, rather than VSMCs, surround capillaries and post-capillary venules and provide vascular stability and microvascular regulation. Finally, the tunica media consists of fibroblasts responsible for producing and maintaining extracellular matrix components including collagen and elastin, providing tensile strength to the vasculature. This figure was created in BioRender.

1.2.2 Neurovascular Unit

CBF is not only regulated by cerebrovascular cells but is also maintained through interdependent mechanisms working in conjunction to maintain cerebral health known as the neurovascular unit (NVU). The NVU is a highly specialised structure acting as a regulatory hub, maintaining and regulating CBF, vascular tone, and the cerebral/cerebrovascular exchange of molecules (Schaeffer and Iadecola, 2021). The NVU is comprised of neurons, glial cells (astrocytes and microglia), pericytes, ECs and VSMCs. Neurons are vital for sending neurotransmitters throughout the central and peripheral nervous system, regulating key processes such as cognition and BP. Furthermore, neural mechanisms contribute to cerebral autoregulatory responses that influence CBF through sympathetic and parasympathetic modulation of vascular tone (Yu *et al*., 2020). Astrocytes play a critical role linking neuronal activity to blood vessel responses and maintaining homeostasis. This is achieved through release of vasoactive substances, most notably NO, that act on nearby vessels leading to vasodilatory effects in response to hypoxia (Christie *et al*., 2023). ECs form the inner layer of the vasculature and the formation of tight junctions known as the blood-brain barrier (BBB), an essential component of the brain that preserves the selective permeability of vital metabolic nutrients to the brain, whilst also preventing harmful molecules and peripheral cells from entering the brain. Furthermore, ECs produce a range of vasoactive substances that regulate vascular tone including the, prostacyclin (PGI_2), thromboxane, endothelin-1, and endothelial nitric oxide synthase (eNOS) derived NO with the most important regulator of vascular tone that diffuses from ECs to mural cells such as pericytes and VSMCs, activating guanylate cyclase and leading to the production of cyclic guanosine monophosphate (cGMP) resulting in pericyte/VSMC relaxation (Sandoo *et al*., 2010, Kadry *et al*., 2020). Pericytes located on capillaries and post-capillary venules, play a key role in cerebrovascular stability and BBB integrity, while VSMCs, which are not present at the capillary level, regulate cerebrovascular tone by contracting or relaxing in response to physiological stimuli, thereby maintaining CBF to ensure adequate cerebral perfusion to meet the metabolic demands of the brain (Yu *et al*., 2020, Kugler *et al*., 2021).

1.2.3 The Blood Brain Barrier

The brain microvasculature forms the foundation of the BBB, possessing key properties that maintain both cerebrovascular and CNS homeostasis and health through precise regulation of molecules entering the brain (Kadry *et al*., 2020). The BBB consists of a single endothelium layer surrounding a basement membrane, enriched with collagens such as collagen type IV, extracellular matrix proteoglycans and laminin, which encase the vessels and provide structural support (Xu *et al*., 2019). Pericytes that form around the basement membrane play a key role in regulating CBF. Moreover, astrocyte end-feet processes surround the basement membrane, providing biochemical support to pericytes and ECs (Xu *et al*., 2019). However, the ECs that form around the BBB differ significantly from those in the peripheral vasculature, exhibiting higher mitochondrial density, low pinocytic activity and lack of fenestrations, limiting non-selective transport from the vasculature to the cerebral interstitial fluid (Erdő *et al*., 2017, Kadry *et al*., 2020). ECs within the BBB are arranged in a continuous tubular structure, held together by specialised tight junction (TJ) proteins that form a highly selective barrier between adjacent ECs to ensure paracellular restriction of cells and molecules between the CNS and circulatory blood (Erdő *et al*., 2017). These TJ's are essential for maintaining neuronal function, protecting the brain from toxins or pathogens that could disrupt brain homeostasis and function (Erdő *et al*., 2017) (**Figure 1-2**).

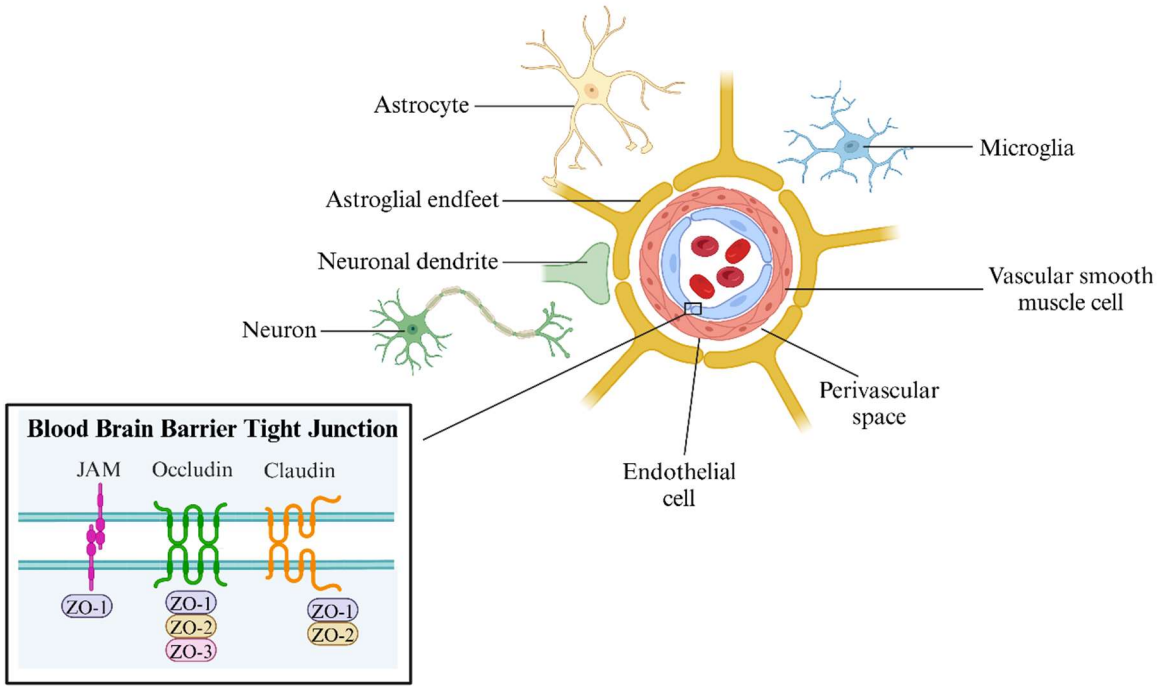

Figure 1-2. The neurovascular unit and the blood brain barrier. Figure illustrating the key components of the NVU in cerebral arteries, highlighting key structural elements of the blood-brain barrier tight junctions and emphasising their role in maintaining cerebral homeostasis. ECs form the inner lining of cerebral blood vessels, interconnected by junctional adhesion molecules (JAM), occludins, claudins and zonula occludins (Z0-1, ZO-2, ZO-3), maintaining BBB integrity by restricting paracellular permeability. Pericytes embedded in the vascular basement membrane regulate capillary diameter, contributing to endothelial function and BBB maintenance. VSMCs surround arteries and arterioles, controlling cerebrovascular tone and CBF. Astrocytes envelop cerebral blood vessels with their astrocytic end-feet, interacting with ECs, regulating neurovascular coupling and BBB function. Neurons and their neuronal dendrites integrate with the NVU, allowing communication with the NVU to support the metabolic demands of neural activity. Finally, the perivascular space, surrounding cerebral blood vessels, facilitates glymphatic system solute exchange and waste clearance. This figure was created in BioRender.

1.2.4 Cerebrovascular Autoregulation

As the brain has limited metabolic storage capacity and a constant metabolic demand, the brain's CBF is maintained by a mechanism known as cerebral autoregulation. Cerebral autoregulation refers to the brain's intrinsic ability to maintain adequate CBF and cerebral perfusion pressure (CPP), critical to brain function (**Figure 1-3**). Physiological CBF is approximately 50-60 mL/100 g/min to maintain cerebral perfusion, provided that mean arterial pressure (MAP) is maintained at a cerebral autoregulatory range within 60 and 150 millilitres of mercury (mmHg) (Claassen *et al*., 2021). Alternatively, when CPP falls below a critical threshold, the cerebral autoregulatory mechanisms fail, leading to CBF becoming directly dependent on alterations to MAP. This loss of autoregulation results in hypoperfusion, leading to hypoxic challenge, increasing ischaemic event risk. Furthermore, in the event of an ischaemic event, the ability for cerebral vessels to autoregulate becomes severely compromised, reinforcing a linear relationship between CBF and CPP whereby reductions in CPP lead to proportional decreases in CBF, exacerbating hypoxia, leading to further ischaemic events and irreversible brain tissue damage (Tzeng and Ainslie, 2014, Claassen *et al*., 2021).

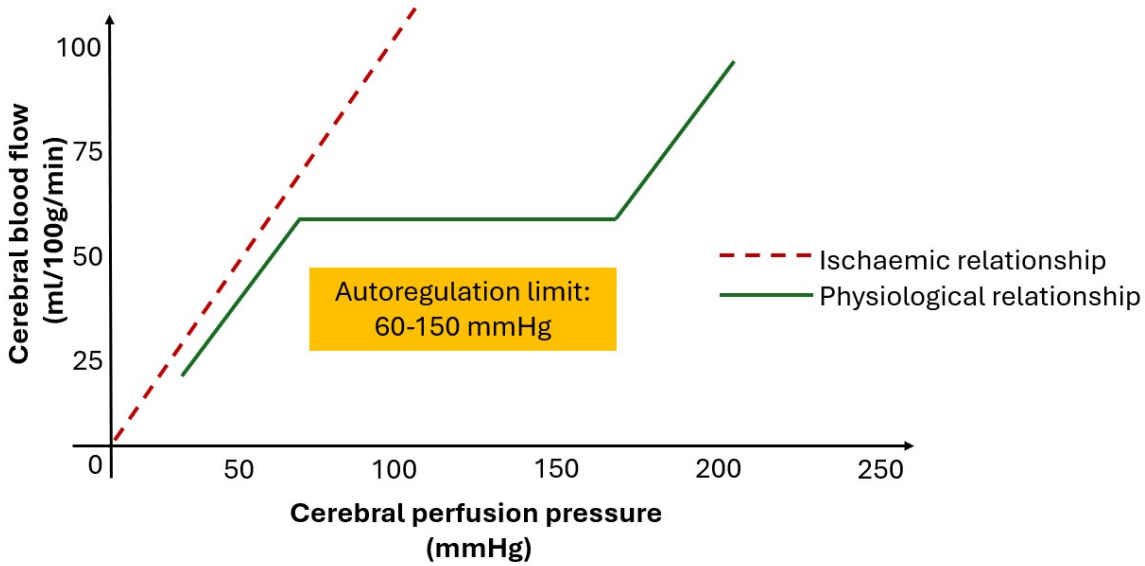

Figure 1-3. Cerebral autoregulatory linear relationship between CBF and CPP. When CPP ranges between 60-150 mmHg, CBF is maintained through effective cerebral autoregulation. Outside this range, CBF becomes directly dependent on MAP. In hypoxia/ischaemia, cerebral autoregulation is lost making CBF linearly dependent on CPP (Lidington *et al*., 2021).

1.2.5 Myogenic Tone in Cerebrovascular Autoregulation

VSMCs are central to the cerebral autoregulatory responses, playing a crucial role in determining CBF to the brain where they modulate the diameter of vessels through contractile and relaxation mechanisms. This process is governed by a complex interplay of signalling pathways to various stimuli such as changes in BP, shear stress, and metabolic cues, preventing insufficient or excessive CBF and damage to vascular and neuronal tissue (Armstead, 2016, Aries *et al*., 2010).

The myogenic component of cerebral autoregulation involves vascular tone responses mediated by VSMCs, which modulate vessel resistance and diameter and play a crucial role in CBF stability. The primary regulator of cerebrovascular tone is through myogenic response. Myogenic tone is primarily driven by VSMC Ca^{2+}concentrations, in response to various stimuli, including intraluminal pressure changes or by G-protein coupled receptor binding of vasoconstrictive agents such as angiotensin II (Ang II), endothelin-1, and noradrenaline, acting on the angiotensin type 1 receptor (AT_1R), engaging ion endothelin receptors alpha and beta (ETα and ETβ), and α_1-adrenergic receptors respectively mediating alterations to Ca^{2+} release and downstream contraction (Nelson *et al*., 1988, Bohm and Pernow, 2007, Touyz *et al*., 2018). These changes also mediate cascades that lead to an influx of Ca^{2+} through CaV and sodium ion (Na^+)/ Ca^{2+} channels, and through VSMC Ca^{2+} storage mechanisms such as the endoplasmic reticulum (ER) through the phosphatidylinositol 4,5-bisphosphate (PIP_2) – phospholipase C (PLC) – inositol 1,4,5-trisphosphate (IP_3) receptor (IP_3R) signalling pathway via G-protein coupled receptor (GPCR) activation. These mechanisms regulate [Ca^{2+}]i levels in response to cerebrovascular tone changes (Wynne *et al*., 2009, Putney and Tomita, 2012).

During vascular contraction, increases in VSMC [Ca^{2+}]i levels lead to the binding of Ca^{2+} to calmodulin (CaM), a regulatory protein that activates myosin light chain kinases (MLCK). MLCK phosphorylates the regulatory myosin light chain (MLC) 20 (MLC_{20}), increasing myosin ATP hydrolysis and triggering the cross-bridge cycling of myosin heads along actin filaments, causing VSMC contraction and vasoconstriction (Brozovich *et al*., 2016, Touyz *et al*., 2018). This Ca^{2+}-dependent contraction is an essential cerebral autoregulatory response to intraluminal pressure. In the context of vasorelaxation, relaxation occurs when [Ca^{2+}]i concentrations are reduced or by inhibitory mechanisms. First, [Ca^{2+}]i efflux occurs through mechanisms such as plasma membrane Ca^{2+} adenosine

triphosphatase (ATPase) and Na^{+}/Ca^{2+} exchange ion pumps that lower cytosolic Ca^{2+} levels as well as the sarco/endoplasmic reticulum Ca^{2+} ATPase (SERCA) that pumps $[Ca^{2+}]i$ back to the ER, with the efflux of VSMC Ca^{2+} leading to reduced activation of the CaM-MLCK-MLC_{20} pathway resulting in VSMC relaxation and vasodilation (Lipskaia *et al*., 2010, Liu and Khalil, 2018). Secondly, interdependent mechanisms such as NO via the eNOS-NO-soluble guanylate cyclase (sGC)-cGMP pathway leads to the dephosphorylation of MLC through activation of MLC phosphatases, leading to VSMC relaxation and vasodilation of cerebral blood vessels. Furthermore, the eNOS-NO-sGC-cGMP pathway contributes to the activation of the SERCA and VSMC $[Ca^{2+}]i$ homeostasis (Zhao *et al*., 2015, Tran *et al*., 2022) (**Figure 1-4**). This balance between VSMC contractile and relaxation mechanisms is essential for normal cerebrovascular physiological function and vascular homeostasis. Conversely, when cerebral autoregulation is impaired, the brain loses its ability to maintain CBF and CPP, and becomes vulnerable to ischaemic events, injury, and cerebrovascular disease prognosis, with ageing and hypertension being key contributors to cerebrovascular pathology.

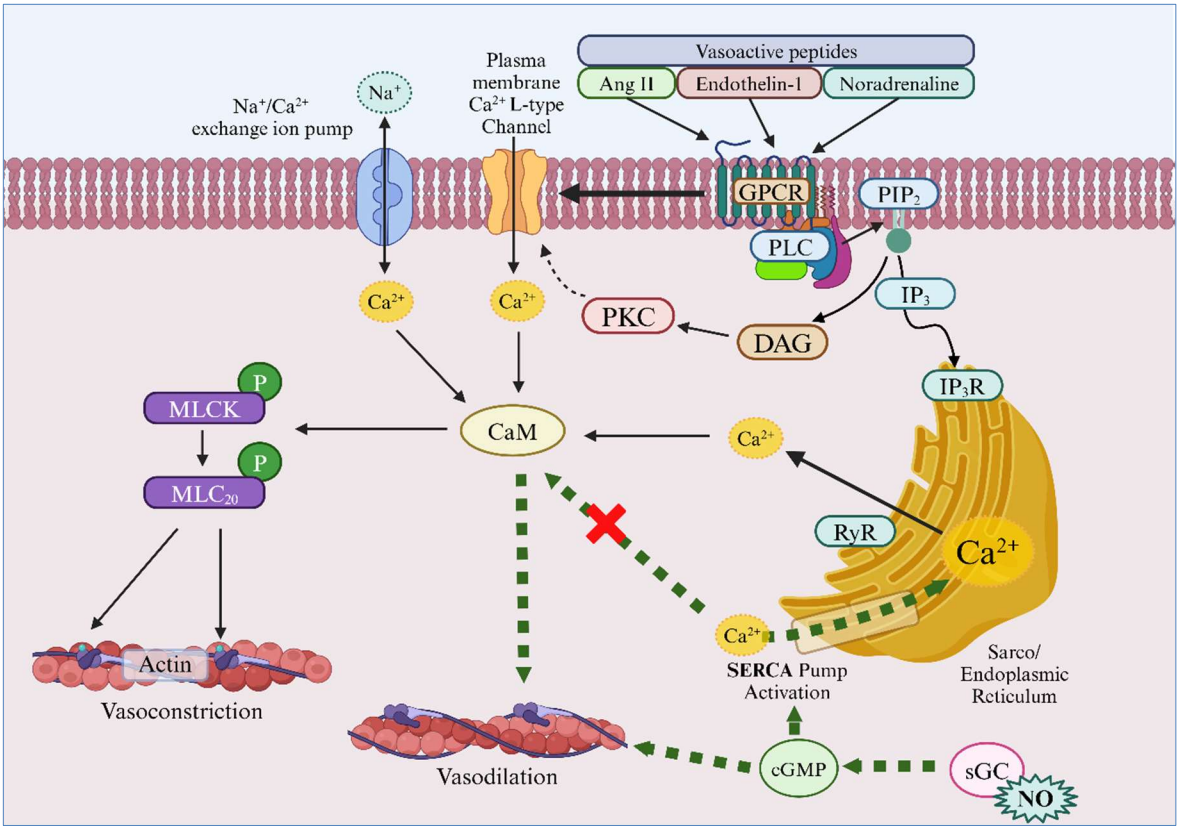

Figure 1-4. Calcium-dependent mechanisms of vascular smooth muscle cell myogenic tone regulation. This figure illustrates the mechanisms of Ca^{2+} regulation underlying the intrinsic ability of blood vessels to mediate vascular tone in response to changes in mean arterial pressure and vascular autoregulation, a process central to myogenic tone. Firstly, pathways that lead to increases in $[Ca^{2+}]i$ and subsequent contraction are indicated by black arrows. Counterregulatory mechanisms such as endothelial-derived factors such as NO counteract vasoconstriction through the sGC-cGMP pathways by reducing Ca^{2+} sensitivity and Ca^{2+} reuptake via the activation of the SERCA pump and are indicated by green arrow pathways. This figure was created in BioRender.

1.3 Cerebrovascular Disease

Impaired cerebrovascular autoregulation and myogenic tone are critical contributors to many forms of cerebrovascular disease. The most prevalent of cerebrovascular diseases to affect the ageing populations are CSVD and stroke (Jokinen *et al*., 2020, Feigin *et al*., 2021). Contextually, CSVD results in chronic, progressive damage, whilst in contrast stroke – whether ischaemic or haemorrhagic in nature – induces sudden severe disruptions to CBF resulting in rapid neuronal injury, neurological necrosis, immediate vascular cognitive impairment (VCI) and increased risk of VaD (Dichgans and Leys, 2017). Furthermore, the relationship between CSVD and stroke is particularly important as CSVD significantly increases the risk of ischaemic stroke, creating a synergetic co-occurrence whereby cognitive decline is exacerbated, leading to a decline in quality of life (Cannistraro *et al*., 2019, Izzo *et al*., 2018). Additionally, ageing is accompanied by a decline in vascular function and integrity leaving the brain vulnerable to CSVD, ischaemic insult, BBB dysfunction, and neurodegeneration, acting as a major contributor to VaD. Cumulatively, CSVD, stroke, and VaD impose an increasing burden on caregivers and healthcare systems, highlighting an urgent need for better preventive therapeutic strategies. However, the pathophysiological mechanisms that drive CSVD and stroke are currently not fully understood with greater knowledge of the complex interplay between these diseases being crucial to developing strategies that reduce CSVD and stroke impact on VaD in aged populations (Zimmerman *et al*., 2021, Hachinski *et al*., 2019).

1.3.1 Cerebral Small Vessel Disease

CSVD has been defined as a spectrum of pathological disorders that acutely or chronically affect cerebral small arteries, arterioles and capillaries in the brain (Li *et al*., 2018). Pathophysiological conditions that alter cerebral small vessel function may alter CBF and presents clinically as lacunar infarcts, white matter hyperintensities (WMH) and cerebral microbleeds that increase stroke risk and contributes to VCI and VaD onset. As CSVD is often presented asymptomatically, the disease is frequently either undiagnosed or misdiagnosed. This leads to significant clinical implications. As such, CSVD is often diagnosed incidentally utilising 1.5–3T magnetic resonance imaging (MRI), identifying clinical CSVD biomarkers such as WMH, cerebral microbleeds, enlarged perivascular

spaces, small subcortical infarcts and lacunar infarcts affecting subcortical white matter and deep grey matter regions of the brain (Cannistraro *et al*., 2019).

1.3.1.1 Cerebral Small Vessel Disease Classification and Pathogenesis

CSVD encompasses a range of subtype classifications, reflecting different underlying pathophysiological mechanisms and pathologies affecting cerebral small vessels and altering CBF, leading to deleterious changes to brain function, contributing to increased stroke risk, cognitive decline and VaD onset (Li *et al*., 2018, Litak *et al*., 2020). According to Litak *et al*. (2020), key features of each CSVD subtype include endothelial dysfunction, BBB-breakdown and impaired vascular tone resulting in chronic hypoperfusion which leads to gradual accumulation of neuronal injury and impaired cognitive function. These CSVD subtype classifications are based on underlying pathophysiological mechanisms:

- Type I: Age-related arteriosclerosis is the most common form of CSVD characterised by impaired vascular tone through small vessel structural changes including thickening, stiffness and narrowing. This causes reductions in CBF, CPP and increased chronic ischaemia, consequently leading to lacunar infarcts, WMH and cognitive decline (Csiszar *et al*., 2024, Litak *et al*., 2020).

- Type II: Amyloid-linked CSVD is considered the second most common CSVD subtype characterised by amyloid-β protein deposition in the walls of cerebral leptomeningeal and cortical small vessels. This leads to impaired vascular function, increased risk of intracerebral haemorrhages and microbleeds particularly in the lobar region and is known as cerebral amyloid angiopathy (CAA). CAA is often associated with ageing populations which are particularly at risk of Alzheimer's pathology (Boulouis *et al*., 2017, Greenberg *et al*., 2020).

- Type III: CSVD with genetic distinctions from CAA pathology, which arises from rare inherited forms of CSVD such as cerebral autosomal dominant arteriopathy with subcortical infarcts and leukoencephalopathy (CADASIL) caused by genetic mutations such as neurogenic locus notch homolog protein 3 (NOTCH3), but also COL4A1/A2; HTRA1 etc. Notably, alterations in NOTCH3 gene expression has been identified to promote early onset of pathological insults such as migraines, strokes, and cognitive decline (Coupland *et al*., 2018).

- Type IV: Autoimmune and inflammatory-mediated CSVD originating from autoimmune or inflammatory insults through T-cell and macrophage infiltration of cerebral small vessels, leading to vascular wall damage, occlusion, ischaemia and brain tissue injury through pathologies such as vasculitis and primary angiitis (Beuker *et al*., 2018, Rouhl *et al*., 2012).

- Type V**:** Periventricular thickening or venous collagenosis characterised by small vessel thickening and collagen deposition associated with ageing and hypertension, leading to chronic hypoperfusion, WMH and cerebral damage (Moody *et al*., 1995, Gronewold *et al*., 2022, Todd *et al*., 2018).

The consequences of CSVD can be diverse, ranging from asymptomatic, to subtle clinical manifestations including cognitive impairments, mental health changes such as depression, apathy and anxiety, and/or disruption to motor functions (Cannistraro *et al*., 2019) (**Figure 1-5)**.

1.3.1.2 Cerebral Small Vessel Disease Epidemiology and Risk Factors

CSVD prevalence increases with age, with the Rotterdam Scan Study identifying that CSVD is prevalent in approximately 5% of 50-year-olds, 90% of individuals older than 80, and almost 100% of individuals by the age of 90 (Cannistraro *et al*., 2019, de Leeuw *et al*., 2001). Furthermore, incidence of cerebral microbleeds increases with age from 6.5% in patients aged between 45-50 years old, and 36% for patients aged between 80-89 years old (Cannistraro *et al*., 2019, Poels *et al*., 2010). Several risk factors have been identified that increase the likelihood of the pathological progression of CSVD including smoking, diabetes, chronic kidney disease and sleep apnoea. However, ageing and hypertension are considered the most notable risk factors with autopsy studies identifying CSVD prevelance in over 50% of hypertensive patients ≥65-years-old (Hainsworth *et al*., 2024, Cannistraro *et al*., 2019). Additionally, CSVD has emerged as a common factor driving age- and hypertension-related diseases such as stroke, whereby CSVD accounts for approximately 25% of stroke onset and doubles the risk of recurrent strokes (Li *et al*., 2018, Elahi *et al*., 2023).

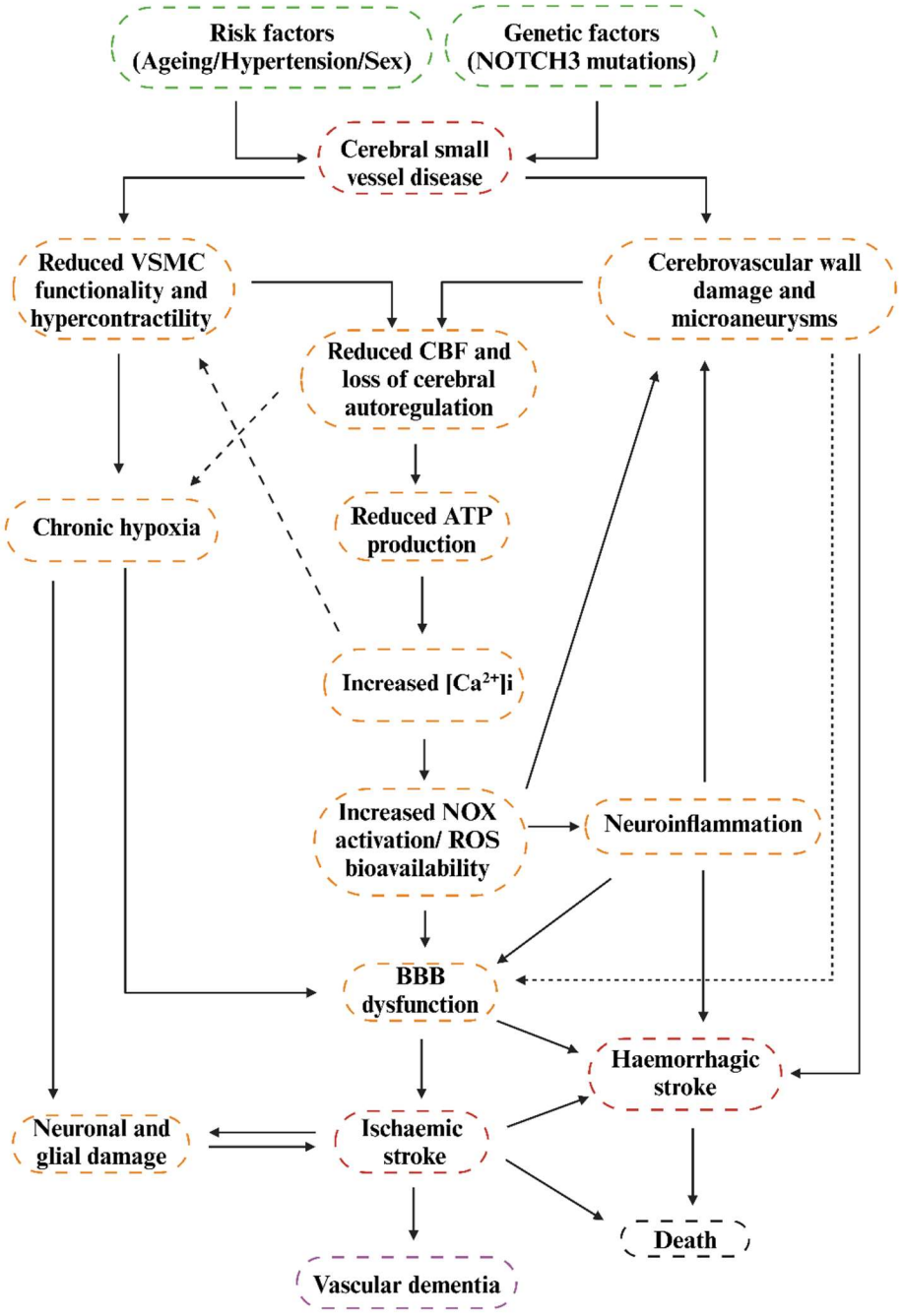

Figure 1-5. Pathogenesis of cerebral small vessel disease and its development in stroke and vascular dementia. This schematic illustrates the pathogenesis of CSVD and its progression to stroke and VaD. Risk factors such as ageing, hypertension, and sex, along with genetic factors such as NOTCH3, COL4A1/A2, and HTR1 contribute to CSVD pathogenesis. These factors can initiate a cascade of pathophysiological outcomes that contribute to cerebrovascular dysfunction and increased risk of ischaemic and haemorrhagic stroke, neuronal and glial damage and risk of developing morbidity such as VCI and VaD, whilst also increasing the risk of mortality. This figure was created in BioRender.

1.3.2 Stroke

Stroke is a complex and devastating neurovascular disorder, representing a major global health challenge, representing the second leading cause of death and the third leading cause of disability worldwide (Katan and Luft, 2018). The World Health Organisation characterises stroke as a vascular condition that occurs when there is an interruption to the blood supply to the brain, causing acute and rapid clinical signs of global and focal cerebrovascular dysfunction lasting from minutes to 24 hours, with longer durations leading to increased risk of irreversible neuronal injury, brain tissue damage and risk of death. Strokes are broadly categorised in two main categories: haemorrhagic and ischaemic. Haemorrhagic stroke results from a rupture of a cerebrovascular vessel leading to an accumulation of blood in the surrounding brain tissue and accounts for approximately 15% of all strokes and a 75% mortality rate of all strokes (Al-Shahi Salman *et al*., 2018). Haemorrhagic strokes are subdivided into two categories: intercranial haemorrhage (ICH) and subarachnoid haemorrhage (SAH) with the common causes of ICH and SAH including CAA, vascular malformations, aneurysms, arteriovenous malformations, chronic hypertension and CSVD (Al-Shahi Salman *et al*., 2018, Heit *et al*., 2017). Ischaemic stroke accounts for the remaining 85% of all strokes and occurs when a blood vessel in the brain is obstructed by a thrombotic or embolic clot, leading to a blockage in CBF to the brain, leading to a radically reduced rate of perfusion (Hasan *et al*., 2021). Ischaemic strokes that are closely associated with CSVD, resulting from an occlusion of the small, deep penetrating arteries are typically due to lipophyalinotic or micro-atheroma formations (Arboix, 2015, Yaghi *et al*., 2021).

1.3.3 Ischaemic Stroke Pathophysiology, Hypoxia and the Ischaemic Cascade

At the onset of an ischaemic stroke, the sudden occlusion impairs cerebral autoregulatory mechanisms, causing an immediate reduction or cessation to CBF leading to the affected brain region. As CPP diminishes, rapid hypoxia accompanied by reduced glucose supply occurs downstream from the occlusion site. Within minutes this leads to a series of devastating pathophysiological events collectively known as the ischaemic cascade (**Figure 1-6**). The ischaemic cascade refers to multiple interdependent pathophysiological states involving a multitude of molecular and cellular mechanisms including bioenergetic

failure, excitotoxicity, Ca^{2+} overload, cytotoxic and vasogenic oedema, inflammation, oxidative stress, BBB-breakdown apoptosis and cell death (Kuriakose and Xiao, 2020).

1.3.3.1 Energy Depletion, and Membrane Depolarisation

Severe decreases of blood perfusion and depletion of oxygen and glucose cause a consequential decline of ATP levels in brain tissue cells (neurons and glial cells). Neurons and glial cells rely extensively on oxidative phosphorylation for metabolic energy production. As ischaemic stroke impairs CBF and CPP, the supply of substrates necessary for oxidative phosphorylation is dramatically reduced leading to ATP loss and neurons and glial cells losing their membrane potential, resulting in cellular depolarisation (Katsura *et al*., 1994). ATP is vital for maintaining ionic gradients through active transport of ion pumps (e.g. Ca^{2+}, potassium ion (K^+) and Na^+ pumps). Reductions of ATP lead to the brain tissue being unable to maintain essential ion transport pumps, with depolarisation leading to a subsequent cellular influx of Na^+, chloride ions (Cl^-), Ca^{2+} and efflux of K^+. Furthermore, ATP-mediated depolarisation also leads to inhibition of neurotransmitter reuptake systems as well as neurotransmitter release of excitatory amino acids, predominantly glutamate, leading to enhanced neurotransmitter accumulation into the extracellular space (Nicholls and Attwell, 1990, Martin *et al*., 1994).

1.3.3.2 Excitotoxicity and Calcium Overload

As pathological depolarisation occurs, the abnormal release of the neurotransmitter glutamate causes it to accumulate in the extracellular space, leading to overactivation of N-methyl-D-aspartate (NMDA), α-amino-3-hydroxy-5-methyl-4-propionate acid (AMPA), and kainite receptors causing uncontrolled cellular influx of Na^+, Cl^-, Ca^{2+} and efflux of K^+. This in turn causes unregulated depolarisation of the cell membrane, resulting in further Ca^{2+} entry and the release of more excitatory amino acids, creating a positive feedback loop that exacerbates injury (Choi, 2020, Lai *et al*., 2014). This excitatory phenomenon not only affects neurons, but also non-neuronal cells such as VSMCs, promoting mechanisms that lead to hypercontractility and further reductions in CBF. Additionally, intracellular Ca^{2+} overload can act as a secondary messenger activating downstream signalling cascades and Ca^{2+}-activated enzymes that lead to pathophysiological mechanisms such as ROS production, mitochondrial dysfunction, lipid

peroxidation and inflammation, promoting secondary damage that drives apoptosis and liquefactive necrosis (Choi, 2020, Lai *et al*., 2014).

1.3.3.3 Cytotoxic and Vasogenic Oedema

Cytotoxic oedema is characterised as cell swelling caused by passive H_2O influx, triggered by abnormal intracellular accumulation of Na^+. The dramatic influx of Na^+ and Cl^- surpasses the efflux of K^+, causing H_2O to follow passively into the cell, resulting in cytotoxic oedema. Vasogenic oedema is mediated by the extracellular accumulation of fluid in the cerebral parenchyma and is caused by BBB-breakdown through pathophysiological mechanisms such as excessive ROS bioavailability and inflammation (Wu *et al*., 2020). Both cytotoxic and vasogenic oedema contribute to increases in brain volume and intercranial pressure, inducing further reductions in CBF, causing hypoperfusion and hypoxia (Michinaga and Koyama, 2015, MartInez-Coria *et al*., 2021).

1.3.3.4 Reactive Oxygen Species Formation

Oxidative stress is a key pathological process of ischaemic stroke that has been identified as a critical driver for ischaemic injury. During cerebral ischaemia, several pathways that produce ROS become overactivated *post* reperfusion. This consequently leads to ROS bioavailability surpassing the ability of endogenous antioxidant response elements to scavenge free radicals, leading to oxidative stress. Once oxidative stress occurs, proteins, lipids and DNA can become oxidised leading to cellular mechanisms that drive apoptosis and necrosis. There are several sources of ROS during ischaemic events such as ischaemic reperfusion injury (IRI), mitochondrial depolarisation and dysfunction, inflammation and Ca^{2+} overload (Rodrigo *et al*., 2013). The primary wave of ROS occurs through mitochondrial dysfunction. Mitochondria are the primary site for ATP production at the mitochondrial respiratory chain within the mitochondrial matrix, where electrons are moved along the electron transport chain. During this some electrons escape rather than leading to ATP synthesis, interacting with O_2 causing the generation of small amounts of superoxide ($O_2^{\bullet-}$), serving as a primary signalling molecule for normal physiological function (Murphy, 2009, Zorov *et al*., 2014). However, during ischaemic events, O_2 in the ischaemic penumbra is depleted, forcing cells to rely on aerobic glycolysis for ATP generation. Consequently, lactic acid builds up, decreasing cellular pH. The combination of decreased pH and ATP loss leads to ER stress and further increases $[Ca^{2+}]i$, leading to

mitochondrial overload and activation of ROS generating enzymes. Collectively this leads to further waves of ROS generation and oxidative stress-mediated cellular damage and inflammation (Cao and Kaufman, 2014, Görlach *et al*., 2015).

1.3.3.5 Ischaemic Inflammatory Response

After ischaemic injury, $[Ca^{2+}]i$ and ROS activate cellular cascades that trigger pro-inflammatory damage associated molecular patterns that activate toll-like receptors (TLRs), leading to cascades that cause the upregulation of transcription factors such as NF-κB (Moskowitz *et al*., 2010). Transcription factors including NF-κB then stimulate the generation of chemokines and cytokines in addition to adhesion molecules that stimulate microglial activity, leading to resting/ramified microglia becoming reactive and accumulating at the lesion necrosis core and in the penumbra (Da Fonseca *et al*., 2014). Primarily, microglia show an M2 anti-inflammatory phenotype, before switching profile to an M1 pro-inflammatory phenotype, releasing ROS and tumour necrosis factor-α (TNF-α), which promote infiltration of circulating neutrophils, leukocytes, lymphocytes and macrophages to the injury site (Hu *et al*., 2012). Furthermore, M1 microglia release cytokines that recruit local astrocytes to perform astrogliosis, forming a glial scar around the necrotic core site, to prevent further neuronal cell death and to initiate recovery of neurons in the ischaemic penumbra (Shen *et al*., 2021, Huang *et al*., 2014).

1.3.3.6 Blood Brain Barrier Breakdown

A major characteristic of ischaemic stroke is BBB-permeability and breakdown. BBB-breakdown clinically presents in a biphasic manner approximately 48-72 hours *post*-stroke through sustained ischaemia and hypoperfusion. BBB-breakdown is primarily driven by altered TJ protein expression, mainly occludins, ZO-1/2/3 and claudin, through pathophysiological mechanisms such as inflammation and oxidative stress (Zheng *et al*., 2023). Inflammatory cytokines such as IL1-β and TNF-α disrupt TJ function, integrity and permeability through pathophysiological mechanisms such as endothelial cell contraction and paracellular gaps. Furthermore, neutrophil infiltration into the ischaemic penumbra exacerbates inflammatory cascades whilst also promoting oxidative stress, amplifying TJ damage and BBB dysfunction (Qiu *et al*., 2021). Enzymes such as NOXs significantly elevate ROS levels leading to the downregulation of TJ components including claudin-5 and occludin, impacting TJ integrity (Hernandes *et al*., 2022). Additionally, ROS and

inflammatory cytokines activate matrix metalloproteinases (MMPs) such as MMP-9, leading to further TJ degradation. This exacerbates ischaemic damage by causing reversible BBB permeability to become irreversible, leading to further complications such as tissue swelling, haemorrhagic transformation, cerebral oedema, extending the penumbra and contributing to further necrosis (Yang and Rosenberg, 2015, Zheng *et al*., 2023).

1.3.3.7 Necrosis and Apoptosis

During an ischaemic stroke event, there are two key areas of the brain, the ischaemic core and ischaemic penumbra. The ischaemic core is characterised by irreversible cell necrosis caused by cellular oedema, excitotoxicity, bioenergetic failure and oxidative stress occurring within minutes of stroke-insult. In contrast, cell death in the ischaemic penumbra occurs mainly by two apoptotic pathways caused by increased Ca^{2+} levels and oxidative stress: the extrinsic (death receptor), and intrinsic (mitochondrial) pathways (Redza-Dutordoir and Averill-Bates, 2016). Oxidative stress causes mitochondrial dysfunction, damaging mitochondrial DNA, disrupting Ca^{2+} homeostasis and causing mitochondrial membrane integrity dysfunction through mitochondrial outer membrane permeabalisation (MOMP) through the release of cytochrome-c which activates caspase signalling cascades such as the Janus kinase/signal transducer and activator of transcription (JAK/STAT) and mitogen-activated protein kinases (MAPK) pathways that commit cells to apoptosis (Kishimoto *et al*., 2019, Redza-Dutordoir and Averill-Bates, 2016).

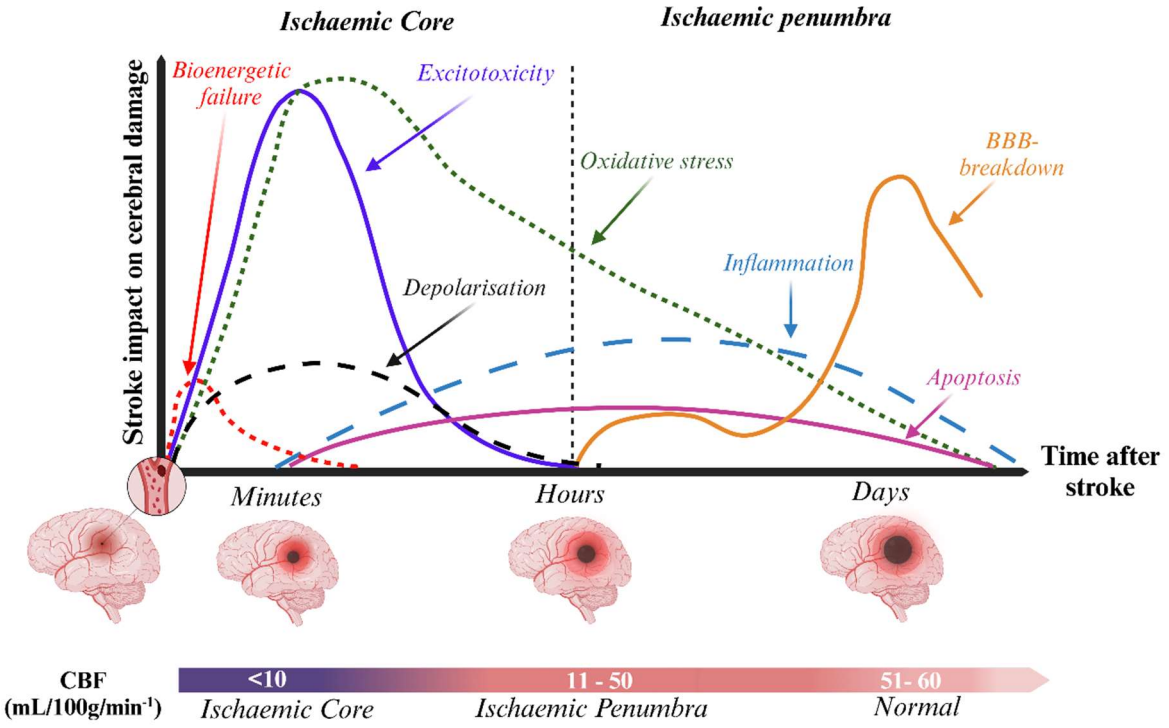

Figure 1-6. The ischaemic cascade. This illustrative graph represents the sequential and overlapping pathophysiological processes that occur following ischaemic stroke, highlighting temporal progression of key stroke events (Bioenergetic failure, excitotoxicity, depolarisation, oxidative stress, inflammation, apoptosis, and BBB-breakdown), occurring minutes, hours, and days within both the ischaemic core and ischaemic penumbra. Additionally, this figure presents CBF thresholds, differentiating thresholds between the ischaemic core (<10mL/100g/min), the ischaemic penumbra (11-50mL/100g/min), and normal "unaffected" brain tissue (51-60mL/100g/min), providing insights into the pathophysiological dynamics of stroke pathology. This figure was created in BioRender.

1.4 Cerebrovascular Risk Factors

Disruption to cerebrovascular homeostasis and function can occur through a variety of both modifiable, and non-modifiable risk factors **(Table 1-1)**. Amongst the most prominent risk factors for CSVD, stroke and VaD are ageing and hypertension, however increasing evidence has shown that sex differences play a critical role in cerebrovascular disease risk, with each risk factor influencing the pathogenesis of cerebrovascular diseases such as CSVD, stroke and VaD through distinct interconnected mechanisms.

CSVD, stroke and VaD risk factors		
Type	**Risk factor**	**Description**
Non-modifiable	Ageing	Cerebrovascular disease risk increases significantly with age, with incidence doubling with each decade after the age of 45.
	Sex	Men have higher CSVD, stroke risk earlier in life, however, CSVD, stroke and VaD risk dramatically increases in women *post* menopause.
	Genetics & family history	Family history of CSVD conditions such as CADASIL or a family history of stroke/traumatic ischaemic attacks increases CSVD, stroke and VaD risk.
	Ethnicity/Race	Non-Hispanic black and Asian populations have increased risk of CSVD, stroke and VaD.
Modifiable	Hypertension	High BP is the leading primary risk factor for CSVD, stroke, and VaD.
	Diabetes	Patients with diabetes are significantly more likely to develop CSVD and VaD, and twice as likely to have a stroke than healthy populations.
	Smoking	Accelerates vascular damage through mechanisms such as oxidative stress, leading to increases risk of CSVD, stroke, and VaD.
	Hyperlipidaemia	High LDL levels contribute to atherosclerotic CSVD, and increased risk of stroke and VaD.
	Obesity/physical inactivity	Increases risk of hypertension, diabetes, hyperlipidaemia, raising risk of CSVD, stroke and VaD.

	Diet	High-salt and high cholesterol diets increase risk of hypertension and hyperlipidaemia, leading to increased susceptibility to CSVD, stroke and VaD.
	Alcohol consumption	Long-term alcoholism increases risks for cerebral microbleed CSVD, increasing stroke risk and subsequent VaD.
	Cardiovascular disease	Conditions like coronary artery disease and atrial fibrillation increase stroke and cerebrovascular disease risk.
	Chronic kidney disease	Impairs BP regulation, leading to hypertension and increased CSVD, stroke and VaD risk.
	Sleep disorders (e.g. sleep apnoea)	Sleep disorders such as obstructive sleep apnoea significantly increases risk of hypertension and oxidative stress, leading to increased risk of CSVD, stroke and VaD.
	Psychological factors	Chronic stress and depression have a bidirectional relationship with CSVD, increased stroke risk and VaD.
	Oral contraception (women)	Oral contraception increases stroke risk through increased risk of blood clotting and altered vascular endocrine levels.
	Inflammation	Chronic inflammation from infection of autoimmune disease is linked to an increased risk of CSVD, stroke and VaD.
	Air pollution	Chronic exposure to pollution increases susceptibility to vascular inflammation, CSVD, stroke and VaD risk.

Table 1-1. **CSVD, stroke, and VaD non-modifiable and modifiable risk factors.** Adapted from (Wang *et al*., 2021, Cannistraro *et al*., 2019, Kelly-Hayes, 2010, Custodero *et al*., 2022, Kulick *et al*., 2023, Lu *et al*., 2024, Li *et al*., 2018, Li *et al*., 2019, Murray *et al*., 2020).

1.4.1 Ageing

Ageing is a key non-modifiable risk factor that greatly influences the cerebrovascular system and brain health. As life-expectancy increases, the prevalence of age-related cerebrovascular diseases significantly contribute to morbidity and mortality in ageing populations, representing a major global health challenge (Hachinski *et al*., 2019). As age advances, vascular structural integrity undergoes progressive deterioration both peripherally and locally in the cerebrovasculature. This deterioration leads to increased risk of pathologies such as CSVD, stroke, and VaD. Age-related decline leads to alterations in the cerebrovascular wall and basement membrane, which has been well documented in both animal and human studies, identifying that as ageing progresses blood vessels display reduced elasticity and reactivity, losing their ability to accommodate BP fluctuations. This causes impairments to cerebral autoregulatory responses, altering CBF and causing chronic and progressive hypoperfusion to the brain. Furthermore, arterial stiffness increases vascular resistance to blood flow both systemically, and in the cerebrovasculature. While this contributes to elevated BP, the relationship between cerebrovasculature changes and the development of hypertension remains complex, warranting further investigation (Pinto, 2007, Zimmerman *et al*., 2021).

1.4.2 Hypertension

Hypertension (high BP) affects more than 1.39 billion people globally, accounting for approximately 21.1% of adults and is the leading preventable risk factor for death worldwide. It is a major risk factor for both cardio- and cerebrovascular diseases including CSVD and stroke, contributing to approximately 7.6 million deaths annually (Mills *et al*., 2020, Arima *et al*., 2011, Zhou *et al*., 2021). Furthermore, hypertension has been intrinsically linked with ageing, with rates of <10% at 20 to >75% at 75 years of age (Mills *et al*., 2020). Additionally, hypertension has been identified to be more prevalent in males during early and middle adulthood; however, this trend is reversed by age 65, where the prevalence becomes higher in females (Ji *et al*., 2021).

Hypertension is characterised as a complex, multifactorial, and multisystem disorder. Under normal physiological BP conditions (normotension), normotension is described as systolic BP ≤120 mmHg and/or diastolic BP ≤80 mmHg. However, when BP is persistently elevated beyond these levels, patients can be defined by two categories or

stages; Stage 1 hypertension is defined as systolic BP 130-139 mmHg and/or diastolic BP 80-89 mmHg and Stage 2 hypertension is defined as systolic BP ≥140 mmHg and/or diastolic BP ≥90 mmHg. However, patients are classified as being at risk of hypertension-linked complications when systolic BP ≥115 mmHg and/or diastolic BP ≥75 mmHg (Whelton *et al*., 2018). Hypertension cases are categorised as primary hypertension (formerly known as essential hypertension) or secondary hypertension. Primary hypertension is the most common form of hypertension, accounting for approximately 95% of cases with the aetiology involving dysregulation of multiple interconnected physiological systems described by Irvine Page's 'Mosaic Theory' (Page, 1949) including: neural, anatomical, hemodynamic, endocrine, genetic and environmental factors. The remaining 5% of hypertension cases are classified as secondary hypertension and are often reversible when the aetiological factor is removed (Touyz *et al*., 2022, Raina *et al*., 2019, Page, 1949). Recently the Mosaic Theory has been revisited with additional hypertensive factors being identified, most notably the renin angiotensin aldosterone system (RAAS).

1.4.2.1 The Renin-Angiotensin-Aldosterone System Axis

The RAAS is a multi-organ peptidergic hormone system consisting of two main axes – the classical and counter-regulatory (non-classical) axis – that plays a fundamental role in regulating BP and the pathophysiology of hypertension. The classical axis is initiated through liver derived angiotensinogen synthesis before being released into the blood circulation. As this occurs, renin, a protease produced by the kidney in response to low BP/low blood volume, catalyses the cleavage of angiotensinogen (AGT) to angiotensin (Ang I). Ang I undergoes further cleavage by angiotensin-converting enzyme (ACE), a zinc metalloproteinase expressed in epithelial cells and ECs of the vasculature and various organs in the body including the lungs, kidney and the brain to generate the octapeptide angiotensin II (Ang II) promoting vasoconstriction (Forrester *et al*., 2018).

Whilst traditionally the classical RAAS system was conceptualised as a linear system whereby Ang II-AT_1R binding promoted pro-fibrotic, pro-inflammatory, and pro-oxidative stress pathophysiological effects that led to a vasoconstrictive phenotype, growing evidence has identified non-classical pathways that mediate protective effects against maladaptive outcomes associated with this pathway. First, the harmful effects of Ang II-mediated AT_1R signalling are balanced by the protective effects of the Ang II type 2 receptor (AT_2R). In physiological conditions, Ang II-AT_2R binding serves as a

protective mechanism against vascular injury, promoting mechanisms that reduce inflammation, inhibit fibrosis, counteract cell proliferation, and promote vasodilation (Sumners *et al*., 2019, Arendse *et al*., 2019). However, the beneficial effects of the Ang II-AT_2R pathway is often overwhelmed by the effects of Ang II-AT_1R signalling leading to impaired vasodilation, progressive vascular remodelling, fibrosis, inflammation and oxidative stress. This imbalance can lead to the pathogenesis of CSVD and increase stroke and VaD risk through pathophysiological mechanisms such as vascular remodelling and BBB-breakdown (Su *et al*., 2021, De Silva and Faraci, 2013).

Alternatively, a counter regulatory 'non-classical' arm exists within the RAAS that diverges from the classical pathway. Similarly to the classical pathway, AGT is broken down to Ang I by renin, however, differentiates through the hydrolysation of Ang I to the nonapeptide Ang (1-9) through the ACE homologue ACE2. Ang (1-9) binds to AT_2R promoting eNOS activation and NO bioavailability, vasodilation, anti-fibrotic, and anti-inflammatory effects, a functional ligand of the AT_2R receptor promoting vasodilatory effects, whilst also lowering Ang II levels through ACE2 competing with ACE enzymatic activity (Ocaranza and Jalil, 2012, Patel and Schultz, 2013, Norambuena-Soto *et al*., 2020). Additionally, ACE and neprilysin (NEP) can further process Ang (1-9) into Ang (1-7) acting on the Mas receptor (MasR), inhibiting fibrosis, cellular proliferation, and pro-inflammatory effects, whilst promoting vasodilation. Furthermore, NEP can directly convert Ang I to Ang (1-7), bypassing the intermediate formation of Ang II. As such, Ang (1-9) and Ang (1-7) represent an additional non-classical RAAS axis pathway that contributes to the overall balance and stability of the RAAS system (Jiang *et al*., 2014, Rukavina Mikusic *et al*., 2021, Rabelo *et al*., 2011) (**Figure 1-7**).

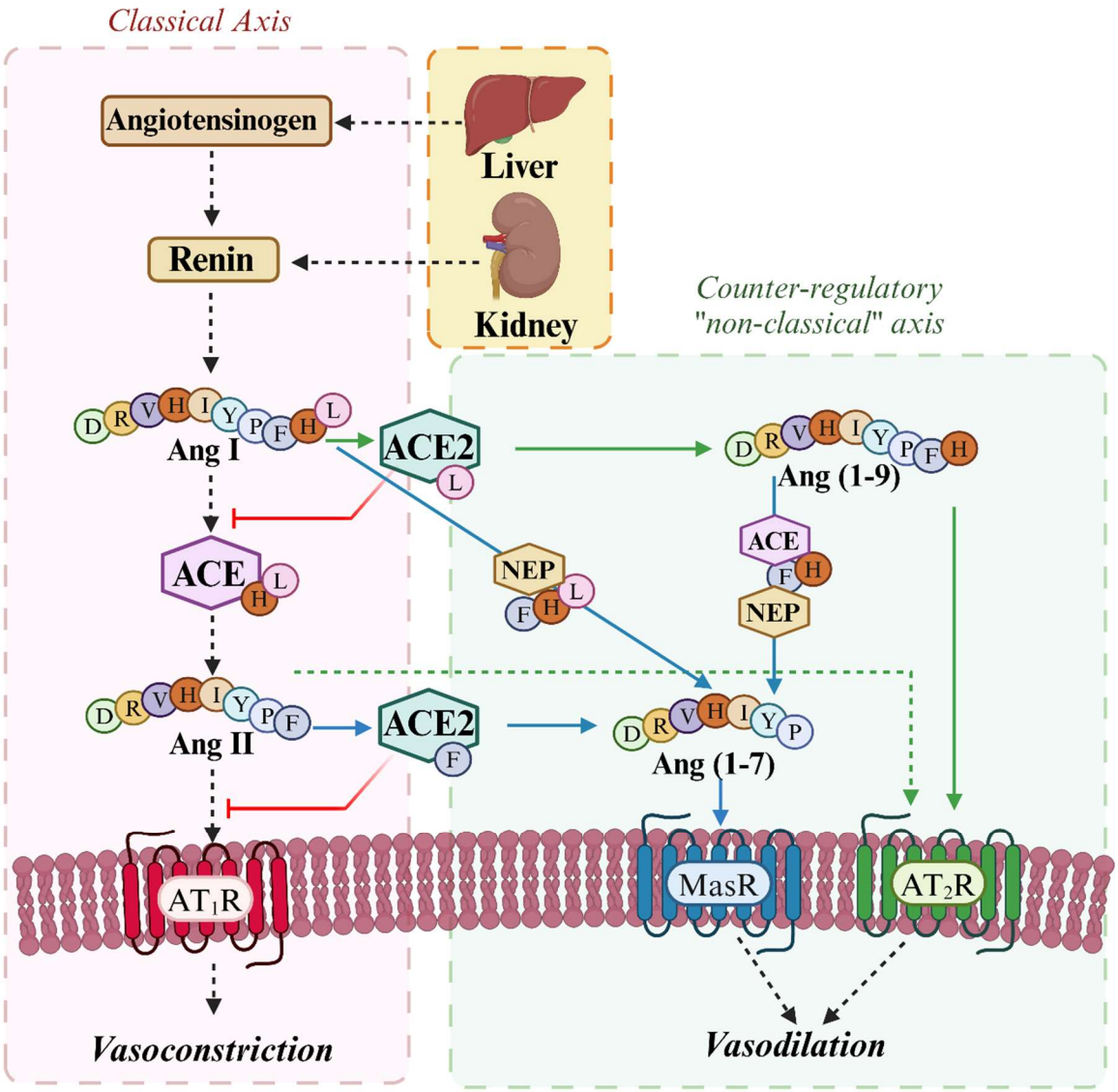

Figure 1-7. The classical and non-classical counter-regulatory axis of the RAAS. This schematic depicts the intricate pathways of the RAAS system, emphasising both the classical and non-classical counter-regulatory axis. Angiotensinogen is produced by the liver and is cleaved by kidney derived renin to generate angiotensin I, which is subsequently converted to angiotensin II (Ang II) by the angiotensin-converting enzyme (ACE). In the classical RAAS axis (black arrow pathway), Ang II binds and activates the angiotensin type 1 receptor (AT_1R), promoting vasoconstriction. Alternatively in the counter-regulatory axis, Ang I can be metabolised to angiotensin (1-9) (Ang (1-9)) by ACE2, acting on the AT_2R, promoting vasodilation (green arrow pathway). Additionally, Ang I, Ang II and Ang (1-9) can be converted to angiotensin (1-7) (Ang (1-9)) through conversion by ACE2, ACE2/NEP and ACE/NEP respectively promoting vasodilatory and protective effects (blue pathway). ACE2 enzymatic activity of the counter-regulatory axis also competed with ACE in the catalytic cleavage of both Ang I and Ang II, reducing AT_1R activation (red pathway). This figure was created in BioRender.

1.4.2.2 Angiotensin II and Angiotensin II Type 1 Receptor on Vascular Function

Angiotensin II is a key regulator of vascular function and a potent vasoconstrictor, playing a crucial role in BP regulation through cellular effects mediated by endothelial and VSMC AT_1R. Ang II binding of AT_1R, initiates the activation of heterotrimeric G-proteins ($G_{\alpha s}$, $G_{\alpha i}$, $G_{\alpha q/11}$ G_{12}, G_{13}) and the initiation of a myriad of deleterious signalling cascades leading to VSMC contractility including Protein kinase C inhibition of MLC phosphatases via CPI-17 (Woodsome *et al*., 2001, Shibata *et al*., 2014), Ras homolog family member A (RhoA)/Rho kinase-(ROCK)- c-jun N-terminal kinases (JNK)-mediated cytoskeletal changes, and VSMC remodelling and phenotypic switch (Tang *et al*., 2018, Nguyen Dinh Cat *et al*., 2013). Additionally Ang II-AT_1R, mediates contraction through the PIP_2-IP_3-IP_3R signalling cascade, activating the ER and initiating increases in $[Ca^{2+}]i$ concentrations and increased VSMC contractility through CaM activation and phosphorylation of MLCK and binding of MLC_{20} to cytoskeletal actin binding (Lin *et al*., 2016, Eid *et al*., 2018). Furthermore, Ang II also stimulates the release of adrenal cortex/zona glomerulosa synthesised aldosterone, leading to aldosterone binding to epithelial mineralocorticoid receptors and the promotion of sodium retention and fluid balance, whilst also inducing processes such as vascular contraction, cardiac output, inflammation and oxidative stress (Rukavina Mikusic *et al*., 2020, Patel *et al*., 2017). Aldosterone can also influence the hypothalamic-pituitary-adrenal axis, modulating the release of the nonapeptide vasopressin, produced primarily in the paraventricular nucleus and supraoptic nucleus of the hypothalamus, and leads to activation of the sympathetic nervous system through vasopressin binding to V1α, V1β, and V2 receptors, mediating vasoconstriction (Touyz *et al*., 2022, Savoia *et al*., 2011).

Deleterious molecular systems activated by the Ang II- AT_1R axis that contribute to vasoconstriction and inflammation also include alterations to redox status most notably through NADPH oxidases (Nguyen Dinh Cat *et al*., 2013). Upon binding to AT_1R, Ang II triggers a cascade of events that involve key signalling molecules such as Rac1, PKC, and PLC, with these molecules being essential in the assembly and activation of NADPH oxidases (Garrido and Griendling, 2009). This in turn leads to the promotion of oxidative stress and a pro-inflammatory environment through ROS-mediated alterations to adhesion molecule expression such as vascular cell adhesion molecule-1 (VCAM-1), intracellular adhesion molecule-1 (ICAM-1), promoting leukocyte adhesion and transmigration into the

tunica intima (Piqueras and Sanz, 2020). Furthermore, Ang II mediated ROS has been identified to promote the phosphorylation and nuclear translocation of NF-κB, resulting in pro-inflammatory cytokine transcription such as tumour necrosis factor-alpha (TNF-α), and interleukins (IL) IL-1β and IL-6 leading to the upregulation and activation of tyrosine kinases, and mitogen-activated protein kinases (MAPK) signalling through pathways such as the extracellular signal-regulated kinases 1/2 (ERK1/2) promoting cell proliferation and hypertrophy (Gorin *et al*., 2004, Guo *et al*., 2006, Jiang *et al*., 2023). Moreover, Ang II can modulate the JNK pathway, promoting transcription of factors such as c-Jun, that imitate proinflammatory, proapoptotic genes, and p38 MAPK that, similarly to JNK, promote inflammation through the upregulation of adhesion molecules, cytokines and matrix metalloproteinases (MMPs), all contributing to inflammation, VSMC phenotypic modulation, proliferation, and vascular injury (Ebrahimian *et al*., 2011, Li *et al*., 2017, Song *et al*., 2013). Additionally, Ang II-mediated AT_1R activation triggers the suppression of peroxisome proliferator-activated receptor gamma coactivator 1-alpha (PGC-1α), a key regulator of mitochondrial biogenesis and cellular metabolism function contributing to mitochondrial dysfunction (Liang and Ward, 2006, Qian *et al*., 2024). Furthermore, downregulation of PGC-1α has significant vascular-specific implications, as suppression leads to decreased eNOS activity, compromising the production of NO and impairment of vasodilatory signalling cascades such NO-sGC-cGMP consequently altering SERCA Ca^{2+} reuptake mechanism functionality (Li *et al*., 2016, Kadlec *et al*., 2016, Moraes *et al*., 2024). All of which promote detrimental pro-inflammatory responses, immune cell activation, cytokine release and reductions in NO bioavailability (Savoia *et al*., 2011, Patel *et al*., 2016, Nguyen Dinh Cat *et al*., 2013).

1.4.2.3 Animal Models of Hypertension

Given the interdependent and dynamic interactions of various interconnected systems involved in hypertension, one of the key challenges in hypertension research is developing a pre-clinical model that replicates the intricacies of a hypertensive phenotype. Currently there are numerous pre-clinical models of hypertension categorised as inducible or genetic (**Table 1-2**). The Ang II-induced hypertensive model is the most widely utilised inducible model of hypertension and ranks second overall following the spontaneously hypertensive stroke prone rat model (SHRSP). Unlike the SHRSP model, which develops hypertension in a spontaneous manner with genetic variability, the Ang II inducible model allows for precise manipulation of BP levels and timing of hypertension onset, allowing for the investigation of specific hypertension-mediated pathophysiological processes in a controlled manner. Furthermore, given the critical role that the RAAS system plays in the pathogenesis of hypertension, the Ang II model represents a reliable pre-clinical model for examining hypertensive pathophysiological mechanisms (Jama *et al*., 2022).

Summary of commonly used pre-clinical rodent models of hypertension					
Category	**Subcategory**	**Model**	**Type**	**Species**	**Description and clinical relevance**
Inducible	Pharmacological and/or surgical	Ang II	Vascular/Immune activity/Renal/ Neurogenic	Mouse/Rat	Models the effect of elevated Ang II. Clinically relevant for RAAS dysregulation in primary hypertension.
		DOCA/Salt	Vascular/Renal/ Immune activity	Mouse/Rat	Mimics excess mineralocorticoid/renin activity and salt-sensitive hypertension, representing secondary form of hypertension.
		Endothelin	Vascular /Renal	Mouse/Rat	Assesses the role of endothelin-1-mediated vasoconstriction, relevant for vascular and renal diseases.
		L-NAME	Vascular/Renal/ Immune activity/ Metabolic	Mouse/Rat	Inhibits eNOS-mediated NO, simulating EC dysfunction, common in hypertension and metabolic disorders.
		Renovascular	Renal/Vascular	Mouse/Rat	Models renovascular hypertension due to renal artery stenosis and is clinically relevant for secondary hypertension.
		Partial nephrectomy	Renal	Mouse/Rat	Mimics impaired renal function and chronic kidney disease-related hypertension.
	Diet	High fat	Metabolic/Vascular/ Renal	Mouse/Rat	Obesity model of hypertension, relevant for metabolic and hyperlipidaemia-mediated hypertension

Summary of commonly used pre-clinical rodent models of hypertension (continued)					
Category	**Subcategory**	**Model**	**Type**	**Species**	**Description and clinical relevance**
Genetic	Monogenic	Congenic	Genetic/Vascular	Mouse/Rat	Examines hypertension linked to single gene mutations, allowing for examination of genetic regulation of BP.
		Transgenic	Genetic/Vascular	Mouse/Rat	Examines genetic modification to knock-out or overexpress specific genes (e.g. LinA3) to assess hypertension.
	Polygenic	SHR/SHRSP	Vascular/Immune activity/Renal/ Neurogenic	Rat	SHR is a genetic model of primary hypertension, whereas SHRSP is a genetic model of chronic hypertension and stroke risk mimicking severe chronic hypertension and cerebrovascular risk.
		Fawn-hooded hypertensive rat	Genetic/Chronic kidney disease	Rat	Genetic model of chronic hypertension-mediated renal lesions and chronic kidney disease.
		Dahl salt-sensitive rat	Vascular/Immune activity/Renal	Rat	Models salt sensitive forms of hypertension and important for investigating the role of low renin in the regulation of BP.

Table 1-2. Summary of commonly used pre-clinical rodent models of hypertension. Adapted from (Lerman *et al*., 2019, Jama *et al*., 2022).

1.4.3 Sex Differences

The role of sex has become increasingly recognised as a major risk factor for the development and clinical progression of diseases for CSVD/hypertension, stroke, and VaD (Colafella and Denton, 2018, Fandler-Höfler *et al*., 2024). These sex differences are shaped by both physiological and hormonal variations between men and women, with premenopausal women having a reduced risk of a cerebrovascular incident than their male counterparts. However, this risk is reversed in postmenopausal women, contributing to accelerated cardiovascular and cerebrovascular disease in older women. This hormonal transition may explain why despite having longer life expectancy, aged women face a greater burden of cerebrovascular pathology with age. This sexual dimorphism has been identified not only in humans, but in most mammals with numerous studies identifying that females exhibit reduced cardiovascular and cerebrovascular risk for the majority of their life span, when compared to their age-matched male counterparts (Akhter *et al*., 2021, Bushnell *et al*., 2018, Lisabeth and Bushnell, 2012, Dos Santos *et al*., 2014). One of the most significant contributors to these hormonal and physiological distinctions is the role of oestrogen signalling, with ovarian sex hormones being identified as having protective effects on the vascular system (Dos Santos *et al*., 2014). This section introduces concepts that are important to the sex-dependent analyses throughout this thesis.

1.4.3.1 Oestrogen Synthesis and Mechanisms of Action

Oestrogens are pleotropic hormones produced from circulating androgens, such as testosterone and androstenedione by aromatase, (also known as oestrogen synthase) to produce oestradiol (Santen *et al*., 2009, Knowlton and Lee, 2012). Humans produce 3 types of oestrogen: oestrone (E_1), 17β-oestradiol (E_2), and oestriol (E_3). In the vasculature, 17β-oestradiol is considered the primary female sex hormone and is the most abundant circulatory oestrogen with the strongest biological activity (Xiang *et al*., 2021, Xing *et al*., 2009). Oestrogen receptors are expressed in both ECs and VSMCs, modulating vascular tone via genomic activation of nuclear oestrogen receptor-alpha (ERα) and oestrogen receptor-beta (ERβ), and by membrane bound non-genomic G-protein-coupled oestrogen receptors (GPER). Activation of these receptors leads to a variety of protective mechanisms including suppression of inflammatory signalling pathways, most notably the inhibition of the TNF-α-NF-κB pathway (Xing *et al*., 2012), and prevention of vascular proliferation and remodelling (Iorga *et al*., 2017). Furthermore, oestrogen promotes

oxidative balance and vascular homeostasis through NO-mediated vasodilation (Mcneill *et al*., 2002), and nuclear factor erythroid 2-related factor 2 (NRF2) upregulation promoting redox homeostasis and DNA repair enzymes (Zárate *et al*., 2017, Xing *et al*., 2009). Furthermore, oestrogen has been shown to be beneficial in the context of hypertension by modulating components of RAAS, with studies identifying that oestrogen can increase beneficial Ang (1-7) production (Connelly *et al*., 2022). Moreover, Ang II-mediated hypertension is exacerbated by lack of ERα (Lu *et al*., 2016, Touyz *et al*., 2022).

In contrast, excessive or alternatively limited androgens, particularly testosterone and its metabolite 5α-dihydrotestosterone (DHT), have shown to contribute to increased vascular risk both systemically and in the cerebrovasculature (Abi-Ghanem *et al*., 2020, Lucas-Herald and Touyz, 2022). Whilst males generally exhibit increased BP levels than premenopausal women and males typically have increased androgen bioavailability (Lucas-Herald and Touyz, 2022). This led to the assumption that male androgens exert a detrimental effect on the vasculature, whilst oestrogen promotes more vasoprotective effects. Androgens such as testosterone and DHT, bind to androgen receptors which are widely expressed in cells such as ECs, VSMCs, fibroblasts and immune cells in both the systemic and cerebrovascular systems (Lucas-Herald *et al*., 2017). Androgens have been implicated in increased cerebrovascular risk through several pathophysiological mechanisms including; BBB-dysfunction, vascular remodelling and vasoconstriction, with pathways such as vascular endothelial growth factor (VEGF) and wingless-type MMTV integration site family (WNT) mediated alterations to endothelial function, inflammation, and oxidative stress being identified as contributing factors (Lucas-Herald *et al*., 2017, Abi-Ghanem *et al*., 2020, Collignon *et al*., 2024). Furthermore, androgens are intrinsically involved in regulating the RAAS system through mechanisms such as increased water and sodium retention, leading to increases in renin production. As a consequence, this leads to increased ACE and AT_1R expression promoting a hypertensive phenotype and increased cerebrovascular risk (Te Riet *et al*., 2015). Collectively, risk factors such as ageing, hypertension and sex differences can contribute to pathophysiological states that promote EC and VSMC dysfunction and cerebrovascular diseases (**Figure 1-8**).

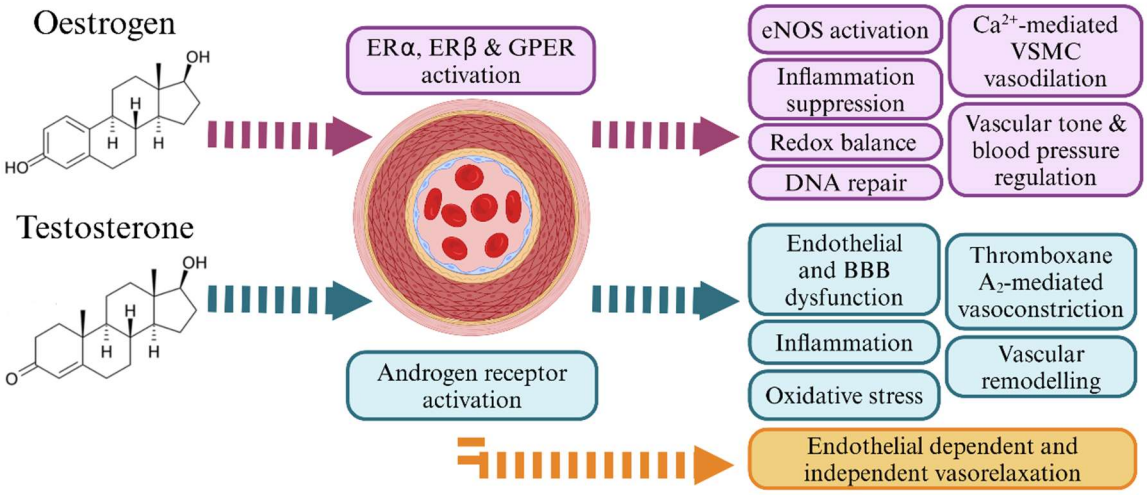

Figure 1-8. Sex hormones and their vascular effects. This figure depicts the vascular expression of sex steroids and their receptors, emphasising the mechanisms through which sex hormones modulate vascular function in health and disease. The purple arrow denotes the oestrogen signalling pathway, the blue arrow illustrates the pathophysiological effects of testosterone signalling, whilst the orange arrow represents the physiological effects of testosterone signalling. Figure adapted from Connelly *et al*. (2019). This figure was created in BioRender.

1.5 Prevention Over Treatment in Cerebrovascular Disease

Given cerebrovascular diseases such as stroke leads to devastating and often irreversible damage, resulting in high rates of mortality and disability, including VaD onset, there is an urgent need for novel therapeutic approaches aimed at not only reducing IRI, but also preventing stroke ons*et al*together. The development of pharmaceutical interventions that target modifiable stroke risk factors such as CSVD and hypertension is essential for decreasing stroke incidence. Whilst anti-hypertensive therapeutic strategies have been shown to significantly reduce the risk of ischaemic (Boncoraglio *et al*., 2021) and haemorrhagic (Benavente *et al*., 2013) strokes, whilst also reducing the risk of recurrent onset, evidence of WMH progression remains mixed with some studies showing benefit, with others showing little to no effect (Goldstein *et al*., 2022, Bath and Wardlaw, 2015). Furthermore, there are no established therapeutic strategies for targeting CSVD as a consequence of factors such as the heterogeneous presentation of CSVD symptoms, limited biomarkers for detection and CSVD diagnosis often being discovered in late-stage development. As such that this often leaves BP management as one of the few modifiable approaches for reducing CSVD and stroke/IRI risk (Gao *et al*., 2022).

1.6 Oxidative Stress: A Unifying Pathophysiological Feature

Throughout this introduction, oxidative stress has been identified as a reoccurring and unifying pathophysiological feature of stroke, stroke IRI, and CSVD alongside cerebrovascular disease risk factors such as ageing, sex differences and hypertension. For over a decade, numerous researchers have explored targeting oxidative stress and ROS producing enzymes as a therapeutic target for vascular diseases. However, applying this strategy specifically to CSVD and stroke/IRI represents a more recent area of investigation and an opportunity for developing strategies that effectively mitigate these conditions and improve patient outcomes.

1.6.1 Oxidative Stress

Oxidative stress is a key pathophysiological feature of cerebrovascular diseases, with brain tissue being exceptionally susceptible to the deleterious effects of oxidative stress due to a combination of the brain having a high O_2 demand for ATP synthesis (as described in section 1.2), high lipid content (Jové *et al*., 2023) and limited antioxidant capacity (Lee *et*

al., 2020). Oxidative stress is characterised as a cellular pathophysiological process that is characterised by excessive bioavailability of ROS that overwhelm endogenous antioxidant response element (ARE) defences, leading to abnormal redox homeostasis. In ECs, VSMCs and fibroblasts, ROS are precisely regulated under normal conditions, allowing them to participate in ROS-mediated physiological signalling, a process known as redox signalling. Redox signalling involves reversible oxidation/reduction-based modification of proteins vital for cell signalling homeostasis. In the vasculature, ROS-mediated redox signalling occurs in response to various stimuli including growth factors, cytokines, hypoxic-inducible factors and shear stress. In turn, many vital signalling cascades are regulated by ROS signalling including NOTCH (Caliceti *et al*., 2014), MAPK, JAK-STAT (Simon *et al*., 1998), NF-κB (Morgan and Liu, 2011) and PI3K/AKT (Byon *et al*., 2016) pathways. These important signalling cascades regulate a wide range of physiological functions including endothelial homeostasis, angiogenesis, VSMC differentiation and vascular tone (Zhou *et al*., 2013).

1.6.2 Reactive Oxygen Species and Antioxidant Response Elements

ROS are chemically reactive molecules derived from O_2, comprising of free radicals and non-free radicals, with O_2 itself being a relatively mild oxidant. Whilst ROS is a generic term that defines a wide range of oxidant molecules, the primary form of ROS is derived through a one-electron reduction of O_2, inducing a negatively charged unpaired electron forming $O_2^{\bullet-}$ (superoxide) as a byproduct (**$O_2 + e^{\bullet-} \rightarrow O_2^{\bullet-}$**). Furthermore the superoxide anion has an extremely short half-life, and as such is a relatively unstable molecule that cannot readily diffuse across cell membranes (Fisher and Paton, 2012). However, $O_2^{\bullet-}$ can act as a precursor of several secondary ROS messengers within cells through a series of enzymatic and non-enzymatic reactions with the most notable secondary reaction being the conversion to hydrogen peroxide (H_2O_2) catalysed by the superoxide dismutase (SOD) antioxidant. This conversive reaction of $O_2^{\bullet-}$ to H_2O_2 (**$2\ O_2^{\bullet-} + 2\ H^+ \rightarrow H_2O_2 + O_2$**) by SOD takes place in multiple cellular compartments including the cytoplasm (SOD1) and mitochondria (SOD2).

Furthermore, H_2O_2 can be generated by some enzymes such as NOX4 (Schröder *et al*., 2012). Unlike $O_2^{\bullet-}$, H_2O_2 is a more chemically stable ROS and can easily diffuse cellular membranes allowing H_2O_2 to participate in autocrine and paracrine signalling (Bienert *et al*., 2006). As such, H_2O_2 may be the most important ROS for physiological cell

signalling, modulating key processes such as migration, proliferation, and differentiation of vascular cells through the modulation of protein function by reversible oxidation of cysteine residues in target proteins (Chung *et al*., 2013). Additionally, H_2O_2 can regulate expression of genes involved in inflammatory cell recruitment and wound repair processes through signalling proteins such as ERK1/2 and NF-κB, MMP and VEGF (Van Der Vliet and Janssen-Heininger, 2014). Moreover, H_2O_2 can act as a vasodilator through increases in cyclic adenosine 3',5'-monophosphate (cAMP) and K^+ channel activation (Iida and Katusic, 2000, Miura *et al*., 2003). However, H_2O_2 has been shown to act as both a vasodilator and vasoconstrictor dependent on H_2O_2 bioavailability with excess H_2O_2 leading to vasoconstriction and vascular damage through mechanisms such as irreversible/reversible lipid peroxidation, oxidation of proteins and DNA and scavenging of vasodilatory NO (Juan *et al*., 2021, Lucchesi *et al*., 2005, Byon *et al*., 2016).

Additionally, in the brain, there are high levels of reduced transition metal ions such as ferrous iron (Fe^{2+}), such that the brain is particularly susceptible to high levels of H_2O_2 reacting with Fe^{2+} through the Fenton and Haber-Weiss reactions (**Figure 1-9**). This leads to the generation of hydroxyl radicals ($^{\bullet}OH$), highly reactive and damaging ROS that contribute to extensive oxidative stress, particularly in hypoxic-ischaemic conditions leading to significant protein oxidation/impaired cleavage of peptides, DNA damage and lipid peroxidation, making $^{\bullet}OH$ a potent mediator of cell injury and death (Gao *et al*., 2023, Halliwell *et al*., 2021, Liu *et al*., 2017).

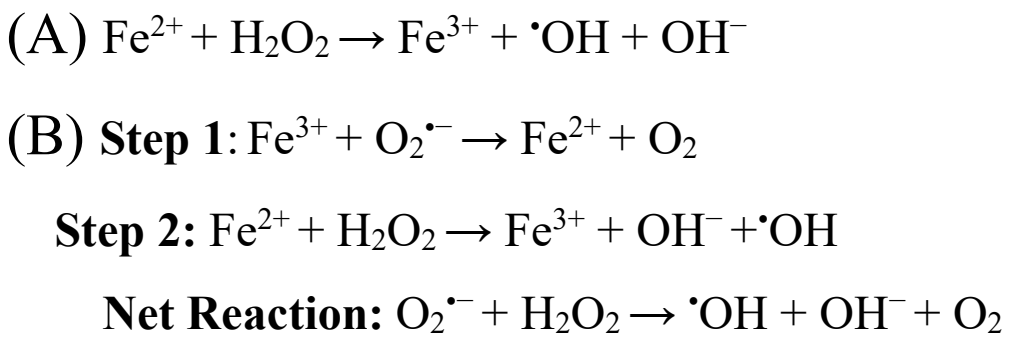

Figure 1-9. Formation of hydroxyl radical through the Fenton and Haber-Weiss reactions involving H_2O_2. The Fenton reaction **(A)** occurs when H_2O_2 reacts with ferrous iron (Fe^{2+}) whereby Fe^{2+} donates an electron to H_2O_2, producing one $^{\bullet}OH$ and one hydroxyl ion OH^- whilst causing the oxidisation of iron to its ferric form (Fe^{3+}). Further $^{\bullet}OH$ can be produced by the Haber-Weiss reaction **(B)**, a two-step process whereby superoxide reduces Fe^{3+} back to Fe^{2+}, causing Fe^{2+} to react with H_2O_2 causing a Fenton reaction **(A)**, and producing further $^{\bullet}OH$.

1.6.3 Nitric Oxide and Reactive Nitrogen Species

In the brain, NO is synthesised by three isoforms of NO synthase. Neuronal NO synthase (nNOS)-derived NO is vital for the regulation of neurotransmitter release, neuronal excitability, synaptic plasticity and long-term potentiation/depression. Inducible NO synthase (iNOS) is expressed in response to pro-inflammatory stimuli as a consequence of vascular dysfunction and inflammation (Kröncke *et al*., 2001, Zhao *et al*., 2015, Prast and Philippu, 2001). However, in the vasculature, NO is mainly generated by eNOS, which plays a critical role in vascular tone, diffusing from ECs to VSMCs leading to vasodilation as previously discussed in 1.4.1. NO is a unique ROS due to its dual functionality as a signalling molecule in physiological conditions, most notably mediating vascular tone through cGMP-dependent mechanisms (Archer *et al*., 1994), and preventing platelet aggregation (Gkaliagkousi *et al*., 2007, Russo *et al*., 2023). However, NO can also act as a reactive nitrogen species (RNS) in pathological contexts. In the context of oxidative stress, overabundance of $O_2^{\bullet-}$ can scavenge NO leading peroxynitrite ($ONOO^-$) formation **($O_2^{\bullet-}$ + NO → $ONOO^-$**) a potent ROS that not only leads to further reductions in NO bioavailability resulting in impaired vascular tone but also increases lipid peroxidation, inflammation, DNA strand breaks and vascular dysfunction (Pérez De La Lastra *et al*., 2022, Szabó, 1996). Furthermore, $ONOO^-$ is capable of diffusing through cell membranes either through passive diffusion, or through anion channels, and may contribute to further cellular and DNA damage, worsening outcomes in both CSVD and stroke pathologies (Radi, 2013).

1.6.4 Antioxidant Response Elements

In the vasculature there are several antioxidant defence mechanisms that act to neutralise ROS production, with enzymatic detoxifiers such as SOD1, SOD2, catalase, haem-oxygenase 1 (HO1), NADPH quinone oxidoreductase 1 (NQO1), and peroxiredoxins (PRDX) being some of the most prevalent (Santilli *et al*., 2015). SOD including cytoplasmic SOD1, and mitochondrial SOD2, catalyse the conversion of $O_2^{\bullet-}$ to H_2O_2 and O_2 (Fukai and Ushio-Fukai, 2011). This conversion is vital for preventing $O_2^{\bullet-}$ from reacting with NO and forming $ONOO^-$, playing a variety of vital roles in the vasculature (see 1.13.1). Catalase is found in the peroxisomes of vascular cells that acts as a highly effective antioxidant neutralising H_2O_2 through its four porphyrin haem iron groups that allow for the decomposition of H_2O_2 to O_2 and H_2O (Li *et al*., 2013). In vascular cells catalase is particularly vital in suppressing levels of H_2O_2 in order to prevent NO

scavenging and the Fenton/Haber-Weiss reactions to reduce secondary production of the highly deleterious $ONOO^-$ and $^{\bullet}OH$ respectively. Indeed, reductions in catalase activity have been linked with ageing and hypertension leading to increased risk of oxidative injury, CSVD and stroke risk (Finkel and Holbrook, 2000, Gomes *et al*., 2013, Nandi *et al*., 2019).

NQO1 is a key cytosolic antioxidant protein in the vasculature that that is upregulated by nuclear factor erythroid 2-regulated factor 2 (NRF2). NQO1 catalyses a two-electron reductase of NADPH to $NAD(P)^+$ by utilising NADPH quinones as reducing cofactors, as such competing with NADPH oxidases and reducing their enzymatic activity, therefore lowering their ROS producing capacity and limiting ROS. As such, NQO1 is a vital antioxidant in the vasculature where oxidative stress is closely linked to NADPH oxidase activity, by lowering the amount of NADPH available to NOX enzymes (Ross *et al*., 2000, Shen *et al*., 2018). Another antioxidant that is mediated by the NRF2 pathway in response to oxidative stress challenge is the inducible antioxidant enzyme HO1. HO1 catalyses the degradation of free cytoplasmic haem into vasodilatory metabolites that protect the vasculature. HO1 degradation of haem increases carbon monoxide (CO) which acts as a vasodilator that mimics NO by activating VSMC soluble guanylate cyclase (sGC), which in turn elevates cGMP levels leading to vasodilation. CO also inhibits VSMC proliferation in hypoxic conditions (Morita *et al*., 1997, Ingi *et al*., 1996). Furthermore, intracellular HO1-mediated CO synthesis has been identified to induce K^+ channel activity leading to reduced $[Ca^{2+}]i$, which in turn leads to reduced VSMC contraction and vasodilation (Leffler *et al*., 2011). In addition, HO1 can also reduce ROS bioavailability through the degradation of haem by limiting the bioavailability of haem as a substrate for NOX enzymatic activity (Jiang *et al*., 2006, Datla *et al*., 2007).

Another key antioxidant in the vasculature are the PRDXs. PRDX are a family of six isoforms of thiol-specific peroxiredoxins that reduce peroxides such as H_2O_2, $ONOO^-$ and other hydroperoxides. Intracellular PRDXs specifically react with H_2O_2, reducing H_2O_2 acting as regulatory sensors during redox signalling transduction and play a key role in cellular defence mechanisms in response to oxidative stress, preventing pathophysiological processes associated with vascular morphological changes and dysfunction that contribute to impaired vascular tone (Jeong *et al*., 2021).

Collectively these antioxidant enzymes act as a network of ARE in vascular cells that maintain ROS balance and protect against oxidative stress. However, chronic ROS production can lead to an imbalance of antioxidant capacity, causing a cascade of deleterious cellular events that contribute to vascular diseases (**Figure 1-10**). Impaired redox status has been identified to have profound impact on cellular structures and mechanisms, particularly in cerebrovascular tissues where oxidative stress plays a key role in disease development. There are several significant pathophysiological features of elevated ROS and oxidative stress including lipid peroxidation, inhibition of protein tyrosine phosphatases (PTPs) and antioxidant hyperoxidation with a critical component of this process being the oxidation of cysteine residues.

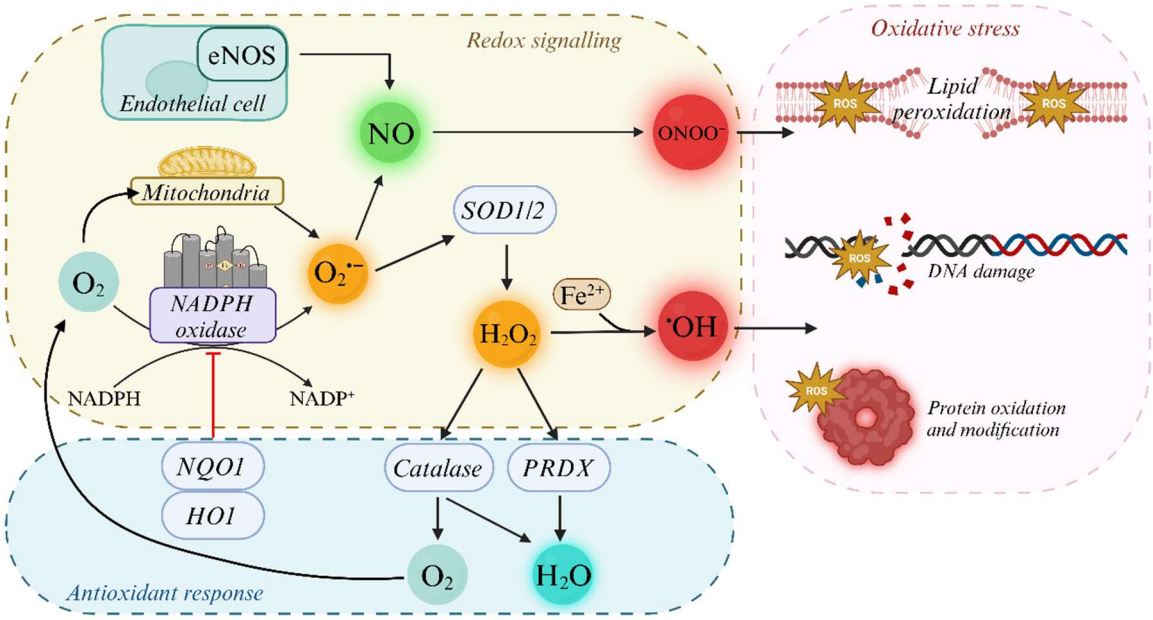

Figure 1-10. Redox signalling, antioxidant response and oxidative stress pathways in the vasculature. NADPH oxidases and the mitochondria are major sources of $O_2^{\bullet-}$ in the systemic and cerebral vascular beds, derived from O_2. $O_2^{\bullet-}$ can subsequently react with eNOS derived NO to form $ONOO^-$, H_2O_2 via SOD, and subsequent Fenton reaction leading to $^{\bullet}OH$ as a consequence of impaired redox status, causing oxidative stress and cellular damage mechanisms. ARE, protect against deleterious ROS formation by the disproportionation of H_2O_2 to H_2O (PRDX) and $H_2O + O_2$ (Catalase). ARE NQO1 and HO1 reduce NADPH oxidase activity by competing with NADPH and haem, both of which are vital for NADPH enzymatic activation. This figure was created in BioRender.

1.6.5 Lipid Peroxidation

Lipid peroxidation is a major consequence of excessive ROS bioavailability, playing a critical role in cellular damage and vascular dysfunction. The process of lipid peroxidation is initiated when ROS, particularly H_2O_2, $ONOO^-$ and $^{\bullet}OH$ interact with cell membrane polyunsaturated fatty acids (PUFA), which are sensitive to ROS due to their Carbon to carbon bonds (Siddique *et al*., 2012, Radi *et al*., 1991). Lipid peroxidation of PUFA leads to the abstraction of H^+, which subsequently leads to the formation of lipid radicals that react with O_2, forming lipid peroxyl radicals. This in turn leads to a peroxidative chain reaction that propagates lipid membrane damage and the generation of highly reactive secondary lipid peroxidation byproducts such as malondialdehyde (MDA) exerting further cellular damage through disruption of normal signalling pathways, impaired membrane damage and membrane permeability (Gianazza *et al*., 2019, Gaschler and Stockwell, 2017). As such, lipid peroxidation can lead to inflammatory cascades and $[Ca^{2+}]i$ dysregulation that can amplify pathophysiological mechanisms such as BBB-breakdown, neurovascular remodelling and neuroinflammation, increasing the risk and progression of diseases such as CSVD and stroke (Baev *et al*., 2022, Lehner *et al*., 2011, Mohan *et al*., 2024).

1.6.6 Reversible/ Irreversible Oxidation of Protein Tyrosine Phosphatases and Peroxiredoxins

Another consequence of oxidative stress is the modification of PTPs. PTPs are a class of signalling enzymes that regulate cell signalling through dephosphorylation of phosphotyrosine residues on target proteins. PTPs regulate a diverse range of cellular processes vital for normal physiological function and homeostasis including vascular permeability, angiogenesis , differentiation and proliferation (Gogiraju *et al*., 2022), as well as mediating vascular inflammation (Vestweber, 2021, Cho *et al*., 2023). Furthermore, PTPs play a crucial role in vascular tone by regulating $[Ca^{2+}]i$ homeostatic processes crucial to VSMC contraction such as Ca^{2+} channels and ER stress signalling pathways (Jeon *et al*., 2017, Thiebaut *et al*., 2018). Dephosphorylation by PTPs involve catalytic cysteine residues that facilitate the removal of phosphate groups from substrates and are therefore essential for catalytic activity and crucial for maintaining appropriate phosphorylation of proteins in cellular signalling cascades (Tautz *et al*., 2013). However,

cysteine residues are extremely sensitive to an environment of oxidative stress due to the nucleophilic nature of their thiol (-SH) groups, making them highly reactive to ROS

(particularly H_2O_2), which result in oxidative modification of cysteines (Meng *et al*., 2002, Welsh and Madan, 2024). Oxidation of cysteine residues in proteins occurs in a stepwise manner, leading to either reversible or irreversible changes, depending on levels of ROS bioavailability (**Figure 1-11**). During redox signalling, the PTP active site cysteine undergoes oxidation by H_2O_2 allowing for temporary regulation of PTP activity. In contrast, during oxidative stress, the cysteine in the active site of PTPs can be irreversibly oxidised, leading to permanent activation or inactivation, dependent on the target enzyme. In vascular cells, loss of PTP activity alters cell signalling homeostasis leading to disruption in kinase activation and other phosphorylation-dependent pathways. In turn, this inactivation or hyperactivation promotes deleterious cellular process such as cell proliferation, inflammation and apoptosis (Kappert *et al*., 2005), promoting vascular pathologies such as endothelial dysfunction (Abdelsalam *et al*., 2019), VSMC fibrosis and hyperplasia (Gogiraju *et al*., 2022), with these pathophysiological outcomes promoting impaired vascular tone that can lead to increased risk of hypertension, CSVD and stroke pathologies.

Furthermore, antioxidants such as PRDX can also become susceptible to hyperoxidation. In normal PRDX cycling, the reaction with hydroperoxides such as H_2O_2 leads to oxidation of cysteines on -SOH, which is then reduced to its active form by other cellular antioxidants. However, in the context of oxidative stress, prolonged ROS exposure can lead to further $-SO_2H$ and $-SO_3H$ hyperoxidised states of cysteines. As a consequence, this hyperoxidisation of PRDX renders its antioxidant capacity inactive, reducing the cellular antioxidant capacity to protect against hydroperoxides such as H_2O_2, leading to increased $ONOO^-$ bioavailability, lipid peroxidation and oxidative stress (Jeong *et al*., 2021). In recent years, research understanding the role of ROS and antioxidants in the pathophysiology of oxidative stress has increased, leading to improved understanding of oxidative stress in the cardio- and cerebrovascular biology. Both the CNS and cerebral vessels express a number of enzymes that produce ROS including the mitochondria respiratory chain and cyclooxygenase, with NOXs the main source of ROS, both in the vasculature and in the brain.

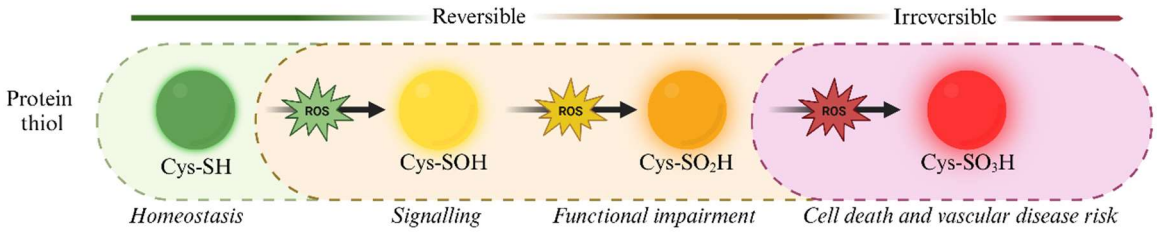

Figure 1-11. Reversible and irreversible protein thiol oxidation pathways. PTPs contain a thiol (-SH) group on their catalytic cysteine (Cys) residue vital for dephosphorylation of target protein tyrosine residues. Exposure to H_2O_2 causes -SH groups to undergo reversible oxidation forming sulfenic acid (-SOH), temporarily inactivating PTPs. During high levels of ROS bioavailability, cysteine residues can undergo further oxidation to sulfinic acid ($-SO_2H$). Prolonged exposure to oxidative stress can lead to irreversible oxidation to sulfonic acid ($-SO_3H$) leading to permanent PTP inactivation. This figure was created in BioRender.

1.7 NADPH Oxidases

NADPH oxidases contribute significantly to cerebrovascular health by producing ROS for cellular signalling. However, under pathological conditions, elevated NADPH oxidase activity leads to cerebrovascular oxidative stress and has been linked to pathophysiological processes such as BBB-breakdown, hypercontractility, increased CSVD and stroke risk. The role of NADPH oxidase enzymes in the pathogenesis of CSVD and stroke is multifaceted with each NADPH oxidase enzyme contributing to a variety of pathophysiological features (Chrissobolis and Faraci, 2008).

The NADPH oxidase enzyme family comprises of seven homologues: NOX1, NOX2, NOX3, NOX4, NOX5, dual oxidase 1 and dual oxidase 2. In the CNS, five NADPH isoforms have been identified (NOX1, NOX2, NOX3, NOX4, and NOX5), with four NOX isoforms (NOX1, NOX2, NOX4, and NOX5) being expressed in both cerebrovascular ECs and VSMCs (Tejero *et al*., 2019, Hernandes *et al*., 2022). Collectively NOXs are a family of transmembrane proteins that transfer electrons across membranes. NOX catalyses the reduction of O_2 to produce $2O_2^{\bullet-}$ (**NADPH + 2O₂ → NADP⁺ + H⁺ → 2O₂•⁻**), with NOX4 spontaneously producing H_2O_2 (Touyz *et al*., 2019, Nisimoto *et al*., 2014). All NOX enzymes share a conserved structural homology comprising of six transmembrane α-helical domains. At the intracellular C-terminus, shared structural features include an NADPH-binding site, a FAD (flavin adenine dinucleotide)-binding region in proximity to the C-terminus transmembrane domain, and four highly conserved haem-binding histidines, with two binding regions being located in transmembrane domain III, and two in transmembrane domain V (**Figure 1-12**). Additionally, the structure of each NOX isoform is modified by specific regulatory subunits required for the modulation of NOX activity and localisation. Of these regulatory subunits, NOX1-4 associate with membrane bound $p22^{phox}$. Following complex formation, NOX isoforms transfer electrons from NADPH to the cytosol through FAD- and haem-binding groups leading to ROS production (Sumimoto, 2008, Rastogi *et al*., 2017, Bedard and Krause, 2007).

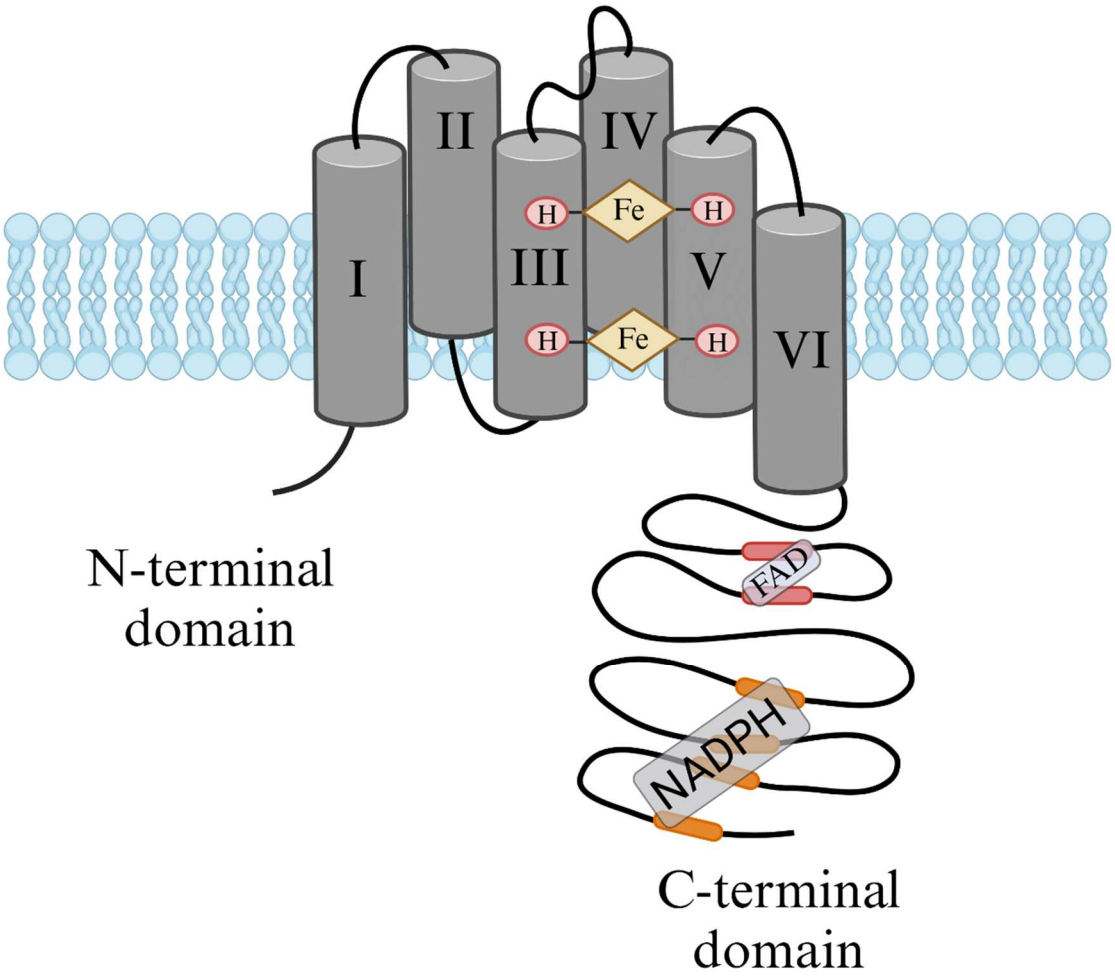

Figure 1-12. Common structural homology of NADPH oxidase. All NOX isoforms share six highly conserved transmembrane domains. NOX transmembrane III and V contain two histidine's, spanning two asymmetrical haem proteins. The cytoplasmic C-terminus contains conserved flavin adenine dinucleotide (FAD) and NADPH binding domains. Electrons are passed from NADPH to FAD to the first haem, and then subsequently second haem, converting to O_2 to ROS. This figure was created in BioRender.

NOX1 is expressed in neurons, astrocytes and microglia, with cerebrovascular NOX1 being predominantly expressed in VSMCs as well as ECs (Vendrov *et al*., 2019, Hernandes *et al*., 2022). NOX1 activation is highly dependent on the presence of cytosolic and membrane-bound subunits, acting together in a series of protein-protein interactions to function effectively (**Figure 1-13**). NOX1 is the most researched NOX isoform, due to NOX1 being considered a 'pathological' NOX, producing $O_2^{\bullet-}$ in response to physiological and pathophysiological stimuli such as shear stress, platelet growth factor (PDGF), and Ang II (Yin and Voit, 2013). Furthermore, NOX activation has been linked with hypoxia-induced increases in ROS and $[Ca^{2+}]i$ by mitochondrial ROS-PKC signalling in VSMCs (Rathore *et al*., 2008). NOX1 has also been linked with hypertension with previous research identifying that Ang II treatment of mice led to upregulation of NOX1 mRNA expression accompanied by increased ROS production when compared to NOX1 knock-out (KO) mice (Matsuno *et al*., 2005), with BP being moderately decreased in Ang II-treated in NOX1-KO mice (Gavazzi *et al*., 2006, Matsuno *et al*., 2005). Additionally, previous research has identified that in a model of *post*-stroke IRI, Mice lacking NOX1 exhibit reduced stroke lesion volume, BBB-permeability and neurological deficits (Kahles *et al*., 2007, Kahles *et al*., 2010). Moreover, in a rat model of bilateral carotid artery occlusion inducing chronic cerebral hypoperfusion, NOX1 was identified to lead to increased ROS, hippocampal death and cognitive dysfunction leading to increased risk of VaD (Choi *et al*., 2014).

NOX2 also known as $gp91^{phox}$, shares 60% homology with NOX1 (**Figure 1-13**) and is also expressed in neurons, astrocytes, microglia, cerebrovascular ECs and VSMCs. NOX2 has been associated with increases in age-related oxidative damage to the cerebral vasculature and neurons (Fan *et al*., 2019). Furthermore, research assessing a bilateral carotid artery stenosis (BCAS) surgical model of chronic hypoperfusion in mice identified that NOX2 was associated with cerebral microvascular oxidative stress, inflammation and white matter pathology leading to VCI (Alfieri *et al*., 2022). Several studies have also implicated NOX2 as a key mediator of post-stroke IRI in the brain, identifying a role for NOX2 using NOX2-KO mice in ischaemic-induced BBB-disruption and vasomotor dysfunction (Walder *et al*., 1997, Chen *et al*., 2009, De Silva *et al*., 2011). Research examining sex differences has identified that NOX2-mediated pro-inflammatory protein expression and infarct volume was greater in males than pre-menopausal female mice (Brait *et al*., 2010).

NOX4. Is expressed in neurons, astrocytes, microglia, ECs, VSMCs (Hernandes *et al*., 2022). Furthermore, NOX4 expression has been identified in human brain pericytes acting as a major source of ROS with NOX4 pericyte expression being regulated by Ang II (Kuroda *et al*., 2014). Unlike other NOX isoforms, NOX4 is constitutively activated with the subunit POLDIP2 regulating activity (**Figure 1-13**) (Lyle *et al*., 2009) . Upregulation of NOX4 mRNA has been identified in response to ER stress (Pedruzzi *et al*., 2004), carotid artery injury (SzöCs *et al*., 2002), hypoxia/ischaemia (Vallet *et al*., 2005, Coucha *et al*., 2016) and Ang II-mediated hypertension (Wingler *et al*., 2001). Studies examining NOX4 deficient mice identified a role for NOX4 in ischaemic brain injury, whereby NOX4-KO mice were identified to have reduced markers of oxidative stress, BBB-dysregulation and prevented neuronal apoptosis *post*-experimental stroke than their NOX4 expressing counterparts. Furthermore, NOX4 expressing mice showed improved post-stroke outcomes after treatment with the NOX4 inhibitor VAS2870 (Kleinschnitz *et al*., 2010). Additionally, recent research examining an endothelial-specific NOX4-KO mouse model experiencing hypoxic/ischaemic challenge reported decreased neuronal toxicity and death and BBB-breakdown after experimental stroke surgery when compared to NOX4 expressing counterparts (Casas *et al*., 2017). However, some studies have suggested that NOX4 may be a beneficial and not a deleterious NOX isoform with NOX4-derived H_2O_2 being identified to act to enhance cerebral vasodilation in in a spontaneously hypertensive rat model of chronic hypertension (Paravicini *et al*., 2004). This is supported by research assessing NOX4 overexpression in mice where NOX4 was identified to lower BP, likely mediated by improved endothelial-dependent vasodilation (Ray *et al*., 2011, Zhang *et al*., 2010).

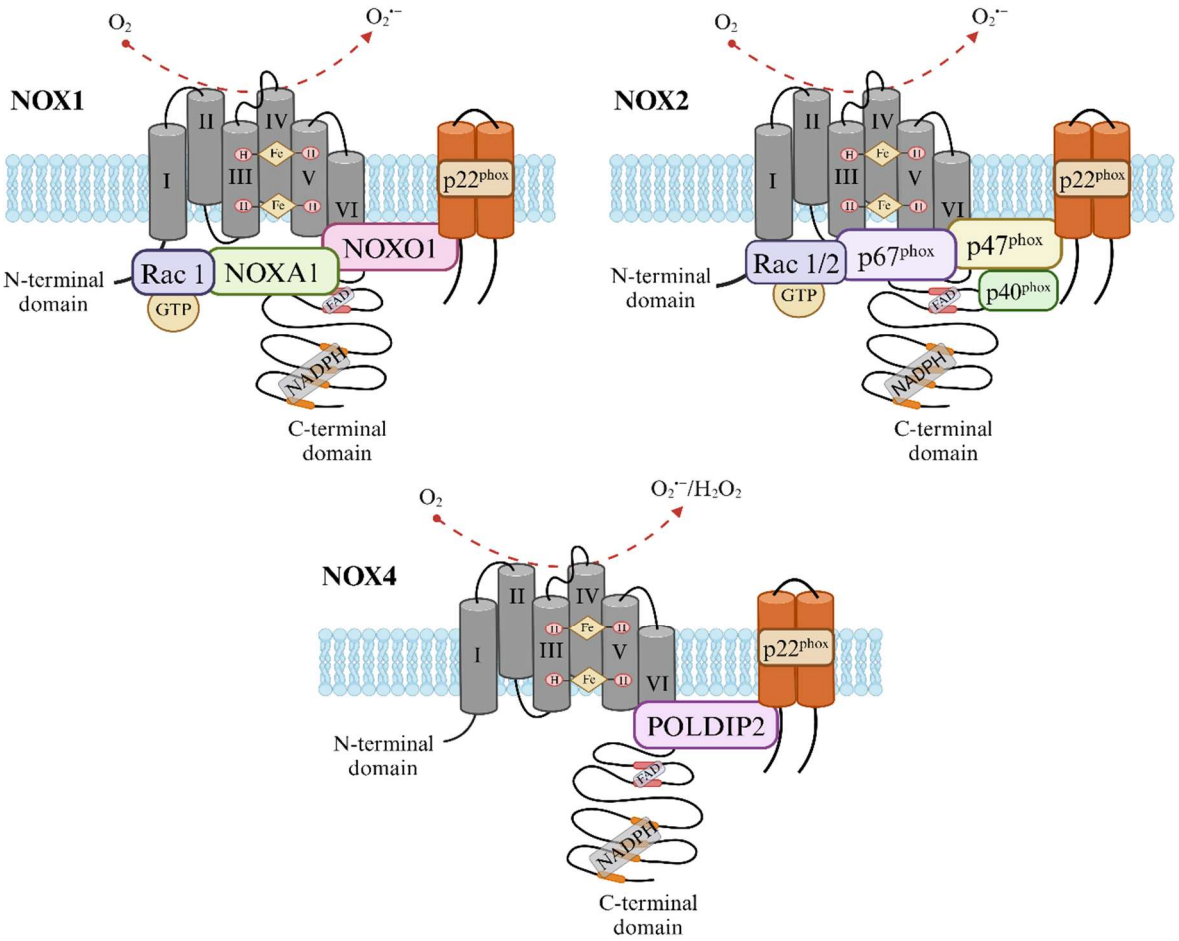

Figure 1-13. NOX1, 2, and 4 structure, activation and ROS production. This figure illustrates the activation mechanisms of NOX1, NOX2 and NOX4 via the recruitment of regulatory subunits. In the resting state, NOX1 is associated with p22phox which stabilises and recruits the following subunits for its enzymatic activity: First, NOXA1 (activator) and NOXO1 (organiser), bind to specific NOX1 and p22phox domains for NOX1 activation, with the GTPase Rac1 phosphorylating NOXA1, and enhancing NOX1 activity, and the transfer of electrons to O2, producing $O2^{\bullet-}$. In its basal state, NOX2 enzymes are located in the plasma membrane as a heterodimer, coupled with the p22phox stabilising enzyme. Activation involved the recruitment of cytosolic proteins including (p47phox (organiser), p67phox (activator) and GTPases Rac1 and 2, promoting the transfer of electrons to O2 and promoting the production of $O2^{\bullet-}$. Unlike NOX1, NOX2, NOX4 is constitutively active with ROS production being produced by its expression levels as opposed to regulatory subunits or binding partners. However, NOX4 is stabilised by p22phox, and enzymatic activity is regulated/enhanced by the interaction of POLDIP2 to the NOX1/p22phox complex, enhancing the production of ROS. NOX4 is further unique by producing both $O2^{\bullet-}$ and H_2O_2 with $O2^{\bullet-}$ being converted to H_2O_2 either enzymatically through rapid dismutation, or spontaneously due to its intracellular location. This figure was created in BioRender.

1.8 NOX5, a Unique NOX Isoform

NOX5 is the most recently characterised NOX isoform and was discovered by the groups of Lambeth (Cheng *et al*., 2001) and Krause (Banfi *et al*., 2001) characterising NOX5 cDNA predicting a protein with 565 and 700 amino acids respectively. Immunoblotting analysis identified that NOX5 has a predicted molecular weight (MW) of 85 kDa, consistent with its predicted molecular mass, further suggesting that NOX5 is not glycosylated and is instead regulated by *post*-translational modifications including phosphorylation and oxidation (Brar *et al*., 2003, Bedard and Krause, 2007, Touyz *et al*., 2019). Similar to other NOX isoforms, NOX5 has six conserved transmembrane α-helices containing putative haem-binding regions and a flavoprotein homology domain, which consists of binding sites for both NADPH and FAD in the intracellular C-terminus (Touyz *et al*., 2019). Unlike NOX1, NOX2 and NOX4 which have membrane bound $p22^{phox}$ that is essential for their stability and enzymatic as well as other subunit regulatory protein-protein interactions that are required for their activation, NOX5 has a unique intracellular NH_2-terminus extension that contains three of four Ca^{2+} binding helix-loop-helix structural (EF-hand) domains for its activation (Bánfi *et al*., 2004, Touyz *et al*., 2019). As such, NOX5 is highly sensitive to $[Ca^{2+}]i$ for enzymatic activity and is activated in a multi-phase process, involving Ca^{2+} binding to the EF-hand motifs, inducing conformational changes that expose specific hydrophobic regions that then bind to the catalytic domain located on the C-terminus (**Figure 1-14**). This binding is essential for conformational changes to NOX5 NADPH- and FAD-binding sites, allowing the initiation of electron transfer and $O_2^{\bullet-}$ production (Touyz *et al*., 2019, Vermot *et al*., 2021).

Another aspect that makes the NOX5 isoform unique is that the NOX5 gene, whilst expressed in higher mammals including humans, is not expressed in mice and rats. It was originally believed that all rodents did not express the *Nox5* gene, however, recent evidence has identified that whilst the gene is not expressed in rats or mice, *Nox5* is expressed in marmots and squirrels (Nazari *et al*., 2023). NOX5 expression in the human cerebrovasculature and brain tissue has not been as well established as other NOX isoforms. However, available data suggests that NOX5 is expressed in human brain EC's (Casas *et al*., 2019, Marqués *et al*., 2022), however, whilst NOX5 is expressed in human VSMCs, the levels of which NOX5 in cerebral VSMCs remains unknown. Furthermore, the cellular and regional expression of NOX5 in cerebrovascular disease is also unknown.

As such, further studies are required to determine precise NOX5 expression patterns and potential changes in cerebrovascular disease states such as CSVD and stroke. Due to the absence of the *Nox5* gene and the dependence of mouse and rat models for pre-clinical research, studies examining the role of NOXs in disease pathophysiology has historically been limited to NOX1, NOX2, and NOX4. However, with the advancement of gene-editing technologies, and with NOX5 being the first NOX isoform to be crystalised, this has allowed researchers new opportunities in understanding the NOX5 structure, regulatory mechanisms and contributions to disease pathologies (Magnani *et al*., 2017).

1.9 NOX5 Regulatory Mechanisms

In humans the *NOX5* gene is located on chromosome 15, and encodes six splice variants with four NOX5 isoforms (NOX5α, -β, -γ, and -δ) being identified by the Krause lab (Banfi *et al*., 2001, Bánfi *et al*., 2004), with two truncated forms of NOX5 (NOX5ε and NOX5ζ) also being further identified (Serrander *et al*., 2007, Fulton, 2009, Touyz *et al*., 2019). In humans, NOX5α, NOX5β splice variants are the primary NOX5 isoforms expressed with NOX5ε acting as a negative regulator of NOX5α and NOX5β, preventing $O_2^{\bullet-}$ generation. Additionally, the *NOX5* gene can be inhibited by epigenetic factors with the overexpression of histone deacetylases 2 (HDAC2) being shown to upregulate *Nox5* gene promotor activity in VSMCs, thereby potentially enhancing NOX5 expression and enzymatic activity (Manea *et al*., 2014). Additionally, NOX5 is known to exhibit a variety of polymorphisms within the NOX5 coding sequence. Research conducted Yang *et al*. (2014) identified several single nucleotide polymorphisms in NOX5 that significantly affect the ROS generation activity of the enzyme. In particular, the M77K mutation was identified to impair Ca^{2+}-mediated ROS production, whilst c-terminus mutants G542R and R530H exhibited little to no changes to enzymatic activity when compared to M77K. However, whether these single nucleotide polymorphisms translate to disease susceptibility remains unclear (Wang *et al*., 2014). Furthermore, recent genome wide association studies (GWAS) have implicated NOX5 single nucleotide polymorphisms in disease phenotypes. In a meta-analysis in a cohort of 475,000 patients, Kraja *et al*. (2017) reported that GWAS identified NOX5 as a novel BP-associated gene, suggesting a potential role in vascular function and hypertension (Kraja *et al*., 2017, Touyz *et al*., 2019). More recently, Azarova *et al*. (2024) demonstrated that NOX5 single nucleotide polymorphism rs35682233 was associated with an increased risk of type 2 diabetes (T2D), with particular susceptibility to patients with a BMI of >25 kg/m^2. Alternatively, a haplotype comprising the NOX5 allele

rs35672233-C was found to be protective against TD2 with elevated antioxidant levels, uric acid, and postprandial plasma glucose level regulation being identified (Azarova *et al*., 2024). While these findings highlight a role for NOX5 genetic variation in cardiovascular and metabolic health, there is no current evidence directly linking NOX5 single nucleotide polymorphisms to cerebrovascular or neurological pathologies. Additionally, no studies have reported NOX5 with linkage disequilibrium in cerebrovascular disease. Given the evidence from GWAS, further investigation is warranted in determining the role of NOX5 genetic variability and its contribution to cerebrovascular disease and neurological disorders.

At a protein level, although NOX5 does not require additional subunits for its activation, NOX5 is modulated by regulatory proteins that impact its stability and sensitivity to Ca^{2+}. Amongst these are CaM, PKCα, caveolin, c-Alb1 and molecular chaperones Hsp70 and Hsp90, each exerting effect on NOX5 functionality (Touyz *et al*., 2019). For instance CaM and PKCα have been identified to increase NOX5 Ca^{2+} sensitivity, facilitating its activation at lower $[Ca^{2+}]i$ concentrations, through phosphorylation of key NOX5 serine and threonine residues (Ser475, Ser490, Ser498, Ser516, and Thr520), enhancing $O_2^{\bullet-}$ production (Jha *et al*., 2017, Jagnandan *et al*., 2007). NOX5 expression and activation are also influenced by pro-inflammatory transcription factors such as NF-κB, STAT1/3 and AP1 in human aortic VSMCs (Pandey and Fulton, 2011), with upstream immune pathways such as TLR activation increasing NOX5 Ca^{2+} sensitivity through IRAK1/4 activity, inducing NOX5-ezymatic activity and $O_2^{\bullet-}$ production (Holterman *et al*., 2019, Touyz *et al*., 2019).

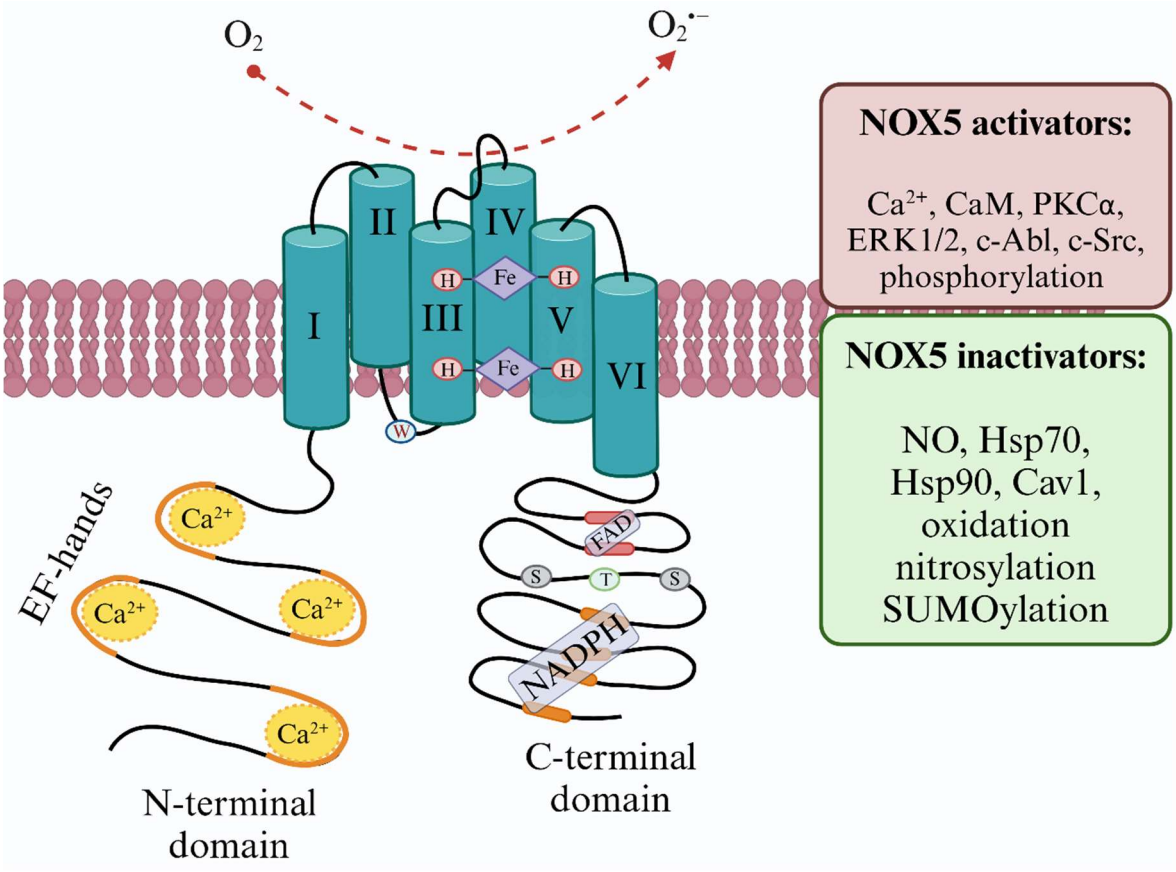

Figure 1-14. Structure and regulation of NOX5 in the vasculature. NOX5 does not require any subunits for its activation, instead utilises Ca^{2+} for its activation. Upon Ca^{2+} binding to EF hands, conformational changes drive electron transfer and the generation of $O_2^{\bullet-}$. NOX5 activity is enhanced by Ca^{2+}/Calmodulin (CaM), binding, and phosphorylation mediated by PKCα, ERK1/2, c-Abl, and c-Src. Alternatively, NO and nitrosylation, Hsp70, Hsp90, caveolin-1, oxidation and SUMOylation inhibit NOX5 function. Figure was adapted from Touyz *et al*., 2019 and was created in BioRender.

1.10 NOX5 in Vascular Dysfunction and Disease

Given that NOX5 is a Ca^{2+}-regulated, $O_2^{\bullet-}$ producing NOX isoform, NOX5 has a wide range of implications in cardiovascular health due to its influence on redox signalling and homeostasis, mediating key vascular responses. For example, research examining NOX5 in a VSMC-specific manner in mice mesenteric arteries suggests that NOX5 directly contributes to enhanced vascular contraction through Ca^{2+}-dependent NOX5-mediated redox signalling, influencing vascular contractility and endothelial-dependent regulation of vascular tone with pro-contractile proteins MLC_{20} and MYPT1 being hyperphosphorylated. These vascular tone impairments identified in VSMC-specific

NOX5 mice were attenuated whith Ca^{2+} channel (Verapamil) and CaM (Calmidazolium) and ER ryanodine receptor (RyR) (Dantrolene) pharmacological inhibition. This research highlights that this effect is dependent on Ca^{2+}-calmodulin and ER-regulated mechanisms and associated NXO5 as an active driver of pro-contractile signalling in both in both mammalian and *Drosophila* models (Ritsick *et al*., 2007, Montezano *et al*., 2018). In humans, NOX5 is the main ROS producing isoform activated by a range of vasoactive agents including endothelin-1 and Ang II (Touyz *et al*., 2019). The importance of NOX5 in ROS-mediated pathophysiology was first observed in human vascular cells, where it localises to the ER and perinuclear regions in microvascular ECs and VSMCs (BelAiba *et al*., 2007, Ahmarani *et al*., 2013). In ECs, increases in NOX5 enzymatic activity has been linked to cell proliferation, angiogenesis, and vascular remodelling, driven by mediators such as JNK3 and stromal cell-derived factor-1α (Pi *et al*., 2014, Wang and Hartnett, 2017).

The role of NOX5 in vascular remodelling extends to conditions involving ageing and hypertension, where it has been identified that NOX5 leads to cell proliferation, fibrosis and inflammation (Guzik and Touyz, 2017, Touyz *et al*., 2019). In hypertension, NOX5 was identified to be associated with redox and proteomic changes, amplifying ER stress and inducing a switch in VSMC phenotype, vascular remodelling and VSMC dysfunction (Camargo *et al*., 2023a). One of the most well-studied regulators of NOX5 expression and enzymatic activity is Ang II, through raising $[Ca^{2+}]i$ levels, influencing myogenic signalling, promoting altered cell growth and vascular remodelling (Montezano *et al*., 2015). Furthermore, the activation of NOX5 in human ECs is regulated by Ang II via $[Ca^{2+}]i$/CaM, signalling pathways (Montezano *et al*., 2010). Additionally, mice expressing NOX5 in an endothelial-specific manner exhibited age-related systolic BP increases through eNOS uncoupling, highlighting a key role for NOX5 in the context of ageing (Elbatreek *et al*., 2020). Collectively these studies indicate that increases in $[Ca^{2+}]i$ could initiate eNOS-uncoupling, thereby reducing NO bioavailability. This in turn reduces NO diffusion to VSMC, reducing the activation of sGC/cGMP production and in turn inducing a positive feedback loop that further impairs endothelial function and deregulation of VSMC myogenic tone regulation. Conversely, NOX5 expression is reduced through the vasoprotective counter-regulatory RAAS axis through angiotensin 1-7 activating AT_2R, leading to reduced oxidative stress, the prevention of cytoskeletal reorganisation and inhibition of vascular-inflammatory processes by reducing NOX5 expression and enzymatic activity (Pai *et al*., 2017). NOX5 is also involved in

hypertension through renal mechanisms. In clinical studies, patients with essential hypertension had increased renal NOX5 expression and enzymatic activity, contributing to significant ROS bioavailability and oxidative stress, amplifying hypertensive pathology (Holterman *et al*., 2015), with mice expressing humanised NOX5 exhibited increased BP leading to a hypertensive phenotype, TLR upregulation, inflammation and renal injury. (Jha *et al*., 2017). Furthermore, in the kidney, NOX5 is highly expressed in proximal tubule cells and is upregulated in diabetic neuropathy, promoting oxidative stress and impacting BP and filtration barrier function (Holterman *et al*., 2015).

NOX5 has also been implicated in the pathology of atherosclerosis, myocardial infraction and coronary artery disease through increased expression and enzymatic activity, resulting in oxidative stress and inflammation in vascular cells, including resident macrophages (Hahn *et al*., 2012, Chen *et al*., 2016). Inflammatory conditions have been shown to increase NOX5 expression in atherogenesis models, driving ROS production and disease progression (Manea *et al*., 2018). However, in primate models of atherosclerosis, NOX2 and not NOX5 was implicated in mediating cardiac inflammatory processes, identifying a context-dependent role for NOX isoforms (Stanic *et al*., 2012, Touyz *et al*., 2019). In the heart, NOX5 has been associated with ROS-mediated alterations to MAPK signalling cascades that promote hypercontractility and hypertrophy in cardiac-specific NOX5-knock in mice (Zhao *et al*., 2020). Additionally, NOX5 has been associated with cardiac microvasculature endothelial dysfunction in COVID-19 patients, suggesting that COVID-19 increases NOX5-mediated cardiovascular dysfunction (Jiang *et al*., 2023). Furthermore, NOX5 acts as a key regulator of oxidative stress, VSMC-specific phenotypic switch and extracellular matrix calcification, with NOX5 overexpression promoting VSMC transitioning to a synthetic phenotype through excessive ROS production, ROS amplification-mediated downregulation of VSMC contractile markers (SM22α and αSMA), and increased Ca^{2+} enriched extracellular vesicle (EV) release with impaired EV reuptake leading to extracellular matrix calcification (Furmanik *et al*., 2020). Given that NOX5 has emerged as a pivotal mediator in pathophysiological processes such as vascular remodelling, hypercontractility, atherosclerosis and hypertension (Touyz *et al*., 2019) Recent research has implicated NOX5 with ER stress, broadening its pathological relevance. Specifically, NOX5-β overexpression in human aortic ECs and endothelial-specific humanised NOX5-β knock-in mice have been identified to upregulate genes associated with unfolded protein response (UPR) and a critical marker of ER stress, such as *binding immunoglobulin protein* (*BIP*). This cascade has been identified to contribute to

adverse cardiac outcomes, through pathophysiological processes such as endothelial dysfunction and apoptosis (Cortés *et al*., 2021a). A significant mechanistic insight relates to the interplay between alterations to ER stress-mediated Ca^{2+} homeostasis and ROS production, whereby ROS has been identified to elevate $[Ca^{2+}]i$ concentrations through activation of Ca^{2+} -permeable channels, IP_3 mobilisation and SERCA pump inhibition. These findings indicate a potential positive feedback loop between ER stress, amplified $[Ca^{2+}]i$, and NOX5 activity leading to further ROS production (Touyz *et al*., 2018). Such a feedback mechanism was identified in research examining VSMC-specific expression of NOX5 identified regulation of smooth muscle contraction and vascular function through a NOX5-$[Ca^{2+}]i$-ROS signalling nexus contributing to vascular hypercontractility and vascular dysfunction contributing to hypertension, coronary artery disease and cerebral vasospasm (Montezano *et al*., 2018).

1.11 NOX5 and NOTCH3 Signalling

Beyond NOX5's established role, NOX5 may also intersect with NOTCH3 signalling, a pivotal pathway in irregular VSMC proliferation and differentiation that leads to severe CSVD pathologies such as CADASIL, primarily in inducing ROS-mediated deleterious outcomes including hypercontractility and vascular dysfunction. In the brain, CADASIL represents the most severe form of CSVD, leading to progressive cerebrovascular damage in arteries, arterioles and small vessels. CADASIL significantly increases the risk of early-onset stroke and VaD with the average age of symptom onset being approximately 30-years old. Moreover, CADASIL is also the most common cause of myogenic stroke. Despite the severity of CADASIL, there are currently no therapeutic treatments for this disease. However, it has been identified that CADASIL is caused by alterations in NOTCH3 expression and activity, and may offer a potential therapeutic target (Papakonstantinou *et al*., 2019).

1.11.1 The Vascular NOTCH3 Signalling Pathway

The NOTCH signalling pathway is a highly conserved mechanism that governs cell fate decisions and differentiation (Artavanis-Tsakonas *et al*., 1999, Morris *et al*., 2019). In mammals, four *Notch* family gene paralogs have been identified encoding NOTCH receptors with NOTCH1 and NOTCH4 being highly expressed in ECs and NOTCH2 and NOTCH3 being more highly expressed in VSMCs, with NOTCH3 being predominantly expressed in adult VSMCs (Morris *et al*., 2019, Baeten and Lilly, 2017). NOTCH3, similar to other NOTCH receptors, consists of a unique NOTCH3 extracellular domain (N3-ECD) containing epidermal growth factor-like (EGF) repeats serving as a platform for ligand binding, and is non-covalently associated with a NOTCH3 intracellular domain (N3-ICD), creating a single-pass heterodimeric transmembrane receptor (Morris *et al*., 2019). NOTCH3 cell transduction is mediated by close proximity cell-to-cell interaction with the EC type I transmembrane Jagged proteins (Jag1 and Jag2) and/or delta-like protein ligands (Delta, 3, and 4), which bind to VSMC N3-ECD receptors, (Baeten and Lilly, 2017). Once Jag/Delta binding occurs, a series of proteolytic processes are initiated, with the most functionally important are cleavage events occurring at site 2 (S2), and site 3 (S3). S2 cleavage occurs upon ligand binding when the sheddase A Disintegrin and Metalloproteinase (ADAM) protease or TNFα-converting enzyme (TACE) mediates the shedding of the N3-ECD from the remainder of the NOTCH receptor. This initiates S3 cleavage by the γ-secretase, releasing the N3-ICD. Cleaved N3-ICD is then released from the cellular membrane into the cytoplasm, triggering nuclear translocation, forming a complex with the nuclear RBP-Jκ (Recombination Signal Binding Protein For Immunoglobulin κ J Region) and binding to DNA and the transcriptional transactivator mastermind-like (MAML) proteins, acting as a signalling cascade for gene transcription (Baeten and Lilly, 2017, Morris *et al*., 2019) (**Figure 1-15**).

In classical NOTCH3 signalling, N3-ICD translocation to the nucleus activates the basic helix-loop-helix (bHLH) transcription factor family genes *hairy and enhancer of split* (*Hes*) and *hairy/enhancer-of-split related with YRPW motif* (*Hey*) which function as key downstream effectors of NOTCH3 signalling, regulating vascular cell fate, proliferation and differentiation by binding to Class C E-box (CACGNG), N-box (CACNAG), and to a lesser extent, Class B E-box (CANNTG) DNA sequences. Once bound, *Hes* and *Hey* gene initiate transcriptional repression of pro-apoptotic and pro-differentiation genes (Grogan *et al*., 2008, Fischer and Gessler, 2007). Furthermore, *Hes* and *Hey* genes regulate the contractile phenotype of VSMCs by modulating the expression of smooth muscle

contractile proteins (e.g., smoothelin, calponin, myosin, and α-SMA). Upregulation of the NOTCH3 signalling axis either promoting an upregulation of *Hey* and *Hes* genes, leading to a synthetic VSMC phenotype, or alternatively, downregulation of *Hes* and *Hey* genes contributing to a hypercontractile phenotype (Morris *et al*., 2019, Wang *et al*., 2008). Alternatively, non-canonical N3-ICD signalling has also been identified, operating independently of traditional ligand-receptor/transcription. This includes interaction with other cytoplasmic proteins and engagement with non-NOTCH3 targets within the nucleus, leading to the activation of downstream signalling targets that occur independently of NOTCH receptor or RBP-Jκ activation. Despite its potential significance, non-canonical NOTCH3 signalling remains poorly understood in the context of vascular biology, warranting further study to clarify its precise mechanisms and functional relevance in pathology (Anderson and Maes, 2014, Morris *et al*., 2019).

1.11.2 NOX5-NOTCH3 Signalling Axis

In a recent study conducted by Neves *et al*. (2019) examining the role of NOTCH3 in CADASIL patient mesenteric arteries, NOTCH3 gain of function was associated with upregulated NOX5 activity, promoting an increased ROS environment, Rho kinase activation, and ER stress. These interrelated pathophysiological pathways underpinned Ca^{2+} signalling, alterations to VSMC phenotype and impaired vascular tone regulation, contributing to cytoskeletal remodelling and a hypercontractile phenotype, suggesting a novel NOX5-NOTCH3 signalling axis whereby NOX5-derived ROS promotes vascular dysfunction. Furthermore, when pharmacological agents such as the Rho kinase inhibitor Fasudil, and the ER stress inhibitor 4-phenylbutyrate (4-PBA) was utilised, ROS production was ameliorated, along with markers of Rho kinase activity, ER stress, and cytoskeletal remodelling, whilst also normalising mesenteric vascular function, pointing to a potential therapeutic strategy that could target the NOX5-NOTCH3 signalling axise and mitigate vascular damage and oxidative stress in CADASIL patients. However the exact mechanisms linking NOTCH3 activation of NOX5 remain unclear with NOTCH3-regulated transcriptional pathways and ER-stress mediated $[Ca^{2+}]_i$ increases promoting NOX5 enzymatic activation and subsequent ROS generation, and therefore requires further study (Neves *et al*., 2019).

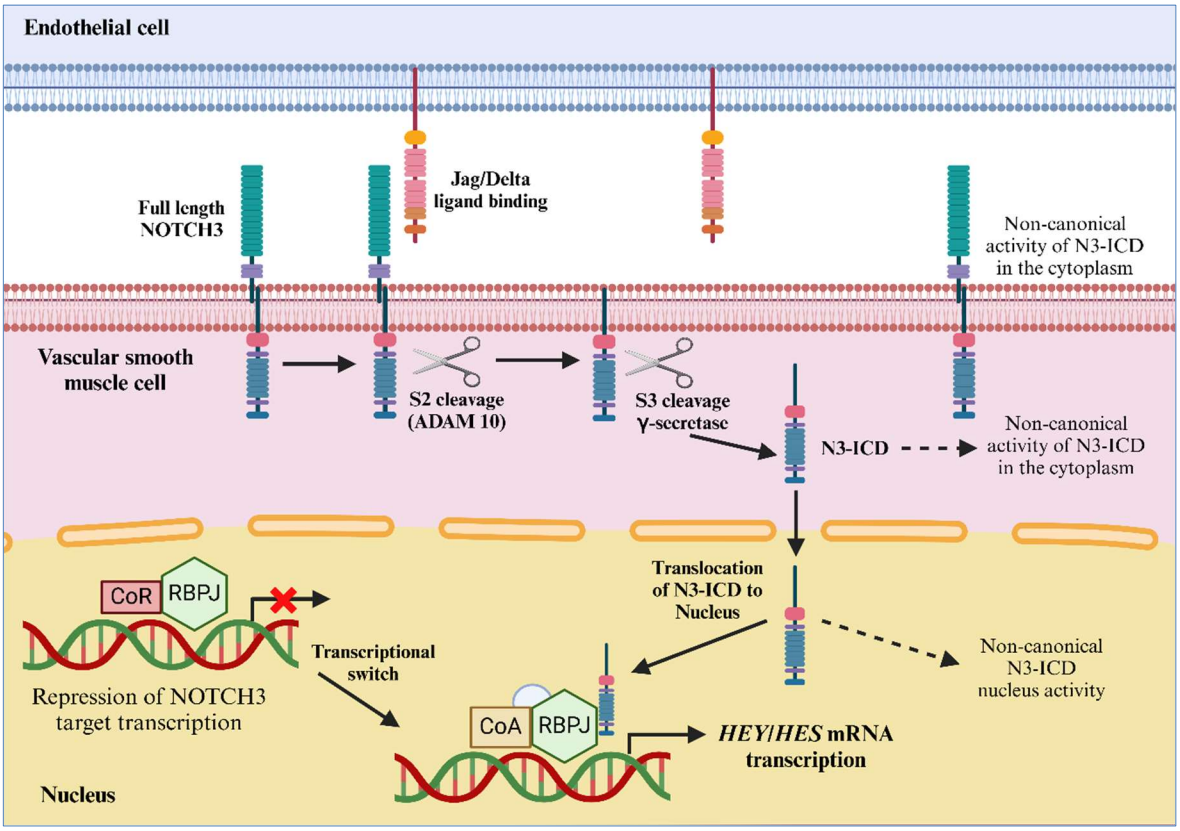

Figure 1-15. The NOTCH3 signalling axis. In the NOTCH3 signalling pathway, adjacent endothelial Jag/Delta protein ligands bind to the neighbouring VSMC full length N3-ECD domain, initiating receptor activation. This interaction triggers sequential proteolytic cleavage. First, cleavage at the S2 NOTCH3 ligand site by the sheddase ADAM10, and secondly at the S3 ligand site by γ-secretase sheddase, releasing N3-ICD into the VSMC cytoplasm. N3-ICD translocates to the nucleus, where it binds to the transcriptional regulator recombinant signal-binding protein for immunoglobulin kappa J region (RBP-Jκ) and recruits Mastermind-like protein (MAML) coactivators. MAML stabilises the N3-ICD-RBP-Jκ complex, promoting the transcription of genes *HEY* and *HES*, which encode transcriptional factors that regulate downstream genes associated with VSMC, survival, differentiation, and phenotypic selection vital for cerebrovascular homeostasis. Additionally, non-canonical NOTCH3 signalling pathways have been described, indicating broader roles for the NOTCH3 signalling axis beyond its canonical signalling. Figure was adapted from Morris *et al*., 2019 and was created in BioRender.

1.12 NOX5 in Cerebrovascular Disease

Whilst there is a growing body of literature exploring the role of NOX5 in peripheral tissues and in the cardiovascular system, its involvement in cerebrovascular disease remains poorly characterised, with only two original research article publications to date examining the role of NOX5. In 2014, preliminary research assessing the role of cerebral NOX5 in an experimental model of humanised endothelial-specific NOX5-KI mice reported that NOX5 was associated with increased hypertension and stroke risk (Kleikers *et al*., 2014). This research was then expanded by Casas and colleagues in 2019 identifying a critical link between *post*-stroke reperfusion Ca^{2+} surges, BBB-breakdown and worsened *post*-stroke neurological outcomes. Furthermore, these effects were specific to the brain as no acute role in myocardial infarction, heart ischaemia or hind limb ischaemia was observed, suggesting that the NOX5 BBB-damage was localised to cerebral endothelial cellular components (Casas *et al*., 2019).

Further research examining vascular dysfunction and cognitive decline in the context of aged endothelial-specific NOX5-KI mice, identified that whilst endothelial-NOX5 was not associated with alterations in BP, locomotor activity deficits, and mortality, it was associated with cognitive decline, with these changes likely mediated by upregulation of the prostaglandin inflammatory pathway including increases in *TXA_2S* (thromboxane A_2 synthase) and *COX2* (cyclooxygenase) mRNA expression. This study also identified that endothelial-NOX5 altered the function of TJ proteins, particularly occludin and ZO-1 becoming dysregulated, contributing to BBB-breakdown evidenced by increased immunoglobulin extravasation, suggesting BBB-permeability and disruption (Cortés *et al*., 2021b). *In vitro* studies examining the role of NOX5 overexpression in human cerebral microvascular endothelial cells (hCMEC/D3) also demonstrated that adenoviral overexpression of NOX5 amplified ROS production particularly when stimulated with NOX5 activators such as Ca^{2+}, Ang II, and PKC activator phorbol 12-myristate 13-acetate (PMA), inducing significant endothelial impairment processes such as cell proliferation and apoptosis and migration, as well as disrupted cellular metabolism though oxidative phosphorylation, and energy expenditure as evidenced by mitochondrial dysfunction, all precursors to cerebrovascular diseases such as CSVD, with these effects being attenuated by pharmaceutical ML-090 inhibition (Marqués *et al*., 2022). Taken together these findings identify a role for endothelial NOX5 in age-associated neuroinflammation, BBB-breakdown, and cognitive decline. These research studies have

identified that inhibition of NOX5 could be used in conjunction with stroke therapeutic strategies to prevent NOX5-mediated *post*-stroke IRI oxidative stress and BBB-breakdown, potentially preventing cognitive decline and, as such, represent a potential neuroprotective strategy. Whilst these studies enhance our understanding of NOX5-ROS-mediated cerebrovascular dysfunction, neuroinflammation, BBB-breakdown and cognitive decline the context of stroke pathophysiology and hypertension.

However, these research studies examining the role on NOX5 in cerebrovascular function has focussed specifically on endothelial cells, leaving significant gaps in research knowledge and do not elucidate the role of NOX5 in VSMCs which are essential regulators of cerebral autoregulation, myogenic tone, structural integrity and vascular remodelling. Therefore, understanding the role of NOX5 in a VSMC-specific manner is critical in understanding the role of NOX5 in pathologies such as CSVD, stroke, *post*-stroke IRI and its effects on VaD onset. As previously discussed, investigation of NOX5 in a VSMC-specific manner have linked NOX5 with critical pathophysiological processes, including ROS-driven oxidative stress, ER stress and hypercontractility in peripheral vessels (Montezano *et al*., 2018). However, whilst VSMC-specific NOX5 has been studied in peripheral vessels, no research has examined the role in the cerebrovasculature. This distinction is critical as NOX activity and its downstream signalling cascades and effects differ significantly between vascular beds. Whilst previous research has identified that NOX activity is significantly higher in cerebral vessels when compared to systemic arteries (Miller *et al*., 2005, Miller *et al*., 2009). Notably, elevated protein expression and activity of cerebrovascular NOX2 (Miller *et al*., 2009) and NOX4 (Miller *et al*., 2005) was identified to be increased in basilar and MCA when compared to systemic vessels. These increases in activity also contributed to increased ROS bioavailability, which was further enhanced in the context of stroke (Kleinschnitz *et al*., 2010, McCann *et al*., 2008). These findings highlight the need to consider regional vascular differences when assessing NOX5 models.

Collectively, the mechanistic findings highlighted in previous research suggest that NOX5 could be a key mediator of *post*-stroke IRI, whereby rapid reoxygenation, combined with acute Ca^{2+}-dependent cellular dysfunction is a hallmark of IRI-mediated oxidative stress and BBB-breakdown contributing to exacerbated damage. Moreover, the role of $[Ca^{2+}]i$ in regulating vascular tone is well documented with excessive ROS production and

unregulated [Ca^{2+}]i being a hallmark of CSVD and hypertensive pathologies (Harraz and Jensen, 2021, Wynne *et al*., 2009, Touyz *et al*., 2018).

Given that NOX5 is a Ca^{2+}-dependent NOX isoform, its expression in VSMCs creates an optimal environment for Ca^{2+}-mediated enzymatic activation of NOX5, driving deleterious levels of ROS and pathophysiological outcomes such as oxidative stress, impaired vascular tone, leading to a CSVD phenotype and increased stroke risk, with a potential NOX5 interaction with NOTCH3 signalling providing further risk of vascular dysfunction and risk of severe CSVD pathologies such as CADASIL. However, the interplay between cerebral NOX5 in a VSMC-specific manner remains unresearched. Furthermore, the effects of cerebral VSMC-specific NOX5 in the context of Ang II-mediated hypertension, age- and sex-differences remains poorly understood, and may offer significant insights into CSVD and stroke pathologies with a broader implication of VaD and potential development of therapeutic strategies.

1.13 Hypothesis and Research Aims

1.13.1 Hypothesis

The central hypothesis of this thesis is that VSMC-specific expression of humanised NOX5 in mice will promote oxidative stress-driven cerebrovascular dysfunction, contributing to neurovascular impairment and pathophysiological processes underlying human diseases. This effect will be exacerbated in the context of ageing, hypertension, and sex differences.

1.13.2 Research Aims

Using a mouse model of VSMC-specific NOX5-KI, the aims that will be addressed by the research in this thesis are:

- To characterise the cerebral effects of male and female mice expressing VSMC-specific NOX5-KI at basal levels (20-weeks-old). Assessing redox sensitive genes and proteins that may influence cerebrovascular function and structure.
- To examine whether NOX5-KI alters vascular reactivity, contributing to a hypercontractile phenotype.
- To further identify whether these effects are worsened in aged (35-weeks-old) and Ang II-treated male and female VSMC-specific NOX5-KI mice.

Chapter 2

Materials and Methods

2.1 Reagents and Suppliers

BioRad Laboratories, Hertfordshire, UK:

Precision Plus Protein™ Dual Xtra Standards (#1610377).

Fisher Scientific, Loughborough, UK:

Methanol (#67-56-1); Chloroform (#67-66-3); Glycine (#56-40-6); Tris Base (#77-86-1); D-Glucose anhydrous (#50-99-7); Sodium chloride (#7647-14-5); Sodium hydrogen carbonate ($NaHCO_3$, #144-55-8); Dimethyl Sulphoxide (DMSO); Amplex™-Red Hydrogen Peroxide/Peroxidase Assay Kit (#10257332).

Applied Biosystems™, Massachusetts, U.S.A:

Applied Biosystems™ High-Capacity cDNA Reverse Transcription Kit (#10400745).

Life Technologies/Invitrogen, Paisley, UK:

Dulbecco's Phosphate Buffered Saline without $CaCl_2$ and $MgCl_2$ (DPBS, #14190-094).

Qiagen, Manchester, UK:

QIAzol Lysis Reagent (#79306); miRNeasy Micro Kit (#74004); RNase-Free DNase set (#79254).

LI-COR Biosciences, Lincoln, U.S.A:

Revert™ 700 Total Protein Stain (#926-11011).

New England Biolabs, Massachusetts, U.S.A:

Deoxynucleotide (dNTP) Solution Mix (#N0447); Quick-Load® 100bp DNA ladder (#N0467S).

ENZO Life Sciences, New York, U.S.A:

U-46619 (#BML-PG023-0001).

Sigma-Aldrich, Dorset, UK:

Ponceau S; Sodium nitroprusside (SNP, #71778); Acetylcholine Chloride (ACh, A-6625) KCl (#7447-40-7); $CaCl_2$ (#10043-52-4); Triton X-100 (#9002-93-1); Tween 20 (#9005-64-5); Bovine Serum Albumin solution (#9048-46-8); Ficoll 400 Type 400-DL Lyophilised powder (#26873-85-8); $MgCl_2$ (25mM, AB0359); REDExtract-N-Amp™ Tissue PCR kit (XNAT2R).

Thermo Fisher Scientific, Renfrew, UK:

Novex WEDGEWELL 4% to 20% Tris Glycine 1.0, Mini protein gel, 15 well (XP04205BOX); Pierce™ BCA Protein Assay Kit (#23227); Nitrocellulose Membrane (#88018); Multiscribe™ Reverse Transcriptase (#4311235), Random Hexamers (#N808127); TaqMan Array Mouse Endogenous Array Card (#4378702)

VWR International, Lutterworth, UK:

Ethanol absolute (#64-17-5); N'-2-Hydroxyethylpiperazine-N'-2 ethane sulphonic acid (HEPES, #7365-45-9); Sodium dodecyl sulphate (SDS, #151-21-3); $MgSO_4 \cdot 7H_2O$ (#10034-99-8); KH_2PO_4 (#7778-77-0).

Cambridge Bioscience:

TBARS (TCA METHOD) Assay Kit (CAY700870-96).

2.2 Solutions and Media

6X Laemmli sample buffer:

SDS (10%, w/v); β-mercaptoethanol (6% v/v); bromophenol blue (0.012% w/v); glycerol (30% v/v); Tris-HCl (260 mM, pH 6.8).

Bovine serum albumin (BSA)-based blocking buffer:

BSA in TBS-T (3% w/v).

High potassium physiological salt solution (KPSS):

KCl (62.5 mM); $MgSO_4$ (1.2 mM); $NaHCO_3$ (25 mM); KH_2PO_4 (1.2 mM); $CaCl_2$ (2.5 mM); D-glucose (11 mM); pH 7.4.

Non-fat dried skimmed milk-based blocking buffer:

Marvel Dried Skimmed Milk in TBS-T (5% w/v).

Phosphate Buffer Saline – PBS (10X):

NaCl – 80g, KCl – 2g, KH_2PO_4– 2g, Na_2HPO_4 – 11.5g in 800mL dH_2O, pH adjusted to 7.4.

Phosphate Buffer Saline PBS (1X):

100mL 10X PBS was diluted in 900 mL dH_2O.

Physiological Salt Solution (PSS):

NaCl (119 mM); KCl (4.7 mM); $MgSO_4$ (1.2 mM); $NaHCO_3$ (25 mM); KH_2PO_4 (1.2 mM); $CaCl_2$ (2.5 mM); D-glucose (11 mM); pH 7.4.

Protein lysis buffer:

HEPES-NaOH (10 mM, pH 7.4); Na3VO4 (2 mM); Triton X-100 (0.5% v/v); Na4P2O7 (50 mM); NaF (50 mM); NaCl (50 mM); Na2EDTA (5 mM); supplemented with PMSF (1 mM); aprotinin (1 µg/ml); leupeptin (1 µg/ml); pepstatin (1 µg/ml).

Sodium dodecyl sulphate polyacrylamide gel electrophoresis (SDS-PAGE) running buffer:

Tris-Base (25 mM); glycine (193 mM); SDS (0.1% w/v).

SDS-PAGE transferring buffer:

Tris-Base (25 mM); glycine (193 mM); methanol (20% v/v).

Stripping solution:

NaOH (200 mM).

Tris-Buffered Saline – TBS (10X):

Tris-HCl– 24.23g, NaCl– 80g – Mixed with 800mL of dH_2O. Adjusted to pH 7.6 using 1M HCl and then added 200mL for final volume of 1L.

1X Tris-Buffered Saline – TBS (10X):

Dilute 100mL of 10X TBS with 900mL of dH_2O.

Tris-buffered saline-Tween 20 (TBS-T):

Tris-Base (20 mM, pH 7.6); NaCl (137 mM); Tween-20 (0.1% v/v).

10X Tris-acetate-EDTA buffer:

1L dH_2O, Tris Base 121.1g, Boric acid, EDTA 7.4g.

1X Tris-acetate-EDTA buffer:

Dilute 100 mL 10X Tris-acetate-EDTA buffer in 900 mL of dH_2O

2.3 Software

Software used for data acquisition and analysis for the research is listed below.

- **GraphPad Prism v8:** GraphPad Software by Dotmatics, San Diego, U.S.A.
- **Lab Chart Reader Windows v8.1.13:** AD Instruments Ltd, Oxford.
- **Empiria Studio Software v2.3: LI-COR** Biotechnology; Cambridge, UK.
- **QuantStudio™ Real-Time PCR Software:** Applied BioSystems, California, USA.
- **NanoDrop 1000 v3.7.1 software:** Thermo Fisher Scientific, Renfrew, UK.

2.4 Animals

2.4.1 Housing and Husbandry

All animal experiments and procedures were conducted in accordance with the United Kingdom Home Office regulations and with the Animals Scientific Procedures Act 1986 under personal (PIL I70208780) and project (PPL 700902 (prior to 10th May 2021), PPL PP0895181), licenses. Research for this thesis was also conducted in accordance with the Animal Research: Reporting of In Vivo Experiments (ARRIVE) guidelines, and National Centre for the Replacement, Refinement & Reduction of Animals in Research (NC3Rs) guidelines. Generation of the transgenic VSMC-specific NOX5 mice was conducted and approved by the Animal Ethics Committee of the Ottawa Hospital Research Institute, University of Ottawa, Canada, and carried out in accordance with the Canadian Council of Animal Care.

Human *NOX5*β (h*NOX5*β) cDNA was PCR amplified from pDONRNOX5β plasmid. Purified PCR hNOX5β gene-coding region was ligated into the Tet-responsive promoter Pbi-1. A fragment of the 3.7-kb TetO/NOX5β was excised, with the resulting band gel-purified and provided to the University of Ottawa Core Transgenic Facility to undergo pronuclear injection into fertilised oocytes from an FVB/N background. Genotyping assessment was utilised for the identification of pBI-hNOX5β founders on a pure FVB/N background as described previously (Montezano *et al*., 2018). The expression of the hNOX5β gene in mice is controlled by the tetracycline response element (TRE) and therefore requires the binding of the tetracycline transactivator (tTA) protein for its activation, which is not present in murine cells, therefore lacking the transcriptional activator for hNOX5β expression. In order to generate VSMC-specific knock-in animals male pBI-hNOX5β mice were cross-bred with female SM22-rtTA-FVB/N producing the $NOX5^{+}SM22^{+}$ transgenic mice used for experimental comparison with WT (FVB/N background) for the research described in this thesis (**Figure 2-1**), with $NOX5^{+}$ and $SM22^{+}$ kept for breeding purposes. Both breeding pairs were heterozygous for the genes of interest. The $NOX5^{+}$, $SM22^{+}$, and $NOX5^{+}SM22^{+}$ mice whilst originally being generated at the Ottawa Hospital Research Institute, University of Ottawa, Canada, where subsequently imported to the University of Glasgow Biological Services facility.

WT, NOX5^{+}SM22^{+}, NOX5^{+} and SM22^{+} mice housed at the University of Glasgow Biological Services facility were then sexed before being placed in cages dependent on sex. Cage environment was regulated and controlled whereby humidity and temperature (22-24^{O}C) and were constantly maintained. Mice were also given a 12-hour light/dark cycle and food and water were accessible. Additional attention was required when feeding these mice. As tTA is sensitive to the antibiotic doxycycline, which can interfere in tTA-to-TRE binding, leading to *NOX5*β gene suppression. Therefore, both chow and water were absent of doxycycline for the research. Animal cages were routinely cleaned, and food and water replaced twice-a-week by animal unit staff. Identification of individual mice were conducted by a 3-step process of: 1) Animal sexing conducted by the animal unit staff. 2) Ear-notch clipping to identify sex and genotype of the mice. 3) Ear-notches were genotyped to differentiate WT, SM22^{+}, NOX5^{+} and NOX5^{+}SM22^{+} genotypes in male and female mice. Confirmation of NOX5^{+}SM22^{+} expression was established using Immunohistochemistry (IHC) as described previously (Montezano *et al*., 2018). However, due to the specific genetic breeding set-up, the probability of Mendelian inheritance for the NOX5^{+}SM22^{+} genotype was determined using a Punnett square (**Table 2-1**) as 25%.

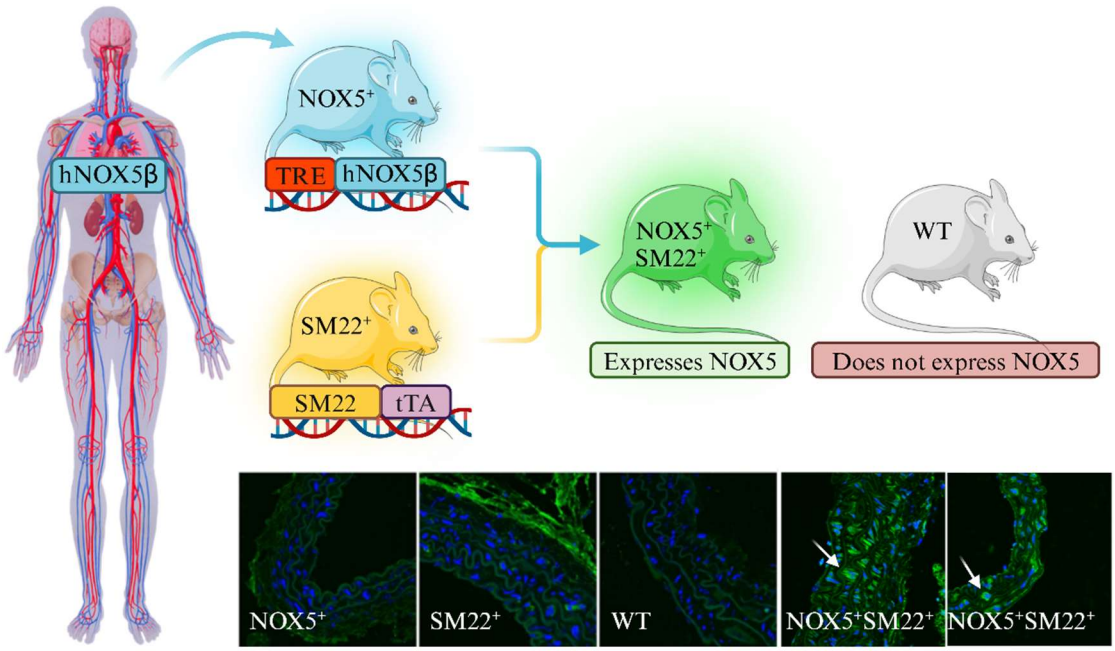

Figure 2-1. Generation of the NOX5 mouse strain and genotypic confirmation. The human NOX5-beta (hNOX5β) gene controlled by a tetracycline response element was introduced to FVB/N mice. Male hNOX5β were bred with female SM22^{+} mice that express appropriate tetracycline transactivator (tTA) to generate mice with an active NOX5 expression. Confirmation was assessed using IHC, with immunolocalization of NOX5 (green fluorescence) and DAPI to localise the nucleus (blue fluorescence) in WT, NOX5^{+}, SM22^{+}, and NOX5^{+}SM22 (Montezano *et al*., 2018). Figure created in BioRender and SMART Servier Medical Art.

		Mendelian Inheritance	
		NOX5	
		NOX5	WT
SM22+	SM22+	NOX5+SM22+ (25%)	WT/SM22+ (25%)
	WT	NOX5 /WT (25%)	WT/WT (25%)

Table 2-1. Mendelian probability of crossbreeding heterozygous NOX5 and SM22 and mice. A punnet square was used to determine the heterozygosity of the NOX5 and SM22 mice. The Mendelian inheritance was 25% for WT, 25% for $NOX5^{+}$, 25% for $SM22^{+}$, and 25% for $NOX5^{+}SM22^{+}$.

2.4.2 Cerebral VSMC-specific NOX5 Study and Experimental Cohort Group Allocation.

Mice were grouped on the basis of genotype, sex, age, and treatment conditions. The study included both WT and $NOX5^{+}SM22^{+}$ genotypes at 20- and 35-weeks of age. Ang II treatment was administered at 600 ng/kg/per-day via minipump implantation for 4-weeks with control sham groups receiving no treatment (**Table 2-2**). The intended number of mice per group for each experimental technique was as follows:

- q-RT PCR: n=7 per group.
- Immunoblotting: n=7 per group.
- Wire Myography n=7 per group.
- ROS measurements (Amplex-Red and TBARS-MDA) n=9 per group.

Outlier analysis was performed using GraphPad Prism software using the ROUT method (Q=1%), and outliers were excluded from analysis. Final sample sizes after outlier removal are reported in graph figure legends of each results chapter. Given the highly quantitative nature of this study with the focus on objective molecular and functional techniques such as immunoblotting, q-RT PCR, myography, and ROS measurements, group randomisation or blinding was not deemed necessary. These techniques provide precise, reproducible data from the predefined experimental groups (genotype, age, sex, and treatment), with the experimental design and all experimental groups controlled for consistency and scientific rigor.

Experimental Groups			
Genotype	**Age (Weeks)**	**Sex**	**Treatment**
WT	20	Male	Non-treated
$NOX5^{+}SM22^{+}$	20	Male	Non-treated
WT	20	Female	Non-treated
$NOX5^{+}SM22^{+}$	20	Female	Non-treated
WT	35	Male	Non-treated
$NOX5^{+}SM22^{+}$	35	Male	Non-treated
WT	35	Female	Non-treated
$NOX5^{+}SM22^{+}$	35	Female	Non-treated
WT	20	Male	Ang II-treated
$NOX5^{+}SM22^{+}$	20	Male	Ang II-treated
WT	20	Female	Ang II-treated
$NOX5^{+}SM22^{+}$	20	Female	Ang II-treated

Table 2-2. Cerebral VSMC-specific NOX5 study experimental cohorts and group allocation. This table summarises the experimental cohorts used in this study categorised by genotype (WT and $NOX5^{+}SM22^{+}$, age (20- or 35-weeks), sex (male or female), and treatment condition (non-treated or Ang II-treated). The planned sample sized for each experimental analysis were n=7 per group for q-RT PCR, immunoblotting, and wire myography. For ROS measurements (Amplex-Red and TBARS-MDA) n=9 per group was planned. Outlier detection and removal was performed using GraphPad Prism ROUT method (Q=1%). Final sample sizes for experiments utilising each experimental group are reported in each graph figure legend in the results chapters.

2.4.3 Subcutaneous Minipump Implantation and Angiotensin-II Treatment of mice.

To assess the role of cerebral $NOX5^{+}SM22^{+}$ in the context of hypertension, male and female 20-week $NOX5^{+}SM22^{+}$ and WT mice were treated with Ang II by subcutaneous implantation of an osmotic minipump 2004 model (Azlet, California, USA) as per manufacturer's instructions. Briefly, one day prior to minipump surgery implantation, pump reservoirs were filled. The total Ang II concentration for treatment was set at 600 ng/kg/per-day over a 4-week period (18 ng in 6 µL released/day for a 30 g mouse). The dosage was selected for studies examining the role of high-dose Ang II treatment of VSMC-specific NOX5 in inducing renal pathophysiology relevant to kidney fibrosis. Total Ang II concentration for the treatment was 600 ng/kg/per-day over a 4-week period (18 ng in 6 µL released/day for a 30 g mouse). On the day of the surgery mice were anesthetized, with the implantation site being washed and shaved before a suitable mid-scapular incision was made adjacent to the implantation site. A homeostat was then inserted into the incision, allowing for the opening of the subcutaneous tissue and the implantation of the Ang II filled minipump. The wound was then closed using haemostatic dressing, before being sutured. For the sham (non-treated) group, an incision was performed, followed by skin detachment with forceps, similar in size to the mice with a minipump implantation. After the 4-week period, the mini-pump was removed, and the animals were humanely killed for molecular studies. Various organs, including the kidney, lungs, aorta, heart, spleen, and brain were collected. While the original study focused on kidney fibrosis, the availability of brain tissue allowed to investigate the role of role of Ang II in the brains of VSMC-specific NOX5 mice. Confirmation of successful Ang II treatment was assessed through phenotypic characterisation of systolic blood pressure as previously published described (Montezano *et al*., 2018) (**Figure 2-2**).

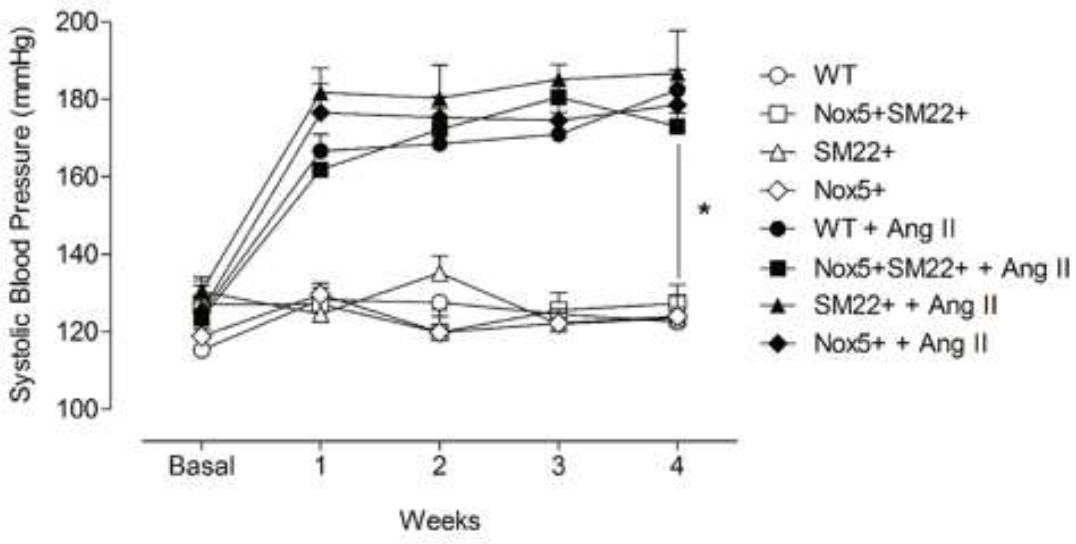

Figure 2-2. Phenotypic characterisation of normotensive and hypertensive WT and NOX5 mice. Tail cuff plethysmography was used to assess systolic blood pressure over a 4-week period using a non-invasive BP recording system which measures changes in the mouse tail blood flow. As the cuff inflates, and deflates, with mice being acclimatised to the procedure over several days to reduce stress-induced variability in BP readings (Harrison *et al*., 2024). In Ang II-treated (600ng/kg/day) and non-treated (Sham) WT, NOX5+ (hNOX5β), SM22+ and NOX5+SM22+ mice. Ang II mice/group showed a significant increase in systolic BP (*P<0.05) compared to the WT control group or untreated group. Data was taken from Montezano *et al*. (2018).

2.5 Molecular and Cellular Techniques

2.5.1 Genotyping

All WT and $NOX5^{+}SM22^{+}$ mice used for experiments in this study were genotyped using the REDExtract-N-Amp™ Tissue PCR kit (Sigma-Aldrich, Dorset, UK). Murine DNA was extracted from collected ear notches, before the ear notch sample was placed into an Eppendorf tube and 100µL of REDExtract-N-AMP extraction solution was to each sample along with 25µL of REDExtract-N-Amp™ Tissue PCR kit tissue solution was added, before being vortex and centrifuge mixed, Samples were then incubated at room temperature for 10 minutes, and then heated at 95ºC using a heating block for a further 3 minutes. 100µL of REDExtract-N-AMP™ Tissue PCR kit neutralising solution was then added to the sample before being vortex mixed and stored at 4ºC until required (as per reagent instructions). Isolated DNA concentration and quality being determined by NanoDrop ND-1000 spectrophotometer (Labtech International, Heathfield, UK) and NanoDrop 1000 v3.7.1 software. The primers to detect hNOX5β, SM22, and γ-actin are described in **Table 2-2**. PCR reactions were undertaken in a PTC-225 Peltier thermal cycler (MJ Research, Massachusetts, USA) under the following conditions:

For hNOX5β: 95°C for 2 min, 95°C for 20 sec; and then 30 cycles of: 60°C for 20 sec (denaturation), 72°C for 30 sec (annealing) and 72°C for 2 min (extension); followed by 4°C for 30 min and held at 12°C.

For rtTA2: 95°C for 5 min, 95°C for 30 sec; and then 33 cycles of: 58°C for 45 sec (denaturation), 72°C for 30 sec (annealing) and 72°C for 5 min (extension); followed by 4°C for 30 min and held at 12°C.

For γ-actin: 95°C for 5 min, 95°C for 30 sec; and then 35 cycles of: 60°C for 45 sec (denaturation), 72°C for 30 sec (annealing) and 72°C for 7 min (extension); followed by 4°C for 30 min and held 12°C.

Amplified PCR products were separated using agarose gel electrophoresis. The agarose gels (2% w/v) were prepared in Tris-acetate-EDTA buffer (40mM Tris-Base, 20mM acetic acid, 1mM EDTA in dH_2O, pH 8.5) and boiled in a microwave until dissolved. Visualisation of double-stranded DNA products, agarose gels were stained with SYBR™ Safe (1:10,000 dilution/0.1 µL/mL). The gel was set at room temperature for 10 minutes

after which, samples were then loaded consisting of; 0.6 µL forward sequence primer, 0.6 µL reverse sequence primer, 4.8 µL dH_2O, and 4 µL of DNA template) see **Table 2-2**. The gels were then run at 100V for 1 hour (BioRad, UK), and visualised using ChemiDoc™ XRS+ Systems (Bio-Rad Laboratories Ltd, Watford, UK) and Image Lab™ software. Mice with a positive hNOX5β, SM22, and γ-actin PCR DNA product were identified as $NOX5^{+}SM22^{+}$ and mice, with a negative PCR DNA sequence to hNOX5β and SM22, and a positive PCR DNA sequence to γ-actin were identified as WT mice (**Figure 2-3**).

Gene	Forward Sequence	Reverse Sequence	Product Length
hNOX5β	**5'** ggc caa ggg ctg tgg cca **3'**	**5'** tgg cct ccg cct gag cct g **3'**	**600bp**
SM22	**5'** cat ggc aag act ttc tgc gg **3'**	**5'** ttg tct cag aag tgg ggg ca **3'**	**450bp**
γ-actin	**5'** gtg tta gac act gtg gac atg g **3'**	**5'** gag aga gcc ata cca aga atg g **3'**	**250bp**
Ladder			**100bp**

Table 2-3. Gene sequences of primers for genotyping. Forward and reverse DNA sequences for hNOX5β, SM22, and γ-actin used for PCR genotyping.

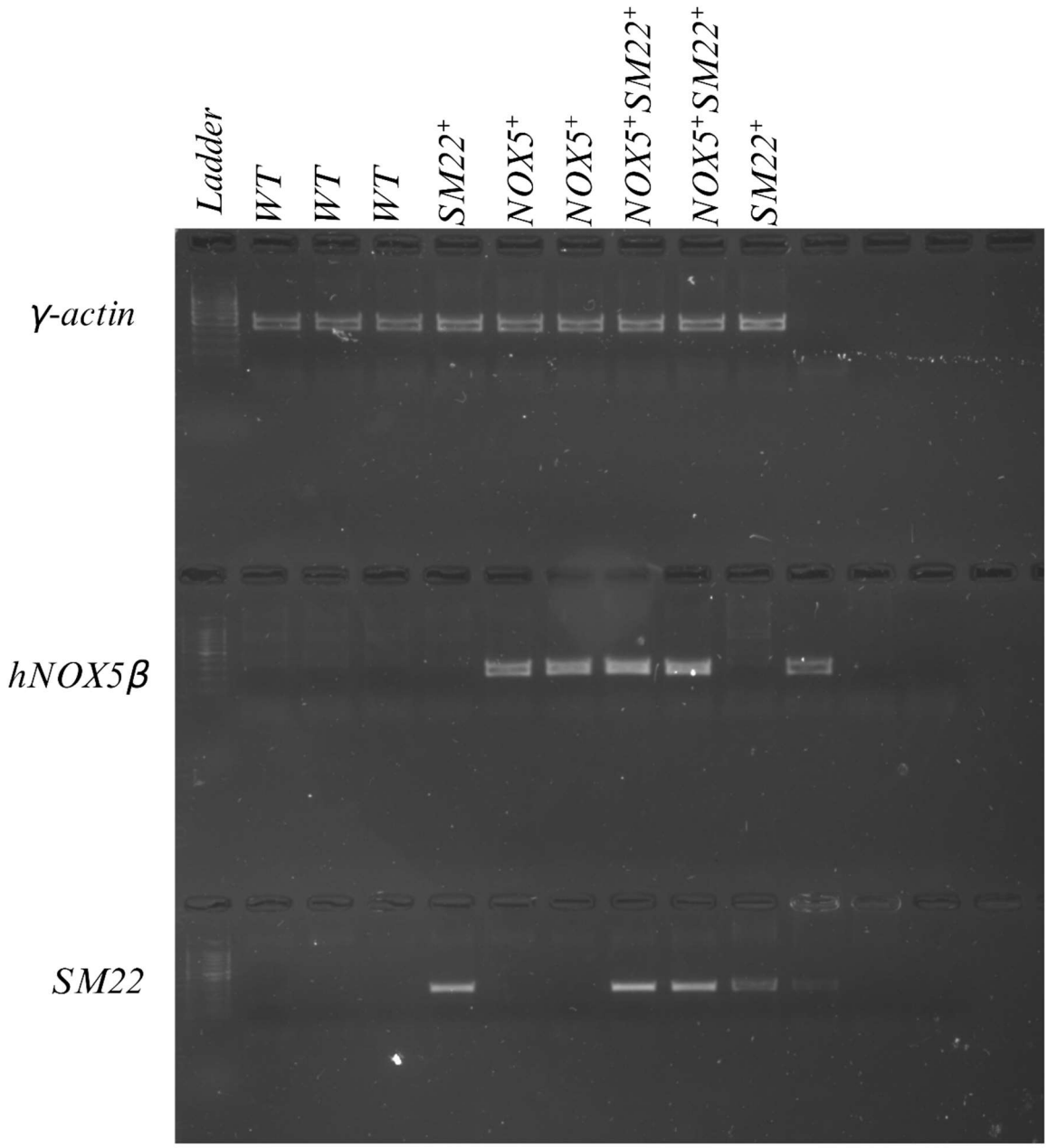

Figure 2-3. Representative genotype gel identifying NOX5$^+$, SM22$^+$, NOX5$^+$SM22$^+$ and WT mice used for this study. For brevity and clarity, NOX5$^+$SM22$^+$ mice will simply be referred to as NOX5 for the remainder of this thesis.

2.5.2 RNA Extraction and Purification using QIAzol® QIAGEN miRNeasy® Minikit

RNA was extracted from murine brain tissues using the QIAGEN QIAzol® isolation and the QIAGEN miRNeasy minikit as per manufacturer's instructions. Briefly, 50mg of frozen brain tissue was placed into a 1.5 ml microcentrifuge tube along with a tungsten steel ball and 700 µl of QIAzol® (**Figure 2-4 (1)**). Samples were then homogenised using a Retsch Qiagen TissueLyser (QIAGEN, Hilden, Germany) at 20Hz for 2x 2 min (**Figure 2-4 (2)**). Subsequently, 140 µl of chloroform was added to each sample, mixed thoroughly for 1 min and incubated at room temperature for 2 min to allow phase separation (**Figure 2-4 (3)**). Samples were centrifuged at 12,000 g, for 10 min, at 4ºC (**Figure 2-4 (4)**). Once centrifugation was complete, the upper (aqueous) phase (approximately 350 µl) was carefully transferred to a new nuclease-free microcentrifuge tube. 100% ethanol was then mixed into the aqueous phase (approximately 1.5x the volume of the aqueous phase) and mixed before 700 µl of sample was added to a miRNeasy mini column (**Figure 2-4 (5)**) and allowed to precipitate before being centrifuged at 8000 g for 30 sec at room temperature (**Figure 2-4 (6)**). Flow through was discarded and the centrifugation repeated to remove excess phenol. 350 µl of QIAGEN RWT buffer was added to the mini column and centrifuged at 8000 g for 20 sec at room temperature to remove residual salt (**Figure 2-4 (7)**). A RNase-Free DNAse kit was used as per the manufacturer's instructions whereby 80 µl of DNAse was added directly to the silica-membrane of the mini-column and incubated for 15 min to allow DNA digestion (**Figure 2-4 (8)**). After this, a further 350 µl of RWT buffer was added to the mini column and centrifuged at 8000 g for 30 sec at room temperature and the flow through discarded. 500 µl of RPE buffer was then added to the mini column and centrifuged at 8000g for 30 sec at room temperature to remove any contaminating proteins through proteinase K digestion (**Figure 2-4 (9)**). Once the flow through was discarded, another 500 µl of RPE buffer was added to the column which was centrifuged at 8000 g for 2 min at room temperature, with the flow through discarded. To remove any residual RPE buffer and to dry the silica membrane, the column was centrifuged at 8000g for 1 min at room temperature (**Figure 2-4 (10)**). The silica membrane spin column was then moved to a new microcentrifuge tube and 30 µl of RNase-free water (RF-H_2O) added before centrifugation at 8000g for 1 min at room temperature (**Figure 2-4 (11)**). The eluted RNA sample was then re-eluted into the spin column to increase isolated RNA concentration before being stored at -80ºC for later use (**Figure 2-4 (12)**).

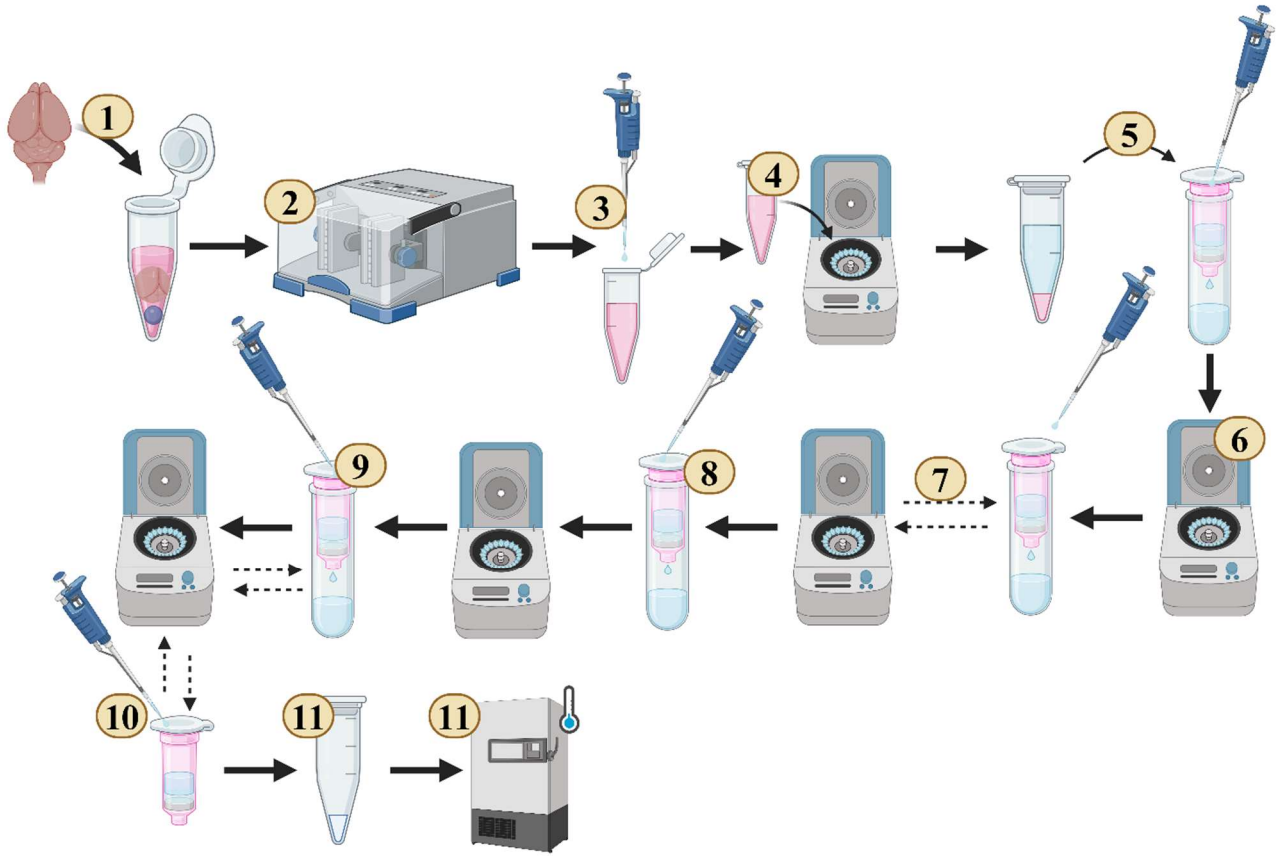

Figure 2-4. Stepwise illustration of RNA extraction and purification using QIAzol® QIAGEN miRNeasy® minikit. RNA was extracted from brain tissue using the QIAGEN miRNeasy minikit with the extraction involving the following steps: 1) Homogenisation, 2) Phase separation, 3) Aqueous phase collection, 4) RNA column binding, 5), RWT buffer-mediated phenol flow-through removal, 6) RWT buffer-mediated salt removal, 7) DNAse treatment, 8) Buffer wash, 9) RPE buffer-mediated protein removal, 10) Silica membrane drying, 11) RNA elution, 12) Re-elution and storage. This method ensured that highly purified RNA was extracted suitable for q-RT PCR experiments. Figure created in BioRender.

2.5.2.1 RNA Analysis and Purity Quantification

RNA concentration and purity was quantified using NanoDrop ND-100 spectrophotometer (Labtech International, Heathfield, UK) utilising NanoDrop 1000 v3.7.1 software. 1.5 µl of RF-H_2O was measured as a "blank" background control. 1.5 µl of the isolated RNA sample was measured in duplication. Concentration of RNA samples were calculated based on the following formula: RNA concentration = $A/\varepsilon l$, where A indicates sample absorbance measured at 260 nm, ε specifies molar extinction coefficient of nucleic acids and l indicates the light path-length. Additional absorbance measurements were made at 230 nm and 280 nm. Samples were used for further experimentation with an A_{260}/A_{280} ratio of ~2.0 indicating purification away from protein contaminants and an A_{260}/A_{230} ratio in the range of ~2.0-2.2, indicating purification away from salts, residual phenol/chloroform, and other organic compounds.

2.5.2.2 Complementary DNA Synthesis of RNA Polymerase Reverse Transcription

Complementary DNA (cDNA) was generated from isolated RNA samples using TaqMan™ cDNA reverse transcription reagents (ThermoFisher, UK and New England Biolabs™, Massachusetts, U.S.A) following the manufacturers recommended protocol. In a 96-well PCR-plate, 12.3 µl of a reaction mix consisting of 10X buffer (1X), 25mM $MgCl_2$ (5.5 mM), 10mM dNTP (deoxyribonucleotide triphosphates (2 mM)), random hexamers (2 U/µL), RNAse Inhibitor (1 u/µl), and Multiscribe reverse transcriptase (2.5 U/µL) was added to each well. RNA samples isolated from murine brain tissues were diluted to 130 ng/µl with RF-H_2O and vortex-mixed before 7.7 µl of diluted RNA was added to each well for a final RNA/reaction mix volume of 20 µl with 1 µg input RNA. A negative template control (NTC) was also included by adding 7.7 µl RF-H_2O to a separate well containing the reaction mixture. The PCR-plate was then sealed using adhesive transparent PCR film and vortex-mixed gently, followed with a quick centrifugation step to spin down the RNA/reaction mix. Subsequent cDNA synthesis was performed using a PTC-225 Peltier Thermal Cycler under the following conditions: 25ºC for 10 min (primer annealing stage), 48ºC for 30 min (cDNA synthesis), 95ºC for 5 min (inactivation of reverse transcriptase), and 4ºC for a minimum of 10 min (reaction termination). 30µl of RF-H_2O was then added to the synthesised cDNA plate leading to a total volume of 50µl and centrifuged prior to storage at -20ºC until required.

2.5.3 TaqMan® Mouse Endogenous Control Array Card

As housekeeping gene expression can vary between experimental conditions such as genotype, treatment, sex, and age, a TaqMan® Mouse Endogenous Control Array Card was used to assess 16 ubiquitously expressed housekeeping genes (HKG (**Table 2-3**)). Briefly, 5 µl of two randomly assigned cDNA samples from each group + 50 µl nuclease-free H_2O and TaqMan no AmpErase® UNG Universal 2x Master Mix (55 µl) was combined and vortex-mixed. 100 µl of each sample was loaded into each reservoir of the microfluidic plate before centrifuging twice at 331 x g for 1 min at room temperature to ensure even distribution of the samples in the array card wells. The array card was then sealed using adhesive transparent q-RT PCR film. A q-RT PCR reaction was then performed using the Quantstudio™ 12K Flex Real-Time PCR System (Applied Biosystems) under the following conditions: Polymerase enzyme activation holding stage at 95ºC for 10 min, then PCR denaturing stage: 40 cycles at 95ºC for 15 sec per cycle, and PCR annealing/extension stage: at 40 cycles at 60ºC 1 min per cycle. Results were then exported and analysed as raw cycle threshold (Ct) values. HKG viability was then considered with a ranged standard deviation of ≤ 0.5. As differences in β-actin gene expression were observed between 20-week and 35-week mice, *Ppia* was used as the HKG.

TaqMan Mouse Endogenous Control Array Card			
18 S-rNA	B2M	GAPDH	GUSB
HMBS	HPRT1	IPO8	PGK1
POLR2a	PPIA	RPLP2	TBP
TFRC	UBC	YWHAZ	β-actin

Table 2-4. TaqMan® Mouse Endogenous Control Array of 16 housekeeping genes: A TaqMan Mouse Endogenous array card containing 16 ubiquitous HKGs was used to determine a viable HKG for male and female non-treated and Ang II treated WT and NOX5 mice.

2.5.4 TaqMan Oligonucleotides and Conditions of Use:

TaqMan gene of interest (GOI) and Housekeeping Gene (HKG) probes used to study quantitative-reverse transcription polymerase chain reaction (q-RT PCR) in this study are summarised in **Table 2-4**.

Target Gene Name	Company	Probe ID	Reporter Dye
Nox1	ThermoFisher	Mm00549170_m1	FAM
Nox2	ThermoFisher	Mm01287743_m1	FAM
Nox4	ThermoFisher	Mm00479246_m1	FAM
Sod1	ThermoFisher	Mm01344232_g1	FAM
Sod2	ThermoFisher	Mm01313000_m1	FAM
Nqo1	ThermoFisher	Mm00500821_m1	FAM
Ho1	ThermoFisher	Mm00516004_m1	FAM
Catalase	ThermoFisher	Mm00437992_m1	FAM
Notch3	ThermoFisher	Mm01345646_m1	FAM
Hey1	ThermoFisher	Mm00468865_m1	FAM
Heyl	ThermoFisher	Mm00516558_m1	FAM
Hes1	ThermoFisher	Mm01342805_m1	FAM
Hes5	ThermoFisher	Mm00439311_g1	FAM
Housekeeping Genes			
Ppia	Thermo Fisher	Mm02342430_g1	FAM

Table 2-5. TaqMan q-RT PCR probes used in this study to determine mRNA levels: All TaqMan probes were purchased from ThermoFisher for q-RT-PCR. Target gene mRNA levels were normalised using HKGs identified using the TaqMan Array Mouse Endogenous Array Card.

2.5.5 Quantitative Real-time Polymerase Chain Reaction

Gene expression of selected genes of interest in NOX5 and WT mice were assessed using TaqMan-based quantitative real-time polymerase chain reaction (q-RT PCR). During the q-RT PCR cycle, TaqMan probes hybridise to the sequence within the target cDNA, the probe is then degraded by the 5' to 3' exonuclease activity, allowing for fluorophore separation from the quencher, and subsequent fluorophore fluorescence emission. The level of fluorescence was measured at the end of each amplification cycle, with the fluorescence intensity being proportional to the amplified PCR product from the initial target gene quantity. Once the fluorescence intensity crosses a predetermined amplification threshold set above the background signal, the Ct number was automatically calculated by the Quantstudio^{TM} 12K Flex Real-Time PCR System (Applied Biosystems). Raw Ct values generated by the q-RT PCR instrument were then calculated using the $2^{-\Delta\Delta Ct}$ method using a housekeeping reference gene (HKG) for normalisation.

In a 384-well reaction plate, 1.5 µl of cDNA product was added along with a mixture of TaqMan no AmpErase® UNG Universal 2x Master Mix (5 µl), FAM-labelled target gene probe (0.5 µl), and RF-H_2O (3 µl), for a total reaction volume of 10 µl. Individual samples were loaded in triplicate with a RF-H_2O along with the NTC cDNA control to separate wells as a negative control, before the plate was sealed using adhesive optically clear qPCR film and vortex-mixed gently before brief centrifugation to spin down the reaction mixture and cDNA. q-RT PCR reactions were then performed using the Quantstudio^{TM} 12K Flex Real-Time PCR System (Applied Biosystems) under the following conditions: Polymerase enzyme activation holding stage at 95ºC for 10 min, then PCR denaturing stage: 40 cycles at 95ºC for 15 sec per cycle, and PCR annealing/extension stage: at 40 cycles at 60ºC 1 min per cycle. Analysis of GOI was performed using the $2^{-\Delta\Delta Ct}$ method, with *Ppia* as the HKG. Briefly, $\Delta\Delta Ct$ was calculated using the following formula: $\Delta Ct = Ct_{GOI} - Ct_{HKG}$, where Ct_{GOI} indicates Ct value of the GOI and Ct_{HKG} indicates Ct value of the HKG, *and* $\Delta\Delta Ct = \Delta Ct_{sample} - \Delta Ct_{control}$, where $\Delta Ct_{control}$ indicates the average ΔCt value of the vehicle-treated control group and ΔCt_{sample} indicates the ΔCt value of stimuli-treated groups. The relative quantity (RQ) value of the target gene was calculated as: $RQ = 2^{-\Delta\Delta Ct}$. TaqMan q-RT PCR mRNA expression results were reported as fold change relative to their control group (**Table 2-5**).

TaqMan q-RT PCR control groups			
	20-weeks	**20-weeks v 35-weeks**	**Normotensive v Ang II-treated Hypertensive**
Mixed sex	20-weeks-old WT	20-weeks-old WT	Non-treated WT
Male	20-weeks-old Male WT	20-weeks-old Male WT	Non-treated Male WT
Female	20-weeks-old Female WT	20-weeks-old Female WT	Non-treated Male WT

Table 2-6. Table representing control group comparisons for 20-week, 20- v 35-week, and normotensive v Ang II-mediated hypertensive analysis of mixed sex, male and female mice.

2.5.6 Protein Isolation and Quantification.

2.5.6.1 Isolation of Total Protein from Mouse Brain Tissues.

Brain tissue samples used for immunoblotting, Amplex-Red, and lipid peroxidation measurement experiments were homogenised in 200µl of lysis buffer, using a Precellys 24 tissue homogeniser (Bertin Instruments, Montigny-le-Bretonneux, France). Samples were homogenised for 2 cycles of 30 sec at 10,000 rpm. Tissue lysates were then centrifuged at 12,000 rpm for 15 min at 4ºC. The resulting supernatant was carefully separated from the tissue pellet and transferred into a new pre-cooled microcentrifuge tube. Samples were then sonicated for 5 sec. Samples were then stored at -80ºC for later experiments (Immunoblotting/Amplex-Red/TBARS).

2.5.6.2 Determination of Protein Concentration and Preparation of Samples.

Protein concentration was determined using Pierce^{TM} BCA Protein Assay Kit according to the manufacturer's instructions. The assay relies on the conversion of Cu^{2+} to Cu^{1+} by proteins in an alkaline environment. By using a reagent containing bicinchoninic acid (BCA), an interaction between cuprous ions and BCA at 37^{O}C for 30 min leads to a purple-coloured reaction complex, allowing for the precise and selective colorimetric quantification of Cu^{1+} characterised by an absorbance peak at 562 nm.

In this assay, standard Bovine Serum Albumin (BSA) across a range of concentrations: 2000 µg/ml, 1000 µg/ml, 500 µg/ml, 250 µg/ml, 125 µg/ml, 62.5 µg/ml was prepared. For a negative control, the lysis buffer for protein extraction was used. To create a working reagent (WR), BCA reagent A containing bicinchoninic acid, and BCA reagent B containing copper (ii) sulphate solution were mixed in a 50:1 ratio. Determination of protein concentrations were established by adding 5 µl of standards to wells of a clean 96-well plate in duplicate. Brain protein lysates were then added to other wells in duplicate. Following this, 50 µl of WR was added to each well and the plate incubated at 37ºC for 30 min in a dark environment. Absorbance at 562nm was measured using a VICTOR$^{2\ TM}$ X3 multilabel plate reader (PerkinElmer, Michigan, USA). The standard curve was accepted if R-squared was > 0.98. Utilising the linear equation derived from the standard curve, the protein concentrations of the samples were determined.

2.5.7 Immunoblotting

2.5.7.1 Sodium Dodecyl Dulphate Polyacrylamide Gel Electrophoresis (SDS-PAGE) for Immunoblotting.

Separation of proteins according to their molecular mass was conducted using SDS-PAGE. Following protein determination, samples were normalised to 30 µg through H_2O dilution. 6X Laemmli sample buffer was then added to protein lysates at a 5:1 ratio and vortex-mixed. The mixture was then heated at 95ºC for 5 min using an Eppendorf ThermoMixer (Eppendorf, Hamburg, Germany) to denature proteins through disrupting non-covalent bonds, resulting in proteins unfolding into linear peptide chains. Protein samples were then stored at -20^{O}C prior to immunoblotting. Invitrogen Novex Tris-Glycine Mini Gels (4-20% containing SDS) were used to separate proteins with a range of 8 to 250 kDa. The Novex Tris-Glycine mini-gels were then placed into an electrophoresis tank filled with 1 l of running buffer. 5 µl of protein standards (Bio-Rad Precision Plus Protein^{TM} Dual Xtra Standards) were loaded into the first lane of the pre-cast wells. Subsequently, wells were loaded with 18 µl of sample containing 30 µg of protein. The electrophoresis tank was then electrophoresed at a constant potential of 165 V for 70 min.

2.5.7.2 Protein Transfer and Immunoblotting.

Following the separation of proteins, gels were removed from the electrophoresis tank and placed into SDS-PAGE transfer buffer. To transfer proteins, the gel was then placed into

an 8-layer “protein transfer sandwich” consisting of: Cassette (Clear end), Sponge, 2x Filter paper, hydrophobic 0.45µm pore nitrocellulose paper, protein separation gel, 2x filter paper, sponge, and cassette (Black end). The sandwich was then placed into a Bio-Rad Tetra Blotting module (Bio-Rad, California, U.S.A) with the clear cassette end orientated to face the positive electrode. The Tetra Blotting module was then filled up with 1 l of transfer buffer. Wet transfer was conducted with a constant voltage of 110 V for 90 min (or for 120 min for proteins such as NOTCH3). Protein transfer efficiency was assessed by Ponceau-S solution or by REVERT^{TM} Total Protein staining of the nitrocellulose membrane, and then destained by 3x 5-min washes of TBS-T. Following de-stain, membranes with adequate protein transfer were then placed into 5% non-fat dried milk-based TBS-T blocking buffer for 1 h at room temperature and agitated at a gentle speed on a laboratory shaker. Blocked membranes were then washed with TBS-T (3 x 5 min) before incubation in primary antibodies (diluted in 5% BSA TBS) with gentle shaking at 4^{O}C overnight. The following day, the primary antibodies were removed, and the membrane washed in TBS-T for 3 x 5 min, followed by incubation with appropriate secondary fluorescence-coupled antibodies (goat-anti-mouse IgG-IRDye 680, and goat-anti-rabbit IgG-IRDye 800 (LI-COR Biosciences, Cambridge, UK)) in 5% BSA/TBS-T solution for 1 h in darkness at room temperature. After incubation, the secondary antibodies were removed, and the membrane washed with TBS-T (3 x 5 min). Immuno-reactive proteins were then imaged using either an Odyssey CLx LI-COR or Odyssey Licor DLx imaging system (LI-COR Biosciences, Cambridge, UK).

Protein levels were analysed using Empiria Studio^{TM} software and normalised to β-actin levels or REVERT^{TM} 700 Total Protein stain depending on the experiment.β-actin was used for normalisation in the early stages of the study whilst conducting research in the Touyz lab group (2021). However, when immunoblotting experiments were conducted in the Salt lab group (2023), the REVERT^{TM} Total Protein stain was utilised as it is now considered the standard for immunoblotting normalisation, providing a more accurate and consistent control that accounts for potential single normalisation protein variations due to genotype, sex, age, and treatment. Additionally, in some instances, antibodies on membranes were stripped with NaOH (200mM) for 5 min at room temperature, before a 5 min wash with TBS, followed by 3 x 5 min washes with TBS-T. Membranes were then re-blocked with fresh blocking buffer for 1 h at room temperature, washed with TBS-T for 3 x 5 min, and re-probed with further primary antibodies.

2.5.7.3 Antibodies and Conditions of use:

Primary and secondary antibodies used in this study are summarised in **Table 2-6**. Primary antibodies were diluted as per manufacturers recommendations in TBS-T with 5% BSA (w/v). β-actin was used for protein normalisation and was diluted to a 1:10,000 dilution in TBS-T with 1% BSA (w/v) or by REVERT™ 700 Total Protein Stain.

Target Protein	Company	Catalogue ID	Host Species	Dilution
NOX1	Sigma-Aldrich	SAB4200097	Rabbit	1:1000
NOX2	Abcam	ab80508	Rabbit	1:1000
NOX4	Abcam	ab133303	Rabbit	1:1000
NOTCH3-FL	Cell Signalling	D11B8-5276s	Rabbit	1:1000
NOTCH3 -ICD	Cell Signalling	D11B8-5276s	Rabbit	1:1000
BIP	BD Biosciences	610978	Mouse	1:1000
PRDX-SO_3	Abcam	ab16830	Rabbit	1:10000
PTP-SO_3	R&D Systems	MAB2844	Mouse	1:1000
ROCK1	Thermo Scientific	PA521130	Rabbit	1:1000
RhoA	Santa Cruz	Sc-418	Mouse	1:1000
VEGFR2	Cell Signalling	2479	Rabbit	1:1000
αSMA	Abcam	Ab5694	Mouse	1:1000
GFAP	St Johns	STJ116876-50	Rabbit	1:200
β-actin	Sigma-Aldrich	A2228	Mouse	1:10000
REVERT™ 700 Total Protein Stain	LI-COR Biosciences	926-11011	N/A	N/A

Secondary Antibody	Company	Catalogue ID	Host Species	Dilution
Anti-Mouse IgG Alexa Fluor 680	ThermoFisher	A21057	Goat	1:10000
Anti-Rabbit IgG Alexa Flour 800	ThermoFisher	A32735	Goat	1:10000

Table 2-7. Primary and Secondary antibodies. Primary and secondary antibodies used for western blotting. For western blot experiments, primary antibody target proteins were then labelled with an appropriate secondary antibody. Blots were normalised to either β-actin or by Revert™ 700 Total Protein Stain, dependent on the experiment.

2.5.8 Reactive Oxygen Species and Oxidative Stress Measurements.

2.5.8.1 Amplex^{TM}-Red Assay

Mouse brain tissue hydrogen peroxide (H_2O_2) levels were measured using an Amplex^{TM}-Red horseradish peroxidase-linked fluorescence assay kit (Life Technologies) used as per manufacturer's instructions. Amplex-Red (10-acetyl-3,7-didroxyphenoxazine) is a colourless and non-fluorescent compound designed to detect H_2O_2 and peroxidase activity in cells and tissue when combined with horseradish peroxidase (HRP). In the presence of peroxidase, Amplex-Red reacts with a 1:1 stoichiometry with H_2O_2 forming resorufin (**Figure 2-5**), which fluoresces at an excitation wavelength of 571nm and emission maxima at 585nm. Amplex-Red standards were created by serial dilution of the 20 mM H_2O_2 working solution with 1x reaction buffer (standard concentrations of 20 µM, 10 µM, 5 µM, 2.5 µM, 1.25 µM, 0.625 µM). A blank standard consisting of 1x reaction buffer was used as a negative control, and the remaining 20 mM working solution was used as a positive control. 50 µl of Amplex-Red reagent was combined with 100 µl of 10 U/ml HRP solution, and 4.85 ml of 1x reaction buffer to create a Amplex-Red+HRP working solution and 50 µl was added to 50 µl of sample or standards in a 96-well plate. Samples were protected from light and absorbance measured at three 30 min intervals using a Wallac 1420 Victor2 plate reader (Perkin Elmer) at 560nm. Sample readings were averaged and normalised to input protein determined by BCA assay (section XX). Amplex-Red was used at a >50 µM to avoid autooxidation of superoxide to H_2O_2, and potential artefacts.

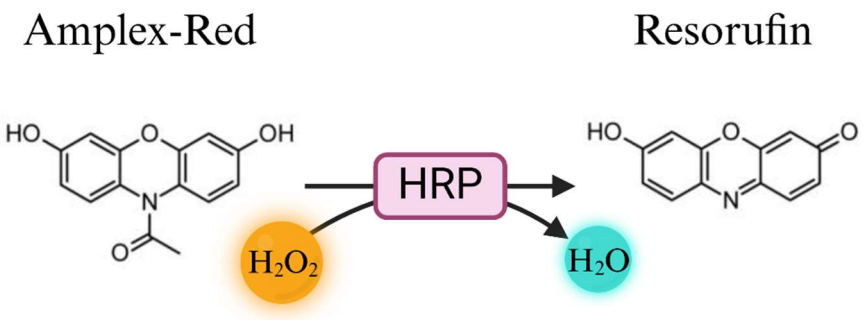

Figure 2-5. Figure illustrating the Amplex-Red to resorufin chemical reaction. This figure illustrates the enzymatic reaction where the non-fluorescent Amplex-Red, is converted into resorufin by the enzymatic action of HRP binding to the active site of H_2O_2, utilising H_2O_2 as a n oxidative agent for Amplex-Red and forming resorufin with this reaction reducing H_2O_2 to H_2O. This figure was created in BioRender.

2.5.8.2 Thiobarbituric Acid Reactive Substances Malondialdehyde Assay

Brain lipid peroxidation was determined by quantifying malondialdehyde (MDA) using a Thiobarbituric Acid Reactive Substances (TBARS) trichloroacetic acid (TCA) method MDA assay kit (Cayman Chemical, Michigan, USA) as per the manufacturer's instructions. Lipid peroxides, a marker of oxidative stress, are produced from polyunsaturated fatty acids and are chemically unstable, producing a series of complex compounds including MDA. When MDA is combined with thiobarbituric acid and heated to a sufficient temperature (95^{O}C), a colorimetric reaction occurs at a readable emission wavelength of 530-540nm (**Figure 2-6**). 100 µl of TCA assay reagent 10% (w/v) was mixed with 100 µl of brain tissue lysate in a microcentrifuge tube and heated at 95ºC for 1 h to precipitate proteins, before being placed on ice for 10 min. Samples were then centrifuged at 1,600 x g for 10 min at 4ºC. MDA colorimetric standards were used, serially diluted to final concentrations of 50 µM, 25 µM, 10 µM, 5 µM, 2.5 µM, 1.25 µM, 0.625 µM. A blank consisting of dH_2O was used as a negative control. Standards (200 µl) and samples (200 µl) were then added to a 96-well plate on ice. Absorbance was then read using a Wallac 1420 Victor^2 plate reader (Perkin Elmer) at 535nm. TBARS was calculated by plotting the absorbance read from the brain tissue samples against the MDA standard curve measurements and normalised to input protein determined by BCA assay and calculated using a linear regression calibration curve (**Figure 2-7**).

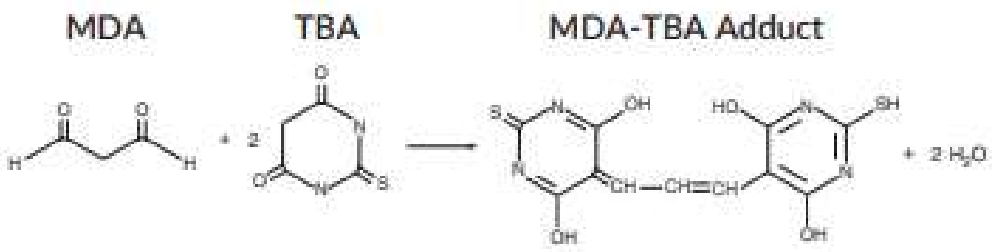

Figure 2-6. Figure illustrating the chemical reaction involved in the detection of malondialdehyde-thiobarbituric acid adduct. One molecule of MDA, a byproduct of lipid peroxidation, reacts with two molecules TBA under acidic and high temperature conditions (90^{o}C) to facilitate the formation of adduct, a colourimetric compound readable at 530-540nm, and utilised for the quantification of lipid peroxidation and oxidative stress.

$$\text{MDA } (\mu\text{M}) = [\frac{(\text{corrected absorbance}) - (\text{y} - \text{intercept})}{\text{Slope}}]$$

Figure 2-7. Colourimetric calculation of malondialdehyde concentration using a linear calibration curve. Corrected MDA absorbance concentration values are calculated by linear regression through measured absorbance of a sample adjusted for blank readings, with the y-intercept accounts for baseline absorbance, with the slope gradient of the calibration curve representing changes in absorbance per unit concentration (1µM).

2.5.9 Carotid Artery Wire Myography

Wire myography is an *in vitro* technique used primarily to assess arterial vessel functionality (Mulvany and Halpern, 1977). On a four-channel wire myograph, carotid artery vessels were carefully dissected from male and female NOX5 and WT mice at 20 and 35-weeks of age. After two wires were carefully placed through the vessel lumen, and vessels were mounted onto the myograph whereby one wire was connected to a micrometre allowing control of vessel circumference, and the other wire was connected to a force transducer, measuring tension developed by the vessel (**Figure 2-8**). After temperature equilibration at 37^{o}C for 30 min, and a normalisation procedure whereby carotid artery vessels were gradually increased to a resting tension of 5mN before being zeroed. The passive length tension was determined before stimuli was added directly to the myograph bath and vessel tension was traced using Lab Chart.

2.5.9.1 Dissection of Carotid Arteries and Preparation for Wire Myography.

20-week and 35-week-old male and female WT and NOX5 mice were humanely killed by a schedule 1 method (CO_2 inhalation). Under a dissecting microscope and using spring scissors, both common carotid arteries were carefully dissected, and placed into ice-cold PSS (pH 7.4). Once in PSS, the vessels were cleaned of surrounding perivascular fat without contacting the vessel wall, before being cut into segments approximately 2mm in length. Before mounting the vessel segments, myograph baths were washed 3 times with dH_2O and 3 times with PSS. After the final wash, the bath was filled with 5 ml of PSS and oxygenated with 95% O_2/5% CO_2. Subsequently, two wires (approx. length 2 cm) were inserted through the vessel segment lumen, carefully avoiding the artery wall. The wires were then mounted onto the myography jaws and micrometre screw was appropriately adjusted to a resting tension, resulting in a final wire myograph system with a mounted carotid artery as shown in **Figure 2-8**.

The myograph bath was connected to the transducer and placed onto the transducer base plate before being washed in 5 ml of PSS and reoxygenated. Vessels were then heated to 37^{o}C, and left to equilibrate for 30 min before being zeroed and normalised by increasing tension incrementally to 5 mN and allowed to rest for 30 min for tension to stabilise before vessels were zeroed, completing normalisation. After normalisation, vessel viability was assessed based on the contractile response to 62.5 mM high potassium physiological salt solution (KPSS)-induced vessel depolarisation. To achieve “wake up” of

the vessels, the vessels were challenged twice with KPSS at 5 min intervals. Vessels that failed to contract were excluded from the experiment.

Vessel endothelial integrity was then assessed by pre-constricting carotid arteries with U-46619 ($3x10^{-8}$ M) and assessing endothelial-dependent vasorelaxation with a single concentration of acetylcholine (ACh $1x10^{-6}$ M). ACh binds to muscarinic receptors on the blood vessel leading to an increase in EC $[Ca^{2+}]_i$ levels, activating EC-specific CaM and subsequently eNOS. The activation of eNOS converts L-arginine to NO which subsequently diffuses from EC's to adjacent VSMCs, activating sGC, promoting an increase in cGMP and the activation of processes such as SERCA pumps that reduce VSMC $[Ca^{2+}]_i$ levels, leading to vasorelaxation (Wilson *et al*., 2016). Endothelial-dependent vasorelaxation was considered functional if the relaxation response had >50% attenuation of the maximum contractile effect induced by U-46619. Consequently, as a substantial number of vessels did not meet this criteria, endothelial-dependent relaxation experiments were excluded from this research.

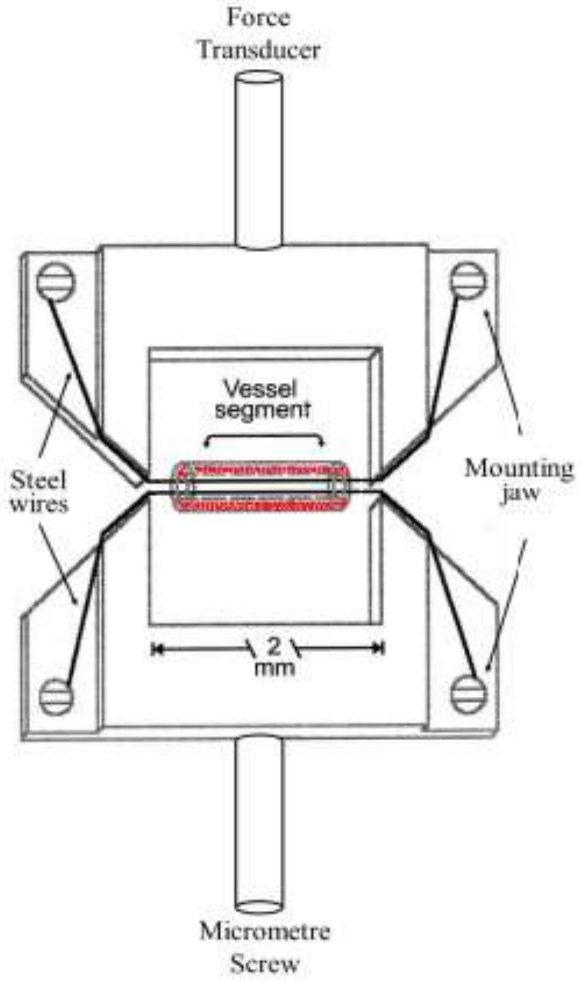

Figure 2-8. Representative schematic of wire myograph. Carotid artery vessel segment was mounted on a myograph by two 40 µm diameter steel wires. One wire was connected to the micrometer to allow vessel circumference control, whilst the other was connected to the myograph force transducer that records changes in vascular tension, allowing for assessment of vascular functionality. Modified from (Wang *et al*., 2000).

2.5.9.2 Concentration Response Curves and Data Analysis.

Cumulative concentration response curves (CCRC) of vasoconstriction were generated in response to the thromboxane A_2 receptor (TXA_2R) agonist U-46619 (Dorn and Becker, 1993). Furthermore, CCRC were also generated to assess endothelial-independent vasodilation to the NO donor sodium nitroprusside (SNP). NO released from SNP stimulates guanylate cyclase, converting guanosine triphosphate (GTP) into cyclic cGMP and activating protein kinase G (PKG), leading to VSMC relaxation (Bonaventura *et al*., 2008) (**Figure 2-9**). Briefly, to assess vasocontractile response, after a plateau in basal tension *post*-normalisation, carotid vessels were exposed to U-46619 in cumulatively increasing concentrations (1×10^{-10} M, 3×10^{-10} M, 1×10^{-9} M, 3×10^{-9} M, 1×10^{-8} M, 3×10^{-8} M, 1×10^{-7} M, 3×10^{-7} M, 1×10^{-6} M, 3×10^{-6} M). Vessel tension was recorded by LabChart software and maximum values were normalised to basal readings. Similarly, endothelial-independent relaxation CCRC in response to SNP was assessed after vessels were pre-constricted with U-46619 (3×10^{-8} M). Following a plateau in the U-46619 mediated contractile response, the tension level was set as 0% relaxation before carotid vessels were cumulatively exposed to increasing concentrations of SNP (1×10^{-9} M, 3×10^{-9} M, 1×10^{-8} M, 3×10^{-8} M, 1×10^{-7} M, 3×10^{-7} M, 1×10^{-6} M, 3×10^{-6} M, 1×10^{-5} M, 3×10^{-5} M). SNP was then expressed as a percentage of vasorelaxation relative to the posited maximum relaxation (The distance between the basal tension recorded prior to the U-46619 dosage and the tension recorded at 0% relaxation). CCRC were then converted and expressed. For contractile dose-response curves, basal readings were subtracted from maximum contractile values and expressed as 'Force millinewtons (mN)' and endothelial-independent relaxation curves were expressed as a percentage of relaxation versus the log concentration of the stimulus (U-46619 or SNP) using a log (stimulus) versus response model in GraphPad Prism software.

Data from the myography experiments were statistically analysed using a non-linear regression model to fit the dose-response curves. LogEC50 (the logarithmic concentration of the stimulus at which 50% of the maximal effect is observed) and the vascular function maximal response (Emax) were derived from the CCRC and used to assess the pharmacological profile of both U-46619- and SNP-mediated vascular responses. The goodness of fit was evaluated using an extra sum-of-squares F-test to assess the significance between experimental conditions. All results were considered statistically

significant when $p < 0.05$ which were then statistically analysed using the non-linear regression model and extra sum-of-squares F test.

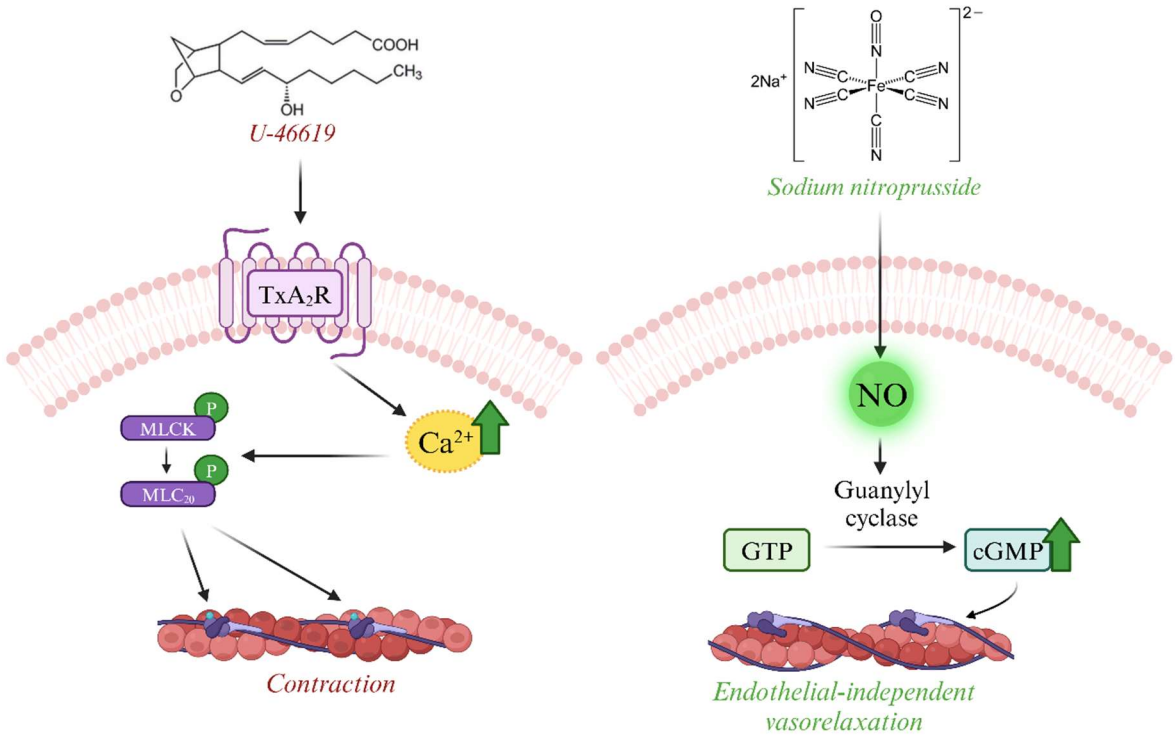

Figure 2-9. Diagram illustrating the mechanisms of action of U-46619 and sodium nitroprusside agonists in vascular pharmacology. U-46619 is a synthetic TxA_2R agonist that initiates $[Ca^{2+}]i$ increases that lead to the phosphorylation of MLCK and subsequently, MLC_{20}, initiating vascular contraction. Alternatively, SNP acts as a NO donor, leading to mechanisms of endothelial-independent vasodilation through guanylate cyclase activation conversion of GTP to cGMP. This figure was created in BioRender.

2.6 Statistical Analysis

Quantitative data was analysed using GraphPad Prism software v8 (San Diego, USA). Results were expressed as mean ± standard error of the mean, and sample size (n), indicating independent biological replicates specified in each figure. Due to the variable factors (Genotype, Age, Treatment, Sex), multiple analyses was performed. For comparisons between two groups, an unpaired and two-tailed students *t*-test was used. When more than two groups were compared a one or two-way analysis of variance (ANOVA) was performed followed by Tukey's or Dunnett's *post*-hoc test. The evaluation of vascular reactivity using wire myography between groups was determined by two parameters: Firstly, the maximum effect (referred to as top or bottom parameter), and the agonist concentration (Log agonist) that produced 50% of the maximal response ($LogEC_{50}$), calculated using a nonlinear regression (curve fit). Statistical significance was determined with a p value < 0.05 considered significant and indicated by asterisks (* $p<0.05$, ** $p<0.01$, *** $p<0.001$, **** $p\leq 0.0001$).

Chapter 3

Cerebral Characterisation of 20-week-old, Male and Female VSMC-NOX5 Knock-in Mice

3.1 Overview

Due to the absence of the *Nox5* gene in mice and rats, there has been a paucity of research investigating the role of NOX5 and its effects on the brain. Limited studies have explored the effects of cerebrovascular NOX5 with previous research examining cerebral vascular NOX5 in transgenic humanised NOX5-knock in mouse model in an endothelial cell-specific manner. These studies revealed that NOX5 is associated with increased ROS production, larger infarct volumes, BBB dysfunction and poorer functional outcomes following a transient middle cerebral artery occlusion (tMCAO) model of experimental stroke (Casas *et al*., 2019). Additionally, previous research examining *Rhodnius prolixus* arthropods, and transgenic mice expressing human NOX5 in a VSMC-specific manner identified a systemic increase in ROS bioavailability in both mesenteric arteries vasculature and in heart tissue, inducing impaired endothelium-dependent vasorelaxation and increased agonist-mediated vasoconstriction (Montezano *et al*., 2018). Moreover NOX5 been linked to ER stress, contributing to increased $[Ca^{2+}]i$, upregulated activation of NOX5-mediated ROS production in resistance arteries from normotensive and hypertensive patients (Camargo *et al*., 2023a). Additionally, Previous studies have identified that in peripheral small arteries of TgNOTCH3^{R169C} mice, a mouse model of CADASIL, uncovered an interaction between NOX5 and NOTCH3, contributing to an impaired ROS environment, ER stress and impaired vascular tone. Furthermore, TgNOTCH3^{R169C} mice have been associated with a reduction in myogenic tone and severe cerebrovascular dysfunction (Capone *et al*., 2016, Neves *et al*., 2019). To date, no research has investigated the role of mice with overexpressed NOX5 in a VSMC-specific manner in the cerebral vasculature. Given that NOX5 is activated by Ca^{2+} binding, coupled with the innate role of $[Ca^{2+}]i$ signalling in VSMC regulation of vascular tone (Montezano *et al*., 2018, García *et al*., 2023). VSMC-NOX5 may play a key role in vascular dysfunction through oxidative stress and aberrant NOTCH3 signalling.

Additionally, existing evidence assessing cerebrovascular risk in male and female populations, identified men have increased susceptibility to CSVDs such as CADASIL and stroke onset when compared to pre-menopausal females (Jiménez-Sánchez *et al*., 2021, Krause *et al*., 2006, Lisabeth and Bushnell, 2012). Redox status has been implicated in this process, with elevated oxidative stress levels being observed predominantly in males, whilst oestrogen has been identified as a protective factor in females. As such, understanding the role of sex differences in VSMC-specific NOX5 in the brain could

highlight NOX5-mediated pathophysiological mechanisms and potential therapeutic targets for cerebrovascular diseases such as CSVD and stroke (Rexrode *et al*., 2022, Jiménez-Sánchez *et al*., 2021, Kander *et al*., 2017).

Here in Chapter 3, this study investigates the baseline vascular function of 20-week-old male and female WT and VSMC-specific NOX5 mice under baseline conditions to understand the fundamental differences between two genotypes at a single time point. As such, the study presented here in Chapter 3 hypothesises that the cerebral expression of NOX5 in a VSMC-specific manner will contribute to a pro-oxidative stress environment that will lead to structural and phenotypic changes in the brain. Furthermore, VSMC-specific NOX5 will contribute to disrupted NOTCH3 signalling and markers of ER stress, contributing to a CSVD phenotype and increased risk of stroke, with these effects worsened in males. The data presented here in chapter 3 will serve as a reference for later analysis for both Chapter 4 and Chapter 5.

3.2 Chapter 3 Hypothesis and Aims:

3.2.1 Hypothesis

Here in Chapter 3, this thesis hypothesises that NOX5 in a VSMC-specific manner will lead to a pro-oxidative stress environment that will contribute to impaired cerebrovascular homeostasis and increased risk of cerebrovascular disease.

3.2.1.1 Predictions of Hypothesis

To test this hypothesis, this study predicts that cerebral VSMC-specific NOX5 will lead to:

1. **Alterations in structural and phenotypic markers:** This study anticipates that VSMC-NOX5-KI mice will exhibit alterations in cerebrovascular proteins (GFAP, RhoA, ROCK1, and VEGFR2) which are vital for typical structure, characteristic phenotype and normal physiological function.
2. **Alternative NOX isoform modulation:** This study predicts that VSMC-NOX5 will cause alterations in NOX1, NOX2, and NOX4 mRNA and protein levels indirectly through compensatory mechanisms to regulate NOX5 activity.
3. **Impaired carotid artery vascular function:** This thesis hypothesises that NOX5 in a VSMC-specific manner would contribute to increased contractility and impaired vasorelaxation in carotid arteries.
4. **NOTCH3 signalling axis alterations:** This study predicts that VSMC-NOX5-KI in the cerebrovasculature of mice will dysregulate the NOTCH3 signalling axis leading to alterations in cerebrovascular function.
5. **Alterations to ROS/antioxidant homeostasis and increased markers of oxidative stress:** This study hypothesises that VSMC-NOX5-KI mice would lead to increase ROS production, markers of oxidative stress, and altered antioxidant gene expression.
6. **Altered protein levels of ER stress UPR marker BIP:** This study further hypothesises that BIP protein expression will be altered by VSMC-NOX5 overexpression in the brains of mice, influencing cellular stress response and calcium homeostasis leading to cerebrovascular dysfunction.

Collectively VSMC-NOX5 overexpression may lead to pathophysiological outcomes that may indicate increased risk of cerebrovascular disease.

3.2.2 Specific Aims

1. *To confirm the presence of NOX5 in a VSMC-specific manner in 20-week-old mice.*
Global confirmation of NOX5 in a VSMC-specific manner was identified previously by immunoblotting (Camargo *et al*., 2022), and immunohistochemistry (Montezano *et al*., 2018). Genotyping of mouse ear notches was also conducted to confirm and differentiate WT and VSMC-NOX5 mice in male and female mice using REDExtract-N-AMP PCR.
2.*Assessment of phenotypic and structural changes in the brains of 20-week-old WT and VSMC NOX5 mice.*
To assess if NOX5 leads to phenotypic and structural changes in the brain, neurovascular unit markers GFAP, α-SMA, VEGFR2, and contractile markers ROCK and RhoA were assessed by immunoblotting.
3. To explore whether VSMC-Nox5 regulates the expression of alternate NOX isoforms (NOX1, NOX2, and NOX4).
NOX1, NOX2, and NOX4 mRNA and protein expression was assessed by q-RT PCR and immunoblotting in the brains of male and female 20-week-old VSMC-specific mice.
4. To assess the effects of VSMC-specific NOX5 overexpression on carotid artery vascular function.
Carotid arteries were derived from male and female 20-week-old WT and VSMC-NOX5 mice. Carotid vessel reactivity was assessed by wire myography using cumulative-concentration curves to assess contraction and endothelial-independent vasorelaxation by incubating carotid artery vessels with U-46619 and sodium nitroprusside (SNP) respectively.
5. To explore if cerebral VSMC-NOX5 regulates the NOTCH3 signalling axis.
Male and female 20-week-old wild-type WT and VSMC-NOX5 mouse brains were used to examine NOTCH3 expression by q-RT PCR and by immunoblotting to assess mRNA expression and protein expression respectively. Genes regulated by NOTCH3 (*Hey* and *Hes* genes) were assessed by q-RT PCR.
6. *To examine the effects of VSMC-NOX5 on redox signalling in the brain.*
Oxidative stress was assessed in the brains of 20-week-old male and female WT and VSMC-NOX5 mice by measuring ROS production (lipid peroxidation and hydrogen peroxide), redox signalling (irreversibly oxidised protein tyrosine phosphatases) and antioxidant genes.
7. *To identify if NOX5 leads to changes in the ER UPR response.*
Immunoblotting was conducted to assess BIP levels in the brains of 20-week-old WT and VSMC-NOX5 mice.

3.3 Results

3.3.1 Confirmation of VSMC-NOX5 Knock-in in Transgenic Mice

To assess VSMC-specific NOX5 in the brains and carotid arteries of mice, this study first needed to confirm the correct genotypes for used for this study (WT and NOX5). Correct genotype identification was conducted using REDExtract-N-AMP PCR on isolated ear notches from colony's containing either WT, non-expressing-NOX5, SM22, and NOX5 mice. Genotypes suitable for study expressed either both NOX5 and SM22 (NOX5) or did not express NOX5 and SM22 genes (WT). Mice that expressed 1 gene were utilised for breeding purposes or were humanely killed by schedule 1 method (**Figure 3-1A**). The WT and VSMC-NOX5 mice were then used for the study. Immunoblotting (**Figure 3-1B**) and immunohistochemistry (**Figure 3-1C**) was conducted in mesenteric arteries and confirmed the expression of VSMC-NOX5 in mice (Camargo *et al*., 2022, Montezano *et al*., 2018).

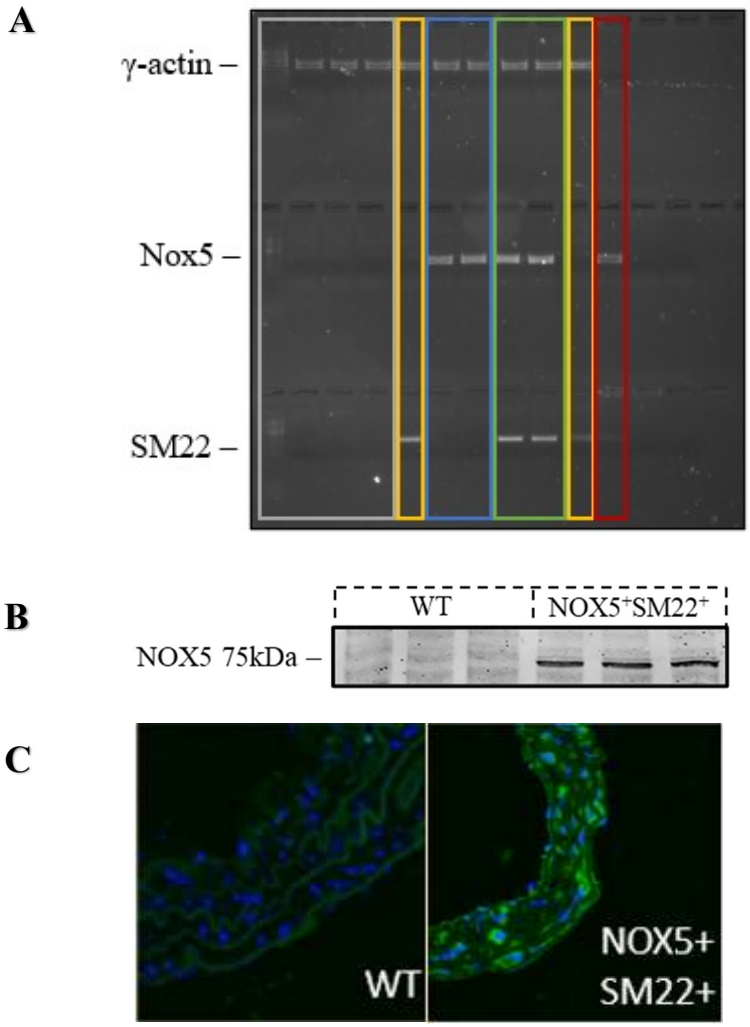

Figure 3-1. Confirmation of VSMC-NOX5 overexpression in mice. (A) Genotyping conducted using mouse ear notches identifying; WT (grey), non-expressing NOX5^{+} (blue), SM22+ (yellow), VSMC-NOX5 (expressing) mice (green), and undefined samples (red) for re-analysis. (B) Immunoblotting confirming NOX5 expression in a VSMC-specific manner in mouse mesenteric arteries of 20-week-old male NOX5^{+}SM22^{+} mice (Camargo *et al*., 2022) (C) Immunofluorescence of male NOX5 mouse aortas confirming NOX5^{+}SM22^{+} expression visualised by green fluorescence (NOX5) and DAPI to localise the nucleus (blue fluorescence) confirming the VSMC-NOX5 mice for the study (Montezano *et al*., 2018).

3.3.2 Housekeeping Gene Suitability for Thesis Studies.

This thesis aimed to examine gene expression of various GOI in the brains of male and female mice VSMC-specific NOX5 overexpression in context of ageing and hypertension. HKG stability of β-actin between sex- and age- was identified, stability between 20-week-old non-treated and Ang II treated mice was not obtained. Therefore, it was important to establish a stable HKG for consistent normalisation of gene expression studies between sex- age-, treatment, and genotype variables. TLDA mouse endogenous array card was utilised with HKG suitability was determine by any HKG that was below a Ct value standard deviation (Std dev) threshold of ≤0.50. Of the 16 genes assessed by TLDA array mouse endogenous array card (**Figure 3-2A**), 2 genes, *Trfc* (Std dev 0.49), and *Ppia* (Std dev 0.42) were below the assigned threshold of suitability with *Ppia* being deemed as the most suitable for this study (**Figure 3-2B**).

A

TaqMan Mouse Endogenous Control Array Card			
18 S-rNA	B2M	GAPDH	GUSB
HMBS	HPRT1	IPO8	PGK1
POLR2a	PPIA	RPLP2	TBP
TFRC	UBC	YWHAZ	β-actin

B

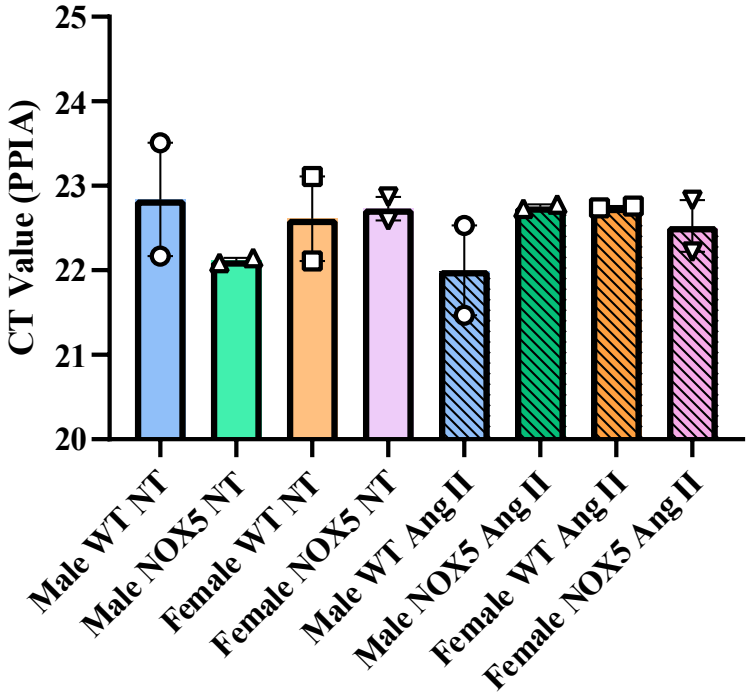

Figure 3-2. TLDA Mouse Endogenous Array Card of 20-week-old non-treated and Ang II treated male and female WT and VSMC-NOX5 mouse brains. HKG suitability was assessed by TLDA mouse endogenous array card in the brains of male and female 20-week-old non-treated (NT) and Ang II-treated WT and NOX5 mice. (**A**) Array table with 16 HKG assessed by TLDA mouse endogenous array card. (**B**) Ct values across male and female non-treated and Ang II treated mouse brains between WT and NOX5 mice.

3.3.3 Systemic Blood Pressure of 20-week-old Male and Female VSMC-specific NOX5 mice.

To assess baseline BP in 20-week-old male and female VSMC-specific NOX5, BP was measured utilising plethysmography. In 20-week-old mixed sex analysis, BP was increased in NOX5 mice (NOX5 122.2±2.2 mmHg vs male WT 117.4±1.2 p=0.04*) when compared to WT mice (**Figure 3-3A**). However, when separated by sex, no differences in BP were identified in male or WT v NOX5 mice (**Figures 3-3B and C**).

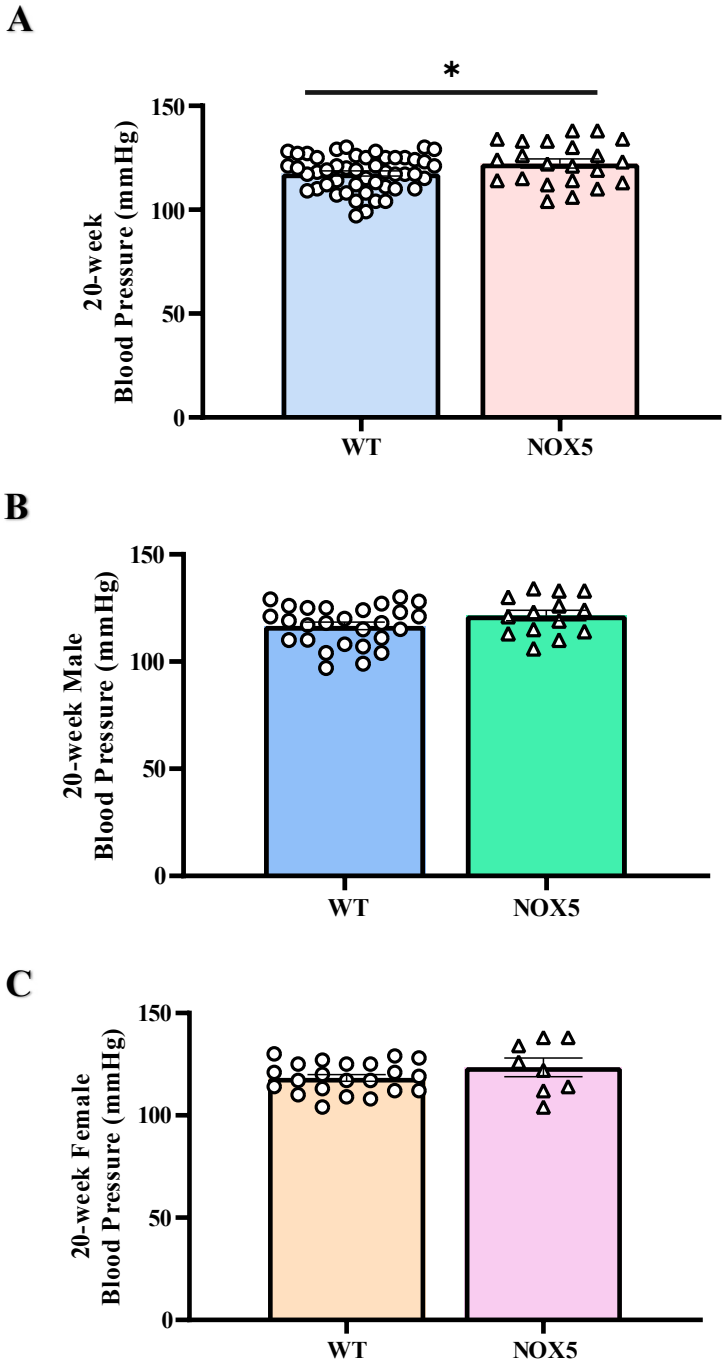

Figure 3-3. Blood pressure assessment of 20-week-old male and female WT and VSMC-specific NOX5 mice. BP assessment of mixed sex (**A**), male (**B**), and female (**C**) WT and NOX5 mice was assessed by plethysmography. Mixed sex study n=22-49, male n=14-27, female study n=8-22 per genotype. Data was presented as mmHg and analysed using a student's t-test and presented as *p≤0.05.

3.3.4 αSMA Protein Level Assessment in the Brains of 20-week-old Male and Female VSMC-specific NOX5 Mice.

NOX5 has been associated with hypercontractility and alterations to VSMC-specific phenotype. As such VSMC contractility and phenotypic marker αSMA was assessed by immunoblotting in whole brain homogenates of 20-week-old male and female WT and NOX5 mice. No differences in αSMA protein levels were observed in male (**Figure 3-4A**), or female (**Figure 3-4B**) NOX5 when compared to WT counterparts. REVERT total protein stain was used to normalise αSMA protein levels.

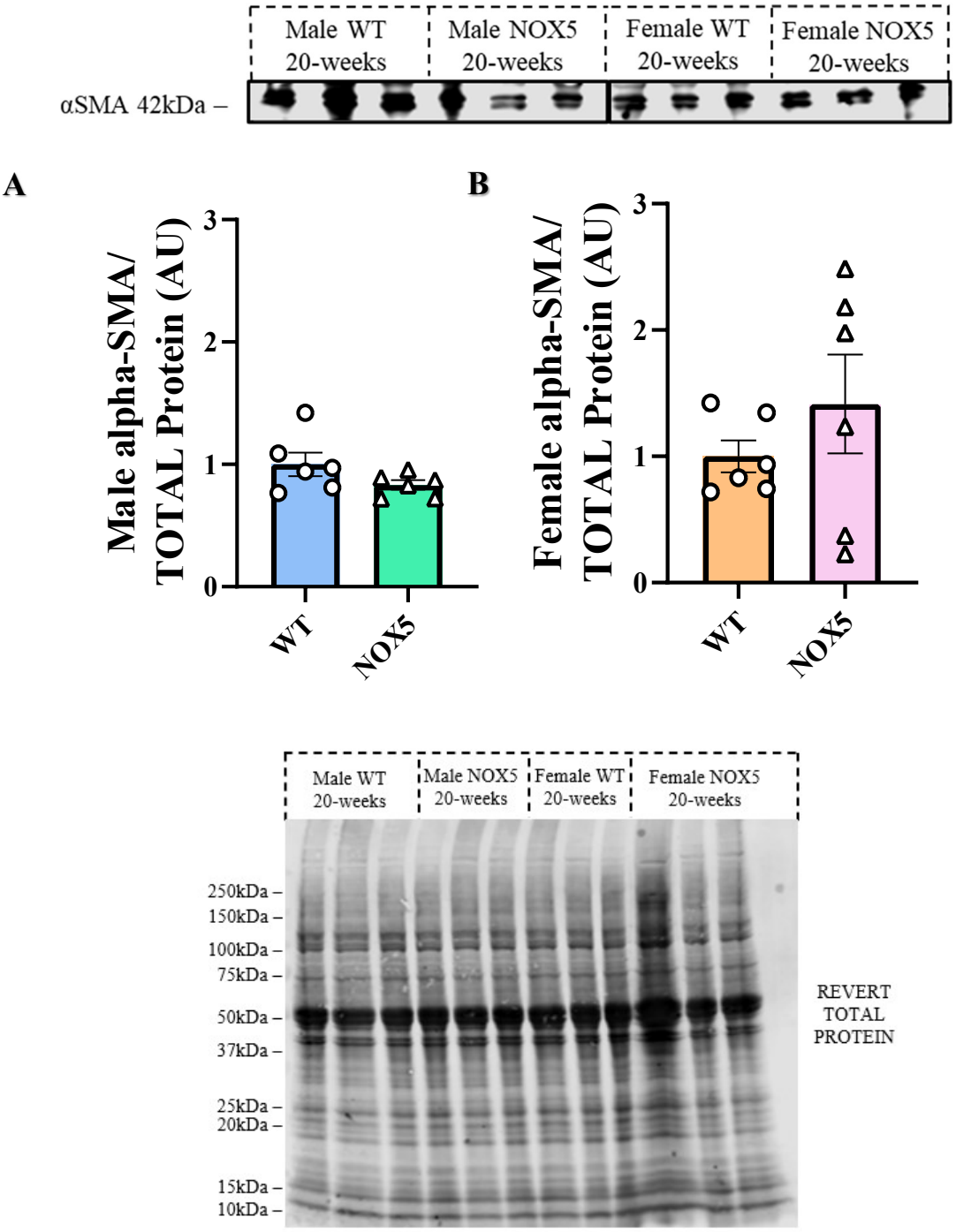

Figure 3-4. Protein assessment of cerebrovascular contractile phenotype marker αSMA in 20-week-old WT and VSMC-NOX5 mice. Protein assessment of αSMA in whole brain homogenates of 20-week-old male (**A**) and female (**B**) WT and NOX5 was assessed by immunoblotting and normalised to REVERT TOTAL protein stain. Male study n=6, female study n=6 per genotype. Data was presented as fold change arbitrary units (AU) and analysed using a student's t-test.

3.3.5 VEGFR2 Protein Level Examination in the Brains of 20-Week-old Male and Female VSMC-specific NOX5 mice.

Previous research has associated NOX5 with endothelial impairment and BBB dysfunction. As such endothelial marker VEGFR2 was assessed by immunoblotting in whole brain homogenates of 20-week-old male and female WT and NOX5 mice. No differences were observed in protein levels were observed in male (**Figure 3-5A**), or female (**Figure 3-5B**) NOX5 when compared to WT counterparts. VEGFR2 protein levels were normalised by REVERT total protein stain.

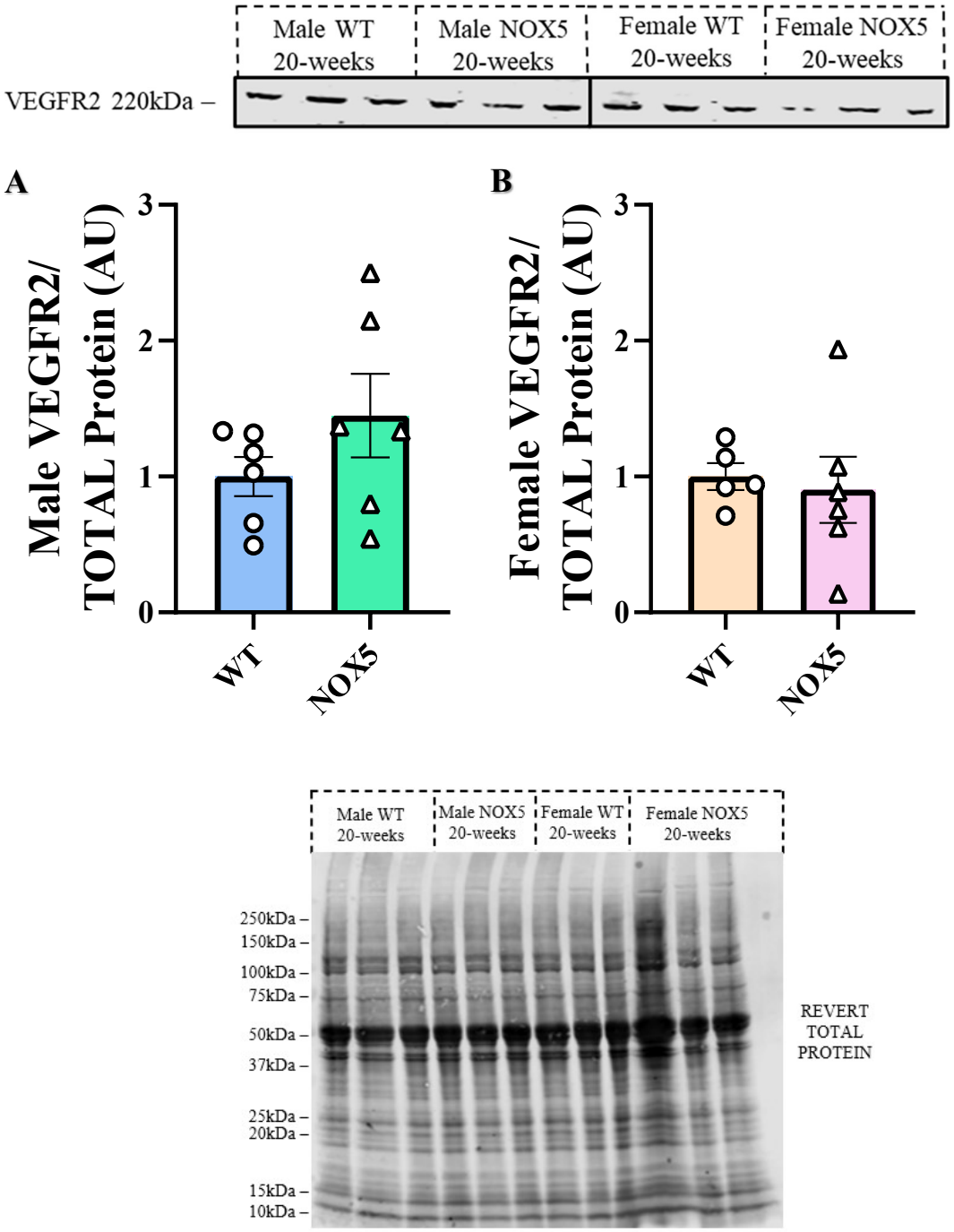

Figure 3-5. Protein assessment of cerebrovascular VEGFR2 in 20-week-old WT and VSMC-NOX5 mice. Protein assessment of VEGFR2 was assessed in whole brain homogenates of male (**A**) and female (**B**) WT and NOX5 mice by immunoblotting and normalised to REVERT TOTAL protein stain (**C**). Data was then presented as fold change AU. Male study n=6, female study n=4-6 per genotype. Data was analysed using a student's t-test.

3.3.6 Assessment of RhoA/ROCK1 Protein Levels in the Brains of 20-week-old Male and Female Mice with VSMC-specific NOX5 Overexpression.

The RhoA/ROCK signalling pathway is a crucial mediator of vascular contractility and cytoskeletal dynamics with NOX5 previously being identified as a mediator of its regulations. As such RhoA and ROCK1 were assessed by immunoblotting in whole brain homogenates of 20-week-old male and female WT and NOX5 mice. No differences were observed in RhoA (**Figures 3-6A-B**), or ROCK1(**Figures 3-6C-D**). protein levels in male or female NOX5 when compared to WT counterparts. RhoA and ROCK1 protein levels were normalised by REVERT total protein stain.

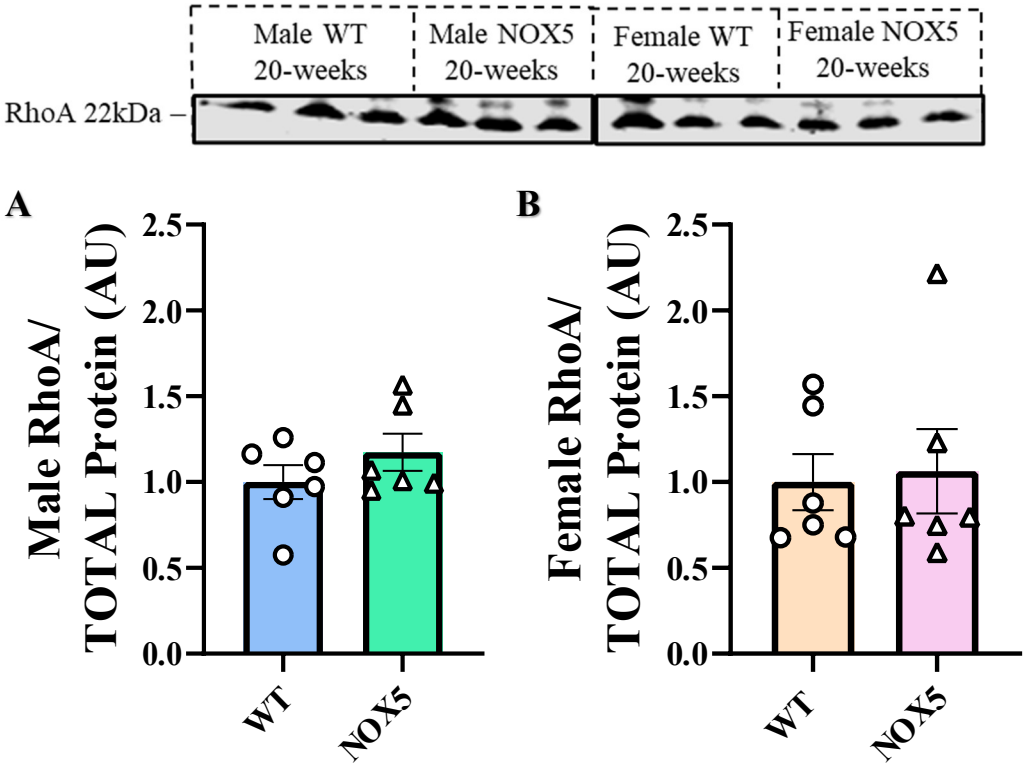

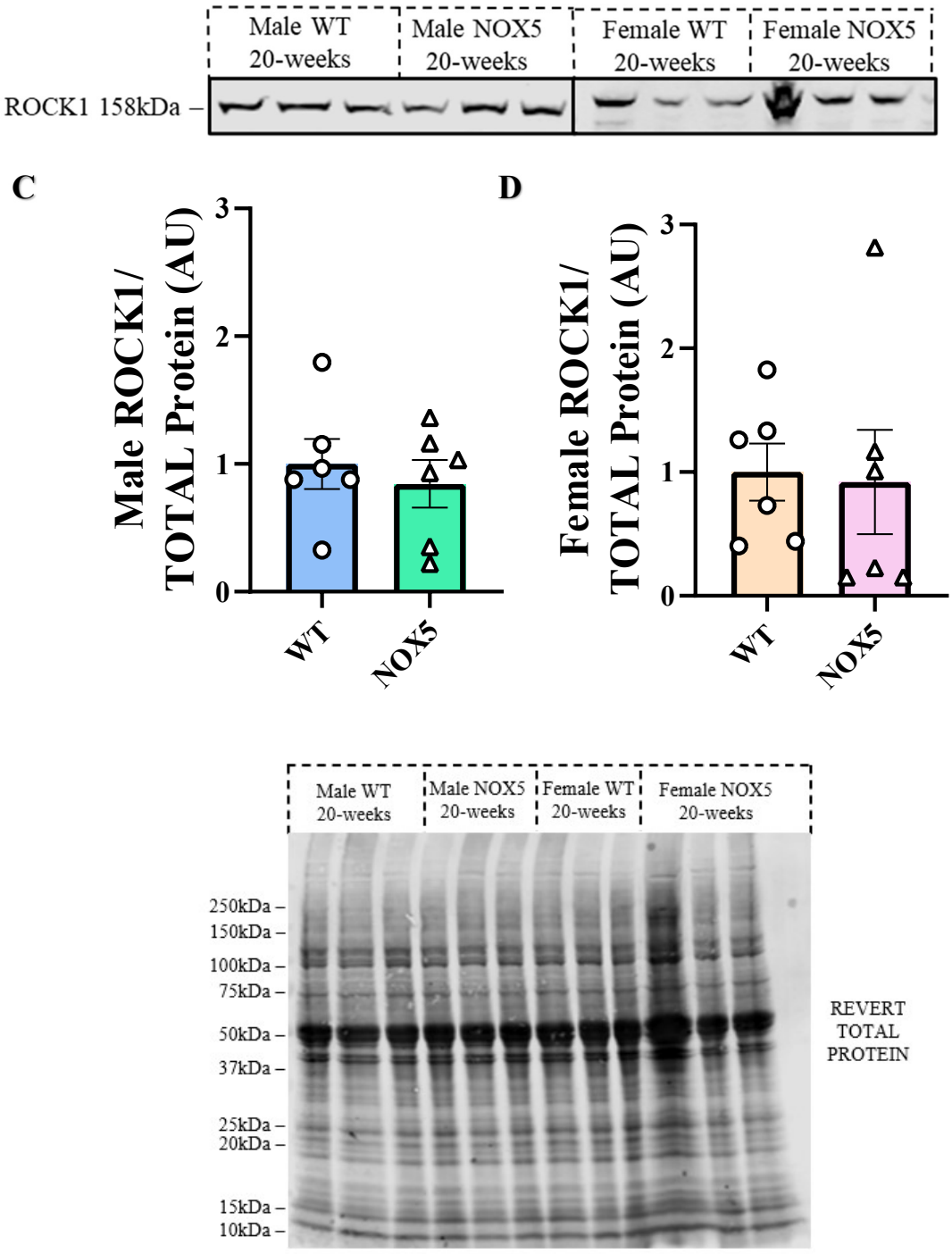

Figure 3-6 Protein assessment of cerebrovascular contractility signalling markers RhoA and ROCK1 in 20-week-old WT and VSMC-NOX5 mice. Protein assessment of contractility signalling proteins markers RhoA and ROCK1 were assessed in whole brain homogenates of male (**A**) and female (**B**) WT and NOX5 mice by immunoblotting and normalised to REVERT TOTAL protein stain. Data was then presented as fold change AU. Male study n=6 and female study n=6 per genotype. Data was analysed using a student's t-test.

3.3.7 Cerebral GFAP Protein Level Examination of 20-week-old Male and Female VSMC-specific NOX5 Mice

GFAP, a marker of NVU function and neuroinflammation was assessed by immunoblotting in whole brain homogenates of 20-week-old male and female WT and NOX5 mice. 20-week-old male VSMC-NOX5 mice were observed to have reduced GFAP protein expression (**Figures 3-7A**) when compared to WT controls (male NOX5 0.36±0.07 vs male WT 1+0.15% p=0.02*). No differences in GFAP expression were observed in 20-week-old female VSMC-NOX5 mice compared to WT (**Figures 3-7B**). GFAP protein levels were normalised by REVERT total protein stain.

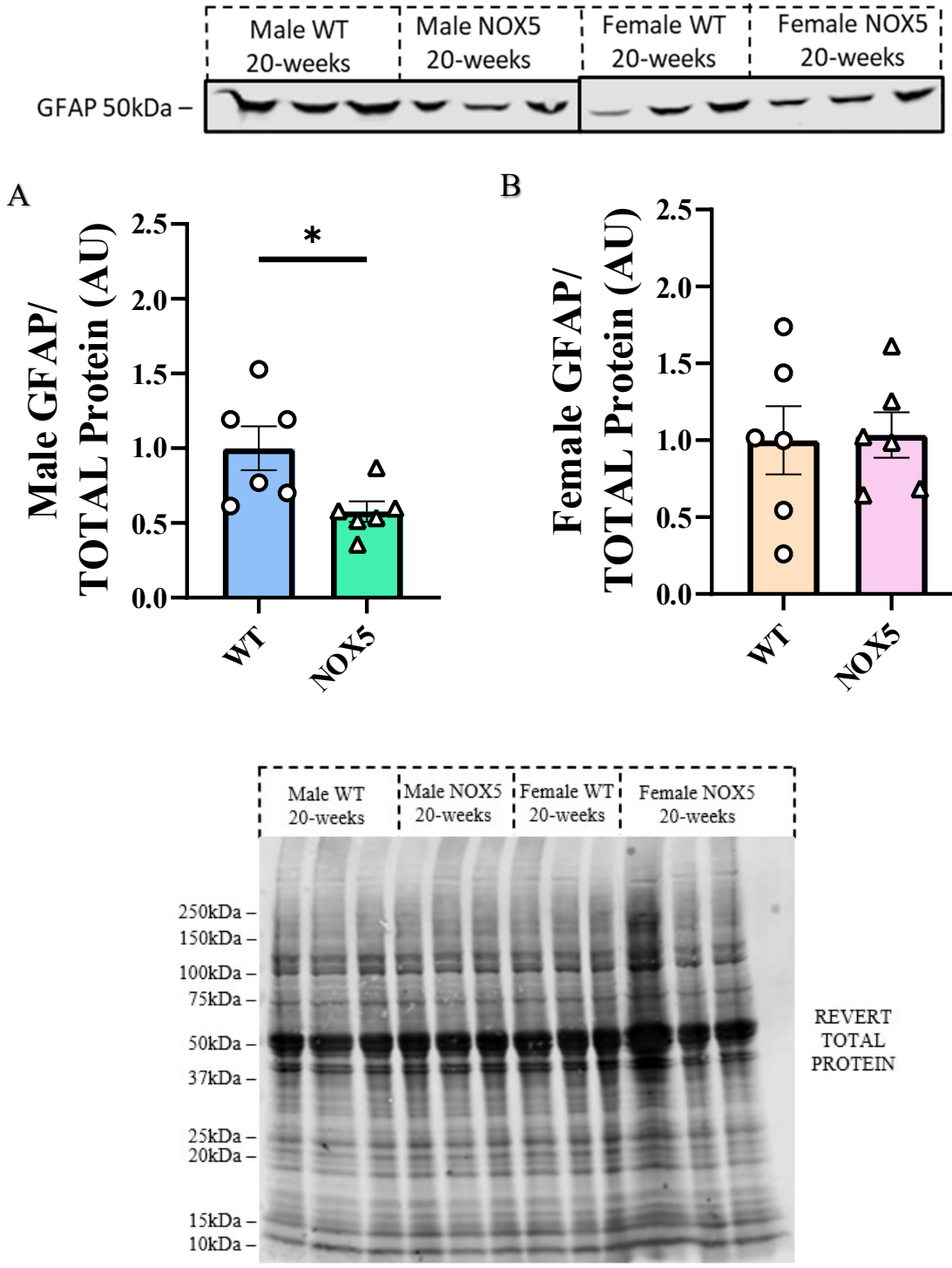

Figure 3-7. Protein assessment of astroglia cell marker GFAP in 20-week-old WT and VSMC-NOX5 mice. Protein assessment of astroglia marker GFAP was assessed in whole brain homogenates of male (**A**) and female (**B**) WT and NOX5 mice by immunoblotting and normalised to REVERT TOTAL protein stain. Data was then presented as fold change AU. Male study n=6 and female study n=6 per genotype. Data was analysed using a student's t-test and presented as *$p \leq 0.05$.

3.3.8 NOX1 mRNA and Protein Expression Assessment in the Brains of 20-week-old VSMC-specific NOX5 Mice.

NOX family members are involved in ROS production in the cerebrovasculature. This study aimed to assess whether other NOX isoforms may be regulated by NOX5 through compensatory or synergistic mechanism. To assess whether VSMC-specific NOX5-KI in a VSMC-specific manner alters the expression or levels of other cerebral NOX isoforms (NOX1, NOX2 and NOX4), RNA and protein was extracted from whole brain homogenates and NOX1 was assessed using q-RT PCR and immunoblotting. 20-week-old samples from WT and VSMC-NOX5 were examined collectively, and separately to assess if differences would be observed in males and females. No differences were identified in *Nox1* mRNA expression (**Figures 3-8A-C**) or NOX1 protein levels (**Figures 3.8E-F)** between genotypes or sexes were identified.

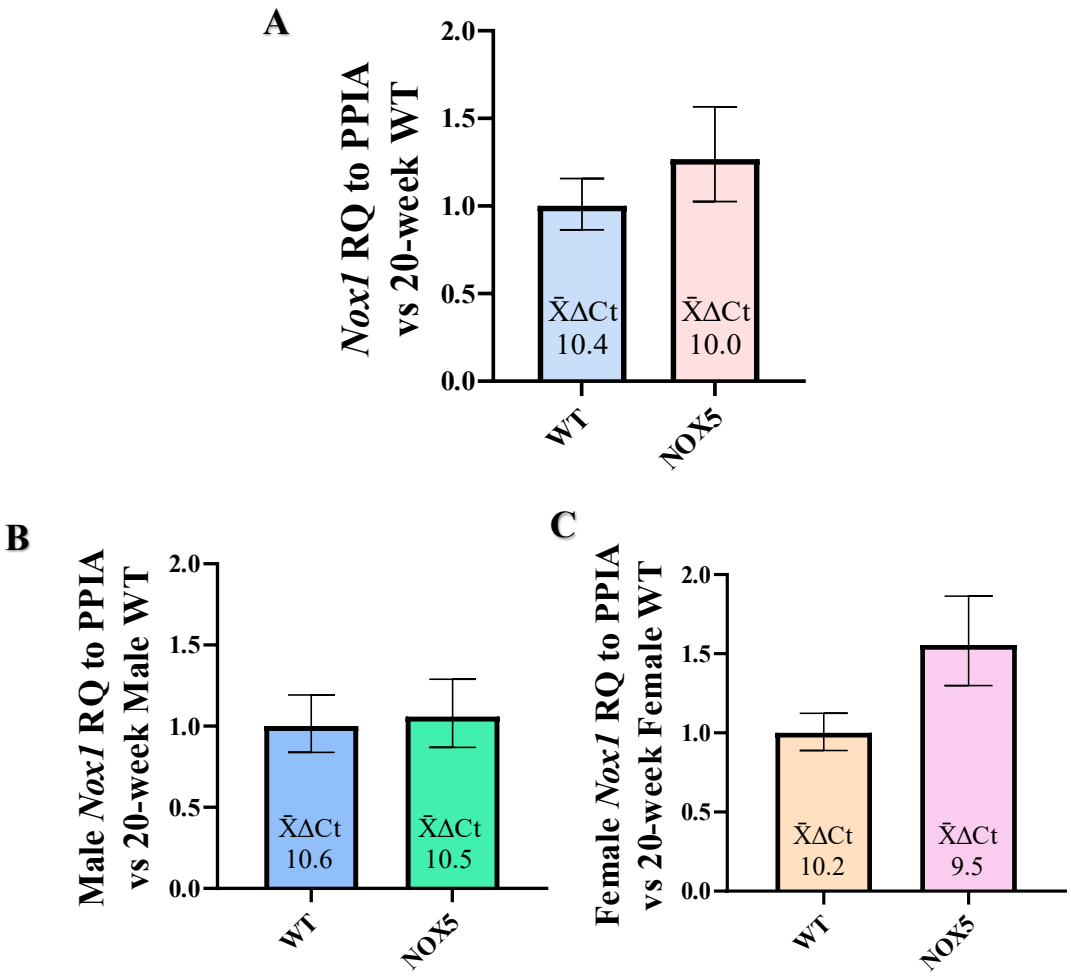

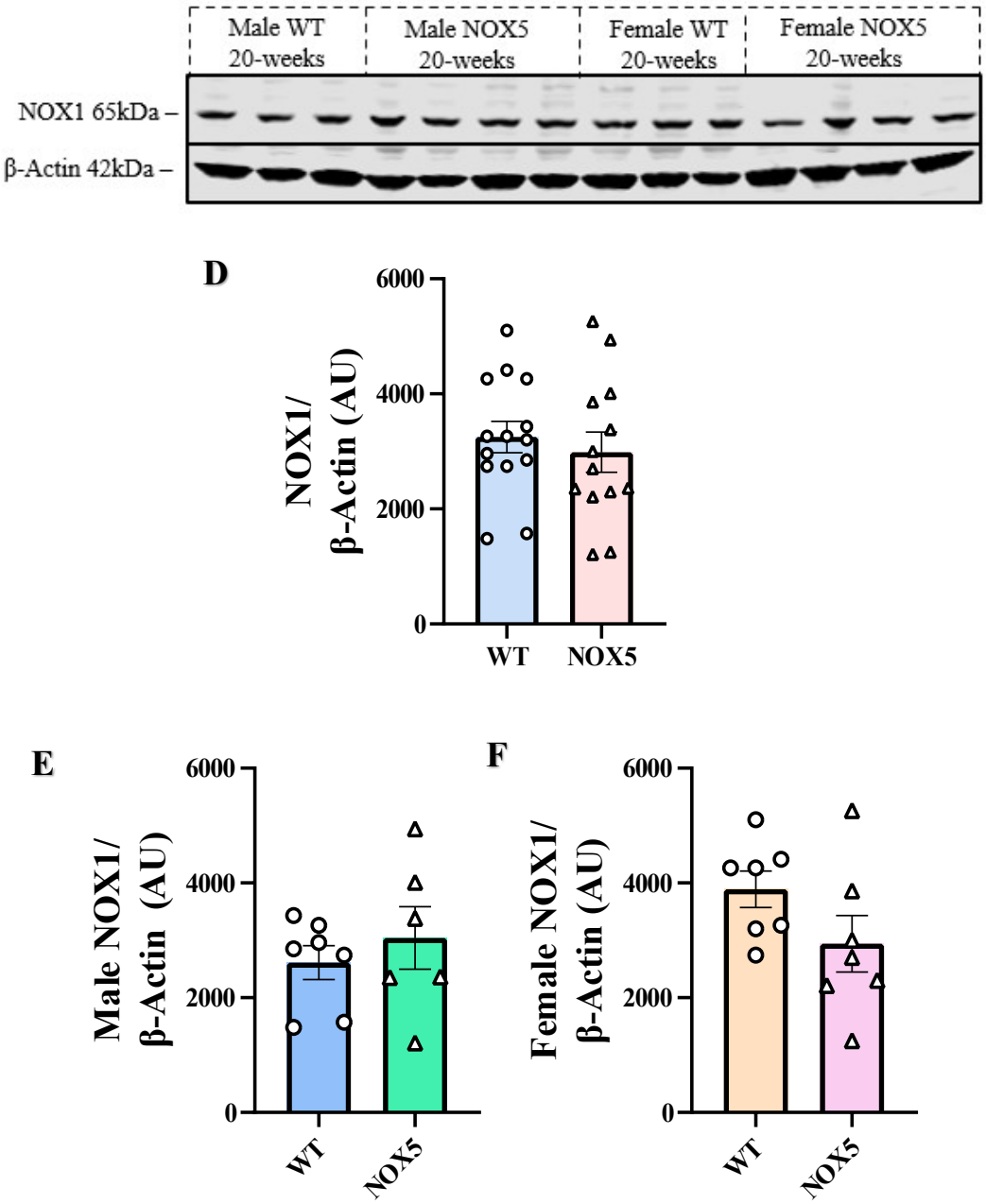

Figure 3-8. Assessment of *Nox1* mRNA and NOX1 protein expression in whole brain homogenates of 20-week-old male and female VSMC-specific NOX5 mice. Cerebral NOX1 mRNA (**A-C**) and protein expression (**D-F**) was assessed in 20-week-old WT and VSMC-NOX5 male and female mice using q-RT PCR and Immunoblotting. ΔCt values in the gene expression was assessed by q-RT PCR with RQ fold change being calculated from ΔΔCt following *Ppia* housekeeping gene normalisation, with immunoblotting normalised to β-actin presented as AU. Mixed sex study n=12-14, male n=6-7, female study n=6-7 per genotype. Data was analysed using a student's t-test.

3.3.9 Cerebral NOX2 mRNA and Protein Level Assessment of 20-week-old Mice Expressing VSMC-specific NOX5.

RNA and protein were extracted from whole brain homogenates and NOX2 was assessed using q-RT PCR and immunoblotting. 20-week-old samples from WT and VSMC-NOX5 were examined collectively, and separately to assess if differences would be observed in males and females. No differences were identified in *Nox2* mRNA expression (**Figures 3-9A-C**) or NOX2 protein levels (**Figures 3.9E-F)** between genotypes or sexes were identified.

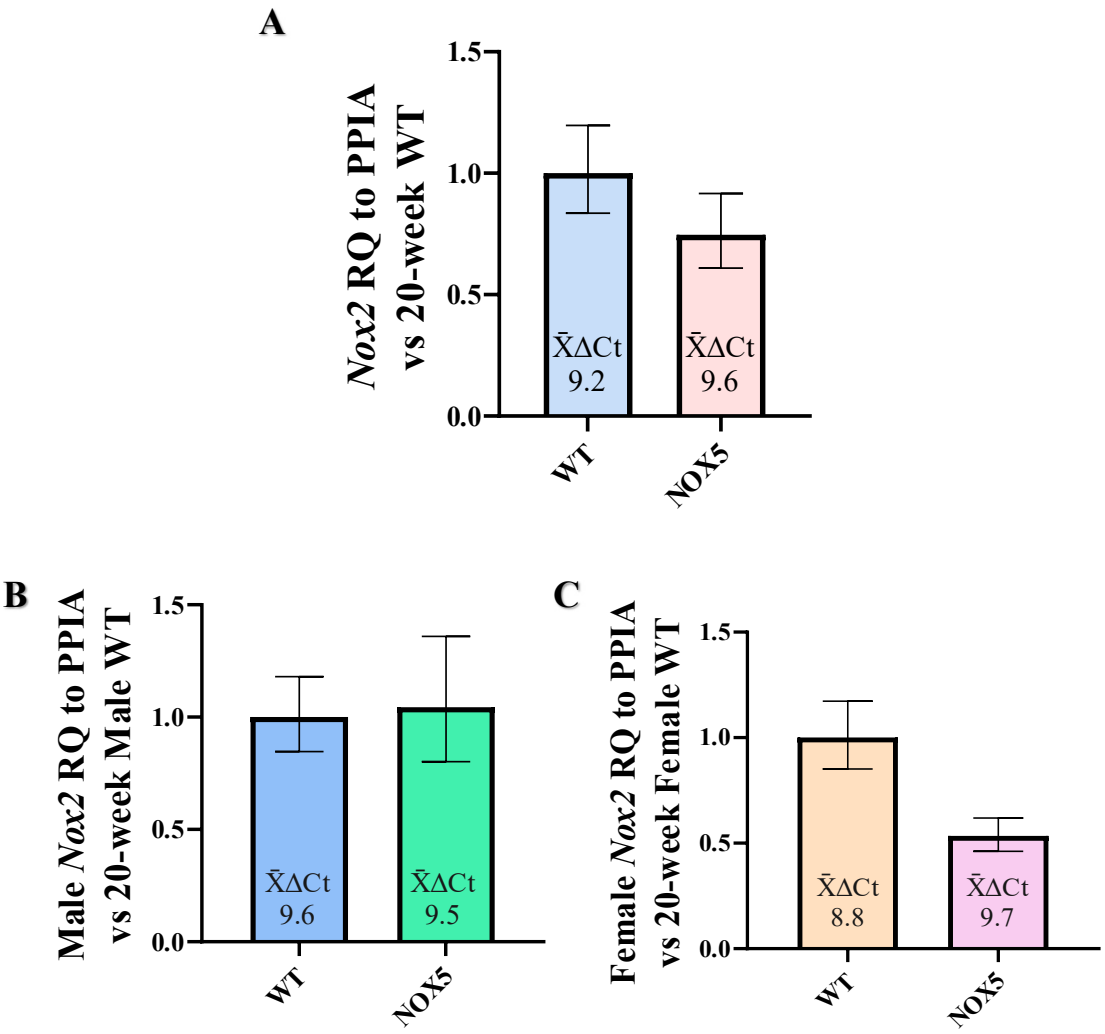

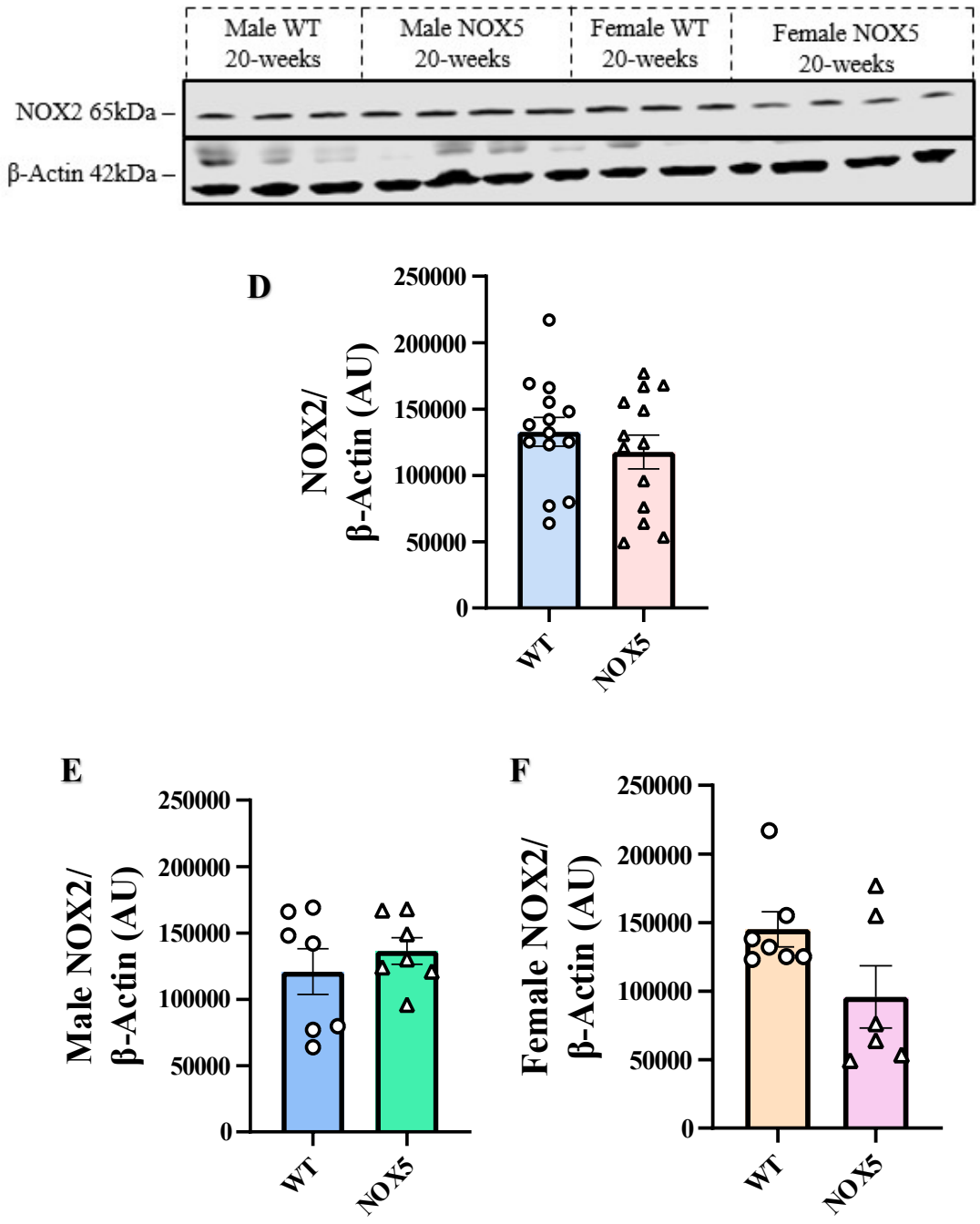

Figure 3-9. Assessment of *Nox2* mRNA and NOX2 protein expression in whole brain homogenates of 20-week-old male and female VSMC-specific NOX5 mice. Cerebral NOX2 (**A-C**) mRNA and protein (**D-F**) expression was assessed in 20-week-old WT and VSMC-NOX5 male and female mice using q-RT PCR and Immunoblotting. ΔCt values in the gene expression was assessed by q-RT PCR with RQ fold change being calculated from ΔΔCt following *Ppia* housekeeping gene normalisation, with immunoblotting normalised to β-actin presented as AU. Mixed sex study n=11-14, male n=6-7, female study n=5-7 per genotype. Data was analysed using a student's t-test.

3.3.10 Assessment of Cerebral NOX4 mRNA and Protein Expression in 20-Week-old Male and Female VSMC-NOX5 Mice.

RNA and protein were extracted from whole brain homogenates and NOX4 was assessed using q-RT PCR and immunoblotting. 20-week-old samples from WT and VSMC-NOX5 were examined collectively, and separately to assess if differences would be observed in males and females. No differences were identified in *Nox1* mRNA expression (**Figures 3-10A-C**) or NOX1 protein levels (**Figures 3.10E-F)** between genotypes or sexes were identified.

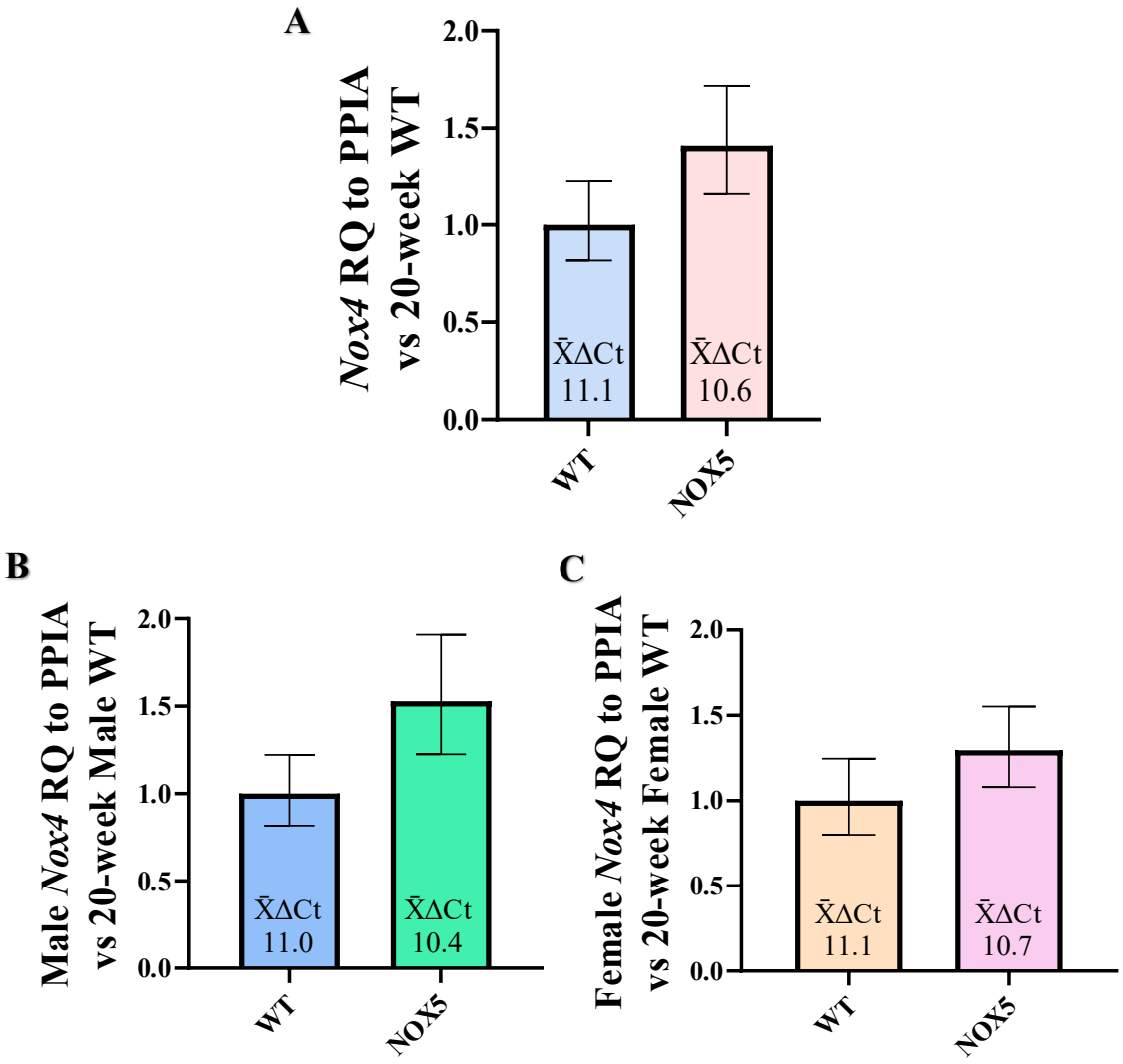

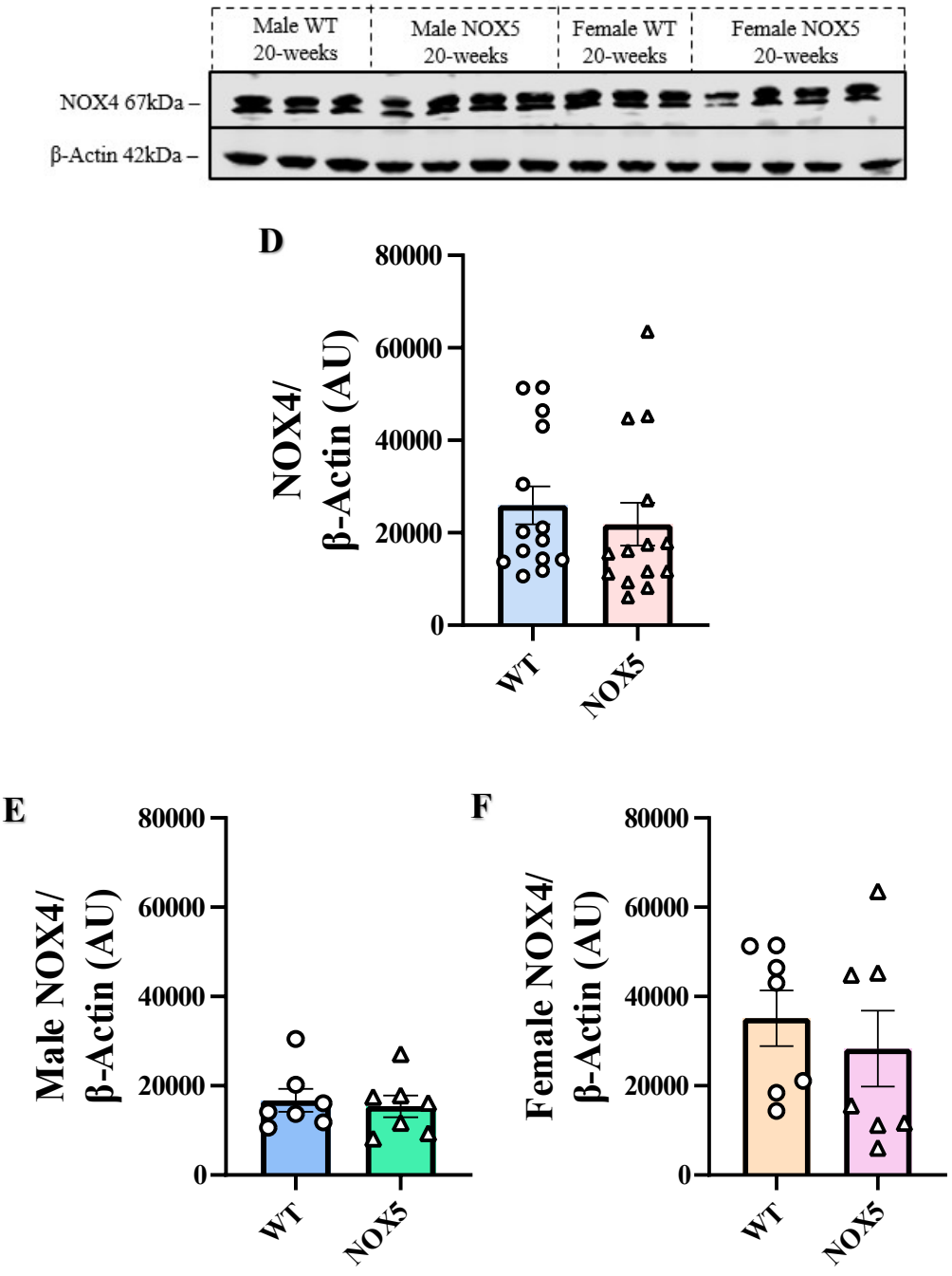

Figure 3.10. Assessment of *Nox4* mRNA and NOX4 protein expression in whole brain homogenates of 20-week-old male and female VSMC-specific NOX5 mice. Cerebral NOX4 mRNA **(A-C)** and protein expression **(D-F)** was assessed in 20-week-old WT and VSMC-NOX5 male and female mice using q-RT PCR and Immunoblotting. ΔCt values in the gene expression was assessed by q-RT PCR with RQ fold change being calculated from ΔΔCt following *Ppia* housekeeping gene normalisation, with immunoblotting normalised to β-actin presented as AU. Mixed sex study n=11-14, male n=5-7, female study n=6-7 per genotype. Data was analysed using a student's *t*-test.

3.3.11 Assessment of U-46619-mediated Contractility in Carotid Arteries of 20-week-old Male and Female VSMC-Specific NOX5 Mice.

Previous research has associated NOX5 with hypercontractility and vascular dysfunction (Montezano *et al*., 2018)To investigate whether VSMC-NOX5 influences vascular function, carotid arteries were isolated from 20-week-old male and female WT and NOX5 mice and pharmacologically treated with U-46619 and were to induce contraction. Carotid arteries were then assessed by wire myography. No differences were identified in U-46619-induced contraction between NOX5 and WT in mixed sex mice (**Figure 3-11A**), male mice (**Figure 3-11B**). or female mice (**Figure 3-11C**).

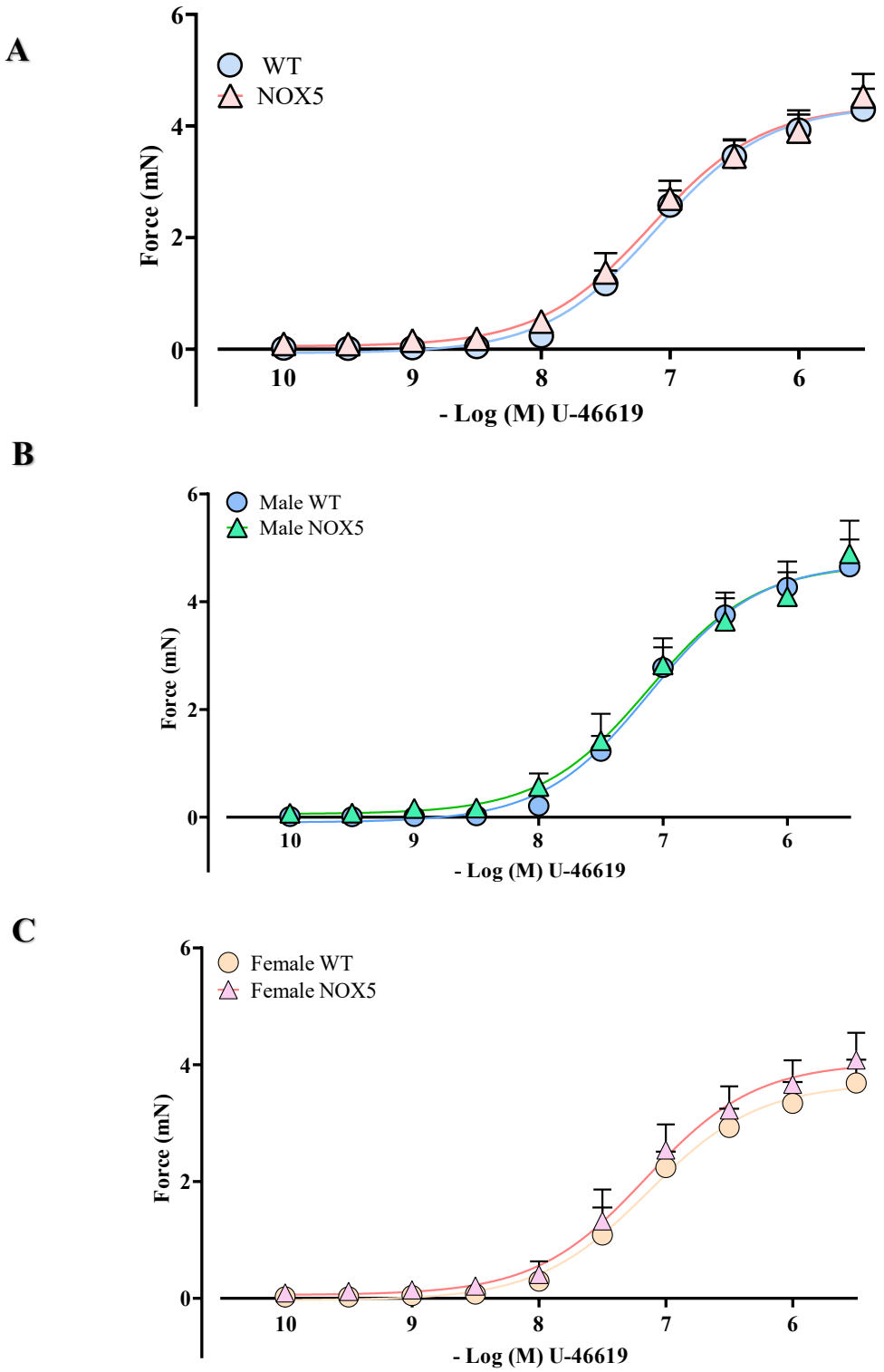

Figure 3-11. U-46619 assessment of carotid arteries in 20-week-old WT and VSMC-NOX5 mice. Vascular reactivity of carotid arteries isolated from 20-week-old male and female WT and VSMC-NOX5 mice. Cumulative concentration-response curves (CCRC) were assessed in response to U-46619-mediated vasoconstriction (**A-C**) results were presented as maximal response to basal levels (mN). Mixed sex study n=9-11, male study n=5-6, female study n=4 per genotype. Myography data was analysed using a non-linear regression model and extra sum-of-squares *F*-test.

3.3.12 Sodium Nitroprusside-mediated Endothelial Independent Vasorelaxation Assessment of 20-week-old male and female VSMC-specific NOX5 mice Carotid Arteries.

To investigate whether VSMC-NOX5 influences endothelial-independent vasorelaxation carotid arteries were isolated from 20-week-old male and female WT and NOX5 mice and were assessed by wire myography. Carotid artery endothelial-independent vasorelaxation was identified to be less responsive when exposed to SNP-induced vasorelaxation in VSMC-NOX5 mice (Emax: NOX5 62±3.2% vs WT 79+2.6% p=0.0005***) (**Figure 3-12A**). This reduced response to a NO donor was maintained when male mice were considered alone (Emax: Male NOX5 63±3.3% vs Male WT 83±3.3% p=0.0008***) (**Figure 3-12B**). However, no differences were observed between female WT and NOX5 mice (**Figure 3-12C**).

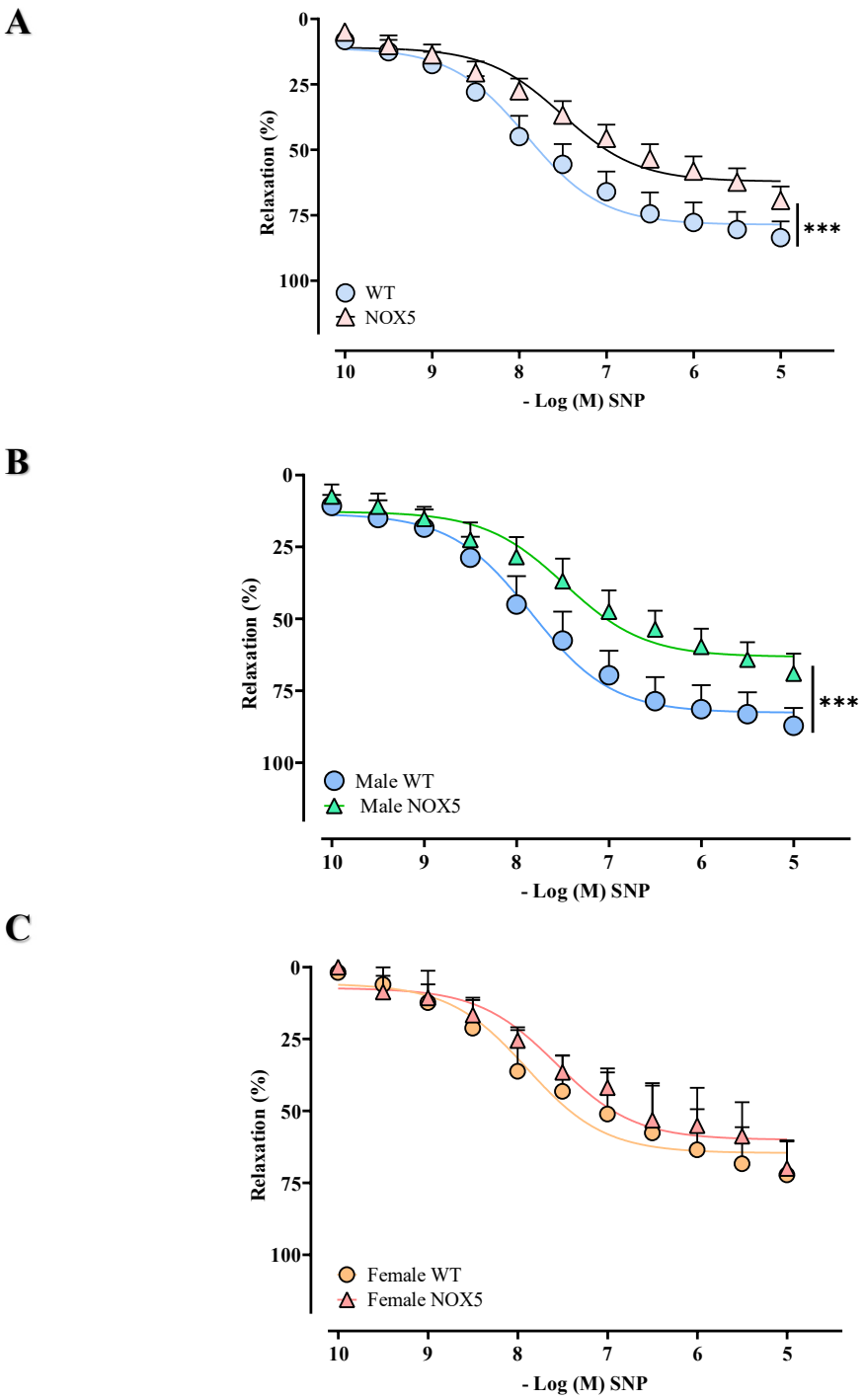

Figure 3-12. Vascular function assessment of carotid arteries in 20-week-old WT and VSMC-NOX5 mice. Endothelia-independent vasorelaxation assessment of carotid arteries isolated from 20-week-old male and female WT and NOX5 mice. CCRC in response to the vasodilator sodium nitroprusside (SNP) after U-46619 pre-constriction were collectively assessed (**A**), and individually assessed by sex (**B-C**). Results were expressed as a percentage of relaxation relative to maximum relaxation (%). Mixed sex study n=10-11, male study n=6-7, female study n=3-7 per genotype. Myography data was analysed using a non-linear regression model and extra sum-of-squares *F*-test and was presented as ***p≤0.001.

3.3.13 Cerebrovascular *Notch3* mRNA Expression and Protein Level Assessment in Male and Female 20-week-old VSMC-Specific Mice.

Previous research has identified an interplay between NOX5 and NOTCH3 signalling in peripheral vessels. As NOTCH3 is linked to severe CSVD onset, this study aimed to explore whether VSMC-NOX5 influences cerebrovascular NOTCH3 mRNA and protein expression. RNA and protein were isolated from whole brain homogenates of 20-week-old-old male and female WT and VSMC-NOX5 mice, utilising q-RT PCR and immunoblotting for the analysis. *Notch3* mRNA expression was significantly decreased in VSMC-NOX5 mice collectively (NOX5 5.9±0.17 ΔCt vs WT 5.4±0.12 ΔCt p=0.02*) (**Figure 3-13A**). When analysed by sex, *Notch3* mRNA expression was decreased only in female VSMC-NOX5 mice (Female NOX5 6.2±0.19 ΔCt vs Female WT 5.3±0.19 ΔCt p=0.006** (**Figure 3-13C**)), with no differences in male mice VSMC-NOX5 (**Figure 3-13B**). No significant differences were observed in full-length NOTCH3 protein levels normalised to β-actin in 20-week-old old WT and VSMC-NOX5 mice (**Figures 3-13D-G**).

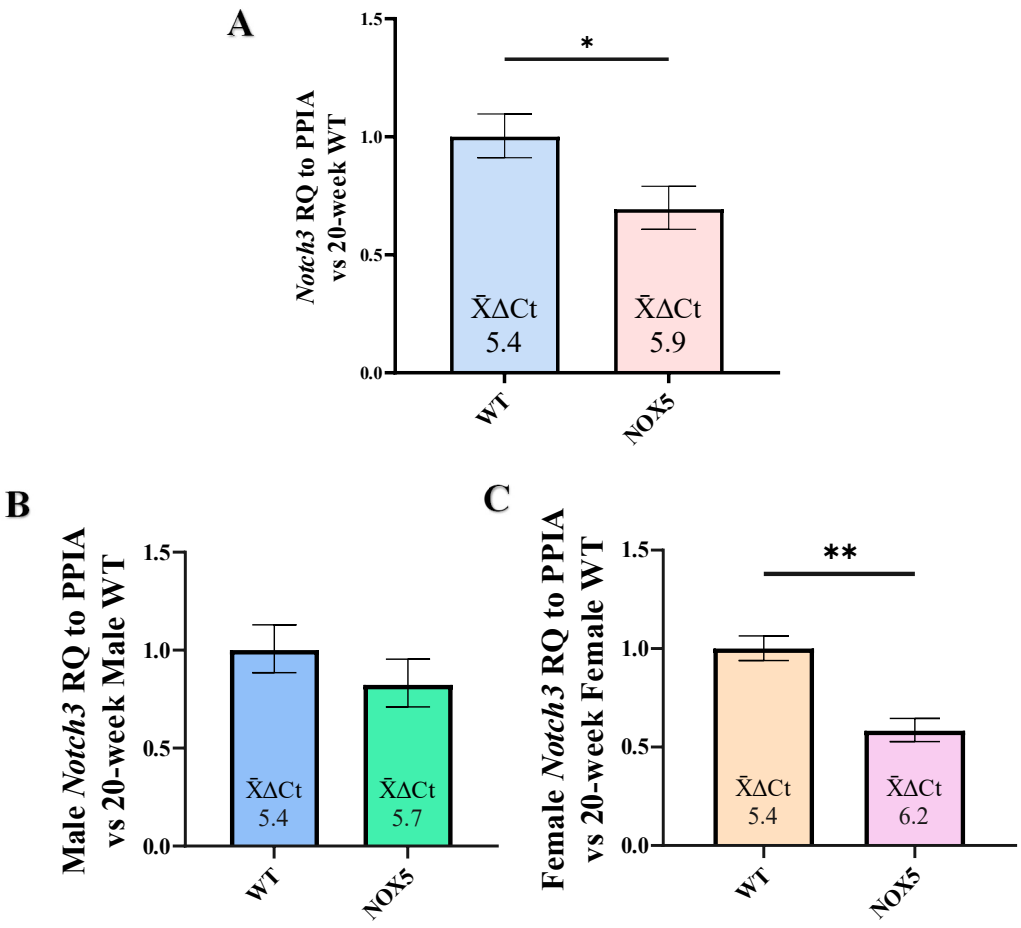

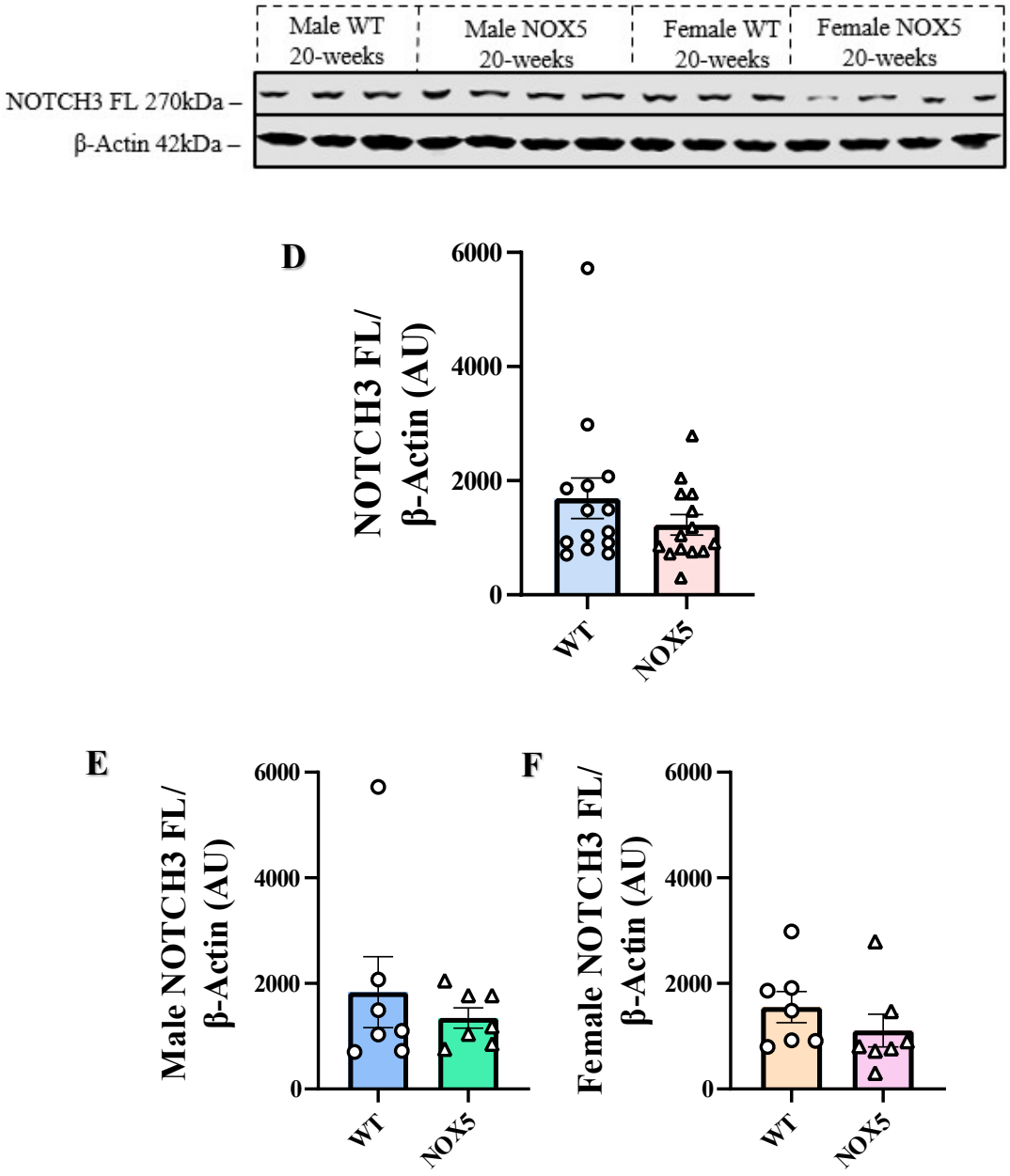

Figure 3-13. NOTCH3 mRNA and protein expression in the cerebrovasculature of 20-week-old female VSMC-NOX5 mice. Whole brain homogenate NOTCH3 mRNA and protein expression was assessed by q-RT PCR and immunoblotting in WT and VSMC-NOX5 mice. NOTCH3 mRNA expression was assessed by q-RT PCR (**A-C**). Full-length NOTCH3 protein expression (**D-F**) protein expression was assessed using immunoblotting and was normalised to β-actin and presented as AU. Gene expression was assessed by q-RT PCR with RQ fold change being calculated from ΔΔCt following *Ppia* housekeeping gene normalisation. Mixed sex study n=12-14, male study n=6-7, female study n=6-7 per genotype. Data was analysed using a student's t-test and presented as *p≤0.05, **p≤0.01.

3.3.14 Intracellular NOTCH3 Protein Level Assessment in the Cerebral Vasculature of 20-week-old Male and Female VSMC-specific NOX5 Mice.

To explore whether VSMC-NOX5 influences cerebrovascular N3-ICD signalling, protein was isolated from whole brain homogenates of 20-week-old male and female WT and VSMC-NOX5 mice, and utilised immunoblotting for the analysis. When levels of the cleaved N3-ICD were examined, there were no differences collectively, or in male 20-week-old VSMC-NOX5 mice (**Figures 3-14A-B**). However, N3-ICD was significantly reduced in 20-week-old old female VSMC-NOX5 mice (**Figure 3-14C**) when compared to WT counterparts (female NOX5 8879±618 AU vs female WT 12036±958 AU p=0.02*).

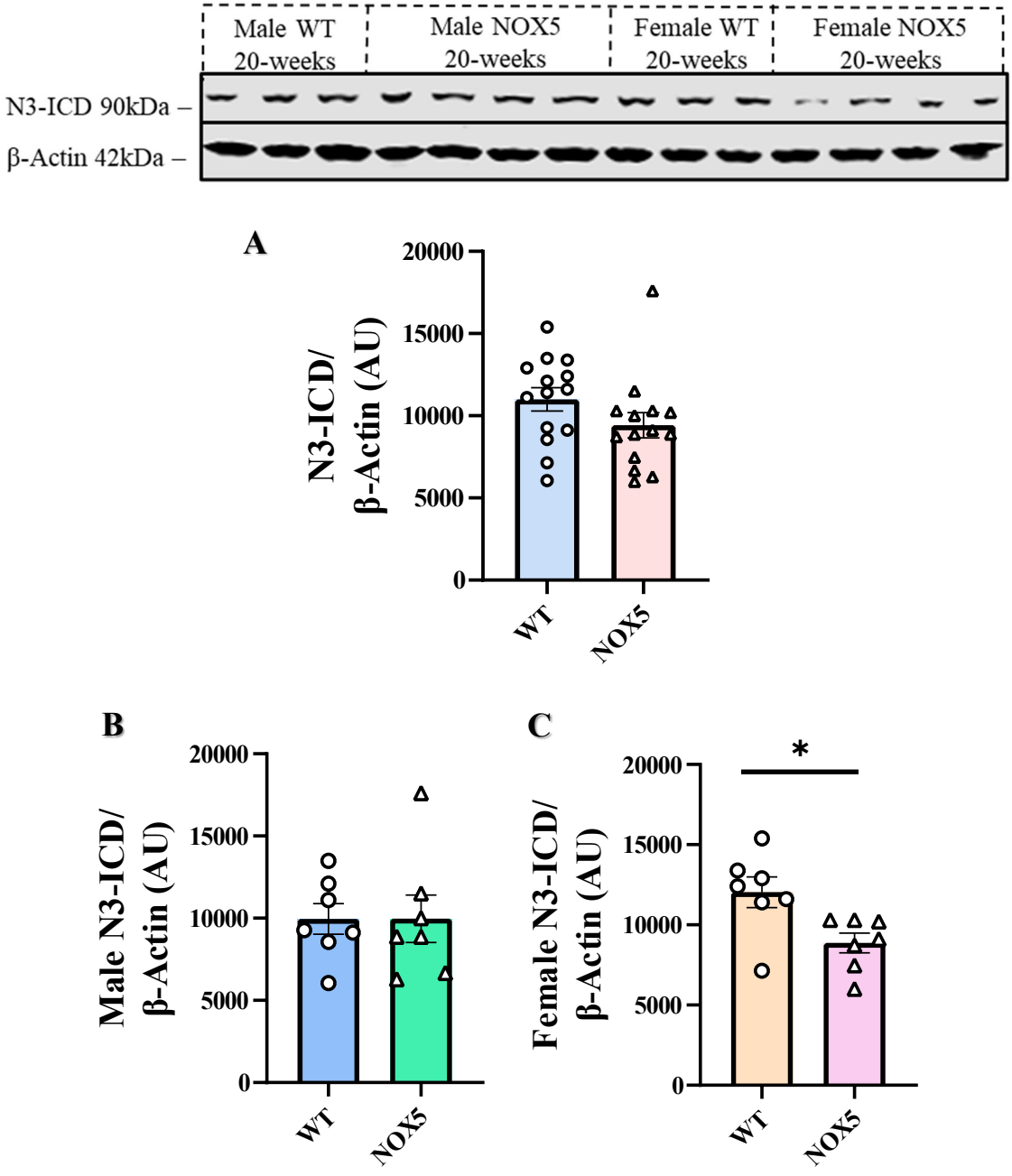

Figure 3-14. Immunoblotting assessment of N3-ICD protein levels in the brains of male and female 20-week-old VSMC-specific NOX5 mice. N3-ICD was assessed by immunoblotting in whole brain homogenates assessing collectively (**A**) and separated by sex in 20-week-old male (**B**) and female (**C**) WT and VSMC-NOX5 mice. N3-ICD protein expression was assessed using immunoblotting and was normalised to β-actin, being presented as AU. Mixed sex study n=14, male study n=7, female study n=7 per genotype. Data was analysed using a student's t-test and presented as *$p \leq 0.05$.

3.3.15 NOTCH3 Downstream Effector *Hes* and *Hey* Gene Expression Assessment in the Brains of 20-week-old Male and Female VSMC-specific NOX5 Mice.

Intracellular domain NOTCH3 can lead to canonical signalling and transcription of *Hey* and *Hes* genes associated with vascular growth and differentiation. To explore whether VSMC-NOX5 influences cerebrovascular downstream canonical NOTCH3 genes, RNA was extracted from whole brain homogenates and q-RT PCR was used. This study identified no differences were identified in mRNA expression of downstream *Hes* (*Hes1*/*Hes5*) and *Hey (*Hey1/HeyL) genes between genotypes when assessed in all mice, or males/females alone (**Figures 3-15A-L**).

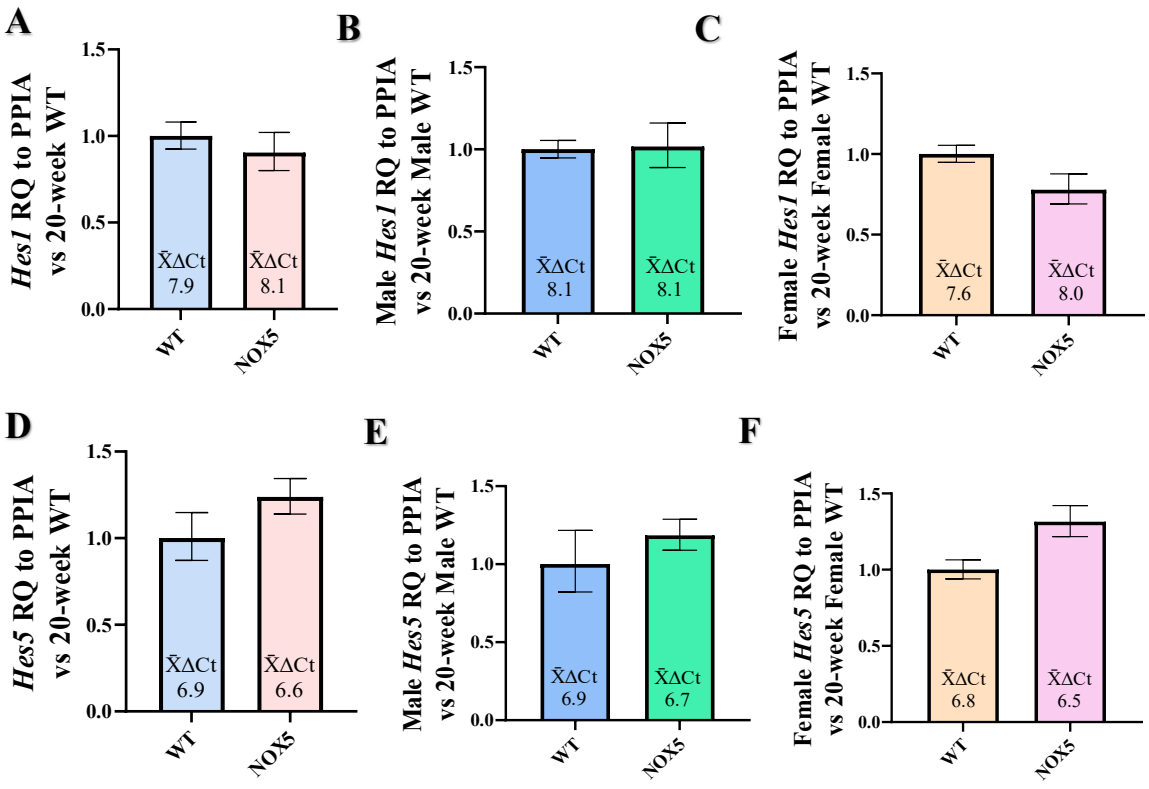

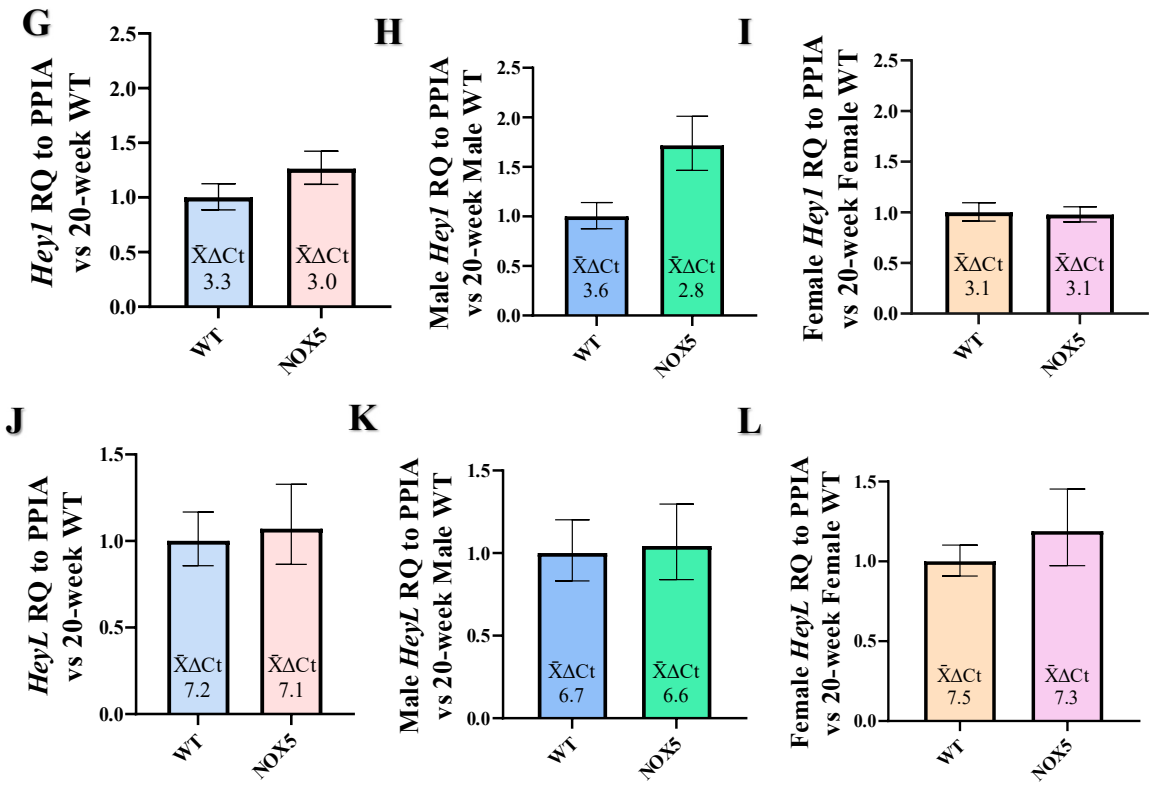

Figure 3-15. Gene expression assessment of canonical NOTCH3 downstream transcription genes in the brains of male and female mice at 20-weeks-old. *Hes1* (**A-C**), *Hes5* (**D-F**), *Hey1* **(G-I)**, and *HeyL* **(J-L)** gene expression was assessed in whole brain homogenates in 20-week male and female WT and NOX5 mice using q-RT PCR. *Notch3* mRNA expression was assessed by q-RT PCR with RQ fold change being calculated from ΔΔCt following *Ppia* housekeeping gene normalisation. Mixed sex study n=12-14, male study n=5-7, female study n=5-7 per genotype. Data was analysed using a student's t-test.

3.3.16 Assessment of Cerebral Hydrogen Peroxide and Lipid Peroxidation Levels in Male and Female VSMC-NOX5 Mice.

To examine the cerebral redox status of 20-week-old male and female VSMC-NOX5 mice, H_2O_2 and lipid peroxidation levels were quantified utilising Amplex-Red and TBARS-MDA respectively. Mixed sex analysis of 20-week-old VSMC-NOX5 mice (**Figure 3.16A**) identified an increase in H_2O_2 levels compared to WT control mice (NOX5 2.04±0.14 vs WT 1.58±0.15 p=0.03*). Assessment of H_2O_2 levels in 20-week-old WT andVSMC-NOX5 mice identified elevated H_2O_2 levels in male VSMC-NOX5 mice (**Figure 3.16B**) relative to male WT controls (male NOX5 2.04±0.14 vs male WT 1.58±0.15 p=0.007**). However, no changes in cerebral H_2O_2 levels were identified between female WT and VSMC-NOX5 at 20-weeks-old (**Figure 3.16C**). Assessment of lipid peroxidation Identified no differences between male and female WT and VSMC-NOX5 mice at 20-week-olds (**Figure 3.16D-F**).

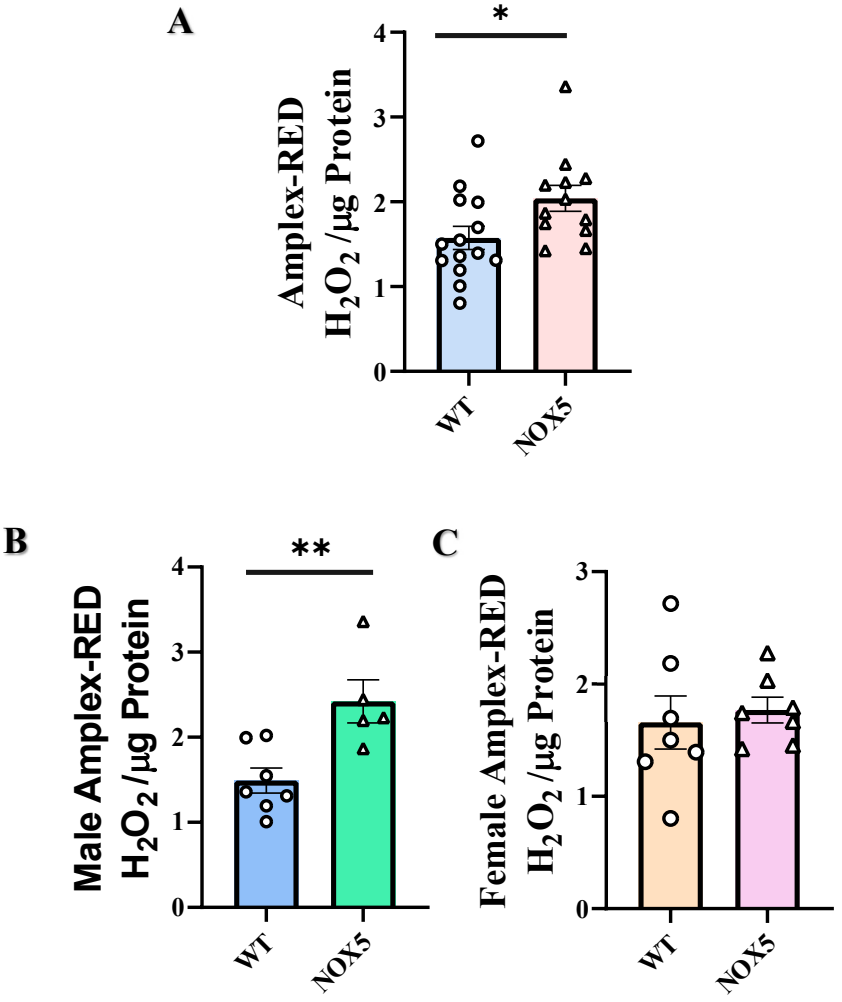

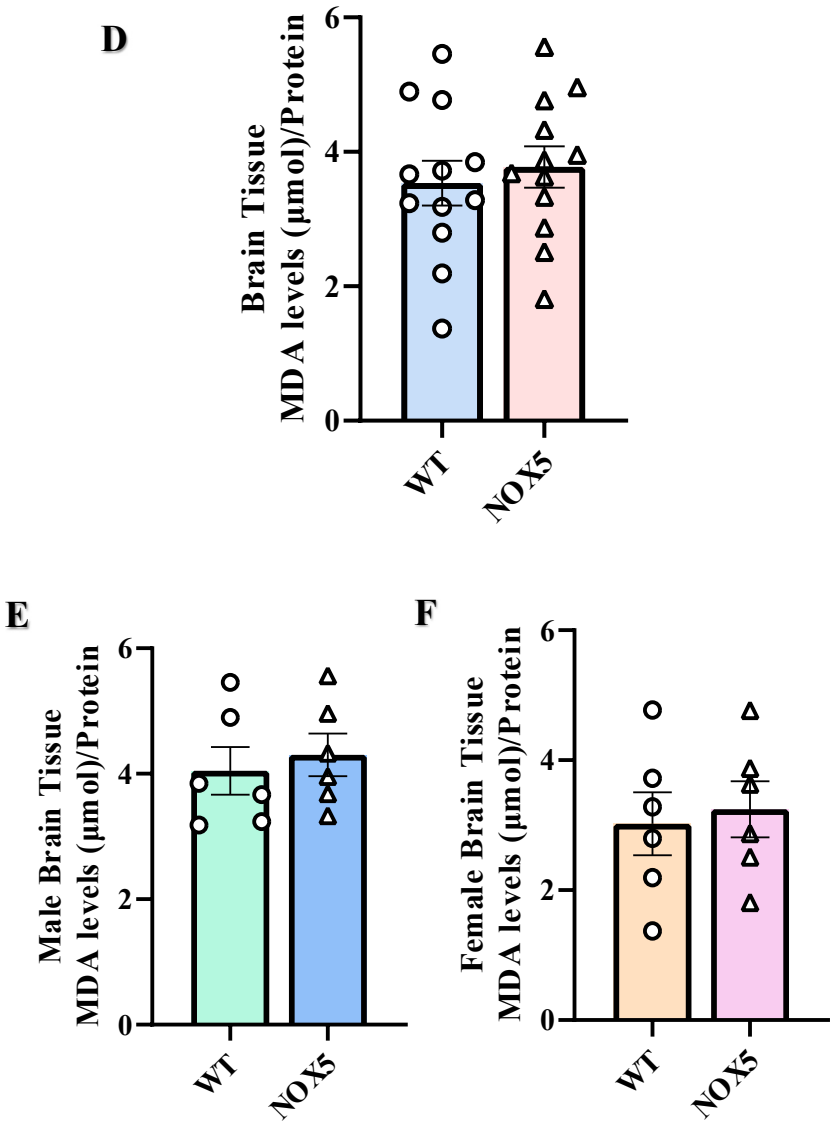

Figure 3-16. Cerebral assessment of hydrogen peroxide and lipid peroxidation levels in the brains of male and female 20-week-old VSMC-NOX5 mice. Cerebral H_2O_2 and lipid peroxidation levels were assessed in whole brain homogenates of 20-week-old male and female WT and VSMC-NOX5 mice using Amplex-Red (**A-C**), and TBARS-MDA (**D-F**). Amplex-Red (µg) and TBARS-MDA (µmol) values were normalised over protein concentration. Mixed sex study n=12-14, males study n=6-7, female study n=6-7 per genotype. Data was analysed using a student's t-test and presented as *p≤0.05, **p≤0.01.

3.3.17 Cerebral PTP-SO_3 and PRDX-SO_3 Assessment of Male and Female 20-week-old VSMC-NOX5 Mice.

Examination of oxidative modifications and overwhelmed cellular antioxidant defence was assessed by examining PRDX-SO_3 and PTP-SO_3 was assessed in 20-week-old male and female NOX5 mice. No difference in cerebral PRDX-SO_3 protein expression was identified in mixed sex, (**Figure 3-17A**) and male (**Figure 3-17B**) analysis identified no changes in PRDX-SO_3 protein levels. When 20-week female WT and NOX5 mice were assessed, NOX5 led to reduced PRDX-SO_3 protein levels (Female NOX5 5740±2968 AU vs Female WT 9811±1122 AU p=0.02*) (**Figure 3-17C**). Assessment of irreversible PTP-SO_3 identified a decrease in levels in 20-week-old female VSMC-NOX5 mice (Female NOX5 58029±7161 AU vs Female WT 81314±7480 AU p=0.04*), but no changes were identified between 20-week-old male genotypes or when all mice were considered together (**Figures 3-17D-F**).

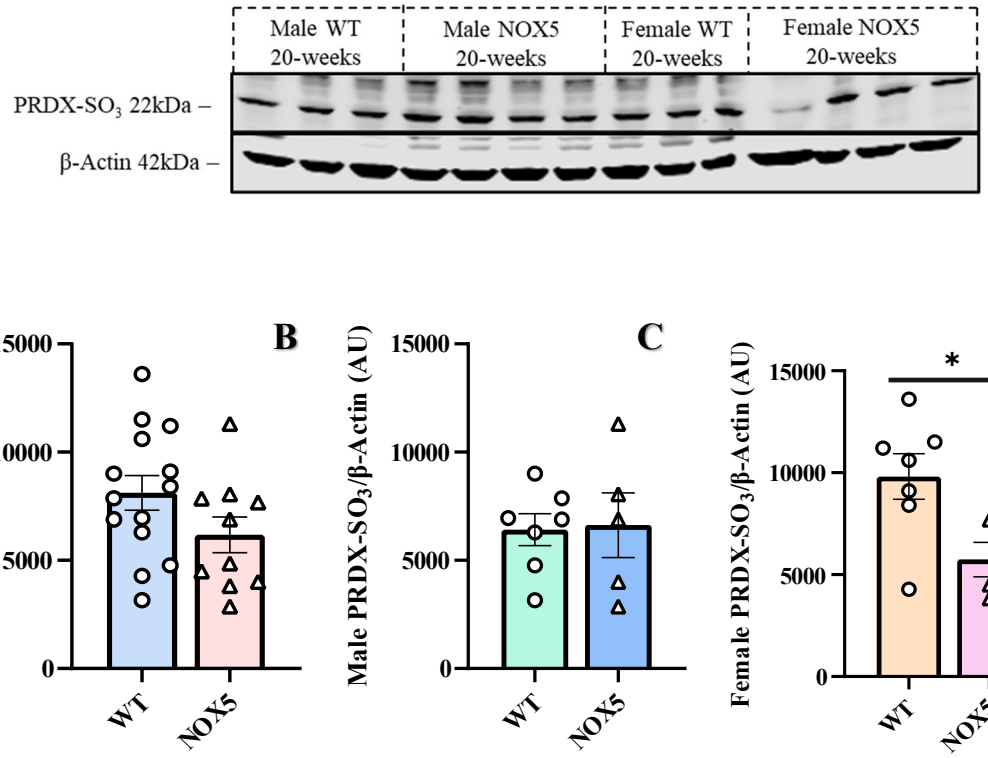

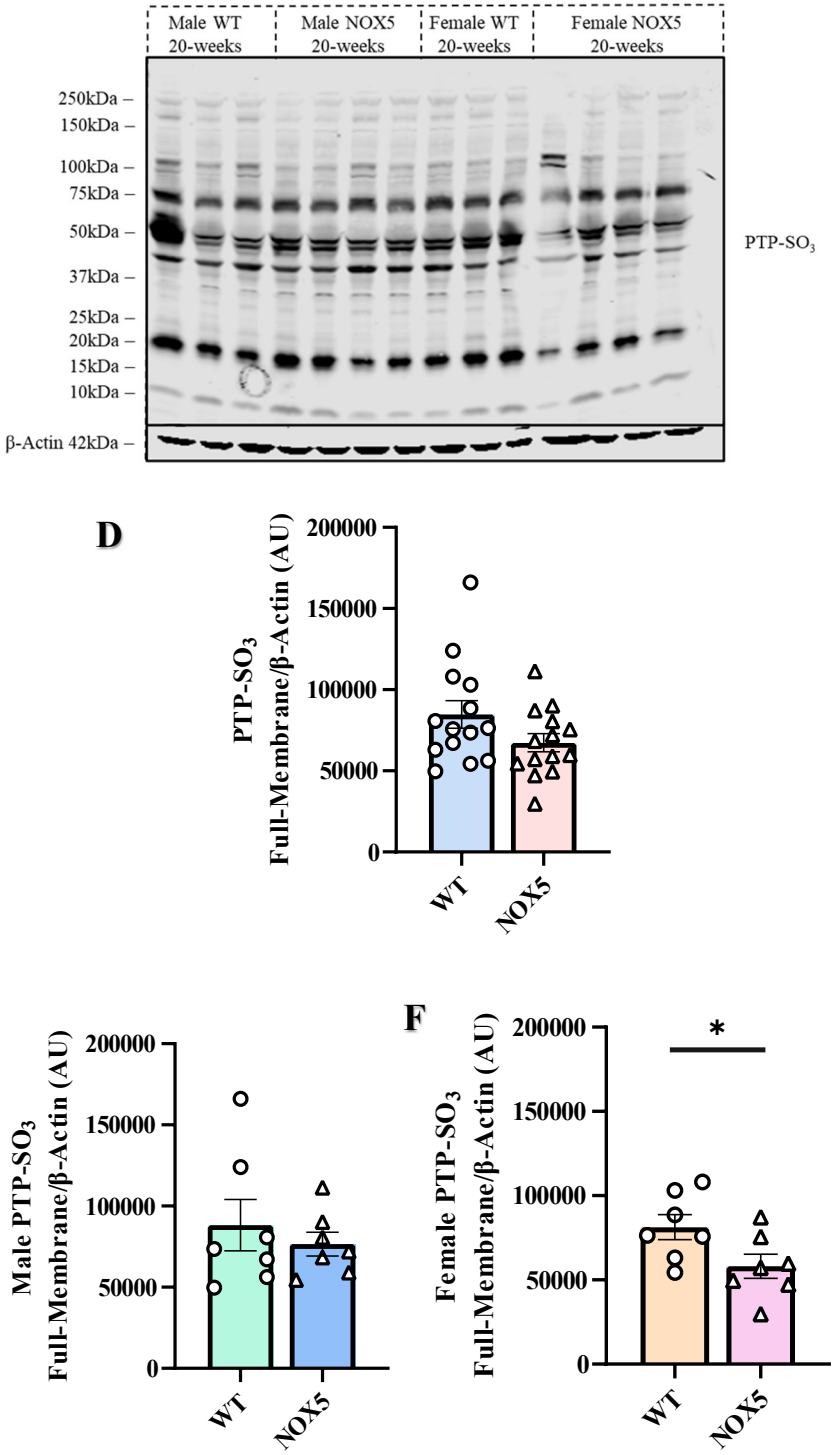

Figure 3-17. Cerebral assessment of peroxiredoxin hyperoxidation and irreversible oxidative protein tyrosine phosphatase in 20-week-old VSMC-specific NOX5 mice. Oxidative stress markers PRDX-SO_3 (**A-C**) and irreversible PTP-ox (**D-F**) were assessed by immunoblotting in whole brain homogenates of male and female 20-week-old $NO5^{+}SM22^{+}$ mice. Results were normalised to β-actin and expressed as AU. Mixed sex study n=10-14, males study n=5-7, female study n=5-7 per genotype. Data was analysed using a student's t-test and presented as *p≤0.05.

3.3.18 Cerebral Assessment of Sod1and Sod2 mRNA Expression of 20-week-old Male and Female VSMC-specific NOX5 Mice.

Transcription of *Sod1* and *Sod2* genes are vital for encoding their relevant antioxidant enzymes that are vital for maintaining cellular redox homeostasis by detoxifying $O_2^{\bullet-}$ to H_2O_2 and protecting against cellular oxidative stress. qRT-PCR assessment of antioxidant response element genes showed no changes in *Sod1* (**Figures 3-18A-C**) or *Sod2* (**Figures 3-18D-F**) mRNA expression in the brains of 20-week-old male and female VSMC-specific NOX5 mice.

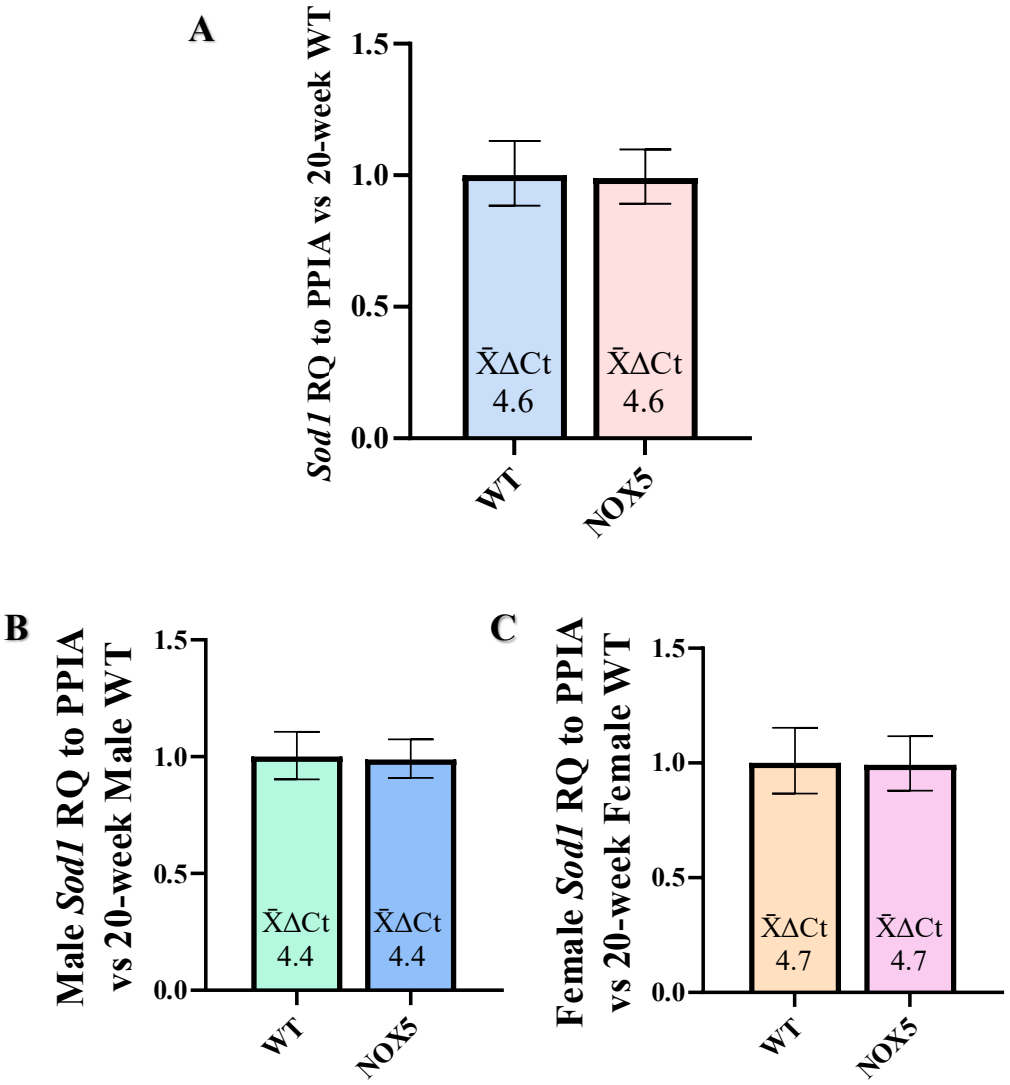

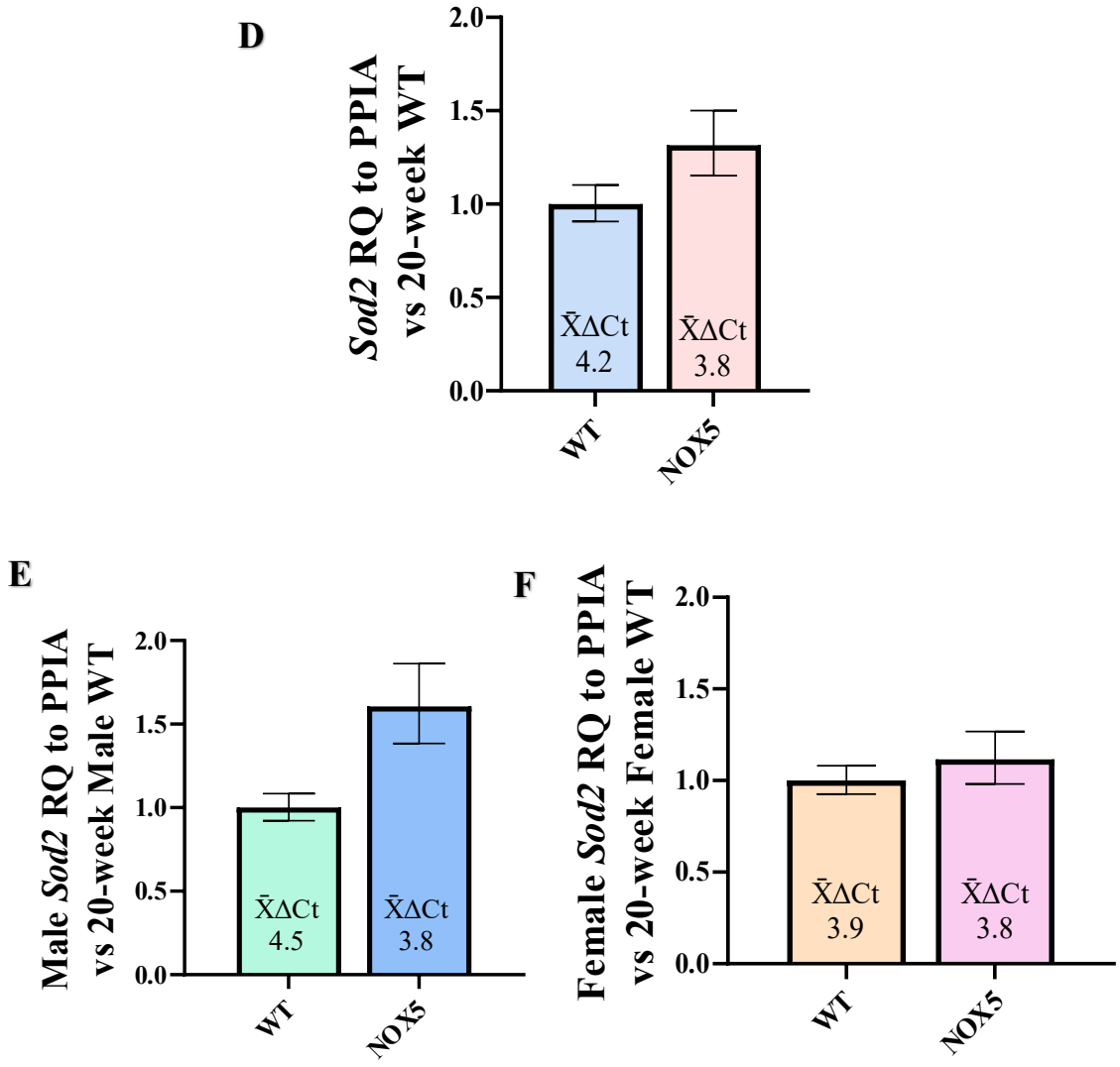

Figure 3-18. Assessment of *Sod1* and *Sod2* in 20-week-old VSMC-NOX5 mice. Cerebral *Sod1* (**A-C**) and *Sod2* (**D-F**). gene expression was assessed in 20-week-old male and female WT and VSMC-specific mouse whole brain homogenates using q-RT PCR. *Sod1* and *Sod2* mRNA expression was assessed by q-RT PCR with RQ fold change being calculated from ΔΔCt following *Ppia* housekeeping gene normalisation. Mixed sex study n=11-14, males study n=5-7, female study n=5-7 per genotype. Data was analysed using a student's t-test.

3.3.19 Cerebral Antioxidant mRNA Expression Assessment of *Nqo1*, *Catalase* and *Ho1* of 20-week-old Male and Female VSMC-specific NOX5-KI Mice.

Transcription of *Nqo1*, C*atalase* and *Ho1* genes are vital for encoding antioxidant response enzymes essential for maintaining cellular redox homeostasis by acting to prevent ROS toxicity and oxidative stress. qRT-PCR assessment of antioxidant response element genes identified no changes in *Nqo1* (**Figures 3-19A-C**), or *Catalase* mRNA expression (**Figures 3-19D-F**) between genotypes or by sex. Assessment of *Ho1* in VSMC-NOX5 mice (Figure 3.3G) identified an increase in mRNA expression compared to WT controls (NOX5 5.26±0.29 vs WT 6.21±0.29 p=0.014*). Further analysis identified no changes in *Ho1* expression in male VSMC-NOX5 mice compared their WT counterparts (**Figure 3-19H**), however, a significant increase in *Ho1* expression in female VSMC-NOX5 mice was observed (female NOX5 5.5±0.54 vs female WT 6.4±0.32 p=0.045* (**Figure 3-19I**).

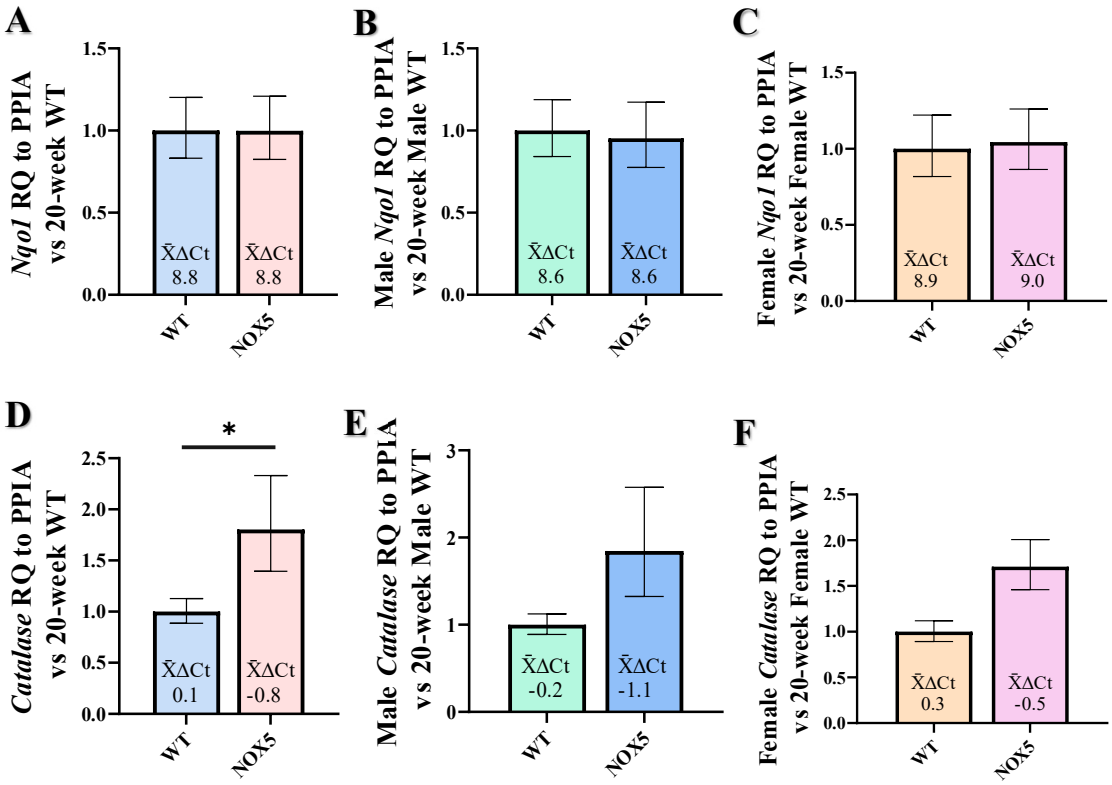

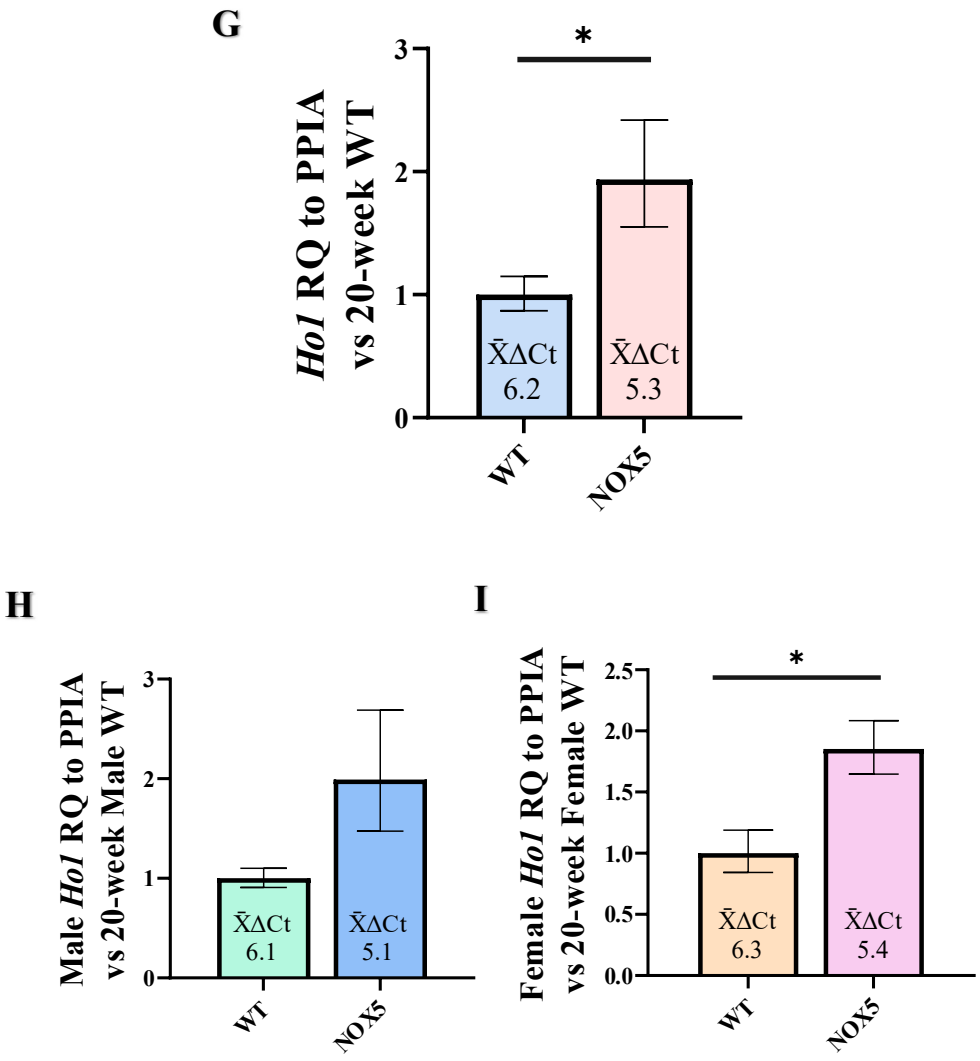

Figure 3-19. Cerebral assessment of antioxidant response element genes NQO1, Catalase, and Ho1 mRNA expression in male and female 20-week-old VSMC-NOX5 mice: 138. Cerebral ARE gene expression (*Nqo1, Catalase* and *Ho1*) was assessed in 20-week-old male and female WT and VSMC-specific mouse whole brain homogenates using q-RT PCR (**A-I**). ARE mRNA expression was assessed by q-RT PCR with RQ fold change being calculated from ΔΔCt following *Ppia* housekeeping gene normalisation. Mixed sex study n=12-14, males study n=12-14, female study n=12-13 per genotype. Data was analysed using a student's t-test and presented as *p≤0.05.

3.3.20 Assessment of BIP Protein Expression in the Brains of 20-week-old Male and Female VSMC-specific NOX5 Mice.

The UPR marker, BIP, an indicator of ER stress, was assessed in 20-week-old male and female VSMC-specific NOX5 mice using immunoblotting on whole brain homogenate protein samples. No differences were observed in mixed sex analysis between 20-week-old WT and NOX5 mice. However, when separated by sex, assessment of BIP identified an increase in expression in 20-week-old male VSMC-NOX5 (Male NOX5 (AU) 3011±533 vs Male WT (AU) 1669±170 p=0.03*), however no differences were observed in 20-week-old female mice (**Figures 3-20C**).

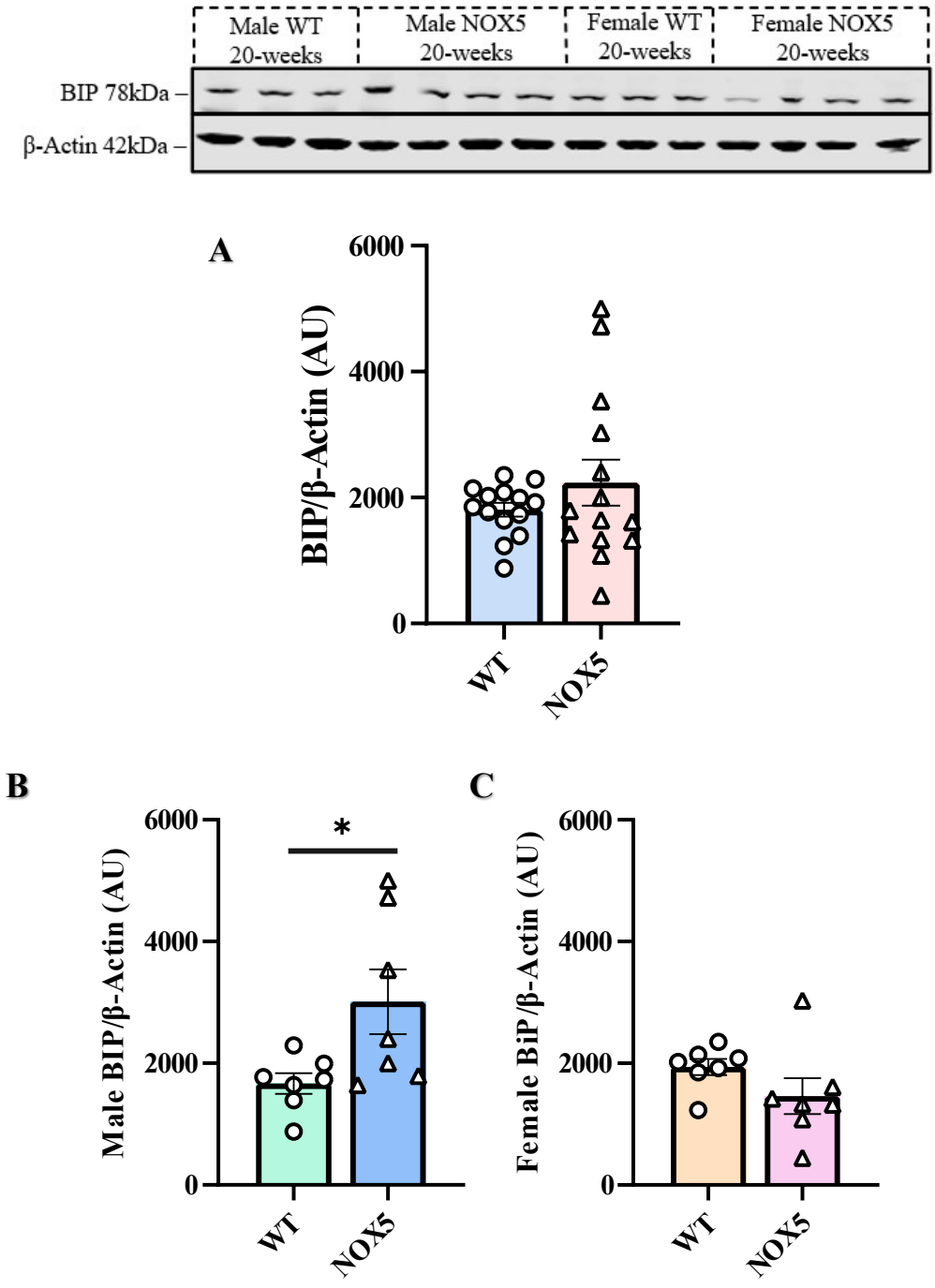

Figure 3-20. Immunoblotting assessment of cerebral BIP levels in 20-week-old VSMC-NOX5 mice. The ER stress marker BIP levels was assessed by immunoblotting respectively on whole brain homogenates of mixed sex, male, and female 20-week-old WT and NOX5 mice (**A-C**). Immunoblotting experiments were normalised to β-actin and expressed as AU. Mixed sex study n=14, males study n=7, female study n=7 per genotype. Data was analysed using a student's t-test and presented as *p≤0.05.

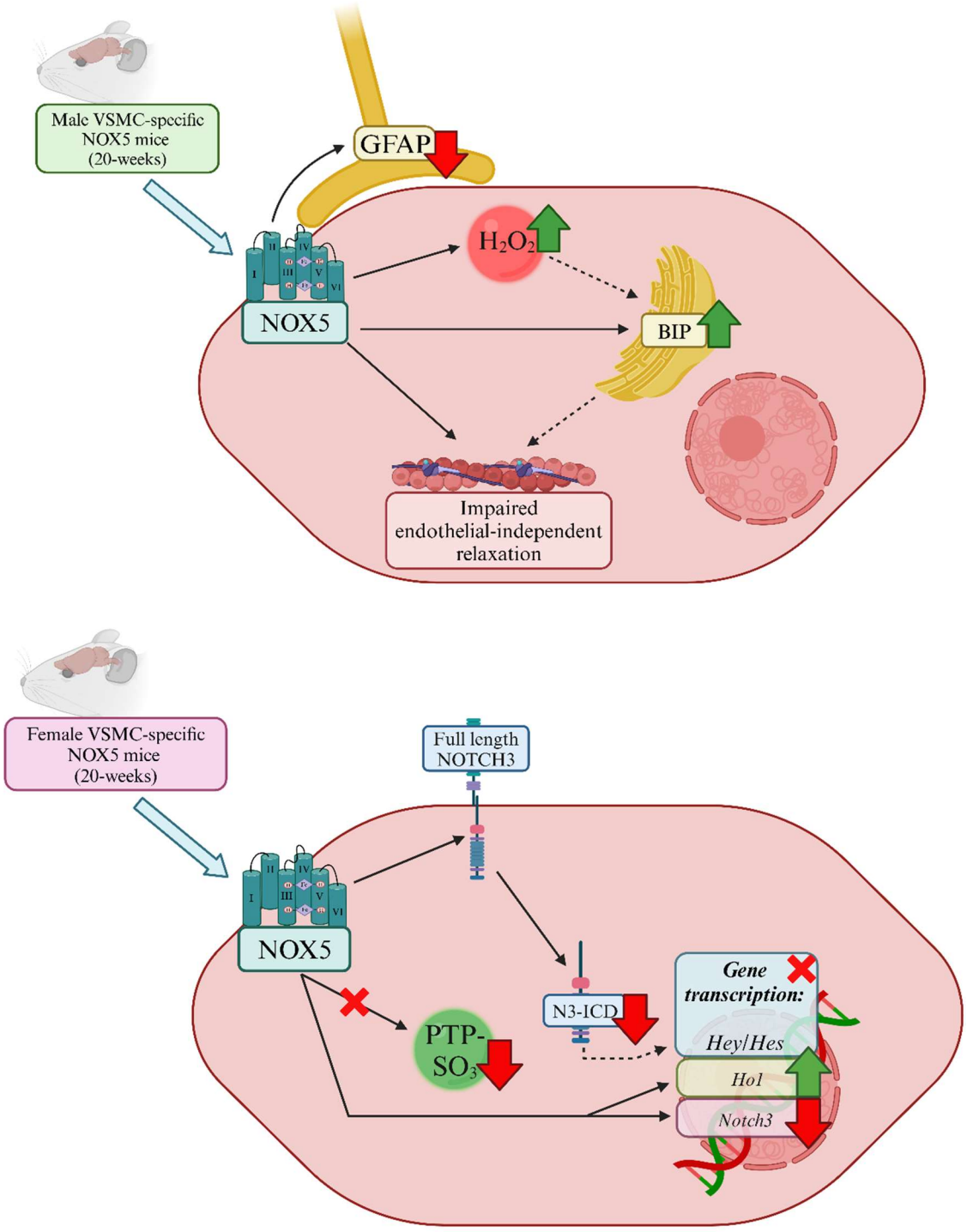

Figure 3-21. Graphical image highlighting the sexual-dimorphic effects of VSMC-specific NOX5 in the brains of 20-week-old mice. In male mice, NOX5 in a VSMC-specific manner was associated with an increased ROS environment, decreased astroglia marker GFAP, increased ER stress marker BIP, and impaired endothelial independent vasorelaxation in carotid arteries. Conversely females were identified to have reduced oxidative stress markers, reduced *Notch3* mRNA expression and N3-ICD protein levels without influencing *Hey* and *Hes* gene expression, and increased antioxidant *Ho1* mRNA expression levels. This image was generated in BioRender.

3.4 Discussion

Previous research has identified NOX5 as a pro-contractile NOX isoform (Montezano *et al*., 2018) that, when researched in an endothelial-specific manner in the brain, leads to deleterious neurological outcomes *post*-stroke (Casas *et al*., 2018). Here in this study presented in chapter 3 aimed to assess the role of VSMC-specific NOX5 on the brain. Our findings suggest that VSMC-NOX5 leads to sex-specific changes in cerebrovascular biology. Firstly, GFAP protein expression was decreased in male VSMC-NOX5 mice, but unchanged in female VSMC-NOX5 mice. Secondly, when assessing vascular reactivity of the common carotid arteries, our study identified that endothelial-independent vasorelaxation was impaired in male VSMC-specific NOX5 mice, with no difference being identified in females. Thirdly, this study identified that NOTCH3 mRNA and protein expression was decreased in female VSMC-NOX5 mice. However, no differences were observed in male VSMC-NOX5 mice. Fourthly, assessment of ROS and oxidative stress markers identified VSMC-specific NOX5 increased cerebral H_2O_2 levels in mice Alternatively in female VSMC-NOX5 mice, PTP-oxidation was decreased and *Ho1* mRNA expression was increased. Finally, BIP protein expression was increased in male VSMC-NOX5 mice (**Figure 3-21**). Collectively, this data may indicate that VSMC-specific NOX5 may lead to sex differences in the brain.

GFAP is the main intermediary filament type III protein present in the cytoskeleton of astroglia. GFAP plays a key role in astroglia integrity, whereby astrocytes play a pivotal role in white matter structural integrity, myelination of neurons, synaptogenesis, regulation of pericyte function in vascular tone, and BBB integrity (Mayer *et al*., 2013, Price *et al*., 2018). Previous research has associated reduced GFAP expression with pathological outcomes, where GFAP knock-out mice have reduced myelination and white matter architecture, and BBB-integrity (Liedtke *et al*., 1996). Furthermore, lower levels of GFAP expression could indicate an early age-related astroglia dysfunction whereby astrocyte structural integrity is reduced, and an inability to respond to inflammatory processes in the brain contributes to cognitive decline (Novakovic *et al*., 2023, Bronzuoli *et al*., 2019). Previous studies examining NOX5 in an endothelial-cell specific manner have linked NOX5 with cognitive decline and BBB-dysfunction (Casas *et al*., 2019). The reduction in GFAP protein expression observed in male VSMC-NOX5 mice could be a biomarker of a similar pathological outcome of BBB-dysfunction and cognitive decline. However, in female VSMC-NOX5 mice, no alterations in GFAP protein expression were observed.

Gonadal steroids have been identified as influencing GFAP immunoreactivity through alterations in testosterone levels (Laping *et al*., 1994). Given that, in previous studies, an association between gonadal steroids such as testosterone with increased NOX5 activation and cardiovascular risk has been identified (Lucas-Herald *et al*., 2022), this could indicate NOX5 activity may directly, or indirectly, influence GFAP expression through testosterone hormone signalling. Alternatively, in females, a possibility for why GFAP expression was unaltered in VSMC-NOX5 mice is the regulation of astrocytes by oestrogen. Previous studies have demonstrated that oestradiol promotes differentiation of astrocytes and alters astroglia morphology, acting neuroprotectivity against neuroinflammation and injury through neurotrophic factors such as brain derived neurotrophic factor (BDNF) and insulin-like growth factor 1 (IGF-1) (Spence *et al*., 2011, Lu *et al*., 2020).

The common carotid arteries are essential for supplying oxygen and nutrients, primarily glucose, to the brain to maintain adequate perfusion for cerebral homeostasis (Khan *et al*., 2021, Harrington *et al*., 2007). NOX5 is associated with increased hypercontractility and impaired vasorelaxation in mesenteric arteries (Montezano *et al*., 2018). Furthermore, a relationship between NOX5-NOTCH3 signalling and impaired endothelial independent vasorelaxation was identified in the small arteries of CADASIL patients (Neves *et al*., 2019). SNP acts as a nitric oxide-releasing compound that initiates vasorelaxation through decreasing VSMC $[Ca^{2+}]i$ concentration, which in turn reduces Ca^{2+}-mediated contractile mechanisms such as the initiation of the CaM-MYTP1-MLCK-MLC_{20} contractile signalling pathway (Cogolludo *et al*., 2001). VSMC-NOX5-mediated impairment of endothelial-independent vasorelaxation could indicate reduced NO signalling in the carotid arteries. One rationale for this is that NOX5-mediated increases in H_2O_2 production may be diffusing from VSMCs to neighbouring ECs, leading to oxidative stress in the endothelium and causing a reduction of NO signalling through pathophysiological mechanisms such as eNOS uncoupling. Furthermore, NOX5-mediated oxidative stress has previously been identified to lower sGC gene expression and increase degradation of sGC (Sharina and Martin, 2017). This would impair the NO-sGC-cGMP pathway in VSMCs and causing reduced endothelial independent vasorelaxation. Alternatively, NOX5 in VSMCs could be increasing ROS bioavailability leading to superoxide and NO scavenging and conversion to $ONOO^-$. Previous studies have identified that reduced NO signalling leads to the alteration of the cGMP-PKG signalling pathway, leading to downregulation of the RyR2 contributing to ER stress and increased $[Ca^{2+}]i$. This in turn could lead to increased activation of NOX5 in the 20-week-old VSMC-

specific NOX5 mice, impairing vasorelaxation and in turn reducing CBF and perfusion in the brain (Ma *et al*., 2015, Camargo *et al*., 2022, Gotoh and Mori, 2006). No changes in vasorelaxation were observed in female VSMC-NOX5 mice in this study. A rationale as to why this study may have observed poorer vasorelaxation outcomes in male, but not female, VSMC-NOX5 mice is that oestrogen is modulating the upregulation of eNOS production in female mice and protecting against the deleterious effects of NOX5 in the common carotid arteries. Previous research has made the association between oestrogen and eNOS upregulation (Chen *et al*., 1999, Chambliss and Shaul, 2002). However, how this mechanism acts in the context of VSMC-NOX5 has yet to be defined.

NOTCH3 is a key signalling protein associated with VSMC survival, proliferation, and cell fate (Bray, 2016, Morris *et al*., 2019). Furthermore, alterations in NOTCH3 mRNA and protein expression are associated classical NOTCH3 signalling pathways that are associated with severe CSVD pathologies, most notably CADASIL (Coupland *et al*., 2018, Hosseini-Alghaderi and Baron, 2020). The classical NOTCH3 pathway is initiated through the binding of endothelial transmembrane ligands, delta or jagged proteins. Subsequently, sheddases ADAM10 or TACE proteases facilitate cleavage by the γ-secretase complex, leading to N3-ICD release and translocation to the nucleus, where acting as a transcription factor regulates HEY and HES genes (Bray, 2016, Morris *et al*., 2019, Hosseini-Alghaderi and Baron, 2020). Previous research has identified an interaction between NOX5 and NOTCH3 signalling leading to an increased ROS environment, impaired endothelial-independent vasorelaxation, and ER stress compared to TgNOTCH3^{WT} mice (Neves *et al*., 2019). In this chapter, this study identified that VSMC-NOX5 in female mice led to downregulation in *Notch3* mRNA and N3-ICD protein expression, without altering HEY and HES gene expression. This suggests that VSMC-NOX5 in females could be activating the non-canonical NOTCH3 pathway, activating targets that are not associated with HEY or HES transcription, such as NF-κB. Previous studies have identified non-canonical NOTCH3 signalling activates transcription of NF-κB activation in response to pathological conditions (López-López *et al*., 2020). Furthermore, no changes were observed in male VSMC-NOX5 mice suggesting that sex plays a key role in the NOX5-NOTCH3 signalling axis and possibly indicating that female hormones act protectively in the context of NOX5 through the activation of non-canonical NOTCH3 pathways. Female mice expressing VSMC-specific NOX5 in the brain may initiate a potential cross talk between NOX5-mediated ROS and enhanced oestrogen signalling that may influence NOTCH3 signalling and NOTCH3 upstream targets. Emerging evidence

has identified a potential cross talk between oestrogens and non-canonical NOTCH signalling through upstream modulation of NOTCH binding targets such as Jag1 through endothelial Erβ receptors (Hao *et al*., 2010). In this study, this could indicate that enhanced oestrogen signalling in response to NOX5-mediated oxidative stress may upregulate the non-canonical pathway in female VSMC-NOX5 mice. However, these effects require further study.

In physiological conditions, redox signalling is vital for a variety of cellular processes and are maintained by a balance of both ROS production and degradation by antioxidant enzymes. Imbalance by excessive ROS generation or diminished antioxidant activity leads to oxidative stress (Montezano *et al*., 2015). A wealth of literature links NOX5 to increased ROS bioavailability and oxidation of protein and protein tyrosine phosphatases (Antony *et al*., 2017, Casas *et al*., 2019, Zhao *et al*., 2020, Marqués *et al*., 2022). This study identified an increase in H_2O_2 levels in the brains of male VSMC-NOX5 mice and is consistent with both previous research and our hypothesis that NOX5 would lead to increases in ROS bioavailability in the brain. However, the origin of the increased cerebral H_2O_2 environment is unclear as H_2O_2 is not spontaneously produced in the vasculature, arising from sources such as NOX4 or through superoxide dismutation. Although the current study did not identify changes in NOX4 (protein and mRNA) SOD1 (mRNA expression), our data suggests a propensity for increased SOD2 mRNA expression in 20-week-old male VSMC-NOX5 mice. This tendency may suggest that the increases in H_2O_2 may be a consequence of mitochondrial oxidative stress and dysfunction leading to increases in mitochondrial manganese superoxide dismutation. The mitochondria are vital for playing the central role of maintaining cellular energy, regulating cellular apoptosis and sustaining cellular metabolism. Mitochondrial dysfunction can lead to severe pathophysiological outcomes in the brain that can promote the onset of CSVD, ischaemic stroke, and vascular dementia (Zong *et al*., 2024). Conversely, this study identified a significant decrease in expression of peroxiredoxin hyperoxidation and irreversible PTP's oxidation levels in female VSMC-NOX5 mice. PTPs regulate system cell signalling by catalysing the removal of phosphates from protein tyrosine residues in normal physiological conditions, acting to modulate key cellular functions such as cellular growth, proliferation, and differentiation. Furthermore, PTPs act to modulate immune responses, control receptor tyrosine kinases (RTKs), and regulate metabolism and vascular function, playing a key role in endothelial function and maintenance of vascular tone (Tautz *et al*., 2013, Kappert *et al*., 2005, Xie *et al*., 2021). In pathophysiological conditions, PRDX and

PTPs become irreversibly oxidised, typically as a consequence of oxidative stress. The active site of PTP cysteine residues go through oxidative modifications including SO_2H and SO_3H formations, leading to permanently activated or inactivated protein function (Meng *et al*., 2002, Sharifi-Rad *et al*., 2020, Östman *et al*., 2011). Given the reduction of irreversible PRDX and PTP oxidation markers observed in female VSMC-NOX5 mice, this could indicate a reduced oxidative stress environment and regulated cellular signalling. Furthermore, this study identified an increase in NRF2-related HO1 mRNA expression. HO1 has previously been shown to catalyse influencing cellular NADPH levels through degradation of haem by HO1, and release of biliverdin, free iron and carbon monoxide (CO). The conversion of haem by HO1 to biliverdin requires the consumption of one molecule of NADPH, with the additional conversion of biliverdin to bilirubin via bilverdine reductase leading to the consumption of two NADPH molecules (Datla *et al*., 2007, Moraes *et al*., 2012). As such, HO1 may be competing with NOX5 for the NADPH coenzyme, leading to reduced NOX5 activity and subsequent ROS production and reduced oxidative stress environment. A potential explanation for the increase in HO1 activity may be that oestrogen is regulating haem oxygenase activity. HO1 is regulated by the NRF2 (Nuclear factor-E2-related factor 2) antioxidant system (Loboda *et al*., 2016) with oestrogen previously been shown to enhance NRF2 signalling, protecting against oxidative stress and improving cardiac function in a rat ovariectomy model (Qian *et al*., 2021). Furthermore, previous research has identified an interplay between oestrogen receptor activity and HO1 production (Baruscotti *et al*., 2010). Taken together, the reduction in irreversible PTP-oxidation and increased HO1 mRNA expression suggests that the inclusion of NOX5 in a VSMC-specific manner leads to protective cerebral effects and homeostatic vascular function in female VSMC-NOX5 mice.

BIP is a chaperone protein of the ER, playing a vital role in synthesising ER proteins in order to prevent misfolded protein aggregation and cellular Ca^{2+} homeostasis (Morris *et al*., 1997). In pathological conditions, BIP dissociates from PERK and IRE1 in order to activate UPR pathways to prevent ER stress, maintaining normal calcium homeostasis within the cell (Kopp *et al*., 2019, Hetz and Papa, 2018). Previous research has identified that NOX5 in an endothelial-specific manner leads to upregulation in BIP expression, leading to ROS induced changes to the UPR pathway (Cortés *et al*., 2021a). In this study, similar changes were identified whereby VSMC-NOX5 led to upregulation of BIP expression in male mice. Furthermore, this links back to the increased ROS production observed in male VSMC-NOX5 mice. The increases in H_2O_2 identified in this study may

be leading to increased levels of UPR, suggesting evidence of a role for H_2O_2 in ER stress. Such a mechanism could also explain this study's observation of upregulated BIP protein expression in male VSMC-NOX5 mice, as previous research has identified a crosstalk between mitochondrial dysfunction and ER stress (Chen *et al*., 2020a, Bilbao-Malavé *et al*., 2021). Furthermore, considering the elevated ROS environment, indicators of ER stress and compromised endothelial-independent vasorelaxation were observed in the brains of male VSMC-NOX5 mice, alongside the attenuation of NOTCH3 gene and intracellular domain protein expression in females without indication of carotid artery vascular dysfunction. These findings could suggest that NOX5-mediated ROS induces an UPR to ER stress in male VSMC-NOX5 mice, with ER stress contributing to increases in $[Ca^{2+}]i$, causing impaired smooth muscle relaxation. Contextually, this suggests that VSMC-NOX5 may lead to heightened ROS bioavailability, mitochondrial oxidative stress, reduced cytosolic ATP levels and impaired ER functionality and poorer outcomes in the brain. In contrast, observations in female VSMC-NOX5 mice revealed no alterations in BIP expression when compared to WT mice. Previous research has identified that in conditions of altered ER stress, oestrogen reduces ER stress by maintaining homeostasis of the ER linked proteins such as BIP and CHOP, inhibiting deleterious processes that contribute to apoptosis (Guo *et al*., 2014, Dreier *et al*., 2022), whilst promoting angiogenesis (Zhang *et al*., 2021). Moreover, oestrogen has been linked with ER stress inhibition whilst upregulating SERCA activation in a rat model of myocardial ischaemic reperfusion (Chen *et al*., 2022). In the context of our current study assessing VSMC-NOX5 in the brain, oestrogen may be preventing changes in BIP expression in female mice, resulting in ER homeostasis.

In summary, Chapter 3 of this thesis demonstrates significant sex-specific effects of VSMC-specific NOX5 in the brains of 20-week-old mice. In male mice, NOX5 in a VSMC-specific manner is associated with increased oxidative stress and ER stress markers, along observed carotid artery endothelial-independent vasorelaxation impairment, which could contribute to vascular dysfunction and cerebrovascular disease progression. However, in females, the data outlined in Chapter 3 suggests a more protective response indicated by reduced oxidative stress markers and increased markers of antioxidant response. Furthermore, female VSMC-specific NOX5 mice were identified to have reduced NOTCH3 signalling without affecting downstream effector genes and may indicate a role for non-canonical NOTCH3 signalling. Whether these changes to NOTCH3 signalling identified in female VSMC-specific NOX5 mice is acting beneficially requires

further study. To conclude, the findings identified in Chapter 3 of this thesis highlight important sex differences in NOX5-mediated cerebrovascular pathology, suggesting that females may possess intrinsic protective mechanisms that mitigate NOX5-induced cerebrovascular dysfunction observed in male VSMC-specific NOX5 mice.

Chapter 4

Evaluating the Impact of Ageing VSMC-specific NOX5 Overexpression in the Brains of 20- and 35-week-old Male and Female Mice

4.1 Overview

As global life expectancy continues to rise, ageing has become a significant contributor to pathophysiological changes in cerebrovascular health. These pathophysiological changes are often associated with compromised CBF, increasing the risk of CSVD and severe outcomes such as stroke and VaD (Zimmerman *et al*., 2021, Hachinski *et al*., 2019). Research literature has associated vascular ageing with molecular and cellular alterations with increased NOX activity (Sahoo *et al*., 2016, Oudot *et al*., 2006), enhanced ROS bioavailability and oxidative stress (Carvalho and Moreira, 2018, Maldonado *et al*., 2023), NOTCH3 dysregulation (Romay *et al*., 2024, Kapoor and Nation, 2021) and heightened ER stress (Brown and Naidoo, 2012, Ma *et al*., 2024) being hallmarks of this process. These age-associated pathophysiological mechanisms can collectively contribute to pathophysiological processes such as VSMC remodelling, endothelial dysfunction, impaired BBB-integrity and CBF contributing increased risk of cerebrovascular pathology (García-Redondo *et al*., 2016, Hernandes *et al*., 2022, Chrissobolis and Faraci, 2008). In the context of NOX5, previous research examining cerebrovascular ageing in endothelial-specific NOX5 mice, NOX5 promoted impaired BBB integrity, contributing to impaired BP, locomotor activity deficits and cognitive decline aetiology (Cortés *et al*., 2021b).

To date, no research has identified the role of VSMC-specific NOX5 in cerebrovascular ageing. Here in chapter 4 this research aims to examine the role of VSMC-specific NOX5 in the context of vascular ageing by assessing male and female mice at 20- and 35-week-old groups, compared to their WT counterparts. Translationally, 35-weeks-old mice represents a transitionary period where early indications of physiological impairments may manifest including vascular ageing and cognitive decline. Furthermore, 35-weeks represents an age whereby mice approach the endocrine equivalent of human perimenopause (Diaz Brinton, 2012).

As previously identified in Chapter 3, VSMC-NOX5 in a VSMC-specific manner contributes to increased levels of ROS and markers of ER stress, impaired endothelial-independent vasorelaxation, leading to downregulation of astroglia GFAP expression in a sex-dependent manner. These findings may indicate a deleterious environment with the possible implication of cerebrovascular dysfunction that could lead to pathologies such as CSVD and increased stroke risk. Moreover, it is well established in research literature, that sex is a critical biological factor in vascular ageing whereby the vasoprotective effects

observed in females declines with age, reducing beneficial physiological mechanisms such as oestrogen mediated ARE upregulation (Miller and Duckles, 2008). This in turn makes females more susceptible to pathophysiological processes such as vascular remodelling and oxidative stress, contributing to increased markers of vascular impairment and cerebrovascular risk (Iorga *et al*., 2017, Zárate *et al*., 2017, Davezac *et al*., 2021).

Chapter 4 builds on the findings presented in Chapter 3 by introducing age comparison (20- vs. 35-week-old mice) within male and female WT and VSMC-specific NOX5 groups. The 20-week-old data from Chapter 3 are included in this chapter to enable direct comparisons between the two age groups. However, the main focus of Chapter 4 is to identify how VSMC-specific NOX5 alters vascular function with age in male and female mice, rather than solely genotypic differences identified in Chapter 3. By assessing a mouse model of VSMC-NOX5 in the context of age, this research could provide valuable insights into the mechanisms that underpin increased cerebrovascular risk between sexes. This study hypothesises that the inclusion of VSMC-NOX in a VSMC-specific manner would accelerate the deleterious effects of ageing, which in turn could be different dependent on sex.

4.2 Chapter 4 Hypothesis and Aims

4.2.1 Hypothesis

Here in Chapter 4, this study hypothesises that VSMC-specific NOX5 in the context of ageing will lead to increased oxidative stress that will disrupt key signalling pathways linked to cerebrovascular dysfunction, thereby accelerating cerebrovascular ageing and disease risk.

4.2.1.1 Predictions of Hypothesis

To test this hypothesis, this study predicts that ageing in the context of cerebral VSMC-specific NOX5 will lead to:

1. **Alterations in structural and phenotypic markers:** This study anticipates that aging in VSMC-NOX5 mice will exhibit alterations in cerebrovascular proteins (GFAP, RhoA, ROCK1, and VEGFR2) which are vital for typical vascular structure, phenotype and physiological function.
2. **Alternative NOX isoform modulation:** This study predicts that VSMC-NOX5 will cause alterations in NOX1, NOX2, and NOX4 mRNA and protein levels either indirectly through compensatory mechanisms to regulate NOX5 activity, or by direct NOX isoform activity as a result of the ageing.
3. **Impaired carotid artery vascular function:** This thesis hypothesises that vascular ageing in VSMC-specific NOX5 mice would contribute to impaired vascular function in carotid arteries.
4. **NOTCH3 signalling axis alterations:** This study predicts that vascular ageing in VSMC-NOX5 mice will dysregulate the NOTCH3 signalling axis leading to alterations in cerebrovascular function.
5. **Alterations to ROS/antioxidant homeostasis and increased markers of oxidative stress:** This study hypothesises that aged VSMC-NOX5 mice would lead to increase ROS production, markers of oxidative stress, and altered antioxidant gene expression.
6. **Altered protein levels of ER stress UPR marker BIP:** This study further hypothesises that BIP protein expression will be altered in the context of aging VSMC-NOX5 mice. These changes may influence cellular stress response and calcium homeostasis leading to cerebrovascular dysfunction.

7. **Sex-dependent changes:** This study also hypothesises that the effects of ageing will lead to progressive decline of potential protective mechanisms in the brains of female VSMC-specific mice, whilst also exacerbating the previously identified deleterious effects observed in the brains of VSMC-specific NOX5 male mice observed in chapter 3.

Collectively VSMC-NOX5 overexpression in the context of ageing may lead to pathophysiological outcomes that may indicate increased risk of cerebrovascular disease.

4.2.2 Specific Aims

1. *Assessment of phenotypic and structural changes in the brains of aged WT and VSMC-NOX5 mice.*

To evaluate if VSMC-NOX5 in a VSMC-specific manner leads to phenotypic and structural changes in the brains of male and female 20- and 35-week-old WT and VSMC-NOX5 mice were assessed by immunoblotting examining neurovascular unit markers GFAP, α-SMA, VEGFR2, and contractile markers ROCK1 and RhoA.

2. To explore whether VSMC-NOX5 regulates the expression of alternative NOX isoforms (NOX1, NOX2, and NOX4) in aged VSMC-NOX5 and WT mice.

To assess whether VSMC-NOX5 leads to changes in alternative NOX isoforms in the brains of 20- and 35-week-old male and female mice, mRNA and protein expression of NOX1, NOX2, and NOX4 were assessed by q-RT PCR and immunoblotting.

3. To assess the effects of VSMC-specific NOX5 overexpression on carotid artery vascular function in in aged VSMC-NOX5 mice.

Carotid arteries were derived from male and female 20- and 35-week-old male and female WT and VSMC-NOX5 mice. Carotid vessel reactivity was assessed by wire myography using cumulative-concentration curves to assess contraction and endothelial-independent vasorelaxation by incubating carotid artery vessels with U46619 and sodium nitroprusside (SNP) respectively.

4. To explore if cerebral VSMC-NOX5 in aged mice regulates the NOTCH3 signalling axis.

Male and female 20- and 35-week-old WT and VSMC-NOX5 mouse brains were used to assess NOTCH3 mRNA and protein (Full-length and intracellular domain) expression by q-RT PCR and immunoblotting. Downstream NOTCH3 transcription genes (*Hey1, HeyL, Hes1, and Hes5*) were also assessed by q-RT PCR.

5. *To examine the effects of VSMC-NOX5 on redox signalling in the brains of aged VSMC-NOX5 mice.*

Oxidative stress was assessed in the brains of 20- and 35-week-old male and female WT and VSMC-NOX5 mice by measuring ROS production (lipid peroxidation and hydrogen peroxide), redox signalling (irreversibly oxidised protein tyrosine phosphatases) and antioxidant genes.

6. To identify if VSMC-NOX5 in the context of age leads to changes in the ER UPR response.

Immunoblotting of whole brain homogenates was conducted in 20- and 35-week-old male and female WT and VSMC-NOX5 mice to assess BIP levels, a marker of ER stress, in the brains of 20-week-old WT and VSMC-NOX5 mice.

4.3 Results

4.3.1 Systemic Blood Pressure Assessment of 20-week and 35-Week-old Male and Female VSMC-specific NOX5 Mice.

BP was measured utilising plethysmography in male and female 20- and 35-week-old WT and NOX5 mice. In 20-week v 35-week-old mixed sex analysis, BP was increased with age in both WT (20-week-old WT 117.4±1.2 mmHg vs 35-week-old WT 127.8±1.56 p=<0.0001****) and NOX5 mice (20-week-old NOX5 122.2±2.2 mmHg vs 35-week-old NOX5 132.9±2.21 mmHg p=0.01*) when compared to their 20-week-old counterparts (**Figure 4-1A)**. Furthermore, when divided by sex, male 20-week v 35-week-old analysis, identified BP increases with age in both male WT (male 20-week-old WT 116.7±1.79 mmHg vs male 35-week-old WT 129.1±1.89 mmHg p=0.0001***) and male NOX5 mice (male 20-week-old NOX5 121.5±2.43 mmHg vs male 35-week-old NOX5 135.4±2.91 mmHg p=0.005**) when compared to their 20-week-old counterparts (**Figure 4-1B)**. However, no differences in BP were identified between 20- and 35-week-old female WT v NOX5 mice (**Figure 4-1C**).

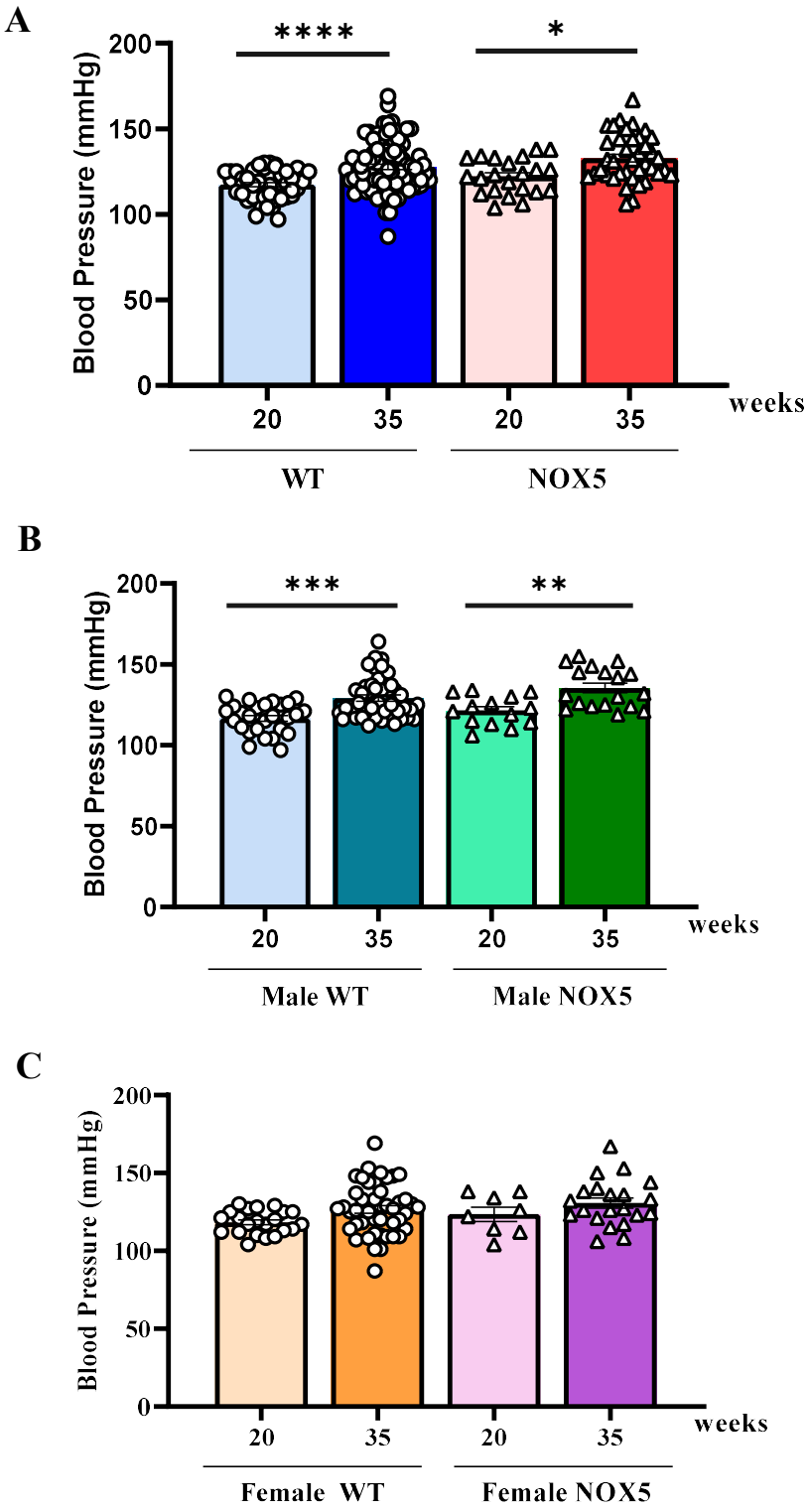

Figure 4-1. Blood pressure assessment of 20-week-old male and female WT and VSMC-specific NOX5 mice. BP assessment of mixed sex, male, and female WT and NOX5 mice was assessed by plethysmography. Mixed sex data n=22-49, male data n=14-27, female data n=8-22 per genotype. Data was presented as mmHg and analysed using a student's t-test and presented as *p≤0.05.

4.3.2 Whole Brain Assessment of αSMA Protein levels in 20- and 35-week-old Male and Female VSMC-specific NOX5 Mice.

NOX5 has been associated with contractility and phenotypic changes. A key marker of contractility and phenotype is αSMA. At 20-weeks-old, αSMA protein levels were not altered in whole brain homogenates of male or female VSMC-specific NOX5 mice. This study aimed to examine whether αSMA protein levels would be altered by VSMC-specific NOX5 overexpression with age. Immunoblotting was utilised to assess αSMA in 35-week-old male (**Figure 4-2A**) and female (**Figure 4-2B**) WT and VSMC-NOX5 mice and normalised to REVERT total protein stain. No differences were observed in αSMA protein levels between sex, age, or genotype when assessed in whole brain homogenates.

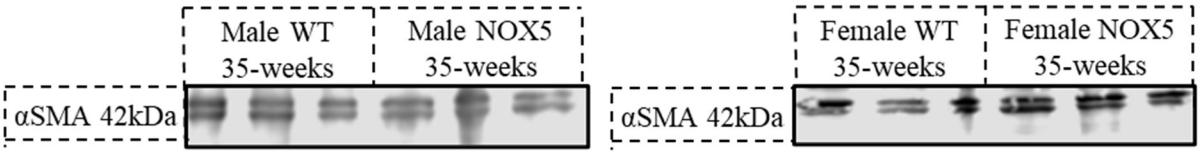

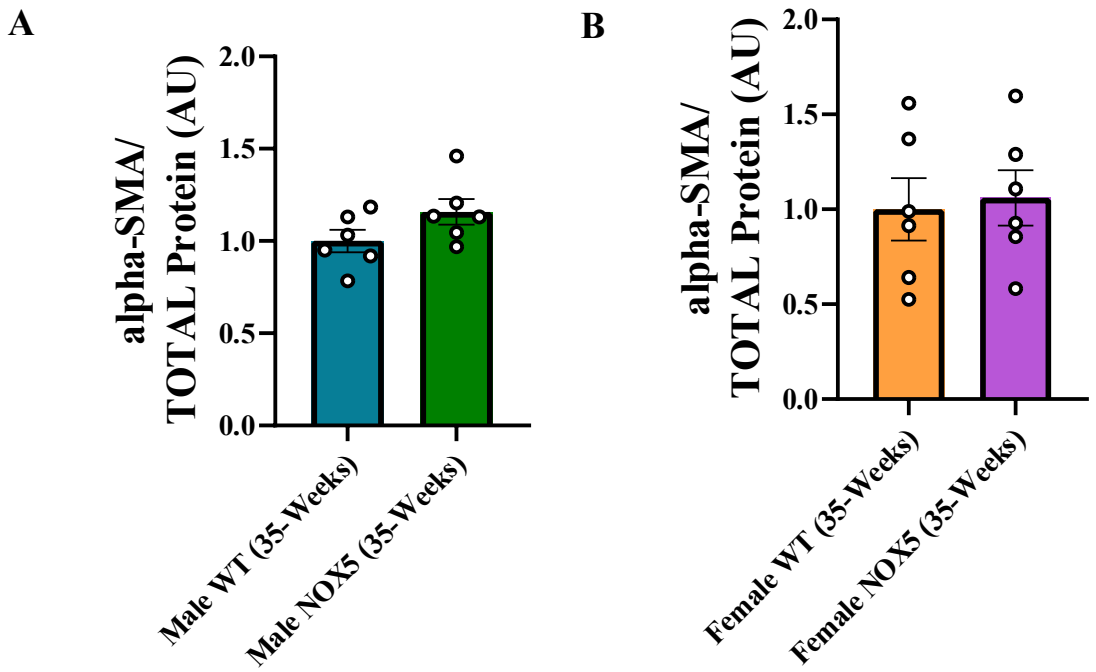

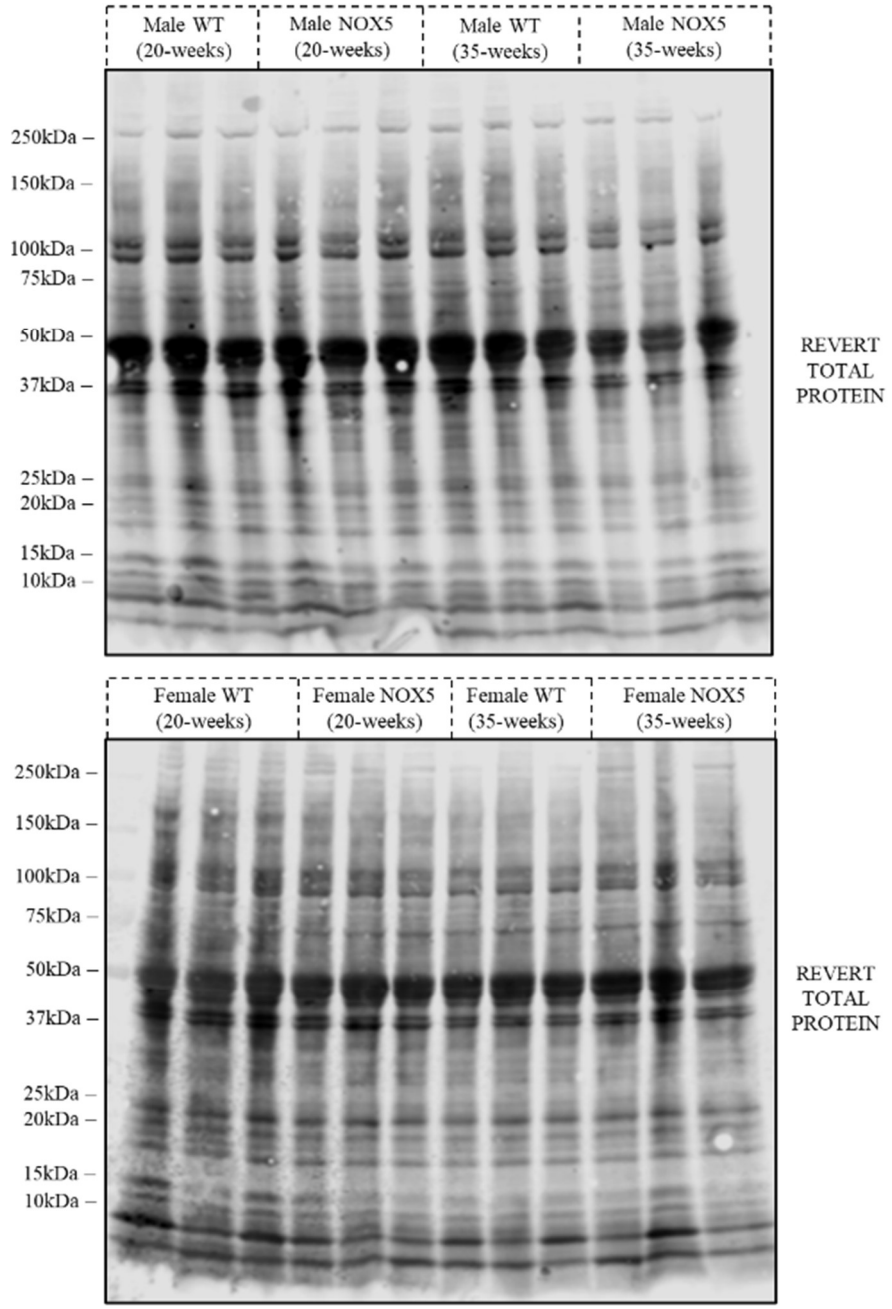

Figure 4-2. Protein assessment of cerebrovascular contractile phenotype marker αSMA in 35-week-old WT and VSMC-NOX5 mice. Protein assessment of αSMA in whole brain homogenates of 35-week-old male (**A**) and female (**B**) WT and NOX5 was assessed by immunoblotting and normalised to REVERT TOTAL protein stain. Male study n=6, female study n=6 per genotype. Data was presented as AU and analysed using a student's t-test.

4.3.3 Whole Brain Assessment of VEGFR2 Protein Levels in 20- and 35-week-old Male and Female VSMC-specific NOX5 Mice.

NOX5 has been associated with endothelial dysfunction. At 20-weeks, no differences were identified in VEGFR2 protein levels when assessed in whole brain homogenates of male or female VSMC-specific NOX5 mice. This study aimed to examine whether VSMC-specific NOX5 mice in the context of ageing would lead to VEGFR2 protein level changes when examined in whole brain homogenates of 35-week-old male and female mice. Immunoblotting was utilised to assess VEGFR2 in 35-week-old male (**Figure 4-3A**) and female (**Figure 4-3B**) WT and VSMC-NOX5 mice and normalised to REVERT total protein stain. No differences were observed in VEGFR2 protein levels between sex, age, or genotype when assessed in whole brain homogenates.

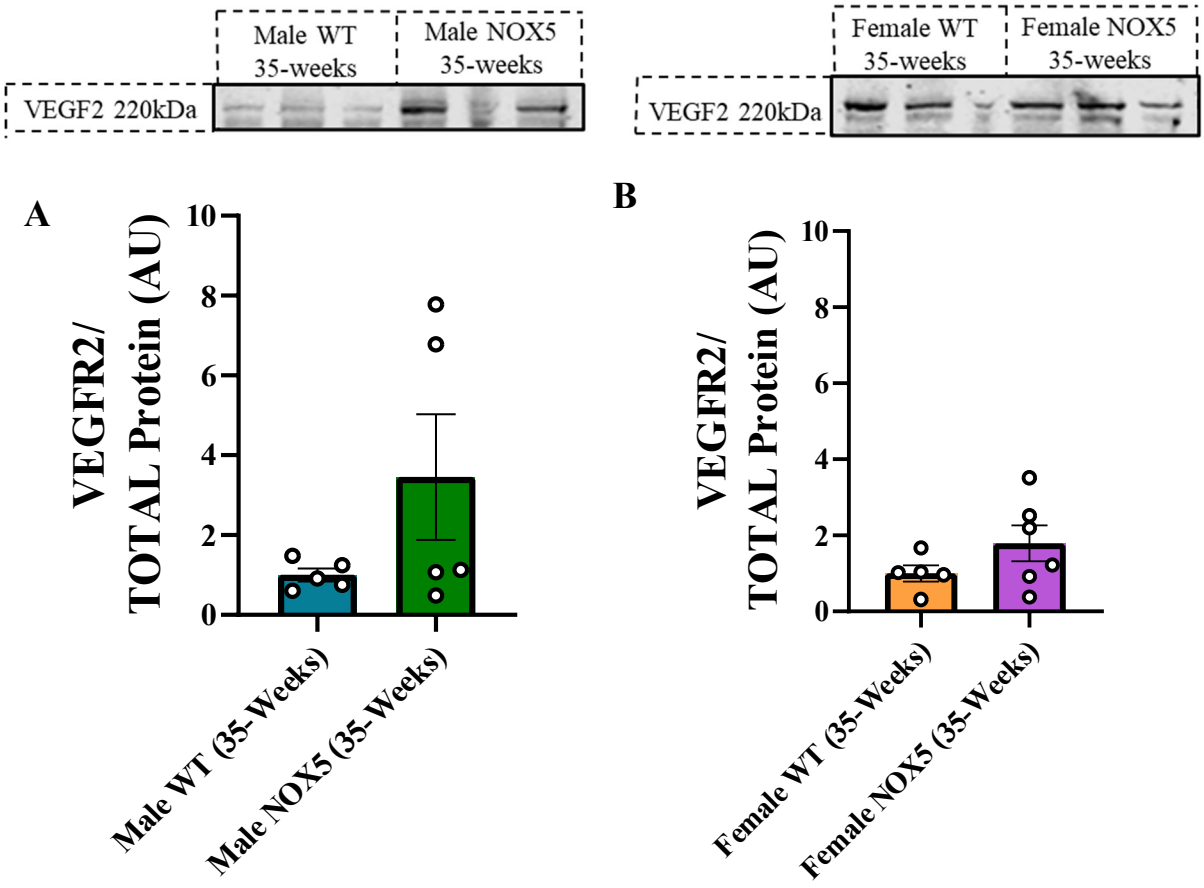

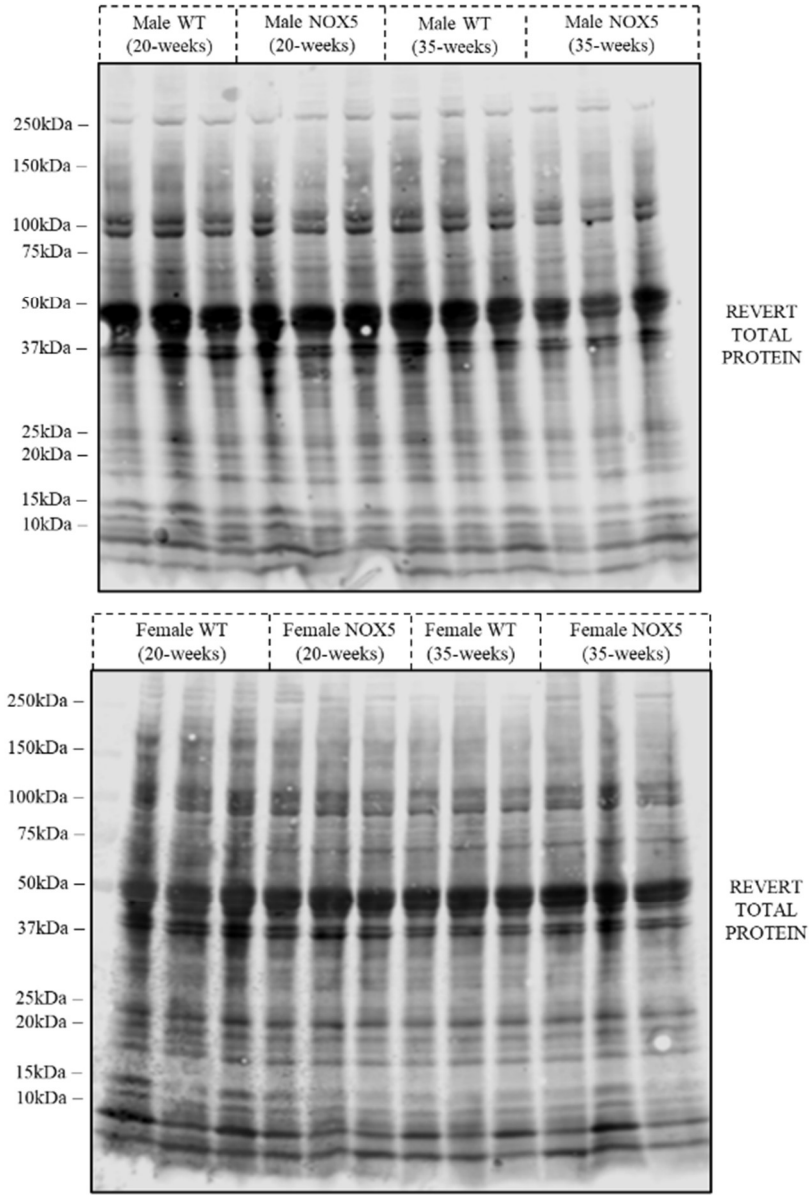

Figure 4-3. Protein assessment of endothelial function marker VEGFR2 in 35-week-old WT and VSMC-specific NOX5 mice. Protein assessment of VEGFR2 in whole brain homogenates of 35-week-old male (**A**) and female (**B**) WT and NOX5 was assessed by immunoblotting and normalised to REVERT TOTAL protein stain. Data was then presented as arbitrary units (AU). Male study n=6, female study n=6 per genotype. Data was presented as fold change AU and analysed using a student's t-test.

4.3.4 Cerebral Assessment of RhoA/ROCK1 Protein Levels of 35-week-old Male and Female Mice with VSMC-specific NOX5 Overexpression.

The RhoA/ROCK1 pathway is a mediator of vascular contractility. At 20-weeks, no differences were identified in protein levels of either RhoA and ROCK1 when assessed in whole brain homogenates of male or female VSMC-specific NOX5 mice. This study aimed to examine whether VSMC-specific NOX5 mice in the context of ageing would lead to VEGFR2 protein level changes when examined in whole brain homogenates of 35-week-old male and female mice. Immunoblotting was utilised to assess RhoA (**Figure 4-4A-B**) and ROCK1(**Figure 4-4B-C**) protein levels in 35-week-old male and female WT and VSMC-NOX5 mice and normalised to REVERT total protein stain. RhoA/ROCK1 protein levels between sex, age, or genotype were not identified to be significantly different when assessed in whole brain homogenates.

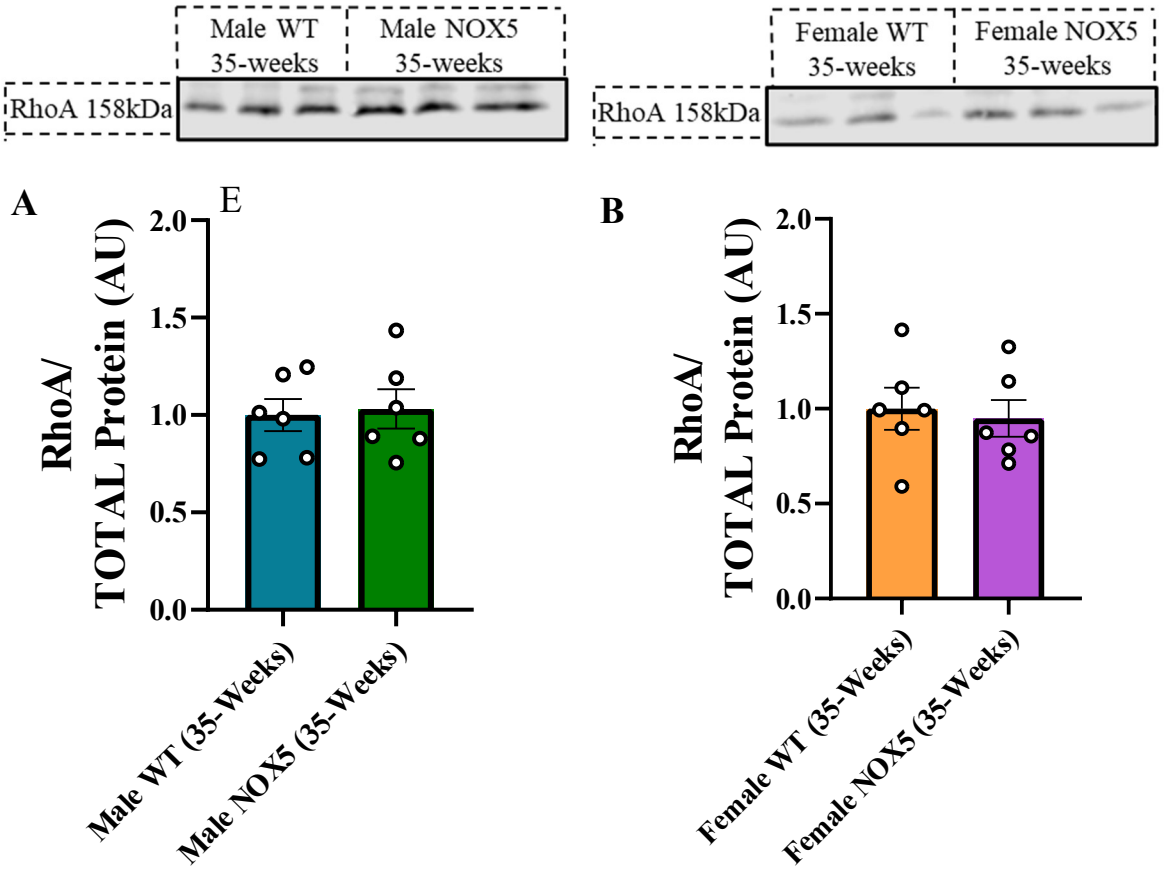

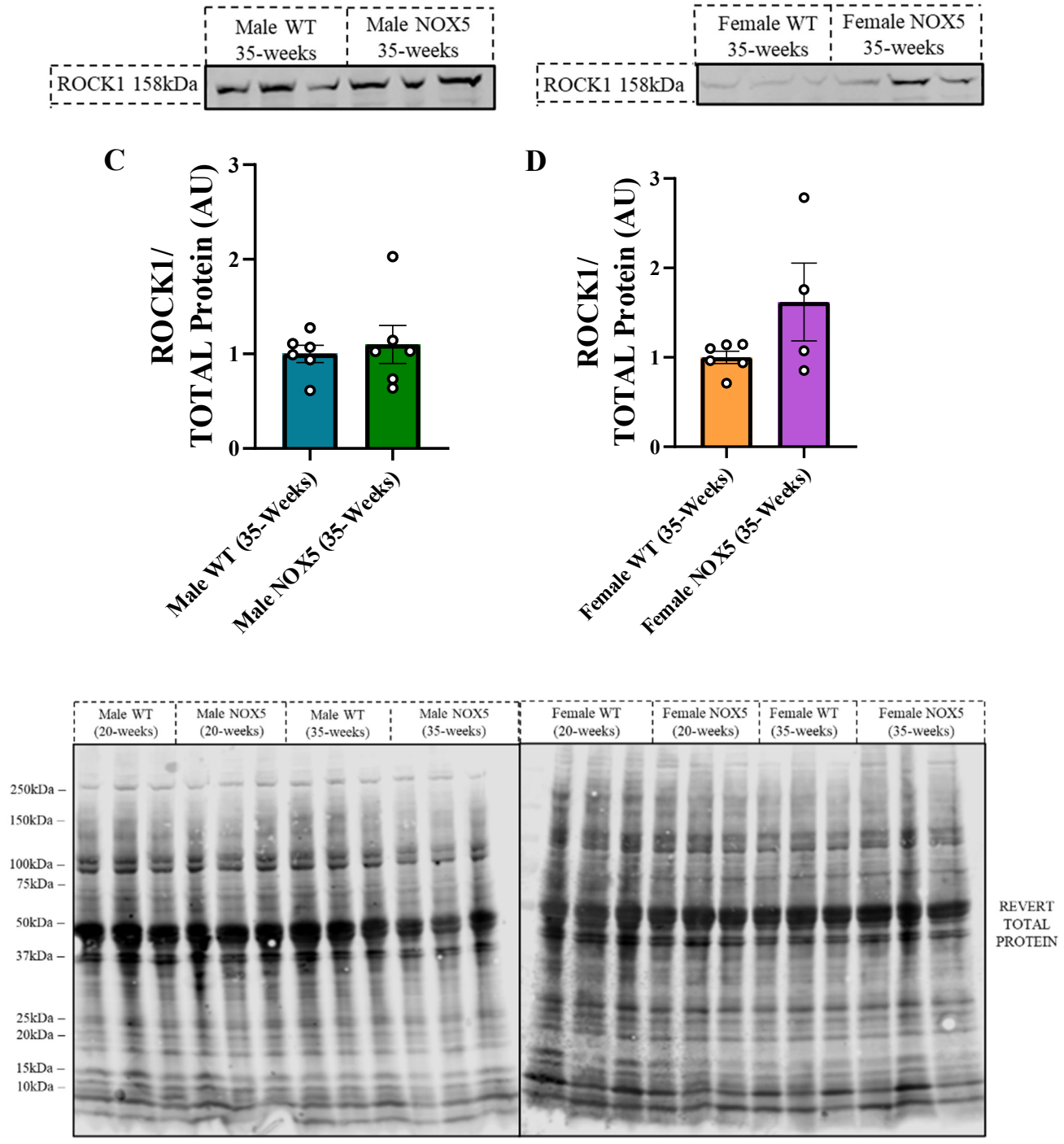

Figure 4-4. Protein assessment of contractile signalling markers RhoA/ROCK1 in 35-week-old WT and VSMC-specific NOX5 mice. Protein assessment of RhoA and ROCK1 in whole brain homogenates of 35-week-old male (**A**) and female (**B**) WT and NOX5 was assessed by immunoblotting and normalised to REVERT TOTAL protein stain **(C & D)**. Data was then presented as arbitrary units (AU). Male study n=6, female study n=6 per genotype. Data was presented as fold change AU and analysed using a student's t-test.

4.3.5 Cerebral GFAP Protein Level Examination of 35-week-old Male and Female VSMC-specific NOX5 Mice.

NOX5 has been associated with contractility and phenotypic changes. A key marker of contractility and phenotype is αSMA. In chapter 3, this thesis research identified that VSMC-specific overexpression in 20-week-old males was associated with downregulated GFAP protein levels indicating a potential astrocyte dysfunctionality. However, no GFAP protein changes were identified in 20-week-old female VSMC-NOX5 mice. This study aimed to examine whether GFAP protein levels would lead be altered in females and further downregulated by age in male VSMC-specific NOX5 mice. GFAP protein was assessed by immunoblotting in 35-week-old male (**Figure 4-5A**) and female (**Figure 4-5B**) WT and VSMC-NOX5 mice and normalised to REVERT total protein stain. No differences were observed in GFAP protein levels between sex, age, or genotype when assessed in whole brain homogenates.

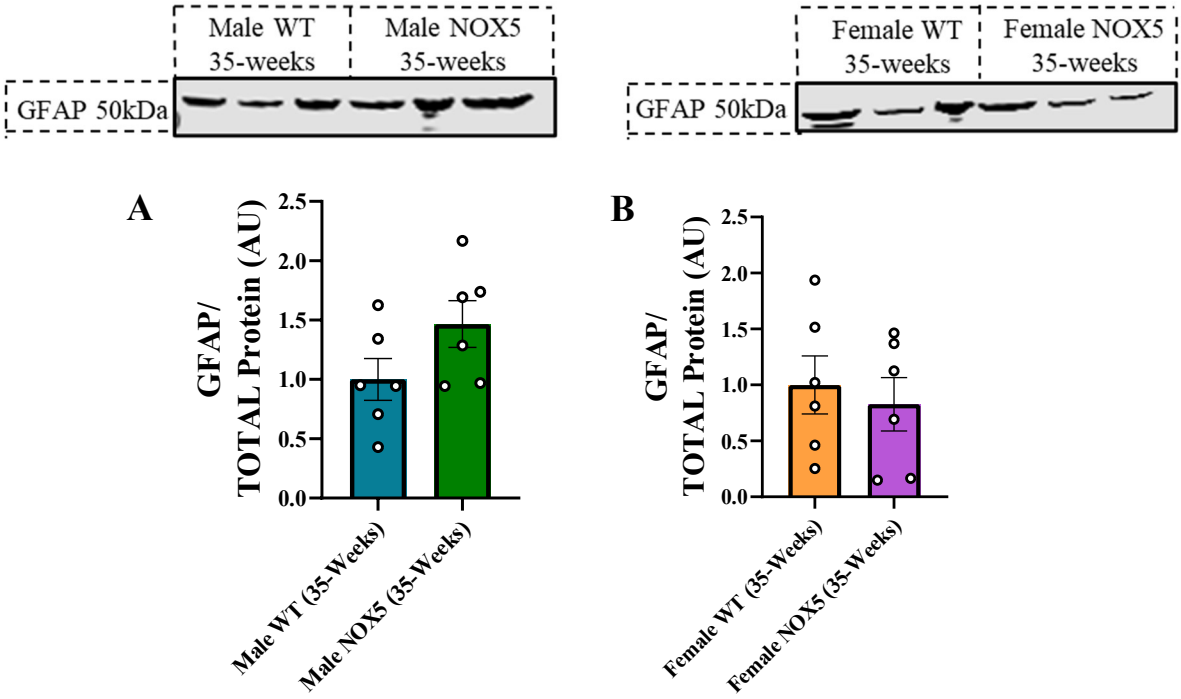

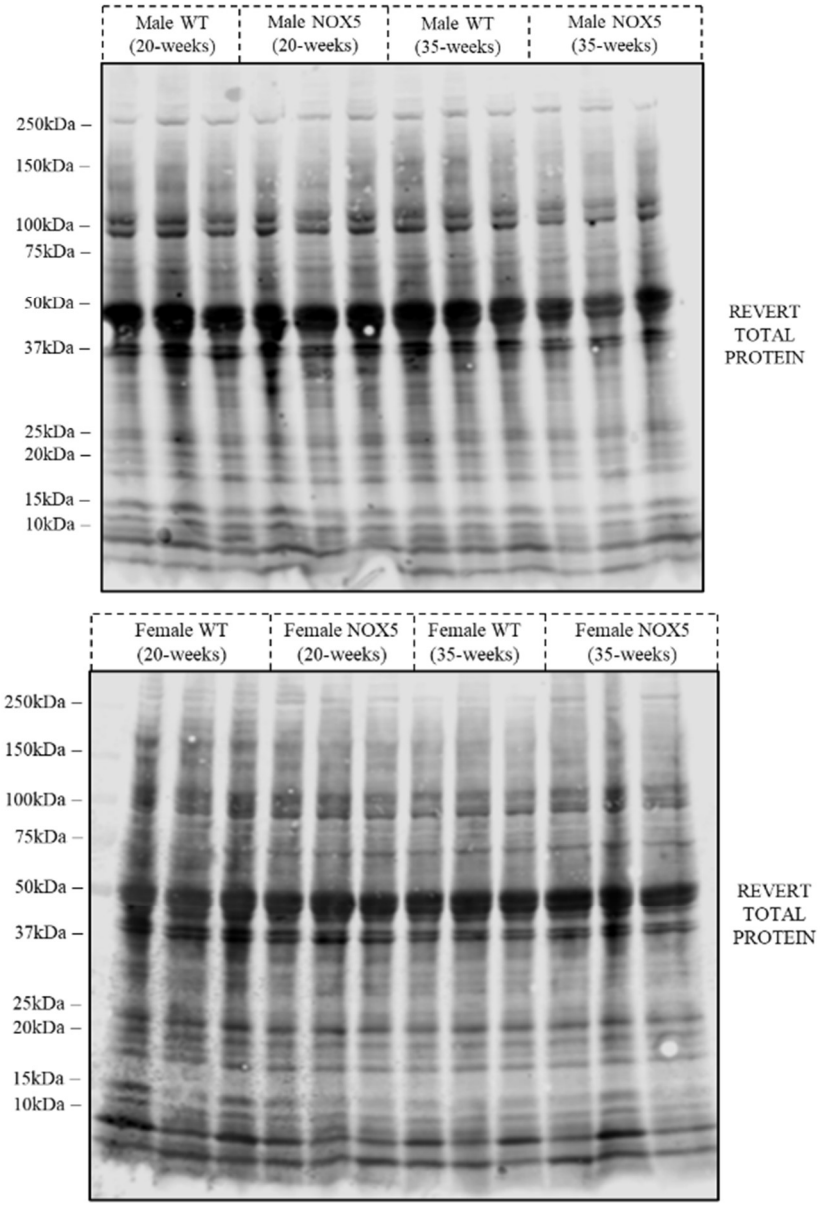

Figure 4-5 Cerebral protein assessment of astroglia marker GFAP in 35-week-old male and female WT and VSMC-specific NOX5 mice. Whole brain lysates were prepared from male and female 35-week-old WT and VSMC-NOX5 mice. Protein assessment of cerebrovascular GFAP levels in male (**A**) and female (**B**) WT and VSMC-specific NOX5 mice were assessed by immunoblotting and presented as AU after normalisation to REVERT total protein. Data was then presented as fold change AU. Male study n=6, female study n=6. Data was analysed using a student's t-test.

4.3.6 Cerebral Assessment of NOX1 Protein and Gene Expression Levels in 20- and 35-week-old Male and Female VSMC-specific NOX5 Mice

To assess NOX1 mRNA expression and protein levels RNA and protein was extracted from whole brain lysates in 20- and 35-week-old male and female WT and VSMC-NOX5 mice using q-RT PCR and immunoblotting. WT and VSMC-NOX5 mice were assessed collectively and as separate sexes. In male VSMC-NOX5 mice, *Nox1* mRNA expression was decreased in 35-week-old mice (**Figure 4-6B**) compared to 20 week-old mice (35-week NOX5 9.01±0.41 ΔCt vs 20-week NOX5 10.5±0.37 ΔCt p=0.03#), No differences were observed in *Nox1* mRNA expression in mixed sex analysis (**Figure 4-6A**) or in female (**Figure 4-6C**) VSMC-NOX5 mice relative to younger mice. Age had no effect on *Nox1* expression in WT mice of either sex or when analysed together.

Mixed sex of NOX1 protein levels identified a significant decrease with age in both 35-week-old WT (20-week WT 3251.43±272.99 AU vs 35-week WT 1337.93±187.89 AU *p*=<0.0001****) and VSMC-NOX5 (20-week NOX5 2986.92±349.69 AU vs 35-week NOX5 818.92±111.72 AU *p*= <0.0001****) mice when compared to their 20-week-old counterparts (**Figure 4-6D**).

When separated by sex, a significant decrease in NOX1 expression in 35-week-old male VSMC-NOX5 mice was identified when compared to 20-week-old VSMC-NOX5 mice (20-week male NOX5 3042±546.32.54 AU vs 35-week male NOX5 1025.14±81.1 AU *p*= 0.008***). NOX1 protein expression was also observed to be increased by age when comparing 20- and 35-week-old male WT mice (20-week-old male WT 2612.86±546.294.81 AU vs 35-week-old male WT 1039.29±201 AU *p*= 0.006**) (**Figure 4-6E**).

Examination of NOX1 protein expression identified that NOX1 expression was significantly reduced by age in both WT and VSMC-NOX5 female mice when compared to their WT counterparts (20-week WT 3890±316.37 AU vs 35-week WT 1636.57±287.84 AU *p*= 0.0006***)/(20-week NOX5 2940±490.1AU vs 35-week NOX5 578.33±184.9 AU *p*= 0.000***). Furthermore, NOX1 protein expression was discovered to be significantly reduced in female 35-week-old VSMC-NOX5 mice when compared to female 35-week-old WT mice (35-week female WT 1636.57±287.84 AU vs 35-week NOX5 578.33±184.9 AU *p*= <0.013#) (**Figure 4-6F**).

A

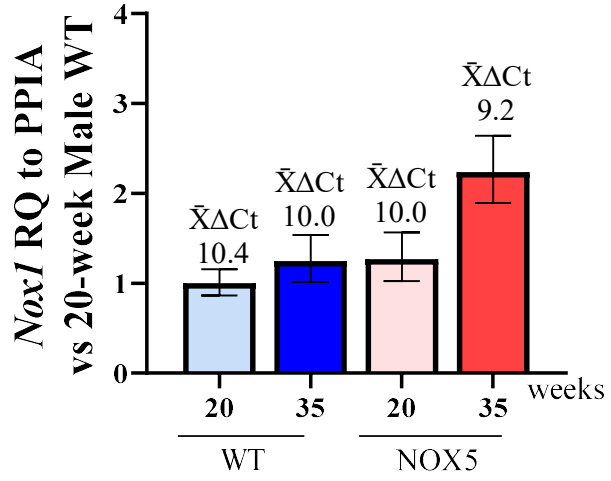
Nox1 RQ to PPIA
vs 20-week Male WT
4
3
2
1
0
X̄ΔCt
10.4
X̄ΔCt
10.0
X̄ΔCt
10.0
X̄ΔCt
9.2
20
35
20
35
weeks
WT
NOX5

B

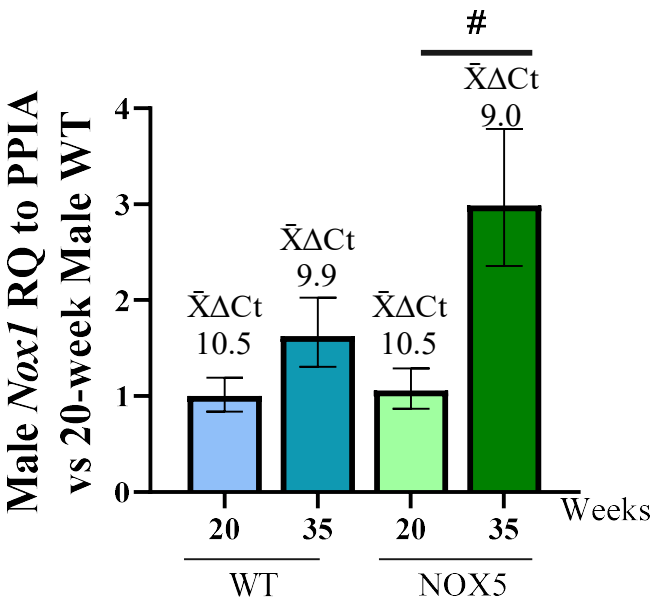
#
Male Nox1 RQ to PPIA
vs 20-week Male WT
4
3
2
1
0
X̄ΔCt
10.5
X̄ΔCt
9.9
X̄ΔCt
10.5
X̄ΔCt
9.0
20
35
20
35
Weeks
WT
NOX5

C

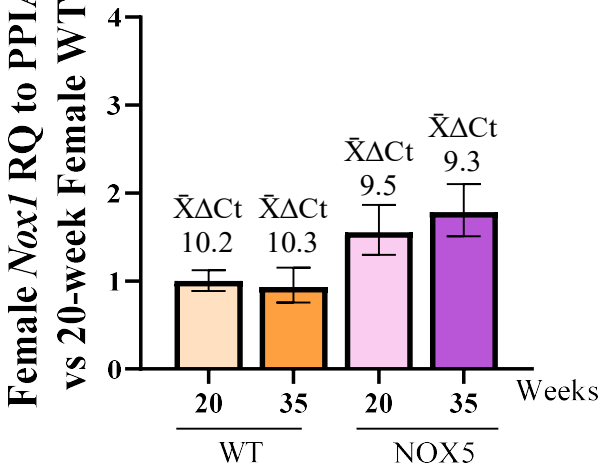
Female Nox1 RQ to PPIA
vs 20-week Female WT
4
3
2
1
0
X̄ΔCt
10.2
X̄ΔCt
10.3
X̄ΔCt
9.5
X̄ΔCt
9.3
20
35
20
35
Weeks
WT
NOX5

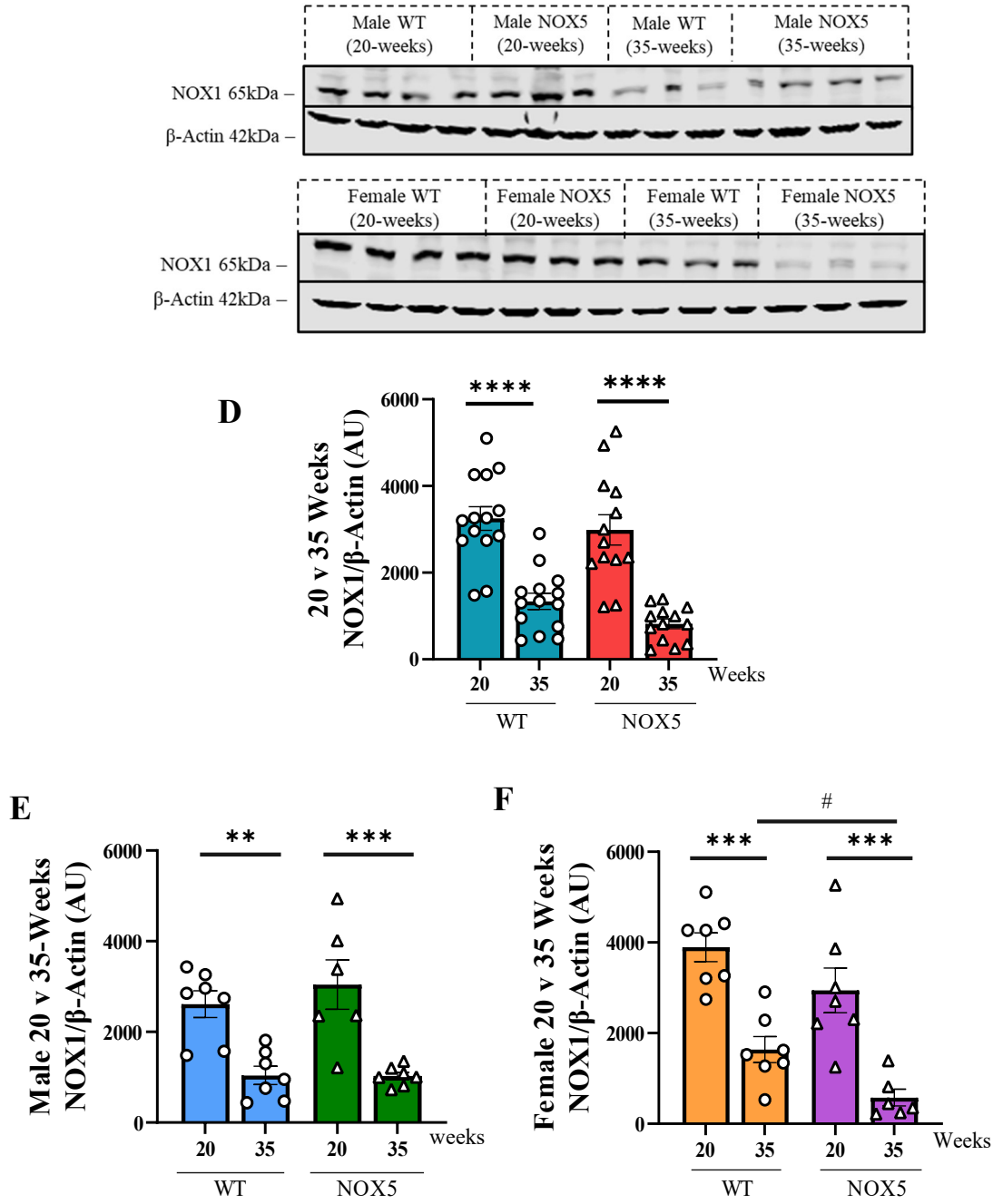

Figure 4-6. Assessment of NOX1 protein and gene expression in the brains of male and female VSMC-specific NOX5 mice the context of age. (**A-C**) *Nox1* mRNA expression or (**D-F**) NOX1 protein and was assessed in whole brain homogenates from male and female WT and VSMC-NOX5 mice aged 20 or 35 weeks-old using q-RT PCR respectively or immunoblotting with anti-NOX1 antibodies respectively. (**A-C**) Gene expression was assessed by q-RT PCR with RQ fold change being calculated from ΔΔCt following *Ppia* housekeeping gene normalisation. Representative immunoblots are shown with molecular masses indicated (**D-F**) Quantification of NOX1 levels is presented as AU after normalisation to β-actin. Mixed sex data n=13-14, male data n=5-7, female data n=5-7 per genotype. Data was analysed using a two-way ANOVA with a Tukey's *post*-hoc test, **p≤0.01, ***p≤0.001, *p<0.0001****. Further analysis was conducted using a student's *t*-test, #p≤0.05.

4.3.7 NOX2 Protein and Gene Expression Levels in the Brains of 20- and 35-week-old Male and Female VSMC-specific NOX5 Mice

NOX2 mRNA and protein expression was assessed in whole brain lysates of 20- and 35-week-old male and female WT and VSMC-NOX5 mice using q-RT PCR and immunoblotting and were assessed collectively and separately by sex. *Nox2* mRNA expression identified no changes in mixed sex (**Figure 4-7A**) or male analysis (**Figure 4-7B**). However, *Nox2* mRNA expression increased in 35-week-old female VSMC-NOX5 mice (**Figure 4-7C**) when compared to 20-week-old female NOX5 mice (female 35-week NOX5 8.73±0.25 ΔCt vs female 20-week NOX5 9.73±0.28 ΔCt p=0.02#). Mixed sex analysis of NOX2 protein levels (**Figure 4-7D**) identified a significant increase with age in VSMC-NOX5 mice (20-week NOX5 134250±20315 AU vs 35-week NOX5 214539±11702 AU p=0.008**). In males (**Figure 4-7E**), NOX2 protein expression in 35-week-old VSMC-NOX5 mice was increased when compared to 20-week-old VSMC-NOX5 mice (20-week NOX5 136414±9956 AU vs 35-week NOX5 219571±15270 AU p=0.009**). Female cerebral NOX2 protein levels were increased in 35-week-old WT mice when compared to 20-week-old WT mice (20-week WT (AU) 145000±12711 vs 35-week WT (AU) 256143±36904 p=0.02#), with no changes being identified between 20- and 35-week-old VSMC-NOX5 mice in females (**Figure 4-7F**).

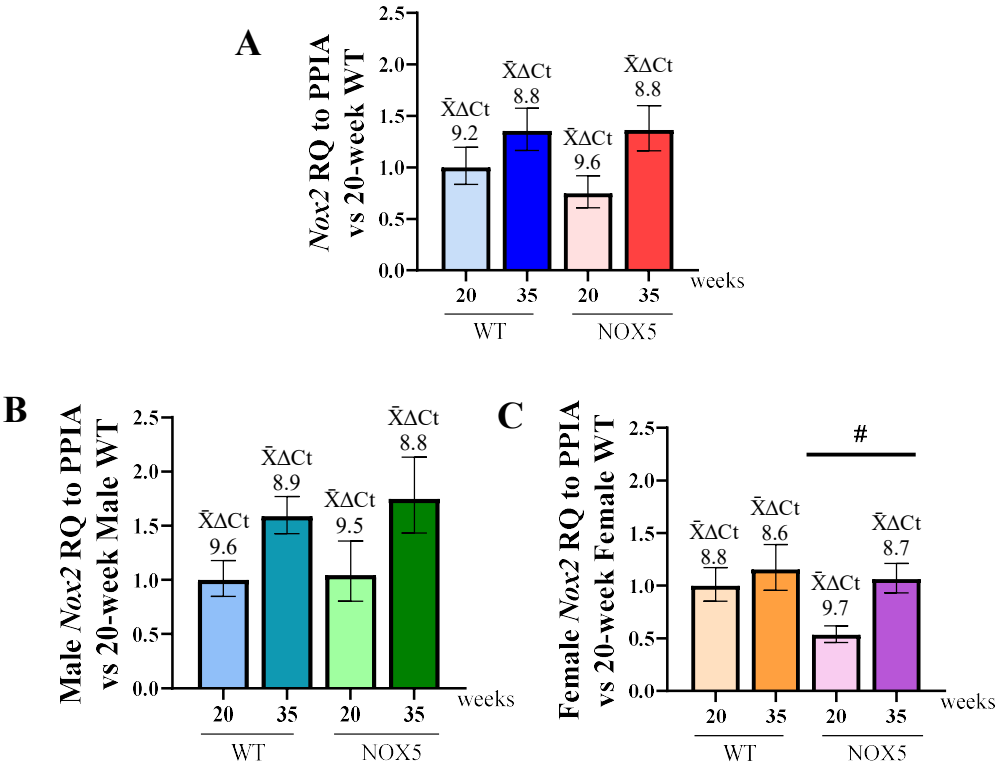

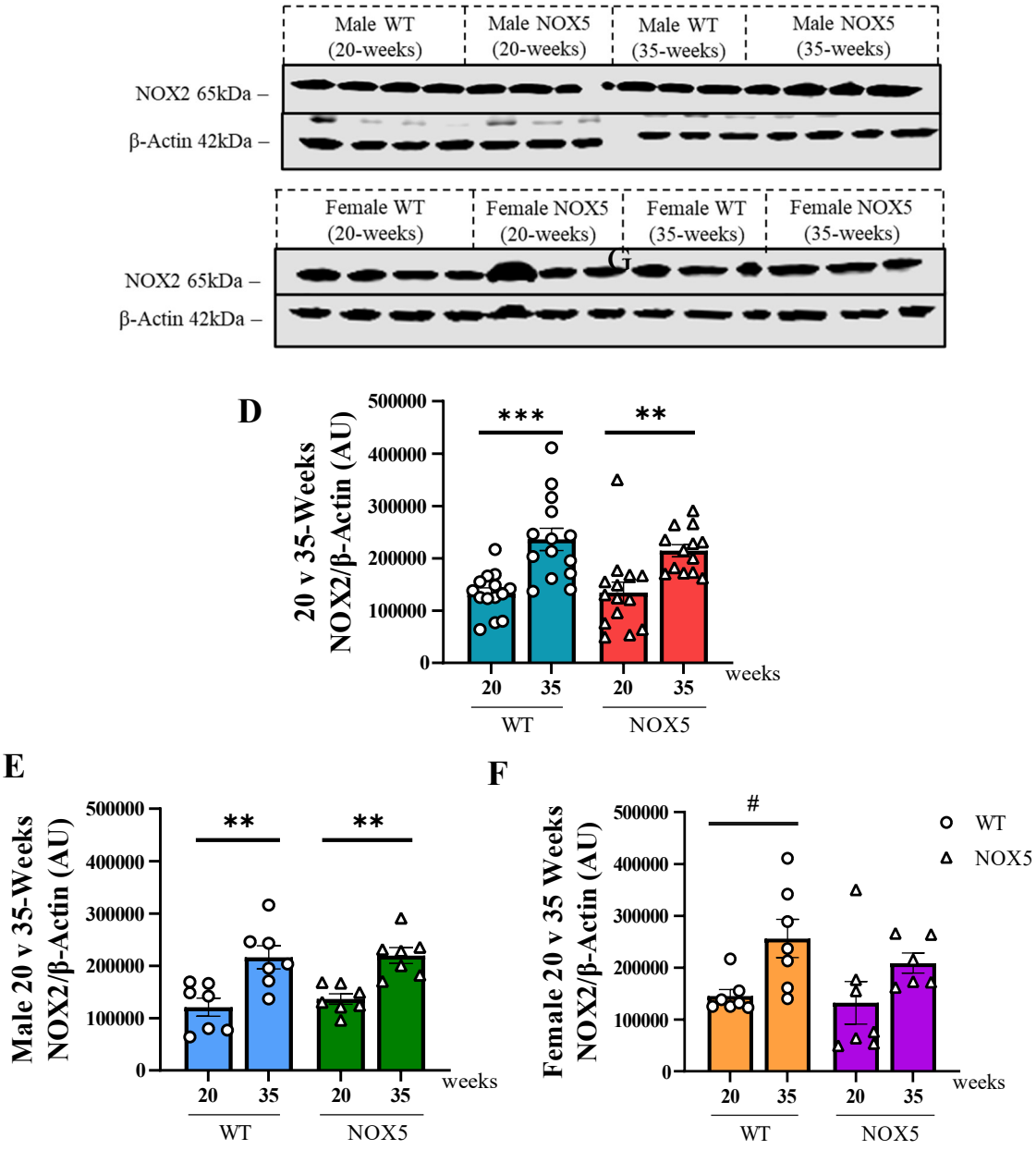

Figure 4-7. Assessment of NOX2 protein and gene expression in the brains of male and female VSMC-specific NOX5 mice the context of age. NOX2 mRNA and protein expression was assessed in whole brain homogenates of male and female WT and VSMC-NOX5 mice at 20- and 35-week-olds-old using q-RT-PCR (**A-C**) and immunoblotting (**D-F**) respectively. Immunoblotting studies were presented as AU after normalisation to β-actin. Gene expression was assessed by q-RT PCR with RQ fold change being calculated from ΔΔCt following *Ppia* housekeeping gene normalisation. Mixed sex data n=12-14, male data n=6-7, female data n=6-7 per genotype. Data was analysed using a two-way ANOVA with a Tukey's *post*-hoc test and presented as **p≤0.01 and ***p≤0.001. Further analysis was conducted using a student's t-test and were presented as #p≤0.05.

4.3.8 Cerebral Assessment of NOX4 Protein and Gene Expression Levels in 20- and 35-week-old Male and Female VSMC-specific NOX5 Mice

Here this study aimed to assess whether modulation of VSMC-NOX5 would alter NOX4 mRNA expression and protein levels with age. Whole brain lysates were extracted from 20- and 35-week-old male and female WT and VSMC-NOX5 mice and were assessed by q-RT PCR and immunoblotting. Assessment of cerebral *Nox4* mRNA expression identified no changes collectively and no sex differences were discovered when assessing VSMC-NOX5 mice in the context of ageing (**Figures 4-8A-C**).

Examination of NOX4 protein levels identified no changes collectively (**Figure 4-8E**) or in male (**Figure 4-8F**) VSMC-NOX5 mice when assessing age. However, 35-week-old female VSMC-NOX5 mice were identified to have decreased NOX4 protein levels when compared to 35-week-old female WT mice (Female 35-week VSMC-NOX5 (AU) 30017±4409 vs Female 35-week WT (AU) 57271±4686 p=0.03*) (**Figure 4-8G**).

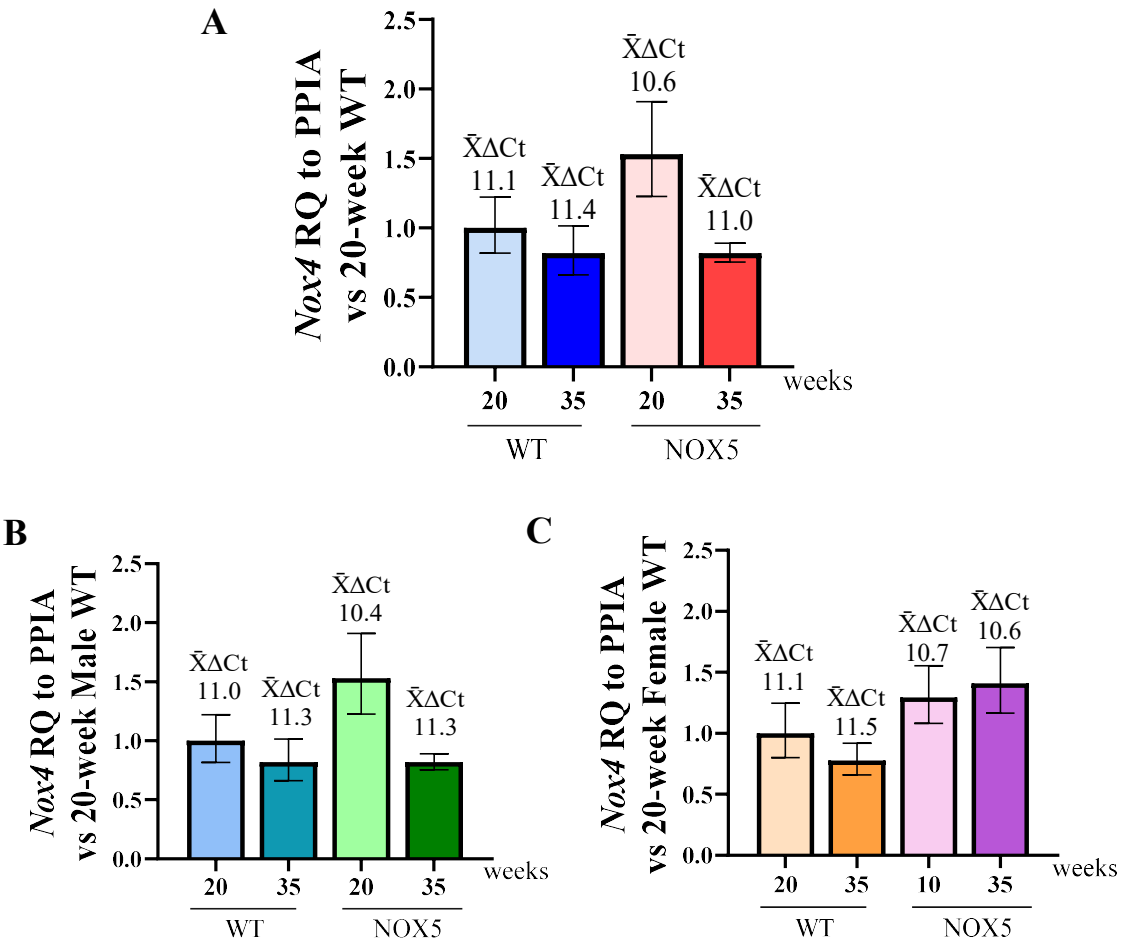

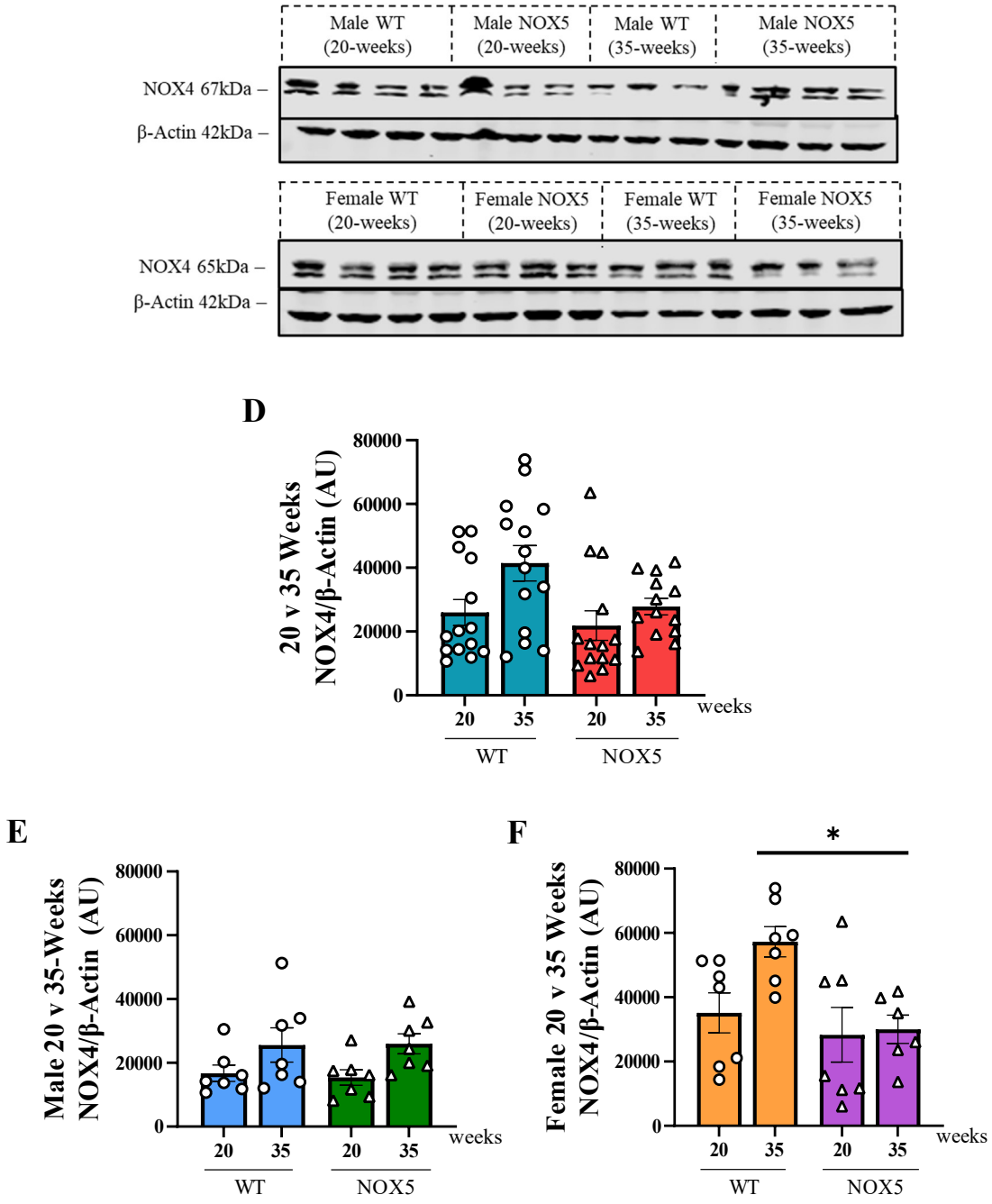

Figure 4-8. Assessment of NOX4 protein and gene expression in the brains of male and female VSMC-specific NOX5 mice the context of age. NOX4 mRNA and protein expression was assessed collectively and in male and female WT and VSMC-NOX5 mouse brain homogenates at 20- and 35-week-old mice using q-RT PCR (**A-C**) immunoblotting (**D-F**). Immunoblotting studies were presented as AU after normalisation to β-actin. Gene expression was assessed by q-RT PCR with RQ fold change being calculated from ΔΔCt following *Ppia* housekeeping gene normalisation. Mixed sex data n=11-14, male data n=5-7, female data n=6-7 per genotype. Data was analysed using a two-way ANOVA with a Tukey's *post*-hoc test and presented as *p≤0.05.

4.3.9 Wire Myography Assessment of Carotid Artery Endothelial-Independent Vasorelaxation in Male and Female VSMC-NOX5 Mice in the Context of Vascular Ageing.

In chapter 3 of this thesis, it was identified that 20-weeks-old, mice expressing VSMC-specific NOX5 have impaired carotid artery endothelial-independent vasorelaxation. VSMC dysfunction was only observed in male, but not female VSMC-NOX5 mice. Ageing, as well as VSMC-NOX5 are important contributors to vascular dysfunction. Here, in chapter 4 this thesis examined whether the effects of VSMC-NOX5 in vascular function is exacerbated by ageing. SNP-mediated endothelial-independent vasorelaxation in mixed sex samples (**Figure 4-9A**) identified an increase in vasorelaxation in 35-week-old VSMC-NOX5 when compared to their 20-week-old counterparts (Emax: 35-week NOX5 74.7%±3.22% vs 20-week NOX5 61.5%±2.63% p=0.0006***).

Assessment of vasorelaxation in the carotid arteries of male 35-week-old VSMC-NOX5 mice identified a significant decrease in SNP-mediated endothelial independent vasorelaxation than their 20-week-old counterparts (Emax: 35-week male NOX5 67.8%±1.96% vs 20-week male NOX5 84.5%±1.95% p=≤0.0001****). This study also identified a significant decrease in SNP-mediated vasorelaxation in male 35-week-old WT when compared to 20-week-old WT mice (Emax: 35-week male WT 62.4%±3.22% vs 20-week male WT 80.3%±4.04% p=0.0028***) (**Figure 4-9B**).

When carotid arteries were assessed in 20- and 35-week-old female WT and VSMC-NOX5 mice, no changes were identified with age in the WT genotype, however, SNP relaxation was significantly increased with age in 35-week-old female VSMC-NOX5 mice, when compared to their 20-week-old counterparts (Emax: 35-week female NOX5 83.1%±3.71% vs 20-week female NOX5 60%±4.39% p=0.0021***) (**Figure 4-9C**).

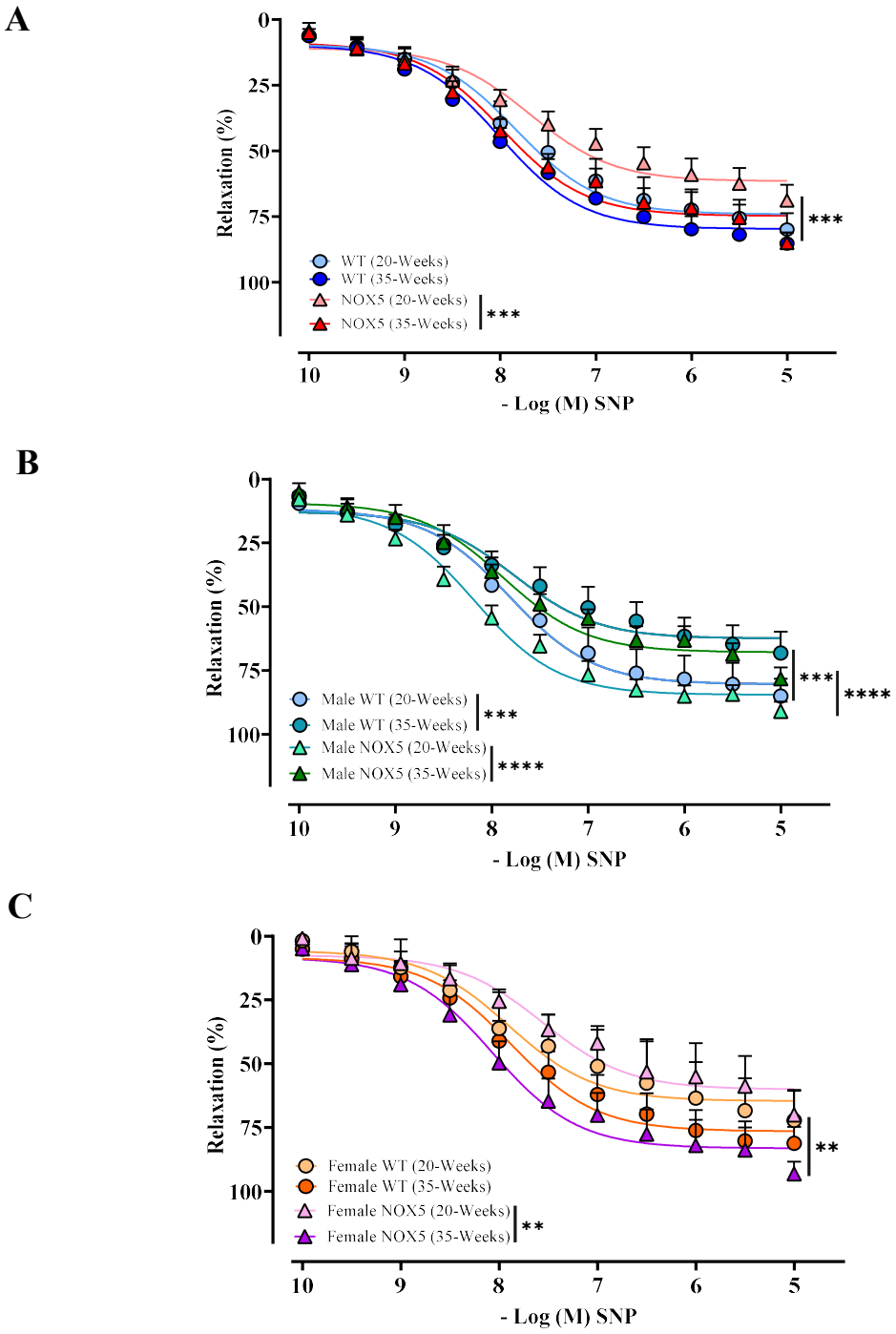

Figure 4-9. Endothelial-independent vasorelaxation in 20- vs 35-week-old male and female VSMC-specific NOX5-KI mice. Assessment of vascular reactivity was conducted using isolated carotid arteries from male and female WT and VSMC-NOX5 mice at 20- and 35-week-olds. Endothelial-independent vasorelaxation (**A-C**) was assessed by CCRC. SNP was used to assess endothelial-independent relaxation after U46619 pre-constriction. Results were presented as a percentage of relaxation relative to maximum relaxation. Mixed sex data n=8-11, male data n=5-7, female data n=6-7 per genotype. Myography data was analysed using a non-linear regression model and extra sum-of-squares *F*-test and was presented as **p≤0.01, ***p≤0.001, ****p≤0.0001.

4.3.10 Wire Myography Assessment of Carotid Artery Contractility in Male and Female VSMC-NOX5 mice in the Context of Vascular Ageing.

In chapter 3, no differences were observed in U-46619-mediated vascular contraction in carotid arteries. Here in chapter4, carotid artery contraction was observed in aged VSMC-specific NOX5 mice. Firstly, a significant increase in U-46619-mediated contraction in 35-week-old VSMC-NOX5 mice collectively, when compared to their 20-week-old counterparts (Emax: 35-week NOX5 4.30±0.29mN vs 35-week WT 3.36±0.41mN p=0.0008***). Furthermore, assessment of aged WT mouse carotid arteries identified decreased U46619 contraction compared to their 20-week-old WT mice (Emax: 35-week WT 3.36±0.41mN vs 20-week WT 4.3±0.37mN p=0.0003***) (**Figure 4-10A**).

Assessment of U46619-contraction in males identified a significant increase in contractility of VSMC-NOX5 mice when compared to 35-week-old male WT mice (Emax: 35-week NOX5 5.08±0.17mN vs 35-week WT 3.37±0.52mN p=<0.0001****). Additionally, this study also identified a significant difference in U46619-mediated contractility between 20-week-old- and 35-week-old male WT mice (Emax: 35-week male WT 3.37±0.52mN vs 20-week WT 4.78±0.58mN p=0.0007***) **Figure 4-10B**).

No differences were identified when assessing contractility of carotid arteries in 20-week-old- and 35-week-old female WT and VSMC-NOX5 mice (**Figure 4-10C**).

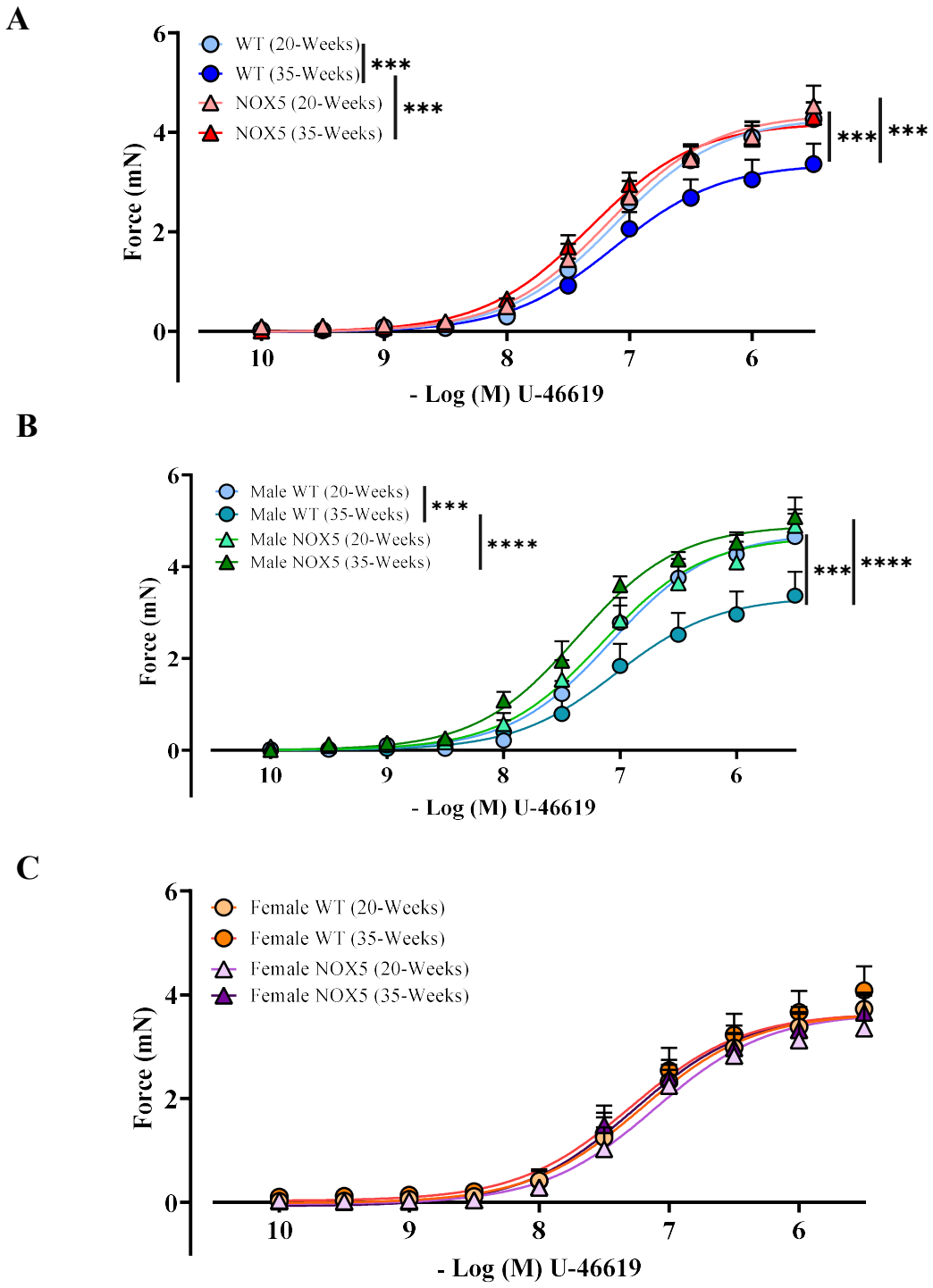

Figure 4-10. Assessment of ageing on contractility of carotid arteries in male and female VSMC-specific NOX5 mice. Assessment of vascular reactivity was conducted using isolated carotid arteries from male and female WT and VSMC-NOX5 mice at 20- and 35-week-olds. U46619-mediated vasoconstriction (**A-C**) was assessed by CCRC. U46619-mediated vasoconstriction results were presented as maximal response to basal levels. Results presented as a percentage of relaxation relative to maximum relaxation. Mixed sex data n=9-12, male data n=5-7, female data n=4-6 per genotype. Myography data was analysed using a non-linear regression model and extra sum-of-squares *F*-test and was presented as ***p≤0.001, ****p≤0.0001.

4.3.11 Cerebrovascular NOTCH3 Protein and Gene Expression Assessment in Male and Female VSMC-NOX5 Mice in the Context of Vascular Ageing.

To assess whether NOTCH3 mRNA and protein levels were altered in VSMC-NOX5 mice in the context of ageing, protein and RNA were isolated from whole brain homogenates of WT and VSMC-NOX5 mice aged 20- and 35-weeks-old. Immunoblotting and q-RT PCR were utilised to assess protein levels and mRNA expression respectively. As described previously in Chapter 3, *Notch3* mRNA expression was reduced in female VSMC-NOX5 mice relative to WT mice. Mixed sex analysis of *Notch3* mRNA expression significantly increased with age in VSMC-NOX5 mice (35-week NOX5 5.1±0.18 ΔCt vs 20-week NOX5 5.9±0.17 ΔCt p=0.001**) (**Figure 4-11A**).

When sexes were separated, *Notch3* mRNA levels were increased with age in male VSMC-specific NOX5 mice (35-week male NOX5 4.7±0.17 ΔCt vs 20-week male NOX5 5.7±0.28 ΔCt p=0.02*). Furthermore, *Notch3* expression was significantly increased in 35-week-old male VSMC-NOX5 mice relative to WT mice (35-week male WT 4.7±0.41 ΔCt vs 35-week male NOX5 5.4±0.2 ΔCt p=0.05# respectively). Age had no effect on *Notch3* expression in male WT mice (**Figure 4-11B**).

In females, *Notch3* mRNA expression was increased between 20-week-old female NOX5 and 20-week-old female WT mice (20-week Female NOX5 6.2±0.19 ΔCt vs 20-week Female WT 5.3±0.19 ΔCt p=0.006**. Additionally, 35-week-old VSMC-NOX5 mice (35-week male NOX5 5.5±0.22 ΔCt vs 20-week male NOX5 6.2±0.19 ΔCt p=0.04#) when compared to 20-week-old VSMC-NOX5 mice (**Figure 4-11C**).

Assessment of full-length NOTCH3 protein expression was normalised to β-actin (**Figures 4-11D-F**). Neither genotype nor age had any significant effect on full-length NOTCH3 levels.

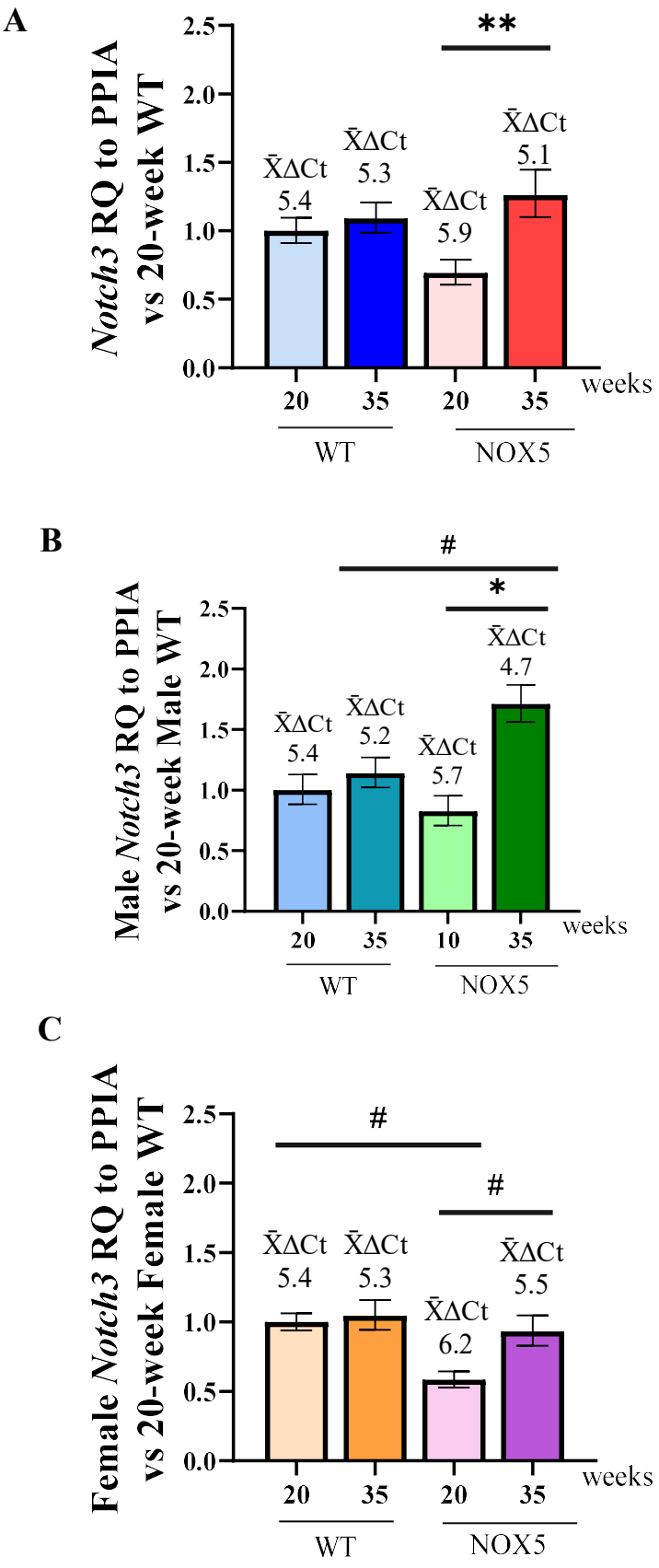
A
Notch3 RQ to PPIA
vs 20-week WT
2.5
2.0
1.5
1.0
0.5
0.0
**
X̄ΔCt
5.4
X̄ΔCt
5.3
X̄ΔCt
5.9
X̄ΔCt
5.1
20
35
20
35
weeks
WT
NOX5
B
Male Notch3 RQ to PPIA
vs 20-week Male WT
#
*
X̄ΔCt
5.4
X̄ΔCt
5.2
X̄ΔCt
5.7
X̄ΔCt
4.7
20
35
10
35
weeks
WT
NOX5
C
Female Notch3 RQ to PPIA
vs 20-week Female WT
#
#
X̄ΔCt
5.4
X̄ΔCt
5.3
X̄ΔCt
6.2
X̄ΔCt
5.5
20
35
20
35
weeks
WT
NOX5

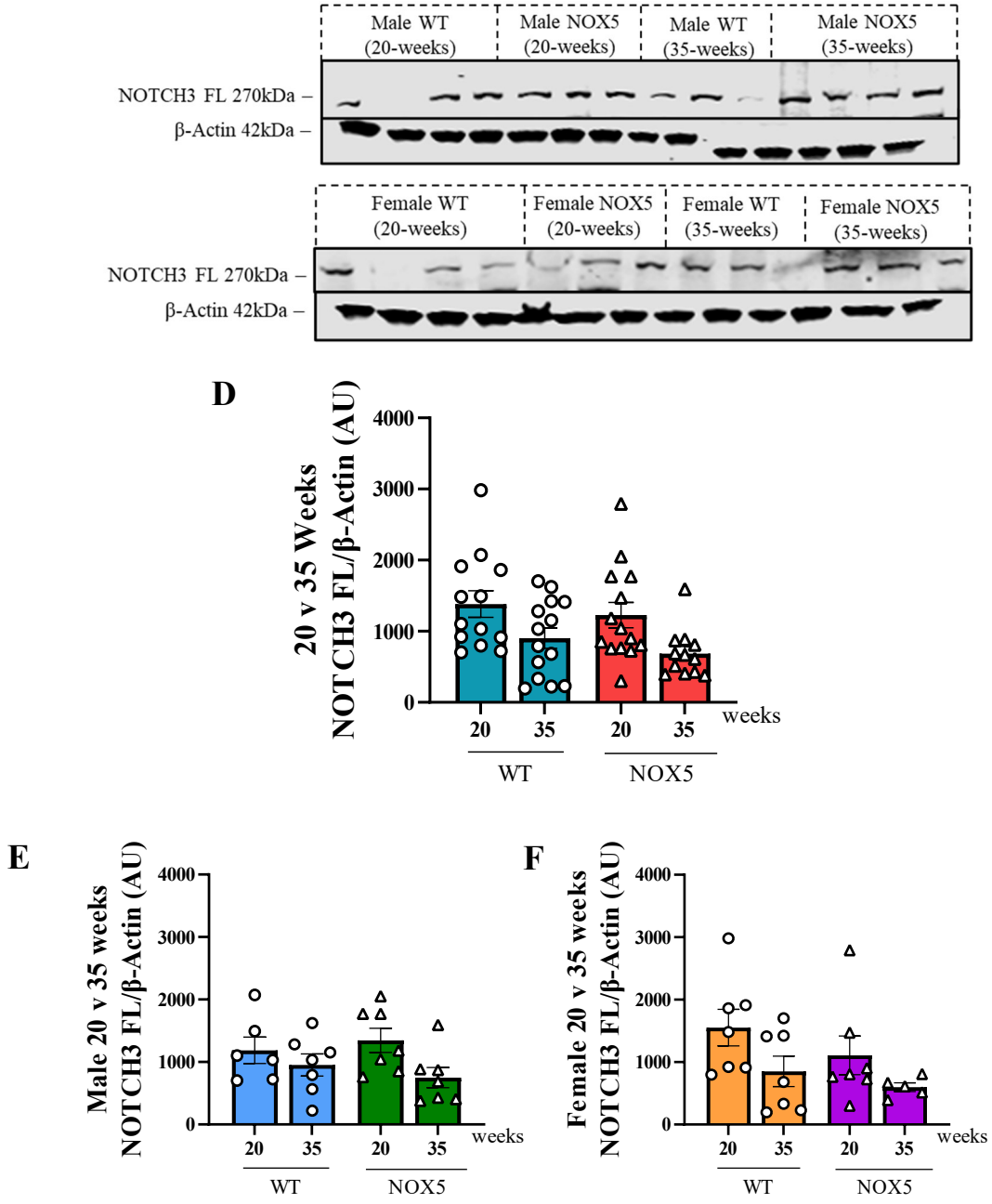

Figure 4-11. Gene and protein expression assessment of *Notch3* gene expression and NOTCH3 full-length protein levels cerebrovasculature of male and female VSMC-specific in the context of ageing. NOTCH3 mRNA and protein expression was assessed in whole brain homogenates of male and female WT and VSMC-NOX5 mice at 20- and 35-week-old age groups. *Notch3* mRNA expression was assessed by q-RT PCR with RQ fold change being calculated from ΔΔCt following *Ppia* housekeeping gene normalisation (**A-C**). Full-length NOTCH3 (**D-F**) protein expression was assessed by immunoblotting and were presented as AU after normalisation by β-actin. Mixed sex data n=11-14, male data n=6-7, female data n=5-7 per genotype. Data was analysed using a two-way ANOVA with a Tukey's *post*-hoc test and presented as *p≤0.05, **p≤0.01. Further analysis was conducted using a student's *t*-test and were presented as #p≤0.05.

4.3.12 Assessment of Cerebrovascular NOTCH3-ICD Protein Levels of Male and Female VSMC-NOX5 Mice in the Context of Vascular Ageing.

In chapter 3, assessment of NOTCH3-ICD in the brains of 20-week-old VSMC-NOX5 mice identified sex-dependent decreases in protein levels, whereby NOTCH3-ICD levels were reduced in female, but not male VSMC-NOX5 mice relative to WT. To assess whether this difference was impacted by age, the levels of NOTCH3-ICD were examined in 20- and 35-week-old WT and VSMC-specific VSMC-NOX5 mice. Whole brain homogenates were immunoblotted with antibodies specific to NOTCH3-ICD and normalised to β-actin levels. N3-ICD protein levels were significantly reduced with age in both VSMC-NOX5 (35-week-old VSMC-NOX5 4122±611 vs 20-week-old VSMC-NOX5 9426±769 p=<0.0001****), and WT (35-week WT 5088±658 AU vs 20-week WT 10998±705 p=<0.0001****) mice (**Figure 4-12A**).

This significant decrease in N3-ICD levels was also observed when male VSMC-NOX5 (35-week 2779±318 vs 20-week 9974±1442 p=0.0001***), and WT mice (35-week 9960±935 AU vs 20-week 4666±880 AU p=0.004**) were analysed separately (**Figure 4-12B**).

Assessment of female mice identified a significant decrease in NOTCH3 levels in 35-week WT mice (35-week 12036±958 AU vs 20-week 5510±1021 AU p=0.0001***) when compared to their 20-week-old counterparts. Subsequent analysis also identified a significant decrease in N3-ICD levels in 35-week-old VSMC-specific VSMC-NOX5 mice (35-week 5690±943 vs 20-week 8879±618 p=0.01#) when compared to 20-week-old VSMC-specific VSMC-NOX5 mice (**Figure 4-12C**).

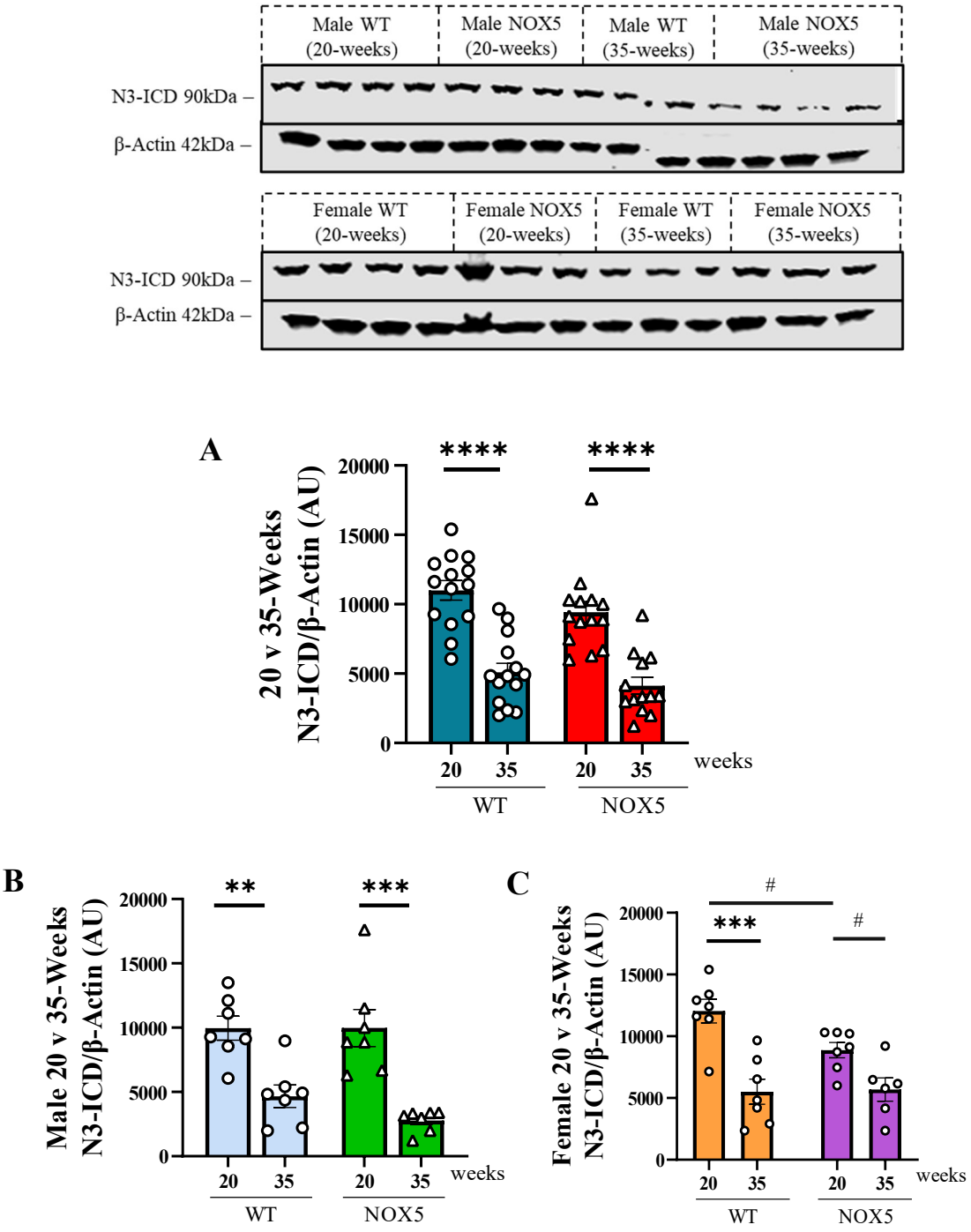

Figure 4.12. Assessment of cerebrovascular N3-ICD protein levels in male and female VSMC-specific in the context of ageing. N3-ICD protein expression was assessed in whole brain homogenates of male and female WT and VSMC-NOX5 mice at 20- and 35-week-old age groups. N3-ICD (**A-C**) protein expression was assessed by immunoblotting and were presented as AU after normalisation by β-actin. Mixed sex data n=13-14, male data n=7, female data n=6-7 per genotype data was analysed using a two-way ANOVA with a Tukey's *post*-hoc test and presented as **p≤0.01, ***p≤0.001, ****p≤0.0001. Further analysis was conducted using a student's *t*-test and were presented as #p≤0.05.

4.3.13 Cerebral NOTCH3 Downstream Effector *Hey1* and *HeyL* mRNA Expression Assessment in Male and Female 20- and 35-week-old VSMC-specific NOX5 Mice.

In chapter 3, no changes were observed in NOTCH3 downstream effector *Hey* genes despite reduced *Notch3* expression and reduced N3-ICD levels in female VSMC-NOX5 mice relative to WT. Given that age led to a downregulation of N3-ICD protein levels in both male and female WT and VSMC-NOX5 mice, (**Figure 4-12A-C**), it would therefore suggest that downstream NOTCH3 transcription targets *Hey* would be altered in mice. NOTCH3 downstream effector gene expression was assessed in 20- and 35-week-old WT and VSMC-NOX5 mice. RNA was isolated from whole brain homogenates of 20- and 35-week-old WT and VSMC-specific VSMC-NOX5 mice and q-RT PCR was utilised.

No changes were observed in *Hey1* (**Figure 4-13A**) mRNA expression when analysed in mixed-sex groups or separately by male mice (**Figures 4-13B**). However, female WT mice, *Hey1* was observed to be reduced in 35-week-old mice when compared to 20-week-old mice (20-week Female WT 3.1±0.17 ΔCt vs 35-week Female WT 3.6±0.2 ΔCt p=0.02#), with no changes were observed with ageing in female VSMC-NOX5 mice (**Figure 4-13C**). No changes were observed in cerebral *HeyL* mRNA expression in both male and female WT and VSMC-NOX5 mice in the context of ageing (**Figures 4-13D-F**).

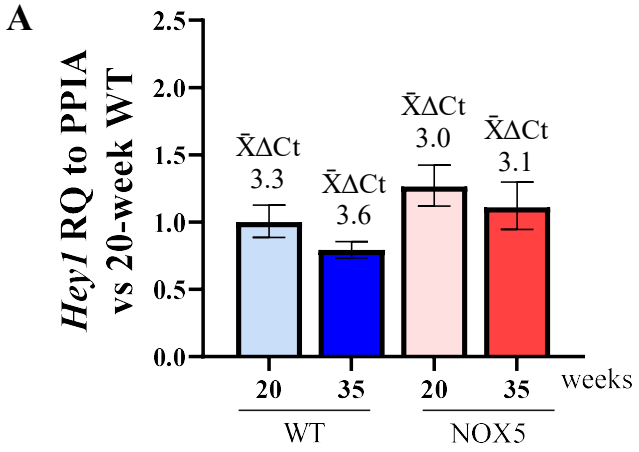

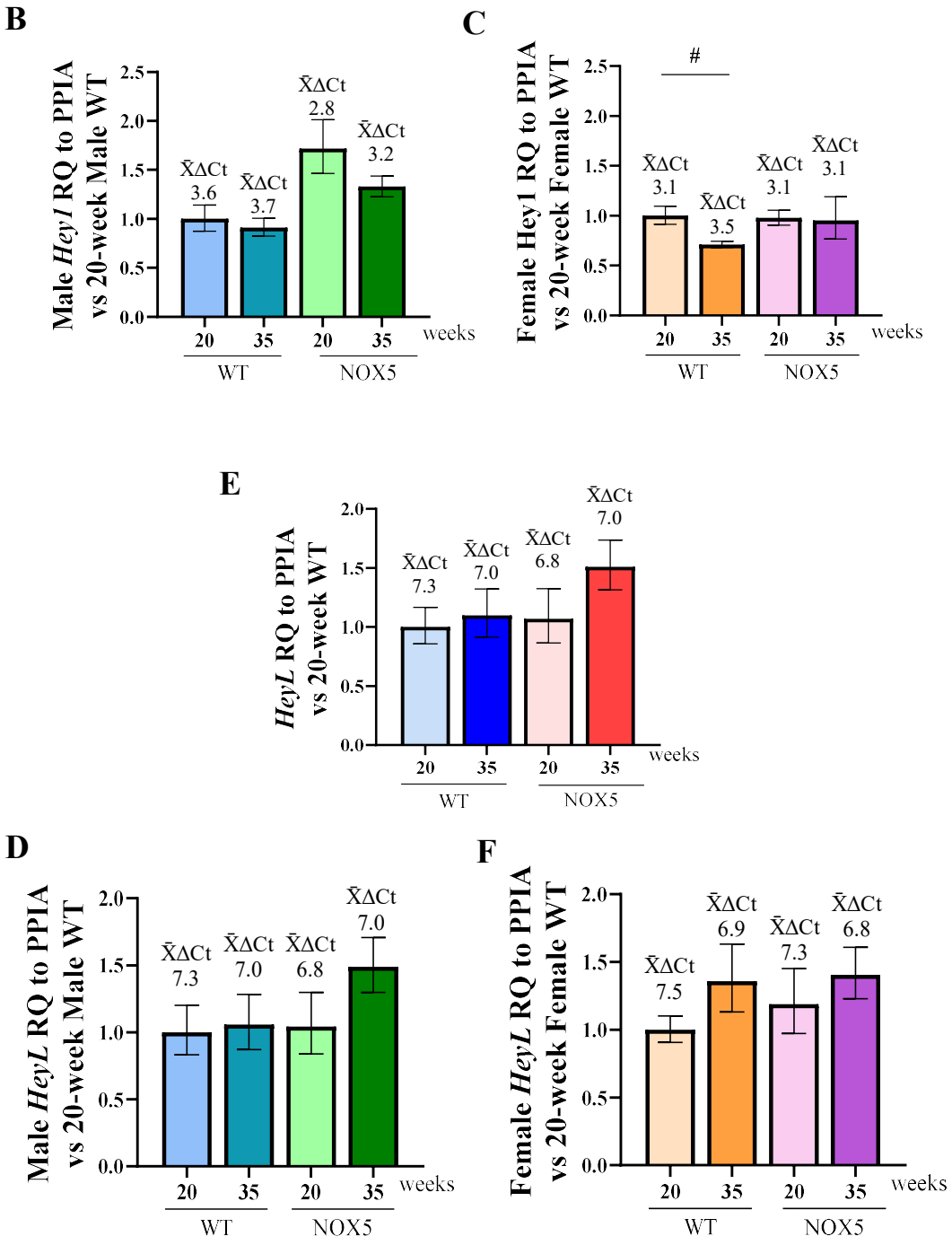

Figure 4-13. Assessment of NOTCH3 target *Hey1* and *HeyL* in the brains of male and female VSMC-specific in the context of ageing. NOTCH3 downstream effector mRNA expression was assessed in whole brain homogenates of male and female WT and VSMC-NOX5 mice at 20- and 35-week-old age groups. NOTCH3 downstream effector genes; *Hey1* (**A-C**), and *HeyL* (**D-F**), were examined using q-RT PCR and with RQ fold change being calculated from ΔΔCt following *Ppia* housekeeping gene normalisation. Mixed sex data n=8-14, male data n=4-7, female data n=4-7. Data was analysed using a student's *t*-test and were presented as #p≤0.05.

4.3.14 Cerebral NOTCH3 Downstream Effector *Hes1* and *Hes5* mRNA Expression Assessment in Male and Female 20- and 35-week-old VSMC-specific NOX5 Mice.

In chapter 3, no changes were observed in NOTCH3 downstream effector genes *Hes1* and *Hes5* despite reduced *Notch3* expression and reduced N3-ICD levels in female VSMC-NOX5 mice relative to WT. No changes were observed in cerebral *Hes1* expression in both male and female WT and VSMC-NOX5 mice in the context of ageing (**Figures 4-14A-C**). No changes were observed in when assessing *Hes5* in mixed sex (**Figure 4-14D**), or female analysis (**Figure 4-14F**). However, an observation of a *Hes5* mRNA upregulation was observed with age in male VSMC-NOX5 mice (35-week Male NOX5 5.9±0.29 ΔCt vs 20-week Male NOX5 6.7±0.29 ΔCt p=0.02#) when compared to their 20-week-old counterparts (**Figure 4-14E**).

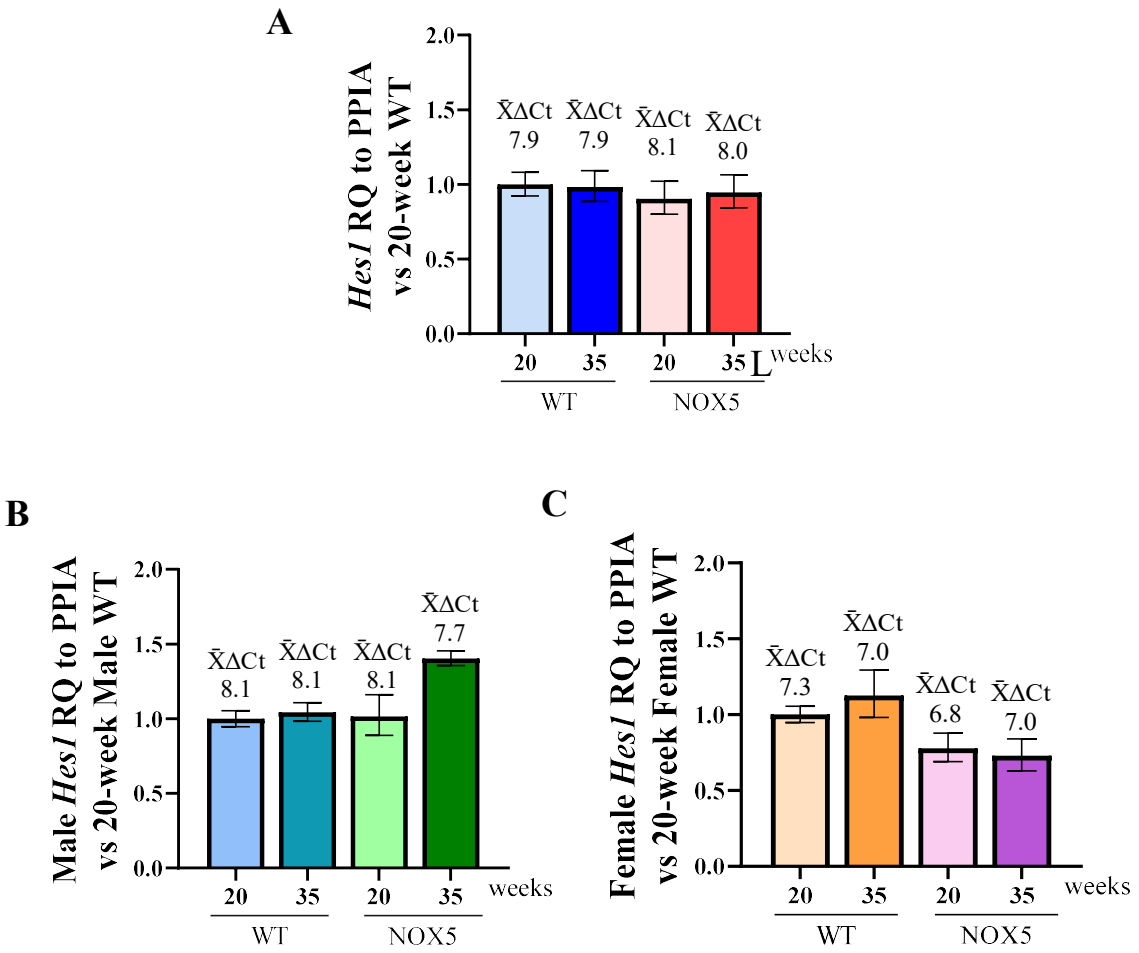

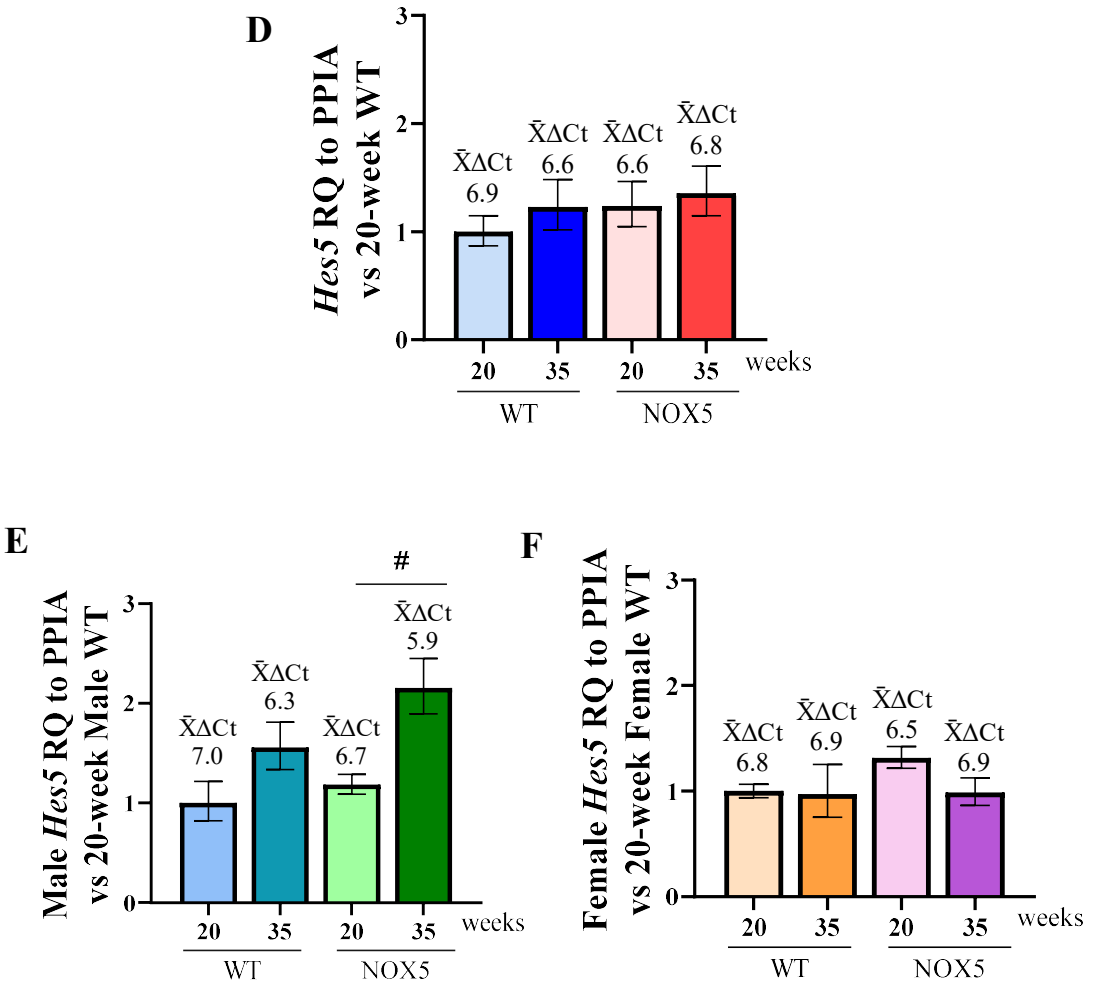

Figure 4-14. Assessment of NOTCH3 target *Hes1* and *Hes5* in the brains of male and female VSMC-specific in the context of ageing. NOTCH3 downstream effector mRNA expression was assessed in whole brain homogenates of male and female WT and VSMC-NOX5 mice at 20- and 35-week-old age groups. NOTCH3 downstream effector genes; *Hes1* (**A-C**), and *Hes5* (**D-F**), mRNA expression was assessed by q-RT PCR with RQ fold change being calculated from ΔΔCt following *Ppia* housekeeping gene normalisation. Mixed sex data n=8-14, male data n=4-7, female data n=4-7. Data was analysed using a student's *t*-test and were presented as #p≤0.05.

4.3.15 Assessment of H_2O_2 Levels by Amplex-Red in 20-week and 35-Week-old Male and Female VSMC-specific NOX5 Mice

Previously in Chapter 3 this study identified alterations in H_2O_2 production in male, but not female 20-week-old VSMC-NOX5 mice. This study aimed to assess whether ageing would lead to alterations in redox environment in whole brain lysates of aged VSMC-NOX5 mice, utilising Amplex-Red and TBARS-MDA. No changes in H_2O_2 were identified in mixed sex (**Figure 4-15A**), and female analysis (**Figures 4-15C**). between 20-week-old mice. However, H_2O_2 levels were found to be significantly increased in 20-week-old male VSMC-NOX5 mice when compared to 20-week-old WT mice (20-week Male NOX5 1.95±0.22 µg vs 20-week WT 1.49±0.39 µg p=0.03#) (**Figure4-15B**), Assessment of Amplex-Red identified no age-related changes in cerebral H_2O_2 levels when analysing mixed sex, male, or female VSMC-NOX5 at 35-weeks (**Figures 4-15A-C**)

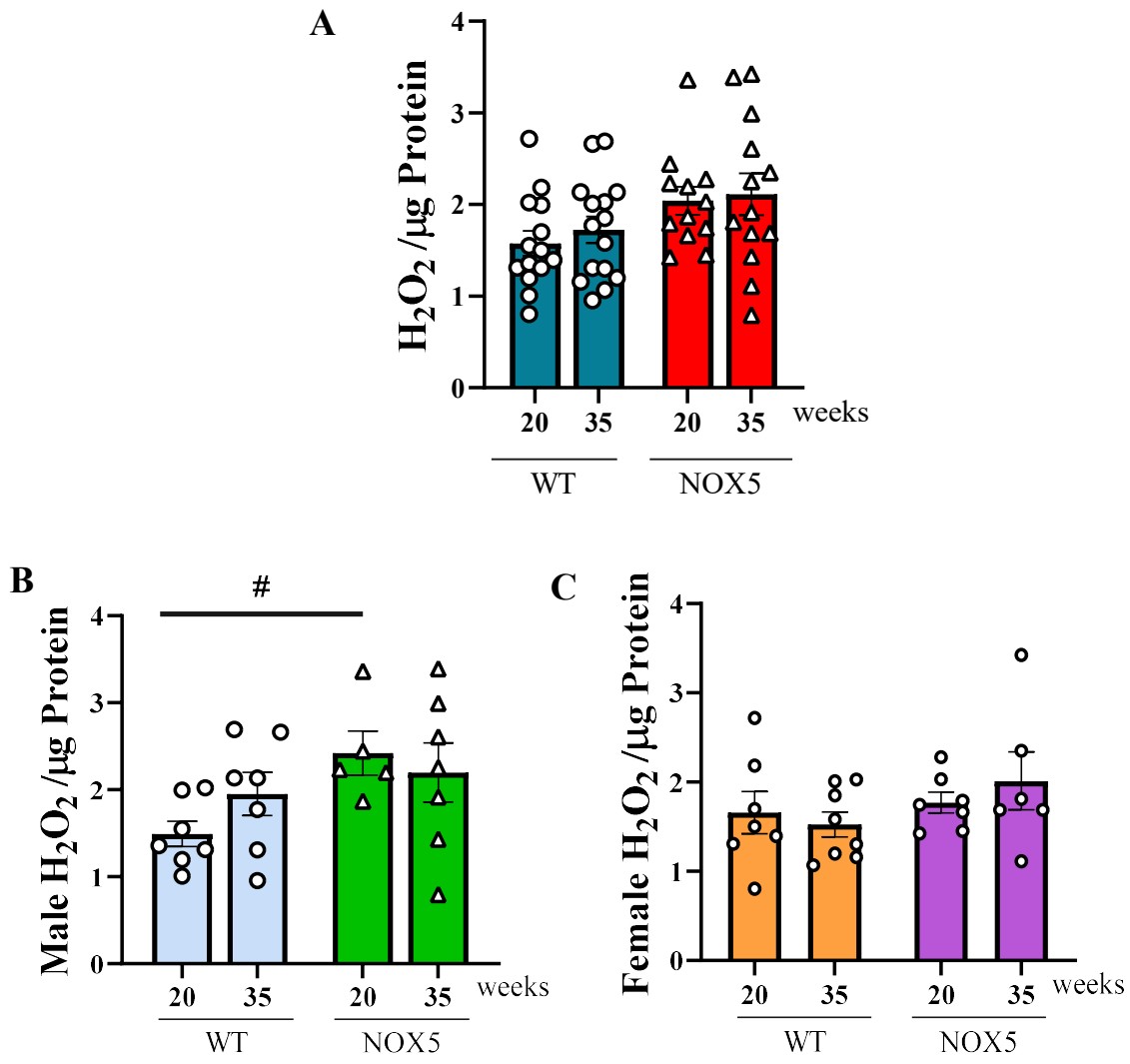

Figure 4-15. Hydrogen peroxide levels in 20- and 35-week-old male and female WT and VSMC-NOX5-KI mice. H_2O_2 levels were assessed in whole brain homogenates of male and female WT and VSMC-NOX5 mice at 20- and 35-week-olds using Amplex-Red (**A-C**). Amplex-Red experimental data was presented as µg and normalised over protein abundance. Mixed sex data n=12-15, male data n=5-7, female data n=6-7 per genotype. Data was analysed using a two-way ANOVA with a Tukey's *post*-hoc test. Further analysis was conducted using a student's *t*-test and were presented as #p≤0.05.

4.3.16 Assessment of Lipid peroxidation Levels by TBARS-MDA Assay in 20-week and 35-Week-old Male and Female VSMC-specific NOX5 Mice

Previously in chapter 3, no differences were identified when assessing lipid peroxidation levels in 20-week VSMC-specific mice. Ageing is a key risk factor for cerebrovascular disease and oxidative stress pathophysiology. Assessment of lipid peroxidation was assessed in whole brain homogenates of male and female WT and VSMC-NOX5 mice at 20- and 35-week-old age groups. Lipid peroxidation levels were increased collectively in mixed sex groups in both WT (35-week WT 7.9±0.30 µmol vs 20-week WT 3.5±0.33 µmol *p*=0.0001****) and VSMC-NOX5 mice (35-week NOX5 8.3±0.31µmol vs 20-week NOX5 3.8±0.31 µmol *p*=0.0001****) (**Figure 4-16A**).

When separated by sex, lipid peroxidation levels were increased in both male WT (male 35-week-old WT 7.7±0.36 µmol vs male 20-week-old WT 4.4±0.38 µmol p=0.0001****) and VSMC-NOX5 mice (male 35-week-old NOX5 8.28±0.55 µmol vs male 20-week-old NOX5 4.31±0.34 µmol p=0.0001****) (**Figure 4-16B**), and in female WT (35-week-old female WT 8.1±0.51 vs 20-week-old female WT 3.0±0.49 *p*=0.0001****) and VSMC-NOX5 (35-week-old female NOX5 8.31±0.36 vs 20-week-old female NOX5 3.3±0.42 *p*=0.0001****) when compared to their 20-week-old VSMC-NOX5 counterparts (**Figure 4-16C**).

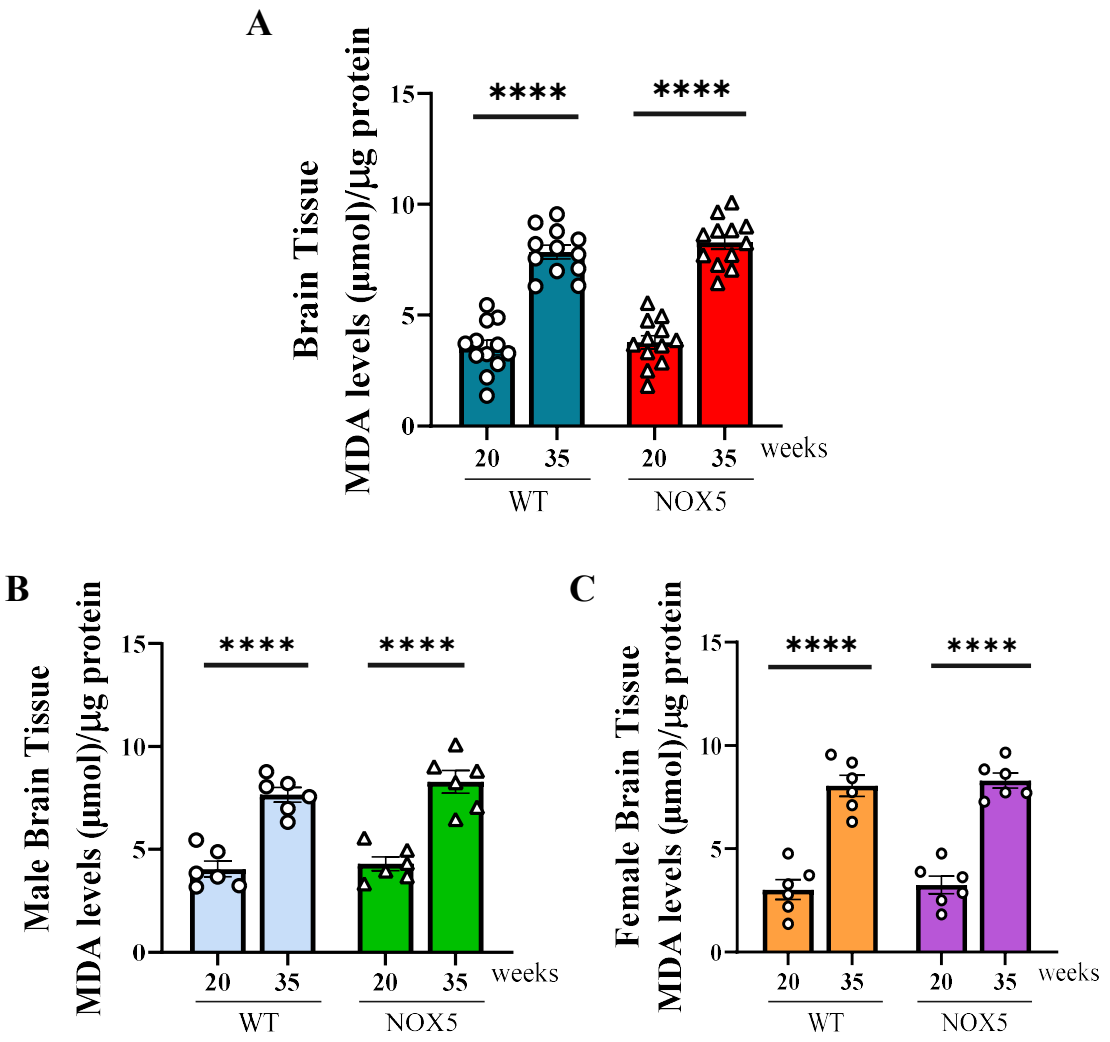

Figure 4-16. Lipid peroxidation levels in 20- and 35-week-old male and female WT and VSMC-NOX5-KI mice. Lipid peroxidation levels were assessed in whole brain homogenates of male and female WT and VSMC-NOX5 mice at 20- and 35-week-olds using TBARS-MDA assay (**A-C**). TBARS-MDA experiments were presented as µmol and normalised over protein abundance. Mixed sex data n=12, male data n=6, female data n=6 per genotype. Data was analysed using a two-way ANOVA with a Tukey's *post*-hoc test and presented as ****p≤0.0001.

4.3.17 Immunoblotting Assessment of Cerebral PTP-SO_3 Levels in 20- and 35-week-old Male and Female VSMC-NOX5 Mice

The research presented in Chapter 3 identified a reduction in PTP-SO_3 in female VSMC-NOX5 at 20-week-olds. Given that ageing is associated with an increased ROS and oxidative stress environment, this study aimed to assess markers of cerebral ROS and oxidative stress in male and female VSMC-NOX5 mice in the context of ageing. PTP-SO_3 oxidation was assessed by immunoblotting (**Figures 4-17A-I**).

In mixed sex groups, this study identified upregulated PTP-SO_3 protein levels when assessed at 20kDa MW in 35-week-old VSMC-NOX5 mice when compared to 20-week-old VSMC-specific mice (male 35-week-old VSMC-NOX5 36009±1954 AU vs male 20-week-old VSMC-NOX5 16868±1954 AU p=0.007**) (**Figure 4-17A**) Full membrane analysis of 35-week-old female VSMC identified a significant decrease in PTP-SO_3 expression when compared to female 35-week-old WT mice (female 35-week-old VSMC-NOX5 54900±8551 AU vs female 35-week-old WT 92686±10835 AU p=0.03*) (**Figure 4-17C**). No differences in full membrane PTP-SO_3 analysis were identified in male mice between age or genotype (**Figure 4-17B**).

Further analysis of PTP-SO_3 at 20kDa MW identified no changes in mixed sex, or male groups (**Figures 4-17D-E**). However, a significant increase in female WT and VSMC-NOX5 mice (female 35-week-old VSMC-NOX5 14006±2481AU vs female 20-week-old VSMC-NOX5 39270±9833 AU p=0.03*) (**Figure 4-17F**).

Examination of PTP-SO_3 at 75kDa MW showing a decrease in expression in 35-week-old WT mice compared to 20-week-old WT mice (35-week-old WT 7471±441 AU vs 20-week-old WT 9289±612 AU p=0.03*) (**Figure 4-17G**), Assessment of PTP-SO_3 levels in males showed a decrease in expression in 35-week-old WT mice compared to 20-week-old WT mice (male 35-week-old WT 6919±436 AU vs 20-week-old male WT 8887±668 AU p=0.03#) at 75kDa MW, with no changes being identified in VSMC-NOX5 mice (**Figure 4-17H**). No changes in PTP-SO_3 at 75kDa were identified in female VSMC-NOX5 mice with age (**Figure 4-17I**).

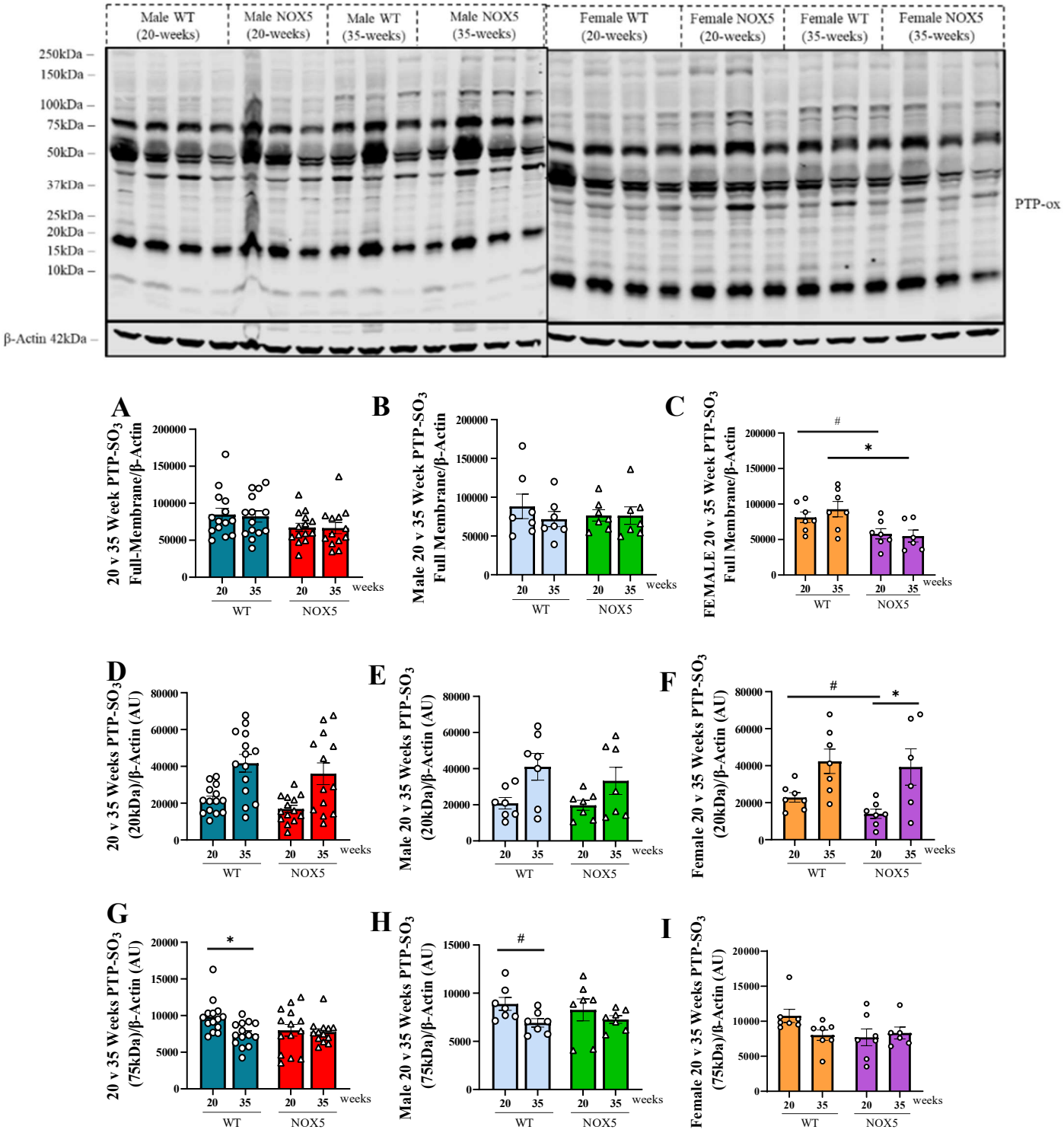

Figure 4-17. Immunoblotting of PTP-SO_3 in male and female 20- and 35-week-old VSMC-NOX5 mice. Oxidative stress marker PTP-SO_3 full membrane (**A-C**), 20kDa (**D-F**), and 75kDa (**G-I**) assessed by immunoblotting in whole brain homogenates of 20- and 35-week-old male and female WT and VSMC-NOX5 mice. Immunoblotting expression was normalised to β-actin and expressed as AU. Mixed sex data n=13-14, male data n=7, female data n=6-7 per genotype. Data was analysed using a two-way ANOVA with a Tukey's *post*-hoc test and presented as *p≤0.05, **p≤0.01. Further analysis was conducted using a student's *t*-test and were presented as #p≤0.05.

4.3.18 Immunoblotting Assessment of Cerebral PRDX-SO_3 Levels in 20- and 35-week-old Male and Female VSMC-NOX5 Mice

Previously in chapter 3, VSMC-specific NOX5 did lead to hyperoxidation of the antioxidant PRDX when assessed in the brains of 20-week-old mice. As antioxidant response is reduced with age and conversely oxidative modification becomes more prevalent, PRDX protein levels in the context of ageing was assessed. Mixed sex analysis of VSMC-NOX5 identified a significant decrease of PRDX-SO_3 protein levels in whole brain homogenates in 35-week-old VSMC-NOX5 mice, when compared to their 20-week-old counterparts (35-week VSMC-NOX5 4077±509 AU vs 20-week VSMC-NOX5 8733±1508 AU p=0.006**) (**Figure 4-18A**).

Separate analysis of male VSMC-NOX5 mice identified no changes with age. However, in 35-week-old male WT mice, PRDX-SO_3 protein expression was significantly reduced when compared to their younger counterparts (35-week Male WT 4720±717 AU vs 20-week Male WT 10033±2347 AU p=0.04#) (**Figure 4-18B**).

Female analysis identified a decrease in PRDX-SO_3 levels between 20-week-old NOX5 and WT mice (20-week Female NOX5 5740±843.77 AU vs 35-week Female WT 9811.43±1121.75 AU p=0.03*). Furthermore, cerebral PRDX-SO_3 was reduced with age in 35-week-old WT mice (20-week Female WT 9811.3±1121.749 AU vs 35-week Female WT 6194±811 AU p=0.03*) when compared to 20-week-old WT mice. Further analysis also identifying that NOX5 was reduced by age in females when compared to their 20-week-old counterparts (20-week Female NOX5 5740±843.77 AU vs 35-week Female NOX5 3326.67±645.42 AU p=0.046#).Comparisons between 35-week-old female WT and VSMCNOX5 mice also identified cerebral PRDX-SO_3 protein levels were reduced in VSMC-NOX5 mice (35-week Female NOX5 3326.67±645AU vs 35-week Female WT 6194±811 AU p=0.02#) (**Figure 4-18C**).

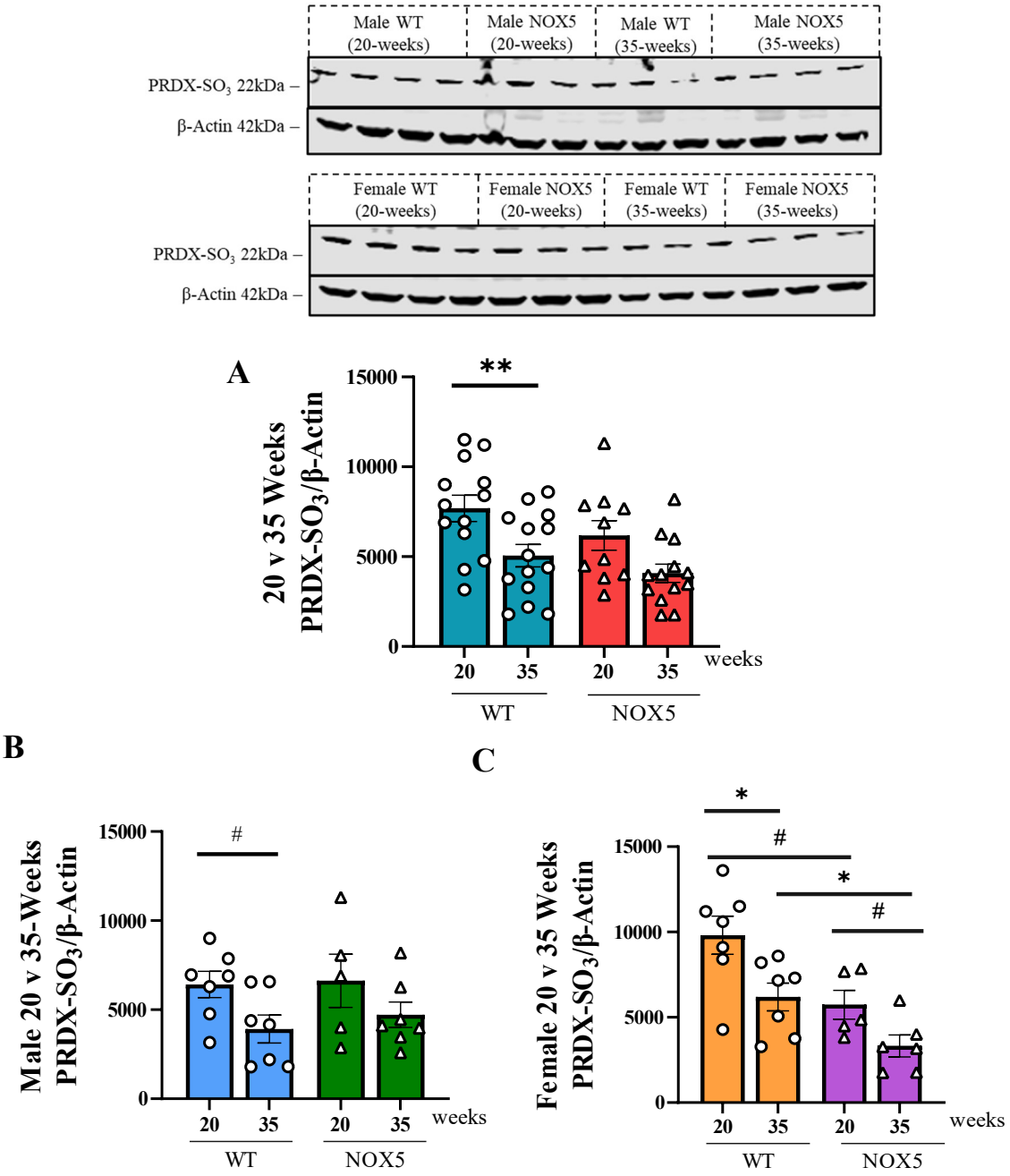

Figure 4-18. Immunoblotting of PRDX-SO_3 in male and female 20- and 35-week-old VSMC-NOX5 mice markers. Oxidative stress markers PRDX-SO_3 (**A-C**) was assessed by immunoblotting in whole brain homogenates of 20- and 35-week-old male and female WT and VSMC-NOX5 mice. Immunoblotting expression was normalised to β-actin and expressed as AU. Mixed sex data n=10-14, male data n=5-7, female data n=5-7 per genotype. Data was analysed using a two-way ANOVA with a Tukey's *post*-hoc test and presented as **p≤0.05 and **p≤0.01. Further analysis was conducted using a student's *t*-test and were presented as #p≤0.05.

4.3.19 Assessment of *Sod1* and *Sod2* Gene Expression in the Brains of 20- and 35-week Male and Female VSMC-NOX5 Mice

Antioxidants *Sod1* and *Sod2* genes play a critical role in the transcription of their respective proteins, acting to dismutase $O_2^{\bullet-}$ to H_2O_2. Ageing is associated with a decline in SOD function. *Sod1* and *Sod2*, expression was assessed in male and female VSMC-NOX5 mice in the context of ageing. Isolated mRNA was extracted from whole brain homogenates of 20- and 35-week-old WT and VSMC-NOX5 mice for q-RT PCR analysis. Assessment of *Sod1* (**Figures 4-19A-C**) identified no changes in expression collectively, or by sex, in 35-week-old VSMC-NOX5 mice. Mixed sex analysis of *Sod2* (**Figure 4-19D**) identified an increase in gene expression when comparing 35-week-old VSMC-NOX5 mice to 35-week-old WT mice (35-week NOX5 4.8±0.13 ΔCt vs 35-week WT 4.3±0.17 ΔCt p=0.03#). No changes in *Sod2* expression were between age or genotype groups in male or female VSMC-NOX5 mice (**Figures 4-19E-F**).

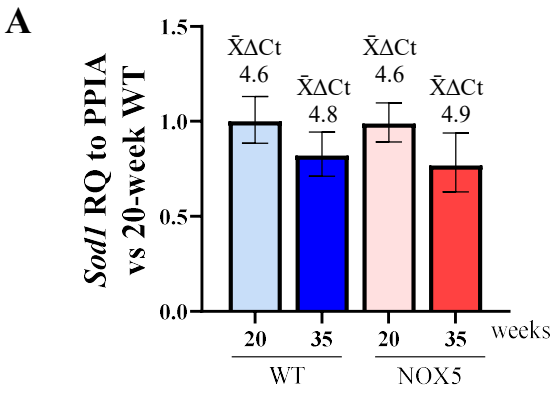

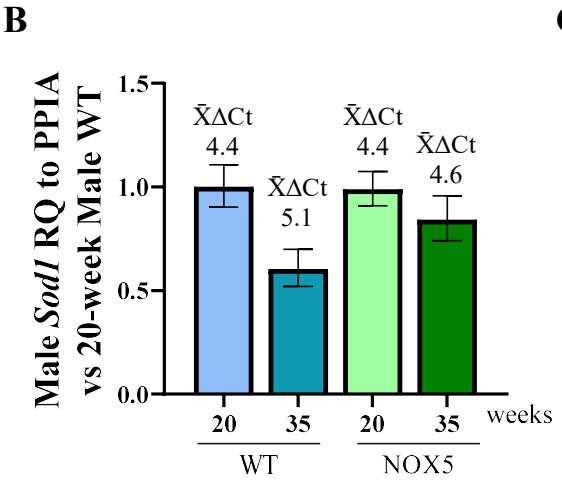

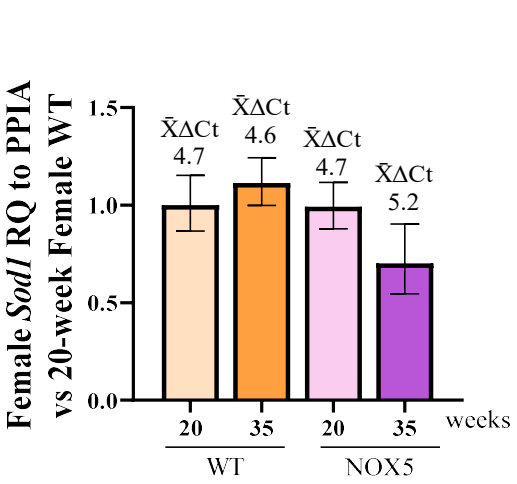

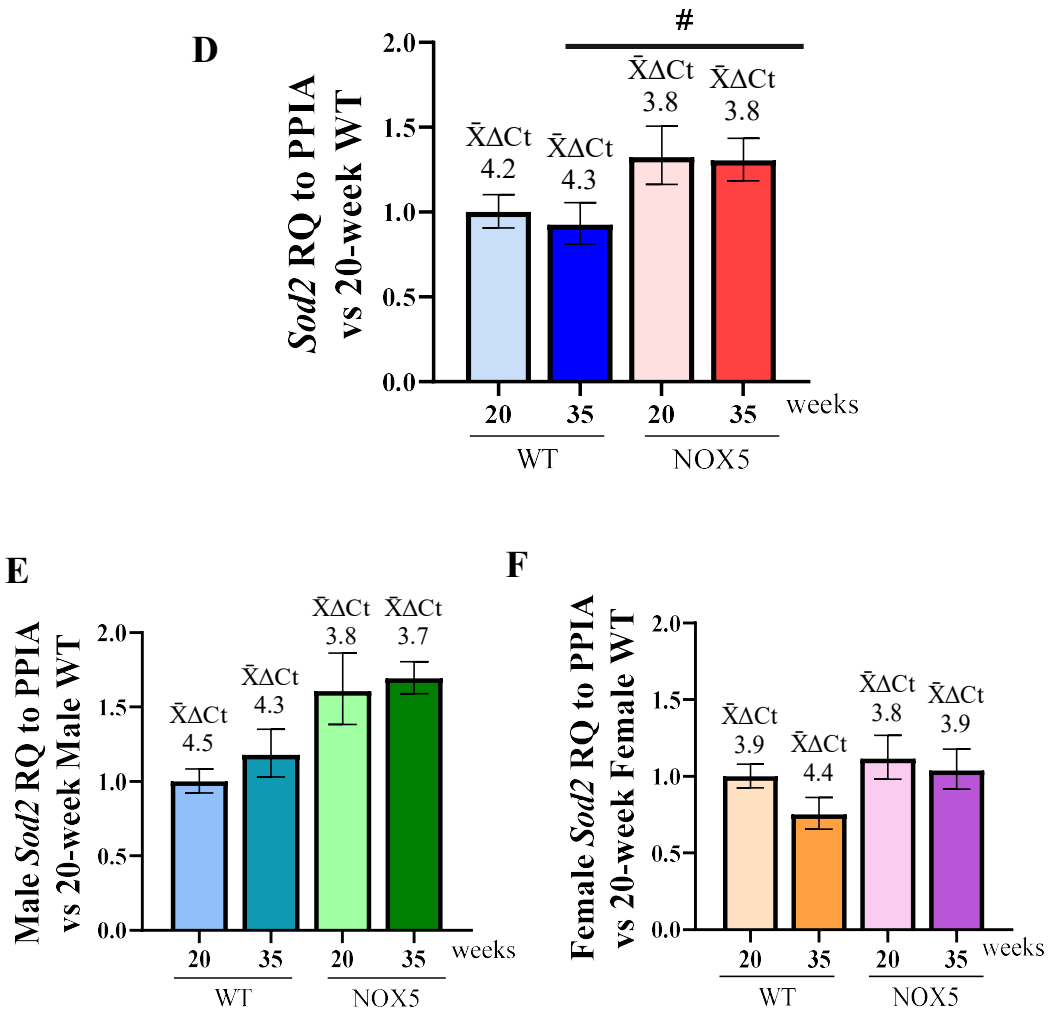

Figure 4-19. Assessment of *Sod1* and *Sod2* mRNA expression in male and female 20- and 35-week-old WT and VSMC-NOX5 mice. *Sod1* (**A-C**), *Sod2* (**D-F**) mRNA expression was assessed in whole brain lysates of 20- and 35-week-old male and female WT and VSMC-NOX5 mice using q-RT PCR. Levels of mRNA expression was assessed by q-RT PCR with RQ fold change being calculated from ΔΔCt following *Ppia* housekeeping gene normalisation. Mixed sex data n=11-12, male data n=5-6, female data n=6 per genotype. Data was analysed using a two-way ANOVA with a Tukey's *post*-hoc test. Further analysis was conducted using a student's *t*-test and were presented as #p≤0.05.

4.3.20 Cerebral Assessment of Antioxidant Response Element Genes *Nqo1*, *Ho1*, and *Catalase* mRNA Expression in 20- and 35-week Male and Female VSMC-NOX5 mice

Previously in chapter 3, *Catalase* mRNA expression was increased in the brains of 20-week-old VSMC-NOX5 mice. This study aimed to assess whether ageing would lead to cerebral alterations in *Nqo1, Ho1,* and *Catalase* mRNA expression in male and female VSMC-NOX5 mice. No changes were identified in, *Nqo1* (**Figures 4-20A-C)** between age, sex, or genotype.

Mixed sex assessment of *Ho1* identified a significant increase between 20-week VSMC-NOX5 (20-week NOX5 5.3±0.29 ΔCt vs 20-week WT 6.2±0.19 ΔCt p=0.02*) and WT mice (**Figure 4-20D**). No differences in *Ho1* gene expression were identified between age- or sex in VSMC-NOX5 and WT genotypes (**Figure 4-20E-F**).

Catalase mRNA expression identified an increase between 20-week VSMC-NOX5 (20-week NOX5 -0.78±0.34 ΔCt vs 20-week WT 0.06±0.17 ΔCt p=0.03#) and WT mice (**Figure 4-20G**) in mixed sex assessment. No differences in *Catalase* gene expression were identified between age- or sex in VSMC-NOX5 and WT genotypes (**Figure 4-20H-I**).

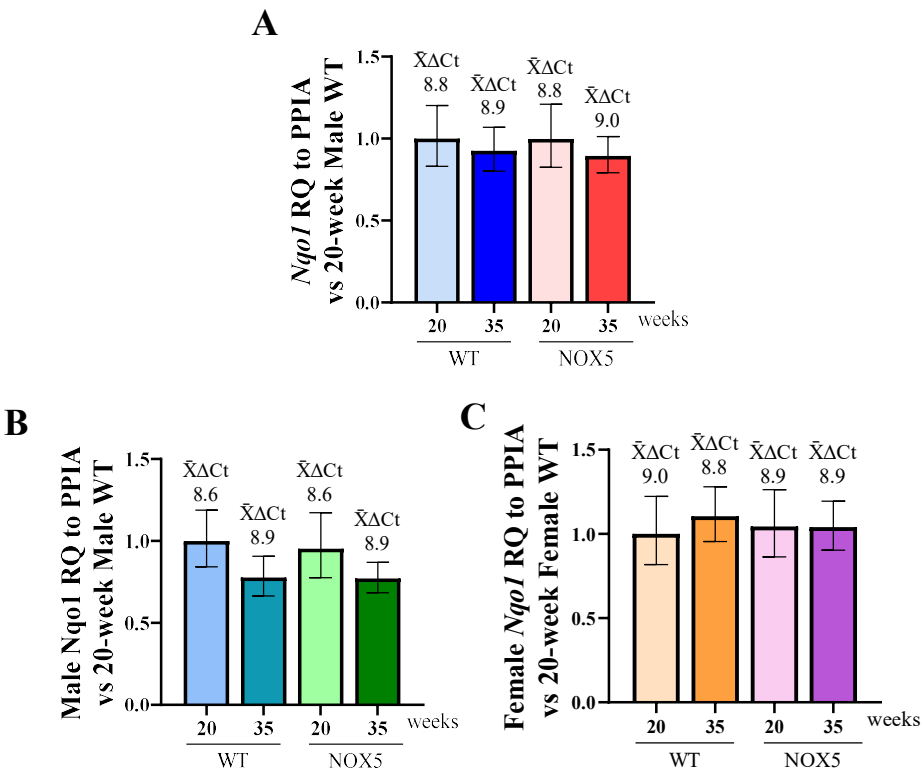

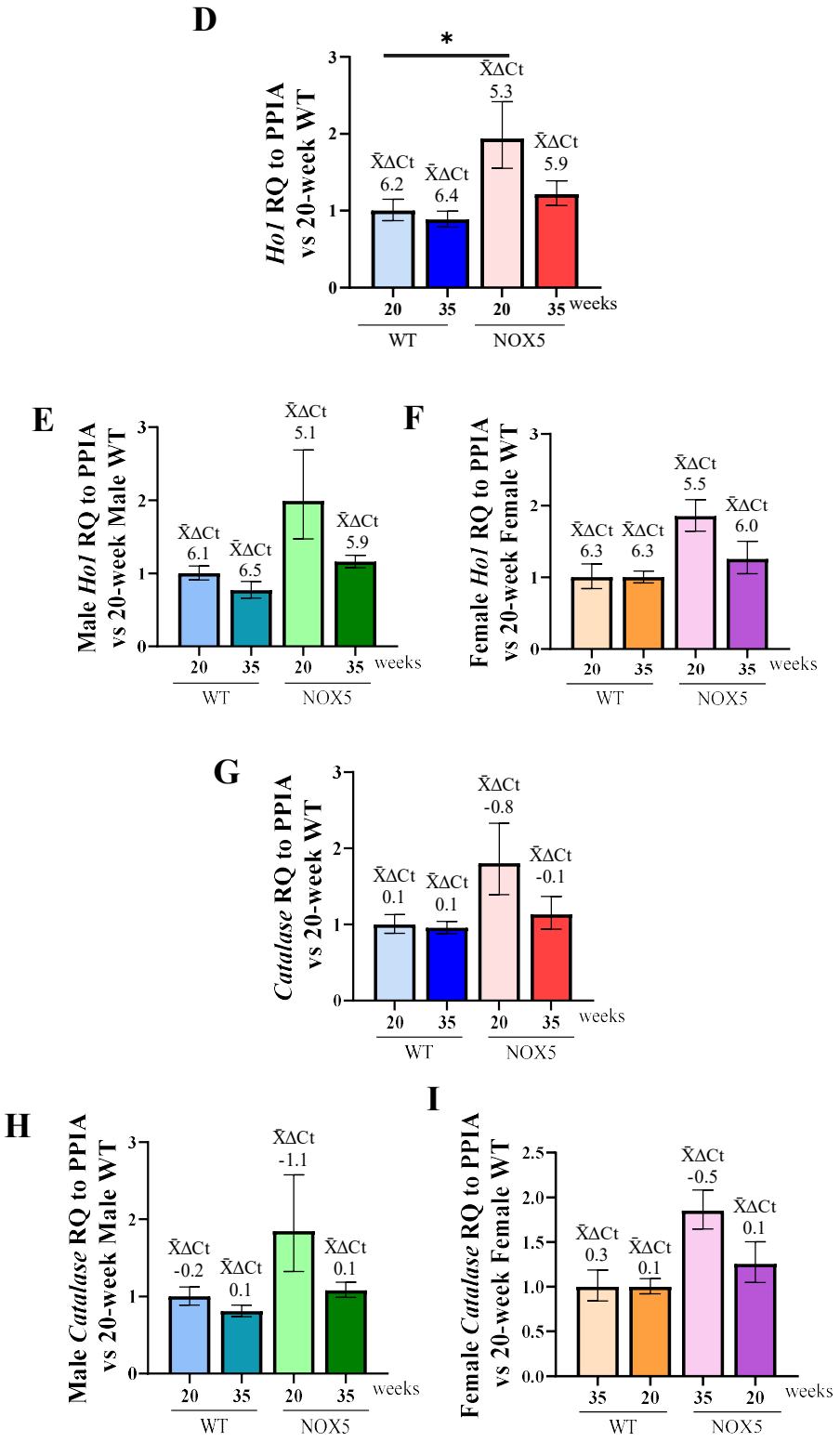

Figure 4-20. Assessment of *Nqo1*, *Ho1*, and *Catalase* mRNA expression in male and female 20- and 35-week-old WT and VSMC-NOX5 mice. *Nqo1*(**A-C**), *Ho1*(**D-F**), and *Catalase* (**G-I**) mRNA expression was assessed in whole brain homogenates of 20- and 35-week-olds-old male and female WT and VSMC-NOX5 mice using q-RT PCR. Gene expression levels were assessed by q-RT PCR with RQ fold change being calculated from ΔΔCt following *Ppia* housekeeping gene normalisation. Mixed sex data n=12, male data n=6, female data n=6 per genotype. Data was analysed using a two-way ANOVA with a Tukey's *post*-hoc test and presented as *p≤0.05. Further analysis was conducted using a student's *t*-test and were presented as #p≤0.05

4.3.21 Whole Brain Immunoblotting Assessment of BIP Protein Levels in Male and Female 20- and 35-week-old VSMC-specific NOX5 Mice.

In chapter 3, NOX5 in a VSMC-specific manner led to sex-specific changes in BIP protein levels. This study aimed to assess BIP expression in whole brain homogenates of 20- and 35-week-old male and female WT and VSMC-NOX5 mice using immunoblotting. BIP expression was identified to be decreased collectively in 35-week-old VSMC-NOX5 mice (**Figure 4-21A**), when compared to 35-week-old WT mice (35-week-old VSMC-NOX5 1625±184 AU vs 35-week-old WT 2370±291 AU p=0.04#).

When separating to male and female subgroups in the context of ageing, 20-week-old male VSMC-NOX5 BIP levels were decreased when compared to 20-week-old male WT counterparts (20-week Male NOX5 (AU) 3011±533 vs 20-week Male WT (AU) 1669±170 p=0.03#). However, no changes were identified with age in both WT and VSMC-NOX5 groups (**Figure 4-21B**).

Analysis of cerebral BIP expression in female VSMC-NOX5 mice was identified to be reduced in 35-week-old VSMC-NOX5 mice when compared to 35-week-old WT mice (female 35-week-old VSMC-NOX5 1345±318 (AU) vs female 35-week-old WT 2509±369 (AU) p=0.04#)(**Figure 4-21C**).

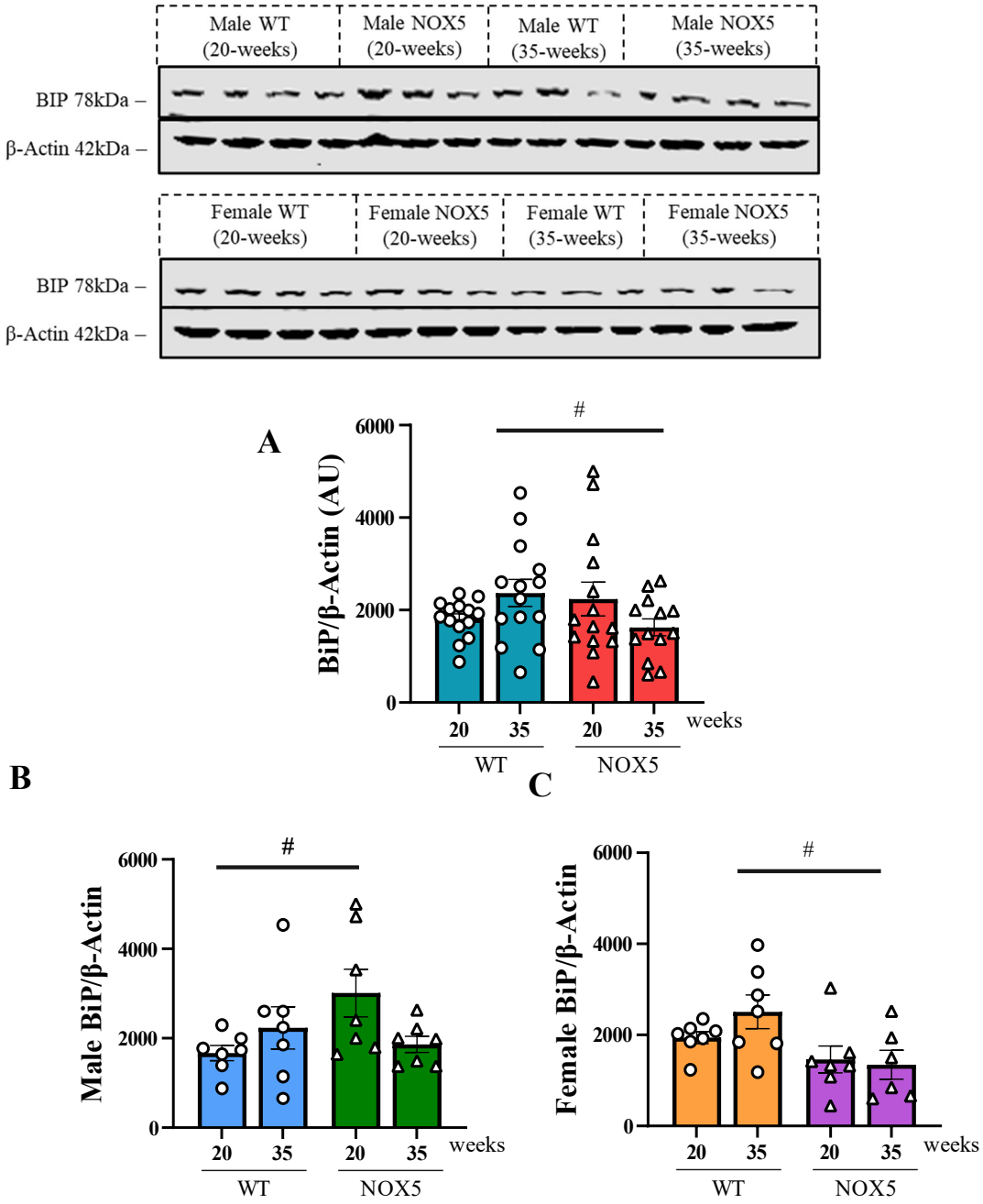

Figure 4-21 Protein expression of the ER stress marker BIP in male and female 20- and 35-week-old WT and VSMC-NOX5 mice. ER stress was assessed by analysing BIP protein levels in whole brain homogenates of 20- and 35-week-old male and female WT and VSMC-NOX5 mice by immunoblotting (**A-C)** Immunoblotting expression was normalised to β-actin and expressed as AU. Mixed sex data n=13-14, male data n=7, female data n=6-7 per genotype Data was analysed using a two-way ANOVA with a Tukey's *post*-hoc test. Further analysis was conducted using a student's *t*-test and were presented as #p≤0.05.

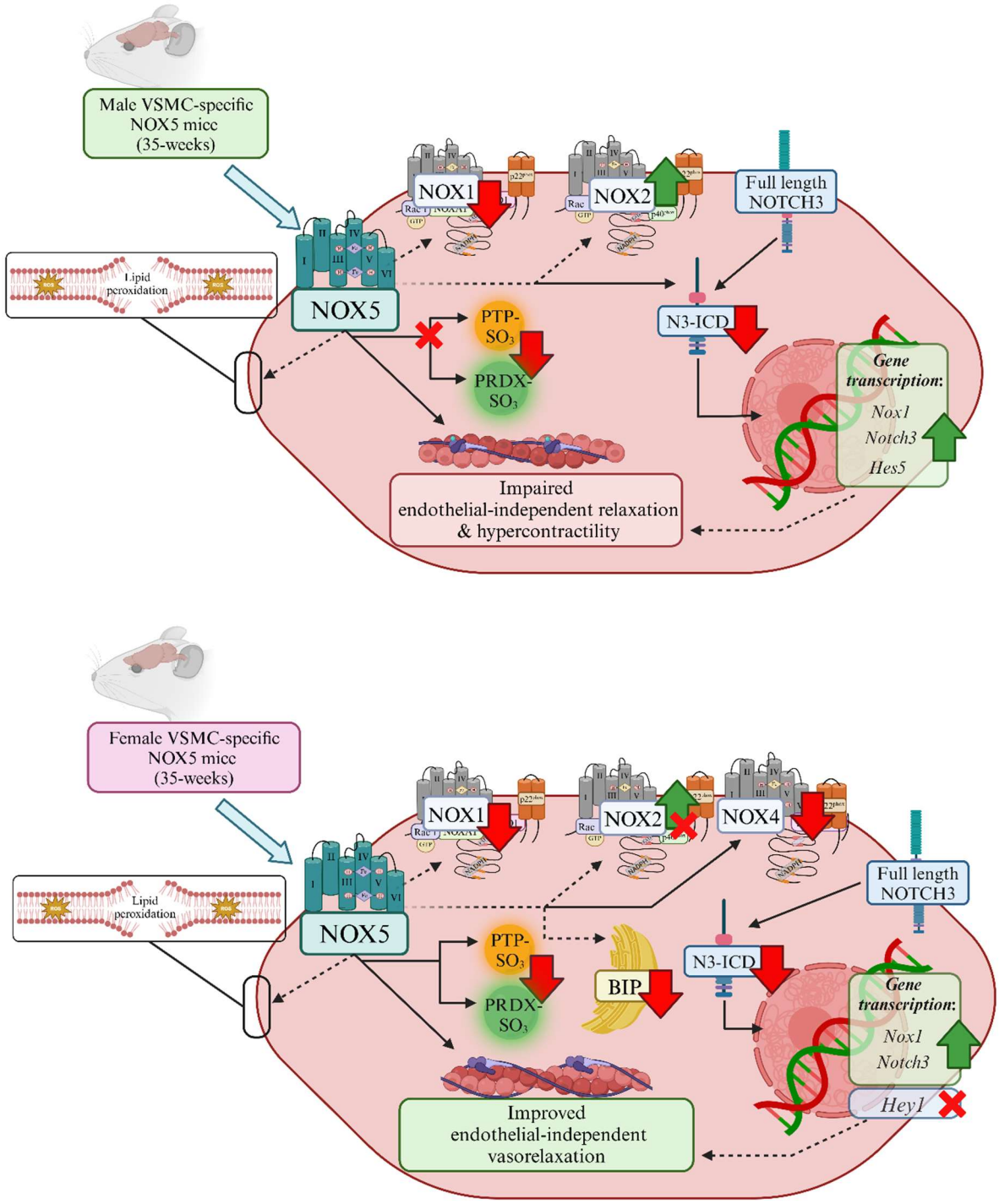

Figure 4-22. Graphical figure highlighting sex-dependent effects of VSMC-specific NOX5 in the brains of 35-week-old mice. In aged male mice, NOX5 in a VSMC-specific manner was associated with alterations to NOX protein and gene expression, prevented decreases of PTP-SO_3 and PRDX-SO_3, lipid peroxidation, altered canonical NOTCH3 signalling, and a hypercontractile phenotype coupled with impaired endothelial-independent relaxation of carotid arteries. In females, NOX1, NOX2, and NOX4 were associated with alterations in protein levels, age-related lipid peroxidation, however, with reduced markers of oxidative and ER stress. Furthermore, females presented with improved endothelial-independent vasorelaxation and decreased N3-ICD protein levels and prevented *Hey1* expression indicating a role for non-canonical NOTCH3 signalling. This image was generated in BioRender.

4.4 Discussion

This study presented in chapter 4 of this thesis aimed to further examine the role of cerebral VSMC-NOX5 in the context of ageing. First, assessment of VSMC-specific NOX5 in the context of ageing identified no changes in markers of cerebrovascular phenotype and contractile markers. Secondly, assessment of NOX1, NOX2, and NOX4 identified sex-dependent alterations to mRNA expression and protein levels with age. Thirdly, assessment of vascular function in carotid arteries identified sustained decreased endothelial-independent vasorelaxation in aged male VSMC-NOX5 mice, with female mice identifying improved endothelial-independent vasorelaxation. Furthermore, U-46619-mediated contraction was identified to be increased with age in male, but not female VSMC-NOX5 mice. Fourthly, VSMC-NOX5 led to changes in NOTCH3 mRNA and ICD protein expression in both aged male and female VSMC-NOX5 mice. Furthermore, decreases in downstream canonical NOTCH3 transcription factor *Hes5* was upregulated with age in male VSMC-specific NOX5 mice while *Hey1* expression was prevented in female VSMC-NOX5 mice with age. Fifthly, lipid peroxidation was increased in both male and female WT and VSMC-NOX5 mice with age. Sixthly, PRDX-SO_3 and PTP-SO_3 expression was observed to be altered with age in VSMC-NOX5 mice in a sex-dependent manner. Furthermore, assessment of antioxidant gene *Sod2* identified changes in mixed sex VSMC-NOX5 mice analysis with age. Finally, BIP expression was identified to be decreased in 35-week-old female, but not male, VSMC-NOX5 mice (**Figure 4-22**). Collectively, the current research findings indicate a sexual dimorphic effect in VSMC-NOX5 mice in the context of ageing.

In normal cerebrovascular function, GFAP is a key protein in astroglial function, regulating cerebrovascular processes such as the BBB and CBF. Furthermore, αSMA, VEGFR2, and RhoA/ROCK1 signalling are vital in maintaining cerebrovascular cytoskeletal dynamics and vascular contraction. Under physiological conditions, these proteins work in concert to ensure appropriate signalling for proper cerebrovascular and neurological function in pathophysiological conditions; dysregulation of these proteins is often associated with cerebrovascular dysfunction and excessive vascular contraction through pathological mechanisms such as oxidative stress and neuroinflammation, contributing to CSVD and stroke onset (Yang and Wang, 2015, Chen *et al*., 2023a, Shibuya, 2011, Lu *et al*., 2023). Previously in chapter 3, this study identified that the inclusion of VSMC-NOX5 in males led to a decrease in the astroglia marker GFAP, potentially indicating disruption to the neurovascular unit/BBB integrity and/or neuronal function.

In the context of ageing, this study hypothesised that this would be exacerbated, and further markers of neuronal (GFAP) and vascular (αSMA, VEGFR2, RhoA/ROCK signalling) dysfunction were profiled. However, no differences in protein levels of vascular αSMA, VEGFR2, RhoA/ROCK signalling, or GFAP levels were found when assessing VSMC-NOX5 mice at 35-weeks-old in either mixed sex or sex-specific analysis. Previous literature has identified that in the context of ageing, astrocyte levels increase as a consequence of oxidative stress and neuroinflammation (Clarke *et al*., 2018, Lawrence *et al*., 2023, Chen *et al*., 2020b). Additionally, in the context of aging JAK/STAT3 has been identified as a common inducer of astrocyte activation (Ben Haim *et al*., 2015). Moreover, when CBF is reduced, astrocytes have been identified to proliferate and migrate leading to increased cell retention of GFAP with H_2O_2 and NO as important for initiating reactive gliosis through the enhancement of the JAK-STAT pathway (Nedergaard and Dirnagl, 2005, Daverey and Agrawal, 2016, Na *et al*., 2007). Given that this study previously identified a decrease in endothelial-independent vasorelaxation in carotid arteries, it is likely that an increased hypoxic cerebral environment occurs in male VSMC-NOX5 mice. However, in 35-week-old VSMC-NOX5 mice, no changes in GFAP expression were identified. This could be as a consequence of VSMC-specific NOX5 males having an increased adaptive astroglia environment with age due to patho-mechanism linked with oxidative stress and neuroinflammation.

As previously described, NOX enzymes play critical roles in normal physiological function generating ROS molecules essential for cellular signalling, host defence and cerebrovascular tone. In pathophysiological conditions, the dysregulation of NOX enzymes can lead to oxidative stress, vascular inflammation, cerebrovascular remodelling and endothelial dysfunction leading to the pathogenesis of conditions such as hypertension and CSVD (De Silva and Miller, 2016, Touyz *et al*., 2019). In the context of ageing, previous literature has established that ageing is directly linked with increased NOX activity and increased risk of vascular dysfunction (Sahoo *et al*., 2016). Previously, assessment of NOX1, NOX2, and NOX4 mRNA expression and protein levels identified no changes in male or female VSMC-NOX5 mice at 20 weeks old. Here in chapter 4, this study hypothesised that VSMC-NOX5 in the brains of aged mice would lead to alterations in NOX1, NOX2, and NOX4 mRNA and protein expression.

Assessment of *Nox1* gene expression identified a sex-dependent increase in *Nox1* mRNA expression in males, but not females with age. However, immunoblotting assessment of NOX1 identified that ageing in VSMC-NOX5 and WT mice led to reduced NOX1 protein expression when assessed collectively or by male or female analysis. However, whilst this seems to be an age-related effect in males, when comparing female 35-week-old WT and VSMC-specific NOX5 mice, NOX5 was identified to have lower cerebral NOX1 protein levels indicating that NOX5 advances the downregulatory effects of ageing. This could indicate that VSMC-NOX5 could directly cause the inactivation of NOX1 impairing normal NOX1-mediated physiological function including impaired adaptive vasodilation. Previous research has identified the beneficial effects of NOX1 activation whereby NOX1 overexpression augments oxidative and contractile responses (Dikalova *et al*., 2005). Alternatively, the decreased NOX1 activity could be as a consequence of regulatory mechanisms reducing the level of cerebrovascular ROS, leading to reduced oxidative stress and improved vascular outcomes preventing further endovascular injury by mediating VSMC migration and proliferation (Vendrov *et al*., 2019). Furthermore, NOX1 inhibition has been identified to be a regulatory mechanism in the context of age-related impaired blood flow (Li *et al*., 2021). In the case of aged VSMC-NOX5 mice, it is unclear whether the downregulation of NOX1 is beneficial or deleterious, warranting further study.

Assessment of 35-week-old female VSMC-NOX5 mice identified an increase in *Nox2* mRNA expression. Analysis of NOX2 protein expression identified increased protein

expression in mixed sex and in male analysis of 35-week-old VSMC-NOX5 mice. The upregulation of NOX2 protein expression may be an indicator of a cerebral inflammatory physiological or pathological insult as a consequence of VSMC-NOX5 causing an oxidative environment in aged male mice. This aligns with previous research identifying that the upregulation of NOX2 in the brain can have deleterious effects linked to microvascular inflammation leading to white matter diseases and cognitive impairment (Alfieri *et al*., 2022). Particularly in the context of ageing, it has also been identified that NOX2 upregulation leads to oxidative stress and DNA damage and loss of cerebral capillary and neuronal function (Fan *et al*., 2019). However, assessment of NOX2 protein expression in female mice identified an increase in NOX2 protein expression in 35-week-old WT mice, with no changes being identified in female 35-week-old VSMC-NOX5 mice, suggesting VSMC-NOX5 in female mice prevents increased NOX2 protein expression with age. Previous research examining NOX2 knockout mice (NOX2-KO) have identified improved outcomes such as the prevention of oxidative stress, cerebral small vessel rarefaction, and increases in tight junction protein expression leading to reduced BBB-disruption and improved neurological outcomes in the context of age (Kahles *et al*., 2007, Fan *et al*., 2019, Song *et al*., 2020). Given that in this study NOX2 protein expression increases were prevented in aged female VSMC-NOX5 mice, it could indicate that NOX5 may result in beneficial effects in the brains of aged female mice leading to a reduced inflammatory profile as well as improved BBB and neurological outcomes.

When examining *Nox4* mRNA expression, this study identified a decrease in expression in female 35-week-old VSMC-NOX5 mice. Previous research has identified NOX4 as a protective NOX in the brain, protecting the cerebrovascular system from neuroinflammation and ischaemia (Schröder *et al*., 2012). In aged female VSMC-NOX5 mice, the downregulation of *Nox4* mRNA expression without affecting NOX4 protein expression may suggest a regulatory post-transcriptional mechanism such as transcriptional efficacy, mRNA stability, and protein regulation. Two regulatory mechanisms that could be affecting the expression of NOX1 and NOX4 in VSMC-NOX5 mice are the JAK-STAT1 and STAT3 and oestradiol signalling pathways. Current research has identified that NOX1 and NOX4 subunits p22phox, p47phox, and p67phox promoters are directly augmented by STAT1 and STAT3 overexpression in human aortic smooth muscle cells (Manea *et al*., 2010). Alternatively, the changes observed in NOX1 and NOX4 expression could be consequences of hormone signalling. Previous research has identified that in pre-

menopausal rats, female mice had suppressed NOX1 and NOX4 NADPH-oxidase activity due to oestrogen-mediated effects (Miller *et al*., 2007).

The cerebrovasculature maintains normal physiological function through a delicate balance of processes that lead to vasoconstriction and vasodilation, ensuring that adequate CBF meets the metabolic demands of the brain. Disruption to this balance leads to cerebrovascular dysfunction, impaired CBF, and reduced perfusion. Previously in chapter 3, wire myography assessments of isolated carotid arteries identified that VSMC-NOX5 in a VSMC-specific manner led to impaired endothelial-independent relaxation in male, but not female, mice. This study aimed to investigate the effects of ageing on vascular function in VSMC-NOX5 overexpressed mice both collectively, and when separated by sex. First, mixed sex assessment of aged VSMC-NOX5 mice led to increased U-46619-mediated contraction when compared to 35-week-old WT mice, and impaired endothelial-independent vasorelaxation when compared to 20-week-old VSMC-NOX5 mice in carotid arteries. Sex-specific analysis identified that in male WT mice, age was linked with a decrease in contractility indicating a loss in elasticity and arterial compliance of vascular carotid arteries (Mcveigh *et al*., 1999, Jani and Rajkumar, 2006). However, assessment of VSMC-NOX5 with age in males was associated with an increase in U-46619-mediated carotid artery contraction and impaired SNP-mediated endothelial-independent vasorelaxation of carotid arteries, consistent with previous studies linking NOX5 to impaired vascular function and hypercontractility (Montezano *et al*., 2018, Neves *et al*., 2019). In the analysis of female VSMC-NOX5 mice, age was associated with improved SNP-mediated vasorelaxation indicating a sex-dependent protective effect in VSMC-NOX5, going against this study's hypothesis that, with age, VSMC-NOX5 would lead to impaired outcomes in females. This sex-specific protection could be mediated by enhanced oestrogen signalling in 35-week-old VSMC-NOX5 female mice, counteracting the vasoconstrictive and vasodilatory impairments observed in male VSMC-NOX5 mice. Previous studies have identified that activation of oestrogen receptors such as ERα, ERβ, GPR30, enhances endothelial and VSMC functionality, leading to improved blood-flow (Iorga *et al*., 2017, Khalil, 2013). Additionally, sex hormones, notably oestrogen, have been identified to upregulate ARE in oxidative stress conditions (Xiang *et al*., 2021, Krause *et al*., 2006). Furthermore, oestrogen has been described to mediate $[Ca^{2+}]i$ homeostasis through K^+ efflux, stabilising Ca^{2+} entry and the membrane potential of VSMC. Moreover, oestrogen has been found to influence endothelial factors such as prostaglandin I2 (PGI2), promoting vasodilation (Golshiri *et al*., 2020, Krause *et al*.,

2006). This oestrogen-mediated mechanism could explain why aged male VSMC-NOX5 mice exhibit contractility in this study, whereas aged VSMC-NOX5 females were identified to have no markers of increased contraction. Further studies are needed to investigate the exact sex-dependent protective mechanisms in cerebrovascular function of aged female VSMC-NOX5 mice.

Normal NOTCH3 signalling plays a critical role in maintaining cerebrovascular homeostasis in VSMCs and is important in VSMC differentiation, proliferation, and survival. Alterations in NOTCH3 signalling contribute to severe cerebrovascular dysfunction leading to impaired vascular tone and inflammation with age (Morris *et al*., 2019, Romay *et al*., 2024). Previously, this study identified that VSMC-NOX5 may lead to non-canonical NOTCH3 alterations in the brains of 20-week-old female mice. This study presented findings that identified that VSMC-NOX5 led to *Notch3* gene expression upregulation in mixed sex, male and female analysis in aged mice. However, this did not translate to increases in full-length NOTCH3 protein expression with ageing leading to no changes in both genotypes when assessed collectively, or in separated male and female assessments. Furthermore, when assessing N3-ICD in both VSMC-NOX5 and WT mice, this study identified that ageing led to decreased N3-ICD protein expression in both genotypes in mixed sex and separated analysis of males and females. Interestingly, when assessing downstream NOTCH3 transcription *Hey* and *Hes* genes, no changes were observed in *Hes1*, and *HeyL* mRNA expression between genotypes in mixed sex analysis of aged mice. However, when separated by sex, *Hes5* gene expression was identified to be upregulated with age in 35-week-old male VSMC-NOX5 mice. Taken collectively, this suggests that with age, VSMC-specific NOX5 in the brains of male mice leads to canonical NOTCH3 signalling, with canonical NOTCH3 signalling indicative of a CSVD phenotype. This is further supported by the findings that in myography analysis of aged male VSMC-NOX5 mice, vascular function was impaired with ageing leading to notable contractility when compared to their aged WT counterparts. Additionally, whilst the assessment of *Hey1* mRNA expression was identified as unchanged in the brains of mixed sex and male analysis with age, *Hey1* mRNA expression was identified to be decreased in female 35-week-old WT mice, when compared to their 20-week-old female WT counterparts. However, no changes were observed between 20- and 35-week-old VSMC-NOX5 mice suggesting that the inclusion of VSMC-NOX5 in a VSMC-specific manner in the brains of aged female mice leads to the prevention of downregulated *Hes1* expression. The decreases in N3-ICD expression identified in female VSMC-specific NOX5 mice

potentially indicate a shift towards non-canonical NOTCH3 signalling. This shift could lead to the activation of pathways that differ from canonical transcription of *Hey* and *Hes* genes with previous research identifying a role for non-canonical NOTCH3 and activation pathways such as the TLR-NF-kB pathway, promoting macrophage activation and an inflammatory cerebrovascular phenotype (López-López *et al*., 2020, Sun, 2017); PI3K-Akt contributing to prototypical leucocyte recruitment and alterations to angiogenesis and vascular tone, (Shiojima and Walsh, 2002, Liu *et al*., 2019); and MAPK pathways that alter vascular growth and differentiation (Lin *et al*., 2017, Baeten and Lilly, 2015). Given that canonical NOTCH3 signalling leads to alterations in *Hey* and *Hes* gene expression as observed in aged female WT mice, this could further indicate that, in the brain, VSMC-NOX5 promotes non-canonical NOTCH3 signalling in both male and female mice.

In physiological homeostasis, redox signalling plays a critical role in maintaining cellular homeostasis with the brain being particularly susceptible to ROS imbalance and oxidative stress. ROS, particularly H_2O_2, act as key signalling molecule's that are vital to cellular homeostasis processes including cell proliferation, differentiation and apoptosis (Miller *et al*., 2006, Gough and Cotter, 2011). In pathophysiological conditions, an increased ROS environment has been linked with oxidative damage including lipid peroxidation and irreversible oxidation of key antioxidant and key cellular signalling enzymes such as PRDX and PTPs with increased susceptibility to oxidation with age (Sharifi-Rad *et al*., 2020). Previously in chapter 3, this study identified an increase in cerebral H_2O_2 levels in male VSMC-NOX5 mice at 20 weeks old. Here in chapter 4, this study identified no differences in H_2O_2 levels in 35-week-old mice. This may indicate that the inclusion of VSMC-NOX5 in a VSMC-specific manner leads to early increases in H_2O_2 production. Assessment of lipid peroxidation in VSMC-NOX5 and WT mice identified that in mixed sex and sex-dependent analysis, lipid peroxidation was significantly increased with age. As lipid peroxidation levels were increased with age in both genotypes regardless of sex, this is likely a response to ageing in the brain and has been well documented previously (Miró *et al*., 2000, Praticò, 2002). Further markers of oxidative stress were assessed, examining PRDX-SO_3 and PTP-SO_3 through immunoblotting and identifying that PRDX-SO_3, when assessed collectively, was significantly reduced in aged 35-week-old VSMC-NOX5 mice. However, when assessing PRDX-SO_3 by sex, 35-week-old male PRDX-SO_3 expression was identified to be prevented in VSMC-NOX5 with age. Furthermore, when assessing female 35-week-old VSMC-NOX5 mice, PRDX-SO_3 protein expression was identified to be reduced with age

in both WT and VSMC-NOX5 mice, however, when VSMC-NOX5 mice were then compared to 35-week-old female WT mice, cerebral PRDX-SO_3 levels were also reduced suggesting that NOX5 in females may be protective against hyperoxidation. Although it is well documented that oestrogen provides an antioxidant defence against free radicals, and notably through peroxiredoxin, (Diaz Brinton, 2012, Xiang *et al*., 2021, Lagranha *et al*., 2018), it is unclear whether this effect is a result of sex-hormone mediated prevention of PRDX hyperoxidation, or, alternatively, whether PRDX enzyme bioavailability is lower as a consequence of reduced oxidative stress or by NOX5 reducing PRDX bioavailability. As such, more research is required.

Assessment of full-membrane PTP-SO_3 identified a significant decrease with age in the brains of female VSMC-NOX5 and WT mice at 35 weeks old. No changes in full-membrane PTP-SO_3 were observed in mixed sex and male analysis. Further analysis identified a significant increase of PTP-SO_3 20kDa in mixed sex 35-week-old WT and VSMC-NOX5 mice. Furthermore, separate analysis of PTP-SO_3 at 20kDa identified a significant increase in 35-week-old female but not male VSMC-NOX5 mice. Assessment at PTP-SO_3 at 65kDa identified that in both mixed sex and male analysis, ageing led to reduced PTP-SO_3 in aged WT mice. However, no differences were observed in aged VSMC-NOX5 mice suggesting that oxidation of PTPs was prevented. NO differences at 65kDa were observed in female mice between age and genotype. Collectively, VSMC-NOX5 is decreased, however, this may be driven by the female results as when assessing by sex, aged female VSMC-NOX5 mice have reduced PRDX-SO_3 and PTP-SO_3, indicating a reduced oxidative environment; whereas in males, decreases in both PRDX-SO_3 and PTP-SO_3 are prevented, further suggesting an increased oxidative environment and sexual dimorphism outcomes in the brains of VSMC-NOX5 mice. This could be due to the protective effects of oestrogen through the ARE system through rapid activation of the transcription factor nuclear factor-E2-related factor 2 (Nrf2), whereby in males, lower testosterone levels as a consequence of ageing may lead to an increased oxidative environment (Ishii and Warabi, 2019, Babcock *et al*., 2022).

Physiologically, antioxidant genes play a crucial role in the transcription of antioxidants vital to maintaining ROS balance and ensuring cellular homeostasis. In pathophysiological conditions, dysregulation of antioxidant gene expression can be a consequence of oxidative stress (Maldonado *et al*., 2023). Previously in chapter 3, VSMC-NOX5 was associated with increased *Ho1* mRNA expression in the brains of 20-week-old

females. In the current study presented in chapter 4, assessment of *Sod1* and *Nqo1*, *Ho1* mRNA expression identified no differences between age and genotype in mixed sex or sex-specific analysis. mixed sex analysis group of 35-week-old VSMC-NOX5 mice identified a significant increase in *Sod2* mRNA expression. This chapter has previously described how the current literature has identified JAK-STAT3 as a regulator of GFAP and NOX1/NOX4 regulation. The JAK-STAT3 signalling axis has also been identified by previous research assessing a *post*-stroke model of cerebrovascular disease as a transcription factor for the *Sod2* gene crucial for neuroprotection in response to oxidative stress, preventing further cell death from ischaemia (Jung *et al*., 2010). Although in this study's VSMC-NOX5 model, stroke was not induced, the upregulation of *Sod2* mRNA expression could be a consequence of a cerebral small vessel disease pathology leading to ischaemia and potential increased stroke risk. Additionally, upregulation of *Sod2* mRNA expression has been associated with neurological dysfunction leading to neurological disorders such as Parkinsons disease, (Santiago *et al*., 2014), and Alzheimer's disease (AD); however in the context of AD, the upregulation of *Sod2* is likely a compensatory mechanism against elevated ROS as a consequence of ageing with the aetiology of altered mitochondrial SOD2 homeostasis being unknown (Flynn and Melov, 2013). This study also assessed the role of catalase identifying no changes when mice were aged to 35 weeks in mixed sex and male or female analysis of VSMC-NOX5 mice.

As previously stated, the ER is critical in protein folding, lipid synthesis, and Ca^{2+}, acting to maintain cellular homeostasis in normal physiology, with BIP playing a key role in the UPR by initiating proper protein folding (Wang *et al*., 2009, Liu *et al*., 2016). During the ageing process, BIP protein levels decrease, leading to a decline in the efficiency of the ER to maintain cellular homeostasis through oxidation of proteins, in turn, leading to the accumulation of misfolded proteins. Previous research has studied this effect whereby in the brain oxidation of ER-linked proteins such as BIP led to declined BIP functionality, initiating an impaired UPR response and causing ER stress (Brown and Naidoo, 2012, Naidoo, 2009). Previously in chapter 3, this study identified that VSMC-NOX5 leads to increased BIP expression in male mice with no effects in females at 20 weeks old. Here in chapter 4, BIP expression was shown to decrease in aged female VSMC-NOX5 mice. This decrease in female VSMC-NOX5 BIP protein expression could be a result of the natural ageing process leading to a functional decline in the UPR response and consequently ER stress. Furthermore, previous research has identified that oestrogen levels are reduced with age, with decreases in oestrogen leading to insufficiency

in oxidative stress defence (Camargo *et al*., 2023b, Xiang *et al*., 2021, Chen *et al*., 2022). This could indicate that in female 35-week-old VSMC-NOX5 mice, a natural age-related reduction in oestrogen could lead to reduced defence against the deleterious nature of VSMC-NOX5 mediated oxidative stress, leading to increased oxidation of chaperone proteins such as BIP.

To summarise, the study presented in chapter 4 identifies that with ageing (35-weeks), the presence of VSMC-specific NOX5 exacerbates cerebrovascular dysfunction in male mice with increased markers of oxidative stress, disrupted canonical-NOTCH3 signalling and upregulated *Hes5* mRNA expression, and sustained impairments to endothelial-independent vasorelaxation and a hypercontractile phenotype supports the hypothesis that NOX5 in a VSMC-specific manner contributes to a CSVD phenotype that may lead to increased risk of further cerebrovascular pathology. In contrast, in the brains and carotid arteries of aged female VSMC-specific mice exhibit further evidence of a distinct protective response whereby markers of irreversible PTP-oxidation and PRDX hyperoxidation were reduced, and endothelial-independent vasorelaxation was maintained. Additionally, similarly to males, NOTCH3 signalling was disrupted, however with prevented changes to *Hey* gene expression levels further indicating a potential role for non-canonical NOTCH3 signalling. To conclude, the findings identified in Chapter 4 highlight a role for VSMC-specific NOX5 in age-related cerebrovascular dysfunction in males, with females showing further evidence of in intrinsic protective mechanisms that may mitigate NOX5-induced cerebrovascular dysfunction, emphasising the need for further research into sex-specific therapeutic targets in cerebrovascular ageing.

Chapter 5

Examining the Role of Ang II-mediated Hypertension in Cerebral VSMC-specific NOX5 Male and Female Mice.

5.1 Overview

Hypertension is a worldwide leading cause of preventable cardio and cerebrovascular pathologies including CSVD, and stroke (Jiménez-Balado *et al*., 2019, Gorelick *et al*., 2020, Touyz *et al*., 2022). Previous studies have extensively linked NOX activity and oxidative stress as a central feature of hypertension pathophysiology (Touyz *et al*., 2020, Datla and Griendling, 2010, Rajagopalan *et al*., 1996). With increased hypertension-mediated NOX activity contributing to key pathophysiological processes including mitochondrial dysfunction (Dikalova *et al*., 2020), NOTCH3 dysregulation (Ragot *et al*., 2016, Baron-Menguy *et al*., 2017), and ER stress (Camargo *et al*., 2018a, Camargo *et al*., 2018b). Moreover, recent research has identified NOX5 as a key mediator of a hypertensive pathological phenotype, initiating pathophysiological processes such as eNOS dysfunction, and hypercontractility, contributing to vascular impairments and vascular pathology (Elbatreek *et al*., 2020, Deliyanti *et al*., 2020, Touyz *et al*., 2019). However, whilst NOX5 has been implicated in hypertensive pathology, its role in cerebral VSMCs remains unknown.

Previously in chapters 3 and 4 of this thesis, VSMC-specific NOX5 was associated with age-dependent pathophysiological effects in the brain and carotid arteries contributing to oxidative stress, canonical NOTCH3 dysregulation and vascular impairment. Alternatively in females, VSMC-NOX5 overexpression was associated with prevented oxidative stress, non-canonical NOTCH3 signalling, and age-dependent delays to vascular dysfunction with these differences potentially being mediated by direct or indirect sex hormone regulation of NOX activity. In the context of hypertension, research evidence suggests that sex hormones such as androgens and oestrogens play a critical role in BP regulation with oestrogen modulating vascular tone in a vasoprotective manner (Connelly *et al*., 2022, Xing *et al*., 2009). Based on findings previously outlined in this thesis, NOX5 in a VSMC-specific manner is linked to worsened outcomes in males. In the context of Ang II-induced hypertension NOX5-mediated ROS production could exacerbate oxidative stress responses and further dysregulate NOTCH3 signalling, contributing to worsened cerebrovascular disease outcomes. Alternatively, female sex hormones may protect the brains of female mice from NOX5-mediated oxidative stress responses in the context of Ang II-induced hypertension.

Given the previous findings identified in this thesis, linking VSMC-specific NOX5 with worsened outcomes in males. In the context of cerebrovascular hypertension, VSMC-specific NOX5 overexpression could lead to exacerbated oxidative stress and NOTCH3 dysregulation in the brains of male mice. Alternatively, females may be further protected through potential sex hormone signalling mechanisms.

Here in Chapter 5, the research presented expands upon Chapter 3 by introducing the effects of Ang II-mediated hypertension on the brains of male and female WT and VSMC-specific NOX5 mice. The 20-week-old data from Chapter 3 are included in this chapter to serve as a baseline for Ang II treatment comparison and will be identified as "non-treated" (NT) male and female WT and VSMC-specific NOX5 mice, with the purpose of providing a control group for evaluating the effects of Ang II treatment in these mice. This allows for an assessment of how Ang II influences vascular responses in VSMC-specific NOX5 and WT mice. By utilising an Ang II mouse model of hypertension, this model induces elevated BP and oxidative stress in pre-clinical experimental conditions, vital for exploration of transgenic models such as VSMC-specific NOX overexpression. Moreover, this model allows for the examination of sex differences in Ang II mediated hypertension (Young and Davisson, 2015, Romero and Reckelhoff, 1999).

5.2 Chapter 5 Hypothesis and Aims

5.2.1 Hypothesis

Here in Chapter 5, this study hypothesises that Ang II-treatment of VSMC-specific NOX5 mice will amplify NOX5-induced oxidative stress, disrupting key signalling pathways that are key to cerebrovascular function, thereby accelerating risk of cerebrovascular pathology.

5.2.1.1 Predictions of Hypothesis

To test this hypothesis, this study predicts that cerebral VSMC-specific NOX5 in the context of Ang II mediated hypertension will lead to:

1. **Alterations in structural and phenotypic markers:** This study anticipates that hypertensive VSMC-NOX5 mice will exhibit alterations in cerebrovascular proteins (GFAP, RhoA, ROCK1, and VEGFR2) which are vital for typical cerebrovascular structure, phenotype and physiological function.
2. **Alternative NOX isoform modulation:** This study predicts that VSMC-NOX5 will cause alterations in NOX1, NOX2, and NOX4 mRNA and protein levels either indirectly through compensatory mechanisms to regulate NOX5 activity, or by direct NOX isoform activity as a result of the hypertensive phenotype through altered redox homeostasis.
3. **NOTCH3 signalling axis alterations:** This study predicts that hypertension in VSMC-NOX5 mice will dysregulate the NOTCH3 signalling axis leading to alterations in cerebrovascular function.
4. **Alterations to ROS/antioxidant homeostasis and increased markers of oxidative stress:** This study hypothesises that a hypertensive phenotype in VSMC-NOX5 mice would lead to increase ROS production, markers of oxidative stress, and altered antioxidant gene expression.
5. **Altered protein levels of ER stress UPR marker BIP:** This study further hypothesises that BIP protein expression will be altered in the context of hypertensive VSMC-NOX5 mice. These changes may influence cellular stress response and calcium homeostasis leading to cerebrovascular dysfunction.
6. **Sex-dependent changes:** This study also hypothesises that the effects of hypertension will diminish the potential protective mechanisms in the brains of female VSMC-specific mice contributing to pathophysiological biomarkers, whilst

also exacerbating the previously identified deleterious effects observed in the brains of VSMC-specific NOX5 male mice observed in chapter 3 and 4.

Collectively VSMC-NOX5 overexpression in the context of hypertension may lead to pathophysiological outcomes that may indicate increased risk of cerebrovascular disease.

5.2.2 Specific Aims

1. *Confirmation of a hypertensive phenotype in Ang II-induced WT and VSMC-NOX5 mice*
To assess the role of hypertension in the brains of WT and VSMC-NOX5 mice, surgical minipump implantation was conducted and mice were treated with Ang II for 4 weeks as previously described (Montezano *et al*., 2018). Tail-cuff plethysmography was used to assess systolic blood pressure (BP) confirming a hypertensive phenotype between Ang II- and non-treated WT and VSMC-NOX5 mice.
2. *Assessment of phenotypic and structural changes in the brains of hypertensive WT and VSMC-NOX5 mice.*
To evaluate if VSMC-NOX5 in a VSMC-specific manner leads to phenotypic and structural changes in the brains of hypertensive VSMC-NOX5 mice, cerebrovascular function and phenotype markers GFAP, RhoA, ROCK1 and VEGFR2 were assessed by immunoblotting.
3. To explore whether VSMC-NOX5 regulates the expression of alternative NOX isoforms (NOX1, NOX2, and NOX4) in Ang II-induced hypertensive VSMC-NOX5 and WT mice.
To assess whether VSMC-NOX5 leads to changes in alternative NOX isoforms in the brains of Ang II- and no-treated male and female mice, mRNA and protein expression of NOX1, NOX2, and NOX4 were assessed by q-RT PCR and immunoblotting.
4. To explore if cerebral VSMC-NOX5 in Ang II-induced hypertensive mice alters the NOTCH3 signalling axis.
Male and female Ang II- and non-treated WT and VSMC-NOX5 mouse brains were used to assess NOTCH3 mRNA and protein (Full-length and intracellular domain) expression by q-RT PCR and immunoblotting respectively. Canonical downstream NOTCH3 transcription genes (*Hey1, HeyL, Hes1, and Hes5*) were also assessed by q-RT PCR.
5. *To examine the effects of VSMC-NOX5 on redox signalling in the brains of Ang II-mediated hypertensive VSMC-NOX5 mice.*
Oxidative stress was assessed in the brains of Ang II- and non-treated male and female WT and VSMC-NOX5 mice by measuring ROS production (lipid peroxidation and hydrogen peroxide), redox signalling (irreversibly oxidised protein tyrosine phosphatases) and antioxidant genes (*Sod1, Sod2, Nqo1, Ho1,* and *Catalase)*.
6. To identify if VSMC-NOX5 leads to changes in the ER UPR response in the context of Ang II mediated hypertension.
Immunoblotting of whole brain homogenates was conducted in Ang II- and non-treated male and female WT and VSMC-NOX5 mice to assess BIP levels, a marker of ER stress, in the brains of male and female WT and VSMC-NOX5 mice.

5.3 Results

5.3.1 Plethysmography Confirms a Hypertensive Phenotype by Surgical Implantation of Ang II in WT and VSMC-specific NOX5 Mice

To assess the role of hypertension in the brains of VSMC-NOX5 mice, mixed sex groups of 20-week-old WT and VSMC-NOX5 mice were treated with Ang II (600ng/kg/per-day) by mini-pump surgical implantation over a 4-week period. BP was measured utilising plethysmography with comparisons made to with comparisons made to 'non treated' (NT) and Ang II treated groups consisting of both male and female WT and VSMC-NOX5 mice. In NT and Ang II mixed sex groups, BP was increased in both WT (WT NT 119.0±14.12 mmHg vs WT+Ang II 179.9±16.41 mmHg p=<0.0001****) and NOX5 mice (NOX5 NT 122.6±11.9 mmHg vs NOX5+Ang II 171.6±10.8 mmHg p=<0.0001****) when compared to their NT counterparts (**Figure 5-1A)**.

When divided by sex, male NT v Ang II analysis, identified BP increases male WT (WT NT 122.6±11.83 mmHg vs WT+Ang II 182.5±17.6 mmHg p=<0.0001****) and male NOX5 mice (NOX5 NT 127.3±11.7 mmHg vs NOX5+Ang II 173.1±9.4 mmHg p=<0.0001****)) when compared to their NT counterparts (**Figure 5-1B)**.

In female NT v Ang II treated analysis, identified increased BP with Ang II treatment in both female WT (WT NT 113.9±16.4 mmHg vs WT+Ang II 173.8±12.54 mmHg p=<0.0001****) and female NOX5 mice (NOX5 NT 119.8±11.6 mmHg vs NOX5+Ang II 170.3±12.2 mmHg p=<0.0001****)) when compared to their NT counterparts (**Figure 5-1C)**. Collectively, these findings indicate a successful Ang II mediated hypertensive phenotype for experiments within this chapter.

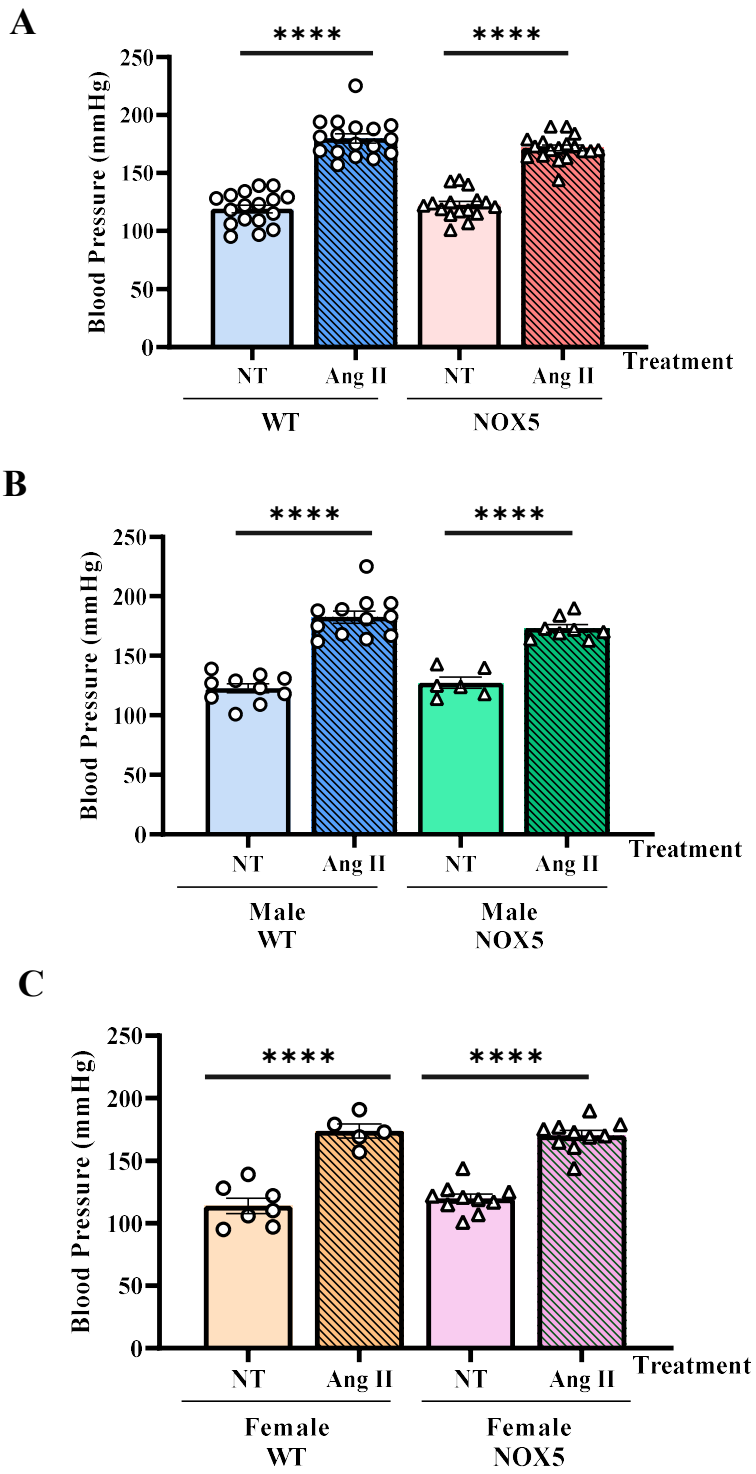

Figure 5-1. Confirmation of Ang II induced hypertensive phenotype in Ang II-treated WT and VSMC-specific NOX5 mice. Mixed sex (**A**), male (**B**) and female (**C**) systolic BP of NT or Ang II-treated WT and VSMC-NOX5 mice systolic BP was assessed using tail-cuff plethysmography over a 4-week period. Systolic BP was presented as mmHg. Mixed sex study n=16-18, male study n=6-12, female study n=6-10. Data was analysed using a one-way ANOVA with a Tukey's *post*-hoc test and presented as p≤0.0001****.

5.3.2 Assessment of GFAP Protein Levels in Whole Brain Homogenates of NT and Ang II-treated Male and Female WT and VSMC-specific NOX5 Mice

GFAP is a key cytoskeletal protein in astroglia homeostasis. Hypertension and oxidative stress have been linked to hypoxic changes that alter NVU dysfunction through impairments to astrocytes. In chapter 3, this thesis identified that NOX5 overexpression in a VSMC-specific manner led to reduced GFAP protein expression in a sex-dependent manner. This study aimed to assess whether hypertension in the context of NOX5 would cause alterations to GFAP protein levels. Protein levels of GFAP were assessed by immunoblotting in whole brain homogenate samples and normalised to REVERT total protein stain in male and female WT and VSMC-NOX5 mice treated with Ang II. No differences were observed in either male (**Figure 5-2A**) or female (**Figure 5-2B**) WT or VSMC-NOX5 genotype when assessing GFAP protein levels in the context of Ang II mediated hypertension.

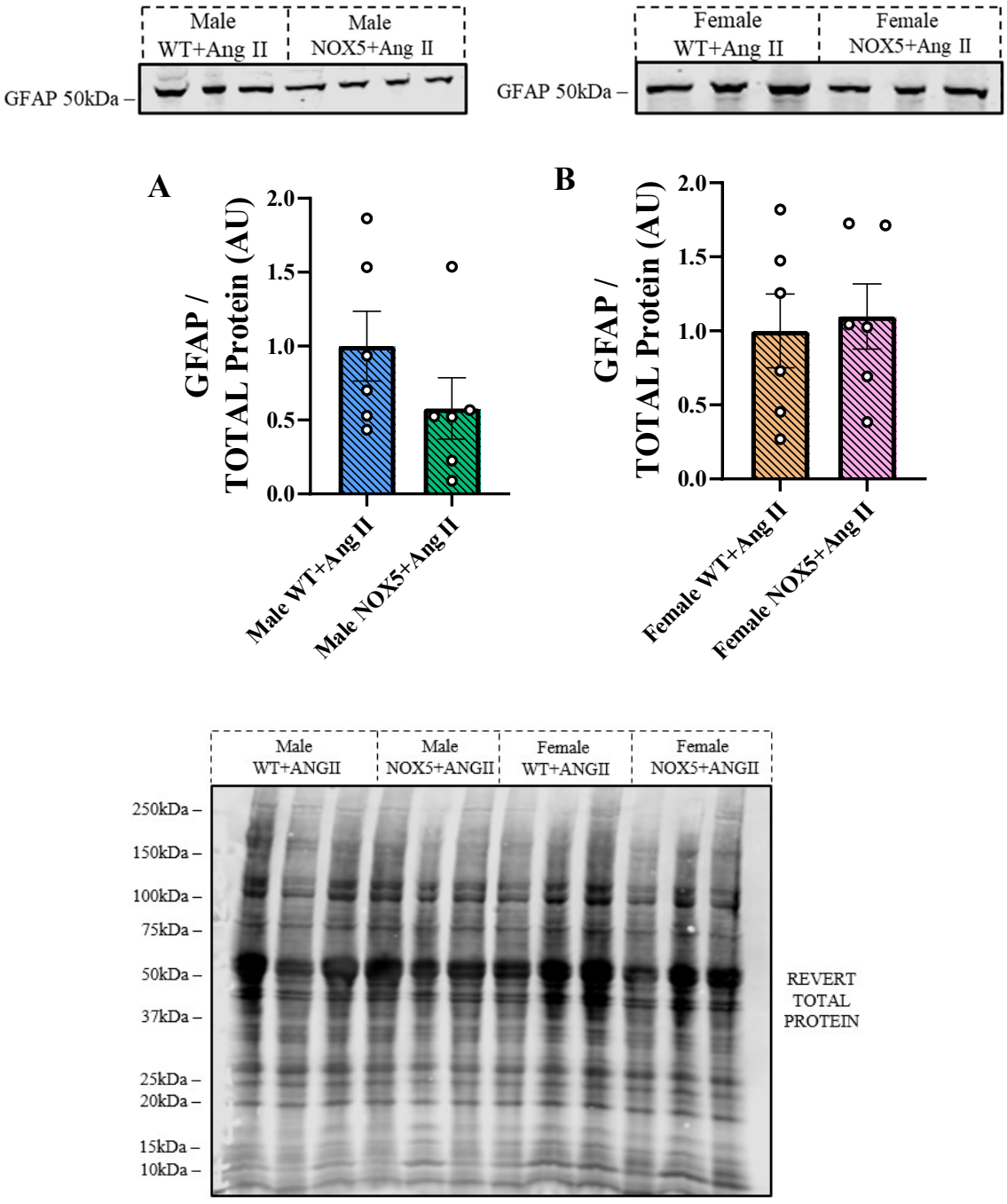

Figure 5-2. Whole brain assessment of GFAP protein levels in male and female Ang II treated WT and NOX5 mice. Whole brain lysates from Ang II-treated male (**A**) and female (**B**) WT and VSMC-NOX5 hypertensive mice were utilised to assess GFAP protein levels by immunoblotting. Protein levels were normalised by REVERT total protein stain and presented as fold change AU. Male study n=6, female study n=6. Data was analysed by a student's *t*-test.

5.3.3 RhoA/ROCK1 Protein Level Assessment in Whole Brain Homogenates of NT and Ang II-treated Male and Female WT and VSMC-specific NOX5 Mice

This study aimed to assess whether hypertension in the context of NOX5 would cause alterations to protein levels of the RhoA/ROCK contractile signalling pathway. Protein levels of RhoA/ROCK1 were assessed by immunoblotting in whole brain homogenate samples and normalised to REVERT total protein stain in male and female WT and VSMC-NOX5 mice treated with Ang II. No differences were observed in either male or female WT or VSMC-NOX5 genotype when assessing RhoA (**Figures 5-3A-B**) or ROCK1 (**Figures 5-3C-D**) protein levels in the context of Ang II mediated hypertension.

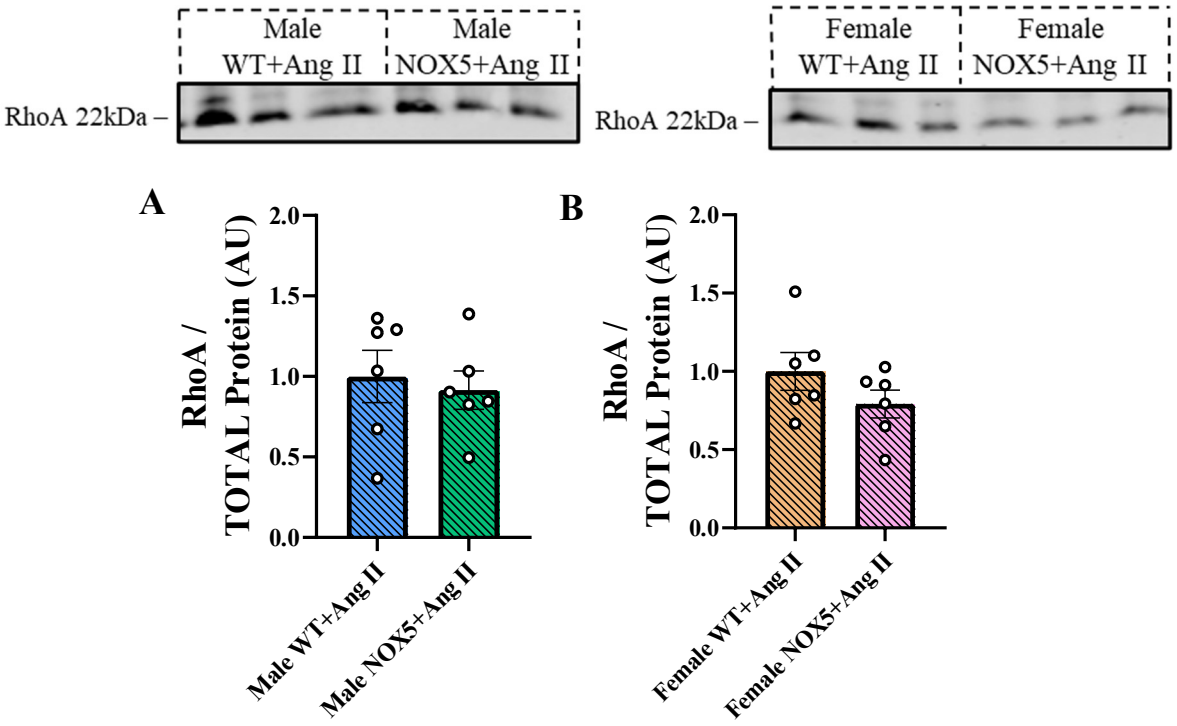

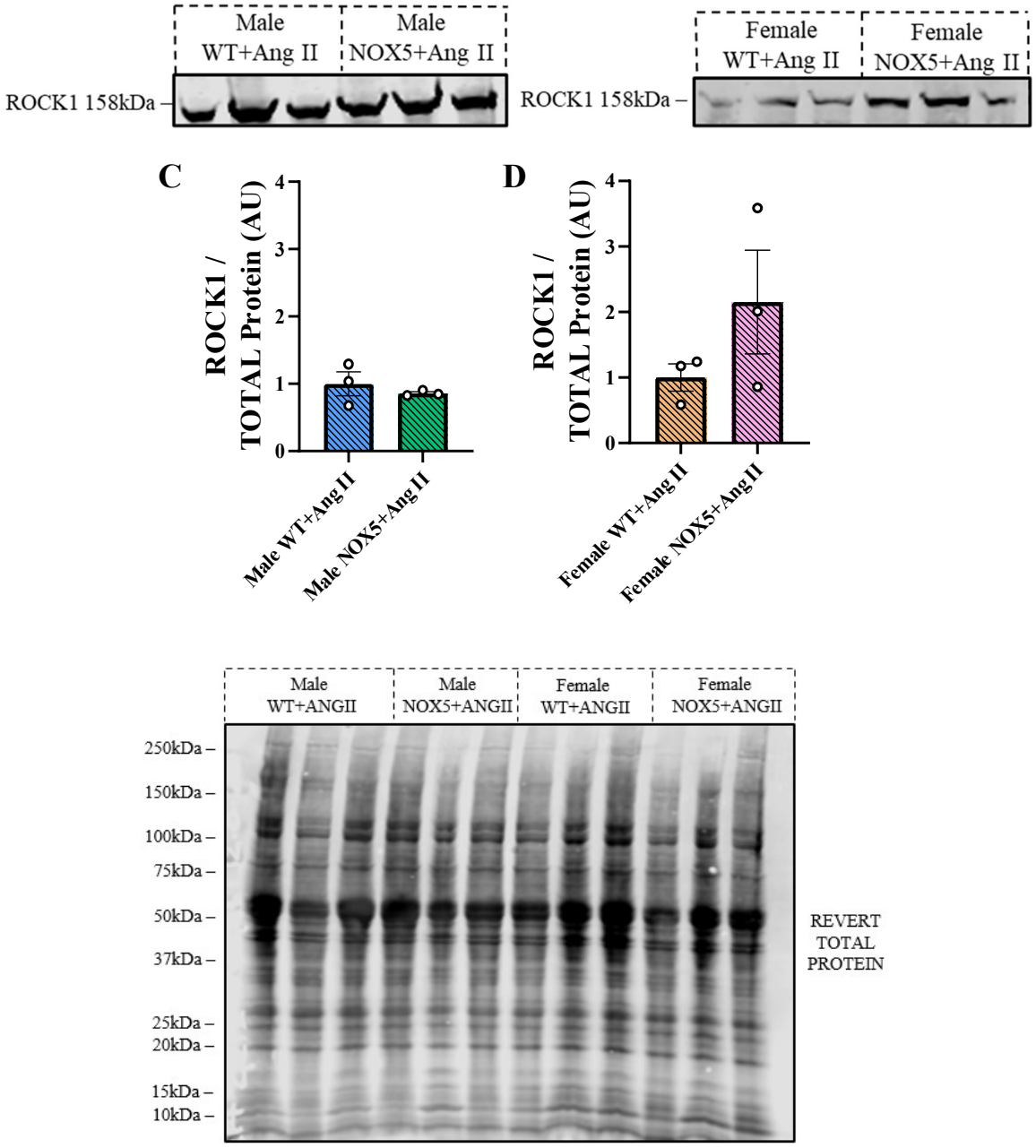

Figure 5-3. Whole brain assessment of RhoA and ROCK1 protein levels in male and female Ang II treated WT and NOX5 mice. Whole brain lysates from Ang II-treated male and female WT and VSMC-NOX5 hypertensive mice were utilised to assess RhoA (**A-B**) and ROCK1 (**C-D**) protein levels by immunoblotting. Protein levels were normalised by REVERT total protein stain and presented as fold change AU. Male study n=3, female study n=3. Data was analysed by a student's *t*-test.

5.3.4 Assessment of VEGFR2 Protein Levels in Whole Brain Homogenates of NT and Ang II-treated Male and Female WT and VSMC-specific NOX5 Mice

Oxidative stress and VEGFR2 plays a key role in BP homeostasis, with changes to VEGFR2 signalling contributing to hypertension. Protein levels of cerebrovascular VEGFR2 were assessed by immunoblotting in whole brain homogenate samples and normalised to REVERT total protein stain in male and female WT and VSMC-NOX5 mice treated with Ang II. Assessment of VEGFR2 identified no changes in male VSMC-NOX5 mice treated with Ang II when compared to WT+Ang II mice (**Figure 5-4A**). Assessment of VEGFR2 in whole brain homogenates of female mice (**Figure 5-4B**) identified that Ang II treatment of VSMC-NOX5 mice led to a significant decrease in VEGFR2 protein levels when compared to WT+Ang II mice (Female NOX5+Ang II 1.00±0.08 AU vs Female WT+Ang II 0.69±0.10 AU p=0.03*).

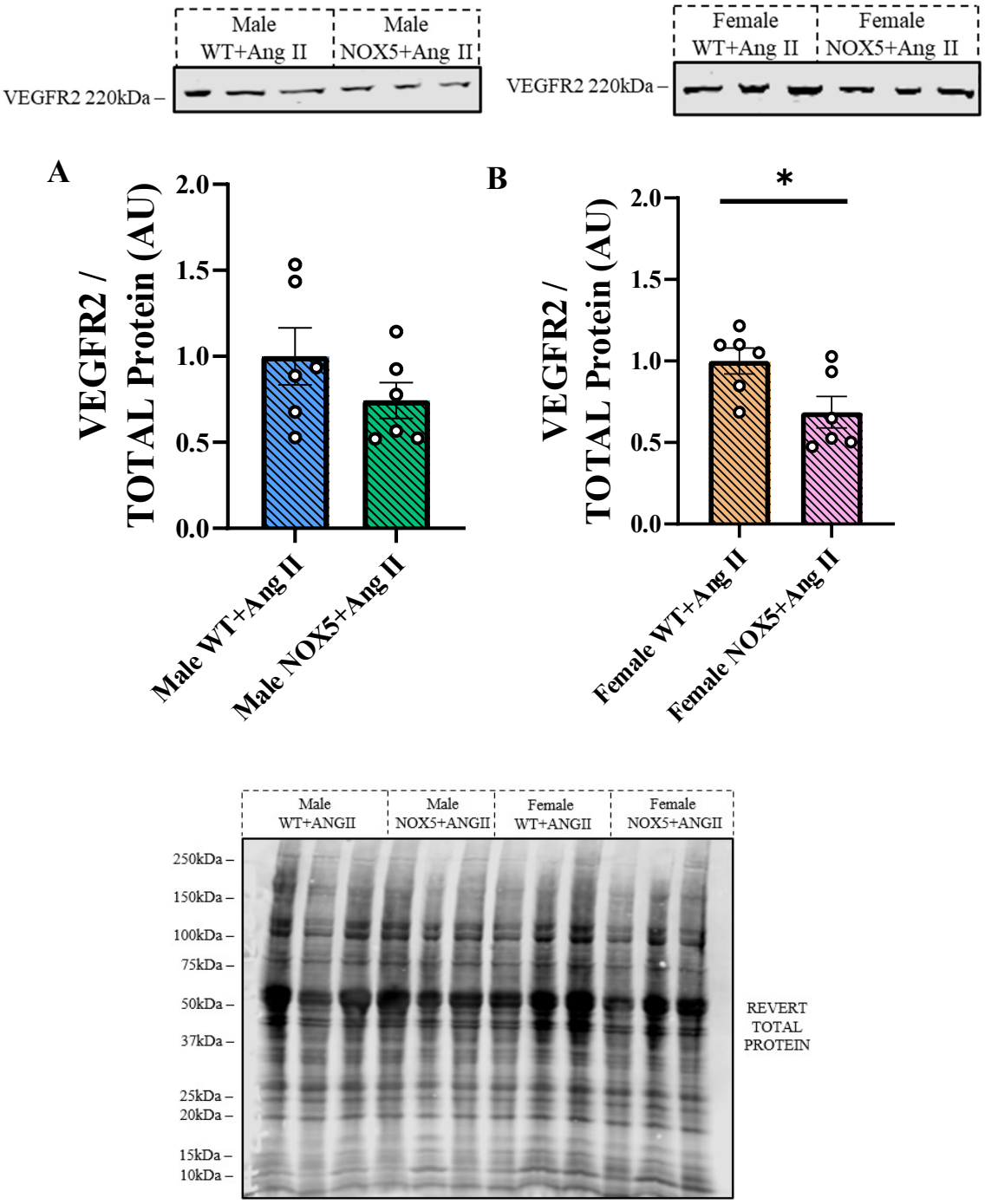

Figure 5-4. Whole brain assessment of VEGFR2 protein levels in male and female Ang II treated WT and NOX5 mice. Whole brain lysates from Ang II-treated male (**A**) and female WT (**B**) and VSMC-NOX5 hypertensive mice were utilised to assess VEGFR2 protein levels by immunoblotting. Protein levels were normalised by REVERT total protein stain and presented as fold change AU. Male study n=6, female study n=6. Data was analysed by a student's *t*-test and presented as *p≤0.05.

5.3.5 Assessment of Cerebral NOX1 Protein and Gene Expression in NT and Ang II-treated Male and Female WT and VSMC-NOX5 Mice

NADPH oxidase expression and activity is upregulated in hypertension, contributing to oxidative stress. In the context of Ang II mediated hypertension, this thesis aimed to elucidate the role of NOX5 on alternative NOX isoform activity. Whole brain homogenates from male and female, NT and Ang II-treated, WT and VSMC-NOX5 mice were used to assess NOX1 mRNA expression and protein levels by q-RT PCR and immunoblotting respectively. *Nox1* mRNA expression was identified to increase in mixed sex analysis (**Figure 5-5A**) of hypertensive WT (WT+Ang II 9.10±0.25 ΔCt vs WT NT 10.35±0.20 ΔCt p=0.004**). When separated by sex, increases in *Nox1* mRNA was identified in both male WT (Male WT+Ang II 9.00±0.54 ΔCt vs Male WT NT 10.59±0.36 ΔCt p=0.03#), and female (Female WT+Ang II 9.176±0.22 ΔCt vs Female WT NT 10.17±0.22 ΔCt p=0.01#) WT mice. No differences were observed collectively or by sex in NOX5+Ang II mice (**Figures 5-5B-C**).

Mixed sex assessment of analysis of NOX1 immunoblotting identified that treatment of Ang II led to increased NOX1 protein levels in whole brain homogenates of both WT (WT+Ang II 1277.14±315.63 AU vs WT NT 360.07±41.00 AU p=0.03*) and NOX5 (NOX5+Ang II 1138.07±311.24 AU vs NOX5 NT 344.57±48.29 AU p=0.02#) mice when compared to NT samples (**Figure 5-5D**).

When separated by sex, male Ang II treated VSMC-specific NOX5 mice were observed to have increased NOX1 protein levels when compared to their normotensive VSMC-NOX5 counterparts (NOX5+Ang II 828.86±162.93 AU vs NOX5 NT 342.29±44.51 AU p=0.02*). Furthermore, no differences were observed in NT or Ang II WT male mice (**Figure 5-5E**). No differences in NOX1 protein levels were observed between treatment or genotype in whole brain homogenates of female WT and VSMC-NOX5 mice (**Figure 5-3F**).

A

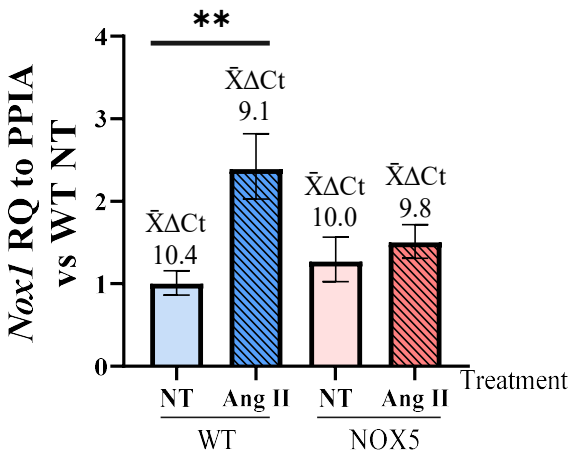
**
Nox1 RQ to PPIA vs WT NT
X̄ΔCt 10.4
X̄ΔCt 9.1
X̄ΔCt 10.0
X̄ΔCt 9.8
NT
Ang II
NT
Ang II
WT
NOX5
Treatment

B

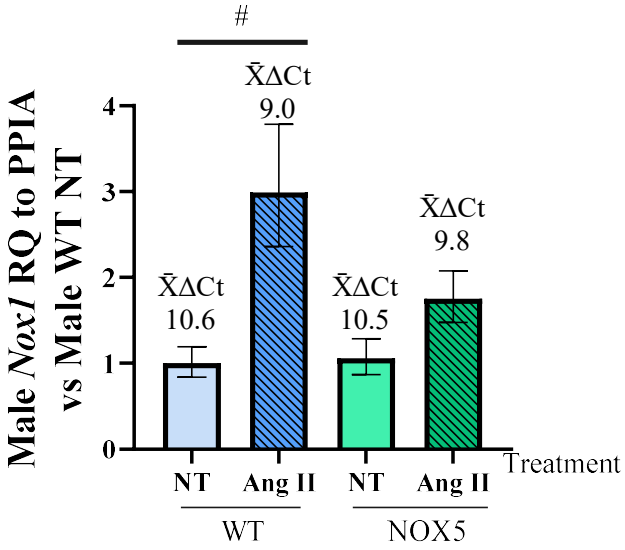
#
Male Nox1 RQ to PPIA vs Male WT NT
X̄ΔCt 10.6
X̄ΔCt 9.0
X̄ΔCt 10.5
X̄ΔCt 9.8
NT
Ang II
NT
Ang II
WT
NOX5
Treatment

C

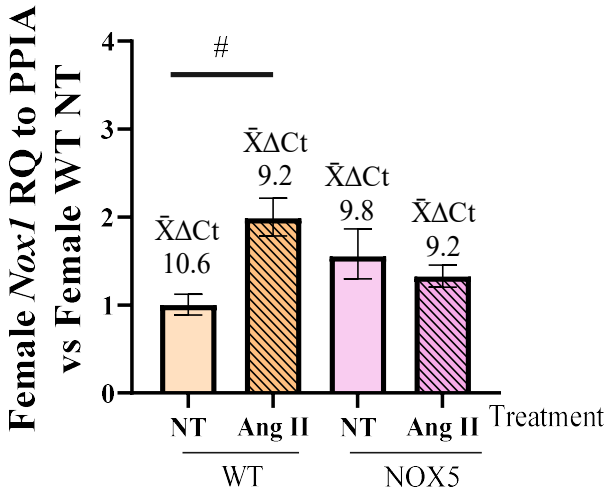
#
Female Nox1 RQ to PPIA vs Female WT NT
X̄ΔCt 10.6
X̄ΔCt 9.2
X̄ΔCt 9.8
X̄ΔCt 9.2
NT
Ang II
NT
Ang II
WT
NOX5
Treatment

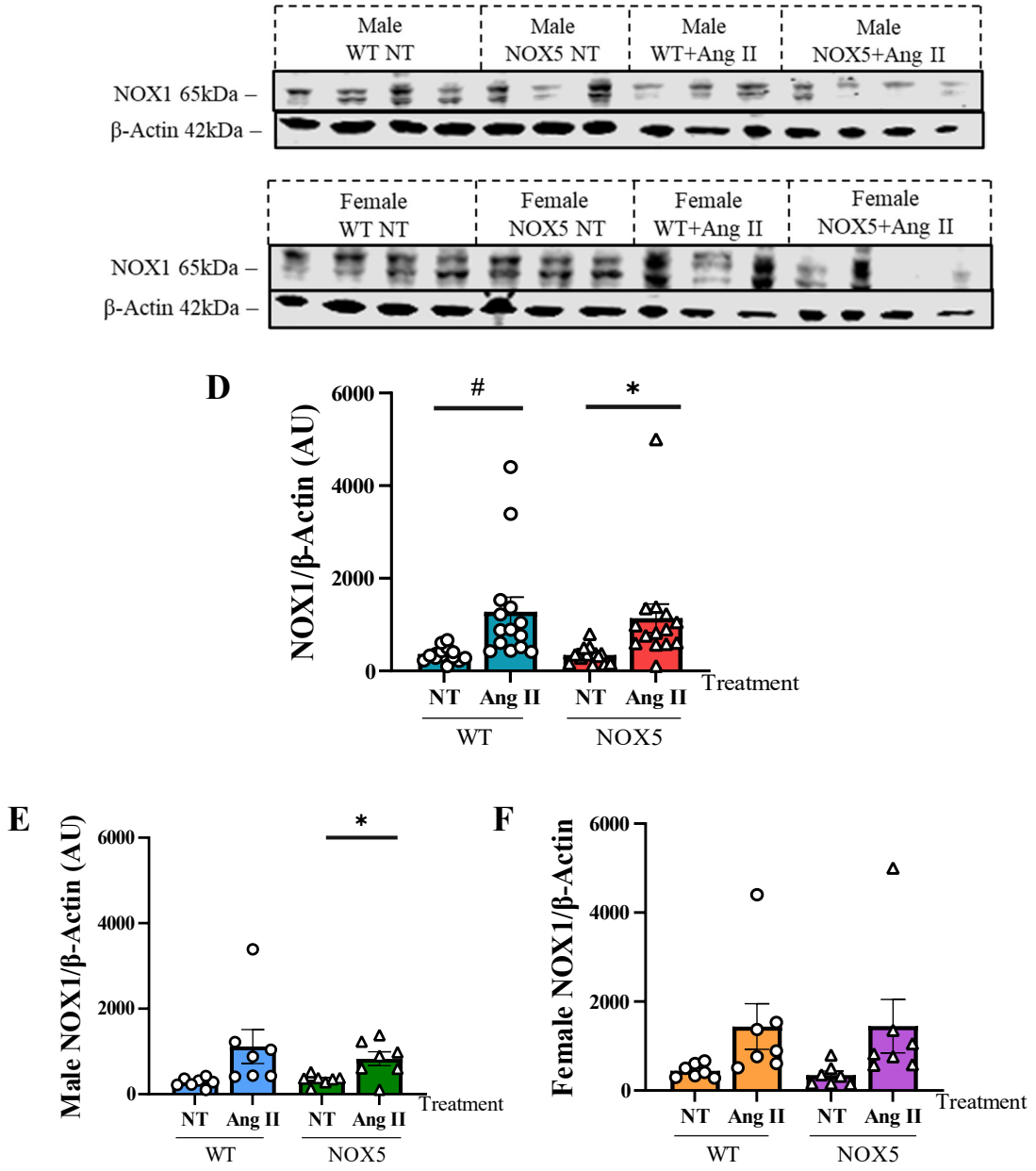

Figure 5-5. Assessment of NOX1 mRNA and protein expression in Ang II- and NT treated male and female WT and VSMC-NOX5 mice. NOX1 mRNA and protein expression was assessed in whole brain homogenates of male and female WT and VSMC-NOX5 mice in Ang II- and non-treated groups. *Nox1* mRNA expression was assessed by q-RT PCR with RQ fold change being calculated from ΔΔCt following *Ppia* housekeeping gene normalisation (**A-C**). Full-length NOX1 protein expression (**D-F**) was assessed by immunoblotting and were presented as AU after normalisation by β-actin. Mixed sex study n=9-14, male study n=4-7, and female study n=5-7. Data was analysed using a two-way ANOVA with a Tukey's *post*-hoc test and presented as *p≤0.05, **p≤0.01. Further analysis was conducted using a student's *t*-test and were presented as #p≤0.05.

5.3.6 Gene and Protein Assessment of Cerebral NOX2 Expression in NT and Ang II-treated Male and Female WT and VSMC-NOX5 Mice

Whole brain homogenates were used to assess NOX2 mRNA expression and protein levels by q-RT PCR and immunoblotting respectively in male and female, NT and Ang II-treated, WT and VSMC-NOX5 mice. Assessment of *Nox2* mRNA expression identified no changes in gene expression in mixed sex or separated-by-sex analysis in both Ang II-treated or NT WT and VSMC-NOX5 mice (**Figures 5-6A-C**). Immunoblotting analysis of NOX2 protein levels identified no changes in mixed sex (**Figures 5-6D**), or in male analysis (**Figures 5-6E)** between treatment or genotype. Assessment of NOX2 protein expression in NT or Ang II-treated female WT and VSMC-NOX5 mouse groups identified a decrease in protein levels in WT mice treated with Ang II, when compared to NT WT samples (WT+Ang II 280571.43±40211.85 AU vs WT NT 171385±29613.88 AU p=0.049#). No differences were observed in NOX2 protein levels in Ang II-treated or non-treated VSMC-NOX5 mice (**Figures 5-6F**).

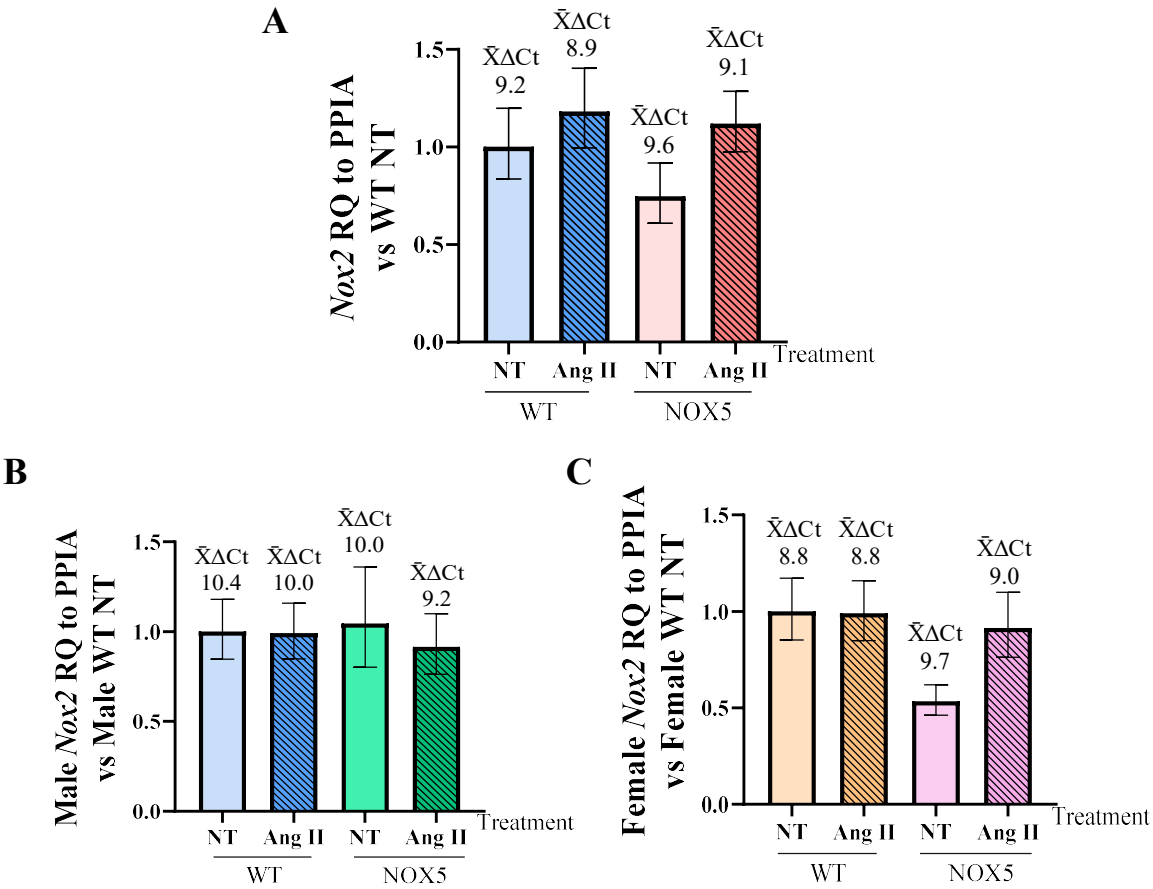

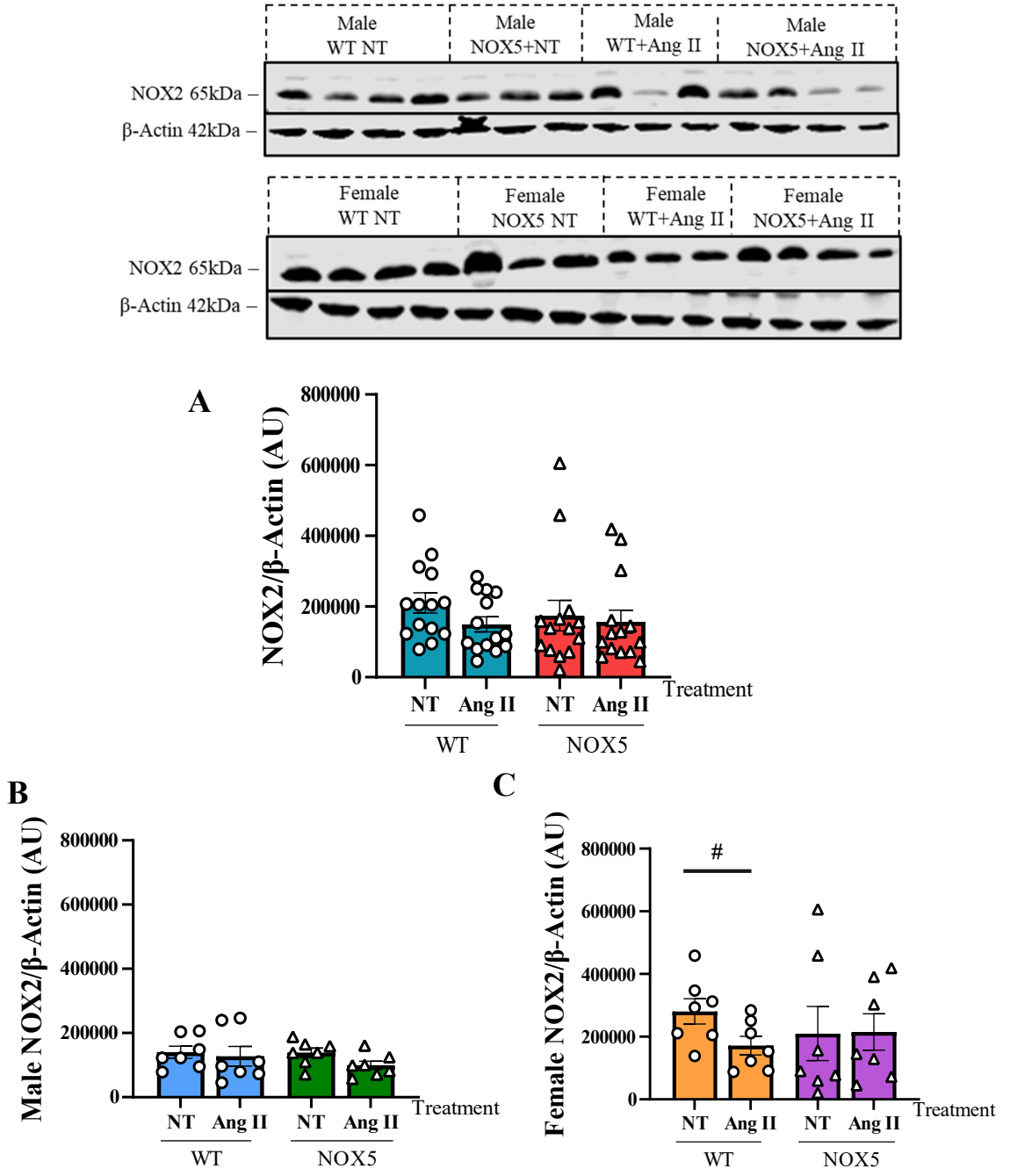

Figure 5-6. NOX2 mRNA and protein expression in Ang II- and NT treated male and female WT and VSMC-NOX5 mice. NOX2 mRNA and protein expression was assessed in whole brain homogenates of male and female WT and VSMC-NOX5 mice in Ang II-and non-treated groups. *Nox2* mRNA expression was assessed by q-RT PCR with RQ fold change being calculated from ΔΔCt following *Ppia* housekeeping gene normalisation (**A-C**). Full-length NOX2 protein expression (**D-F**) was assessed by immunoblotting and were presented as AU after normalisation by β-actin. Mixed sex study n=14, male study n=7, and female study n=7. Data was analysed using a two-way ANOVA with a Tukey's *post*-hoc test with *p≤0.05.

5.3.7 Examination of Cerebral NOX4 protein and Gene Expression in NT and Ang II-treated Male and Female WT and VSMC-NOX5 Mice

NOX4 mRNA expression and protein levels were assessed using q-RT PCR and immunoblotting in whole brain homogenates of male and female, NT and Ang II-treated, WT and VSMC-NOX5 mice. *Nox4* mRNA expression data identified no changes in gene expression in mixed sex or separated-by-sex analysis in both Ang II-treated or NT WT and VSMC-NOX5 mice (**Figures 5-7A-C**).

Mixed sex immunoblotting analysis of NOX4 protein levels identified a significant increase in hypertensive VSMC-NOX5 mice (**Figure 5-7D**), when compared to normotensive VSMC-NOX5 mice (VSMC-NOX5+Ang II 19177.14±3988.15 AU vs VSMC-NOX5 NT 9590.74±1788.68 AU p=0.037#). When separated by sex, assessment of males identified a significant increase in NOX4 protein levels between male WT NT and male WT+Ang II mice (Male WT+Ang II 23571.43±3343.84 AU vs Male WT NT 12745.71±1638.40 AU p=0.013#), with no differences being identified between treatments in male VSMC-NOX5 mice (**Figure 5-7E**). No differences in NOX4 protein levels were observed between treatment or genotype in female WT and VSMC-NOX5 mice (**Figure 5-7F**).

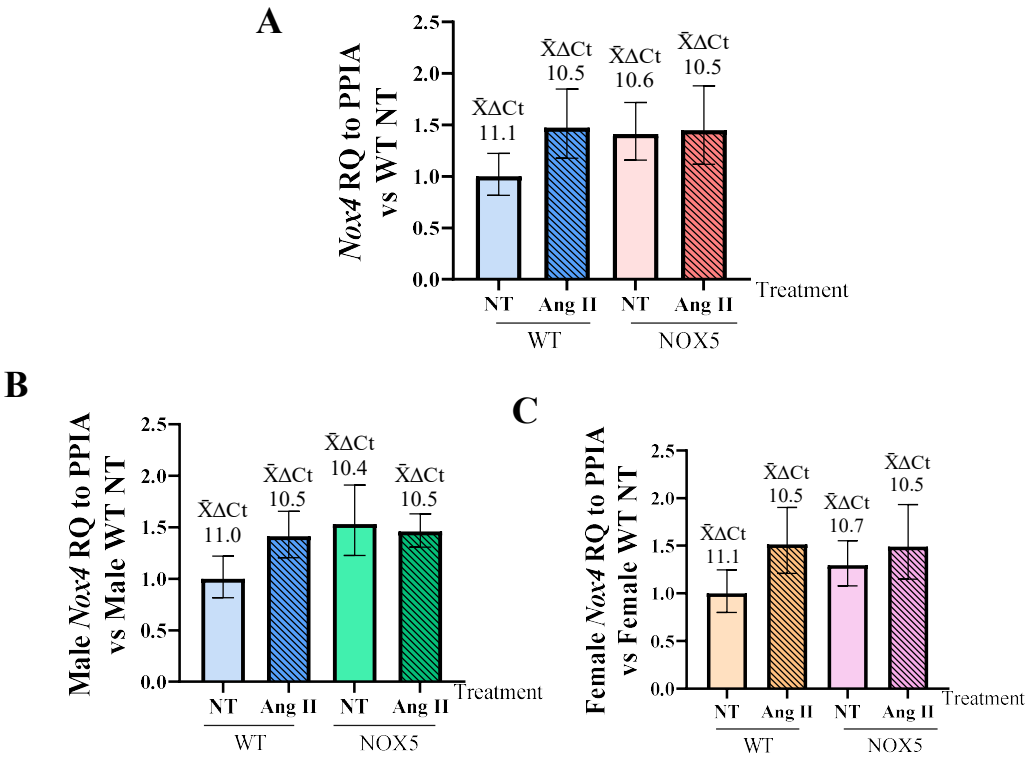

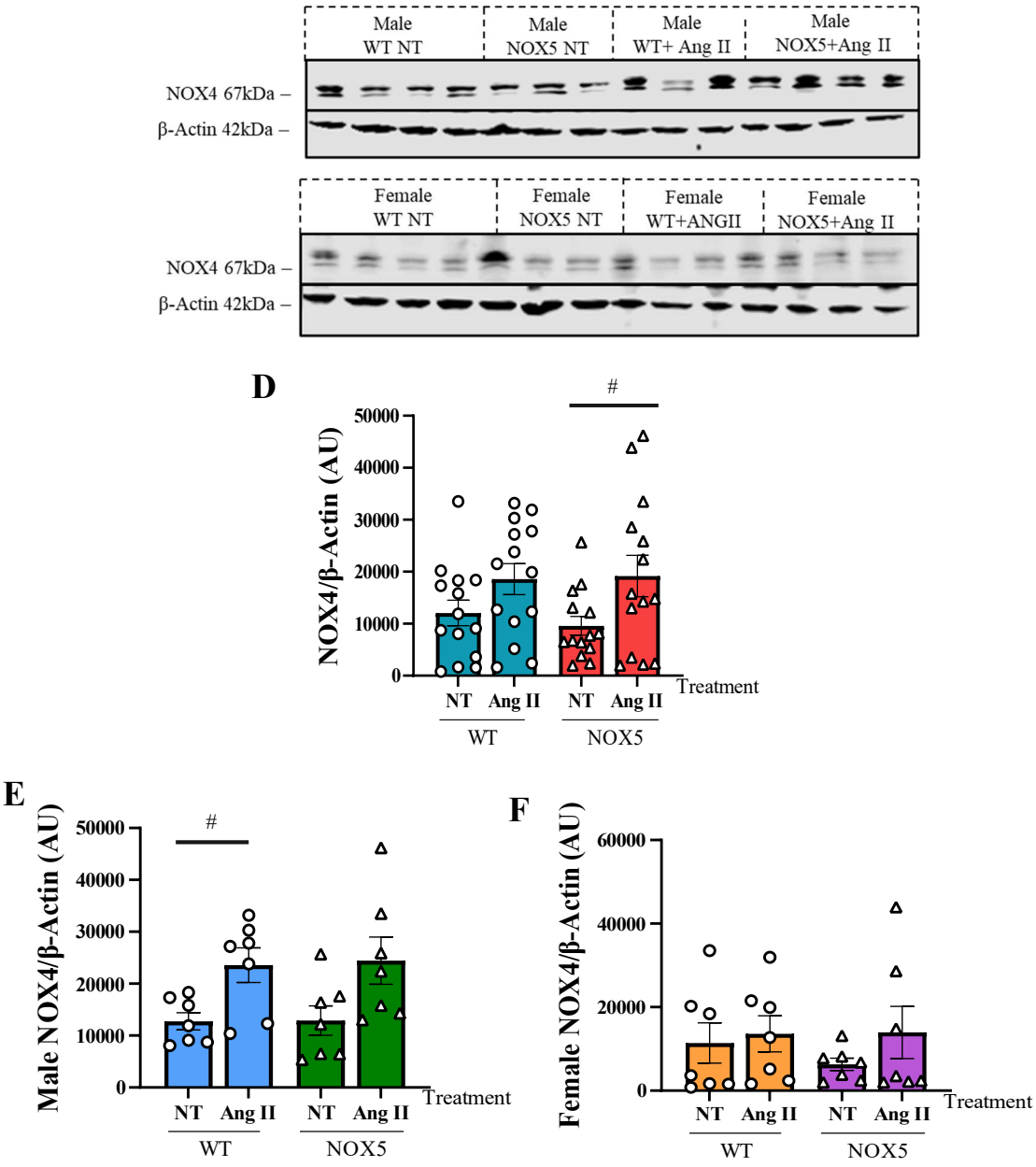

Figure 5-7. Assessment of NOX4 mRNA and protein expression in Ang II- and NT treated male and female WT and VSMC-NOX5 mice. NOX4 mRNA and protein expression was assessed in whole brain homogenates of male and female WT and VSMC-NOX5 mice in Ang II- and non-treated groups. *Nox4* mRNA expression was assessed by q-RT PCR with RQ fold change being calculated from ΔΔCt following *Ppia* housekeeping gene normalisation (**A-C**). Full-length NOX4 protein expression (**D-F**) was assessed by immunoblotting and were presented as AU after normalisation by β-actin. Mixed sex study n=13-14, male study n=6-7, and female study n=6-7. Data was analysed using a two-way ANOVA with a Tukey's *post*-hoc test with *p≤0.05.

5.3.8 NOTCH3 mRNA expression and protein levels assessment of cerebral VSMC-NOX5 mice in the context of Ang II-mediated hypertension

Whole brain homogenates of male and female normotensive and hypertensive WT and NOX5 mice were used to assess *Notch3* mRNA expression and Full length NOTCH3 protein levels by q-RT PCR and immunoblotting. Assessment of *Notch3* mRNA expression identified that NT VSMC-NOX5 led to a significant decrease in levels in mixed sex (WT NT 5.40±0.12 ΔCt vs NOX5 NT 5.93±0.17 ΔCt p=0.02#) **Figure 5-8A**)) and female analyses (Female WT NT 5.38±0.12 ΔCt vs Female NOX5 NT 6.15±0.19 ΔCt p=0.006## (**Figure 5-8C**)) VSMC-NOX5 led to a significant decrease in gene expression compared to WT NT mice. No changes were observed in *Notch3* mRNA expression between genotypes and treatment in male mice (**Figure 5-8B**).

Assessment of Full-Length NOTCH3 protein levels identified a significant increase in protein levels when examined collectively between Ang II mediated hypertensive and NT WT (WT+Ang II 2006.14±349.08 AU vs WT NT 619.90±138.79 AU p=0.02*), and VSMC-NOX5 mice (VSMC-NOX5+Ang II 2362.79±467.68 AU vs VSMC-NOX5 NT 689.46±143.46 AU p=0.003**) **Figure 5-8D**)).

Sex-specific analysis identified that treatment of Ang II also increased Full-length NOTCH3 protein levels in male WT (Male WT+Ang II 2433.57±588.96 AU vs Male WT NT 501.00±198.06 AU p=0.045*) and male VSMC-NOX5 (Male VSMC-NOX5+Ang II 3512.86±636.20 AU vs Male VSMC-NOX5 NT 480.00±110.74 AU p=0.001**) mice when compared to their NT counterparts (**Figures 5-8E**). No differences in Full-Length NOTCH3 protein levels were identified between genotype and treatment in female mice (**Figure 5-8F**).

A

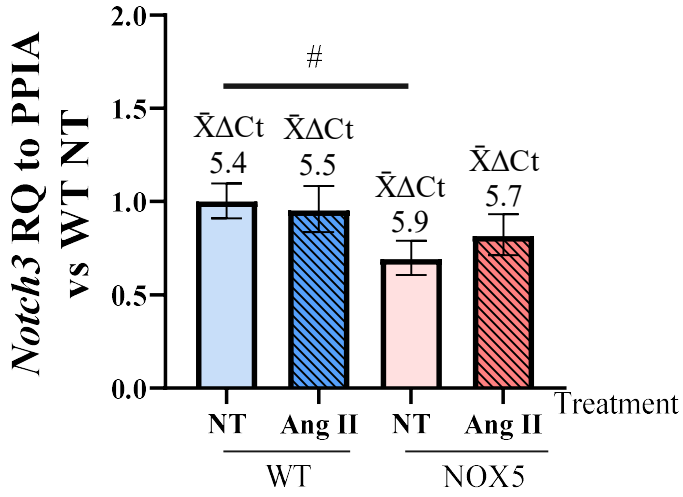
Notch3 RQ to PPIA
vs WT NT
2.0
1.5
1.0
0.5
0.0
#
X̄ΔCt
5.4
X̄ΔCt
5.5
X̄ΔCt
5.9
X̄ΔCt
5.7
NT
Ang II
NT
Ang II
Treatment
WT
NOX5

B

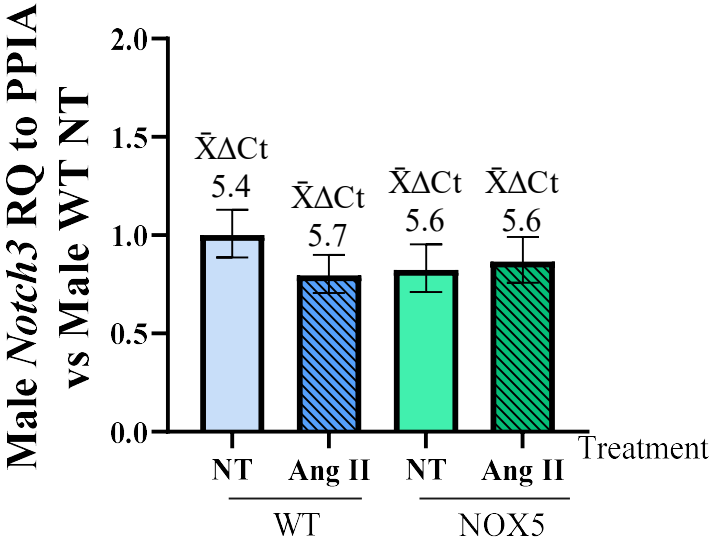
Male Notch3 RQ to PPIA
vs Male WT NT
2.0
1.5
1.0
0.5
0.0
X̄ΔCt
5.4
X̄ΔCt
5.7
X̄ΔCt
5.6
X̄ΔCt
5.6
NT
Ang II
NT
Ang II
Treatment
WT
NOX5

C

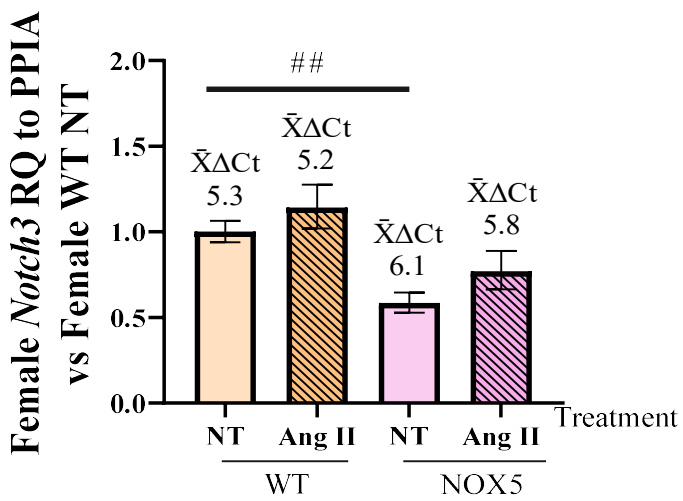
Female Notch3 RQ to PPIA
vs Female WT NT
2.0
1.5
1.0
0.5
0.0
##
X̄ΔCt
5.3
X̄ΔCt
5.2
X̄ΔCt
6.1
X̄ΔCt
5.8
NT
Ang II
NT
Ang II
Treatment
WT
NOX5

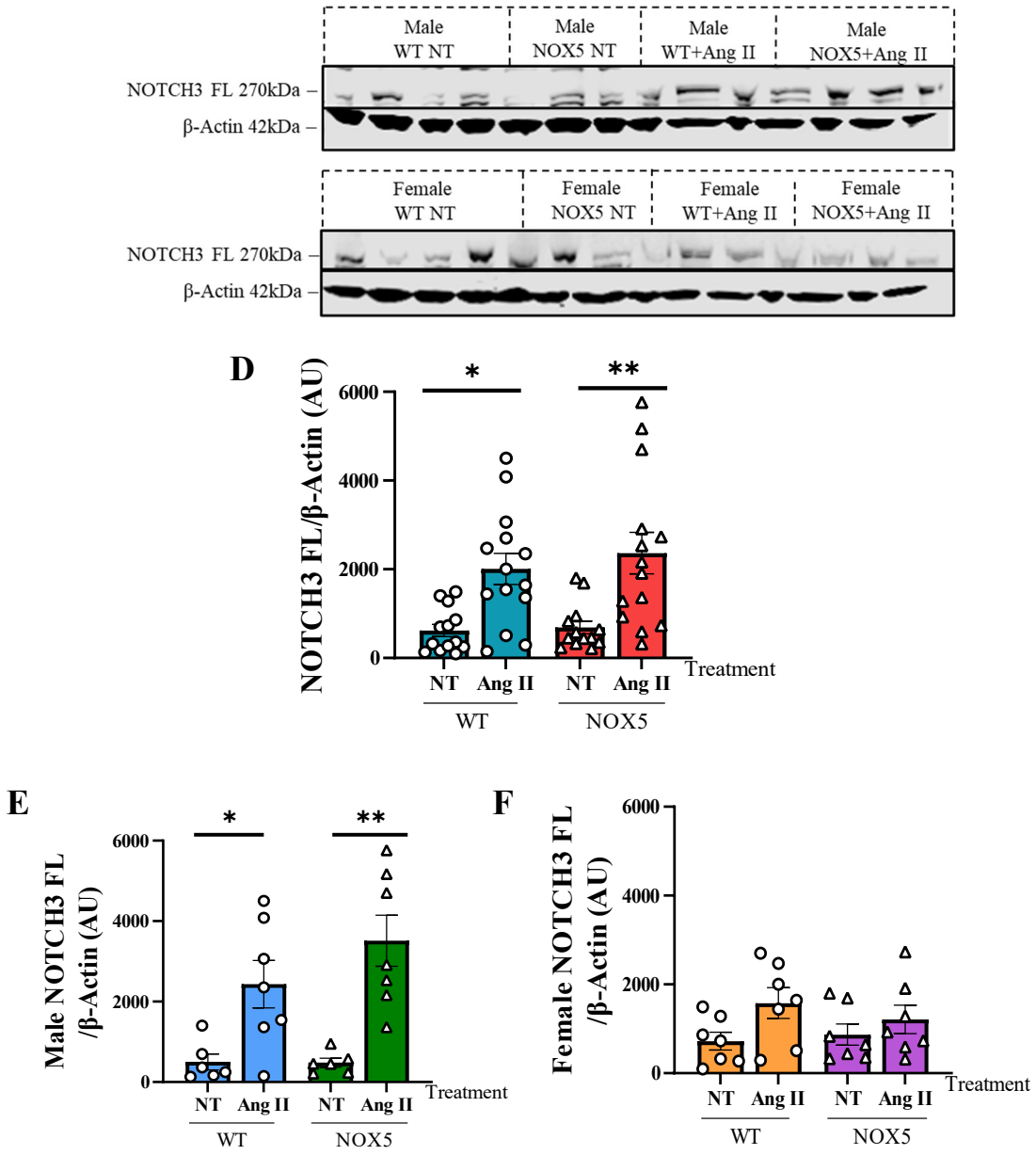

Figure 5-8. Assessment of NOTCH3 mRNA and protein expression in Ang II- and NT treated male and female WT and VSMC-NOX5 mice. NOTCH3 mRNA and protein expression was assessed in whole brain homogenates of male and female WT and VSMC-NOX5 mice in Ang II- and non-treated groups. *Notch3* mRNA expression was assessed by q-RT PCR with RQ fold change being calculated from ΔΔCt following *Ppia* housekeeping gene normalisation (**A-C**). Full-length NOTCH3 protein expression (**D-F**) was assessed by immunoblotting and were presented as AU after normalisation by β-actin. Mixed sex study n=13-14, male study n=6-7, and female study n=7. Data was analysed using a two-way ANOVA with a Tukey's *post*-hoc test and presented as *p≤0.05, **p≤0.01. Further analysis was conducted using a student's *t*-test and were presented as #p≤0.05, ##p≤0.01.

5.3.9 N3-ICD Protein Level Assessment of Cerebral VSMC-NOX5 Mice in the Context of Ang II-mediated Hypertension.

N3-ICD protein levels were assessed by immunoblotting in whole brain lysates of normotensive and Ang II-induced hypertensive male and female WT and VSMC-NOX5 mice. In mixed sex analysis, Ang II WT mice were identified to have increased N3-ICD protein levels when compared to NT WT mice (WT+Ang II 6792.14±995.03 AU vs WT NT 3337.86±545.51 AU p=0.008**). No differences were observed collectively in VSMC-NOX5 mice (**Figure 5-9A**).

Sex-specific assessment of Ang II-induced hypertension led to increased N3-ICD protein levels in male WT (Male WT+Ang II 7824.29±1513.68 AU vs Male WT NT 2832.86±127.55 AU p=0.03*) and male VSMC-NOX5 (Male WT+Ang II 6662.86±1411.01 AU vs Male WT NT 3010.00±248.82 AU p=0.03#), when compared to their normotensive counterparts (**Figure 5-9B**).

No differences were identified between treatment and genotype in female mice treated with Ang II (**Figure 5-9C**).

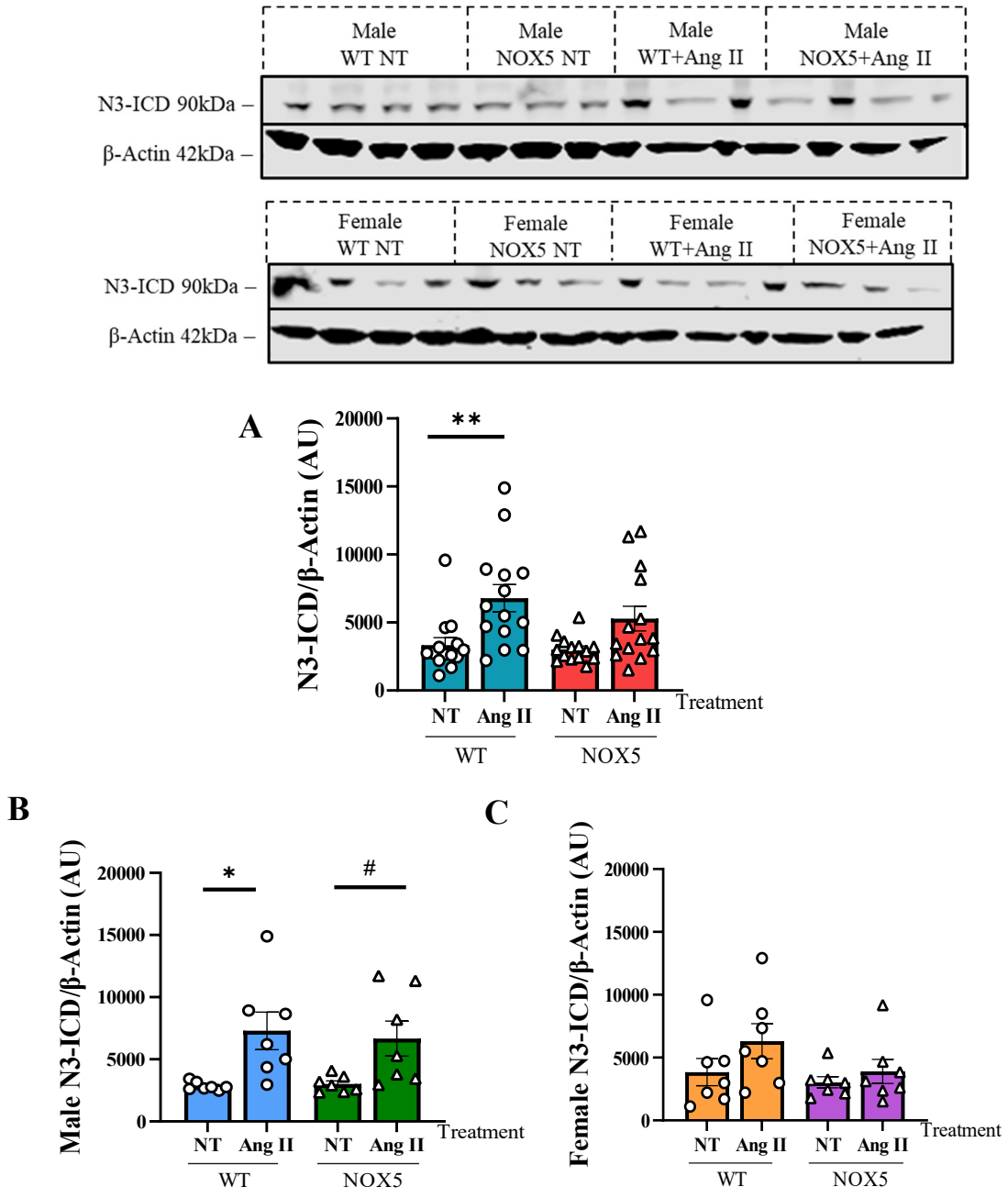

Figure 5-9. Assessment of intracellular domain NOTCH3 protein levels in Ang II- and NT treated male and female WT and VSMC-NOX5 mice. Whole brain homogenates of Ang II-treated and on-treated male and female WT and VSMC-NOX5 mice were used to assess N3-ICD protein expression by immunoblotting (**A-C).** Immunoblotting expression was normalised to β-actin and expressed as (AU). Mixed sex study n=13-14, male study n=6-7, and female study n=7. Data was analysed using a two-way ANOVA with a Tukey's *post*-hoc test and presented as *p≤0.05, **p≤0.01. Further analysis was conducted using a student's *t*-test and were presented as #p≤0.05.

5.3.10 Downstream NOTCH3 Transcription Factor *Hes* mRNA Expression Assessment in Cerebral VSMC-NOX5 Mice in the Context of Ang II-Mediated Hypertension

Downstream NOTCH3 transcription *Hes* genes were assessed to examine whether the alterations in N3-ICD contributed to canonical NOTCH3 signalling. Whole brain homogenates of male and female normotensive and Ang II-induced hypertensive WT and NOX5 mice were used to assess downstream classical NOTCH3 signalling axis *Hes1* and *Hes5* transcriptional genes by q-RT PCR. *Hes1* mRNA expression was not found to change between normotensive and hypertensive WT and VSMC-NOX5 genotypes in mixed sex (**Figure 5-10A**), or by sex specific (**Figures 5-10B-C**) analyses. Similarly, *Hes5* gene expression was also identified to be unaltered between normotensive and hypertensive WT and VSMC-NOX5 genotypes in mixed sex (**Figure 5-10D**), or by sex specific (**Figures 510E-F**) analyses.

A

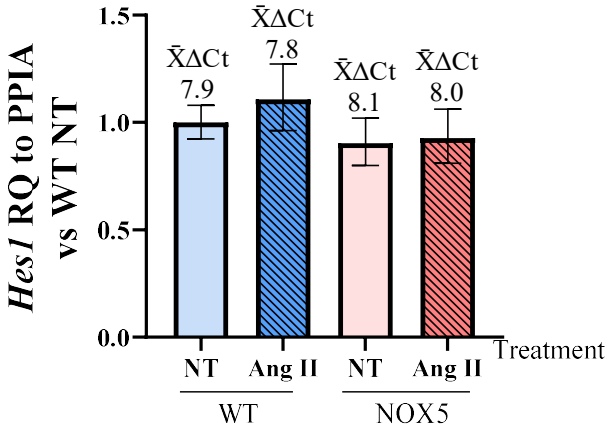
Hes1 RQ to PPIA
vs WT NT
1.5
1.0
0.5
0.0
X̄ΔCt
7.9
X̄ΔCt
7.8
X̄ΔCt
8.1
X̄ΔCt
8.0
NT
Ang II
NT
Ang II
Treatment
WT
NOX5

B

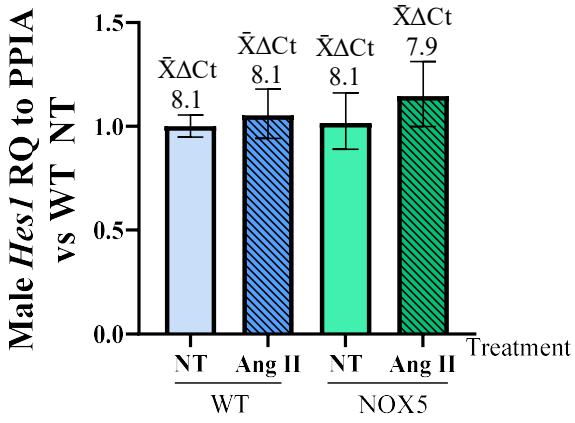
Male Hes1 RQ to PPIA
vs WT NT
1.5
1.0
0.5
0.0
X̄ΔCt
8.1
X̄ΔCt
8.1
X̄ΔCt
8.1
X̄ΔCt
7.9
NT
Ang II
NT
Ang II
Treatment
WT
NOX5

C

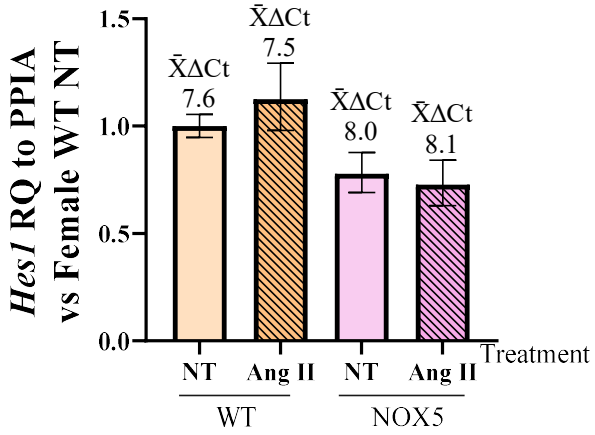
Hes1 RQ to PPIA
vs Female WT NT
1.5
1.0
0.5
0.0
X̄ΔCt
7.6
X̄ΔCt
7.5
X̄ΔCt
8.0
X̄ΔCt
8.1
NT
Ang II
NT
Ang II
Treatment
WT
NOX5

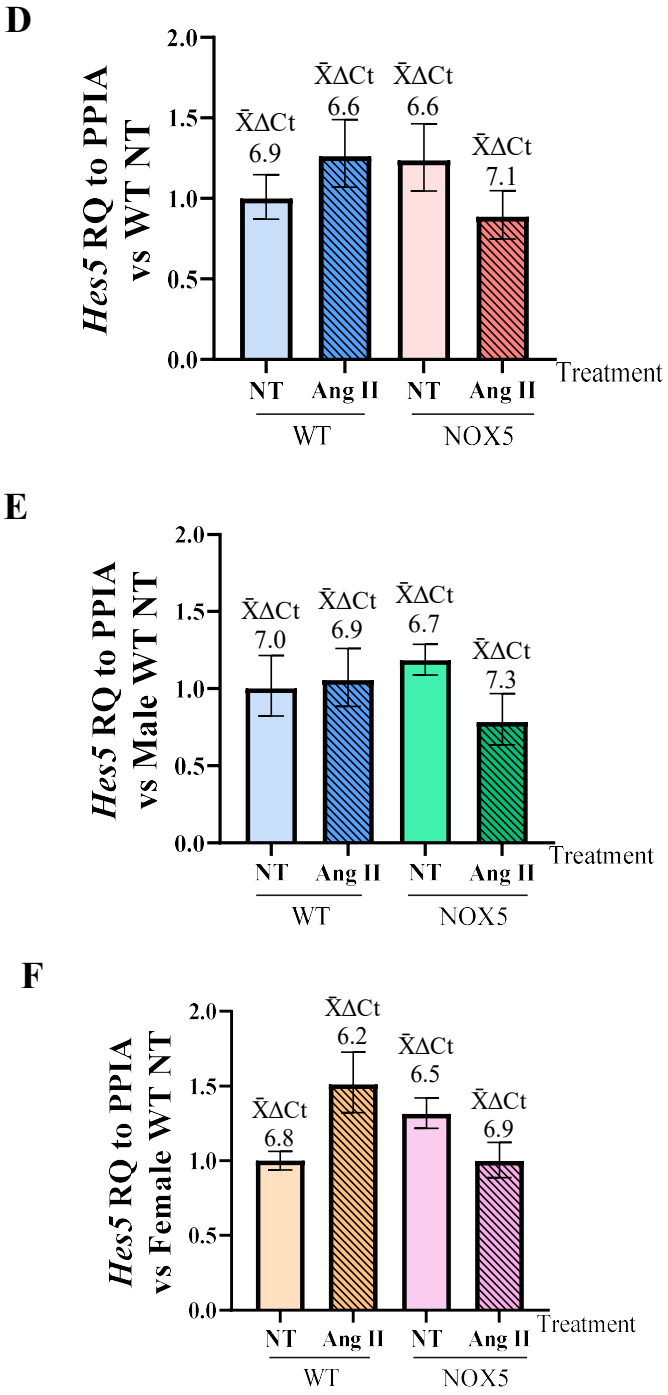

Figure 5-10. Downstream 'classical' NOTCH3 transcription targets *Hes1* and *Hes5* mRNA expression in Ang II- and non-treated male and female WT and VSMC-NOX5 mice. Downstream NOTCH3 targets; *Hes1* (**A-C**)*, Hes5* (**D-F**) mRNA expression was assessed collectively and in Ang II- and non-treated male and female WT and VSMC-NOX5 mouse brain homogenates using q-RT PCR. Gene expression was assessed by q-RT PCR with RQ fold change being calculated from ΔΔCt following *Ppia* housekeeping gene normalisation. Mixed sex study n=13-14, male study n=7, and female study n=6-7. Data was analysed using a two-way ANOVA with a Tukey's *post*-hoc test.

5.3.11 Downstream NOTCH3 Transcription Factor *Hey* mRNA Expression Assessment in the Brains of Ang II-treated VSMC-NOX5 Mice

Downstream NOTCH3 transcription *Hey* genes were also assessed to examine whether the alterations in N3-ICD contributed to canonical NOTCH3 signalling. Whole brain homogenates of male and female normotensive and Ang II-induced hypertensive WT and NOX5 mice were used to assess downstream classical NOTCH3 signalling axis *Hey1* and *HeyL* transcriptional genes by q-RT PCR. *HeyL* mRNA expression was unaltered between genotype or treatment in mixed sex and sex-dependent analyses (**Figures 5-11A-C**). However, when examining *Hey1* mRNA expression, collectively, Ang II-treatment led to decreases in *Hey1* gene expression in both WT (WT+Ang II 3.89±0.09 ΔCt vs WT NT 3.3±0.16 ΔCt p=0.004##) and VSMC-NOX5 (VSMC-NOX5+Ang II 3.97±0.18 ΔCt vs VSMC-NOX5 NT 2.95±0.17 ΔCt p=0.0002***) mice when assessed collectively (**Figure 5-11D**).

When split by sex, Ang II-treatment of VSMC-NOX5 mice led to a significant decrease in *Hey1* expression when compared to VSMC NT mice (Male VSMC-NOX5+Ang II 3.91±0.13 ΔCt vs Male VSMC-NOX5 NT 2.78±0.33 ΔCt p=0.007***). No differences in *Hey1* mRNA expression were observed between Ang II-treated and NT male WT mice (**Figure 5-11E**).

Assessment of female WT and VSMC-NOX5 mice identified that Ang II-treatment led to a significant decrease in *Hey1* gene expression in both WT (Female WT+Ang II 3.64±0.08 ΔCt vs Female WT NT 3.06±0.17 ΔCt p=0.01#) and VSMC-NOX5 (Female VSMC-NOX5+Ang II 4.04±0.39 ΔCt vs Female VSMC-NOX5 NT 3.09±0.14 ΔCt p=0.02*), when compared to their NT counterparts (**Figure 5-11F**).

A

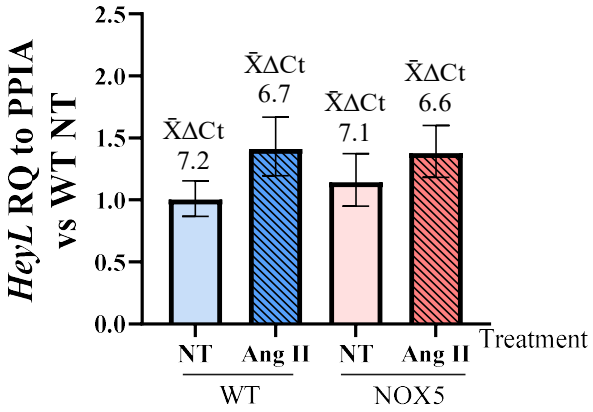
HeyL RQ to PPIA
vs WT NT
2.5
2.0
1.5
1.0
0.5
0.0
X̄ΔCt
7.2
X̄ΔCt
6.7
X̄ΔCt
7.1
X̄ΔCt
6.6
NT
Ang II
NT
Ang II
Treatment
WT
NOX5

B

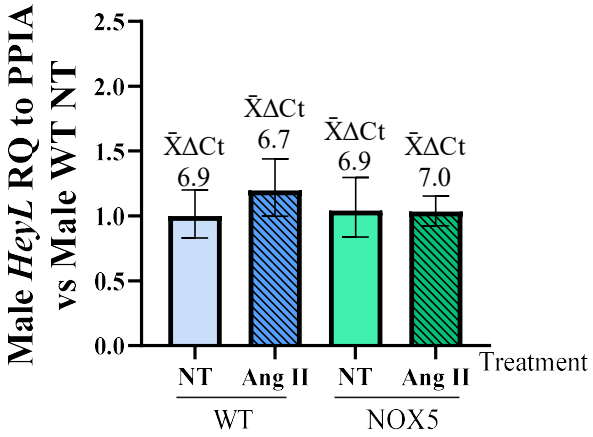
Male HeyL RQ to PPIA
vs Male WT NT
2.5
2.0
1.5
1.0
0.5
0.0
X̄ΔCt
6.9
X̄ΔCt
6.7
X̄ΔCt
6.9
X̄ΔCt
7.0
NT
Ang II
NT
Ang II
Treatment
WT
NOX5

C

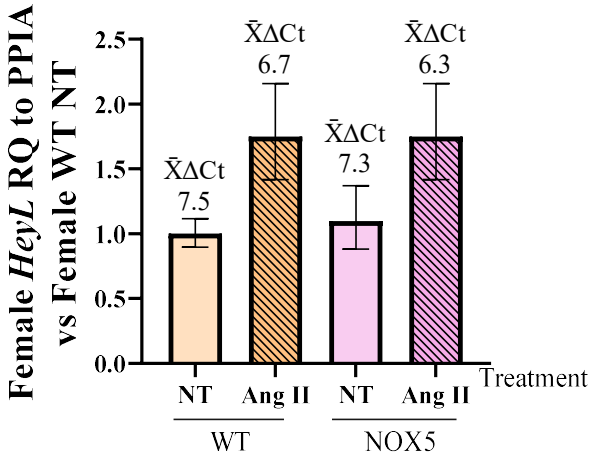
Female HeyL RQ to PPIA
vs Female WT NT
2.5
2.0
1.5
1.0
0.5
0.0
X̄ΔCt
7.5
X̄ΔCt
6.7
X̄ΔCt
7.3
X̄ΔCt
6.3
NT
Ang II
NT
Ang II
Treatment
WT
NOX5

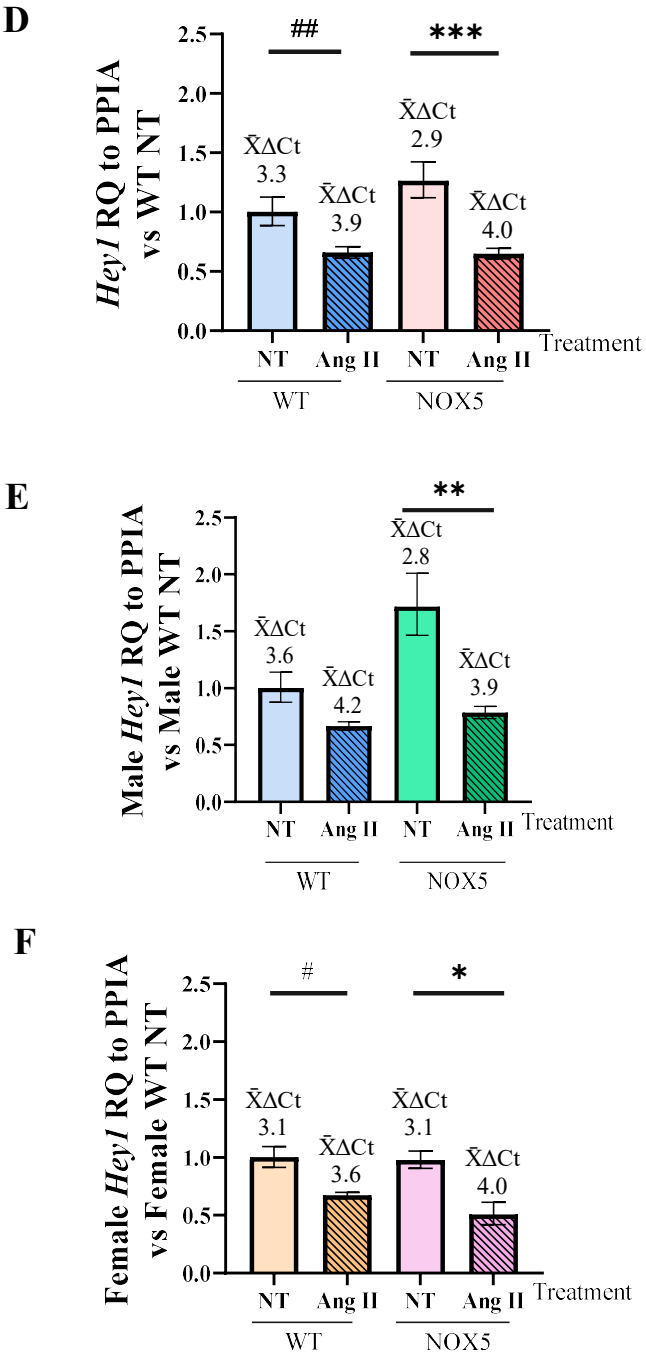

Figure 5-11. Downstream 'classical' NOTCH3 transcription targets *HeyL*, and *Hey1* mRNA expression in Ang II- and non-treated male and female WT and VSMC-NOX5 mice.
Downstream NOTCH3 targets; *HeyL* (**A-C**)*, and Hey1* (**D-F**) mRNA expression was assessed collectively and in Ang II- and non-treated male and female WT and VSMC-NOX5 mouse brain homogenates using q-RT PCR. Gene expression was assessed by q-RT PCR with RQ fold change being calculated from ΔΔCt following *Ppia* housekeeping gene normalisation. Mixed sex study n=12-14, male study n=5-7, and female study n=5-7. Data was analysed using a two-way ANOVA with a Tukey's *post*-hoc test and presented as *p≤0.05, **p≤0.01, ***p≤0.001. Further analysis was conducted using a student's *t*-test and were presented as #p≤0.05.

5.3.12 Assessment of Cerebral H_2O_2 Levels in NT and Ang II-treated Male and Female WT and VSMC-specific NOX5 Mice

To assess whether VSMC-NOX5 leads altered ROS status in the context of hypertension, this study assessed H_2O_2 and lipid peroxidation levels in whole brain homogenates of normotensive and Ang II-induced hypertensive male and female WT and VSMC-NOX5 mice. To do this, Amplex-Red and TBARS MDA experiments were utilised. In mixed sex analysis, cerebral H_2O_2 levels remained unchanged by Ang II-induced hypertension in both WT and VSMC-NOX5 mice when compared to their NT counterparts (**Figure 5-12A**).

Sex-specific analysis identified H_2O_2 levels were decreased in Ang II-induced hypertensive VSMC-NOX5 males when compared to male VSMC-NOX5 NT mice (Male VSMC-NOX5+Ang II 1.29±0.08 µg/protein vs Male VSMC-NOX5 NT 2.26±0.24 µg/protein p=0.002##), with no changes being observed between treatments of male WT mice (**Figure 5-12B**).

No changes were observed in female H_2O_2 mice regardless of treatment or genotype (**Figure 5-12C**).

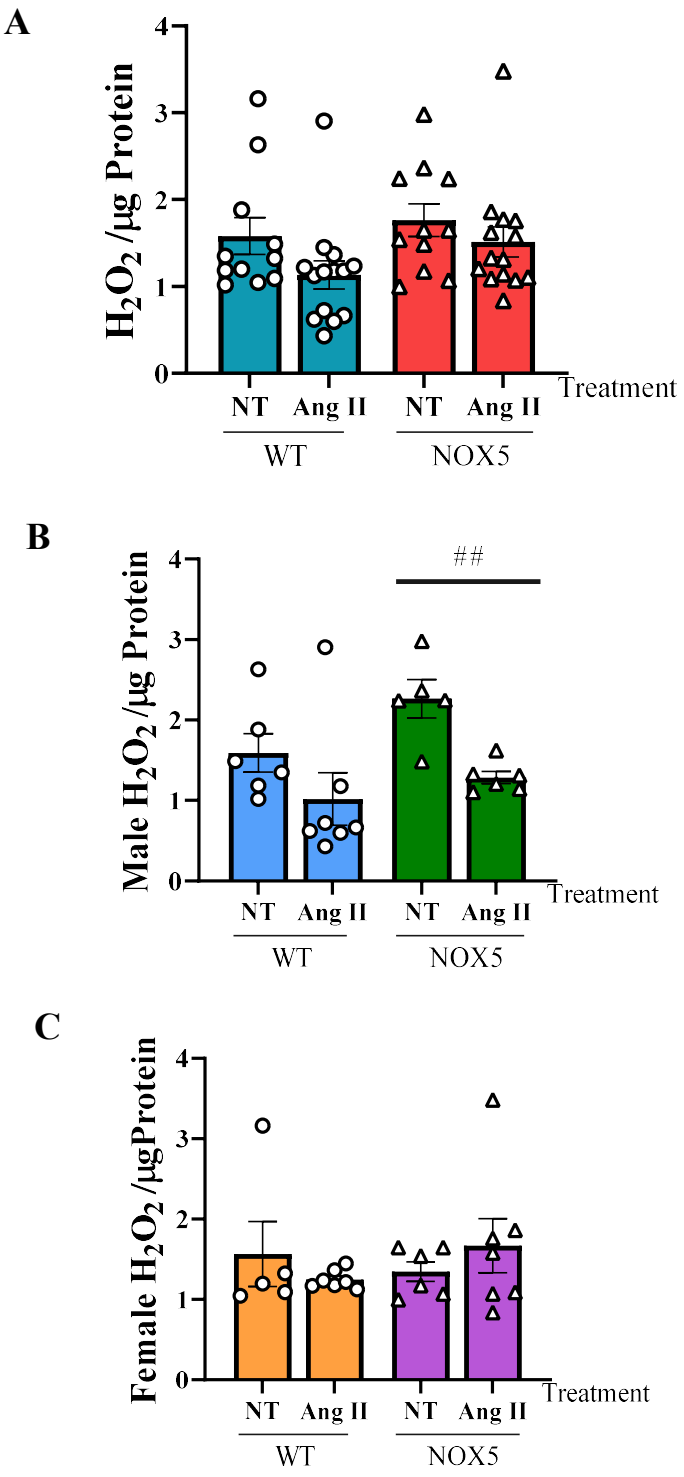

Figure 5-12. Assessment of H_2O_2 levels in Ang II- and NT treated male and female WT and VSMC-NOX5 mice. Whole brain homogenates of Ang II-treated and on-treated male and female WT and VSMC-NOX5 mice were used to assess H_2O_2 levels by Amplex-Red (**A-C**). Samples used for Amplex-Red experiments were normalised to protein (µg/protein) using BCA protein assessment. Mixed sex study n=11-14, male study n=5-7, and female study n=4-7. Data was analysed using a two-way ANOVA with a Tukey's *post*-hoc test. Further analysis was conducted using a student's *t*-test and were presented as #p≤0.05, ##p≤0.01.

5.3.13 Assessment of Cerebral Lipid Peroxidation Levels in NT and Ang II treated Male and Female WT and VSMC-specific NOX5 Mice

To assess whether VSMC-specific NOX5-KI in the context of Ang II mediated hypertension contributes to exacerbated oxidative stress. TBARS-MDA was utilised to assess lipid peroxidation levels. Mixed sex analysis of TBARS-MDA identified that Ang II-treatment leads to a decrease in markers of lipid peroxidation in VSMC-NOX5 mice (VSMC-NOX5+Ang II 2.76±0.33 µmol/protein vs VSMC-NOX5 NT 2.76±0.47 µmol/protein p=0.02*), with no changes being identified between Ang II and non-treated WT mice (**Figure 5-13A**).

Sex specific analysis of males and females were also assessed with male Ang II-treated VSMC-NOX5 mice leading to a decrease in lipid peroxidation levels (Male VSMC-NOX5+Ang II 3.00±0.42 µmol/protein vs Male VSMC-NOX5 NT 4.31±0.34 µmol/protein p=0.04#). No changes were identified between WT Ang II-treated and NT male mice (**Figure 5-13B**).

Assessment of female mice identified a significant decrease between Ang II-treated VSMC-NOX5 and VSMC-NOX5 NT mice (Female VSMC-NOX5+Ang II 1.28±0.26 µmol/protein vs Female VSMC-NOX5+NT 3.25±0.43 µmol/protein p=0.006**). Furthermore, *post*-hoc analysis also identified a significant difference between Ang II-treated VSMC-NOX5 and WT female mice (Female VSMC-NOX5+Ang II 1.28±0.26 µmol/protein vs Female WT+Ang II 2.63±0.25 µmol/protein p=0.004##). No differences were observed between female Ang II-treated and NT WT mice (**Figure 5-13C**).

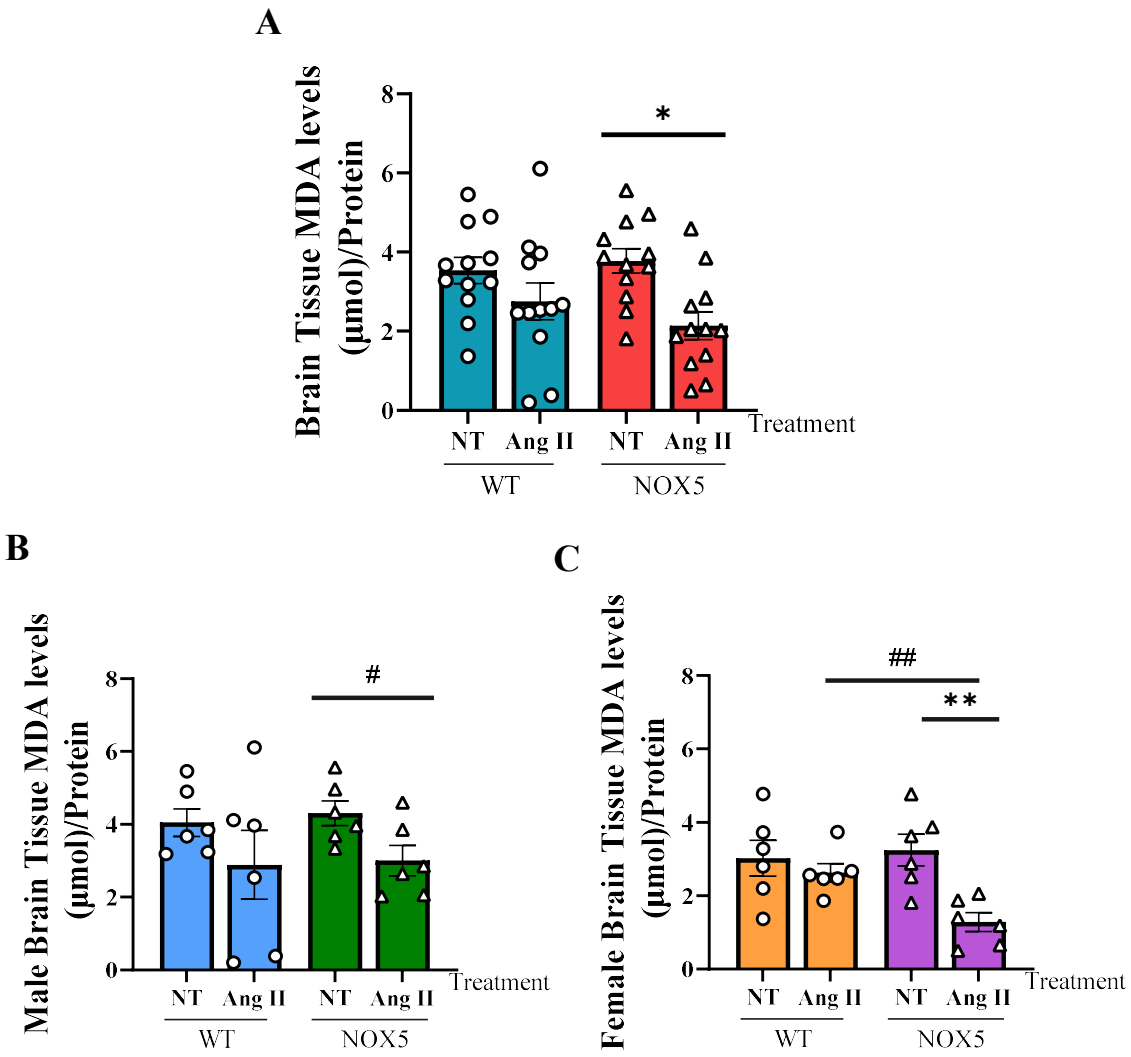

Figure 5-13. Assessment of lipid peroxidation levels in Ang II- and NT treated male and female WT and VSMC-NOX5 mice. Whole brain homogenates of Ang II-treated and on-treated male and female WT and VSMC-NOX5 mice were used to assess lipid peroxidation levels by TBARS-MDA (**A-C**). Samples used for TBARS experiments were normalised to protein (µmol) using BCA protein assessment. Mixed sex study n=11-12, male study n=6-7, and female study n=6. Data was analysed using a two-way ANOVA with a Tukey's *post*-hoc test and presented as *p≤0.05, **p≤0.01. Further analysis was conducted using a student's *t*-test and were presented as #p≤0.05, ##p≤0.01.

5.3.14 Assessment of Cerebral PRDX-SO_3 Protein Levels of VSMC-NOX5 Mice in the Context of Ang II-mediated Hypertension

Hyperoxidation of proteins is a hallmark feature of oxidative stress and hypertension. PRDX hyperoxidation contributes to reduced antioxidant response and deleterious outcomes. Oxidative stress marker PRDX-SO_3 protein levels were assessed by immunoblotting in whole brain lysates of normotensive and Ang II-induced hypertensive male and female WT and VSMC-NOX5 mice.

No differences were identified in immunoblotting analysis of PRDX-SO_3 analysis between Ang II and non-treated WT and VSMC-NOX5 mice when assessed collectively (**Figure 5-14A**), or by sex in male (**Figure 5-14B**) and female (**Figure 5-14C**) mice.

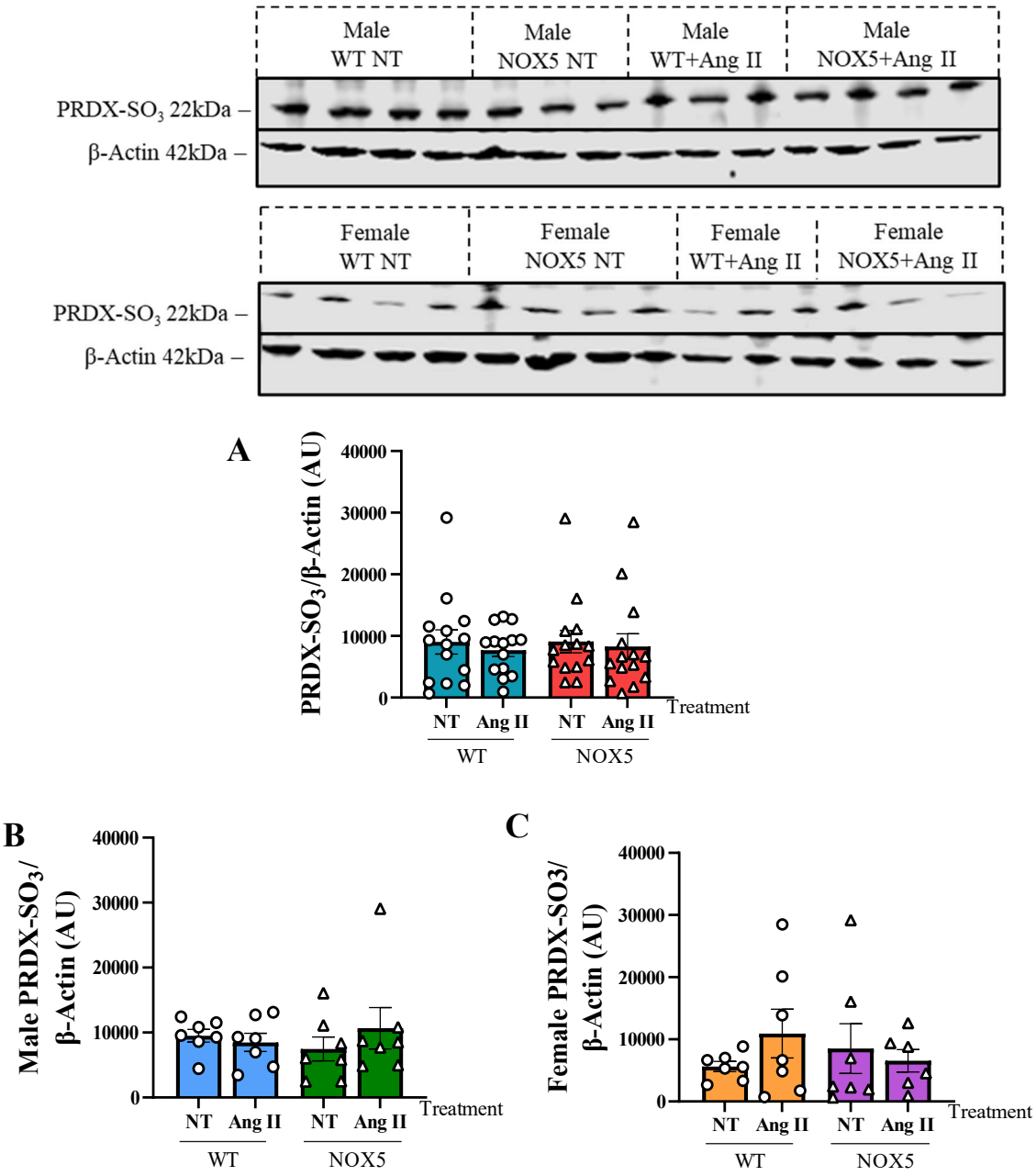

Figure 5-14. Immunoblotting of PRDX-SO_3 levels in Ang II- and non-treated male and female WT and VSMC-NOX5 mice. Whole brain homogenates of Ang II-treated and on-treated male and female WT and VSMC-NOX5 mice were used to assess PRDX-SO_3 by immunoblotting (**A-C**). Immunoblotting expression was normalised to β-actin and expressed as AU. Mixed sex study n=14, male study n=7, and female study n=7. Data was analysed using a two-way ANOVA with a Tukey's *post*-hoc test.

5.3.15 Whole Brain Assessment of Irreversible PTP-oxidation in Male and Female Ang II treated VSMC-specific NOX5 Mice

PTP-SO_3 protein levels were assessed by immunoblotting in whole brain lysates of normotensive and Ang II-induced hypertensive male and female WT and VSMC-NOX5 mice. Mixed sex assessment of full membrane PTP-SO_3 identified a significant increase in PTP-SO_3 levels in WT+Ang II mice when compared to WT NT mice (WT+Ang II 60878.70±7570.70 AU vs WT NT 37901.07±4340.86 AU p=0.04*), with no changes being identified between Ang II- and non-treated VSMC-NOX5 mice (**Figure 5-15A**). Sex-specific analysis of male full membrane PTP-SO_3 levels identified a significant increase in Ang II-treated VSMC-NOX5 mice when compared to their non-treated VSMC-NOX5 counterparts (Male VSMC+Ang II 64852.02±9870.45 AU vs Male VSMC-NOX5 NT 31861.43±3157.28 AU p=0.008##), with no changes being identified between treatments in male WT mice (**Figure 5-15B**). Full membrane analysis identified no changes in full membrane PTP-SO_3 levels were identified between treatment and genotypes in female mice (**Figure 5-15C**).

Further analysis of PTP-SO_3 levels at 20kDa and 50kDa were also assessed. First, mixed sex analysis of PTP-SO_3 at 20kDa identified that Ang II treatment led to an increase in PTP-SO_3 levels in WT (WT+Ang II 24910.14±.3852.00 AU vs WT NT 12749.52±1764.58 AU p=0.02*), and VSMC-NOX5 (VSMC-NOX5+Ang II 20625.40±3452.38 AU vs VSMC-NOX5 NT 11436.40±1326.54 AU p=0.02#) mice (**Figure 5-15D**). Sex-specific assessment at 20kDa identified a significant increase in PTP-SO_3 levels in Ang II-treated WT mice WT (Male WT+Ang II 26582.86±6595.61 AU vs Male WT NT 11212.61±1667.18 AU p=0.04#), with no changes being identified in male VSMC-NOX5 between Ang II and non-treated mice (**Figure 5-15E**). Furthermore, no changes were also observed regardless of genotype or treatment in female mice when assessing PTP-SO_3 levels at 20kDa (**Figure 5-15F**).

Secondly, mixed sex assessment of PTP-SO_3 at 50kDa (**Figure 5-15G**) identified a significant increase in PTP-SO_3 levels in VSMC-NOX5+Ang II when compared to VSMC-NOX5 NT mice (VSMC-NOX5+Ang II 11182.98±1801.31 AU vs VSMC-NOX5 NT 6224.74±907.78 AU p=0.02#). Analysis of PTP-SO_3 at 50kDa in males (**Figure 5-15H**) also identified a significant increase between Ang II-induced hypertensive VSMC-NOX5 and non-treated VSMC-NOX5 mice (Male VSMC-NOX5+Ang II 14528.10±3002.91 AU vs Male VSMC-NOX5 NT 6136.13±1201.13 AU p=0.02#). Assessment of PTP-SO_3 levels

at 50kDa in female mice were unchanged regardless of treatment or genotype (**Figure 5-15I**).

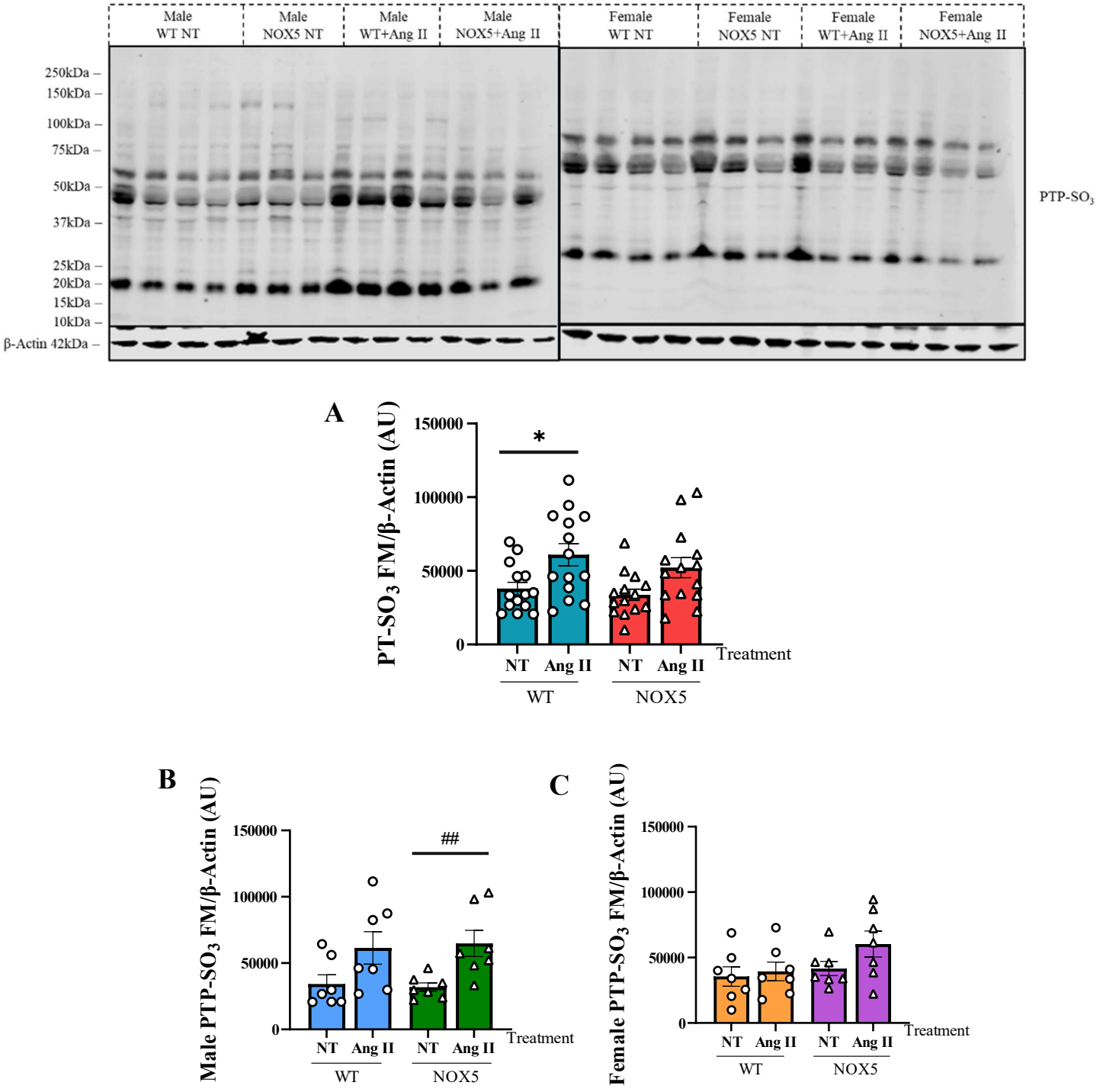

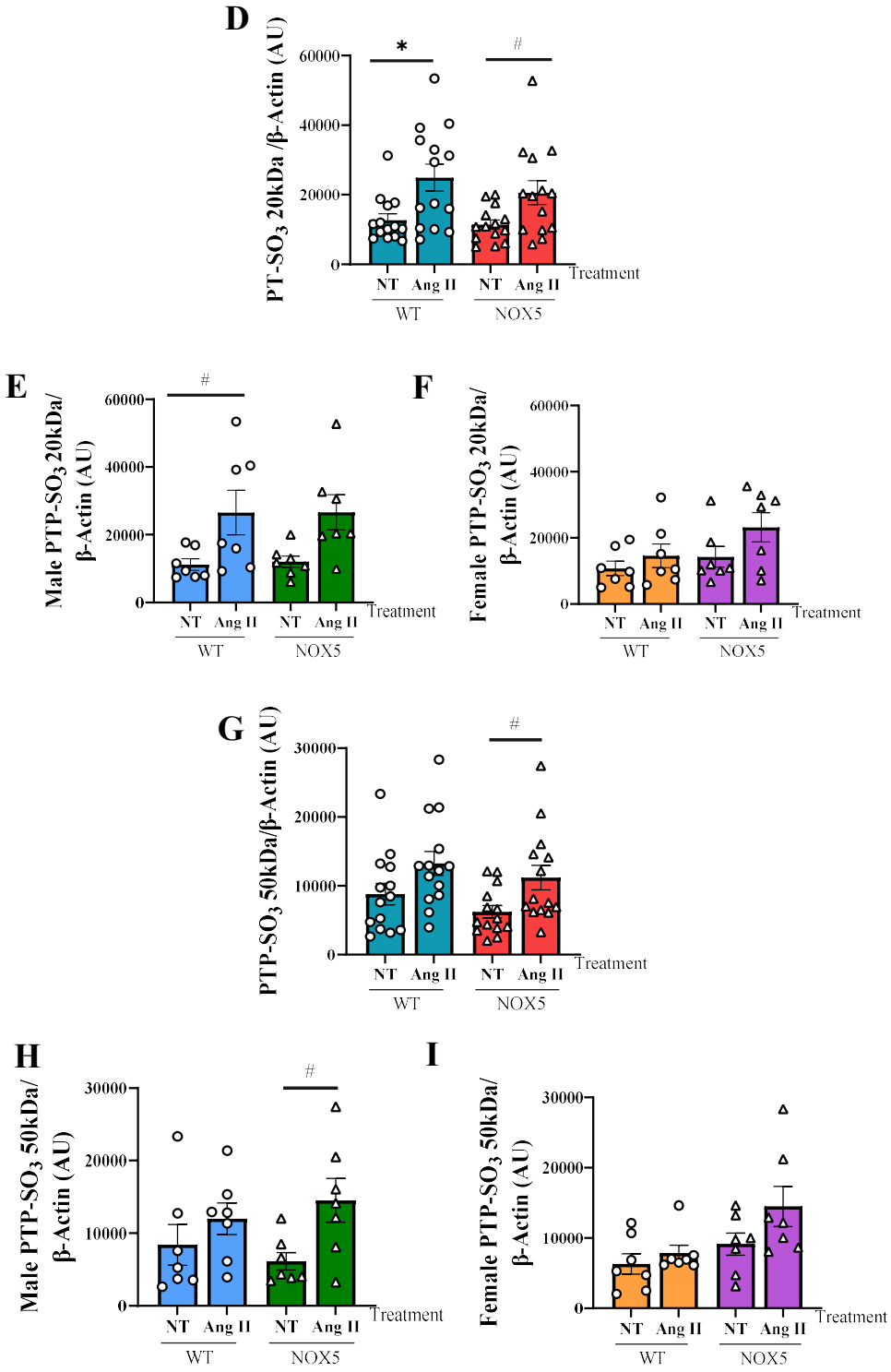

Figure 5-15. Immunoblotting of PTP-SO_3 levels in Ang II- and NT male and female WT and VSMC-NOX5 mice. Whole brain homogenates of Ang II-treated and on-treated male and female WT and VSMC-NOX5 mice were used to assess PTP-SO_3 by immunoblotting at FM (**A-C)** 20kDa (**D-F)**, and 50kDa levels (**G-I)**. Immunoblotting expression was normalised to β-actin and expressed as AU. Mixed sex study n=14, male study n=7, and female study n=7. Data was analysed using a two-way ANOVA with a Tukey's *post*-hoc test and presented as *p≤0.05. Further analysis was conducted using a student's *t*-test and were presented as #p≤0.05, ##p≤0.01.

5.3.16 Assessment of *Sod1* and *Sod2* mRNA Expression in Male and Female Ang II Mediated Hypertensive VSMC-NOX5 Mice.

To assess *Sod1* and *Sod2* mRNA expression in male and female WT and VSMC-NOX5 in the context of Ang II-induced hypertension, whole brain lysate cDNA was utilised using q-RT PCR. First, when assessing *Sod1* mRNA expression in mixed sex (**Figure 5-16A**), and sex-specific analyses in male (**Figure 5-16B**) and female mice (**Figure 5-16C**), Ang II-treatment did not alter *Sod1* gene expression in WT or VSMC-NOX5 mice.

Mixed sex assessment of WT and VSMC-NOX5 mice in either Ang II-treated or non-treated groups identified a significant decrease in *Sod2* mRNA expression in both WT+Ang II (WT+Ang II 4.76±0.17 ΔCt vs WT NT 4.19±0.13 ΔCt p=0.02#) and VSMC-NOX5+Ang II (VSMC-NOX5+Ang II 3.97±0.18 ΔCt vs VSMC-NOX5 NT 2.95±0.17 ΔCt p=0.0008***) mice, when compared to their non-treated counterparts (**Figure 5-16D**).

Sex specific analysis of male mice identified decrease in *Sod2* mRNA expression in VSMC-NOX5+Ang II mice (Male VSMC-NOX5+Ang II 4.73±0.14 ΔCt vs Male VSMC-NOX5 NT 3.80±0.28 ΔCt p=0.03*). No changes were observed between treatments in male WT mice (**Figure 5-16E**).

In females, *Sod2* mRNA expression was decreased in both hypertensive female WT (Female WT+Ang II 4.68±0.26 ΔCt vs Female WT NT 3.94±0.15 ΔCt p=0.04#) and VSMC-NOX5 (Female VSMC-NOX5+Ang II 4.77±0.24 ΔCt vs Female VSMC-NOX5 NT 3.78±0.24 ΔCt p=0.03#) when compared to their NT counterparts (**Figure 5-16F**).

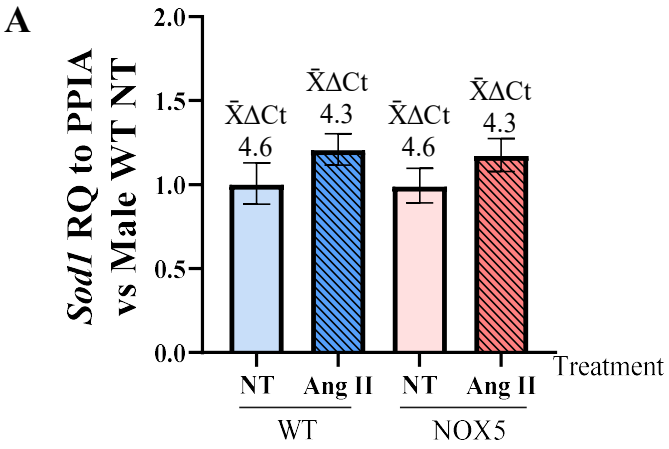

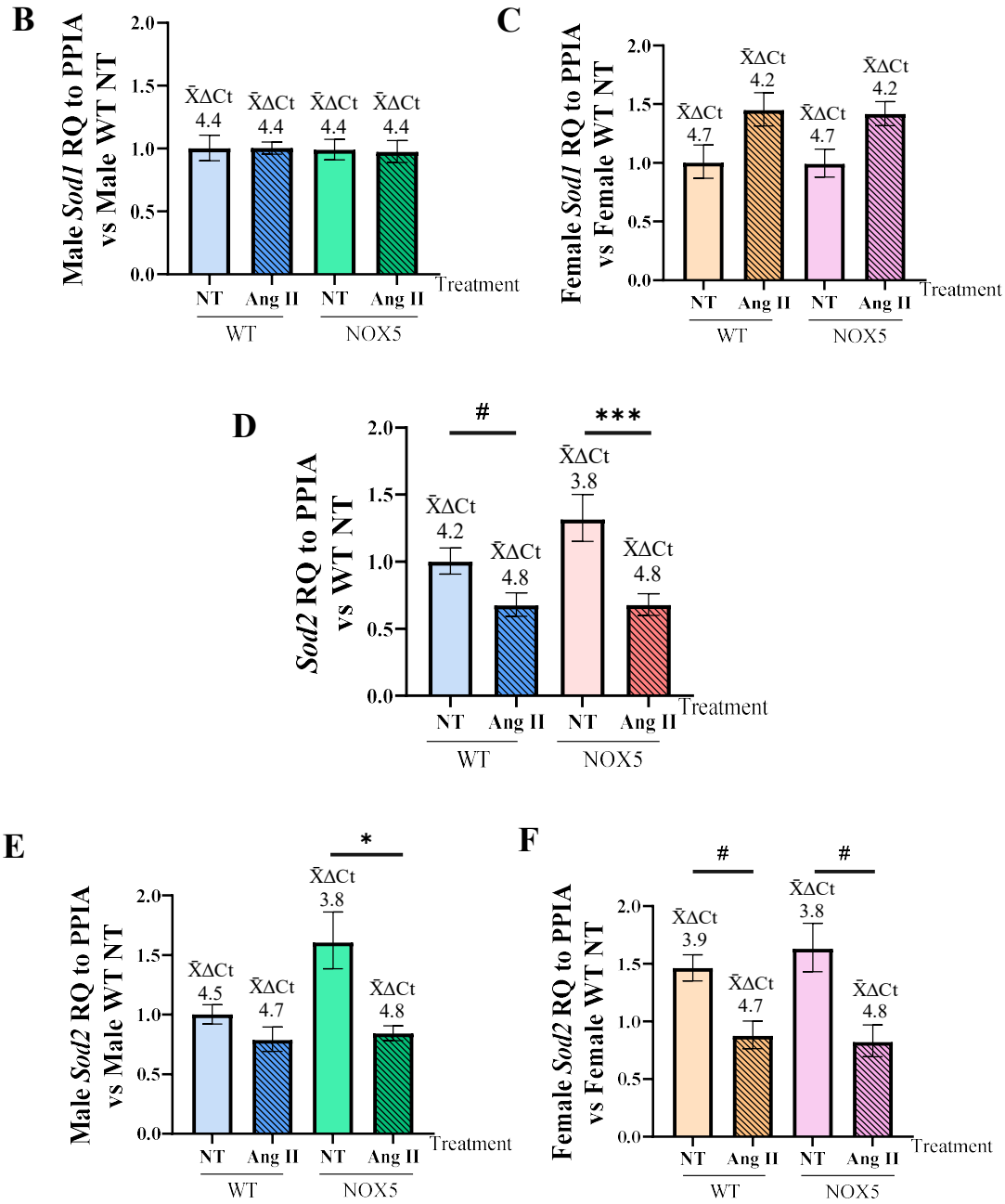

Figure 5-16. *Sod1* and *Sod2* mRNA expression in Ang II- and non-treated male and female WT and VSMC-NOX5 mice. *Sod1* and *Sod2* mRNA expression was assessed collectively and in Ang II- and non-treated male and female WT and VSMC-NOX5 mouse brain homogenates using q-RT PCR. Gene expression was assessed by q-RT PCR with RQ fold change being calculated from ΔΔCt following *Ppia* housekeeping gene normalisation. Mixed sex study n=12-14, male study n=6-7, and female study n=6-7. Data was analysed using a two-way ANOVA with a Tukey's *post*-hoc test and presented as *p≤0.05, ***p≤0.001. Further analysis was conducted using a student's *t*-test and were presented as #p≤0.05.

5.3.17 *Nqo1*, *Ho1*, and *Catalase* mRNA Expression Assessment by q-RT PCR in Ang II-treated Male and Female VSMC-NOX5 Mice.

Assessment of *Nqo1*, *Ho1,* and *Catalase* mRNA expression was assessed by q-RT PCR in whole brain lysates of male and female WT and VSMC-NOX5 in the context of Ang II-induced hypertension. First, no changes were identified in mixed sex and sex-specific analysis of *Nqo1* mRNA expression in VSMC-NOX5 mice in the context of Ang II-induced hypertension (**Figures 5-17A-C**).

Mixed sex assessment of *Ho1* mRNA expression was identified to increase between non-treated WT and VSMC-NOX5 genotypes (WT+NT 6.21±0.19 ΔCt vs VSMC-NOX5 NT 5.26±0.29 ΔCt p=0.02*). Furthermore, *Ho1* mRNA expression was identified to be decreased in mixed sex analysis of Ang II-induced hypertensive VSMC-NOX5 mice (**Figure 5-17D**) when compared to their NT treated counterparts (VSMC-NOX5+Ang II 6.49±0.23 ΔCt vs VSMC-NOX5 NT 5.26±0.29 ΔCt p=0.0017**).

When separated by sex, *Ho1* mRNA expression was significantly decreased in male VSMC-NOX5+Ang II mice (Male VSMC-NOX5+Ang II 6.59±0.53 ΔCt vs Male VSMC-NOX5 NT 5.45±0.22 ΔCt p=0.043*) when compared to their NT counterparts. No differences were observed between male normotensive and Ang II-treated hypertensive WT mice (**Figure 5-17E**).

No differences were observed between female WT and VSMC-NOX5 mice in the context of hypertension. However, in NT samples, VSMC-NOX5 led to an increase in *Ho1* expression (Female WT+NT 6.34±0.32 ΔCt vs Female VSMC-NOX5 NT 5.45±0.22 ΔCt p=0.02*) when compared to WT NT mice (**Figure 5-17F**).

Mixed sex assessment of *Catalase* mRNA expression was identified to increase between non-treated samples of WT and VSMC-NOX5 mice (WT+NT 0.06±0.17 ΔCt vs VSMC-NOX5 NT -0.79±0.34 ΔCt p=0.045*). Furthermore, analysis of VSMC-NOX5+Ang II was identified to be significantly decreased (VSMC-NOX5=Ang II 0.24±0.18 ΔCt vs VSMC-NOX5 NT -0.79±0.34 ΔCt p=0.045*) when compared to VSMC-NOX5 NT mice (**Figure 5-17G**).

When *Catalase* mRNA expression was analysed by sex, assessment of Ang II-treatment of male VSMC-NOX5 led to a decrease in mRNA expression when compared to NT VSMC-NOX5 male mice (Male VSMC-NOX5 0.44±0.19 ΔCt vs Male VSMC-NOX5 NT -1.06±0.62 ΔCt p=0.045*). No differences were observed between treatment in male WT mice (**Figure 5-17H**). Finally, no differences were observed between genotype or treatment in female mice (**Figure 5-17I**).

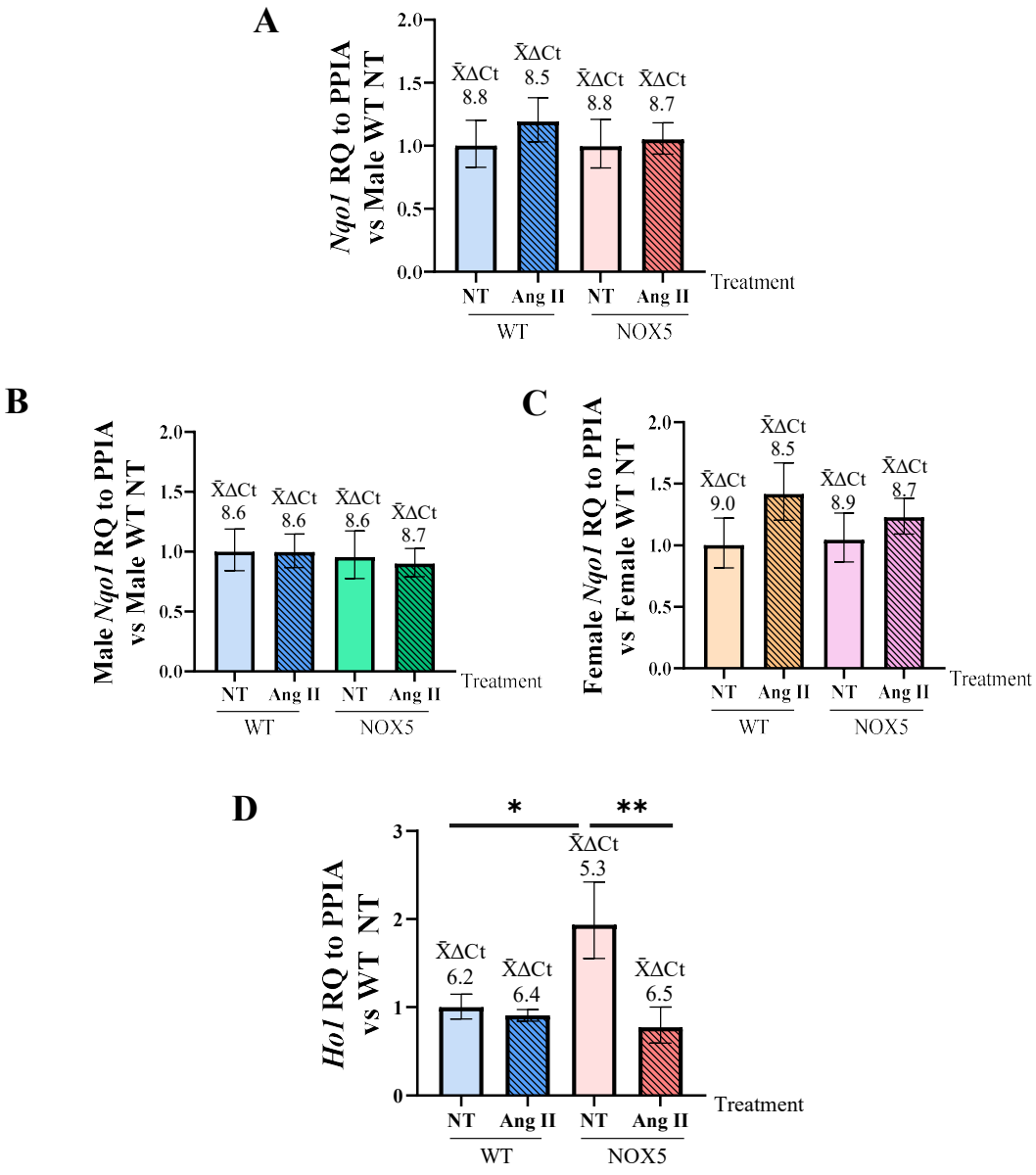

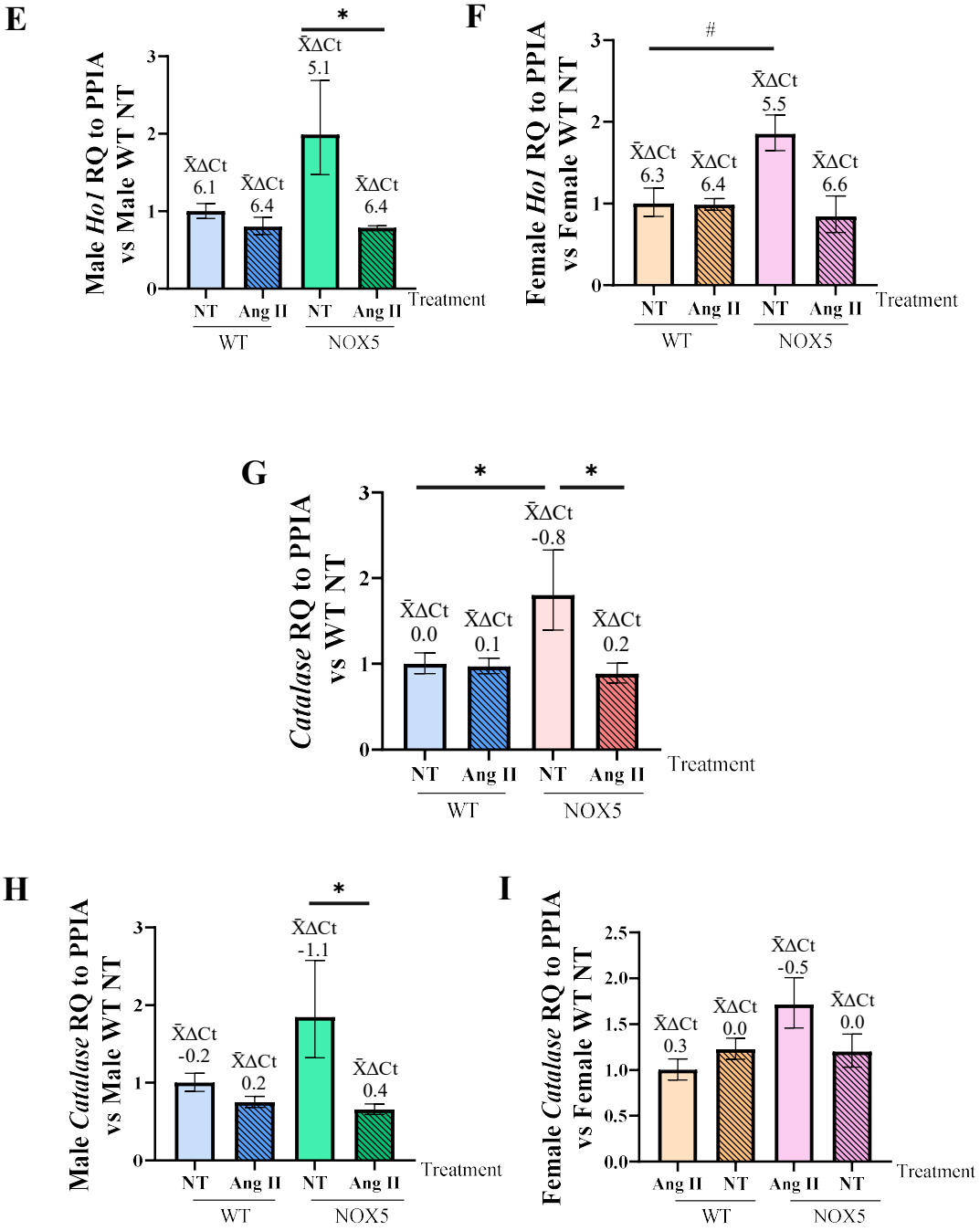

Figure 5-17. Antioxidant genes *Nqo1*, *Ho1*, and *Catalase* mRNA expression in Ang II- and non-treated male and female WT and VSMC-NOX5 mice. *Nqo1* (**A-C**), *Ho1* (**D-F**), and *Catalase* (**G-I**) mRNA expression was assessed collectively and in Ang II- and non-treated male and female WT and VSMC-NOX5 mouse brain homogenates using q-RT PCR. Gene expression was assessed by q-RT PCR with RQ fold change being calculated from ΔΔCt following *Ppia* housekeeping gene normalisation. Mixed sex study n=10-14, male study n=5-7, and female study n=5-7. Data was analysed using a two-way ANOVA with a Tukey's *post*-hoc test and presented as *p≤0.05, **p≤0.01. Further analysis was conducted using a student's *t*-test and were presented as #p≤0.05.

5.3.18 Immunoblotting Assessment of BIP Protein Levels in Ang II-treated Male and Female VSMC-specific NOX5 mice

BIP protein levels were assessed by immunoblotting in whole brain homogenates of normotensive and Ang II induced hypertensive male and female WT and VSMC-NOX5 mice. In mixed sex analysis, BIP protein levels are increased in Ang II-treated WT mice when compared to WT NT (WT+Ang II 621.36±81.81 (AU) vs WT NT 311.14±40.50 (AU) p=0.0089*). Furthermore, BIP levels were also increased between Ang II treated and NT VSMC-NOX5 mice (VSMC-NOX5+Ang II 547.46±93.02 (AU) vs VSMC-NOX5 NT 293.50±37.89 (AU) p=0.049* (**Figure 5-18A**)).

Sex-specific analysis of males identified that WT mice treated with Ang II led to a significant increase in BIP levels when compared to their non-treated WT counterparts (Male WT+Ang II 495.00±82.56 (AU) vs Male WT NT 276.00±47.39 (AU) p=0.04#). However, no changes in protein levels were identified in male VSMC-NOX5 mice between Ang II- and non-treated controls (**Figure 5-18B**).

Finally, female analysis identified that when treated with Ang II, WT (Female WT+Ang II 747.71±129.86 (AU) vs Female WT NT 346.29±66.71 (AU) p=0.02#) and VSMC-NOX5 (Female VSMC-NOX5+Ang II 672.43±156.21 (AU) vs Female VSMC-NOX5 NT 291.50±44.25 (AU) p=0.04#) mice led to a significant increase in BIP protein levels when compared to their WT counterparts (**Figure 5-18C**).

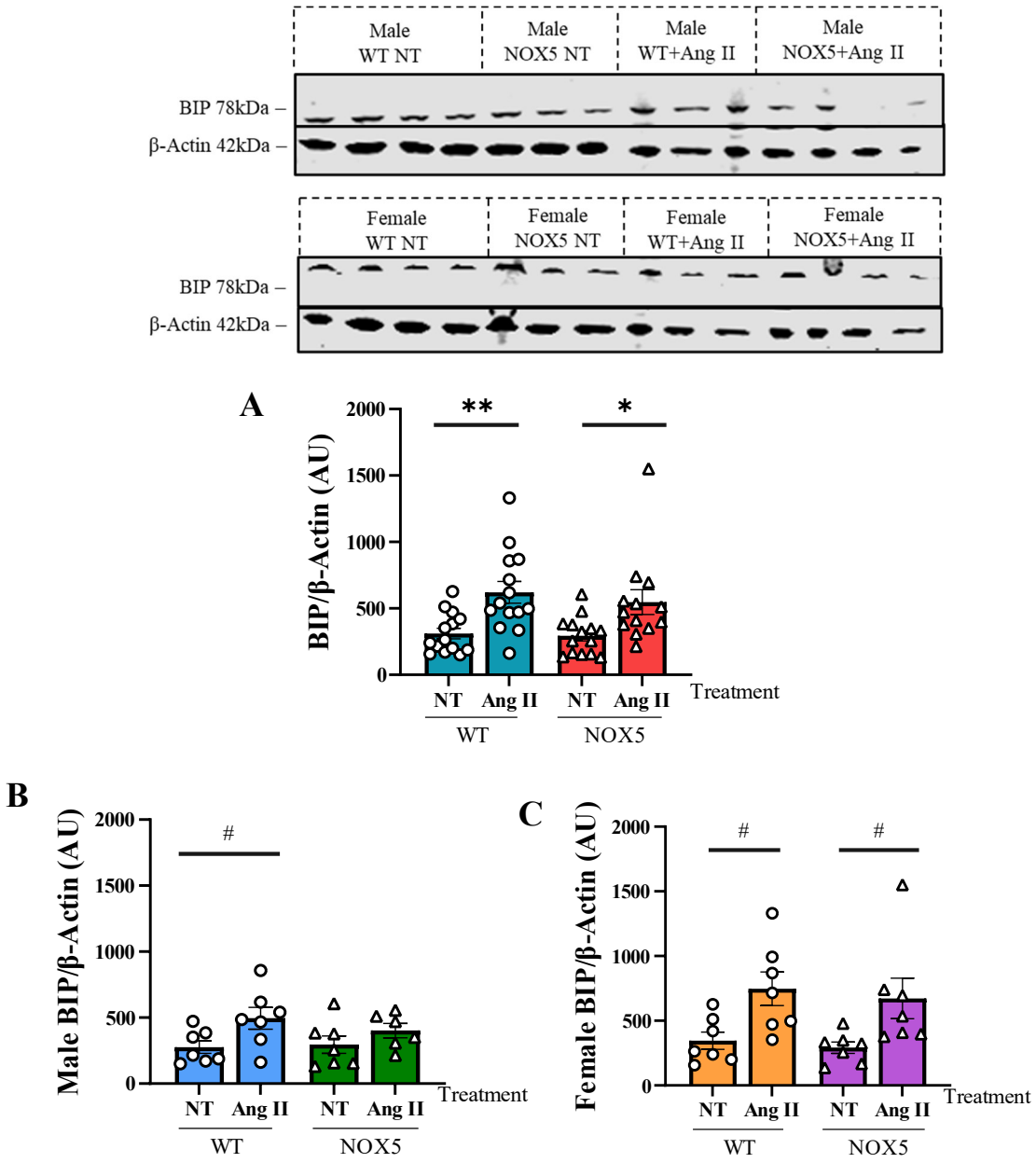

Figure 5-18. Immunoblotting of BIP protein levels in NT and Ang II treated male and female WT and VSMC-NOX5 mice. ER stress was assessed by analysing BIP protein levels in whole brain homogenates of Ang II-treated and non-treated male and female WT and VSMC-NOX5 mice by immunoblotting (**A-C)** Immunoblotting expression was normalised to β-actin and expressed as (AU). Mixed sex study n=12-14, male study n=6-7, and female study n=6-7. Data was analysed using a two-way ANOVA with a Tukey's *post*-hoc test and presented as *p≤0.05, **p≤0.01. Further analysis was conducted using a student's *t*-test and were presented as #p≤0.05.

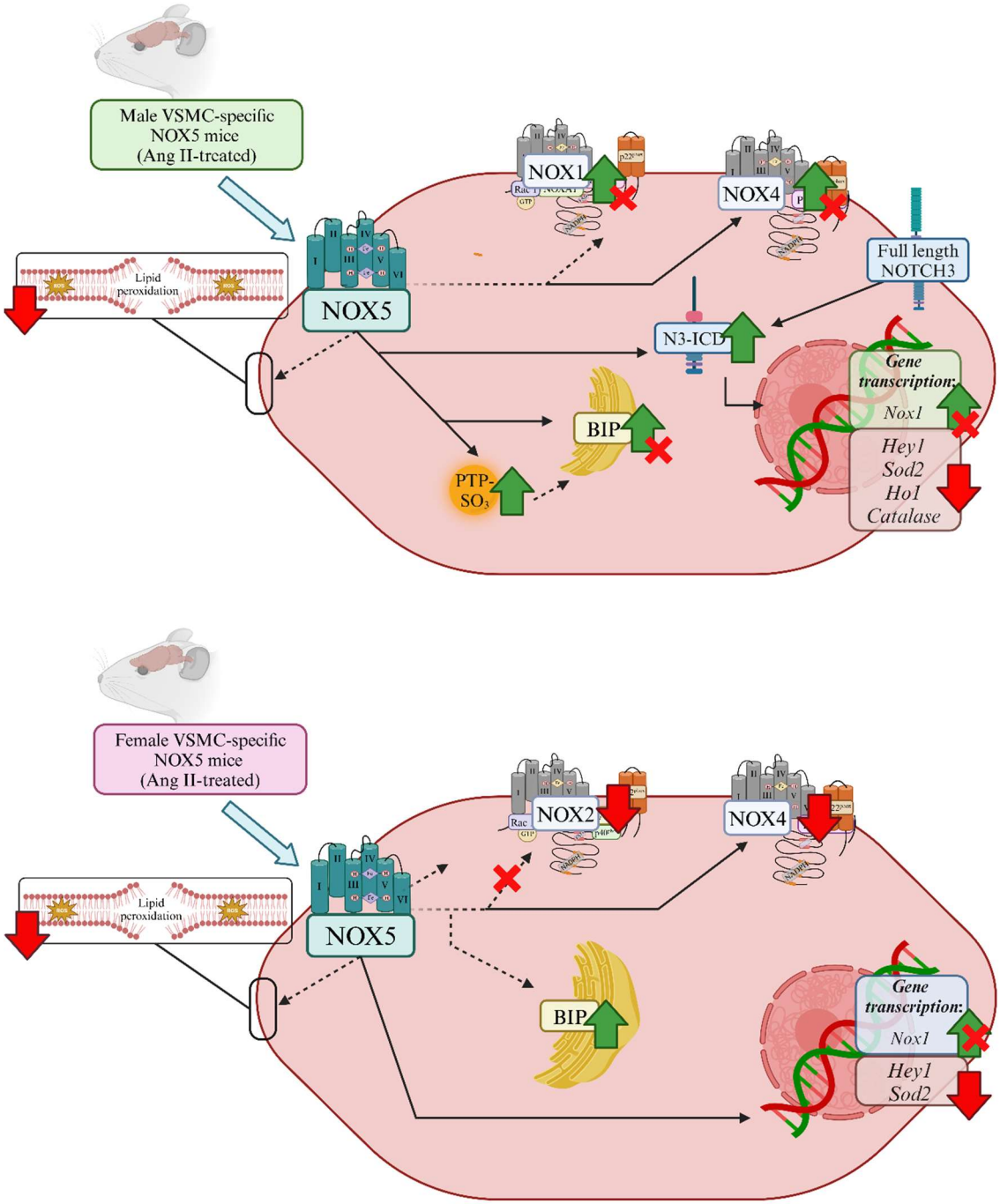

Figure 5-19. Graphical figure highlighting the effects of Ang II-treatment in the brains of male and female VSMC-specific NOX5 mice. In male Ang II-treated mice, VSMC-specific NOX5 was associated with increased PTP-SO_3 oxidative stress markers despite reduced lipid peroxidation levels, prevented increases in NOX1 mRNA/protein levels, NOX4 protein and ER stress response BIP protein levels, increased N3-ICD protein levels, with reduced *Hey1*, *Sod2*, and *Catalase* mRNA levels. Conversely in females, *Nox1* mRNA expression increases with NOX2 and NOX4 protein levels being decreased. Furthermore, lipid peroxidation levels were decreased with ER stress marker protein levels were increased and *Hey1* and *Sod2* mRNA expression levels also being decreased by VSMC-specific NOX5. This image was generated in BioRender.

5.4 Discussion

This study presented in Chapter 5 aimed to assess the role of cerebral VSMC-specific NOX5 in the context of Ang II mediated hypertension. First, VSMC-NOX5 in the context of hypertension was associated with downregulated VEGFR2 protein levels in females. Secondly, assessment of NOX1, NOX2, and NOX4 identified prevented upregulation of *Nox1* mRNA expression in Ang II treatment of VSMC-NOX5 mice, whilst also identifying sex-dependent alterations to NOX1, NOX2, and NOX4 protein expression. Thirdly, VSMC-NOX5 in the context of Ang II led to upregulation of cerebrovascular NOTCH3 signalling in males, but not females. Furthermore, NOTCH3 target *Hey1* mRNA expression was altered by VSMC-NOX5 in a sex-dependent manner. Examination of ROS and oxidative stress markers identified decreased H_2O_2 levels in male VSMC-NOX5 mice, with lipid peroxidation being reduced in both male and female VSMC-NOX5 mice. Furthermore, assessment of PTP-SO_3 identified a sex-dependent increase in VSMC-NOX5 mice. Assessment of ARE genes also identified a VSMC-NOX5 mediated decrease in *Sod2* mRNA expression; however, *Ho1* and *Catalase* mRNA expression was reduced by VSMC-NOX5 in males, but not females. Finally, BIP protein level upregulation was prevented by VSMC-NOX5 in male mice.

As previously described, GFAP, RhoA/ROCK1 and VEGFR2 are vital in maintaining cerebrovascular dynamics crucial for regulating BP. In the context of Ang II mediated hypertension, this study hypothesised that VSMC-specific NOX5 would contribute to dysregulation of these proteins. Whilst the study presented in chapter 5 identified no changes in GFAP and RhoA/ROCK1 protein levels, VEGFR2 protein level assessments identified a decrease of VEGFR2 in the brains of Ang II-mediated hypertensive female VSMC-NOX5 mice with no changes in expression in the brains of male VSMC-specific mice. Under physiological conditions, VEGFR2 acts as a cell-surface receptor playing a key role in the regulating of key vascular functions including vascular permeability, angiogenesis, vasculogenesis, and BP control via eNOS production of NO (Holmes *et al*., 2007, Wang *et al*., 2020, Facemire *et al*., 2009).

Looking at the literature, there is little evidence to link the findings of this study whereby VEGFR2 protein levels were decreased in female Ang II-treated VSMC-NOX5 mice and this likely arises from sex-specific oxidative responses. Whilst literature suggests that oestrogen leads to an upregulation of VEGF/VEGFR2 signalling (Mueller *et al*.,

2000), this is contrary to the findings established in this thesis. It is plausible that, in female VSMC-specific NOX5 mice, the increases in BP induced by Ang II could cause hypoxic challenge. As such, the upregulation of hypoxic sensitive pathways including factor 1-alpha (HIF-1α) could occur in this context, with HIF-1α known to transactivate genes including VEGF and downregulate VEGFR2 activity (Rey and Semenza, 2010, Ulyatt *et al*., 2011). Previous research examining coronary artery endothelial cells has identified that HIF-1α mediates the downregulation of VEGFR2 (Olszewska-Pazdrak *et al*., 2009, Ulyatt *et al*., 2011). This may offer a potential explanation of why VEGFR2 downregulation was observed in Ang II-related female VSMC-NOX5 mice. However, why this was not observed in males is unknown and requires further study, and whether the downregulation of VEGFR2 is acting as a vasoprotective or deleterious mechanism remains unknown.

Additionally, it is important to contextualise that the assessment of VEGFR2 protein levels in this study was conducted by whole brain analysis. This could therefore suggest that the decreases in VEGFR2 is attributable to other cellular sources. For example, neurons and oligodendrocytes express VEGFR2 with previous studies linking neuronal and oligodendrocyte VEGFR2 with angiogenesis and hippocampal-dependent cognition in adult rat models (Cao *et al*., 2004, Jin *et al*., 2002, De Rossi *et al*., 2016). Therefore, the VEGFR2 protein level reductions identified in whole brain homogenate assessment of Ang II-treated female VSMC-NOX5 mice could also indicate a biomarker of cognitive decline. As such further examination into the sex differences identified in VEGF2 protein levels in Ang II mediated hypertension requires further study.
It has been extensively characterised that Ang II binding of AT_1R contributes to hypertensive pathophysiological processes including the stimulation, assembly and activation of NOX activity, contributing to ROS production and oxidative stress (Matsuno *et al*., 2005, Touyz *et al*., 2022, Garrido and Griendling, 2009). This study hypothesised that protein levels and mRNA expression of cerebral NOX1, NOX2 and NOX4 in male and female VSMC-specific NOX5 mice would be increased in the context of Ang II mediated hypertension.

When assessing the effects of Ang II-mediated VSMC-NOX5 mice, this study identified that *Nox1* mRNA expression is increased in both male and female WT mice treated with Ang II when compared to NT WT mice. However, no differences were observed between Ang II and NT male or female VSMC-NOX5 mice suggesting *Nox1*

mRNA upregulation was prevented by VSMC-NOX5 in mice. Upregulation of *Nox1* mRNA expression has previously been established in mesenteric arteries of SHR (Androwiki *et al*., 2015). Additionally, previous research findings have associated upregulation of NOX1 in Ang II-mediated hypertensive transgenic mouse models, contributing to NOX1-mediated $[Ca^{2+}]i$ signalling generation and contraction, VSMC hypertrophy and eNOS uncoupling (Park *et al*., 2022, Dikalova *et al*., 2005, Dikalova *et al*., 2010). A possible rationale may be that the downregulation of *Nox1* mRNA expression in the brains of Ang II induced hypertensive VSMC-specific NOX5 mice may be a consequence of feedback inhibition and functional redundancy whereby cellular sensory mechanisms such as thioredoxins/thioredoxin-interacting proteins, peroxiredoxins, hypoxic inducible factors, NRF2 and mitochondrial ROS detection may be reducing the transcription of *Nox1*. These processes may be adjusting cellular metabolism in response to the NOX5-mediated ROS and oxidative stress environment in hypertensive mice. However, when assessing cerebral NOX1 protein levels, this study identified an increase in NOX1 protein expression in the brains of male but not female Ang II-treated NOX5 mice suggesting that sex hormones such as androgens and oestrogens may be regulating cerebral NOX1 protein levels in a sex dependent manner. Previous research has associated downregulation of NOX1 activity and expression in cerebral arteries in an oestrogen-dependent manner (Miller *et al*., 2007). Furthermore, increases in NOX1 activity in VSMC-NOX5 males may be a consequence of Ang II-treatment leading to mechanisms whereby androgens potentiate NOX1 activity and oxidative stress leading to pathological outcomes such as vascular remodelling and increased inflammation in VSMC-NOX5 mice and may be indicative of worsened outcomes (Montezano and Touyz, 2014).

Assessment of *Nox2* mRNA expression identified no changes in in the brains of both male and female Ang II-treated VSMC-specific NOX5 mice. Furthermore, NOX2 protein expression was unchanged by Ang II treatment in the brains of male VSMC-specific NOX5 mice. However, when assessed in females, Ang II treatment in WT mice led to a significant increase in NOX2 expression, however, this was not observed in female mice, suggesting that VSMC-specific NOX5 prevented increased cerebral NOX2 protein levels. The findings of this study could further indicate that oestrogen may play a protective role in the context of VSMC-NOX5 whereby NOX2 protein levels are being downregulated by sex-hormone mediated compensatory mechanisms. Previous research examining human umbilical vein endothelial cells has identified that oestrogen can play a protective regulatory role in NOX2 expression in endothelial cells by shifting the balance

of NOX mediated superoxide production to an increase in vasodilatory NO production (Wagner *et al*., 2001).A similar oestrogen mediated mechanism could also be modulating NOX5 activity directly to counter balance NOX5-mediated ROS, or indirectly modulate NOX5-NOX2 activity through mechanisms such as inhibition of the NF-κB and promotion of Nrf2 signalling pathways.

This study also identified that Ang II-treatment led to an increase in NOX4 expression in males WT mice whereas no differences were observed in VSMC-NOX5 mice when compared to NT counterparts, suggesting that NOX4 protein upregulation was prevented in male VSMC-NOX5 mice. The decreased NOX4 protein levels could be as a direct cause of Ang II-mediated activation of NOX5 however whether this is leading to a deleterious or protective effect is unknown with research studies examining the role of NOX4 in disease being contentious (Schröder *et al*., 2012, Casas *et al*., 2017, Basuroy *et al*., 2009, Paravicini *et al*., 2004). Research examining the role of NOX4 in the vasculature has identified NOX4 upregulation as a major cause of oxidative stress in pathological circumstances such as ischemia and hypertension leading to chronic hypoxia, apoptosis, BBB-breakdown and worsened neurological outcomes (Casas *et al*., 2017, Vallet *et al*., 2005, Basuroy *et al*., 2009). In this context it would appear that in Ang II-treated mice, VSMC-NOX5 males are being protected from potential NOX4 mediated damages. However, NOX4 has also been highlighted to play a protective role in the vasculature by playing a key role in eNOS mediated vasodilation through H_2O_2 ROS signalling (Ray *et al*., 2011). Furthermore, NOX4 downregulation has been linked to impairment of $[Ca^{2+}]i$ homeostasis leading to endothelial dysfunction which is exacerbated by hypertension, identifying a vasoprotective role for NOX4 in the vasculature, with endothelial-specific NOX4 overexpression leading to a decrease in BP (Alves-Lopes *et al*., 2023, Ray *et al*., 2011) It is therefore unclear whether the prevention of NOX4 expression in the brains of male VSMC-NOX5 mice acts protectively or deleteriously. No changes in NOX4 mRNA or protein levels were identified in female WT or VSMC-NOX5 mice in ANG-II treated or NT groups.

Abnormal NOTCH3 signalling is a hallmark of several cardiovascular and cerebrovascular diseases playing a role in vascular remodelling and switching VSMC phenotype from synthetic to hypercontractile through transcription of HEY and HES genes (Morris *et al*., 2019, Zhou *et al*., 2022). In this study, *Notch3* mRNA expression was identified to be prevented in female WT and VSMC-NOX5 Ang II-mediated hypertensive

mice, with no changes being identified in males. Indicating that genotype played no role in mRNA expression changes and was a treatment-based effect. Furthermore, when assessing full-length and ICD NOTCH3 protein expression, males were identified to have upregulated protein levels in both male Ang II-treated WT and VSMC-NOX5 mice when compared to their NT counterparts with no changes being identified in female mice between treatment and genotype. Whilst the changes in male WT and VSMC-NOX5 mice may suggest a treatment- and not genotype-mediated effect, this study also identified a significant change in downstream transcription with *Hey1* mRNA expression downregulated in Ang II-treated VSMC-NOX5 mice, and not Ang II-treated WT mice when compared to their NT counterparts. The upregulation of full-length and ICD NOTCH3 protein levels may be resulting in the activation of classical NOTCH signalling in Ang II-treated VSMC-NOX5 mice, and non-canonical NOTCH3 signalling in Ang II-treated WT mice. Interestingly, *Hey1* mRNA expression was also downregulated in both female WT and VSMC-NOX5 mice when treated with Ang II despite no changes in full-length or ICD NOTCH3 signalling. This may indicate alternative signalling cascades could be involved in the regulation of *Hey1* gene expression.

One alternative cellular mechanism that could be altering *Hey1* mRNA expression in females is through Sonic hedgehog signalling which has been identified previously as an upstream transcriptional repressor of *Hey* gene expression (Benito-Gonzalez and Doetzlhofer, 2014). Alternatively, Ang II-treated female VSMC-specific NOX5 mice exhibiting an upregulation of *Hey1* mRNA, without concurrent changes in *Notch3* mRNA or full length-NOTCH3 and N3-ICD protein expression, may indicate alternative signalling pathways to canonical and non-canonical NOCTH3 signalling that may lead to *Hey1* transcription. *Hey1* gene expression transcription is not exclusive to NOTCH3 and may be influenced by other members of the NOTCH family, for example NOTCH1 and NOTCH2 are also expressed in the brain, playing key roles in neuronal and glial cell fate and differentiation (Gaiano and Fishell, 2002, Guo *et al*., 2023) and may be acting in response to Ang II treatment and VSMC-specific NOX5-mediated changes in CBF and perfusion. Additionally, upregulation of *Hey1* mRNA expression could be in response to hypoxic challenge and *Sod2* mRNA downregulation. Previous research has demonstrated that ROS-mediated hypoxia regulates mitochondrial activity through HIF-1 pathway leading to the upregulation of *HEY1*, albeit in hepatocellular carcinoma cells (Kung-Chun Chiu *et al*., 2019).

It is well established that hypertension is linked with excessive ROS bioavailability and oxidative stress (Loperena and Harrison, 2017, Touyz *et al*., 2020, Griendling *et al*., 2021). In this study, Amplex-Red assessment identified that cerebral H_2O_2 levels are significantly decreased in Ang II-treated male VSMC-NOX5 mice. Furthermore, markers of cerebral lipid peroxidation were decreased in both male and female Ang II-treated VSMC-NOX5 mice when compared to their NT VSMC-NOX5 counterparts. Conversely however, full-membrane and 50kDa analysis of PTP-SO_3 identified a significant increase in hypertensive Ang II-treated male VSMC-NOX5 mice when compared to male VSMC-NOX5 NT mice. However, PTP-SO_3 at 20kDA was prevented in male VSMC-NOX5 mice. The reduction of H_2O_2 levels in mice could be a consequence of prevented increase in cerebral NOX4 protein levels observed in male Ang II-treated VSMC-NOX5 mice.

NOX4 has been well established in the literature to constitutively produce H_2O_2 through rapid dismutation of $^{\bullet}O_2^-$ when induced by Ang II (Takac *et al*., 2011, Montezano and Touyz, 2014). Furthermore, NOX4 downregulation could be affecting vasoprotective pathways whereby downregulated NOX4/H_2O_2 production could be altering signalling pathways such as PARP/TRPM7/Ca^{2+} that would lead to impaired eNOS-derived NO production and may be indicative of endothelial dysfunction (Alves-Lopes *et al*., 2023). This could indicate why, in the context of Ang II, a decrease in markers of cellular lipid peroxidation levels in the brains of both male and female VSMC-NOX5 mice were observed. Moreover, with male NOX4 downregulation and the reduced VEGFR2 expression in females, VSMC-specific NOX5 may potentially be reducing eNOS derived NO bioavailability that would lead to reduced $^{\bullet}O_2^-$ scavenging of NO to, deleterious $ONOO^-$, contributing to cytotoxic effects (Szabó and Módis, 2010). However, this study identified increased levels of PTP-oxidation in male VSMC-NOX5 mice, despite also displaying the classical H_2O_2 oxidation of PTPs (Östman *et al*., 2011). One mechanism could be that VSCM-specific NOX5 in males could be leading to localised bursts of $^{\bullet}O_2^-$ leading to specific damage in microdomains of specific PTP residues leading to irreversible oxidation. This also could be potentially as a consequence of, the reductions observed could be a consequence of reduced dismutation of $^{\bullet}O_2^-$ in the brains of male Ang II-treated VSMC-NOX5 mice. Furthermore, it is possible that the increases in PTP-SO_3 is a consequence of alternative ROS reactions such as $^{\bullet}OH$ that were not investigated in this study.

SOD2 is a key to maintaining mitochondrial homeostasis and function through dismutation of mitochondrial $^{\bullet}O_2^-$ production (Flynn and Melov, 2013). Previous research

has associated hypertension with SOD2 hyperacetylation and inactivation leading to dysfunction in vascular cells that contributes to a contractile phenotype (Dikalova *et al*., 2017). Furthermore, it has also been well characterised that SOD2 deficiency with mitochondrial dysfunction leads to neurodegenerative and cardiovascular disease risk (Flynn and Melov, 2013, Sharma *et al*., 2020). Previous research has associated Ang II with alterations to *Sod2* mRNA expression in rat cardiac fibroblasts (Lijnen *et al*., 2010). Additionally, SOD activity was identified to be downregulated by Ang II in rat mesenteric arteries, (Kang *et al*., 2018). In this study, *Sod2* mRNA expression was significantly reduced in male Ang II-treated VSMC-NOX5 mice. This could indicate mitochondrial dysfunction in male VSMC-NOX5 mice and also explain the reduction observed in H_2O_2 levels. Whilst in females *Sod2* mRNA expression was reduced in both Ang II-treated WT and VSMC-NOX5 mice indicating that this is likely a treatment-mediated effect.

This study also identified that male VSMC-NOX5 mice, cerebral *Ho1* mRNA levels were reduced and may further support the concept that $^{\bullet}OH$ may be forming in the brains of VSMC-NOX5 mice. HO1 has previously been identified to act defensively against oxidative stress and $^{\bullet}OH$ damage through the degradation of haem and the sequestration of iron (Fraser *et al*., 2011, Araujo *et al*., 2012). Furthermore, HO1 has previously been identified to reduce the hypertensive effect of Ang II by protecting against oxidative stress and inflammatory insults leading to vasodilation (Martínez-Casales *et al*., 2021, Yang *et al*., 2004, Mazza *et al*., 2003). Given that the brain is an iron rich environment (Gao *et al*., 2023, Reinert *et al*., 2019), the reduction of *Ho1* mRNA expression could further support a deleterious $^{\bullet}OH$ environment. Additionally, *Catalase* mRNA levels were reduced in the brains of male VSMC-NOX5 mice indicating a ROS-to-antioxidant imbalance and oxidative stress. Reductions in catalase have previously been identified to lead to reduced oxidative stress tolerance in a rat model of hypertension (Gomes *et al* 2012). One potential reason for the downregulation of catalase in male Ang II-treated VSMC-NOX5 mice is due to low H_2O_2 abundance, higher levels of cellular catalase production are not required to catalyse the reduction of H_2O_2 to oxygen and water.

Finally, this study identified that BIP protein levels were prevented in male Ang II mediated hypertensive VSMC-NOX5 mice. Previous studies have identified that BIP expression is often upregulated in models of pathophysiological stimuli including Ang II-mediated hypertension, in response to increased unfolded protein in an attempt to mitigate ER Stress (Menikdiwela *et al*., 2019, Camargo *et al*., 2023b, Chen *et al*., 2023b). This may

indicate that in hypertensive male VSMC-NOX5 mice leads to impaired UPR response leading to prolonged ER stress and apoptosis. Furthermore, the prevented BIP increase in hypertensive VSMC-NOX5 males identified in this study may potentially indicate an increased $[Ca^{2+}]i$ environment and unregulated activation of NOX5 as identified in previous studies (Cortés *et al*., 2021a, Camargo *et al*., 2023a). In females BIP protein levels were increased in both WT and VSMC-NOX5 mice when treated with Ang II.

To summarise, the study presented in Chapter 5 of this thesis demonstrates that Ang II-induced hypertension interacts with cerebral VSMC-specific NOX5 to produce sex-specific cerebrovascular effects. In males, the presence of VSMC-specific NOX5 contributes to markers of oxidative and ER stress response, with impaired antioxidant response to mitigate these effects. Furthermore, Ang II-treatment also alters canonical NOTCH3 signalling and downstream effector gene expression and could promote cerebrovascular dysfunction, a CSVD/CADASIL phenotype and increased stroke susceptibility. Conversely, in the brains of Ang II-treated female VSMC-specific NOX5 mice, despite reduced antioxidant responses, the absence oxidative stress markers and NOTCH3 signalling changes suggests the presence of compensatory mechanisms with a potential role for oestrogen signalling or other sex-specific influences that may mitigate the deleterious markers observed in males. To conclude, these findings identified in Chapter 5 provide critical insights into how Ang II-mediated hypertension contributes to a sexual dimorphism of VSMC-specific NOX5-mediated oxidative stress responses and alterations to NOTCH3 signalling in cerebrovascular health and disease, highlighting a role for sex-specific therapeutic strategies.

Chapter 6

General Discussion

6.1 General Discussion

NOX5 has previously been identified as a deleterious NOX isoform playing a key role in oxidative stress-mediated vascular pathology. Whilst NOX5 is expressed in human tissues and vascular cells, the *Nox5* gene is absent in rodents. As such, pre-clinical research examining its role in disease pathophysiology has been limited, particularly in the context of the brain. Previous research has associated NOX5 with increases in ROS bioavailability, BBB-breakdown and worsened cognitive decline following a tMCAO model of ischaemic stroke (Casas *et al*., 2019). Additionally, NOX5 has been associated with age-related hypertension, eNOS uncoupling, BBB-breakdown and cognitive decline (Cortés *et al*., 2021b, Elbatreek *et al*., 2020). Whilst these studies provided critical insight into the deleterious role of NOX5, they were assessed in an endothelial-specific manner and therefore did not consider the role of VSMC-specific NOX5 in cerebrovascular function. VSMCs are critical to cerebral autoregulatory responses by altering vascular tone in response to BP changes through cerebral autoregulatory and $[Ca^{2+}]i$ dynamics, that ensure adequate CBF and perfusion. Oxidative stress is a key pathophysiological feature of impaired cerebral autoregulation and disrupted CBF in cerebrovascular pathology. Given the intrinsic Ca^{2+} activated properties of NOX5 in producing ROS, NOX5 may have a unique role in the cerebrovasculature, particularly in VSMC-mediated mechanism of cerebrovascular dysfunction. Furthermore, previous research has identified that VSMC-specific NOX5 impairs myogenic tone by impairing $[Ca^{2+}]i$ and redox signalling homeostasis, contributing to hyperco ntractility and vascular dysfunction in mesenteric arteries (Montezano *et al*., 2018). By employing a transgenic mouse model that expresses NOX5 specifically in VSMCs, this thesis sought to elucidate how the expression of NOX5 influences vascular function.

The rationale for studying VSMC-specific NOX5-KI in the brains of mice is deeply rooted in understanding VSMCs unique role in cerebrovascular health and pathology, playing a critical role in maintaining CBF and cerebral perfusion by regulating myogenic tone and integrity through key mechanisms such as $[Ca^{2+}]i$ and redox signalling. This allowed for focused investigation of its direct effects on VSMC function and vascular tone regulation, processes which are critical to maintaining CBF. Furthermore, this model enables the investigation of NOX5s contribution to key regulatory processes of VSMC function including redox and NOTCH3 signalling with the ability to examine these effects in the context of age and hypertension. Given the known importance of ROS in

cerebrovascular disease, it was hypothesised that NOX5 would lead to exacerbated oxidative stress, dysregulated NOTCH3 signalling and impaired vascular function, with these processes being exacerbated in the context of ageing and Ang II-mediated hypertension.

Additionally, this model allowed examination of sex differences, a key yet overlooked aspect in relation to the contributory role of NOX5 in vascular biology. Previous research has demonstrated that cerebrovascular response to oxidative stress, particularly in the context of ageing and hypertension, differs between males and females, largely due to the protective effects of sex hormones such as oestrogen, with ageing diminishing the protective effects of oestrogen in the vasculature (Lisabeth and Bushnell, 2012, Nicholson *et al*., 2017, Krause *et al*., 2006, Deer and Stallone, 2016) The work detailed in this thesis identified a multifaceted role of VSMC-specific NOX5 overexpression in the brains of mice, with novel sex-dependent effects in oxidative stress responses, maladaptive signalling pathways and cerebrovascular dysfunction, emphasised by ageing and Ang II mediated hypertension. In female mice, VSMC-specific NOX5 was associated with age-related delays in vascular dysfunction, age/Ang II mediated non-canonical NOTCH3 signalling, and reduced/localised oxidative stress. Meanwhile, male VSMC-specific NOX5 mice were associated with progressive age-related oxidative stress, contributing to vascular dysfunction and hypercontractility, whilst also identifying age-/Ang II-mediated canonical NOTCH3 signalling. The findings identified in male mice align with previous studies linking NOX5 in ROS-mediated vascular dysfunction and a bidirectional relationship with NOX5-NOTCH3 signalling (Montezano *et al*., 2018, Neves *et al*., 2019).

6.1.1 VSMC-specific NOX5 May Influence Oxidative Responses in a Sex-Dependent Manner

Although it is well established that NOX5 leads to an oxidative stress environment, the role of sex, age and hypertension is still unclear. Whilst one previous study has assessed the cerebral effects of endothelial-specific NOX5 in the context of ageing and hypertension (Elbatreek *et al*., 2020), most existing literature has failed to, or overlooked the impact of sex differences, focusing on mixed, or male-specific experimental designs. This thesis provides new sex-dependent insights into the role of VSMC-specific NOX5-KI in mediating oxidative stress in the brains of mice. In the brains of male mice expressing VSMC-specific NOX5, ageing was associated with elevated markers of oxidative stress, indicating a progressively reduced capacity to manage oxidative insults. Moreover, this effect was exacerbated by Ang II treatment with antioxidant response genes being downregulated, highlighting a role for ageing and hypertension in amplifying an oxidative stress in the brains of male mice consistent with previous research (Elbatreek *et al*., 2020). In contrast, females may be protected by the deleterious effects of VSMC-specific NOX5 overexpression in the context of age and Ang II hypertension, relative to males. These findings are consistent with research previously identifying a role for female sex hormones, most notably oestrogen, in mitigating oxidative stress-mediated vascular dysfunction (Rettberg *et al*., 2014, Behl *et al*., 1997, Zhang *et al*., 2009). In animal models, oestrogen is known to act protectively through the downregulation of NOX activity, enhancing ARE defences, and promoting NO bioavailability which leads to increased vasorelaxation capabilities (Zhang *et al*., 2009, Miller *et al*., 2007, Dantas *et al*., 2002). However, it is well established that ageing is associated with a decline in oestrogen levels, contributing to increased cardiovascular and cerebrovascular vulnerability and stroke risk that eventually exceeds that of males (Lisabeth and Bushnell, 2012, Kumar and Mccullough, 2021).

Whilst these findings indicate that sex differences in a model of VSMC-specific NOX5 influence both the physiological and pathophysiological response to oxidative stress, it is plausible that distinct ROS production pathways and oxidative stress markers such as oxidative DNA damage not assessed in this study may be differentially expressed between males and females and may identify a different pathophysiological role between sexes. As such a more comprehensive examination of ROS and oxidative stress mechanisms may be required in future research.

6.1.2 NOX5 a Potential Upstream Regulator of Alternative NOX Isoforms Members

Whilst oxidative stress was identified in a sex-dependent manner in VSMC-NOX5 mice, a novel finding of this study is the identification of VSMC-specific NOX5 as a potential upstream regulator of alternative NOX isoforms (NOX1, NOX2, and NOX4), modulating both gene expression and protein expression, potentially through direct or indirect mechanisms.

Notably, VSMC-specific NOX5-KI in the context of ageing led to upregulated *Nox1* mRNA expression in the brains of male mice, whilst also leading to decreased NOX1 protein levels and upregulated NOX2 protein levels. In female counterparts, VSMC-specific NOX5 overexpression led to a decrease in NOX1 protein levels. Assessment of NOX2 protein and mRNA expression identified that ageing contributed to upregulated *Nox2* mRNA expression in the brains of female VSMC-specific NOX5 mice. However, although NOX2 protein levels were increased with age in the brains of female WT mice, NOX2 protein level increases were unchanged suggesting VSMC-specific NOX5 prevents NOX2 protein level increases in aged female mice.

In the context of Ang II-mediated hypertension, *Nox1 mRNA* levels were unchanged in the brains of both male and female VSMC-specific NOX5 mice despite upregulation of *Nox1* mRNA expression being identified in male and female Ang II treated WT mice. Assessment of protein levels in the brains of Ang II-treated VSMC-NOX5 mice identified that Ang II-treatment in male VSMC-NOX5 contributes to upregulated NOX1 protein levels, whilst simultaneously preventing the upregulation of NOX4 levels identified in Ang II-treated WT counterparts. In female assessments, NOX2 protein levels were increases in Ang II-treated WT, but not Ang II-treated VSMC-NOX5 mice suggesting that NOX2 protein levels were prevented by VSMC-specific NOX5 overexpression.

The findings indicate that ageing and hypertension in VSMC-specific NOX5 induces complex changes in NOX isoform expression potentially through ROS-mediated alterations to downstream signalling cascades that contribute to gene transcription, translational and post-translational modifications which is further altered in a sex-dependent manner. These cascades may allude to redox-sensitive transcription factors such as HIF-1α (Diebold *et al*., 2010), NF-kB (Morgan and Liu, 2011, Wu *et al*., 2021), STAT,

and AP-1 (Manea *et al*., 2012, Manea *et al*., 2008) which have previously been implicated in the regulation of *NOX1, NOX2*, *NOX4,* and *NOX5* gene expression. Alternatively, these changes in NOX isoform gene and protein expression may act as a compensatory response to NOX5-mediated oxidative stress with signalling cascades such as NRF2/ARE (Ma, 2013), SIRT1/FoXO (Salminen *et al*., 2013), cAMP/PKA (Kim *et al*., 2007, Raad *et al*., 2020), AMPK (Marino *et al*., 2021, Song and Zou, 2012), and suppression of the PI3K/Akt/PTEN (Nakanishi, 2014, Vermot *et al*., 2021) being identified in playing a role in preventing pro-oxidant transcription of complexes such as NADPH oxidases. As such, exploring upstream and downstream protein and gene expression of potential compensatory signalling cascades is necessary. In a future study, this could be assessed by utilising specific NOX isoform ELISA kits and protein expression of cytosolic subunits to assess NOX activity and whether NOX5 regulates these processes would elucidate the role of NOX5 on alternative NOX isoform regulation.

6.1.3 Canonical and Non-canonical NOTCH3 Signalling in a Sex-dependent Manner and May Influence Vascular Function.

A notable finding identified in this thesis is that NOX5 is associated with age-dependent vascular dysfunction. In the carotid arteries of aged males, VSMC-specific NOX5 mice contributed to a hypercontractility consistent with previous findings observed by Montezano and colleagues that NOX5 in a VSMC-specific manner contributes to hypercontractility in mesenteric arteries (Montezano *et al*., 2018). Another novel finding of this thesis is that VSMC-specific male mice were identified to have early onset of impaired endothelial-independent vasorelaxation, which progressed with age. In contrast, female VSMC-specific NOX5 mice exhibited improved endothelial-independent vasorelaxation in aged carotid arteries. These changes in vascular function could be indicative of progressive sex-specific oxidative impairments in the brains of VSMC-specific mice that progressively become more pronounced with age. Specifically, excessive ROS in VSMCs may lead to the scavenging of NO, reducing bioavailability vital for cGMP-dependent pathway activation and cerebrovascular relaxation. Furthermore, progressive cGMP downregulation has been associated with phenotypic alterations and vascular remodelling in VSMCs (Golshiri *et al*., 2020). Therefore, it could be assumed that this progressive loss of cerebral vascular relaxation mechanisms could lead to the development of vascular remodelling and contractile response observed with age in male VSMC-NOX5 mice. This difference could potentially be attributed to sex hormones, in part oestrogen signalling, through the

upregulation of antioxidant defences and reduction of the sensitivity of VSMC contractile mechanism to ROS. As such, the age-related oxidative and vascular impairments observed in the brain and carotid arteries of female mice expressing VSMC-specific NOX5 could mirror clinical observations of increased oxidative stress-mediated vascular pathologies following menopause (Lisabeth and Bushnell, 2012, Ruediger *et al*., 2021). In males, the findings of this thesis concur with previous research that male sex hormones and androgen signalling may play a key role in driving NOX5-mediated vascular impairments (Lucas-Herald *et al*., 2017, Lucas-Herald *et al*., 2022).

Another critical mediator of these sex-specific cerebrovascular changes is the NOTCH3 signalling axis, a key signalling axis that is integral in maintaining cerebrovascular phenotype, integrity and function and has also been identified to maintain BBB stability and functionality (Henshall *et al*., 2015). Furthermore, NOTCH3 mutations and N3-ICD ligand canonical translocation promotes genes associated with maladaptive remodelling, reinforcing a contractile VSMC phenotype (Henshall *et al*., 2015, Baron-Menguy *et al*., 2017, Morris *et al*., 2019). Previous research has identified a link between NOX5 and NOTCH3 signalling and a CADASIL phenotype when assessed in mutant NOTCH3 mice (Neves *et al*., 2019).

A key finding of this thesis is the role of VSMC-specific NOX5 in modulating the NOTCH3 signalling axis, highlighting a critical sex-dependent divergence in cerebrovascular responses in the context of ageing. Ageing and canonical signalling has been well established in the pathology of CADASIL, a hereditary form of CSVD characterised by WMH, increased stroke risk and VCI clinically (Romay *et al*., 2024, Morris *et al*., 2019, Hack *et al*., 2022). As such, male mice expressing VSMC-specific NOX5 may be predisposed to a CSVD/CADASIL phenotype that may explain the age associated impairments to vascular function. In males, VSMC-specific NOX5 driven oxidative stress was deemed to preferentially activate canonical NOTCH3 signalling in the context of ageing. As such, canonical NOTCH3 signalling may be driving vascular hypercontractility and vascular dysfunction in aged mice. This finding also aligns with previous research that identified NOTCH3 induces vascular dysfunction by transcription of *Hes5* (Morris *et al*., 2023)**.** This thesis also demonstrated that Ang II-mediated hypertensive male mice expressing VSMC-specific NOX led to canonical NOTCH3 signalling suggesting that hypertension drives early onset CSVD. However, assessment of vascular function in Ang II treated mice was not assessed and therefore this study cannot

determine whether this contributes to a hypercontractile phenotype similarly observed in aged male VSMC-specific NOX5 mice warranting further study. Alternatively in females, the relationship between VSMC-specific NOX5 and NOTCH3 signalling is distinct to their male counterparts, with a shift toward non-canonical NOTCH3 signalling in the context of both ageing and hypertension. Given that VSMC-NOX5-mediated hypercontractility was not observed in females and endothelial-independent vasorelaxation was improved with age, this may suggest that non-canonical NOTCH3 signalling does not contribute to vascular dysfunction. Whilst research is limited in non-canonical NOTCH3 signalling, particularly in the role of oestrogen in mediating this axis in VSMCs, previous studies suggest a bidirectional relationship between NOTCH and oestrogen signalling, identifying that oestrogen can activate and be activated by NOTCH ligands (Soares *et al*., 2004). As such, this study may have identified a key role for sex-dependent hormone modulation of the NOTCH3 signalling axis and its effects on vascular function. Whilst there is limited literature assessing non-canonical NOTCH3, previous studies have identified a role for oestrogen and non-canonical NOTCH3 signalling as a tumour suppressor, preventing angiogenesis through its apoptotic effects in the context of cancer suggesting a protective role(Lin *et al*., 2017). However, whether, non-canonical NOTCH3 acts beneficially in the cerebrovasculature of VSMC-specific NOX5 is unknown and requires further study. Collectively, the identification of VSMC-specific NOX5 modulation of the NOTCH3 signalling axis identified in this thesis extends previous work by Neves and colleagues, associating NOX5 with aberrant NOTCH3 signalling and pathological features of CSVD and CADASIL (Neves *et al*., 2019), whilst contributing new knowledge to the sex-dependent activation of alternative NOTCH3 signalling axes.

6.2 Clinical Implications

The findings of this thesis contribute key clinical considerations and implications for the management of age- and hypertension related cerebrovascular diseases. The novel discovery of sex-specific responses to VSMC-specific NOX5 overexpression underscores the importance of considering gender in cerebrovascular disease pathogenesis and potential therapeutic strategies. In the brains of male mice expressing VSMC-specific NOX5, markers of early onset oxidative stress and vascular dysfunction was observed, which progressed with age. Furthermore, Ang II-mediated hypertension led to markers of oxidative and ER stress, and perturbed canonical NOTCH3 signalling suggesting a drive toward severe CSVD pathologies such as CADASIL. Conversely, female mice exhibited a

more vasoprotective phenotype characterised by improved vascular function and non-canonical NOTCH3 signalling. This suggests a possible oestrogen-mediated protective mechanisms that counter the deleterious nature of NOX5. The findings in this thesis support clinical observations that premenopausal women have delayed risk of cerebrovascular impairments (Lisabeth and Bushnell, 2012, Welten *et al*., 2021). Furthermore, the findings of this thesis may also implicate NOX5 in ischaemic stroke risk pathology, specifically through its role in oxidative stress and the observations of hypercontractility and impaired vasorelaxation. In conditions such as post-stroke IRI, VSMC-specific NOX5-mediated oxidative stress during reperfusion could contribute to a hypercontractile state post-stroke, potentially delaying the beneficial effects of reperfusion, and amplifying ischaemic damage. By selective targeting NOX5 activity during thrombolysis or thrombectomy interventions, NOX5 inhibition could improve outcomes by mitigating ROS-mediated damage in the ischaemic penumbra, whilst reducing infarct core expansion. As such, the development of a NOX5 inhibitor could enhance post-stroke recovery and prevent subsequent cognitive and neurological damage. Whilst Casas *et al*. (2019) demonstrated that ML090 inhibition of NOX5-mediated ROS bioavailability contributed to reduced BBB permeability post-stroke. ML090 has been identified to have incomplete selectivity resulting in off-target effects including inhibition of other NOX isoforms (Casas *et al*., 2019, Dao *et al*., 2020). As such, a more selective NOX5 inhibitor would be required.

These findings also highlight a need to consider sex-specific aetiology on NOX5 function in order to develop therapeutic strategies for managing hypertension, CSVD, CADASIL, and preventing stroke risk. For males, interventions directly targeting NOX5 and associated pathways such as NOTCH3 signalling, may help prevent CSVD/CADASIL, stroke risk, VCI impairments, and VaD onset. For females, targeting NOX5 and preventing hormone decline may mitigate the risk of cerebrovascular disease for female populations where the protective effects of female hormones such as oestrogens diminish with age (in peri and post-menopausal women). Further research is required to fully elucidate the role of NOX5 in cerebrovascular diseases and the interplay between NOX5 and oestrogen-mediated signalling cascades on vascular effects. By furthering research in VSMC-specific NOX5 pre-clinically, these efforts could pave the way for clinical studies to examine NOX5 in CSVD, CADASIL and stroke patients are where current research is limited and would greatly enhance the translatability of the findings identified in this thesis. This could also lead to the development of improved diagnostic accuracy of CSVD/CADASIL and

stroke risk pathologies, whilst also leading to the development of tailored therapeutic interventions that could potentially reduce the deleterious effects of NOX5. These strategies could further enhance cognitive and neurological outcomes for patients with CSVD, stroke and related cerebrovascular conditions.

6.3 Study Limitations

This model presented in this thesis allowed for an in-depth investigation of how VSMC-specific NOX5 expression in male and female mice impacts cerebrovascular function by addressing these sex differences in the context of ageing and Ang II mediated hypertension. It provides critical insight into the role of NOX5 in cerebrovascular health and dysfunction with important implications for further understanding cerebrovascular disease pathophysiology in both men and women. While the research findings presented in this thesis provide novel contributions in examining the role of VSMC-specific NOX5 in cerebrovascular function and cerebral health, it is not without its limitations.

First, whilst VSMC-specific NOX5 overexpression was observed in these mice through genotyping and through IHC and immunoblotting conformation of VSMC-specific expression in mesenteric arteries (Montezano *et al*., 2018, Camargo *et al*., 2022), a key limitation of this study was the inability to directly measure NOX5 mRNA and protein levels or its enzymatic activity in the brains of VSMC-specific NOX5 mice. As such, the lack of direct NOX5 activity and expression assessments leaves uncertainty whether the observations identified in this thesis are directly attributable to VSMC-specific overexpression or through changes in other compensatory mechanisms not identified in this study. Furthermore, as VSMC-NOX5 has been associated with increased oxidative stress contributing to vascular hypercontractility and vascular remodelling in peripheral vessels (Montezano *et al*., 2018, Camargo *et al*., 2022), it also raises the possibility that systemic vascular changes may exacerbate cerebrovascular dysfunction, even in the absence of NOX5 activity in the brain. As such it is imperative that future studies utilise techniques such as specific NOX5 antibodies, NOX5 enzymatic activity assays and/or proteomics to provide a clear and direct assessment of VSMC-specific NOX5 activity and its role in cerebrovascular pathology.

Secondly, the VSMC-specific NOX5 mice used in this study employed the use of a tetracycline-controlled transactivator (tet-on/tet-off) system whereby if doxycycline was added to chow, NOX5 expression would be turned off. In this study, doxycycline was not added to chow resulting in chronic *NOX5* gene expression and activation in these mice, contrasting potential observations of pathological context-specific NOX5 expression and activation observed in humans (García *et al*., 2023). As such, persistent expression could lead to sustained oxidative stress or compensatory changes such as upregulation of ARE defences or shifts in alternative NOX isoform expression. Future studies should assess and compare NOX5 expression and activity between mice and human tissues while also exploring inducible expression of VSMC-specific NOX5 in mice to better replicate the physiological dynamics of NOX5 activity and expression observed in humans. Furthermore, rodents do not normally express the *NOX5* gene and therefore may not have the required transcriptional activators for protein expression and activity. The insertion of NOX5 into the murine genome in a VSMC-specific manner could potentially result in non-physiological expression patterns not observed in humans. As such, regulatory elements in humans and mechanisms that govern NOX5 activity and expression may be absent or altered in mice potentially impacting NOX5 functionality and its contribution to cerebrovascular dysfunction. Furthermore, NOX5 has been shown to be expressed in other cerebral cell types such as endothelial cells (Hernandes *et al*., 2022) and components of the NVU including astrocytes in humans (Sheng *et al*., 2013). Therefore, the reliance on a mouse model of VSMC-specific NOX5 mice may not fully recapitulate human cerebrovascular physiological function and/or NOX5 expression levels. However, it is important to note that the VSMC-specific NOX5-KI model utilised in this study was identified to share a similar phenotype to rabbits, which naturally express NOX5, indicating a level of translatability (Prof. Touyz, McGill University, personal communication). Another limitation of this thesis is the inability to assess mRNA expression, protein levels, and the overall activity of NOX5 in the brains of VSMC-specific NOX5 mice. This is likely due to the dilution of VSMC-specific expression by the presence of other brain tissue cell types. To overcome this limitation, future research could employ advanced techniques such as laser capture microdissection and vessel enrichment fractionation to selectively assess NOX5 expression. Additionally, the use of spatial transcriptomics, or single cell RNA sequencing could allow for precise gene expression mapping, distinguishing VSMC-specific NOX5 expression from other cerebral cell populations.

Thirdly, another key limitation of the study is in some experiments, a relatively small sample size was examined which may limit statistical power and the ability to detect biologically relevant differences. As a result of the COVID-19 pandemic, the number of animals allowed to be housed in the University of Glasgow Biological Services facility were significantly reduced and breeding of the VSMC-specific NOX5 mouse model was significantly scaled back as per the requirements set by the U.K. Home Office. As the models used were 20- and 35-week-old models, this meant that *in vivo* experiments or experiments such as wire myography which required the immediate dissection of arteries was significantly delayed. Consequently, pre-collected brain tissues for molecular studies were prioritised. Furthermore, due to the high variability in the breeding efficiency of VSMC-specific NOX5 mice as outlined in Chapter 2.4.1 (Table 2-1), certain segments of this study, particularly the female analysis in wire myography experiments were underpowered (n=3). Additionally, due to different schedule 1 methods for tissue collection, with CO_2 method used to collect carotid arteries cervical dislocation used to collect whole brains for whole brain homogenate molecular experiments, due to the differences in schedule 1 method, brain tissues were not collected in wire myography studies. This further led to a reduction in the amount of brain tissue available for the study. With the limited availability of biological materials, RNA and protein extracted from brain tissues from individual mice were used across multiple experiments including q-RT PCR, immunoblotting, and oxidative stress assays. This strategy optimised tissue usage and minimalised inter-animal variability. However, such an approach also introduces statistical dependencies as measurements from the same brain tissue sample may not be fully independent and may introduce variation in RNA/protein efficiency. To address this issue, future studies should prioritise larger cohort studies to ensure statistical power. Additionally, applying statistical methods that account for same sample repeated measurements such as linear mixed-effect models, would not only improve data robustness, by incorporating individual mice as a random effect with genotype, sex, age, and treatment accounting for fixed effects, controlling inter-sample variability and allowing for within-subject correlations, but also allow for investigation correlations in changes between target proteins and target genes. By implementing a linear mixed-effect model, future research can strengthen the reliability of the data results and provide deeper insights into potential molecular interactions.

Fourthly, whilst the molecular techniques utilised in this study, mainly immunoblotting and oxidative stress measurement assays which are valuable in understanding the molecular and functional pathophysiological roles of enzymes such as NOX5, they are with inherent limitations that may affect data interpretation. For example, whilst immunoblotting is useful for detecting protein expression, it is a semi-quantitative technique and may not reliably detect proteins of interest. Whilst this study used commercially available antibodies and the use of a MW ladder for the identification of specific proteins, there is a theoretical possibility that the target protein bands observed in this study, could be a consequence of cross-reactivity with other proteins of a similar epitope. As such future studies should establish conformation of the proteins of interest used in this study by using additional confirmation methods such as mass spectrometry or positive control tissues with high target protein abundance. For example, the NOX1 protein is highly abundant in the colon making it an ideal positive control for evaluating NOX1 expression in brain tissue (Wang *et al*., 2016). Furthermore, whilst assessing oxidative stress levels utilising assays such as Amplex-Red and TBARS-MDA are useful in measuring H_2O_2 and lipid peroxidation level respectively, they do have their limitations when assessing NOX5 activity. For example, H_2O_2 can arise from multiple sources, both locally within cells, and can diffuse between cells (Breton-Romero and Lamas, 2014). However, the protein of interest, NOX5 primarily produces $O_2^{\bullet-}$ which has a short half-life and as such is only stable for a short duration. As such measuring $O_2^{\bullet-}$ levels in whole brain homogenates is crucial for directly measuring changes in ROS levels mediated by VSMC-specific NOX5. Whilst this study attempted to measure $O_2^{\bullet-}$ production using lucigenin chemiluminescence, the approach was unsuccessful due to high variability in output between samples, likely caused by lipid concentrations in whole brain homogenate samples. A future study should employ a more accurate and direct assessment of $O_2^{\bullet-}$ levels in the brains of VSMC-specific NOX5 mice utilising electron paramagnetic resonance (EPR) spectrometry to provide real-time detection of $O_2^{\bullet-}$ levels allowing for a precise characterisation of NOX5 activity in the brain.

Another aspect to consider is the use of whole brain approaches for molecular experiments such as ROS measurements, immunoblotting, and q-RT PCR. Whilst whole brain approaches are useful for assessing global changes to ROS, protein and mRNA levels, a major limitation of this is the cellular heterogeneity whereby the identified changes observed in the VSMC-specific NOX5 mice in these studies, most notably changes in alternative NOX isoform expression, oxidative stress levels and antioxidant

mRNA expression, may be diluted or masked by other cell types, therefore this can make it challenging to precisely attribute molecular changes to VSMC-specific NOX5 overexpression. To overcome these limitations, future studies could employ vessel enrichment fractionation that would allow for the analysis of separate vascular and neuronal fractions to be analysed to give a more targeted analysis of how VSMC-specific NOX5 overexpression in the brains of these mice affect the cerebrovasculature and neuronal and glial cells. Another valuable approach to consider is the use of laser capture microdissection which would allow for the precise isolation of VSMC- and EC-rich regions from brain sections and enable a direct assessment of how VSMC-specific NOX5 affects both VSMCs and ECs, whilst reducing the risk of contamination from non-vascular cell types. These approaches could also be crucial in establishing NOX5 mRNA and protein expression, as well as NOX5 enzymatic activity levels.

Another limitation of the study is the sole use of wire myography to assess carotid artery function. Whilst wire myography is a valuable technique for assessing vascular function, it is an *ex vivo* method that does not fully replicate *in vivo* conditions, whereby systemic factors such as blood flow/CBF, circulating hormones, and neuronal inputs influence cerebrovascular function. For instance, while this research highlights that VSMC-specific NOX5-KI of mice contributes to vascular dysfunction in the context of ageing, the absence of CBF measures represents a gap whereby the observed VSMC-specific NOX5-mediated vascular dysfunction in carotid arteries prevents direct assessment on how carotid artery dysfunction correlates with functional impairments such as reduced perfusion and increased ischemia susceptibility, central to cerebrovascular disease pathophysiology. As such, techniques such as pressure myography and laser speckle contrast imaging would be crucial in establishing whether arterial response and CBF is altered by VSMC-specific NOX5 overexpression. Furthermore, the isolation and mounting of carotid arteries performed in the study may also introduce mechanical stress altering cerebrovascular responses. Additionally, this study did not assess endothelial-dependent vasorelaxation due to variable responses in ACh, limiting insights into endothelial function and how ECs influence cerebrovascular responses in VSMC-specific NOX5 mouse arteries. Given the critical importance of the endothelium in regulating vascular tone, future studies should assess whether VSMC-specific NOX5 impairs key vasorelaxation mechanisms such as eNOS derived NO contributing to increased risk of cerebrovascular dysfunction. Moreover, whilst this study did assess carotid artery SNP-mediated endothelial-independent vasorelaxation and U-46619-mediated contractility in

20- and 35-week-old mice, this was not performed in the context of Ang II-mediated hypertension. As such, these studies would need to be repeated in the context of Ang II along with the recommendations outlined here in the study limitations to fully assess the role of cerebrovascular dysfunction in Ang II-treated VSMC-specific NOX5 mice. To further compliment the role of cerebrovascular function studies and how VSMC-specific NOX5 may alter CBF, and cerebral perfusion is assessing the direct implications on neurological and cognitive function in the brains of VSMC-specific NOX5 mice. Whilst this study did identify markers of CSVD in males, this study did not assess any cognitive or neurological assessments of NOX5. Future studies should also employ a Y-maze test (testing to assess working memory), grip strength tests (to assess muscle strength and neuromuscular function) and open field test (assessing anxiety and depression behaviours) to assess whether VSMC-NOX5 leads to worsened cognitive and neurological decline before assessing VSMC-specific NOX5 in *pre*- and *post*- surgical model intervention models.

Another potential limitation to consideration is the hypertension model utilised in this study. While the 4-week Ang II hypertension model identified short-term alterations in VSMC-NOX5 pathophysiology, the acute response to elevated BP is limited in fully understanding the impact of long-term cerebral damage as hypertension is usually chronic and progressive in nature. The Low-dose Ang II and NOS inhibition (LinA3) model may (Alves-Lopes *et al*., 2020, Alves-Lopes *et al*., 2023) be more suitable in assessing VSMC-NOX5 in the context of hypertension as it offers a more accurate representation of chronic hypertension, offering progressive metabolic, and neuroinflammatory components to chronic hypertension in the brain. For instance, progressive impairments to NO signalling, oxidative stress, and inflammation common to hypertensive patients (Touyz *et al*., 2020). Additionally, LinA3 has also been utilised in transgenic mouse models previously (Alves-Lopes *et al*., 2023) and could be cross-bred with the VSMC-specific NOX5 mice utilised in this thesis. As such, the LinA3 model may offer a better translational model for assessing VSMC-NOX5 in the context of hypertension.

Given that this thesis identified that cerebral VSMC-NOX5 leads to sex-differences throughout this study, future research assessing sex hormones would be vital to understand the role of sex in the context of VSMC-NOX5 with oestrogen signalling being a logical starting point given the protective effects of oestrogen in preventing cerebrovascular disease in premenopausal patients (Lisabeth 2012, Shekhar 2017). *In vivo* models such as

ovariectomy and male castration could be utilised to assess whether sudden hormonal depletion would lead to worsened or improved outcomes in the brains of VSMC-specific NOX5 mice (Souza *et al*., 2019, Valkenburg *et al*., 2016). Furthermore, hormonal replacement therapy could be utilised to assess whether the effects of these in vivo models could be reversed. Alternatively, progressive hormone inhibition utilising pharmacological agents such as 4-vinylcyclohexene and antiandrogens such as flutamide in VSMC-specific NOX5 mice could be used to assess the progressive decline of oestrogen, progesterone and testosterone in VSMC-specific NOX5 mice. These interventions would give clarity to the sex-specific effects observed in this thesis (Konhilas *et al*., 2020, Ba *et al*., 2002).

Finally, throughout this thesis, NOX5 was attributed to changes in oxidative status, NOTCH3 signalling and alterations to vascular function with males displaying a deleterious phenotype and females being observed to have a protective phenotype. However, despite comparisons to WT controls, whether these changes were directly attributable to NOX5 in a VSMC-specific manner was not fully established. As such an intervention study is required in order to determine a cause-and-effect relationship between VSMC-specific NOX5 and the findings identified in this study to provide critical validation. Previous cell culture studies examining NOX5 have utilised agents such as melittin (Camargo *et al*., 2022) and ML090 (Casas *et al*., 2019) to inhibit NOX5 showing reduced NOX5-mediated activity and improved outcomes, however these pharmacological agents, are with some limitations, as neither specifically inhibit NOX5. For example, melittin also inhibits CaM. In an *in vivo* model this may lead to adverse effects most notably, the indirect inhibition of NO, a key vasodilatory molecule through the endothelial CaM-eNOS-NO pathway. Furthermore, ML090 may lead to off-target effects and inhibit other NOX isoforms, which, despite NOX1, NOX2, and NOX4 also being ROS producing enzymes. Taken together, these methods for validating the cause/effect relationship of VSMC-specific NOX5 in the cerebrovasculature may introduce confounding effects. As such, future studies could explore precise suppression of VSMC-specific NOX5 utilising NOX5 small interfering RNA (siRNA) to assess whether NOX5 is directly attributable to the changes in oxidative status, NOTCH3 signalling and cerebrovascular function identified in this study. Previous research has confirmed that in NOX5 siRNA attenuates oxidative stress in VSMC culture from arteries isolated from hypertensive patients, validating NOX5 as a mediator of oxidative stress and vascular dysfunction (Camargo *et al*., 2022). As such, the use of NOX5 siRNA could be used as a validating step in understanding how VSMC-specific NOX5 influences cerebrovascular function.

6.4 Future Directions

Future studies should aim to address the limitations identified in this discussion. These findings also provide compelling evidence to explore VSMC-specific overexpression in the context of severe cerebrovascular pathologies CSVD such as BCAS for modelling chronic hypoperfusion and tMCAO induced ischaemic stoke. Given the role the sex-dependent role of NOX5 in impaired vascular function identified in this thesis, these effects are likely to play a role in the progression of cerebrovascular pathology. Additionally, given that stroke reperfusion is associated with cellular Ca^{2+} influx and oxidative damage, this creates a perfect environment for NOX5 activation and with this thesis identifying that VSMC-specific NOX5 contributes to hypercontractility and dysfunction of carotid arteries potentially impairing blood flow to the brain, NOX5 could therefore be key in driving post-stroke IRI oxidative stress mediated hypercontractility, exacerbated infarct size, brain tissue necrosis, and cognitive decline. By utilising the tMCAO model in VSMC-specific NOX5 mice could further highlight key mechanisms that drive IRI and elucidate potential therapeutic targets in reducing these deleterious effects. Whilst a model BCAS model could provide beneficial insights into the molecular mechanisms of cerebral hypoperfusion and vascular remodelling. Furthermore, these models also allow for exploration as to whether sex hormones such as oestrogen in the context of VSMC-NOX5 modulates disease severity.

An additional future direction for this study could be to assess the validity as to whether or not NOX5 in a VSMC-specific manner produces a CSVD. Whilst this thesis assessed VSMC-specific NOX5-KI in two age groups (20- and 35-weeks-old), revealing sex-specific alterations to oxidative stress status, dysregulation in NOTCH3 signalling, and changes to vascular function. However, it is important to note that translationally, the age groups selected in this study equate to approximately 30-years, and 50-years old-respectively (Jackson *et al*., 2017, Dutta and Sengupta, 2016). Whilst the findings of this study did indicate suggestions of a CSVD phenotype, in humans, CSVD prevalence significantly increases around the human equivalent age of 65-years-old (Smith *et al*., 2015). As such, future studies should evaluate aged mice at an older time point (e.g. 60-weeks) to see whether VSMC-specific NOX5 alone, at a translational age of 65-years old in humans, at baseline conditions, induces a CSVD phenotype and increased risk of ischaemic stroke, without the use of surgical interventions such as tMCAO and BCAS.

This would validate the hypothesis that NOX5 serves as an initiating factor in CSVD, rather than an exacerbating factor in response to cerebrovascular diseases such as ischaemic stroke identified in (Casas *et al*., 2019).

Additionally, a future study should assess NOX5 as a pharmacological target for preventing cerebrovascular diseases including CSVD and ischaemic stroke pathologies, that may lead to the prevention of VCI and VaD. The recent advances identifying the crystallisation of the NOX5 enzyme (Magnani *et al*., 2017) offers an opportunity for designing highly selective NOX5 inhibitors. As NOX5 activation is Ca^{2+}-dependent, requiring no cytosolic subunits for its activation (Touyz *et al*., 2019), future research could identify unique NOX5-specific peptide sequences in the EF-hand domains to directly inhibit enzymatic activation and ROS production, without affecting other key proteins that contain EF-hands for Ca^{2+} binding such as CaM. Alternatively, specific NOX5 FAD/NADPH binding domain sequences could be targeted to interfere with electron transfer, without affecting activity of other NOX isoforms. Given that NOX5 is associated with severe pathologies including but not limited to cerebrovascular disease, the development of a NOX5 pharmacological target represents a promising avenue for study and potential target for precision medicine-based strategies in a wide range of diseases.

.

6.5 Final Conclusions

This thesis provides a cohesive and multi-dimensional examination of mice expressing VSMC-specific NOX5 overexpression in cerebrovascular physiology, establishing novel evidence that NOX5 in a VSMC-specific manner leads to sex-dependent pathophysiological effects to the brain in the context of both ageing and hypertension. In the brains of male mice, VSMC-NOX5 contributes to oxidative stress and ER-stress mediated pathophysiological process that contribute to impaired vascular function with age, and canonical NOTCH3 dysregulation in the context of Ang II-mediated hypertension, indicating the VSMC-specific NOX5 contributes to a CSVD phenotype. In female VSMC-specific NOX5 mice, carotid artery vascular function was seemingly improved by age, with a potential role for cerebrovascular non-canonical NOTCH3 signalling also being identified. Collectively, these findings support previous research identifying NOX5 as a mediator of vascular dysfunction whilst also suggesting sex hormones as a regulator of NOX5-mediated ROS bioavailability, providing new perspectives for the role of NOX5 in cerebrovascular dysfunction. Whilst limitations to the study do exist, this research provides a roadmap for future research through assessing the role of VSMC-specific NOX5 in the context of pathologies such as stroke, CSVD and cognitive decline. While the novel findings presented throughout this thesis do not directly lead to the development of new therapies, they do highlight the need for NOX5 inhibitors, whilst also identifying sex hormones regulation and NOTCH3 signalling cascades as promising therapeutic targets to prevent cerebrovascular disease pathology and cognitive decline.

References

ABDELSALAM, S. S., KORASHY, H. M., ZEIDAN, A. & AGOUNI, A. 2019. The Role of Protein Tyrosine Phosphatase (PTP)-1B in Cardiovascular Disease and Its Interplay with Insulin Resistance. *Biomolecules,* 9**,** 286.

ABI-GHANEM, C., ROBISON, L. S. & ZULOAGA, K. L. 2020. Androgens' effects on cerebrovascular function in health and disease. *Biology of Sex Differences,* 11.

AGARWAL, N. & CARARE, R. O. 2021. Cerebral Vessels: An Overview of Anatomy, Physiology, and Role in the Drainage of Fluids and Solutes. *Frontiers in Neurology,* 11.

AHMARANI, L., AVEDANIAN, L., AL-KHOURY, J., PERREAULT, C., JACQUES, D. & BKAILY, G. 2013. Whole-cell and nuclear NADPH oxidases levels and distribution in human endocardial endothelial, vascular smooth muscle, and vascular endothelial cells. *Can J Physiol Pharmacol,* 91**,** 71-9.

AHN, S. & PRINCE, E. 2013. Basic Vascular Neuroanatomy of the Brain and Spine: What the General Interventional Radiologist Needs to Know. *Seminars in Interventional Radiology,* 30**,** 234-239.

AKHTER, F., PERSAUD, A., ZAOKARI, Y., ZHAO, Z. & ZHU, D. 2021. Vascular Dementia and Underlying Sex Differences. *Frontiers in Aging Neuroscience,* 13.

AL-SHAHI SALMAN, R., FRANTZIAS, J., LEE, R. J., LYDEN, P. D., BATTEY, T. W. K., AYRES, A. M., GOLDSTEIN, J. N., MAYER, S. A., STEINER, T., WANG, X., ARIMA, H., HASEGAWA, H., OISHI, M., GODOY, D. A., MASOTTI, L., DOWLATSHAHI, D., RODRIGUEZ-LUNA, D., MOLINA, C. A., JANG, D.-K., DAVALOS, A., CASTILLO, J., YAO, X., CLAASSEN, J., VOLBERS, B., KAZUI, S., OKADA, Y., FUJIMOTO, S., TOYODA, K., LI, Q., KHOURY, J., DELGADO, P., SABÍN, J. Á., HERNÁNDEZ-GUILLAMON, M., PRATS-SÁNCHEZ, L., CAI, C., KATE, M. P., MCCOURT, R., VENKATASUBRAMANIAN, C., DIRINGER, M. N., IKEDA, Y., WORTHMANN, H., ZIAI, W. C., D'ESTERRE, C. D., AVIV, R. I., RAAB, P., MURAI, Y., ZAZULIA, A. R., BUTCHER, K. S., SEYEDSAADAT, S. M., GROTTA, J. C., MARTÍ-FÀBREGAS, J., MONTANER, J., BRODERICK, J., YAMAMOTO, H., STAYKOV, D., CONNOLLY, E. S., SELIM, M., LEIRA, R., MOON, B. H., DEMCHUK, A. M., DI NAPOLI, M., FUJII, Y., ANDERSON, C. S., ROSAND, J., HANLEY, D. F., BUTCHER, K. S., DAVIS, S., GREGSON, B., LEES, K. R., LYDEN, P. D., MAYER, S. A., MUIR, K. W., STEINER, T., XIE, P., BAKHSHAYESH, B., MCDONALD, M., BROTT, T., PENNATI, P., PARRY-JONES, A. R., SMITH, C. J., HOPKINS, S. J., SLEVIN, M., CAMPI, V., SINGH, P., PAPA, F., POPA-WAGNER, A., TUDORICA, V., TAKAGI, R., TERAMOTO, A., WEISSENBORN, K. & LANFERMANN, H. 2018. Absolute risk and predictors of the growth of acute spontaneous intracerebral haemorrhage: a systematic review and meta-analysis of individual patient data. *The Lancet Neurology,* 17**,** 885-894.

ALARCON-MARTINEZ, L., YILMAZ-OZCAN, S., YEMISCI, M., SCHALLEK, J., KILIÇ, K., CAN, A., DI POLO, A. & DALKARA, T. 2018. Capillary pericytes express α-smooth muscle actin, which requires prevention of filamentous-actin depolymerization for detection. *Elife,* 7.

ALFIERI, A., KOUDELKA, J., LI, M., SCHEFFER, S., DUNCOMBE, J., CAPORALI, A., KALARIA, R. N., SMITH, C., SHAH, A. M. & HORSBURGH, K. 2022. Nox2 underpins microvascular inflammation and vascular contributions to cognitive decline. *Journal of Cerebral Blood Flow & Metabolism***,** 42(7):1176-1191.

ALVES-LOPES, R., LACCHINI, S., NEVES, K. B., HARVEY, A., MONTEZANO, A. C. & TOUYZ, R. M. 2023. Vasoprotective effects of NOX4 are mediated via

polymerase and transient receptor potential melastatin 2 cation channels in endothelial cells. *J Hypertens,* 41**,** 1389-1400.

ALVES-LOPES, R., NEVES, K. B., ANAGNOSTOPOULOU, A., RIOS, F. J., LACCHINI, S., MONTEZANO, A. C. & TOUYZ, R. M. 2020. Crosstalk Between Vascular Redox and Calcium Signaling in Hypertension Involves TRPM2 (Transient Receptor Potential Melastatin 2) Cation Channel. *Hypertension,* 75**,** 139-149.

ANDERSON, G. & MAES, M. 2014. Oxidative/Nitrosative Stress and Immuno-inflammatory Pathways in Depression: Treatment Implications. *Current Pharmaceutical Design,* 20**,** 3812-3847.

ANDROWIKI, A. C. D., CAMARGO, L. V. D. L., SARTORETTO, S., COUTO, G. K., RIBEIRO, I. M. R., VERÃ-SSIMO-FILHO, S., ROSSONI, L. V. & LOPES, L. R. 2015. Protein disulfide isomerase expression increases in resistance arteries during hypertension development. Effects on Nox1 NADPH oxidase signaling. *Frontiers in Chemistry,* 3.

ANTONY, S., JIANG, G., WU, Y., MEITZLER, J. L., MAKHLOUF, H. R., HAINES, D. C., BUTCHER, D., HOON, D. S., JI, J., ZHANG, Y., JUHASZ, A., LU, J., LIU, H., DAHAN, I., KONATE, M., ROY, K. K. & DOROSHOW, J. H. 2017. NADPH oxidase 5 (NOX5)induced reactive oxygen signaling modulates normoxic HIF-1 and p27(Kip1) expression in malignant melanoma and other human tumors. *Molecular Carcinogenesis,* 56**,** 2643-2662.

ARAUJO, J. A., ZHANG, M. & YIN, F. 2012. Heme Oxygenase-1, Oxidation, Inflammation, and Atherosclerosis. *Frontiers in Pharmacology,* 3.

ARBOIX, A. 2015. Cardiovascular risk factors for acute stroke: Risk profiles in the different subtypes of ischemic stroke. *World J Clin Cases,* 3**,** 418-29.

ARCHER, S. L., HUANG, J. M., HAMPL, V., NELSON, D. P., SHULTZ, P. J. & WEIR, E. K. 1994. Nitric oxide and cGMP cause vasorelaxation by activation of a charybdotoxin-sensitive K channel by cGMP-dependent protein kinase. *Proceedings of the National Academy of Sciences,* 91**,** 7583-7587.

ARENDSE, L. B., DANSER, A. H. J., POGLITSCH, M., TOUYZ, R. M., BURNETT, J. C., LLORENS-CORTES, C., EHLERS, M. R. & STURROCK, E. D. 2019. Novel Therapeutic Approaches Targeting the Renin-Angiotensin System and Associated Peptides in Hypertension and Heart Failure. *Pharmacological Reviews,* 71**,** 539-570.

ARIES, M. J. H., ELTING, J. W., DE KEYSER, J., KREMER, B. P. H. & VROOMEN, P. 2010. Cerebral Autoregulation in Stroke A Review of Transcranial Doppler Studies. *Stroke,* 41**,** 2697-2704.

ARIMA, H., BARZI, F. & CHALMERS, J. 2011. Mortality patterns in hypertension. *J Hypertens,* 29 Suppl 1**,** S3-7.

ARMSTEAD, W. M. 2016. Cerebral Blood Flow Autoregulation and Dysautoregulation. *Anesthesiology Clinics,* 34**,** 465-477.

ARTAVANIS-TSAKONAS, S., RAND, M. D. & LAKE, R. J. 1999. Notch signaling: cell fate control and signal integration in development. *Science,* 284**,** 770-6.

AZAROVA, I., KLYOSOVA, E., AZAROVA, V. & POLONIKOV, A. 2024. NADPH oxidase 5 is a novel susceptibility gene for type 2 diabetes mellitus. *Archives of Endocrinology and Metabolism,* 68.

BA, Z. F., WANG, P., KUEBLER, J. F., RUE, L. W., BLAND, K. I. & CHAUDRY, I. H. 2002. Flutamide induces relaxation in large and small blood vessels. *Arch Surg,* 137**,** 1180-6.

BABCOCK, M. C., DUBOSE, L. E., WITTEN, T. L., STAUFFER, B. L., HILDRETH, K. L., SCHWARTZ, R. S., KOHRT, W. M. & MOREAU, K. L. 2022. Oxidative Stress and Inflammation Are Associated With Age-Related Endothelial Dysfunction in

Men With Low Testosterone. *The Journal of Clinical Endocrinology & Metabolism,* 107**,** e500-e514.

BAETEN, J. T. & LILLY, B. 2015. Differential Regulation of NOTCH2 and NOTCH3 Contribute to Their Unique Functions in Vascular Smooth Muscle Cells. *Journal of Biological Chemistry,* 290**,** 16226-16237.

BAETEN, J. T. & LILLY, B. 2017. Notch Signaling in Vascular Smooth Muscle Cells. *Advances in pharmacology (San Diego, Calif.),* 78**,** 351-382.

BAEV, A. Y., VINOKUROV, A. Y., NOVIKOVA, I. N., DREMIN, V. V., POTAPOVA, E. V. & ABRAMOV, A. Y. 2022. Interaction of Mitochondrial Calcium and ROS in Neurodegeneration. *Cells,* 11**,** 706.

BANFI, B., MOLNAR, G., MATURANA, A., STEGER, K., HEGEDUS, B., DEMAUREX, N. & KRAUSE, K. H. 2001. A Ca2+-activated NADPH oxidase in testis, spleen, and lymph nodes. *Journal of Biological Chemistry,* 276**,** 37594-37601.

BARON-MENGUY, C., DOMENGA-DENIER, V., GHEZALI, L., FARACI, F. M. & JOUTEL, A. 2017. Increased Notch3 Activity Mediates Pathological Changes in Structure of Cerebral Arteries. *Hypertension,* 69**,** 60-70.

BARUSCOTTI, I., BARCHIESI, F., JACKSON, E. K., IMTHURN, B., STILLER, R., KIM, J.-H., SCHAUFELBERGER, S., ROSSELLI, M., HUGHES, C. C. W. & DUBEY, R. K. 2010. Estradiol Stimulates Capillary Formation by Human Endothelial Progenitor Cells. *Hypertension,* 56**,** 397-404.

BASUROY, S., BHATTACHARYA, S., LEFFLER, C. W. & PARFENOVA, H. 2009. Nox4 NADPH oxidase mediates oxidative stress and apoptosis caused by TNF-alpha in cerebral vascular endothelial cells. *Am J Physiol Cell Physiol,* 296**,** C422-32.

BATH, P. M. & WARDLAW, J. M. 2015. Pharmacological Treatment and Prevention of Cerebral Small Vessel Disease: A Review of Potential Interventions. *International Journal of Stroke,* 10**,** 469-478.

BEDARD, K. & KRAUSE, K. H. 2007. The NOX family of ROS-generating NADPH oxidases: physiology and pathophysiology. *Physiol Rev,* 87**,** 245-313.

BEHL, C., SKUTELLA, T., LEZOUALC'H, F., POST, A., WIDMANN, M., NEWTON, C. J. & HOLSBOER, F. 1997. Neuroprotection against oxidative stress by estrogens: structure-activity relationship. *Mol Pharmacol,* 51**,** 535-41.

BELAIBA, R. S., DJORDJEVIC, T., PETRY, A., DIEMER, K., BONELLO, S., BANFI, B., HESS, J., POGREBNIAK, A., BICKEL, C. & GÖRLACH, A. 2007. NOX5 variants are functionally active in endothelial cells. *Free Radic Biol Med,* 42**,** 446-59.

BEN HAIM, L., CEYZÉRIAT, K., CARRILLO-DE SAUVAGE, M. A., AUBRY, F., AUREGAN, G., GUILLERMIER, M., RUIZ, M., PETIT, F., HOUITTE, D., FAIVRE, E., VANDESQUILLE, M., ARON-BADIN, R., DHENAIN, M., DÉGLON, N., HANTRAYE, P., BROUILLET, E., BONVENTO, G. & ESCARTIN, C. 2015. The JAK/STAT3 Pathway Is a Common Inducer of Astrocyte Reactivity in Alzheimer's and Huntington's Diseases. *The Journal of Neuroscience,* 35**,** 2817-2829.

BENAVENTE , O., R., COFFEY , C., S., CONWIT , R., HART , R., G., MCCLURE , L., A., PEARCE , L., A., PERGOLA , P., E. & SZYCHOWSKI , J., M. 2013. Blood-pressure targets in patients with recent lacunar stroke: the SPS3 randomised trial. *The Lancet,* 382**,** 507-515.

BENITO-GONZALEZ, A. & DOETZLHOFER, A. 2014. Hey1 and Hey2 Control the Spatial and Temporal Pattern of Mammalian Auditory Hair Cell Differentiation Downstream of Hedgehog Signaling. *Journal of Neuroscience,* 34**,** 12865-12876.

BERGERS, G. & SONG, S. 2005. The role of pericytes in blood-vessel formation and maintenance. *Neuro-Oncology,* 7**,** 452-464.

BEUKER, C., SCHMIDT, A., STRUNK, D., SPORNS, P. B., WIENDL, H., MEUTH, S. G. & MINNERUP, J. 2018. Primary angiitis of the central nervous system: diagnosis and treatment. *Ther Adv Neurol Disord,* 11**,** 1756286418785071.

BIENERT, G. P., SCHJOERRING, J. K. & JAHN, T. P. 2006. Membrane transport of hydrogen peroxide. *Biochim Biophys Acta,* 1758**,** 994-1003.

BILBAO-MALAVÉ, V., GONZÁLEZ-ZAMORA, J., DE LA PUENTE, M., RECALDE, S., FERNANDEZ-ROBREDO, P., HERNANDEZ, M., LAYANA, A. G. & SAENZ DE VITERI, M. 2021. Mitochondrial Dysfunction and Endoplasmic Reticulum Stress in Age Related Macular Degeneration, Role in Pathophysiology, and Possible New Therapeutic Strategies. *Antioxidants,* 10**,** 1170.

BOEHME, A. K., ESENWA, C. & ELKIND, M. S. V. 2017. Stroke Risk Factors, Genetics, and Prevention. *Circulation Research,* 120**,** 472-495.

BOHM, F. & PERNOW, J. 2007. The importance of endothelin-1 for vascular dysfunction in cardiovascular disease. *Cardiovascular Research,* 76**,** 8-18.

BONAVENTURA, D., LUNARDI, C. N., RODRIGUES, G. J., NETO, M. A. & BENDHACK, L. M. 2008. A novel mechanism of vascular relaxation induced by sodium nitroprusside in the isolated rat aorta. *Nitric Oxide,* 18**,** 287-95.

BONCORAGLIO, G. B., DEL GIOVANE, C. & TRAMACERE, I. 2021. Antihypertensive Drugs for Secondary Prevention After Ischemic Stroke or Transient Ischemic Attack: A Systematic Review and Meta-Analysis. *Stroke,* 52**,** 1974-1982.

BOULOUIS, G., CHARIDIMOU, A., JESSEL, M. J., XIONG, L., ROONGPIBOONSOPIT, D., FOTIADIS, P., PASI, M., AYRES, A., MERRILL, M. E., SCHWAB, K. M., ROSAND, J., GUROL, M. E., GREENBERG, S. M. & VISWANATHAN, A. 2017. Small vessel disease burden in cerebral amyloid angiopathy without symptomatic hemorrhage. *Neurology,* 88**,** 878-884.

BRAIT, V. H., JACKMAN, K. A., WALDUCK, A. K., SELEMIDIS, S., DIEP, H., MAST, A. E., GUIDA, E., BROUGHTON, B. R., DRUMMOND, G. R. & SOBEY, C. G. 2010. Mechanisms Contributing to Cerebral Infarct Size after Stroke: Gender, Reperfusion, T Lymphocytes, and Nox2-Derived Superoxide. *Journal of Cerebral Blood Flow & Metabolism,* 30**,** 1306-1317.

BRAR, S. S., CORBIN, Z., KENNEDY, T. P., HEMENDINGER, R., THORNTON, L., BOMMARIUS, B., ARNOLD, R. S., WHORTON, A. R., STURROCK, A. B., HUECKSTEADT, T. P., QUINN, M. T., KRENITSKY, K., ARDIE, K. G., LAMBETH, J. D. & HOIDAL, J. R. 2003. NOX5 NAD(P)H oxidase regulates growth and apoptosis in DU 145 prostate cancer cells. *Am J Physiol Cell Physiol,* 285**,** C353-69.

BRAY, S. J. 2016. Notch signalling in context. *Nat Rev Mol Cell Biol,* 17**,** 722-735.

BRETON-ROMERO, R. & LAMAS, S. 2014. Hydrogen peroxide signaling in vascular endothelial cells. *Redox Biology,* 2**,** 529-534.

BRONZUOLI, M. R., FACCHINETTI, R., VALENZA, M., CASSANO, T., STEARDO, L. & SCUDERI, C. 2019. Astrocyte Function Is Affected by Aging and Not Alzheimer's Disease: A Preliminary Investigation in Hippocampi of 3xTg-AD Mice. *Frontiers in Pharmacology,* 10.

BROWN, M. K. & NAIDOO, N. 2012. The endoplasmic reticulum stress response in aging and age-related diseases. *Frontiers in Physiology,* 3.

BROZOVICH, F. V., NICHOLSON, C. J., DEGEN, C. V., GAO, Y. Z., AGGARWAL, M. & MORGAN, K. G. 2016. Mechanisms of Vascular Smooth Muscle Contraction and the Basis for Pharmacologic Treatment of Smooth Muscle Disorders. *Pharmacological Reviews,* 68**,** 476-532.

BUSHNELL, C. D., CHATURVEDI, S., GAGE, K. R., HERSON, P. S., HURN, P. D., JIMÉNEZ, M. C., KITTNER, S. J., MADSEN, T. E., MCCULLOUGH, L. D., MCDERMOTT, M., REEVES, M. J. & RUNDEK, T. 2018. Sex differences in

stroke: Challenges and opportunities. *Journal of Cerebral Blood Flow & Metabolism,* 38**,** 2179-2191.

BYON, C. H., HEATH, J. M. & CHEN, Y. 2016. Redox signaling in cardiovascular pathophysiology: A focus on hydrogen peroxide and vascular smooth muscle cells. *Redox Biol,* 9**,** 244-253.

BÁNFI, B., TIRONE, F., DURUSSEL, I., KNISZ, J., MOSKWA, P., MOLNÁR, G. Z., KRAUSE, K.-H. & COX, J. A. 2004. Mechanism of Ca2+ Activation of the NADPH Oxidase 5 (NOX5). *Journal of Biological Chemistry,* 279**,** 18583-18591.

CALICETI, C., NIGRO, P., RIZZO, P. & FERRARI, R. 2014. ROS, Notch, and Wnt Signaling Pathways: Crosstalk between Three Major Regulators of Cardiovascular Biology. *BioMed Research International,* 2014**,** 1-8.

CAMARGO, L., MARY, S., LILLA, S., HARTLEY, R., DELLES, C., FULLER, W., WANG, Y., RIOS, F., MONTEZANO, A. & TOUYZ, R. 2023a. Nox5 links oxidative stress and endoplasmic reticulum stress to enable vascular smooth muscle cell phenotypic switcing in hypertension. 47.

CAMARGO, L. L., HARVEY, A. P., RIOS, F. J., TSIROPOULOU, S., SILVA, R. D. O., CAO, Z. B., GRAHAM, D., MCMASTER, C., BURCHMORE, R. J., HARTLEY, R. C., BULLEID, N., MONTEZANO, A. C. & TOUYZ, R. M. 2018a. Vascular Nox (NADPH Oxidase) Compartmentalization, Protein Hyperoxidation, and Endoplasmic Reticulum Stress Response in Hypertension. *Hypertension,* 72**,** 235-246.

CAMARGO, L. L., HARVEY, A. P., RIOS, F. J., TSIROPOULOU, S. A., SILVA, R. D. D., CAO, Z. B., MCMASTER, C., BURCHMORE, R. J., HARTLEY, R. C., BULLEID, N., MONTEZANO, A. & TOUYZ, R. M. 2018b. Interplay between NOX-regulated oxidative stress and ER stress response in experimental hypertension. *Journal of Hypertension,* 36**,** E57-E58.

CAMARGO, L. L., MONTEZANO, A. C., HUSSAIN, M., WANG, Y., ZOU, Z., RIOS, F. J., NEVES, K. B., ALVES-LOPES, R., AWAN, F. R., GUZIK, T. J., JENSEN, T., HARTLEY, R. C. & TOUYZ, R. M. 2022. Central role of c-Src in NOX5-mediated redox signalling in vascular smooth muscle cells in human hypertension. *Cardiovascular Research,* 118**,** 1359-1373.

CAMARGO, L. L., WANG, Y., RIOS, F. J., MCBRIDE, M., MONTEZANO, A. C. & TOUYZ, R. M. 2023b. Oxidative Stress and Endoplasmic Reticular Stress Interplay in the Vasculopathy of Hypertension. *Can J Cardiol,* 39**,** 1874-1887.

CANNISTRARO, R. J., BADI, M., EIDELMAN, B. H., DICKSON, D. W., MIDDLEBROOKS, E. H. & MESCHIA, J. F. 2019. CNS small vessel disease. *Neurology,* 92**,** 1146-1156.

CAO, L., JIAO, X., ZUZGA, D. S., LIU, Y., FONG, D. M., YOUNG, D. & DURING, M. J. 2004. VEGF links hippocampal activity with neurogenesis, learning and memory. *Nat Genet,* 36**,** 827-35.

CAO, S. S. & KAUFMAN, R. J. 2014. Endoplasmic Reticulum Stress and Oxidative Stress in Cell Fate Decision and Human Disease. *Antioxidants & Redox Signaling,* 21**,** 396-413.

CAPONE, C., COGNAT, E., GHEZALI, L., BARON-MENGUY, C., AUBIN, D., MESNARD, L., STÖHR, H., DOMENGA-DENIER, V., NELSON, M. T. & JOUTEL, A. 2016. Reducing Timp3 or vitronectin ameliorates disease manifestations in CADASIL mice. *Ann Neurol,* 79**,** 387-403.

CARVALHO, C. & MOREIRA, P. I. 2018. Oxidative Stress: A Major Player in Cerebrovascular Alterations Associated to Neurodegenerative Events. *Frontiers in Physiology,* 9**,** 14.

CASAS, A. I., GEUSS, E., KLEIKERS, P. W. M., MENCL, S., HERRMANN, A. M., BUENDIA, I., EGEA, J., MEUTH, S. G., LOPEZ, M. G., KLEINSCHNITZ, C. & SCHMIDT, H. 2017. NOX4-dependent neuronal autotoxicity and BBB breakdown

explain the superior sensitivity of the brain to ischemic damage. *Proceedings of the National Academy of Sciences of the United States of America,* 114**,** 12315-12320.

CASAS, A. I., KLEIKERS, P. W. M., GEUSS, E., LANGHAUSER, F., ADLER, T., BUSCH, D. H., GAILUS-DURNER, V., DE ANGELIS, M. H., EGEA, J., LOPEZ, M. G., KLEINSCHNITZ, C. & SCHMIDT, H. 2019. Calcium-dependent blood-brain barrier breakdown by NOX5 limits postreperfusion benefit in stroke. *Journal of Clinical Investigation,* 129**,** 1772-1778.

CHAMBLISS, K. L. & SHAUL, P. W. 2002. Estrogen modulation of endothelial nitric oxide synthase. *Endocr Rev,* 23**,** 665-86.

CHEN, F., LI, X., AQUADRO, E., HAIGH, S., ZHOU, J., STEPP, D. W., WEINTRAUB, N. L., BARMAN, S. A. & FULTON, D. J. R. 2016. Inhibition of histone deacetylase reduces transcription of NADPH oxidases and ROS production and ameliorates pulmonary arterial hypertension. *Free Radical Biology and Medicine,* 99**,** 167-178.

CHEN, H., SONG, Y. S. & CHAN, P. H. 2009. Inhibition of NADPH Oxidase is Neuroprotective after Ischemia—Reperfusion. *Journal of Cerebral Blood Flow & Metabolism,* 29**,** 1262-1272.

CHEN, J., LIU, Y., PAN, D., XU, T., LUO, Y., WU, W., WU, P., ZHU, H. & LI, D. 2022. Estrogen inhibits endoplasmic reticulum stress and ameliorates myocardial ischemia/reperfusion injury in rats by upregulating SERCA2a. *Cell Communication and Signaling,* 20.

CHEN, Q., SAMIDURAI, A., THOMPSON, J., HU, Y., DAS, A., WILLARD, B. & LESNEFSKY, E. J. 2020a. Endoplasmic reticulum stress-mediated mitochondrial dysfunction in aged hearts. *Biochim Biophys Acta Mol Basis Dis,* 1866**,** 165899.

CHEN, R., MCVEY, D. G., SHEN, D., HUANG, X. & YE, S. 2023a. Phenotypic Switching of Vascular Smooth Muscle Cells in Atherosclerosis. *Journal of the American Heart Association,* 12.

CHEN, X., SHI, C., HE, M., XIONG, S. & XIA, X. 2023b. Endoplasmic reticulum stress: molecular mechanism and therapeutic targets. *Signal Transduction and Targeted Therapy,* 8.

CHEN, Y., QIN, C., HUANG, J., TANG, X., LIU, C., HUANG, K., XU, J., GUO, G., TONG, A. & ZHOU, L. 2020b. The role of astrocytes in oxidative stress of central nervous system: A mixed blessing. *Cell Proliferation,* 53.

CHEN, Z., YUHANNA, I. S., GALCHEVA-GARGOVA, Z., KARAS, R. H., MENDELSOHN, M. E. & SHAUL, P. W. 1999. Estrogen receptor α mediates the nongenomic activation of endothelial nitric oxide synthase by estrogen. *Journal of Clinical Investigation,* 103**,** 401-406.

CHENG, G. J., CAO, Z. H., XU, X. X., VAN MEIR, E. G. & LAMBETH, J. D. 2001. Homologs of gp91phox: cloning and tissue expression of Nox3, Nox4, and Nox5. *Gene,* 269**,** 131-140.

CHO, M. J., LEE, D. G., LEE, J. W., HWANG, B., YOON, S. J., LEE, S. J., PARK, Y. J., PARK, S. H., LEE, H. G., KIM, Y. H., LEE, C. H., LEE, J., LEE, N. K., HAN, T. S., CHO, H. S., MOON, J. H., LEE, G. S., BAE, K. H., HWANG, G. S., LEE, S. H., CHUNG, S. J., SHIM, S., CHO, J., OH, G. T., KWON, Y. G., PARK, J. G. & MIN, J. K. 2023. Endothelial PTP4A1 mitigates vascular inflammation via USF1/A20 axis-mediated NF-κB inactivation. *Cardiovasc Res,* 119**,** 1265-1278.

CHOI, D.-H., LEE, K.-H., KIM, J.-H., SEO, J.-H., KIM, H. Y., SHIN, C. Y., HAN, J.-S., HAN, S.-H., KIM, Y.-S. & LEE, J. 2014. NADPH Oxidase 1, a Novel Molecular Source of ROS in Hippocampal Neuronal Death in Vascular Dementia. *Antioxidants & Redox Signaling,* 21**,** 533-550.

CHOI, D. W. 2020. Excitotoxicity: Still Hammering the Ischemic Brain in 2020. *Frontiers in Neuroscience,* 14.

CHRISSOBOLIS, S. & FARACI, F. M. 2008. The role of oxidative stress and NADPH oxidase in cerebrovascular disease. *Trends in Molecular Medicine,* 14**,** 495-502.

CHRISTIE, I. N., THEPARAMBIL, S. M., BRAGA, A., DORONIN, M., HOSFORD, P. S., BRAZHE, A., MASCARENHAS, A., NIZARI, S., HADJIHAMBI, A., WELLS, J. A., HOBBS, A., SEMYANOV, A., ABRAMOV, A. Y., ANGELOVA, P. R. & GOURINE, A. V. 2023. Astrocytes produce nitric oxide via nitrite reduction in mitochondria to regulate cerebral blood flow during brain hypoxia. *Cell Reports,* 42**,** 113514.

CHUNG, H. S., WANG, S.-B., VENKATRAMAN, V., MURRAY, C. I. & VAN EYK, J. E. 2013. Cysteine Oxidative Posttranslational Modifications. *Circulation Research,* 112**,** 382-392.

CLAASSEN, J. A. H. R., THIJSSEN, D. H. J., PANERAI, R. B. & FARACI, F. M. 2021. Regulation of cerebral blood flow in humans: physiology and clinical implications of autoregulation. *Physiol Rev,* 101**,** 1487-1559.

CLARKE, L. E., LIDDELOW, S. A., CHAKRABORTY, C., MÜNCH, A. E., HEIMAN, M. & BARRES, B. A. 2018. Normal aging induces A1-like astrocyte reactivity. *Proceedings of the National Academy of Sciences,* 115**,** E1896-E1905.

COGOLLUDO, A. L., PÉREZ-VIZCAÍNO, F., ZARAGOZÁ-ARNÁEZ, F., IBARRA, M., LÓPEZ-LÓPEZ, G., LÓPEZ-MIRANDA, V. & TAMARGO, J. 2001. Mechanisms involved in SNP-induced relaxation and [Ca2+]i reduction in piglet pulmonary and systemic arteries. *British Journal of Pharmacology,* 132**,** 959-967.

COLAFELLA, K. M. M. & DENTON, K. M. 2018. Sex-specific differences in hypertension and associated cardiovascular disease. *Nat Rev Nephrol,* 14**,** 185-201.

COLLIGNON, A., DION-ALBERT, L., MÉNARD, C. & COELHO-SANTOS, V. 2024. Sex, hormones and cerebrovascular function: from development to disorder. *Fluids and Barriers of the CNS,* 21.

CONNELLY, P. J., CASEY, H., MONTEZANO, A. C., TOUYZ, R. M. & DELLES, C. 2022. Sex steroids receptors, hypertension, and vascular ageing. *Journal of Human Hypertension,* 36**,** 120-125.

CORTÉS, A., PEJENAUTE, Á., MARQUÉS, J., IZAL, Í., CENOZ, S., ANSORENA, E., MARTÍNEZ-IRUJO, J. J., DE MIGUEL, C. & ZALBA, G. 2021a. NADPH Oxidase 5 Induces Changes in the Unfolded Protein Response in Human Aortic Endothelial Cells and in Endothelial-Specific Knock-in Mice. *Antioxidants,* 10**,** 194.

CORTÉS, A., SOLAS, M., PEJENAUTE, Á., ABELLANAS, M. A., GARCIA-LACARTE, M., AYMERICH, M. S., MARQUÉS, J., RAMÍREZ, M. J. & ZALBA, G. 2021b. Expression of Endothelial NOX5 Alters the Integrity of the Blood-Brain Barrier and Causes Loss of Memory in Aging Mice. *Antioxidants,* 10**,** 1311.

COUCHA, M., ABDELSAID, M., LI, W., JOHNSON, M. H., ORFI, L., EL-REMESSY, A. B., FAGAN, S. C. & ERGUL, A. 2016. Nox4 contributes to the hypoxia-mediated regulation of actin cytoskeleton in cerebrovascular smooth muscle. *Life Sciences,* 163**,** 46-54.

COUPLAND, K., LENDAHL, U. & KARLSTROM, H. 2018. Role of NOTCH3 Mutations in the Cerebral Small Vessel Disease Cerebral Autosomal Dominant Arteriopathy With Subcortical Infarcts and Leukoencephalopathy. *Stroke,* 49**,** 2793-2800.

CSISZAR, A., UNGVARI, A., PATAI, R., GULEJ, R., YABLUCHANSKIY, A., BENYO, Z., KOVACS, I., SOTONYI, P., KIRKPARTRICK, A. C., PRODAN, C. I., LIOTTA, E. M., ZHANG, X. A., TOTH, P., TARANTINI, S., SOROND, F. A. & UNGVARI, Z. 2024. Atherosclerotic burden and cerebral small vessel disease: exploring the link through microvascular aging and cerebral microhemorrhages. *GeroScience,* 46**,** 5103-5132.

CUSTODERO, C., CIAVARELLA, A., PANZA, F., GNOCCHI, D., LENATO, G. M., LEE, J., MAZZOCCA, A., SABBÀ, C. & SOLFRIZZI, V. 2022. Role of inflammatory markers in the diagnosis of vascular contributions to cognitive impairment and dementia: a systematic review and meta-analysis. *GeroScience,* 44**,** 1373-1392.

DA FONSECA, A. C. C., MATIAS, D., GARCIA, C., AMARAL, R., GERALDO, L. H., FREITAS, C. & LIMA, F. R. S. 2014. The impact of microglial activation on blood-brain barrier in brain diseases. *Frontiers in Cellular Neuroscience,* 8.

DANTAS, A. P. V., TOSTES, R. C. A., FORTES, Z. B., COSTA, S. G., NIGRO, D. & CARVALHO, M. H. C. 2002. In Vivo Evidence for Antioxidant Potential of Estrogen in Microvessels of Female Spontaneously Hypertensive Rats. *Hypertension,* 39**,** 405-411.

DAO, V. T., ELBATREEK, M. H., ALTENHÖFER, S., CASAS, A. I., PACHADO, M. P., NEULLENS, C. T., KNAUS, U. G. & SCHMIDT, H. H. H. W. 2020. Isoform-selective NADPH oxidase inhibitor panel for pharmacological target validation. *Free Radic Biol Med,* 148**,** 60-69.

DATLA, S. R., DUSTING, G. J., MORI, T. A., TAYLOR, C. J., CROFT, K. D. & JIANG, F. 2007. Induction of Heme Oxygenase-1 In Vivo Suppresses NADPH Oxidase–Derived Oxidative Stress. *Hypertension,* 50**,** 636-642.

DATLA, S. R. & GRIENDLING, K. K. 2010. Reactive Oxygen Species, NADPH Oxidases, and Hypertension. *Hypertension,* 56**,** 325-330.

DAVEREY, A. & AGRAWAL, S. K. 2016. Curcumin alleviates oxidative stress and mitochondrial dysfunction in astrocytes. *Neuroscience,* 333**,** 92-103.

DAVEZAC, M., BUSCATO, M., ZAHREDDINE, R., LACOLLEY, P., HENRION, D., LENFANT, F., ARNAL, J.-F. & FONTAINE, C. 2021. Estrogen Receptor and Vascular Aging. *Frontiers in Aging,* 2.

DE LEEUW, F. E., DE GROOT, J. C., ACHTEN, E., OUDKERK, M., RAMOS, L. M., HEIJBOER, R., HOFMAN, A., JOLLES, J., VAN GIJN, J. & BRETELER, M. M. 2001. Prevalence of cerebral white matter lesions in elderly people: a population based magnetic resonance imaging study. The Rotterdam Scan Study. *J Neurol Neurosurg Psychiatry,* 70**,** 9-14.

DE ROSSI, P., HARDE, E., DUPUIS, J. P., MARTIN, L., CHOUNLAMOUNTRI, N., BARDIN, M., WATRIN, C., BENETOLLO, C., PERNET-GALLAY, K., LUHMANN, H. J., HONNORAT, J., MALLERET, G., GROC, L., ACKER-PALMER, A., SALIN, P. A. & MEISSIREL, C. 2016. A critical role for VEGF and VEGFR2 in NMDA receptor synaptic function and fear-related behavior. *Molecular Psychiatry,* 21**,** 1768-1780.

DE SILVA, T. M., BRAIT, V. H., DRUMMOND, G. R., SOBEY, C. G. & MILLER, A. A. 2011. Nox2 Oxidase Activity Accounts for the Oxidative Stress and Vasomotor Dysfunction in Mouse Cerebral Arteries following Ischemic Stroke. *PLoS ONE,* 6**,** e28393.

DE SILVA, T. M. & FARACI, F. M. 2013. Effects of angiotensin II on the cerebral circulation: role of oxidative stress. *Frontiers in Physiology,* 3.

DE SILVA, T. M. & MILLER, A. A. 2016. Cerebral Small Vessel Disease: Targeting Oxidative Stress as a Novel Therapeutic Strategy? *Frontiers in Pharmacology,* 7**,** 18.

DEER, R. R. & STALLONE, J. N. 2016. Effects of estrogen on cerebrovascular function: age-dependent shifts from beneficial to detrimental in small cerebral arteries of the rat. *Am J Physiol Heart Circ Physiol,* 310**,** H1285-94.

DELIYANTI, D., ALRASHDI, S. F., TOUYZ, R. M., KENNEDY, C. R., JHA, J. C., COOPER, M. E., JANDELEIT-DAHM, K. A. & WILKINSON-BERKA, J. L. 2020. Nox (NADPH Oxidase) 1, Nox4, and Nox5 Promote Vascular Permeability and Neovascularization in Retinopathy. *Hypertension,* 75**,** 1091-1101.

DIAZ BRINTON, R. 2012. Minireview: translational animal models of human menopause: challenges and emerging opportunities. *Endocrinology,* 153**,** 3571-8.

DICHGANS, M. & LEYS, D. 2017. Vascular Cognitive Impairment. *Circulation Research,* 120**,** 573-591.

DIEBOLD, I., PETRY, A., HESS, J. & GOERLACH, A. 2010. The NADPH Oxidase Subunit NOX4 Is a New Target Gene of the Hypoxia-inducible Factor-1. *Molecular Biology of the Cell,* 21**,** 2087-2096.

DIKALOVA, A., CLEMPUS, R., LASSEGUE, B., CHENG, G. J., MCCOY, J., DIKALOV, S., MARTIN, A. S., LYLE, A., WEBER, D. S., WEISS, D., TAYLOR, R., SCHMIDT, H., OWENS, G. K., LAMBETH, J. D. & GRIENDLING, K. K. 2005. Nox1 overexpression potentiates angiotensin II-induced hypertension and vascular smooth muscle hypertrophy in transgenic mice. *Circulation,* 112**,** 2668-2676.

DIKALOVA, A. E., GÓNGORA, M. C., HARRISON, D. G., LAMBETH, J. D., DIKALOV, S. & GRIENDLING, K. K. 2010. Upregulation of Nox1 in vascular smooth muscle leads to impaired endothelium-dependent relaxation via eNOS uncoupling. *Am J Physiol Heart Circ Physiol,* 299**,** H673-9.

DIKALOVA, A. E., ITANI, H. A., NAZAREWICZ, R. R., MCMASTER, W. G., FLYNN, C. R., UZHACHENKO, R., FESSEL, J. P., GAMBOA, J. L., HARRISON, D. G. & DIKALOV, S. I. 2017. Sirt3 Impairment and SOD2 Hyperacetylation in Vascular Oxidative Stress and Hypertension. *Circulation Research,* 121**,** 564-574.

DIKALOVA, A. E., PANDEY, A., XIAO, L., ARSLANBAEVA, L., SIDOROVA, T., LOPEZ, M. G., BILLINGS, F. T., VERDIN, E., AUWERX, J., HARRISON, D. G. & DIKALOV, S. I. 2020. Mitochondrial Deacetylase Sirt3 Reduces Vascular Dysfunction and Hypertension While Sirt3 Depletion in Essential Hypertension Is Linked to Vascular Inflammation and Oxidative Stress. *Circulation Research,* 126**,** 439-452.

DORN, G. W. & BECKER, M. W. 1993. Thromboxane A2 stimulated signal transduction in vascular smooth muscle. *J Pharmacol Exp Ther,* 265**,** 447-56.

DOS SANTOS, R. L., DA SILVA, F. B., RIBEIRO, R. F. & STEFANON, I. 2014. Sex hormones in the cardiovascular system. *Hormone Molecular Biology and Clinical Investigation,* 18**,** 89-103.

DREIER, R., ISING, T., RAMROTH, M. & RELLMANN, Y. 2022. Estradiol Inhibits ER Stress-Induced Apoptosis in Chondrocytes and Contributes to a Reduced Osteoarthritic Cartilage Degeneration in Female Mice. *Frontiers in Cell and Developmental Biology,* 10.

DUTTA, S. & SENGUPTA, P. 2016. Men and mice: Relating their ages. *Life Sci,* 152**,** 244-8.

EBRAHIMIAN, T., LI, M. W., LEMARIÉ, C. A., SIMEONE, S. M. C., PAGANO, P. J., GAESTEL, M., PARADIS, P., WASSMANN, S. & SCHIFFRIN, E. L. 2011. Mitogen-Activated Protein Kinase–Activated Protein Kinase 2 in Angiotensin II–Induced Inflammation and Hypertension. *Hypertension,* 57**,** 245-254.

EID, A. H., EL-YAZBI, A. F., ZOUEIN, F., ARREDOUANI, A., OUHTIT, A., RAHMAN, M. M., ZAYED, H., PINTUS, G. & ABOU-SALEH, H. 2018. Inositol 1,4,5-Trisphosphate Receptors in Hypertension. *Frontiers in Physiology,* 9.

ELAHI, F. M., WANG, M. M. & MESCHIA, J. F. 2023. Cerebral Small Vessel Disease–Related Dementia: More Questions Than Answers. *Stroke,* 54**,** 648-660.

ELBATREEK, M. H., SADEGH, S., ANASTASI, E., GUNEY, E., NOGALES, C., KACPROWSKI, T., HASSAN, A. A., TEUBNER, A., HUANG, P.-H., HSU, C.-Y., SCHIFFERS, P. M. H., JANSSEN, G. M., KLEIKERS, P. W. M., WIPAT, A., BAUMBACH, J., DE MEY, J. G. R. & SCHMIDT, H. H. H. W. 2020. NOX5-induced uncoupling of endothelial NO synthase is a causal mechanism and

theragnostic target of an age-related hypertension endotype. *PLOS Biology,* 18**,** e3000885.

ERDŐ, F., DENES, L. & DE LANGE, E. 2017. Age-associated physiological and pathological changes at the blood–brain barrier: A review. *Journal of Cerebral Blood Flow & Metabolism,* 37**,** 4-24.

FACEMIRE, C. S., NIXON, A. B., GRIFFITHS, R., HURWITZ, H. & COFFMAN, T. M. 2009. Vascular Endothelial Growth Factor Receptor 2 Controls Blood Pressure by Regulating Nitric Oxide Synthase Expression. *Hypertension,* 54**,** 652-658.

FAN, L. M., GENG, L., CAHILL-SMITH, S., LIU, F., DOUGLAS, G., MCKENZIE, C.-A., SMITH, C., BROOKS, G., CHANNON, K. M. & LI, J.-M. 2019. Nox2 contributes to age-related oxidative damage to neurons and the cerebral vasculature. *Journal of Clinical Investigation,* 129**,** 3374-3386.

FANDLER-HÖFLER, S., EPPINGER, S., AMBLER, G., NASH, P., KNEIHSL, M., LEE, K.-J., LIM, J.-S., SHIOZAWA, M., KOGA, M., LI, L., LOVELOCK, C., CHABRIAT, H., HENNERICI, M., WONG, Y. K., MAK, H. K. F., PRATS-SANCHEZ, L., MARTÍNEZ-DOMEÑO, A., INAMURA, S., YOSHIFUJI, K., ARSAVA, E. M., HORSTMANN, S., PURRUCKER, J., LAM, B. Y. K., WONG, A., KIM, Y. D., SONG, T.-J., LEMMENS, R., UYSAL, E., TANRIVERDI, Z., BORNSTEIN, N. M., BEN ASSAYAG, E., HALLEVI, H., MOLAD, J., NISHIHARA, M., TANAKA, J., COUTTS, S. B., POLYMERIS, A., WAGNER, B., SEIFFGE, D. J., LYRER, P., KAPPELLE, L. J., SALMAN, R. A.-S., HERNANDEZ, M. V., JÄGER, H. R., LIP, G. Y. H., FISCHER, U., EL-KOUSSY, M., MAS, J.-L., LEGRAND, L., KARAYIANNIS, C., PHAN, T., GUNKEL, S., CHRIST, N., ABRIGO, J., CHU, W., LEUNG, T., CHAPPELL, F., MAKIN, S., HAYDEN, D., WILLIAMS, D. J., MESS, W. H., KOOI, M. E., BARBATO, C., BROWNING, S., TULADHAR, A. M., MAAIJWEE, N., GUEVARRA, A. C., MENDYK, A.-M., DELMAIRE, C., KÖHLER, S., VAN OOSTENBRUGGE, R., ZHOU, Y., XU, C., HILAL, S., ROBERT, C., CHEN, C., LOU, M., STAALS, J., BORDET, R., KANDIAH, N., DE LEEUW, F.-E., SIMISTER, R., BOS, D., KELLY, P. J., WARDLAW, J., SOO, Y., FLURI, F., SRIKANTH, V., CALVET, D., JUNG, S., KWA, V. I. H., ENGELTER, S. T., PETERS, N., SMITH, E. E., HARA, H., YAKUSHIJI, Y., ORKEN, D. N., THIJS, V., HEO, J. H., MOK, V., et al. 2024. Sex Differences in Frequency, Severity, and Distribution of Cerebral Microbleeds. *JAMA Network Open,* 7**,** e2439571.

FEIGIN, V. L., STARK, B. A., JOHNSON, C. O., ROTH, G. A., BISIGNANO, C., ABADY, G. G., ABBASIFARD, M., ABBASI-KANGEVARI, M., ABD-ALLAH, F., ABEDI, V., ABUALHASAN, A., ABU-RMEILEH, N. M., ABUSHOUK, A. I., ADEBAYO, O. M., AGARWAL, G., AGASTHI, P., AHINKORAH, B. O., AHMAD, S., AHMADI, S., AHMED SALIH, Y., AJI, B., AKBARPOUR, S., AKINYEMI, R. O., AL HAMAD, H., ALAHDAB, F., ALIF, S. M., ALIPOUR, V., ALJUNID, S. M., ALMUSTANYIR, S., AL-RADDADI, R. M., AL-SHAHI SALMAN, R., ALVIS-GUZMAN, N., ANCUCEANU, R., ANDERLINI, D., ANDERSON, J. A., ANSAR, A., ANTONAZZO, I. C., ARABLOO, J., ÄRNLÖV, J., ARTANTI, K. D., ARYAN, Z., ASGARI, S., ASHRAF, T., ATHAR, M., ATREYA, A., AUSLOOS, M., BAIG, A. A., BALTATU, O. C., BANACH, M., BARBOZA, M. A., BARKER-COLLO, S. L., BÄRNIGHAUSEN, T. W., BARONE, M. T. U., BASU, S., BAZMANDEGAN, G., BEGHI, E., BEHESHTI, M., BÉJOT, Y., BELL, A. W., BENNETT, D. A., BENSENOR, I. M., BEZABHE, W. M., BEZABIH, Y. M., BHAGAVATHULA, A. S., BHARDWAJ, P., BHATTACHARYYA, K., BIJANI, A., BIKBOV, B., BIRHANU, M. M., BOLOOR, A., BONNY, A., BRAUER, M., BRENNER, H., BRYAZKA, D., BUTT, Z. A., CAETANO DOS SANTOS, F. L., CAMPOS-NONATO, I. R., CANTU-BRITO, C., CARRERO, J. J., CASTAÑEDA-ORJUELA, C. A.,

CATAPANO, A. L., CHAKRABORTY, P. A., CHARAN, J., CHOUDHARI, S. G., CHOWDHURY, E. K., CHU, D.-T., CHUNG, S.-C., COLOZZA, D., COSTA, V. M., COSTANZO, S., CRIQUI, M. H., DADRAS, O., DAGNEW, B., DAI, X., DALAL, K., DAMASCENO, A. A. M., D'AMICO, E., DANDONA, L., DANDONA, R., DAREGA GELA, J., et al. 2021. Global, regional, and national burden of stroke and its risk factors, 1990–2019: a systematic analysis for the Global Burden of Disease Study 2019. *The Lancet Neurology,* 20**,** 795-820.

FINKEL, T. & HOLBROOK, N. J. 2000. Oxidants, oxidative stress and the biology of ageing. *Nature,* 408**,** 239-47.

FISCHER, A. & GESSLER, M. 2007. Delta-Notch--and then? Protein interactions and proposed modes of repression by Hes and Hey bHLH factors. *Nucleic Acids Res,* 35**,** 4583-96.

FISHER, J. P. & PATON, J. F. R. 2012. The sympathetic nervous system and blood pressure in humans: implications for hypertension. *Journal of Human Hypertension,* 26**,** 463-475.

FLYNN, J. M. & MELOV, S. 2013. SOD2 in mitochondrial dysfunction and neurodegeneration. *Free Radical Biology and Medicine,* 62**,** 4-12.

FORRESTER, S. J., BOOZ, G. W., SIGMUND, C. D., COFFMAN, T. M., KAWAI, T., RIZZO, V., SCALIA, R. & EGUCHI, S. 2018. Angiotensin II Signal Transduction: An Update on Mechanisms of Physiology and Pathophysiology. *Physiological Reviews,* 98**,** 1627-1738.

FRASER, S. T., MIDWINTER, R. G., BERGER, B. S. & STOCKER, R. 2011. Heme Oxygenase-1: A Critical Link between Iron Metabolism, Erythropoiesis, and Development. *Adv Hematol,* 2011**,** 473709.

FUKAI, T. & USHIO-FUKAI, M. 2011. Superoxide Dismutases: Role in Redox Signaling, Vascular Function, and Diseases. *Antioxidants & Redox Signaling,* 15**,** 1583-1606.

FULTON, D. J. R. 2009. Nox5 and the Regulation of Cellular Function. *Antioxidants & Redox Signaling,* 11**,** 2443-2452.

FURMANIK, M., CHATROU, M., VAN GORP, R., AKBULUT, A., WILLEMS, B., SCHMIDT, H., VAN EYS, G., BOCHATON-PIALLAT, M.-L., PROUDFOOT, D., BIESSEN, E., HEDIN, U., PERISIC, L., MEES, B., SHANAHAN, C., REUTELINGSPERGER, C. & SCHURGERS, L. 2020. Reactive Oxygen-Forming Nox5 Links Vascular Smooth Muscle Cell Phenotypic Switching and Extracellular Vesicle-Mediated Vascular Calcification. *Circulation Research,* 127**,** 911-927.

GAIANO, N. & FISHELL, G. 2002. The role of notch in promoting glial and neural stem cell fates. *Annu Rev Neurosci,* 25**,** 471-90.

GAO, G., YOU, L., ZHANG, J., CHANG, Y.-Z. & YU, P. 2023. Brain Iron Metabolism, Redox Balance and Neurological Diseases. *Antioxidants,* 12**,** 1289.

GAO, Y., LI, D., LIN, J., THOMAS, A. M., MIAO, J., CHEN, D., LI, S. & CHU, C. 2022. Cerebral small vessel disease: Pathological mechanisms and potential therapeutic targets. *Frontiers in Aging Neuroscience,* 14.

GARCÍA, J. G., ANSORENA, E., IZAL, I., ZALBA, G., DE MIGUEL, C. & MILAGRO, F. I. 2023. Structure, regulation, and physiological functions of NADPH oxidase 5 (NOX5). *Journal of Physiology and Biochemistry,* 79**,** 383-395.

GARCÍA-REDONDO, A. B., AGUADO, A., BRIONES, A. M. & SALAICES, M. 2016. NADPH oxidases and vascular remodeling in cardiovascular diseases. *Pharmacol Res,* 114**,** 110-120.

GARRIDO, A. M. & GRIENDLING, K. K. 2009. NADPH oxidases and angiotensin II receptor signaling. *Molecular and Cellular Endocrinology,* 302**,** 148-158.

GASCHLER, M. M. & STOCKWELL, B. R. 2017. Lipid peroxidation in cell death. *Biochem Biophys Res Commun,* 482**,** 419-425.

GAVAZZI, G., BANFI, B., DEFFERT, C., FIETTE, L., SCHAPPI, M., HERRMANN, F. & KRAUSE, K. H. 2006. Decreased blood pressure in NOX1-deficient mice. *FEBS Lett,* 580**,** 497-504.

GIANAZZA, E., BRIOSCHI, M., FERNANDEZ, A. M. & BANFI, C. 2019. Lipoxidation in cardiovascular diseases. *Redox Biol,* 23**,** 101119.

GKALIAGKOUSI, E., RITTER, J. & FERRO, A. 2007. Platelet-Derived Nitric Oxide Signaling and Regulation. *Circulation Research,* 101**,** 654-662.

GOGIRAJU, R., GACHKAR, S., VELMEDEN, D., BOCHENEK, M. L., ZIFKOS, K., HUBERT, A., MÜNZEL, T., OFFERMANNS, S. & SCHÄFER, K. 2022. Protein Tyrosine Phosphatase 1B Deficiency in Vascular Smooth Muscle Cells Promotes Perivascular Fibrosis following Arterial Injury. *Thrombosis and Haemostasis,* 122**,** 1814-1826.

GOLDSTEIN, E. D., WOLCOTT, Z., GARG, G., NAVARRO, K., DELIC, A., YAGHI, S., SEDERHOLM, B., PRABHAKARAN, S., WONG, K.-H., MCLEAN, K. & DE HAVENON, A. H. 2022. Effect of Antihypertensives by Class on Cerebral Small Vessel Disease: A Post Hoc Analysis of SPRINT-MIND. *Stroke,* 53**,** 2435-2440.

GOLSHIRI, K., ATAEI ATAABADI, E., PORTILLA FERNANDEZ, E. C., JAN DANSER, A. H. & ROKS, A. J. M. 2020. The importance of the nitric oxide-cGMP pathway in age-related cardiovascular disease: Focus on phosphodiesterase-1 and soluble guanylate cyclase. *Basic & Clinical Pharmacology & Toxicology,* 127**,** 67-80.

GOMES, P., SIMÃO, S., LEMOS, V., AMARAL, J. S. & SOARES-DA-SILVA, P. 2013. Loss of oxidative stress tolerance in hypertension is linked to reduced catalase activity and increased c-Jun NH2-terminal kinase activation. *Free Radic Biol Med,* 56**,** 112-22.

GORELICK, P. B., WHELTON, P. K., SOROND, F. & CAREY, R. M. 2020. Blood Pressure Management in Stroke. *Hypertension,* 76**,** 1688-1695.

GORIN, Y., RICONO, M., JILL, WAGNER, B., KIM, N.-H., BHANDARI, B., CHOUDHURY, G., GOUTAM & ABBOUD, E., HANNA 2004. Angiotensin II-induced ERK1/ERK2 activation and protein synthesis are redox-dependent in glomerular mesangial cells. *Biochemical Journal,* 381**,** 231-239.

GOTOH, T. & MORI, M. 2006. Nitric Oxide and Endoplasmic Reticulum Stress. *Arteriosclerosis, Thrombosis, and Vascular Biology,* 26**,** 1439-1446.

GOUGH, D. R. & COTTER, T. G. 2011. Hydrogen peroxide: a Jekyll and Hyde signalling molecule. *Cell Death & Disease,* 2**,** e213-e213.

GREENBERG, S. M., BACSKAI, B. J., HERNANDEZ-GUILLAMON, M., PRUZIN, J., SPERLING, R. & VAN VELUW, S. J. 2020. Cerebral amyloid angiopathy and Alzheimer disease - one peptide, two pathways. *Nat Rev Neurol,* 16**,** 30-42.

GRIENDLING, K. K., CAMARGO, L. L., RIOS, F. J., ALVES-LOPES, R., MONTEZANO, A. C. & TOUYZ, R. M. 2021. Oxidative Stress and Hypertension. *Circulation Research,* 128**,** 993-1020.

GROGAN, S. P., OLEE, T., HIRAOKA, K. & LOTZ, M. K. 2008. Repression of chondrogenesis through binding of notch signaling proteins HES-1 and HEY-1 to N-box domains in the COL2A1 enhancer site. *Arthritis & Rheumatism,* 58**,** 2754-2763.

GRONEWOLD, J., JOKISCH, M., SCHRAMM, S., HIMPFEN, H., GINSTER, T., TENHAGEN, I., DOEPPNER, T. R., JOCKWITZ, C., MILLER, T., LEHMANN, N., MOEBUS, S., JÖCKEL, K. H., ERBEL, R., CASPERS, S. & HERMANN, D. M. 2022. Periventricular rather than deep white matter hyperintensities mediate effects of hypertension on cognitive performance in the population-based 1000BRAINS study. *J Hypertens,* 40**,** 2413-2422.

GUO, R., HAN, D., SONG, X., GAO, Y., LI, Z., LI, X., YANG, Z. & XU, Z. 2023. Context-dependent regulation of Notch signaling in glial development and tumorigenesis. *Science Advances,* 9.

GUO, R. W., YANG, L. X., LI, M. Q., LIU, B. & WANG, X. M. 2006. Angiotensin II induces NF-kappa B activation in HUVEC via the p38MAPK pathway. *Peptides,* 27**,** 3269-75.

GUO, Y.-S., SUN, Z., MA, J., CUI, W., GAO, B., ZHANG, H.-Y., HAN, Y.-H., HU, H.-M., WANG, L., FAN, J., YANG, L., TANG, J. & LUO, Z.-J. 2014. 17β-Estradiol inhibits ER stress-induced apoptosis through promotion of TFII-I-dependent Grp78 induction in osteoblasts. *Laboratory Investigation,* 94**,** 906-916.

GUZIK, T. J. & TOUYZ, R. M. 2017. Oxidative Stress, Inflammation, and Vascular Aging in Hypertension. *Hypertension,* 70**,** 660-667.

GÖRLACH, A., BERTRAM, K., HUDECOVA, S. & KRIZANOVA, O. 2015. Calcium and ROS: A mutual interplay. *Redox Biol,* 6**,** 260-271.

HACHINSKI, V., EINHÄUPL, K., GANTEN, D., ALLADI, S., BRAYNE, C., STEPHAN, B. C. M., SWEENEY, M. D., ZLOKOVIC, B., ITURRIA-MEDINA, Y., IADECOLA, C., NISHIMURA, N., SCHAFFER, C. B., WHITEHEAD, S. N., BLACK, S. E., ØSTERGAARD, L., WARDLAW, J., GREENBERG, S., FRIBERG, L., NORRVING, B., ROWE, B., JOANETTE, Y., HACKE, W., KULLER, L., DICHGANS, M., ENDRES, M. & KHACHATURIAN, Z. S. 2019. Preventing dementia by preventing stroke: The Berlin Manifesto. *Alzheimer's & Dementia,* 15**,** 961-984.

HACK, R. J., CERFONTAINE, M. N., GRAVESTEIJN, G., TAP, S., HAFKEMEIJER, A., VAN DER GROND, J., WITJES-ANÉ, M.-N., BAAS, F., RUTTEN, J. W. & LESNIK OBERSTEIN, S. A. J. 2022. Effect of N*OTCH3* EGFr Group, Sex, and Cardiovascular Risk Factors on CADASIL Clinical and Neuroimaging Outcomes. *Stroke,* 53**,** 3133-3144.

HAHN, N. E., MEISCHL, C., KAWAHARA, T., MUSTERS, R. J. P., VERHOEF, V. M. J., VAN DER VELDEN, J., VONK, A. B. A., PAULUS, W. J., VAN ROSSUM, A. C., NIESSEN, H. W. M. & KRIJNEN, P. A. J. 2012. NOX5 Expression Is Increased in Intramyocardial Blood Vessels and Cardiomyocytes after Acute Myocardial Infarction in Humans. *The American Journal of Pathology,* 180**,** 2222-2229.

HAINSWORTH, A. H., MARKUS, H. S. & SCHNEIDER, J. A. 2024. Cerebral Small Vessel Disease, Hypertension, and Vascular Contributions to Cognitive Impairment and Dementia. *Hypertension,* 81**,** 75-86.

HALL, C. N., REYNELL, C., GESSLEIN, B., HAMILTON, N. B., MISHRA, A., SUTHERLAND, B. A., O'FARRELL, F. M., BUCHAN, A. M., LAURITZEN, M. & ATTWELL, D. 2014. Capillary pericytes regulate cerebral blood flow in health and disease. *Nature,* 508**,** 55-60.

HALLIWELL, B., ADHIKARY, A., DINGFELDER, M. & DIZDAROGLU, M. 2021. Hydroxyl radical is a significant player in oxidative DNA damage in vivo. *Chem Soc Rev,* 50**,** 8355-8360.

HAO, L., RIZZO, P., OSIPO, C., PANNUTI, A., WYATT, D., CHEUNG, L. W., SONENSHEIN, G., OSBORNE, B. A. & MIELE, L. 2010. Notch-1 activates estrogen receptor-alpha-dependent transcription via IKKalpha in breast cancer cells. *Oncogene,* 29**,** 201-13.

HARRAZ, O. F. & JENSEN, L. J. 2021. Vascular calcium signalling and ageing. *J Physiol,* 599**,** 5361-5377.

HARRINGTON, D. K., FRAGOMENI, F. & BONSER, R. S. 2007. Cerebral Perfusion. *The Annals of Thoracic Surgery,* 83**,** S799-S804.

HARRISON, D. G., BADER, M., LERMAN, L. O., FINK, G., KARUMANCHI, S. A., RECKELHOFF, J. F., SEQUEIRA-LOPEZ, M. L. S. & TOUYZ, R. M. 2024. Tail-

Cuff Versus Radiotelemetry to Measure Blood Pressure in Mice and Rats. *Hypertension,* 81**,** 3-5.
HASAN, T. F., HASAN, H. & KELLEY, R. E. 2021. Overview of Acute Ischemic Stroke Evaluation and Management. *Biomedicines,* 9**,** 1486.
HEIT, J. J., IV, M. & WINTERMARK, M. 2017. Imaging of Intracranial Hemorrhage. *Journal of Stroke,* 19**,** 11-27.
HENSHALL, T. L., KELLER, A., HE, L., JOHANSSON, B. R., WALLGARD, E., RASCHPERGER, E., MÄE, M. A., JIN, S., BETSHOLTZ, C. & LENDAHL, U. 2015. Notch3 Is Necessary for Blood Vessel Integrity in the Central Nervous System. *Arteriosclerosis, Thrombosis, and Vascular Biology,* 35**,** 409-420.
HERNANDES, M. S., XU, Q. & GRIENDLING, K. K. 2022. Role of NADPH Oxidases in Blood–Brain Barrier Disruption and Ischemic Stroke. *Antioxidants,* 11**,** 1966.
HETZ, C. & PAPA, F. R. 2018. The Unfolded Protein Response and Cell Fate Control. *Molecular Cell,* 69**,** 169-181.
HILL, A., ROBERT, TONG, L., YUAN, P., MURIKINATI, S., GUPTA, S. & GRUTZENDLER, J. 2015. Regional Blood Flow in the Normal and Ischemic Brain Is Controlled by Arteriolar Smooth Muscle Cell Contractility and Not by Capillary Pericytes. *Neuron,* 87**,** 95-110.
HOLMES, K., ROBERTS, O. L., THOMAS, A. M. & CROSS, M. J. 2007. Vascular endothelial growth factor receptor-2: structure, function, intracellular signalling and therapeutic inhibition. *Cell Signal,* 19**,** 2003-12.
HOLTERMAN, C. E., BOISVERT, N. C., THIBODEAU, J. F., KAMTO, E., NOVAKOVIC, M., ABD-ELRAHMAN, K. S., FERGUSON, S. S. G. & KENNEDY, C. R. J. 2019. Podocyte NADPH Oxidase 5 Promotes Renal Inflammation Regulated by the Toll-Like Receptor Pathway. *Antioxid Redox Signal,* 30**,** 1817-1830.
HOLTERMAN, C. E., THIBODEAU, J. F. & KENNEDY, C. R. 2015. NADPH oxidase 5 and renal disease. *Curr Opin Nephrol Hypertens,* 24**,** 81-7.
HOSSEINI-ALGHADERI, S. & BARON, M. 2020. Notch3 in Development, Health and Disease. *Biomolecules,* 10**,** 485.
HU, X., LI, P., GUO, Y., WANG, H., LEAK, R. K., CHEN, S., GAO, Y. & CHEN, J. 2012. Microglia/Macrophage Polarization Dynamics Reveal Novel Mechanism of Injury Expansion After Focal Cerebral Ischemia. *Stroke,* 43**,** 3063-3070.
HUANG, L., WU, Z.-B., ZHUGE, Q., ZHENG, W., SHAO, B., WANG, B., SUN, F. & JIN, K. 2014. Glial Scar Formation Occurs in the Human Brain after Ischemic Stroke. *International Journal of Medical Sciences,* 11**,** 344-348.
IIDA, Y. & KATUSIC, Z. S. 2000. Mechanisms of Cerebral Arterial Relaxations to Hydrogen Peroxide. *Stroke,* 31**,** 2224-2230.
INGI, T., CHENG, J. & RONNETT, G. V. 1996. Carbon Monoxide: An Endogenous Modulator of the Nitric Oxide–Cyclic GMP Signaling System. *Neuron,* 16**,** 835-842.
IORGA, A., CUNNINGHAM, C. M., MOAZENI, S., RUFFENACH, G., UMAR, S. & EGHBALI, M. 2017. The protective role of estrogen and estrogen receptors in cardiovascular disease and the controversial use of estrogen therapy. *Biology of Sex Differences,* 8.
ISHII, T. & WARABI, E. 2019. Mechanism of Rapid Nuclear Factor-E2-Related Factor 2 (Nrf2) Activation via Membrane-Associated Estrogen Receptors: Roles of NADPH Oxidase 1, Neutral Sphingomyelinase 2 and Epidermal Growth Factor Receptor (EGFR). *Antioxidants,* 8**,** 69.
IZZO, C., CARRIZZO, A., ALFANO, A., VIRTUOSO, N., CAPUNZO, M., CALABRESE, M., DE SIMONE, E., SCIARRETTA, S., FRATI, G., OLIVETI, M., DAMATO, A., AMBROSIO, M., DE CARO, F., REMONDELLI, P. &

VECCHIONE, C. 2018. The Impact of Aging on Cardio and Cerebrovascular Diseases. *International Journal of Molecular Sciences,* 19**,** 481.

JACKSON, S. J., ANDREWS, N., BALL, D., BELLANTUONO, I., GRAY, J., HACHOUMI, L., HOLMES, A., LATCHAM, J., PETRIE, A., POTTER, P., RICE, A., RITCHIE, A., STEWART, M., STREPKA, C., YEOMAN, M. & CHAPMAN, K. 2017. Does age matter? The impact of rodent age on study outcomes. *Laboratory Animals,* 51**,** 160-169.

JAGNANDAN, D., CHURCH, J. E., BANFI, B., STUEHR, D. J., MARRERO, M. B. & FULTON, D. J. R. 2007. Novel Mechanism of Activation of NADPH Oxidase 5. *Journal of Biological Chemistry,* 282**,** 6494-6507.

JAMA, H. A., MURALITHARAN, R. R., XU, C., O'DONNELL, J. A., BERTAGNOLLI, M., BROUGHTON, B. R. S., HEAD, G. A. & MARQUES, F. Z. 2022. Rodent models of hypertension. *British Journal of Pharmacology,* 179**,** 918-937.

JANI, B. & RAJKUMAR, C. 2006. Ageing and vascular ageing. *Postgraduate Medical Journal,* 82**,** 357-362.

JEON, Y. M., LEE, S., KIM, S., KWON, Y., KIM, K., CHUNG, C. G., LEE, S. B. & KIM, H. J. 2017. Neuroprotective Effects of Protein Tyrosine Phosphatase 1B Inhibition against ER Stress-Induced Toxicity. *Mol Cells,* 40**,** 280-290.

JEONG, S.-J., PARK, J.-G. & OH, G. T. 2021. Peroxiredoxins as Potential Targets for Cardiovascular Disease. *Antioxidants,* 10**,** 1244.

JHA, J. C., WATSON, A. M. D., MATHEW, G., DE VOS, L. C. & JANDELEIT-DAHM, K. 2017. The emerging role of NADPH oxidase NOX5 in vascular disease. *Clin Sci (Lond),* 131**,** 981-990.

JI, H., NIIRANEN, T. J., RADER, F., HENGLIN, M., KIM, A., EBINGER, J. E., CLAGGETT, B., MERZ, C. N. B. & CHENG, S. 2021. Sex Differences in Blood Pressure Associations With Cardiovascular Outcomes. *Circulation,* 143**,** 761-763.

JIANG, F., ROBERTS, S. J., DATLA, S. R. & DUSTING, G. J. 2006. NO Modulates NADPH Oxidase Function Via Heme Oxygenase-1 in Human Endothelial Cells. *Hypertension,* 48**,** 950-957.

JIANG, F., YANG, J., ZHANG, Y., DONG, M., WANG, S., ZHANG, Q., LIU, F. F., ZHANG, K. & ZHANG, C. 2014. Angiotensin-converting enzyme 2 and angiotensin 1–7: novel therapeutic targets. *Nature Reviews Cardiology,* 11**,** 413-426.

JIANG, Z., WU, L., VAN DER LEEDEN, B., VAN ROSSUM, A. C., NIESSEN, H. W. M. & KRIJNEN, P. A. J. 2023. NOX2 and NOX5 are increased in cardiac microvascular endothelium of deceased COVID-19 patients. *Int J Cardiol,* 370**,** 454-462.

JIMÉNEZ-BALADO, J., RIBA-LLENA, I., ABRIL, O., GARDE, E., PENALBA, A., OSTOS, E., MAISTERRA, O., MONTANER, J., NOVIEMBRE, M., MUNDET, X., VENTURA, O., PIZARRO, J. & DELGADO, P. 2019. Cognitive Impact of Cerebral Small Vessel Disease Changes in Patients With Hypertension. *Hypertension,* 73**,** 342-349.

JIMÉNEZ-SÁNCHEZ, L., HAMILTON, O. K. L., CLANCY, U., BACKHOUSE, E. V., STEWART, C. R., STRINGER, M. S., DOUBAL, F. N. & WARDLAW, J. M. 2021. Sex differences in Cerebral Small Vessel Disease: a systematic review and meta-analysis. *Frontiers in neurology***,** 1960 %@ 1664-2295.

JIN, K., ZHU, Y., SUN, Y., MAO, X. O., XIE, L. & GREENBERG, D. A. 2002. Vascular endothelial growth factor (VEGF) stimulates neurogenesis in vitro and in vivo. *Proceedings of the National Academy of Sciences,* 99**,** 11946-11950.

JOKINEN, H., KOIKKALAINEN, J., LAAKSO, H. M., MELKAS, S., NIEMINEN, T., BRANDER, A., KORVENOJA, A., RUECKERT, D., BARKHOF, F., SCHELTENS, P., SCHMIDT, R., FAZEKAS, F., MADUREIRA, S., VERDELHO, A., WALLIN, A., WAHLUND, L.-O., WALDEMAR, G., CHABRIAT, H.,

HENNERICI, M., O'BRIEN, J., INZITARI, D., LÖTJÖNEN, J., PANTONI, L. & ERKINJUNTTI, T. 2020. Global Burden of Small Vessel Disease–Related Brain Changes on MRI Predicts Cognitive and Functional Decline. *Stroke,* 51**,** 170-178.

JOVÉ, M., MOTA-MARTORELL, N., OBIS, È., SOL, J., MARTÍN-GARÍ, M., FERRER, I., PORTERO-OTÍN, M. & PAMPLONA, R. 2023. Lipid Adaptations against Oxidative Challenge in the Healthy Adult Human Brain. *Antioxidants,* 12**,** 177.

JUAN, C. A., PÉREZ DE LA LASTRA, J. M., PLOU, F. J. & PÉREZ-LEBEÑA, E. 2021. The Chemistry of Reactive Oxygen Species (ROS) Revisited: Outlining Their Role in Biological Macromolecules (DNA, Lipids and Proteins) and Induced Pathologies. *International Journal of Molecular Sciences,* 22**,** 4642.

JUNG, J. E., KIM, G. S., CHEN, H., MAIER, C. M., NARASIMHAN, P., SONG, Y. S., NIIZUMA, K., KATSU, M., OKAMI, N., YOSHIOKA, H., SAKATA, H., GOEDERS, C. E. & CHAN, P. H. 2010. Reperfusion and Neurovascular Dysfunction in Stroke: from Basic Mechanisms to Potential Strategies for Neuroprotection. *Molecular Neurobiology,* 41**,** 172-179.

KADLEC, A. O., CHABOWSKI, D. S., AIT-AISSA, K. & GUTTERMAN, D. D. 2016. Role of PGC-1α in Vascular Regulation. *Arteriosclerosis, Thrombosis, and Vascular Biology,* 36**,** 1467-1474.

KADRY, H., NOORANI, B. & CUCULLO, L. 2020. A blood–brain barrier overview on structure, function, impairment, and biomarkers of integrity. *Fluids and Barriers of the CNS,* 17.

KAHLES, T., KOHNEN, A., HEUMUELLER, S., RAPPERT, A., BECHMANN, I., LIEBNER, S., WITTKO, I. M., NEUMANN-HAEFELIN, T., STEINMETZ, H., SCHROEDER, K. & BRANDES, R. P. 2010. NADPH oxidase Nox1 contributes to ischemic injury in experimental stroke in mice. *Neurobiology of Disease,* 40**,** 185-192.

KAHLES, T., LUEDIKE, P., ENDRES, M., GALLA, H. J., STEINMETZ, H., BUSSE, R., NEUMANN-HAEFELIN, T. & BRANDES, R. P. 2007. NADPH oxidase plays a central role in blood-brain barrier damage in experimental stroke. *Stroke,* 38**,** 3000-3006.

KANDER, M. C., CUI, Y. & LIU, Z. 2017. Gender difference in oxidative stress: a new look at the mechanisms for cardiovascular diseases. *Journal of Cellular and Molecular Medicine,* 21**,** 1024-1032.

KANG, K.-T., SULLIVAN, J. C. & POLLOCK, J. S. 2018. Superoxide Dismutase Activity in Small Mesenteric Arteries Is Downregulated by Angiotensin II but Not by Hypertension. *Toxicological Research,* 34**,** 363-370.

KAPOOR, A. & NATION, D. A. 2021. Role of Notch signaling in neurovascular aging and Alzheimer's disease. *Semin Cell Dev Biol,* 116**,** 90-97.

KAPPERT, K., PETERS, K. G., BÖHMER, F. D. & OSTMAN, A. 2005. Tyrosine phosphatases in vessel wall signaling. *Cardiovasc Res,* 65**,** 587-98.

KATAN, M. & LUFT, A. 2018. Global Burden of Stroke. *Seminars in Neurology,* 38**,** 208-211.

KATSURA, K., KRISTIÁN, T. & SIESJÖ, B. K. 1994. Energy metabolism, ion homeostasis, and cell damage in the brain. *Biochem Soc Trans,* 22**,** 991-6.

KELLY-HAYES, M. 2010. Influence of Age and Health Behaviors on Stroke Risk: Lessons from Longitudinal Studies. *Journal of the American Geriatrics Society,* 58**,** S325-S328.

KHALIL, R. A. 2013. Estrogen, vascular estrogen receptor and hormone therapy in postmenopausal vascular disease. *Biochemical Pharmacology,* 86**,** 1627-1642.

KHAN, A. A., PATEL, J., DESIKAN, S., CHRENCIK, M., MARTINEZ-DELCID, J., CARABALLO, B., YOKEMICK, J., GRAY, V. L., SORKIN, J. D., CEBRAL, J., SIKDAR, S. & LAL, B. K. 2021. Asymptomatic carotid artery stenosis is associated with cerebral hypoperfusion. *J Vasc Surg,* 73**,** 1611-1621.e2.

KIM, J.-S., DIEBOLD, B. A., BABIOR, B. M., KNAUS, U. G. & BOKOCH, G. M. 2007. Regulation of Nox1 Activity via Protein Kinase A-mediated Phosphorylation of NoxA1 and 14-3-3 Binding. *Journal of Biological Chemistry,* 282**,** 34787-34800.

KISHIMOTO, M., SUENAGA, J., TAKASE, H., ARAKI, K., YAO, T., FUJIMURA, T., MURAYAMA, K., OKUMURA, K., UENO, R., SHIMIZU, N., KAWAHARA, N., YAMAMOTO, T. & SEKO, Y. 2019. Oxidative stress-responsive apoptosis inducing protein (ORAIP) plays a critical role in cerebral ischemia/reperfusion injury. *Scientific Reports,* 9.

KLEIKERS, P. W. M., DAO, V. T., GÖB, E., HOOIJMANS, C., DEBETS, J., VAN ESSEN, H., KLEINSCHNITZ, C. & SCHMIDT, H. H. H. W. 2014. NOXing out stroke: Identification of NOX4 and 5as targets in blood-brain-barrier stabilisation and neuroprotection. *Free Radical Biology and Medicine,* 75**,** S16.

KLEINSCHNITZ, C., GRUND, H., WINGLER, K., ARMITAGE, M. E., JONES, E., MITTAL, M., BARIT, D., SCHWARZ, T., GEIS, C., KRAFT, P., BARTHEL, K., SCHUHMANN, M. K., HERRMANN, A. M., MEUTH, S. G., STOLL, G., MEURER, S., SCHREWE, A., BECKER, L., GAILUS-DURNER, V., FUCHS, H., KLOPSTOCK, T., DE ANGELIS, M. H., JANDELEIT-DAHM, K., SHAH, A. M., WEISSMANN, N. & SCHMIDT, H. 2010. Post-Stroke Inhibition of Induced NADPH Oxidase Type 4 Prevents Oxidative Stress and Neurodegeneration. *Plos Biology,* 8**,** 13.

KNOWLTON, A. A. & LEE, A. R. 2012. Estrogen and the cardiovascular system. *Pharmacology & Therapeutics,* 135**,** 54-70.

KONHILAS, J. P., SANCHEZ, J. N., REGAN, J. A., CONSTANTOPOULOS, E., LOPEZ-PIER, M., CANNON, D. K., SKARIA, R., MCKEE, L. A., CHEN, H., LIPOVKA, Y., POLLOW, D. & BROOKS, H. L. 2020. Using 4-vinylcyclohexene diepoxide as a model of menopause for cardiovascular disease. *Am J Physiol Heart Circ Physiol,* 318**,** H1461-H1473.

KOPP, M. C., LARBURU, N., DURAIRAJ, V., ADAMS, C. J. & ALI, M. M. U. 2019. UPR proteins IRE1 and PERK switch BiP from chaperone to ER stress sensor. *Nat Struct Mol Biol,* 26**,** 1053-1062.

KORTE, N., BARKAWAY, A., WELLS, J., FREITAS, F., SETHI, H., ANDREWS, S. P., SKIDMORE, J., STEVENS, B. & ATTWELL, D. 2024. Inhibiting Ca2+ channels in Alzheimer's disease model mice relaxes pericytes, improves cerebral blood flow and reduces immune cell stalling and hypoxia. *Nature Neuroscience,* 27**,** 2086-2100.

KRAJA, A. T., COOK, J. P., WARREN, H. R., SURENDRAN, P., LIU, C., EVANGELOU, E., MANNING, A. K., GRARUP, N., DRENOS, F., SIM, X., SMITH, A. V., AMIN, N., BLAKEMORE, A. I. F., BORK-JENSEN, J., BRANDSLUND, I., FARMAKI, A.-E., FAVA, C., FERREIRA, T., HERZIG, K.-H., GIRI, A., GIULIANINI, F., GROVE, M. L., GUO, X., HARRIS, S. E., HAVE, C. T., HAVULINNA, A. S., ZHANG, H., JØRGENSEN, M. E., KÄRÄJÄMÄKI, A., KOOPERBERG, C., LINNEBERG, A., LITTLE, L., LIU, Y., BONNYCASTLE, L. L., LU, Y., MÄGI, R., MAHAJAN, A., MALERBA, G., MARIONI, R. E., MEI, H., MENNI, C., MORRISON, A. C., PADMANABHAN, S., PALMAS, W., POVEDA, A., RAURAMAA, R., RAYNER, N. W., RIAZ, M., RICE, K., RICHARD, M. A., SMITH, J. A., SOUTHAM, L., STANČÁKOVÁ, A., STIRRUPS, K. E., TRAGANTE, V., TUOMI, T., TZOULAKI, I., VARGA, T. V., WEISS, S., YIORKAS, A. M., YOUNG, R., ZHANG, W., BARNES, M. R., CABRERA, C. P., GAO, H., BOEHNKE, M., BOERWINKLE, E., CHAMBERS, J. C., CONNELL, J. M., CHRISTENSEN, C. K., DE BOER, R. A., DEARY, I. J., DEDOUSSIS, G., DELOUKAS, P., DOMINICZAK, A. F., DÖRR, M., JOEHANES, R., EDWARDS, T. L., ESKO, T., FORNAGE, M., FRANCESCHINI, N., FRANKS, P. W., GAMBARO, G., GROOP, L., HALLMANS, G., HANSEN,

T., HAYWARD, C., HEIKKI, O., INGELSSON, E., TUOMILEHTO, J., JARVELIN, M.-R., KARDIA, S. L. R., KARPE, F., KOONER, J. S., LAKKA, T. A., LANGENBERG, C., LIND, L., LOOS, R. J. F., LAAKSO, M., MCCARTHY, M. I., et al. 2017. New Blood Pressure–Associated Loci Identified in Meta-Analyses of 475 000 Individuals. *Circulation: Cardiovascular Genetics,* 10.

KRAUSE, D. N., DUCKLES, S. P. & PELLIGRINO, D. A. 2006. Influence of sex steroid hormones on cerebrovascular function. *J Appl Physiol (1985),* 101**,** 1252-61.

KREMER, C., LORENZANO, S. & KRUUSE, C. 2023. Editorial: Sex differences in cerebrovascular diseases. *Frontiers in Neurology,* 13.

KRÖNCKE, K.-D., FEHSEL, K. & KOLB-BACHOFEN, V. 2001. Inducible nitric oxide synthase in human diseases. *Clinical and Experimental Immunology,* 113**,** 147-156.

KUGLER, E. C., GREENWOOD, J. & MACDONALD, R. B. 2021. The "Neuro-Glial-Vascular" Unit: The Role of Glia in Neurovascular Unit Formation and Dysfunction. *Frontiers in Cell and Developmental Biology,* 9.

KULICK, E. R., KAUFMAN, J. D. & SACK, C. 2023. Ambient Air Pollution and Stroke: An Updated Review. *Stroke,* 54**,** 882-893.

KUMAR, A. & MCCULLOUGH, L. 2021. Cerebrovascular disease in women. *Therapeutic Advances in Neurological Disorders,* 14**,** 175628642098523.

KUNG-CHUN CHIU, D., PUI-WAH TSE, A., LAW, C.-T., MING-JING XU, I., LEE, D., CHEN, M., KIT-HO LAI, R., WAI-HIN YUEN, V., WING-SUM CHEU, J., WAI-HUNG HO, D., WONG, C.-M., ZHANG, H., NG, I. O.-L. & CHAK-LUI WONG, C. 2019. Hypoxia regulates the mitochondrial activity of hepatocellular carcinoma cells through HIF/HEY1/PINK1 pathway. *Cell Death & Disease,* 10.

KURIAKOSE, D. & XIAO, Z. 2020. Pathophysiology and Treatment of Stroke: Present Status and Future Perspectives. *International Journal of Molecular Sciences,* 21**,** 7609.

KURODA, J., AGO, T., NISHIMURA, A., NAKAMURA, K., MATSUO, R., WAKISAKA, Y., KAMOUCHI, M. & KITAZONO, T. 2014. Nox4 Is a Major Source of Superoxide Production in Human Brain Pericytes. *Journal of Vascular Research,* 51**,** 429-438.

LAGRANHA, C. J., SILVA, T. L. A., SILVA, S. C. A., BRAZ, G. R. F., DA SILVA, A. I., FERNANDES, M. P. & SELLITTI, D. F. 2018. Protective effects of estrogen against cardiovascular disease mediated via oxidative stress in the brain. *Life Sci,* 192**,** 190-198.

LAI, T. W., ZHANG, S. & WANG, Y. T. 2014. Excitotoxicity and stroke: identifying novel targets for neuroprotection. *Prog Neurobiol,* 115**,** 157-88.

LAPING, N. J., TETER, B., NICHOLS, N. R., ROZOVSKY, I. & FINCH, C. E. 1994. Glial Fibrillary Acidic Protein: Regulation by Hormones, Cytokines, and Growth Factors. *Brain Pathology,* 4**,** 259-275.

LAWRENCE, J. M., SCHARDIEN, K., WIGDAHL, B. & NONNEMACHER, M. R. 2023. Roles of neuropathology-associated reactive astrocytes: a systematic review. *Acta Neuropathologica Communications,* 11.

LEE, D. H., KANG, D.-W., AHN, J. S., CHOI, C. G., KIM, S. J. & SUH, D. C. 2005. Imaging of the Ischemic Penumbra in Acute Stroke. *Korean Journal of Radiology,* 6**,** 64.

LEE, K. H., CHA, M. & LEE, B. H. 2020. Neuroprotective Effect of Antioxidants in the Brain. *International Journal of Molecular Sciences,* 21**,** 7152.

LEFFLER, C. W., PARFENOVA, H. & JAGGAR, J. H. 2011. Carbon monoxide as an endogenous vascular modulator. *Am J Physiol Heart Circ Physiol,* 301**,** H1-H11.

LEHNER, C., GEHWOLF, R., TEMPFER, H., KRIZBAI, I., HENNIG, B., BAUER, H.-C. & BAUER, H. 2011. Oxidative Stress and Blood–Brain Barrier Dysfunction Under Particular Consideration of Matrix Metalloproteinases. *Antioxidants & Redox Signaling,* 15**,** 1305-1323.

LERMAN, L. O., KURTZ, T. W., TOUYZ, R. M., ELLISON, D. H., CHADE, A. R., CROWLEY, S. D., MATTSON, D. L., MULLINS, J. J., OSBORN, J., EIRIN, A., RECKELHOFF, J. F., IADECOLA, C. & COFFMAN, T. M. 2019. Animal Models of Hypertension: A Scientific Statement From the American Heart Association. *Hypertension,* 73.

LI, B., WANG, Z., HU, Z., ZHANG, M., REN, Z., ZHOU, Z., HUANG, J. & HU, X. 2017. P38 MAPK Signaling Pathway Mediates Angiotensin II-Induced miR143/145 Gene Cluster Downregulation during Aortic Dissection Formation. *Ann Vasc Surg,* 40**,** 262-273.

LI, F., ZHU, L., ZHANG, J., HE, H., QIN, Y., CHENG, Y. & XIE, Z. 2019. Oral Contraceptive Use and Increased Risk of Stroke: A Dose–Response Meta-Analysis of Observational Studies. *Frontiers in Neurology,* 10.

LI, H., HORKE, S. & FÖRSTERMANN, U. 2013. Oxidative stress in vascular disease and its pharmacological prevention. *Trends Pharmacol Sci,* 34**,** 313-9.

LI, J., GENG, X. Y. & CONG, X. L. 2016. PGC-1α ameliorates AngiotensinII-induced eNOS dysfunction in human aortic endothelial cells. *Vascul Pharmacol,* 83**,** 90-7.

LI, Q., YANG, Y., REIS, C., TAO, T., LI, W. W., LI, X. G. & ZHANG, J. H. 2018. Cerebral Small Vessel Disease. *Cell Transplantation,* 27**,** 1711-1722.

LI, Y., KRAČUN, D., DUSTIN, C. M., EL MASSRY, M., YUAN, S., GOOSSEN, C. J., DEVALLANCE, E. R., SAHOO, S., ST. HILAIRE, C., GURKAR, A. U., FINKEL, T., STRAUB, A. C., CIFUENTES-PAGANO, E. & PAGANO, P. J. 2021. Forestalling age-impaired angiogenesis and blood flow by targeting NOX: Interplay of NOX1, IL-6, and SASP in propagating cell senescence. *Proceedings of the National Academy of Sciences,* 118**,** e2015666118.

LIANG, H. & WARD, W. F. 2006. PGC-1alpha: a key regulator of energy metabolism. *Adv Physiol Educ,* 30**,** 145-51.

LIDINGTON, D., WAN, H. & BOLZ, S.-S. 2021. Cerebral Autoregulation in Subarachnoid Hemorrhage. *Frontiers in Neurology,* 12.

LIEDTKE, W., EDELMANN, W., BIERI, P. L., CHIU, F.-C., COWAN, N. J., KUCHERLAPATI, R. & RAINE, C. S. 1996. GFAP Is Necessary for the Integrity of CNS White Matter Architecture and Long-Term Maintenance of Myelination. *Neuron,* 17**,** 607-615.

LIJNEN, P. J., VAN PELT, J. F. & FAGARD, R. H. 2010. Downregulation of manganese superoxide dismutase by angiotensin II in cardiac fibroblasts of rats: Association with oxidative stress in myocardium. *Am J Hypertens,* 23**,** 1128-35.

LIN, Q., ZHAO, G., FANG, X., PENG, X., TANG, H., WANG, H., JING, R., LIU, J., LEDERER, W. J., CHEN, J. & OUYANG, K. 2016. IP3 receptors regulate vascular smooth muscle contractility and hypertension. *JCI Insight,* 1.

LIN, S., NEGULESCU, A., BULUSU, S., GIBERT, B., DELCROS, J.-G., DUCAROUGE, B., RAMA, N., GADOT, N., TREILLEUX, I., SAINTIGNY, P., MEURETTE, O. & MEHLEN, P. 2017. Non-canonical NOTCH3 signalling limits tumour angiogenesis. *Nature Communications,* 8**,** 16074.

LIPSKAIA, L., CHEMALY, E. R., HADRI, L., LOMPRE, A.-M. & HAJJAR, R. J. 2010. Sarcoplasmic reticulum Ca²⁺ATPase as a therapeutic target for heart failure. *Expert Opinion on Biological Therapy,* 10**,** 29-41.

LISABETH, L. & BUSHNELL, C. 2012. Stroke risk in women: the role of menopause and hormone therapy. *The Lancet Neurology,* 11**,** 82-91.

LITAK, J., MAZUREK, M., KULESZA, B., SZMYGIN, P., KAMIENIAK, P. & GROCHOWSKI, C. 2020. Cerebral Small Vessel Disease. *Int J Mol Sci,* 21.

LIU, F., LAI, S., TONG, H., LAKEY, P. S. J., SHIRAIWA, M., WELLER, M. G., PÖSCHL, U. & KAMPF, C. J. 2017. Release of free amino acids upon oxidation of peptides and proteins by hydroxyl radicals. *Analytical and Bioanalytical Chemistry,* 409**,** 2411-2420.

LIU, L., ZHANG, L., ZHAO, S., ZHAO, X.-Y., MIN, P.-X., MA, Y.-D., WANG, Y.-Y., CHEN, Y., TANG, S.-J., ZHANG, Y.-J., DU, J. & GU, L. 2019. Non-canonical Notch Signaling Regulates Actin Remodeling in Cell Migration by Activating PI3K/AKT/Cdc42 Pathway. *Frontiers in Pharmacology,* 10.

LIU, M.-Q., CHEN, Z. & CHEN, L.-X. 2016. Endoplasmic reticulum stress: a novel mechanism and therapeutic target for cardiovascular diseases. *Acta Pharmacologica Sinica,* 37**,** 425-443.

LIU, Z. & KHALIL, R. A. 2018. Evolving mechanisms of vascular smooth muscle contraction highlight key targets in vascular disease. *Biochem Pharmacol,* 153**,** 91-122.

LLORET, A., ESTEVE, D., LLORET, M. A., MONLLOR, P., LÓPEZ, B., LEÓN, J. L. & CERVERA-FERRI, A. 2021. Is Oxidative Stress the Link Between Cerebral Small Vessel Disease, Sleep Disruption, and Oligodendrocyte Dysfunction in the Onset of Alzheimer's Disease? *Frontiers in Physiology,* 12.

LOBODA, A., DAMULEWICZ, M., PYZA, E., JOZKOWICZ, A. & DULAK, J. 2016. Role of Nrf2/HO-1 system in development, oxidative stress response and diseases: an evolutionarily conserved mechanism. *Cellular and Molecular Life Sciences,* 73**,** 3221-3247.

LOPERENA, R. & HARRISON, D. G. 2017. Oxidative Stress and Hypertensive Diseases. *Medical Clinics of North America,* 101**,** 169-193.

LU, H., WANG, H., LI, X., LIN, X., LI, C., CHEN, W., ZOU, L., PAN, J., ZHANG, X., HE, L., RONG, X. & PENG, Y. 2024. Chronic alcohol exposure induces cerebral microbleeds by TGF-β1/Smad signaling pathway mediated remodeling of cerebral small vessels. Cold Spring Harbor Laboratory.

LU, K.-T., KEEN, H. L., WEATHERFORD, E. T., SEQUEIRA-LOPEZ, M. L. S., GOMEZ, R. A. & SIGMUND, C. D. 2016. Estrogen Receptor α Is Required for Maintaining Baseline Renin Expression. *Hypertension,* 67**,** 992-999.

LU, W., CHEN, Z. & WEN, J. 2023. The role of RhoA/ROCK pathway in the ischemic stroke-induced neuroinflammation. *Biomed Pharmacother,* 165**,** 115141.

LU, Y., SAREDDY, G. R., WANG, J., ZHANG, Q., TANG, F.-L., PRATAP, U. P., TEKMAL, R. R., VADLAMUDI, R. K. & BRANN, D. W. 2020. Neuron-Derived Estrogen Is Critical for Astrocyte Activation and Neuroprotection of the Ischemic Brain. *The Journal of Neuroscience,* 40**,** 7355-7374.

LUCAS-HERALD, A., K.,, ALVES-LOPES, R., MONTEZANO, A., C.,, AHMED, S., FAISAL., & TOUYZ, R., M. 2017. Genomic and non-genomic effects of androgens in the cardiovascular system: clinical implications. *Clinical Science,* 131**,** 1405-1418.

LUCAS-HERALD, A. K., MONTEZANO, A. C., ALVES-LOPES, R., HADDOW, L., ALIMUSSINA, M., O'TOOLE, S., FLETT, M., LEE, B., AMJAD, S. B., STEVEN, M., BROOKSBANK, K., MCCALLUM, L., DELLES, C., PADMANABHAN, S., AHMED, S. F. & TOUYZ, R. M. 2022. Vascular dysfunction and increased cardiovascular risk in hypospadias. *European Heart Journal,* 43**,** 1832-1845.

LUCAS-HERALD, A. K. & TOUYZ, R. M. 2022. Androgens and Androgen Receptors as Determinants of Vascular Sex Differences Across the Lifespan. *Canadian Journal of Cardiology,* 38**,** 1854-1864.

LUCCHESI, P. A., BELMADANI, S. & MATROUGUI, K. 2005. Hydrogen peroxide acts as both vasodilator and vasoconstrictor in the control of perfused mouse mesenteric resistance arteries. *J Hypertens,* 23**,** 571-9.

LYLE, A. N., DESHPANDE, N. N., TANIYAMA, Y., SEIDEL-ROGOL, B., POUNKOVA, L., DU, P., PAPAHARALAMBUS, C., LASSÈGUE, B. & GRIENDLING, K. K. 2009. Poldip2, a Novel Regulator of Nox4 and Cytoskeletal Integrity in Vascular Smooth Muscle Cells. *Circulation Research,* 105**,** 249-259.

LÓPEZ-LÓPEZ, S., MONSALVE, E. M., ROMERO DE ÁVILA, M. J., GONZÁLEZ-GÓMEZ, J., HERNÁNDEZ DE LEÓN, N., RUIZ-MARCOS, F., BALADRÓN, V., NUEDA, M. L., GARCÍA-LEÓN, M. J., SCREPANTI, I., FELLI, M. P., LABORDA, J., GARCÍA-RAMÍREZ, J. J. & DÍAZ-GUERRA, M. J. M. 2020. NOTCH3 signaling is essential for NF-κB activation in TLR-activated macrophages. *Scientific Reports,* 10.

MA, C., LIU, Y. & FU, Z. 2024. Implications of endoplasmic reticulum stress and autophagy in aging and cardiovascular diseases. *Frontiers in Pharmacology,* 15.

MA, H., BUTLER, M. R., THAPA, A., BELCHER, J., YANG, F., BAEHR, W., BIEL, M., MICHALAKIS, S. & DING, X.-Q. 2015. cGMP/Protein Kinase G Signaling Suppresses Inositol 1,4,5-Trisphosphate Receptor Phosphorylation and Promotes Endoplasmic Reticulum Stress in Photoreceptors of Cyclic Nucleotide-gated Channel-deficient Mice. *Journal of Biological Chemistry,* 290**,** 20880-20892.

MA, Q. 2013. Role of Nrf2 in Oxidative Stress and Toxicity. *Annual Review of Pharmacology and Toxicology,* 53**,** 401-426.

MAGNANI, F., NENCI, S., MILLANA FANANAS, E., CECCON, M., ROMERO, E., FRAAIJE, M. W. & MATTEVI, A. 2017. Crystal structures and atomic model of NADPH oxidase. *Proceedings of the National Academy of Sciences,* 114**,** 6764-6769.

MALDONADO, E., MORALES-PISON, S., URBINA, F. & SOLARI, A. 2023. Aging Hallmarks and the Role of Oxidative Stress. *Antioxidants,* 12**,** 651.

MANEA, A., MANEA, S. A., FLOREA, I. C., LUCA, C. M. & RAICU, M. 2012. Positive regulation of NADPH oxidase 5 by proinflammatory-related mechanisms in human aortic smooth muscle cells. *Free Radic Biol Med,* 52**,** 1497-507.

MANEA, A., MANEA, S. A., GAFENCU, A. V., RAICU, M. & SIMIONESCU, M. 2008. AP-1–Dependent Transcriptional Regulation of NADPH Oxidase in Human Aortic Smooth Muscle Cells. *Arteriosclerosis, Thrombosis, and Vascular Biology,* 28**,** 878-885.

MANEA, A., TANASE, L. I., RAICU, M. & SIMIONESCU, M. 2010. JAK/STAT Signaling Pathway Regulates Nox1 and Nox4-Based NADPH Oxidase in Human Aortic Smooth Muscle Cells. *Arteriosclerosis, Thrombosis, and Vascular Biology,* 30**,** 105-112.

MANEA, S. A., ANTONESCU, M. L., FENYO, I. M., RAICU, M., SIMIONESCU, M. & MANEA, A. 2018. Epigenetic regulation of vascular NADPH oxidase expression and reactive oxygen species production by histone deacetylase-dependent mechanisms in experimental diabetes. *Redox Biol,* 16**,** 332-343.

MANEA, S. A., TODIRITA, A., RAICU, M. & MANEA, A. 2014. C/EBP transcription factors regulate NADPH oxidase in human aortic smooth muscle cells. *Journal of Cellular and Molecular Medicine,* 18**,** 1467-1477.

MARINO, A., HAUSENLOY, D. J., ANDREADOU, I., HORMAN, S., BERTRAND, L. & BEAULOYE, C. 2021. AMP-activated protein kinase: A remarkable contributor to preserve a healthy heart against ROS injury. *Free Radic Biol Med,* 166**,** 238-254.

MARQUÉS, J., FERNÁNDEZ-IRIGOYEN, J., AINZÚA, E., MARTÍNEZ-AZCONA, M., CORTÉS, A., RONCAL, C., ORBE, J., SANTAMARÍA, E. & ZALBA, G. 2022. NADPH Oxidase 5 (NOX5) Overexpression Promotes Endothelial Dysfunction via Cell Apoptosis, Migration, and Metabolic Alterations in Human Brain Microvascular Endothelial Cells (hCMEC/D3). *Antioxidants,* 11**,** 2147.

MARTIN, R. L., LLOYD, H. G. & COWAN, A. I. 1994. The early events of oxygen and glucose deprivation: setting the scene for neuronal death? *Trends Neurosci,* 17**,** 251-7.

MARTINEZ-CORIA, H., ARRIETA-CRUZ, I., CRUZ, M. E. & LÓPEZ-VALDÉS, H. E. 2021. Physiopathology of ischemic stroke and its modulation using memantine: evidence from preclinical stroke. *Neural Regen Res,* 16**,** 433-439.

MARTÍNEZ-CASALES, M., HERNANZ, R. & ALONSO, M. J. 2021. Vascular and Macrophage Heme Oxygenase-1 in Hypertension: A Mini-Review. *Frontiers in Physiology,* 12.

MATSUNO, K., YAMADA, H., IWATA, K., JIN, D., KATSUYAMA, M., MATSUKI, M., TAKAI, S., YAMANISHI, K., MIYAZAKI, M., MATSUBARA, H. & YABE-NISHIMURA, C. 2005. Nox1 is involved in angiotensin II-mediated hypertension - A study in Nox1-deficient mice. *Circulation,* 112**,** 2677-2685.

MAYER, C. A., BRUNKHORST, R., NIESSNER, M., PFEILSCHIFTER, W., STEINMETZ, H. & FOERCH, C. 2013. Blood Levels of Glial Fibrillary Acidic Protein (GFAP) in Patients with Neurological Diseases. *PLoS ONE,* 8**,** e62101.

MAZZA, F., GOODMAN, A., LOMBARDO, G., VANELLA, A. & ABRAHAM, N. G. 2003. Heme oxygenase-1 gene expression attenuates angiotensin II-mediated DNA damage in endothelial cells. *Exp Biol Med (Maywood),* 228**,** 576-83.

MCCANN, S. K., DUSTING, G. J. & ROULSTON, C. L. 2008. Early increase of Nox4 NADPH oxidase and superoxide generation following endothelin-1-induced stroke in conscious rats. *J Neurosci Res,* 86**,** 2524-34.

MCNEILL, A. M., ZHANG, C., STANCZYK, F. Z., DUCKLES, S. P. & KRAUSE, D. N. 2002. Estrogen Increases Endothelial Nitric Oxide Synthase via Estrogen Receptors in Rat Cerebral Blood Vessels. *Stroke,* 33**,** 1685-1691.

MCVEIGH, G. E., BRATTELI, C. W., MORGAN, D. J., ALINDER, C. M., GLASSER, S. P., FINKELSTEIN, S. M. & COHN, J. N. 1999. Age-Related Abnormalities in Arterial Compliance Identified by Pressure Pulse Contour Analysis. *Hypertension,* 33**,** 1392-1398.

MENG, T. C., FUKADA, T. & TONKS, N. K. 2002. Reversible oxidation and inactivation of protein tyrosine phosphatases in vivo. *Molecular Cell,* 9**,** 387-399.

MENIKDIWELA, K. R., RAMALINGAM, L., ALLEN, L., SCOGGIN, S., KALUPAHANA, N. S. & MOUSTAID-MOUSSA, N. 2019. Angiotensin II Increases Endoplasmic Reticulum Stress in Adipose Tissue and Adipocytes. *Scientific Reports,* 9.

MICHINAGA, S. & KOYAMA, Y. 2015. Pathogenesis of Brain Edema and Investigation into Anti-Edema Drugs. *International Journal of Molecular Sciences,* 16**,** 9949-9975.

MILLER, A. A., DRUMMOND, G. R., DE SILVA, T. M., MAST, A. E., HICKEY, H., WILLIAMS, J. P., BROUGHTON, B. R. & SOBEY, C. G. 2009. NADPH oxidase activity is higher in cerebral versus systemic arteries of four animal species: role of Nox2. *Am J Physiol Heart Circ Physiol,* 296**,** H220-5.

MILLER, A. A., DRUMMOND, G. R., MAST, A. E., SCHMIDT, H. H. H. W. & SOBEY, C. G. 2007. Effect of gender on NADPH-oxidase activity, expression, and function in the cerebral circulation - Role of estrogen. *Stroke,* 38**,** 2142-2149.

MILLER, A. A., DRUMMOND, G. R., SCHMIDT, H. & SOBEY, C. G. 2005. NADPH oxidase activity and function are profoundly greater in cerebral versus systemic arteries. *Circulation Research,* 97**,** 1055-1062.

MILLER, A. A., DRUMMOND, G. R. & SOBEY, C. G. 2006. Reactive oxygen species in the cerebral circulation: are they all bad? *Antioxid Redox Signal,* 8**,** 1113-20.

MILLER, V. M. & DUCKLES, S. P. 2008. Vascular Actions of Estrogens: Functional Implications. *Pharmacological Reviews,* 60**,** 210-241.

MILLS, K. T., STEFANESCU, A. & HE, J. 2020. The global epidemiology of hypertension. *Nat Rev Nephrol,* 16**,** 223-237.

MIRÓ, O., CASADEMONT, J., CASALS, E., PEREA, M., URBANO-MÁRQUEZ, A., RUSTIN, P. & CARDELLACH, F. 2000. Aging is associated with increased lipid peroxidation in human hearts, but not with mitochondrial respiratory chain enzyme defects. *Cardiovasc Res,* 47**,** 624-31.

MIURA, H., BOSNJAK, J. J., NING, G., SAITO, T., MIURA, M. & GUTTERMAN, D. D. 2003. Role for Hydrogen Peroxide in Flow-Induced Dilation of Human Coronary Arterioles. *Circulation Research,* 92**,** 31e-40.

MOHAN, S., ALHAZMI, H. A., HASSANI, R., KHUWAJA, G., MAHESHKUMAR, V. P., ALDAHISH, A. & CHIDAMBARAM, K. 2024. Role of ferroptosis pathways in neuroinflammation and neurological disorders: From pathogenesis to treatment. *Heliyon,* 10**,** e24786.

MONTEZANO, A. C., BURGER, D., PARAVICINI, T. M., CHIGNALIA, A. Z., YUSUF, H., ALMASRI, M., HE, Y., CALLERA, G. E., HE, G., KRAUSE, K.-H., LAMBETH, D., QUINN, M. T. & TOUYZ, R. M. 2010. Nicotinamide Adenine Dinucleotide Phosphate Reduced Oxidase 5 (Nox5) Regulation by Angiotensin II and Endothelin-1 Is Mediated via Calcium/Calmodulin-Dependent, Rac-1-Independent Pathways in Human Endothelial Cells. *Circulation Research,* 106**,** 1363-1373.

MONTEZANO, A. C., CAMARGO, L. D., PERSSON, P., RIOS, F. J., HARVEY, A. P., ANAGNOSTOPOULOU, A., PALACIOS, R., GANDARA, A. C. P., ALVES-LOPES, R., NEVES, K. B., DULAK-LIS, M., HOLTERMAN, C. E., DE OLIVEIRA, P. L., GRAHAM, D., KENNEDY, C. & TOUYZ, R. M. 2018. NADPH Oxidase 5 Is a Pro-Contractile Nox Isoform and a Point of Cross-Talk for Calcium and Redox Signaling-Implications in Vascular Function. *Journal of the American Heart Association,* 7**,** 33.

MONTEZANO, A. C. & TOUYZ, R. M. 2014. Reactive Oxygen Species, Vascular Noxs, and Hypertension: Focus on Translational and Clinical Research. *Antioxidants & Redox Signaling,* 20**,** 164-182.

MONTEZANO, A. C., TSIROPOULOU, S., DULAK-LIS, M., HARVEY, A., CAMARGO, L. D. & TOUYZ, R. M. 2015. Redox signaling, Nox5 and vascular remodeling in hypertension. *Current Opinion in Nephrology and Hypertension,* 24**,** 425-433.

MOODY, D. M., BROWN, W. R., CHALLA, V. R. & ANDERSON, R. L. 1995. Periventricular venous collagenosis: association with leukoaraiosis. *Radiology,* 194**,** 469-76.

MORAES, J. A., BARCELLOS-DE-SOUZA, P., RODRIGUES, G., NASCIMENTO-SILVA, V., SILVA, S. V., ASSREUY, J., ARRUDA, M. A. & BARJA-FIDALGO, C. 2012. Heme modulates smooth muscle cell proliferation and migration via NADPH oxidase: A counter-regulatory role for heme oxygenase system. *Atherosclerosis,* 224**,** 394-400.

MORAES, R. A., BRITO, D. S., ARAUJO, F. A., JESUS, R. L. C., SILVA, L. B., SÁ, D. S., SILVA DA SILVA, C. D., PERNOMIAN, L., WENCESLAU, C. F., PRIVIERO, F., WEBB, R. C. & SILVA, D. F. 2024. NONO2P, a novel nitric oxide donor, causes vasorelaxation through NO/sGC/PKG pathway, K. *Eur J Pharmacol,* 979**,** 176822.

MORGAN, M. J. & LIU, Z. G. 2011. Crosstalk of reactive oxygen species and NF-κB signaling. *Cell Res,* 21**,** 103-15.

MORITA, T., MITSIALIS, S. A., KOIKE, H., LIU, Y. & KOUREMBANAS, S. 1997. Carbon monoxide controls the proliferation of hypoxic vascular smooth muscle cells. *J Biol Chem,* 272**,** 32804-9.

MORRIS, H., E.,, NEVES, K., B.,, MONTEZANO, A., C.,, MACLEAN, M., R., & TOUYZ, R., M. 2019. Notch3 signalling and vascular remodelling in pulmonary arterial hypertension. *Clinical Science,* 133**,** 2481-2498.

MORRIS, H. E., NEVES, K. B., NILSEN, M., MONTEZANO, A. C., MACLEAN, M. R. & TOUYZ, R. M. 2023. Notch3/Hes5 Induces Vascular Dysfunction in Hypoxia-Induced Pulmonary Hypertension Through ER Stress and Redox-Sensitive Pathways. *Hypertension,* 80**,** 1683-1696.

MORRIS, J. A., DORNER, A. J., EDWARDS, C. A., HENDERSHOT, L. M. & KAUFMAN, R. J. 1997. Immunoglobulin Binding Protein (BiP) Function Is Required to Protect Cells from Endoplasmic Reticulum Stress but Is Not Required for the Secretion of Selective Proteins. *Journal of Biological Chemistry,* 272**,** 4327-4334.

MOSKOWITZ, M. A., LO, E. H. & IADECOLA, C. 2010. The science of stroke: mechanisms in search of treatments. *Neuron,* 67**,** 181-98.

MUELLER, M. D., VIGNE, J.-L., MINCHENKO, A., LEBOVIC, D. I., LEITMAN, D. C. & TAYLOR, R. N. 2000. Regulation of vascular endothelial growth factor (VEGF) gene transcription by estrogen receptors α and β. *Proceedings of the National Academy of Sciences,* 97**,** 10972-10977.

MULVANY, M. J. & HALPERN, W. 1977. Contractile properties of small arterial resistance vessels in spontaneously hypertensive and normotensive rats. *Circulation Research,* 41**,** 19-26.

MURPHY, P., MICHAEL 2009. How mitochondria produce reactive oxygen species. *Biochemical Journal,* 417**,** 1-13.

MURRAY, C. J. L., ARAVKIN, A. Y., ZHENG, P., ABBAFATI, C., ABBAS, K. M., ABBASI-KANGEVARI, M., ABD-ALLAH, F., ABDELALIM, A., ABDOLLAHI, M., ABDOLLAHPOUR, I., ABEGAZ, K. H., ABOLHASSANI, H., ABOYANS, V., ABREU, L. G., ABRIGO, M. R. M., ABUALHASAN, A., ABU-RADDAD, L. J., ABUSHOUK, A. I., ADABI, M., ADEKANMBI, V., ADEOYE, A. M., ADETOKUNBOH, O. O., ADHAM, D., ADVANI, S. M., AGARWAL, G., AGHAMIR, S. M. K., AGRAWAL, A., AHMAD, T., AHMADI, K., AHMADI, M., AHMADIEH, H., AHMED, M. B., AKALU, T. Y., AKINYEMI, R. O., AKINYEMIJU, T., AKOMBI, B., AKUNNA, C. J., ALAHDAB, F., AL-ALY, Z., ALAM, K., ALAM, S., ALAM, T., ALANEZI, F. M., ALANZI, T. M., ALEMU, B. W., ALHABIB, K. F., ALI, M., ALI, S., ALICANDRO, G., ALINIA, C., ALIPOUR, V., ALIZADE, H., ALJUNID, S. M., ALLA, F., ALLEBECK, P., ALMASI-HASHIANI, A., AL-MEKHLAFI, H. M., ALONSO, J., ALTIRKAWI, K. A., AMINI-RARANI, M., AMIRI, F., AMUGSI, D. A., ANCUCEANU, R., ANDERLINI, D., ANDERSON, J. A., ANDREI, C. L., ANDREI, T., ANGUS, C., ANJOMSHOA, M., ANSARI, F., ANSARI-MOGHADDAM, A., ANTONAZZO, I. C., ANTONIO, C. A. T., ANTONY, C. M., ANTRIYANDARTI, E., ANVARI, D., ANWER, R., APPIAH, S. C. Y., ARABLOO, J., ARAB-ZOZANI, M., ARIANI, F., ARMOON, B., ÄRNLÖV, J., ARZANI, A., ASADI-ALIABADI, M., ASADI-POOYA, A. A., ASHBAUGH, C., ASSMUS, M., ATAFAR, Z., ATNAFU, D. D., ATOUT, M. M. D. W., AUSLOOS, F., AUSLOOS, M., AYALA QUINTANILLA, B. P., AYANO, G., AYANORE, M. A., AZARI, S., AZARIAN, G., AZENE, Z. N., BADAWI, A., et al. 2020. Global burden of 87 risk factors in 204 countries and territories, 1990–2019: a systematic analysis for the Global Burden of Disease Study 2019. *The Lancet,* 396**,** 1223-1249.

NA, Y. J., JIN, J. K., KIM, J. I., CHOI, E. K., CARP, R. I. & KIM, Y. S. 2007. JAK-STAT signaling pathway mediates astrogliosis in brains of scrapie-infected mice. *J Neurochem,* 103**,** 637-49.

NAIDOO, N. 2009. ER and aging-Protein folding and the ER stress response. *Ageing Res Rev,* 8**,** 150-9.

NAKANISHI, A. 2014. Link between PI3K/AKT/PTEN Pathway and NOX Proteinin Diseases. *Aging and Disease,* 5**,** 203.

NANDI, A., YAN, L.-J., JANA, C. K. & DAS, N. 2019. Role of Catalase in Oxidative Stress- and Age-Associated Degenerative Diseases. *Oxidative Medicine and Cellular Longevity,* 2019**,** 1-19.

NAZARI, B., JAQUET, V. & KRAUSE, K. H. 2023. NOX family NADPH oxidases in mammals: Evolutionary conservation and isoform-defining sequences. *Redox Biol,* 66**,** 102851.

NEDERGAARD, M. & DIRNAGL, U. 2005. Role of glial cells in cerebral ischemia. *Glia,* 50**,** 281-286.

NELSON, M. T., STANDEN, N. B., BRAYDEN, J. E. & WORLEY, J. F. 1988. Noradrenaline contracts arteries by activating voltage-dependent calcium channels. *Nature,* 336**,** 382-5.

NEVES, K. B., HARVEY, A. P., MORETON, F., MONTEZANO, A. C., RIOS, F. J., ALVES-LOPES, R., CAT, A. N. D., ROCCHICCIOLLI, P., DELLES, C., JOUTEL, A., MUIR, K. & TOUYZ, R. M. 2019. ER stress and Rho kinase activation underlie the vasculopathy of CADASIL. *Jci Insight,* 4**,** 21.

NGUYEN DINH CAT, A., MONTEZANO, A. C., BURGER, D. & TOUYZ, R. M. 2013. Angiotensin II, NADPH Oxidase, and Redox Signaling in the Vasculature. *Antioxidants & Redox Signaling,* 19**,** 1110-1120.

NICHOLLS, D. & ATTWELL, D. 1990. The release and uptake of excitatory amino acids. *Trends Pharmacol Sci,* 11**,** 462-8.

NICHOLSON, C. J., SWEENEY, M., ROBSON, S. C. & TAGGART, M. J. 2017. Estrogenic vascular effects are diminished by chronological aging. *Scientific Reports,* 7.

NISIMOTO, Y., DIEBOLD, B. A., COSENTINO-GOMES, D. & LAMBETH, J. D. 2014. Nox4: a hydrogen peroxide-generating oxygen sensor. *Biochemistry,* 53**,** 5111-20.

NORAMBUENA-SOTO, I., OCARANZA, M. P., CANCINO-ARENAS, N., SANHUEZA-OLIVARES, F., VILLAR-FINCHEIRA, P., LEIVA-NAVARRETE, S., MANCILLA-MEDINA, C., MOYA, J., NOVOA, U., JALIL, J. E., CASTRO, P. F., LAVANDERO, S. & CHIONG, M. 2020. Angiotensin-(1-9) prevents vascular remodeling by decreasing vascular smooth muscle cell dedifferentiation through a FoxO1-dependent mechanism. *Biochem Pharmacol,* 180**,** 114190.

NOVAKOVIC, M. M., KORSHUNOV, K. S., GRANT, R. A., MARTIN, M. E., VALENCIA, H. A., BUDINGER, G. R. S., RADULOVIC, J. & PRAKRIYA, M. 2023. Astrocyte reactivity and inflammation-induced depression-like behaviors are regulated by Orai1 calcium channels. *Nature Communications,* 14.

OCARANZA, M. P. & JALIL, J. E. 2012. Protective Role of the ACE2/Ang-(1–9) Axis in Cardiovascular Remodeling. *International Journal of Hypertension,* 2012**,** 1-12.

OLSZEWSKA-PAZDRAK, B., HEIN, T. W., OLSZEWSKA, P. & CARNEY, D. H. 2009. Chronic hypoxia attenuates VEGF signaling and angiogenic responses by downregulation of KDR in human endothelial cells. *Am J Physiol Cell Physiol,* 296**,** C1162-70.

OUDOT, A., MARTIN, C., BUSSEUIL, D., VERGELY, C., DEMAISON, L. & ROCHETTE, L. 2006. NADPH oxidases are in part responsible for increased cardiovascular superoxide production during aging. *Free Radic Biol Med,* 40**,** 2214-22.

PAGE, I. H. 1949. Pathogenesis of arterial hypertension. *J Am Med Assoc,* 140**,** 451-8.

PAI, W.-Y., LO, W.-Y., HSU, T., PENG, C.-T. & WANG, H.-J. 2017. Angiotensin-(1-7) Inhibits Thrombin-Induced Endothelial Phenotypic Changes and Reactive Oxygen Species Production via NADPH Oxidase 5 Downregulation. *Frontiers in Physiology,* 8.

PANDEY, D. & FULTON, D. J. 2011. Molecular regulation of NADPH oxidase 5 via the MAPK pathway. *Am J Physiol Heart Circ Physiol,* 300**,** H1336-44.

PAPAKONSTANTINOU, E., BACOPOULOU, F., BROUZAS, D., MEGALOOIKONOMOU, V., D'ELIA, D., BONGCAM-RUDLOFF, E. & VLACHAKIS, D. 2019. NOTCH3 and CADASIL syndrome: a genetic and structural overview. *EMBnet.journal,* 24**,** e921.

PARAVICINI, T. M., CHRISSOBOLIS, S., DRUMMOND, G. R. & SOBEY, C. G. 2004. Increased NADPH-Oxidase Activity and Nox4 Expression During Chronic Hypertension Is Associated With Enhanced Cerebral Vasodilatation to NADPH In Vivo. *Stroke,* 35**,** 584-589.

PARK, J.-M., DO, V. Q., SEO, Y.-S., KIM, H. J., NAM, J. H., YIN, M. Z., KIM, H. J., KIM, S. J., GRIENDLING, K. K. & LEE, M.-Y. 2022. NADPH Oxidase 1 Mediates Acute Blood Pressure Response to Angiotensin II by Contributing to Calcium Influx in Vascular Smooth Muscle Cells. *Arteriosclerosis, Thrombosis, and Vascular Biology,* 42.

PATEL, K. P. & SCHULTZ, H. D. 2013. Angiotensin Peptides and Nitric Oxide in Cardiovascular Disease. *Antioxidants & Redox Signaling,* 19**,** 1121-1132.

PATEL, S., RAUF, A., KHAN, H. & ABU-IZNEID, T. 2017. Renin-angiotensin-aldosterone (RAAS): The ubiquitous system for homeostasis and pathologies. *Biomed Pharmacother,* 94**,** 317-325.

PATEL, V. B., ZHONG, J.-C., GRANT, M. B. & OUDIT, G. Y. 2016. Role of the ACE2/Angiotensin 1–7 Axis of the Renin–Angiotensin System in Heart Failure. *Circulation Research,* 118**,** 1313-1326.

PEDRUZZI, E., GUICHARD, C., OLLIVIER, V., DRISS, F., FAY, M., PRUNET, C., MARIE, J.-C., POUZET, C., SAMADI, M., ELBIM, C., O'DOWD, Y., BENS, M., VANDEWALLE, A., GOUGEROT-POCIDALO, M.-A., LIZARD, G. & OGIER-DENIS, E. 2004. NAD(P)H Oxidase Nox-4 Mediates 7-Ketocholesterol-Induced Endoplasmic Reticulum Stress and Apoptosis in Human Aortic Smooth Muscle Cells. *Molecular and Cellular Biology,* 24**,** 10703-10717.

PI, X., XIE, L., PORTBURY, A. L., KUMAR, S., LOCKYER, P., LI, X. & PATTERSON, C. 2014. NADPH Oxidase–Generated Reactive Oxygen Species Are Required for Stromal Cell–Derived Factor-1α–Stimulated Angiogenesis. *Arteriosclerosis, Thrombosis, and Vascular Biology,* 34**,** 2023-2032.

PINTO, E. 2007. Blood pressure and ageing. *Postgraduate Medical Journal,* 83**,** 109-114.

PIQUERAS, L. & SANZ, M. J. 2020. Angiotensin II and leukocyte trafficking: New insights for an old vascular mediator. Role of redox-signaling pathways. *Free Radic Biol Med,* 157**,** 38-54.

POELS, M. L. M. F., VERNOOIJ, M. W., IKRAM, M. A., HOFMAN, A., KRESTIN, G. P., VAN DER LUGT, A. & BRETELER, M. M. B. 2010. Prevalence and Risk Factors of Cerebral Microbleeds. *Stroke,* 41**,** S103-S106.

PRAST, H. & PHILIPPU, A. 2001. Nitric oxide as modulator of neuronal function. *Prog Neurobiol,* 64**,** 51-68.

PRATICÒ, D. 2002. Lipid Peroxidation and the Aging Process. *Science of Aging Knowledge Environment,* 2002**,** 5re-5.

PRICE, B. R., NORRIS, C. M., SOMPOL, P. & WILCOCK, D. M. 2018. An emerging role of astrocytes in vascular contributions to cognitive impairment and dementia. *Journal of Neurochemistry,* 144**,** 644-650.

PUTNEY, J. W. & TOMITA, T. 2012. Phospholipase C signaling and calcium influx. *Advances in Biological Regulation,* 52**,** 152-164.

PÉREZ DE LA LASTRA, J. M., JUAN, C. A., PLOU, F. J. & PÉREZ-LEBEÑA, E. 2022. The Nitration of Proteins, Lipids and DNA by Peroxynitrite Derivatives-Chemistry Involved and Biological Relevance. *Stresses,* 2**,** 53-64.

QIAN, L., ZHU, Y., DENG, C., LIANG, Z., CHEN, J., CHEN, Y., WANG, X., LIU, Y., TIAN, Y. & YANG, Y. 2024. Peroxisome proliferator-activated receptor gamma coactivator-1 (PGC-1) family in physiological and pathophysiological process and diseases. *Signal Transduction and Targeted Therapy,* 9.

QIAN, X., WANG, J., CAI, M., SUN, H., XU, H., WEN, H. & ZHU, H. 2021. Estradiol Valerate Enhances Cardiac Function via the Nrf2 Signaling Pathway to Protect

Against Oxidative Stress by the Nrf2 Signaling Pathway in an Ovariectomized Rat Model. *Curr Pharm Des,* 27**,** 4716-4725.

QIU, Y.-M., ZHANG, C.-L., CHEN, A.-Q., WANG, H.-L., ZHOU, Y.-F., LI, Y.-N. & HU, B. 2021. Immune Cells in the BBB Disruption After Acute Ischemic Stroke: Targets for Immune Therapy? *Frontiers in Immunology,* 12.

RAAD, H., MOUAWIA, H., HASSAN, H., EL-SEBLANI, M., ARABI-DERKAWI, R., BOUSSETTA, T., GOUGEROT-POCIDALO, M. A., DANG, P. M. & EL-BENNA, J. 2020. The protein kinase A negatively regulates reactive oxygen species production by phosphorylating gp91phox/NOX2 in human neutrophils. *Free Radic Biol Med,* 160**,** 19-27.

RABELO, L. A., ALENINA, N. & BADER, M. 2011. ACE2–angiotensin-(1–7)–Mas axis and oxidative stress in cardiovascular disease. *Hypertension Research,* 34**,** 154-160.

RADI, R. 2013. Peroxynitrite, a stealthy biological oxidant. *J Biol Chem,* 288**,** 26464-72.

RADI, R., BECKMAN, J. S., BUSH, K. M. & FREEMAN, B. A. 1991. Peroxynitrite-induced membrane lipid peroxidation: the cytotoxic potential of superoxide and nitric oxide. *Arch Biochem Biophys,* 288**,** 481-7.

RAGOT, H., MONFORT, A., BAUDET, M., AZIBANI, F., FAZAL, L., MERVAL, R., POLIDANO, E., COHEN-SOLAL, A., DELCAYRE, C., VODOVAR, N., CHATZIANTONIOU, C. & SAMUEL, J.-L. 2016. Loss of Notch3 Signaling in Vascular Smooth Muscle Cells Promotes Severe Heart Failure Upon Hypertension. *Hypertension,* 68**,** 392-+.

RAINA, R., KRISHNAPPA, V., DAS, A., AMIN, H., RADHAKRISHNAN, Y., NAIR, N. R. & KUSUMI, K. 2019. Overview of Monogenic or Mendelian Forms of Hypertension. *Frontiers in Pediatrics,* 7.

RAJAGOPALAN, S., KURZ, S., MÜNZEL, T., TARPEY, M., FREEMAN, B. A., GRIENDLING, K. K. & HARRISON, D. G. 1996. Angiotensin II-mediated hypertension in the rat increases vascular superoxide production via membrane NADH/NADPH oxidase activation. Contribution to alterations of vasomotor tone. *Journal of Clinical Investigation,* 97**,** 1916-1923.

RASTOGI, R., GENG, X. K., LI, F. W. & DING, Y. C. 2017. NOX Activation by Subunit Interaction and Underlying Mechanisms in Disease. *Frontiers in Cellular Neuroscience,* 10**,** 13.

RATHORE, R., ZHENG, Y., NIU, C., LIU, Q., KORDE, A., HO, Y. & WANG, Y. 2008. Hypoxia activates NADPH oxidase to increase [ROS]i and [Ca2+]i through the mitochondrial ROS-PKCε signaling axis in pulmonary artery smooth muscle cells. *Free Radical Biology and Medicine,* 45**,** 1223-1231.

RAY, R., MURDOCH, C. E., WANG, M., SANTOS, C. X., ZHANG, M., ALOM-RUIZ, S., ANILKUMAR, N., OUATTARA, A., CAVE, A. C., WALKER, S. J., GRIEVE, D. J., CHARLES, R. L., EATON, P., BREWER, A. C. & SHAH, A. M. 2011. Endothelial Nox4 NADPH Oxidase Enhances Vasodilatation and Reduces Blood Pressure In Vivo. *Arteriosclerosis, Thrombosis, and Vascular Biology,* 31**,** 1368-1376.

REDZA-DUTORDOIR, M. & AVERILL-BATES, D. A. 2016. Activation of apoptosis signalling pathways by reactive oxygen species. *Biochim Biophys Acta,* 1863**,** 2977-2992.

REINERT, A., MORAWSKI, M., SEEGER, J., ARENDT, T. & REINERT, T. 2019. Iron concentrations in neurons and glial cells with estimates on ferritin concentrations. *BMC Neuroscience,* 20.

RETTBERG, J. R., YAO, J. & BRINTON, R. D. 2014. Estrogen: A master regulator of bioenergetic systems in the brain and body. *Frontiers in Neuroendocrinology,* 35**,** 8-30.

REXRODE, K. M., MADSEN, T. E., YU, A. Y. X., CARCEL, C., LICHTMAN, J. H. & MILLER, E. C. 2022. The Impact of Sex and Gender on Stroke. *Circulation Research,* 130**,** 512-528.

REY, S. & SEMENZA, G. L. 2010. Hypoxia-inducible factor-1-dependent mechanisms of vascularization and vascular remodelling. *Cardiovascular Research,* 86**,** 236-242.

RITSICK, D. R., EDENS, W. A., FINNERTY, V. & LAMBETH, J. D. 2007. Nox regulation of smooth muscle contraction. *Free Radical Biology and Medicine,* 43**,** 31-38.

RODRIGO, R., FERNÁNDEZ-GAJARDO, R., GUTIÉRREZ, R., MATAMALA, J. M., CARRASCO, R., MIRANDA-MERCHAK, A. & FEUERHAKE, W. 2013. Oxidative stress and pathophysiology of ischemic stroke: novel therapeutic opportunities. *CNS Neurol Disord Drug Targets,* 12**,** 698-714.

ROMAY, M. C., KNUTSEN, R. H., MA, F., MOMPEÓN, A., HERNANDEZ, G. E., SALVADOR, J., MIRKOV, S., BATRA, A., SULLIVAN, D. P., PROCISSI, D., BUCHANAN, S., KRONQUIST, E., FERRANTE, E. A., MULLER, W. A., WALSHON, J., STEFFENS, A., MCCORTNEY, K., HORBINSKI, C., TOURNIER-LASSERVE, E., SONABEND, A. M., SOROND, F. A., WANG, M. M., BOEHM, M., KOZEL, B. A. & IRUELA-ARISPE, M. L. 2024. Age-related loss of Notch3 underlies brain vascular contractility deficiencies, glymphatic dysfunction, and neurodegeneration in mice. *Journal of Clinical Investigation,* 134.

ROMERO, J. C. & RECKELHOFF, J. F. 1999. Role of Angiotensin and Oxidative Stress in Essential Hypertension. *Hypertension,* 34**,** 943-949.

ROSS, D., KEPA, J. K., WINSKI, S. L., BEALL, H. D., ANWAR, A. & SIEGEL, D. 2000. NAD(P)H:quinone oxidoreductase 1 (NQO1): chemoprotection, bioactivation, gene regulation and genetic polymorphisms. *Chem Biol Interact,* 129**,** 77-97.

ROUHL, R. P., DAMOISEAUX, J. G., LODDER, J., THEUNISSEN, R. O., KNOTTNERUS, I. L., STAALS, J., HENSKENS, L. H., KROON, A. A., DE LEEUW, P. W., TERVAERT, J. W. & VAN OOSTENBRUGGE, R. J. 2012. Vascular inflammation in cerebral small vessel disease. *Neurobiol Aging,* 33**,** 1800-6.

RUEDIGER, S. L., KOEP, J. L., KEATING, S. E., PIZZEY, F. K., COOMBES, J. S. & BAILEY, T. G. 2021. Effect of menopause on cerebral artery blood flow velocity and cerebrovascular reactivity: Systematic review and meta-analysis. *Maturitas,* 148**,** 24-32.

RUKAVINA MIKUSIC, N. L., PINEDA, A. M. & GIRONACCI, M. M. 2021. Angiotensin-(1-7) and Mas receptor in the brain. *Exploration of Medicine,* 2**,** 268-293.

RUKAVINA MIKUSIC, N. L., SILVA, M. G., PINEDA, A. M. & GIRONACCI, M. M. 2020. Angiotensin Receptors Heterodimerization and Trafficking: How Much Do They Influence Their Biological Function? *Frontiers in Pharmacology,* 11.

RUSSO, I., BARALE, C., MELCHIONDA, E., PENNA, C. & PAGLIARO, P. 2023. Platelets and Cardioprotection: The Role of Nitric Oxide and Carbon Oxide. *International Journal of Molecular Sciences,* 24**,** 6107.

SAHOO, S., MEIJLES, D. N. & PAGANO, P. J. 2016. NADPH oxidases: key modulators in aging and age-related cardiovascular diseases? *Clin Sci (Lond),* 130**,** 317-35.

SALMINEN, A., KAARNIRANTA, K. & KAUPPINEN, A. 2013. Crosstalk between Oxidative Stress and SIRT1: Impact on the Aging Process. *International Journal of Molecular Sciences,* 14**,** 3834-3859.

SANDOO, A., VELDHUIJZEN VAN ZANTEN, J. J. C. S., METSIOS, G. S., CARROLL, D. & KITAS, G. D. 2010. The Endothelium and Its Role in Regulating Vascular Tone. *The Open Cardiovascular Medicine Journal,* 4**,** 302-312.

SANTEN, R. J., BRODIE, H., SIMPSON, E. R., SIITERI, P. K. & BRODIE, A. 2009. History of aromatase: saga of an important biological mediator and therapeutic target. *Endocr Rev,* 30**,** 343-75.

SANTIAGO, J. A., SCHERZER, C. R. & POTASHKIN, J. A. 2014. Network Analysis Identifies SOD2 mRNA as a Potential Biomarker for Parkinson's Disease. *PLoS ONE,* 9**,** e109042.

SANTILLI, F., D'ARDES, D. & DAVÌ, G. 2015. Oxidative stress in chronic vascular disease: From prediction to prevention. *Vascul Pharmacol,* 74**,** 23-37.

SAVOIA, C., BURGER, D., NISHIGAKI, N., MONTEZANO, A. & TOUYZ, R. M. 2011. Angiotensin II and the vascular phenotype in hypertension. *Expert Rev Mol Med,* 13**,** e11.

SCHAEFFER, S. & IADECOLA, C. 2021. Revisiting the neurovascular unit. *Nat Neurosci,* 24**,** 1198-1209.

SCHRÖDER, K., ZHANG, M., BENKHOFF, S., MIETH, A., PLIQUETT, R., KOSOWSKI, J., KRUSE, C., LUEDIKE, P., MICHAELIS, U. R., WEISSMANN, N., DIMMELER, S., SHAH, A. M. & BRANDES, R. P. 2012. Nox4 Is a Protective Reactive Oxygen Species Generating Vascular NADPH Oxidase. *Circulation Research,* 110**,** 1217-1225.

SERRANDER, L., JAQUET, V., BEDARD, K., PLASTRE, O., HARTLEY, O., ARNAUDEAU, S., DEMAUREX, N., SCHLEGEL, W. & KRAUSE, K. H. 2007. NOX5 is expressed at the plasma membrane and generates superoxide in response to protein kinase C activation. *Biochimie,* 89**,** 1159-67.

SHARIFI-RAD, M., ANIL KUMAR, N. V., ZUCCA, P., VARONI, E. M., DINI, L., PANZARINI, E., RAJKOVIC, J., TSOUH FOKOU, P. V., AZZINI, E., PELUSO, I., PRAKASH MISHRA, A., NIGAM, M., EL RAYESS, Y., BEYROUTHY, M. E., POLITO, L., IRITI, M., MARTINS, N., MARTORELL, M., DOCEA, A. O., SETZER, W. N., CALINA, D., CHO, W. C. & SHARIFI-RAD, J. 2020. Lifestyle, Oxidative Stress, and Antioxidants: Back and Forth in the Pathophysiology of Chronic Diseases. *Frontiers in Physiology,* 11.

SHARINA, I. G. & MARTIN, E. 2017. The Role of Reactive Oxygen and Nitrogen Species in the Expression and Splicing of Nitric Oxide Receptor. *Antioxidants & Redox Signaling,* 26**,** 122-136.

SHARMA, S., BHATTARAI, S., ARA, H., SUN, G., ST CLAIR, D. K., BHUIYAN, M. S., KEVIL, C., WATTS, M. N., DOMINIC, P., SHIMIZU, T., MCCARTHY, K. J., SUN, H., PANCHATCHARAM, M. & MIRIYALA, S. 2020. SOD2 deficiency in cardiomyocytes defines defective mitochondrial bioenergetics as a cause of lethal dilated cardiomyopathy. *Redox Biol,* 37**,** 101740.

SHEN, A., KIM, H.-J., OH, G.-S., LEE, S.-B., LEE, S., PANDIT, A., KHADKA, D., SHARMA, S., KIM, S. Y., CHOE, S.-K., YANG, S.-H., CHO, E.-Y., SHIM, H., PARK, R., KWAK, T. H. & SO, H.-S. 2018. Pharmacological stimulation of NQO1 decreases NADPH levels and ameliorates acute pancreatitis in mice. *Cell Death & Disease,* 10.

SHEN, X.-Y., GAO, Z.-K., HAN, Y., YUAN, M., GUO, Y.-S. & BI, X. 2021. Activation and Role of Astrocytes in Ischemic Stroke. *Frontiers in Cellular Neuroscience,* 15.

SHENG, W. S., HU, S., FENG, A. & ROCK, R. B. 2013. Reactive Oxygen Species from Human Astrocytes Induced Functional Impairment and Oxidative Damage. *Neurochemical Research,* 38**,** 2148-2159.

SHIBATA, S., ARROYO, J. P., CASTAÑEDA-BUENO, M., PUTHUMANA, J., ZHANG, J., UCHIDA, S., STONE, K. L., LAM, T. T. & LIFTON, R. P. 2014. Angiotensin II signaling via protein kinase C phosphorylates Kelch-like 3, preventing WNK4 degradation. *Proceedings of the National Academy of Sciences,* 111**,** 15556-15561.

SHIBUYA, M. 2011. Vascular Endothelial Growth Factor (VEGF) and Its Receptor (VEGFR) Signaling in Angiogenesis: A Crucial Target for Anti- and Pro-Angiogenic Therapies. *Genes & Cancer,* 2**,** 1097-1105.

SHIOJIMA, I. & WALSH, K. 2002. Role of Akt Signaling in Vascular Homeostasis and Angiogenesis. *Circulation Research,* 90**,** 1243-1250.

SIDDIQUE, Y. H., ARA, G. & AFZAL, M. 2012. Estimation of Lipid Peroxidation Induced by Hydrogen Peroxide in Cultured Human Lymphocytes. *Dose-Response,* 10**,** dose-response.1.

SIMON, A. R., RAI, U., FANBURG, B. L. & COCHRAN, B. H. 1998. Activation of the JAK-STAT pathway by reactive oxygen species. *Am J Physiol,* 275**,** C1640-52.

SMITH, E. E., O'DONNELL, M., DAGENAIS, G., LEAR, S. A., WIELGOSZ, A., SHARMA, M., POIRIER, P., STOTTS, G., BLACK, S. E., STROTHER, S., NOSEWORTHY, M. D., BENAVENTE, O., MODI, J., GOYAL, M., BATOOL, S., SANCHEZ, K., HILL, V., MCCREARY, C. R., FRAYNE, R., ISLAM, S., DEJESUS, J., RANGARAJAN, S., TEO, K. & YUSUF, S. 2015. Early cerebral small vessel disease and brain volume, cognition, and gait. *Annals of Neurology,* 77**,** 251-261.

SOARES, R., BALOGH, G., GUO, S., GÄRTNER, F., RUSSO, J. & SCHMITT, F. 2004. Evidence for the Notch Signaling Pathway on the Role of Estrogen in Angiogenesis. *Molecular Endocrinology,* 18**,** 2333-2343.

SONG, B., JIN, H., YU, X., ZHANG, Z., YU, H., YE, J., XU, Y., ZHOU, T., OUDIT, G. Y., YE, J. Y., CHEN, C., GAO, P., ZHU, D., PENNINGER, J. M. & ZHONG, J. C. 2013. Angiotensin-converting enzyme 2 attenuates oxidative stress and VSMC proliferation via the JAK2/STAT3/SOCS3 and profilin-1/MAPK signaling pathways. *Regul Pept,* 185**,** 44-51.

SONG, K., LI, Y., ZHANG, H., AN, N., WEI, Y., WANG, L., TIAN, C., YUAN, M., SUN, Y., XING, Y. & GAO, Y. 2020. Oxidative Stress-Mediated Blood-Brain Barrier (BBB) Disruption in Neurological Diseases. *Oxidative Medicine and Cellular Longevity,* 2020**,** 1-27.

SONG, P. & ZOU, M.-H. 2012. Regulation of NAD(P)H oxidases by AMPK in cardiovascular systems. *Free Radical Biology and Medicine,* 52**,** 1607-1619.

SOUZA, V. R., MENDES, E., CASARO, M., ANTIORIO, A. T. F. B., OLIVEIRA, F. A. & FERREIRA, C. M. 2019. Description of Ovariectomy Protocol in Mice. *Methods in Molecular Biology.* Springer New York.

SPENCE, R. D., HAMBY, M. E., UMEDA, E., ITOH, N., DU, S., WISDOM, A. J., CAO, Y., BONDAR, G., LAM, J., AO, Y., SANDOVAL, F., SURIANY, S., SOFRONIEW, M. V. & VOSKUHL, R. R. 2011. Neuroprotection mediated through estrogen receptor-α in astrocytes. *Proceedings of the National Academy of Sciences,* 108**,** 8867-8872.

STANIC, B., PANDEY, D., FULTON, D. J. & MILLER, F. J. 2012. Increased Epidermal Growth Factor–Like Ligands Are Associated With Elevated Vascular Nicotinamide Adenine Dinucleotide Phosphate Oxidase in a Primate Model of Atherosclerosis. *Arteriosclerosis, Thrombosis, and Vascular Biology,* 32**,** 2452-2460.

SU, C., LIU, W. C., LI, G. M. & HUANG, Y. 2021. Association Between the Angiotensin-Converting Enzyme I/D Polymorphism and Risk of Cerebral Small Vessel Disease: A Meta-Analysis Based on 7186 Subjects. *J Stroke Cerebrovasc Dis,* 30**,** 105579.

SUMIMOTO, H. 2008. Structure, regulation and evolution of Nox-family NADPH oxidases that produce reactive oxygen species. *The FEBS Journal,* 275**,** 3249-3277.

SUMNERS, C., PELUSO, A. A., HAUGAARD, A. H., BERTELSEN, J. B. & STECKELINGS, U. M. 2019. Anti-fibrotic mechanisms of angiotensin AT₂-receptor stimulation. *Acta Physiologica,* 227**,** e13280.

SUN, S. C. 2017. The non-canonical NF-κB pathway in immunity and inflammation. *Nat Rev Immunol,* 17**,** 545-558.

SZABÓ, C. 1996. The pathophysiological role of peroxynitrite in shock, inflammation, and ischemia-reperfusion injury. *Shock,* 6**,** 79-88.

SZABÓ, C. & MÓDIS, K. 2010. Pathophysiological roles of peroxynitrite in circulatory shock. *Shock,* 34 Suppl 1**,** 4-14.

SZÖCS, K., LASSÈGUE, B., SORESCU, D., HILENSKI, L. L., VALPPU, L., COUSE, T. L., WILCOX, J. N., QUINN, M. T., LAMBETH, J. D. & GRIENDLING, K. K. 2002. Upregulation of Nox-Based NAD(P)H Oxidases in Restenosis After Carotid Injury. *Arteriosclerosis, Thrombosis, and Vascular Biology,* 22**,** 21-27.

TAKAC, I., SCHRÖDER, K., ZHANG, L., LARDY, B., ANILKUMAR, N., LAMBETH, J. D., SHAH, A. M., MOREL, F. & BRANDES, R. P. 2011. The E-loop Is Involved in Hydrogen Peroxide Formation by the NADPH Oxidase Nox4. *Journal of Biological Chemistry,* 286**,** 13304-13313.

TANG, L., DAI, F., LIU, Y., YU, X., HUANG, C., WANG, Y. & YAO, W. 2018. RhoA/ROCK signaling regulates smooth muscle phenotypic modulation and vascular remodeling via the JNK pathway and vimentin cytoskeleton. *Pharmacol Res,* 133**,** 201-212.

TAUTZ, L., CRITTON, D. A. & GROTEGUT, S. 2013. Protein tyrosine phosphatases: structure, function, and implication in human disease. *Methods Mol Biol,* 1053**,** 179-221.

TE RIET, L., VAN ESCH, J. H. M., ROKS, A. J. M., VAN DEN MEIRACKER, A. H. & DANSER, A. H. J. 2015. Hypertension. *Circulation Research,* 116**,** 960-975.

TEJERO, J., SHIVA, S. & GLADWIN, M. T. 2019. Sources of Vascular Nitric Oxide and Reactive Oxygen Species and Their Regulation. *Physiological Reviews,* 99**,** 311-379.

THIEBAUT, P. A., DELILE, E., COQUEREL, D., BRUNEL, J. M., RENET, S., TAMION, F. & RICHARD, V. 2018. Protein tyrosine phosphatase 1B regulates endothelial endoplasmic reticulum stress; role in endothelial dysfunction. *Vascul Pharmacol,* 109**,** 36-44.

TODD, K. L., BRIGHTON, T., NORTON, E. S., SCHICK, S., ELKINS, W., PLETNIKOVA, O., FORTINSKY, R. H., TRONCOSO, J. C., MOLFESE, P. J., RESNICK, S. M. & CONOVER, J. C. 2018. Ventricular and Periventricular Anomalies in the Aging and Cognitively Impaired Brain. *Frontiers in Aging Neuroscience,* 9.

TOUYZ, R. M., ALVES-LOPES, R., RIOS, F. J., CAMARGO, L. L., ANAGNOSTOPOULOU, A., ARNER, A. & MONTEZANO, A. C. 2018. Vascular smooth muscle contraction in hypertension. *Cardiovascular Research,* 114**,** 529-539.

TOUYZ, R. M., ANAGNOSTOPOULOU, A., RIOS, F., MONTEZANO, A. C. & CAMARGO, L. L. 2019. NOX5: Molecular biology and pathophysiology. *Experimental Physiology,* 104**,** 605-616.

TOUYZ, R. M., CAMARGO, L. L., RIOS, F. J., ALVES-LOPES, R., NEVES, K. B., ELUWOLE, O., MASEKO, M. J., LUCAS-HERALD, A., **BLAIKIE, Z**., MONTEZANO, A. C. & FELDMAN, R. D. 2022. Arterial Hypertension. *Comprehensive Pharmacology.* Elsevier.

TOUYZ, R. M., RIOS, F. J., ALVES-LOPES, R., NEVES, K. B., CAMARGO, L. L. & MONTEZANO, A. C. 2020. Oxidative Stress: A Unifying Paradigm in Hypertension. *Canadian Journal of Cardiology,* 36**,** 659-670.

TRAN, N., GARCIA, T., ANIQA, M., ALI, S., ALLY, A. & NAULI, S. M. 2022. Endothelial Nitric Oxide Synthase (eNOS) and the Cardiovascular System: in Physiology and in Disease States. *Am J Biomed Sci Res,* 15**,** 153-177.

TZENG, Y.-C. & AINSLIE, P. N. 2014. Blood pressure regulation IX: cerebral autoregulation under blood pressure challenges. *European Journal of Applied Physiology,* 114**,** 545-559.

ULYATT, C., WALKER, J. & PONNAMBALAM, S. 2011. Hypoxia differentially regulates VEGFR1 and VEGFR2 levels and alters intracellular signaling and cell migration in endothelial cells. *Biochem Biophys Res Commun,* 404**,** 774-9.

VALKENBURG, K. C., AMEND, S. R. & PIENTA, K. J. 2016. Murine Prostate Micro-dissection and Surgical Castration. *Journal of Visualized Experiments*.

VALLET, P., CHARNAY, Y., STEGER, K., OGIER-DENIS, E., KOVARI, E., HERRMANN, F., MICHEL, J. P. & SZANTO, I. 2005. Neuronal expression of the NADPH oxidase NOX4, and its regulation in mouse experimental brain ischemia. *Neuroscience,* 132**,** 233-238.

VAN DER VLIET, A. & JANSSEN-HEININGER, Y. M. W. 2014. Hydrogen Peroxide as a Damage Signal in Tissue Injury and Inflammation: Murderer, Mediator, or Messenger? *Journal of Cellular Biochemistry,* 115**,** 427-435.

VENDROV, A. E., SUMIDA, A., CANUGOVI, C., LOZHKIN, A., HAYAMI, T., MADAMANCHI, N. R. & RUNGE, M. S. 2019. NOXA1-dependent NADPH oxidase regulates redox signaling and phenotype of vascular smooth muscle cell during atherogenesis. *Redox Biol,* 21**,** 101063.

VERDELHO, A., WARDLAW, J., PAVLOVIC, A., PANTONI, L., GODEFROY, O., DUERING, M., CHARIDIMOU, A., CHABRIAT, H. & BIESSELS, G. J. 2021. Cognitive impairment in patients with cerebrovascular disease: A white paper from the links between stroke ESO Dementia Committee. *European Stroke Journal,* 6**,** 5-17.

VERMOT, A., PETIT-HÄRTLEIN, I., SMITH, S. M. E. & FIESCHI, F. 2021. NADPH Oxidases (NOX): An Overview from Discovery, Molecular Mechanisms to Physiology and Pathology. *Antioxidants,* 10**,** 890.

VESTWEBER, D. 2021. Vascular Endothelial Protein Tyrosine Phosphatase Regulates Endothelial Function. *Physiology (Bethesda),* 36**,** 84-93.

WAGNER, A. H., SCHROETER, M. R. & HECKER, M. 2001. 17β-Estradiol inhibition of NADPH oxidase expression in human endothelial cells. *The FASEB Journal,* 15**,** 2121-2130.

WALDER, C. E., GREEN, S. P., DARBONNE, W. C., MATHIAS, J., RAE, J., DINAUER, M. C., CURNUTTE, J. T. & THOMAS, G. R. 1997. Ischemic stroke injury is reduced in mice lacking a functional NADPH oxidase. *Stroke,* 28**,** 2252-2258.

WANG, D., IVERSEN, J. & STRANDGAARD, S. 2000. Endothelium-dependent relaxation of small resistance vessels is impaired in patients with autosomal dominant polycystic kidney disease. *J Am Soc Nephrol,* 11**,** 1371-1376.

WANG, H. & HARTNETT, M. 2017. Roles of Nicotinamide Adenine Dinucleotide Phosphate (NADPH) Oxidase in Angiogenesis: Isoform-Specific Effects. *Antioxidants,* 6**,** 40.

WANG, H. P., WANG, X., GONG, L. F., CHEN, W. J., HAO, Z., FENG, S. W., WU, Y. B., YE, T. & CAI, Y. K. 2016. Nox1 promotes colon cancer cell metastasis via activation of the ADAM17 pathway. *Eur Rev Med Pharmacol Sci,* 20**,** 4474-4481.

WANG, M., WEY, S., ZHANG, Y., YE, R. & LEE, A. S. 2009. Role of the Unfolded Protein Response Regulator GRP78/BiP in Development, Cancer, and Neurological Disorders. *Antioxidants & Redox Signaling,* 11**,** 2307-2316.

WANG, T., BARON, M. & TRUMP, D. 2008. An overview of Notch3 function in vascular smooth muscle cells. *Progress in Biophysics and Molecular Biology,* 96**,** 499-509.

WANG, X., BOVE, A. M., SIMONE, G. & MA, B. 2020. Molecular Bases of VEGFR-2-Mediated Physiological Function and Pathological Role. *Frontiers in Cell and Developmental Biology,* 8.

WANG, Y., CHEN, F., LE, B., STEPP, D. W. & FULTON, D. J. R. 2014. Impact of Nox5 Polymorphisms on Basal and Stimulus-Dependent ROS Generation. *PLoS ONE,* 9**,** e100102.

WANG, Z., CHEN, Q., CHEN, J., YANG, N. & ZHENG, K. 2021. Risk factors of cerebral small vessel disease: A systematic review and meta-analysis. *Medicine (Baltimore),* 100**,** e28229.

WELSH, C. L. & MADAN, L. K. 2024. Protein Tyrosine Phosphatase regulation by Reactive Oxygen Species. *Adv Cancer Res,* 162**,** 45-74.

WELTEN, S. J. G. C., ONLAND-MORET, N. C., BOER, J. M. A., VERSCHUREN, W. M. M. & VAN DER SCHOUW, Y. T. 2021. Age at Menopause and Risk of Ischemic and Hemorrhagic Stroke. *Stroke,* 52**,** 2583-2591.

WHELTON, P. K., CAREY, R. M., ARONOW, W. S., CASEY, D. E., COLLINS, K. J., DENNISON HIMMELFARB, C., DEPALMA, S. M., GIDDING, S., JAMERSON, K. A., JONES, D. W., MACLAUGHLIN, E. J., MUNTNER, P., OVBIAGELE, B., SMITH, S. C., SPENCER, C. C., STAFFORD, R. S., TALER, S. J., THOMAS, R. J., WILLIAMS, K. A., WILLIAMSON, J. D. & WRIGHT, J. T. 2018. 2017 ACC/AHA/AAPA/ABC/ACPM/AGS/APhA/ASH/ASPC/NMA/PCNA Guideline for the Prevention, Detection, Evaluation, and Management of High Blood Pressure in Adults: A Report of the American College of Cardiology/American Heart Association Task Force on Clinical Practice Guidelines. *J Am Coll Cardiol,* 71**,** e127-e248.

WILSON, C., LEE, M. D. & MCCARRON, J. G. 2016. Acetylcholine released by endothelial cells facilitates flow-mediated dilatation. *The Journal of Physiology,* 594**,** 7267-7307.

WINGLER, K., WÜNSCH, S., KREUTZ, R., ROTHERMUND, L., PAUL, M. & SCHMIDT, H. H. 2001. Upregulation of the vascular NAD(P)H-oxidase isoforms Nox1 and Nox4 by the renin-angiotensin system in vitro and in vivo. *Free Radic Biol Med,* 31**,** 1456-64.

WOODSOME, T. P., ETO, M., EVERETT, A., BRAUTIGAN, D. L. & KITAZAWA, T. 2001. Expression of CPI-17 and myosin phosphatase correlates with Ca(2+) sensitivity of protein kinase C-induced contraction in rabbit smooth muscle. *J Physiol,* 535**,** 553-64.

WU, L., XIONG, X., WU, X., YE, Y., JIAN, Z., ZHI, Z. & GU, L. 2020. Targeting Oxidative Stress and Inflammation to Prevent Ischemia-Reperfusion Injury. *Frontiers in Molecular Neuroscience,* 13.

WU, W., LI, L., SU, X., ZHU, Z., LIN, X., ZHANG, J., ZHUANG, Z., CAI, H. & HUANG, W. 2021. Nuclear factor-kappaB regulates the transcription of NADPH oxidase 1 in human alveolar epithelial cells. *BMC Pulmonary Medicine,* 21.

WYNNE, B. M., CHIAO, C.-W. & WEBB, R. C. 2009. Vascular smooth muscle cell signaling mechanisms for contraction to angiotensin II and endothelin-1. *Journal of the American Society of Hypertension,* 3**,** 84-95.

XIANG, D., LIU, Y., ZHOU, S., ZHOU, E. & WANG, Y. 2021. Protective Effects of Estrogen on Cardiovascular Disease Mediated by Oxidative Stress. *Oxidative Medicine and Cellular Longevity,* 2021**,** 1-15.

XIE, F., DONG, H. & ZHANG, H. 2021. Regulatory Functions of Protein Tyrosine Phosphatase Receptor Type O in Immune Cells. *Frontiers in Immunology,* 12.

XING, C.-Y., TARUMI, T., LIU, J., ZHANG, Y., TURNER, M., RILEY, J., TINAJERO, C. D., YUAN, L.-J. & ZHANG, R. 2017. Distribution of cardiac output to the brain across the adult lifespan. *Journal of Cerebral Blood Flow & Metabolism,* 37**,** 2848-2856.

XING, D., NOZELL, S., CHEN, Y.-F., HAGE, F. & OPARIL, S. 2009. Estrogen and Mechanisms of Vascular Protection. *Arteriosclerosis, Thrombosis, and Vascular Biology,* 29**,** 289-295.

XING, D., OPARIL, S., YU, H., GONG, K., FENG, W., BLACK, J., CHEN, Y.-F. & NOZELL, S. 2012. Estrogen Modulates NFκB Signaling by Enhancing IκBα

Levels and Blocking p65 Binding at the Promoters of Inflammatory Genes via Estrogen Receptor-β. *PLoS ONE,* 7**,** e36890.

XU, L., NIRWANE, A. & YAO, Y. 2019. Basement membrane and blood–brain barrier. *Stroke and Vascular Neurology,* 4**,** 78-82.

XU, X., WU, X., ZHU, C., ZHANG, R., JIAERKEN, Y., WANG, S., HONG, H., YU, W., LI, K., ZENG, Q., LUO, X., YU, X., SUN, J., ZHANG, M. & HUANG, P. 2021. Characterization of Lenticulostriate Arteries and Its Associations With Vascular Risk Factors in Community-Dwelling Elderly. *Frontiers in Aging Neuroscience,* 13.

YAGHI, S., RAZ, E., YANG, D., CUTTING, S., MAC GRORY, B., ELKIND, M. S. & DE HAVENON, A. 2021. Lacunar stroke: mechanisms and therapeutic implications. *Journal of Neurology, Neurosurgery & Psychiatry,* 92**,** 823-830.

YANG, L., QUAN, S., NASJLETTI, A., LANIADO-SCHWARTZMAN, M. & ABRAHAM, N. G. 2004. Heme Oxygenase-1 Gene Expression Modulates Angiotensin II–Induced Increase in Blood Pressure. *Hypertension,* 43**,** 1221-1226.

YANG, Y. & ROSENBERG, G. A. 2015. Matrix metalloproteinases as therapeutic targets for stroke. *Brain Research,* 1623**,** 30-38.

YANG, Z. & WANG, K. K. W. 2015. Glial fibrillary acidic protein: from intermediate filament assembly and gliosis to neurobiomarker. *Trends in Neurosciences,* 38**,** 364-374.

YAO, Y., CHEN, Z.-L., NORRIS, E. H. & STRICKLAND, S. 2014. Astrocytic laminin regulates pericyte differentiation and maintains blood brain barrier integrity. *Nature Communications,* 5.

YIN, W. & VOIT, E. O. 2013. Function and design of the Nox1 system in vascular smooth muscle cells. *BMC Systems Biology,* 7**,** 20.

YOUNG, C. N. & DAVISSON, R. L. 2015. Angiotensin-II, the Brain, and Hypertension. *Hypertension,* 66**,** 920-926.

YU, X., JI, C. & SHAO, A. 2020. Neurovascular Unit Dysfunction and Neurodegenerative Disorders. *Frontiers in Neuroscience,* 14.

ZHANG, M., BREWER, A. C., SCHRÖDER, K., SANTOS, C. X. C., GRIEVE, D. J., WANG, M., ANILKUMAR, N., YU, B., DONG, X., WALKER, S. J., BRANDES, R. P. & SHAH, A. M. 2010. NADPH oxidase-4 mediates protection against chronic load-induced stress in mouse hearts by enhancing angiogenesis. *Proceedings of the National Academy of Sciences,* 107**,** 18121-18126.

ZHANG, Q.-G., RAZ, L., WANG, R., HAN, D., DE SEVILLA, L., YANG, F., VADLAMUDI, R. K. & BRANN, D. W. 2009. Estrogen Attenuates Ischemic Oxidative Damage via an Estrogen Receptor α-Mediated Inhibition of NADPH Oxidase Activation. *The Journal of Neuroscience,* 29**,** 13823-13836.

ZHANG, Y., CAO, C., DU, S., FAN, L., ZHANG, D., WANG, X. & HE, M. 2021. Estrogen Regulates Endoplasmic Reticulum Stress–Mediated Apoptosis by ERK-p65 Pathway to Promote Endometrial Angiogenesis. *Reproductive Sciences,* 28**,** 1216-1226.

ZHAO, G.-J., ZHAO, C.-L., OUYANG, S., DENG, K.-Q., ZHU, L., MONTEZANO, A. C., ZHANG, C., HU, F., ZHU, X.-Y., TIAN, S., LIU, X., JI, Y.-X., ZHANG, P., ZHANG, X.-J., SHE, Z.-G., TOUYZ, R. M. & LI, H. 2020. Ca2+-Dependent NOX5 (NADPH Oxidase 5) Exaggerates Cardiac Hypertrophy Through Reactive Oxygen Species Production. *Hypertension (Dallas, Tex. : 1979)***,** HYPERTENSIONAHA12015558.

ZHAO, Y., VANHOUTTE, P. M. & LEUNG, S. W. S. 2015. Vascular nitric oxide: Beyond eNOS. *Journal of Pharmacological Sciences,* 129**,** 83-94.

ZHENG, X., REN, B. & GAO, Y. 2023. Tight junction proteins related to blood-brain barrier and their regulatory signaling pathways in ischemic stroke. *Biomed Pharmacother,* 165**,** 115272.

ZHOU, B., LIN, W., LONG, Y., YANG, Y., ZHANG, H., WU, K. & CHU, Q. 2022. Notch signaling pathway: architecture, disease, and therapeutics. *Signal Transduction and Targeted Therapy,* 7.

ZHOU, B., PEREL, P., MENSAH, G. A. & EZZATI, M. 2021. Global epidemiology, health burden and effective interventions for elevated blood pressure and hypertension. *Nature Reviews Cardiology,* 18**,** 785-802.

ZHOU, Y., YAN, H., GUO, M., ZHU, J., XIAO, Q. & ZHANG, L. 2013. Reactive Oxygen Species in Vascular Formation and Development. *Oxidative Medicine and Cellular Longevity,* 2013**,** 1-14.

ZIMMERMAN, B., RYPMA, B., GRATTON, G. & FABIANI, M. 2021. Age-related changes in cerebrovascular health and their effects on neural function and cognition: A comprehensive review. *Psychophysiology,* 58.

ZONG, Y., LI, H., LIAO, P., CHEN, L., PAN, Y., ZHENG, Y., ZHANG, C., LIU, D., ZHENG, M. & GAO, J. 2024. Mitochondrial dysfunction: mechanisms and advances in therapy. *Signal Transduction and Targeted Therapy,* 9.

ZOROV, D. B., JUHASZOVA, M. & SOLLOTT, S. J. 2014. Mitochondrial reactive oxygen species (ROS) and ROS-induced ROS release. *Physiol Rev,* 94**,** 909-50.

ZÁRATE, S., STEVNSNER, T. & GREDILLA, R. 2017. Role of Estrogen and Other Sex Hormones in Brain Aging. Neuroprotection and DNA Repair. *Frontiers in Aging Neuroscience,* 9.

ÖSTMAN, A., FRIJHOFF, J., SANDIN, Å. & BÖHMER, F.-D. 2011. Regulation of protein tyrosine phosphatases by reversible oxidation. *The Journal of Biochemistry,* 150**,** 345-356.